



# Venus Flagship Mission Study

April 17, 2009







## Venus Flagship Mission Study:

### Report of the Venus Science and Technology Definition Team

Task Order NMO710851

17 April 2009

A handwritten signature of Jeffery L. Hall.

Jeffery L. Hall  
Study Lead  
California Institute of Technology,  
Jet Propulsion Laboratory

A handwritten signature of Mark A. Bullock.

Mark Bullock  
co-Chair, Science and Technology  
Definition Team  
Southwest Research Institute

A handwritten signature of David A. Senske.

David A. Senske  
co-Chair, Science and Technology Definition Team  
California Institute of Technology,  
Jet Propulsion Laboratory

A handwritten signature of James A. Cutts.

James A. Cutts  
Manager, Strategic Missions and Advanced  
Concepts Office  
California Institute of Technology  
Jet Propulsion Laboratory

A handwritten signature of Rick Grammer.

Rick Grammer  
Director, Solar System Exploration Directorate  
California Institute of Technology,  
Jet Propulsion Laboratory





# NASA's Flagship Mission to Venus

A Future Mission Concept

## Venus Flagship Science Themes and Objectives

Science Theme	Science Objective
What does the Venus greenhouse tell us about climate change?	Understand radiation balance in the atmosphere and the cloud and chemical cycles that affect it
	Understand how superrotation and the general circulation work
	Look for evidence of climate change at the surface
How active is Venus?	Identify evidence of current geologic activity and understand the geologic history
	Understand how surface/atmosphere interactions affect rock chemistry and climate
	Place constraints on the structure and dynamics of the interior
When and where did the water go?	Determine how the early atmosphere evolved
	Identify chemical and isotopic signs of a past ocean
	Understand crustal composition differences and look for evidence of continent-like crust

## Science Payload for the Design Reference Mission

Orbiter	2 Balloons	2 Landers	
Lifetime (4 years)	(1 month)	Descent Phase (1–1.5 hour)	Landed Phase (5 hours)
InSAR — Interferometric Synthetic Aperture Radar	ASI — Atmospheric Science Instrument (pressure, temperature, wind speed.)	ASI	Microscopic imager
Vis-NIR Imaging Spectrometer	GC/MS — Gas Chromatograph / Mass Spectrometer	Vis-NIR Cameras with spot spectrometry	XRD / XRF
Neutral Ion Mass Spectrometer	Nephelometer	GC / MS	Heat Flux Plate
Sub-mm Sounder	Vis-NIR camera	Magnetometer	Passive Gamma Ray Detector
Magnetometer	Magnetometer	Net Flux Radiometer	Sample acquisition, transfer, and preparation
Langmuir Probe	Radio tracking	Nephelometer	Drill to ~10 cm
Radio Subsystem (USO — Ultra Stable Oscillator)			Microwave corner reflector

## Mission Elements



Orbiter S/C

Launch Vehicle
Atlas V-551 (w/ 5-m diameter fairing)
Mass (CBE + Cont.)
5308 kg (wet); 2275 kg (dry); Payload mass: 290.4 kg
Power
32 square meter solar panels (9868 W EOL)
Telecom
4-m Ka/X-band (Orbiter-to-Earth to 34-m DSN antennas); 0.5-m S-band (Orbiter-to-in situ); 2.5-m S-band (Orbiter-to-in situ)
Functions
Relay telecom support for in situ elements (30 days); 6 months of aerobraking to science orbit; Science orbiter (2 years baseline & 2 years extended); Overall Mission Science Data Return ~300 Tbits of data to Earth over 2 years of science operations

Mass (CBE + Cont.)
686 kg; Payload mass: 106.2 kg
Lander Design
0.9-m diameter titanium shell (1-cm wall thickness); Rotating pressure vessel; Drill to 10-cm (2 samples)
Thermal Design
Passive thermal management; Lithium nitrate phase change material (PCM); Silica insulation: 5-cm external; 1-cm internal; Carbon dioxide backfilled pressure vessel
Power
Lithium-thionyl chloride primary batteries (the same cells used on the balloons), (6 kWh, 12.6 kg)
Telecom
S-band LGA to Orbiter with Electra (backup to flyby s/c)
Functions
Descent science for ~1 hour; Surface science for 5 hours



Landers (2)



Balloons (2)

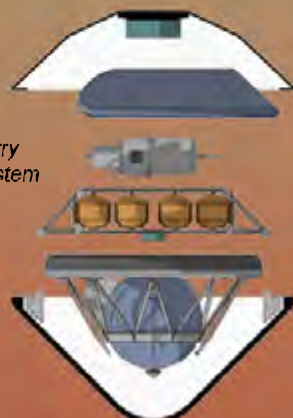
Mass (CBE + Cont.)
162.5 kg; Payload mass: 22.5 kg
Balloon design
7.1-m diameter helium filled superpressure balloon; Teflon coated for sulfuric acid resistance; Vectran fabric plus Mylar film construction; Metalized for low solar heating
Power
Lithium-thionyl chloride (Li-SOCl2) primary batteries (10.5 kWh, 22 kg)
Telecom
S-band to Orbiter (w/ backup to carrier flyby s/c); (plus carrier signal to Earth for Doppler and VLBI data)
Functions
30 days science operation at 55.5 km float altitude

## Carrier S/C

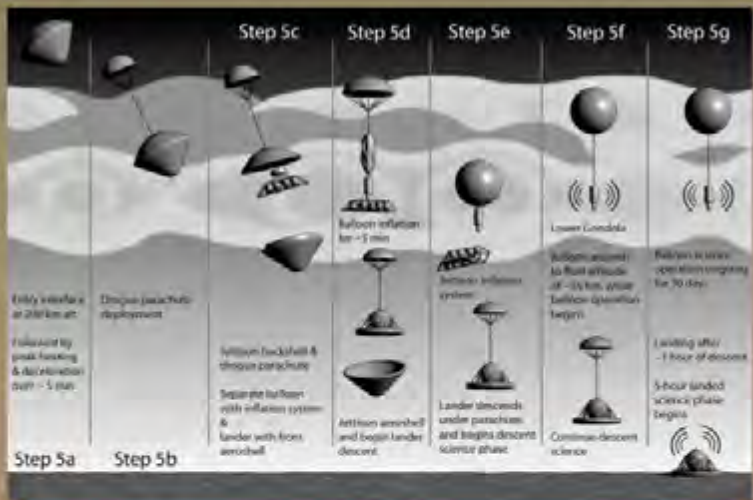
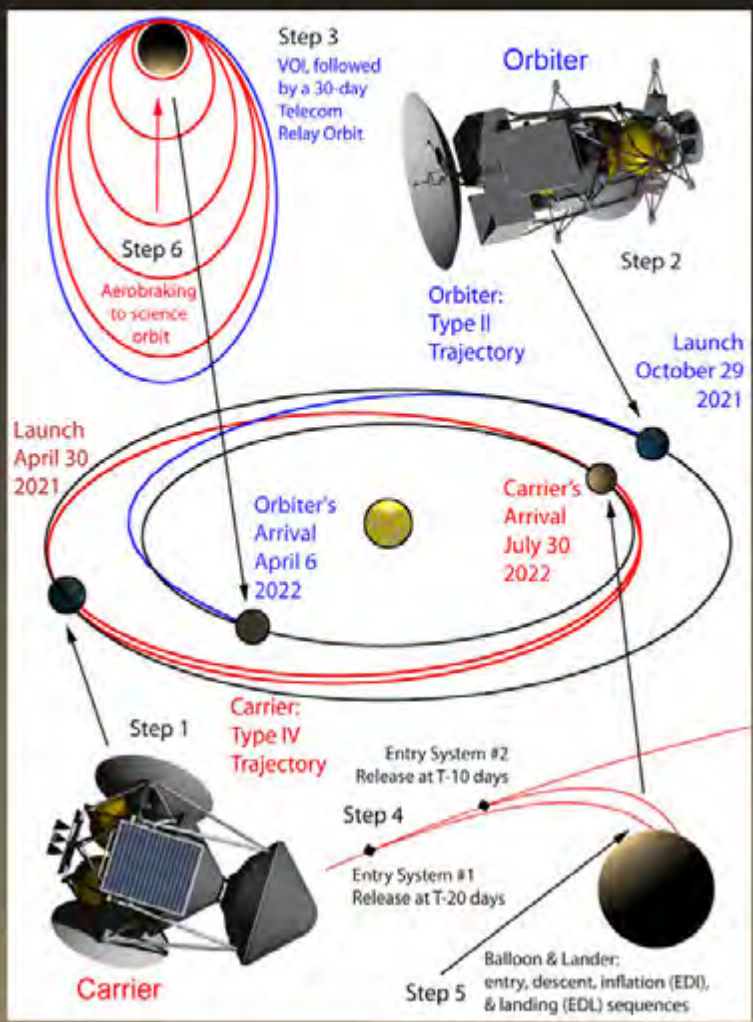
Launch Vehicle
Atlas V-551 (5-m diameter fairing)
Mass (CBE + Cont.)
5578 kg (wet) w/ entry systems; 1640 kg (wet) w/o the carried two entry systems
Power
4.4 square meter solar panels
Attitude Control
3-axis stabilized; (Spin up for release of entry systems)
Telecom
2.5-m dual-feed X/S-band HGA (Carrier-to-Earth to 34-m DSN antennas; and Carrier-to-in situ); 2.5-m S-band fixed HGA (Carrier-to-in situ)
Functions
Delivery & deployment of entry systems; & backup relay telecom

## Entry Systems (2)

Mass (CBE + Cont.)
1969 kg each entry system
Design
Thermal Protection System: Carbon-Phenolic
Aeroshell
45° half cone angle (Pioneer-Venus heritage); 2.65-m diameter; Spin stabilized after release from carrier
Functions
Entry systems deliver the in situ elements safely through the atmosphere; Each entry system carries a balloon & a lander with supporting subsystems



# Mission Architecture Overview



- Step 1:** Carrier spacecraft launch April 30, 2021 on an Atlas V-551 L/V (w/ 5-m diameter fairing) Type IV trajectory to Venus (arrives second after orbiter)
- Step 2:** Orbiter spacecraft launch October 29, 2021 on an Atlas V-551 L/V (w/ 5-m diameter fairing) Type II trajectory to Venus (arrives first before carrier)
- Step 3:** Orbiter arrives on April 6, 2022 (after 159-day cruise) Venus Orbit Insertion (VOI) maneuver 300 km × 40000 km orbit for telecom relay support for (balloons & landers)
- Step 4:** Carrier flyby on July 30, 2022 (after 436 days of cruise) Entry system #1 release: 20 days before carrier's Venus flyby Entry system #2 release: 10 days before carrier's Venus flyby Backup relay telecom support during lander's lifetime
- Step 5:** Staggered entry for entry systems (13 hours phasing – one orbiter revolution)
  - Entry, Descent, & Inflation (EDI) phases for the balloons
  - Entry, Descent, & Landing (EDL) phases for the landers
  - Step 5a:** Pre-entry phase: entry system (w/ balloon & lander) cruises to Venus
  - Step 5b:** Atmospheric entry; entry heating; deceleration; Deployment of drogue parachute.
  - Step 5c:** Separation of aeroshell into two parts; Main chutes open for balloon & lander elements
  - Balloon released from backshell storage container.
  - Step 5d:** Full balloon inflation in ~5 minutes
  - Step 5e:** Helium inflation system jettisoned; Balloon rises to 55.5 km equilibrium altitude; Lander continues its descent to the surface; descent science
  - Step 5f:** Balloon cord extended
  - One-month balloon science mission phase begins
  - Balloon data relayed to orbiter, then relayed to Earth
  - Step 5g:** Lander reaches the ground after 1 hour of descent
  - Begins 5-hour surface science operations phase
  - Lander data relayed to orbiter, then relayed to Earth
- Step 6:** Orbiter completes relay telecom support phase: 6 months of aerobraking to 230 km circular orbit; 2 years of orbiter science operations in prime mission (sufficient propellant for 2-year extended mission)

## Mission Cost Estimate

- Mission cost: \$2.7B to \$3.8B in FY09

### Cost assumptions:

- Technology Readiness Level: TRL-6 by 2016.
- Schedule: 24 month duration for Phases A & B, 52 month duration for Phases C & D.
- Mission class: the overall mission is Class A, as is the orbiter.
- Landers & balloons: single-string, redundancy through multiple mission elements.
- No contributed hardware from foreign partners.
- Pre-Phase A technology development funding at the level of 1-2% of the total mission cost.

## Team Members

### Venus STDT Members

Chair: Mark Bullock (SwRI)  
Co-Chair: David Senske (JPL)

### NASA & JPL

Jim Cutts (JPL)  
Adriana Ocampo (NASA HQ)

### Ex Officio

Ellen Stofan (VEXAG Chair)  
Tibor Kremic (NASA GRC)

### Atmosphere Sub-Group

David Grinspoon (Lead) (DMNS)  
Eric Chassefiere (France)  
Anthony Colaprete (NASA ARC)  
George Hashimoto (Japan)  
Sanjay Limaye (UW Madison)  
Hakan Svedhem (ESA)  
Dimitri Titov (Germany)  
Mikhail Y. Marov (Russia)

### Geochemistry Sub-Group

Allan Treiman (Lead) (LPI)  
Natasha Johnson (NASA GSFC)  
Steve Mackwell (LPI)

### Geology & Geophysics Sub-Group

Dave Senske (Lead) (JPL)  
Bruce Campbell (Smithsonian)  
Lori Glaze (NASA GSFC)  
Jim Head (Brown U.)  
Walter Kiefer (LPI)  
Gerald Schubert (UCLA)

### Technology Sub-Group

Elizabeth Kolawa (Lead) (JPL)  
Steve Gorevan (Honeybee)  
Gary Hunter (NASA GRC)  
Viktor Kerzhanovich (JPL)

### JPL Venus Flagship Team

Jeffery L. Hall (Study Lead) (JPL)  
Tibor Balint (JPL)  
Craig Peterson (JPL)  
Alexis Benz (JPL)  
Team-X Design Team

## Contents

1	EXECUTIVE SUMMARY .....	1-1
1.1	Science Goals and Objectives .....	1-1
1.2	Science and Technology Approach .....	1-2
1.3	The Venus Flagship Design Reference Mission .....	1-3
1.4	Recommended Technology Development.....	1-5
1.5	Conclusion .....	1-5
2	VENUS SCIENCE GOALS AND OBJECTIVES .....	2-1
2.1	Introduction: Mysteries of Venus .....	2-1
2.1.1	Venus Flagship Science Traceability .....	2-3
2.2	Exploring Venus to Better Understand the Earth .....	2-6
2.3	Science Background, Goals, and Objectives .....	2-9
2.3.1	The Venus Atmosphere.....	2-13
2.3.2	Venus Geology .....	2-25
2.3.3	Venus Interior Structure .....	2-38
2.3.4	Venus Geochemistry .....	2-42
2.4	Venus and Planets Around Other Stars.....	2-47
2.5	Scientific Advancement to be Achieved by a Venus Flagship Mission .....	2-49
3	CHOOSING THE MISSION ARCHITECTURE.....	3-1
3.1	Mission Architectures Analysis of Alternatives .....	3-1
3.2	Design Reference Mission Trades .....	3-7
3.2.1	Selection of the Science Instruments .....	3-7
3.2.2	Major Architectural Trades .....	3-8
3.2.3	In Situ Vehicle Trades.....	3-10
3.3	Design Reference Mission Synopsis.....	3-13
4	DESIGN REFERENCE MISSION .....	4-1
4.1	Introduction.....	4-1
4.2	Design Reference Mission Summary.....	4-1
4.3	Science Payload Description.....	4-3
4.3.1	Orbiter Instruments .....	4-3
4.3.2	Balloon Instruments .....	4-10
4.3.3	Lander Instruments.....	4-13
4.3.4	Data Taking Scenario and Data Volumes .....	4-30
4.4	Mission Design and Trajectories .....	4-35
4.4.1	Overview .....	4-35
4.4.2	Trajectories and Launch Vehicle.....	4-35
4.4.3	Orbit Design and Landing Sites .....	4-39

4.4.4	Orbiter Science Mission Design.....	4-43
4.4.5	Mission Options .....	4-43
4.4.6	Mission Timeline Details .....	4-44
4.5	Vehicle Descriptions for Mission Elements .....	4-47
4.5.1	Orbiter .....	4-47
4.5.2	Carrier .....	4-61
4.5.3	Entry Vehicle.....	4-69
4.5.4	Balloons .....	4-75
4.5.5	Lander .....	4-84
4.5.6	Mission Operations .....	4-96
4.5.7	Ground Systems .....	4-96
4.6	Planetary Protection Considerations .....	4-98
4.7	Open Issues and Identified Risks.....	4-99
4.8	New Technology Requirements for the DRM .....	4-102
4.8.1	Surface Sample Acquisition System .....	4-102
4.8.2	Rotating Pressure Vessel.....	4-107
4.8.3	Rugged Terrain Landing System.....	4-107
4.8.4	Instruments .....	4-107
4.9	Mission Cost Estimate .....	4-109
5	MISSION AND PAYLOAD ENHANCEMENTS FOR EXTRAORDINARY SCIENCE RETURN .....	5-1
5.1	Background: Path to a Venus Surface Sample Return Mission.....	5-1
5.2	Enhancements to the Landed Mission .....	5-2
5.2.1	In-situ Science at the Venus Surface .....	5-2
5.2.2	Extended Surface Life Landers .....	5-3
5.3	Enhancements to the Balloon Mission.....	5-5
5.3.1	In-situ Atmospheric Science at Venus .....	5-5
5.3.2	Enhanced Mid-Altitude Balloons.....	5-5
5.4	Mission Architecture Enhancements .....	5-8
5.4.1	Surface Exploration.....	5-8
5.4.2	Technologies for Exploring the Surface of Venus .....	5-20
5.4.3	Atmospheric Exploration .....	5-38
5.4.4	Orbiter Science Enhancements.....	5-43
5.5	Recommended Technology Priorities.....	5-46
6	SUMMARY AND CONCLUSIONS.....	6-1
6.1	Acknowledgements and Notes.....	6-2
7	REFERENCES .....	7-1

A	CHOOSING THE MISSION ARCHITECTURE.....	A-1
A.1	Venus Flagship Mission Science .....	A-2
A.2	Constructing the Science Analysis Matrix.....	A-3
A.3	Mission Architecture Assessment Methodology .....	A-5
A.3.1	Science Figures of Merit .....	A-5
A.3.2	Technological Difficulty .....	A-5
A.3.3	Mission Architecture Elements .....	A-6
A.3.4	Rapid Cost Estimates .....	A-6
A.4	Mission Architectures .....	A-9
B	ADVANCED IN SITU EXPLORATION CONCEPTS .....	B-1
B.1	Rovers .....	B-1
B.1.1	Scientific Objectives of a Venus Rover .....	B-2
B.1.2	Technologies for Venus Rovers .....	B-2
B.2	Atmospheric Exploration by Aircraft .....	B-4
B.2.1	Scientific Objectives for the Exploration of Venus by Aircraft.....	B-5
B.2.2	Technologies for Venus Aircraft.....	B-5
B.2.3	Solar Power Generation Technology for Venus Exploration.....	B-7



## 1 EXECUTIVE SUMMARY

---

### 1.1 Science Goals and Objectives

There is a compelling motivation of great global concern for exploring Venus: As we discover how climate and geology work on a world similar to our own, we gain a deeper understanding of the processes at work in our own environment. With the realization that the Earth's climate system is not sufficiently well understood, and the threat of accelerating anthropogenic changes to the atmosphere, comes a valid concern about the natural vulnerability of the world in which we have thrived. What are the limits of stability of the global system under the influence of human consumption and effluent? Could rapid or irreversible changes be triggered by the current unprecedented pace of greenhouse gas input to the atmosphere (IPCC, 2007)? Are there climate tipping points beyond which there is no return? To this last question, because of planetary exploration, we know the answer. Yes. Venus' oceans boiled away in a dramatic runaway greenhouse and were eventually lost to space. If this happened to Venus, could it happen to Earth? Again, the answer is yes. Earth will someday pass the tipping point, its oceans will boil, and a desiccated, hot Earth will be like Venus today. We know this because main sequence stars like the Sun slowly increase in luminosity as their fuel is used up. Subtler discontinuities in climate, with real consequences for society, are certainly possible and climate feedbacks that might be difficult to discern in the Earth system might be illuminated by the deeper understanding of planetary climate gained by studying the climate of Venus.

Our great progress in exploring Mars illustrates how in-depth exploration of a nearby terrestrial planet can successfully illuminate Earth processes. Mars's dynamic surface, accessible to our eyes for centuries and comparatively benign as an environment for spacecraft exploration, has revealed how physics and chemistry have shaped another rocky world. This cold, dry planet has a

history of water, climate, and potential habitability starkly different from our own. Other planets will, of course, offer radically different comparisons. Venus, too, we believe, had early oceans but lost this habitable environment for completely different reasons. Verifying and quantifying this story will immensely improve our understanding of how Earth-like worlds come to be and how they might evolve to either encourage life or extinguish it. More immediately, the nature of climate feedbacks that might ultimately determine the physical safety and economic security of society must be understood. Some of the most revealing secrets to the formation of the solar system, the evolution of climate on our own planet, and the habitability of terrestrial planets around other stars can be found only on Venus. But the searching is difficult: Venus' obscuring cloud layer and hostile environment have made it a challenging planet to explore. Nevertheless, many of the scientific investigations that should be done to understand the Venus system and relate those results to our own world can be achieved by a flagship mission to Venus. This report 1) describes in detail the important science that should be done at Venus in the coming decades to achieve these goals and 2) details a flagship Design Reference Mission (DRM) to accomplish many of them.

Why is Venus so different from Earth? The science driving a flagship-class mission to Venus can be summarized by its three themes:

1. What does the Venus greenhouse tell us about climate change? The Venus greenhouse is poorly understood because it is coupled to the still mysterious atmospheric dynamics and cloud physics. To better understand the atmosphere, experiments that simultaneously probe dynamics, chemical cycles, energy balance, and isotopic abundances must be performed, mostly in situ.

**Table 1.1:** Top-Level Science Themes and Objectives for the Venus Flagship Mission.

Science Theme	Science Objective
What does the Venus greenhouse tell us about climate change?	Understand radiation balance in the atmosphere and the cloud and chemical cycles that affect it
	Understand how superrotation and the general circulation work
	Look for evidence of climate change at the surface
How active is Venus?	Identify evidence of current geologic activity and understand the geologic history
	Understand how surface/atmosphere interactions affect rock chemistry and climate
	Place constraints on the structure and dynamics of the interior
When and where did the water go?	Determine how the early atmosphere evolved
	Identify chemical and isotopic signs of a past ocean
	Understand crustal composition differences and look for evidence of continent-like crust

2. How active is Venus? The search for Venus' activity ranges from detecting active volcanic processes, to tracking the clouds and logging meteorological data such as the winds, pressures, and temperatures. Detecting ground movement at one location and monitoring the planet globally for seismic events are the most definitive tests for internal structure and activity.

3. When and where did the water go? Mineralogical and chemical analyses of Venus' surface, if done with sufficient precision, have the potential to revolutionize our understanding of Venus' geology. The ability to analyze both rocks and soils and to drill to depths within pristine rocks holds the key to past changes in atmospheric conditions, volcanism, and climate. Volcanism, tectonism, and weathering affect the climate of Earth in profound ways.

The top-level science objectives for a Venus flagship mission can be traced directly from these three science themes in Table 1.1. A comprehensive discussion of our current knowledge of Venus and of open science questions is presented in Chapter 2.

## 1.2 Science and Technology Approach

The Venus Science and Technology Definition Team was created by NASA's Science Mission Directorate to formulate the

science goals and objectives and to design the mission architecture, science investigations, and instrument payload for a flagship-class mission to Venus. It was also tasked with developing a prioritized technology roadmap to bring the necessary technologies and instruments to sufficient technology readiness levels. This was facilitated by a JPL engineering study team and JPL's Advanced Projects Design Team (Team X). This \$3- to \$4-B flagship mission, to launch in the 2020 - 2025 timeframe, should revolutionize our understanding of how climate works on terrestrial planets, including the close relationship between volcanism, tectonism, interiors, and atmospheres. Details of methods the STDT used and the process by which we selected an optimum architecture are briefly given in Chapter 3 and in more depth in Appendix A.

The work of the STDT was divided into two phases. Phase 1 was a very broad look at the science objectives for a Venus flagship mission and a detailed consideration of a large range of mission architecture options. The STDT drew upon the successful multi-year community Venus Exploration and Analysis Group (VEXAG) effort to define the science goals and objectives for the exploration of Venus (VEXAG, 2007), as well as the NRC Solar System Decadal Survey (National Research Council, 2003) and its update (National Research Council, 2008) and the

2006 NASA Roadmap (NASA, 2006). Phase 2 focused on creating a flagship-class Design Reference Mission that would provide optimal science return for a detailed exploration of Venus. This point design provides preliminary estimates of the mass, power, data, and cost resources needed for a flagship mission to Venus, along with a set of technology development requirements. The team also studied science and technology enhancements to the flagship mission that could be done if, for example, one or more smaller missions advances knowledge of Venus before the flagship is flown. These enhanced science investigations, not part of the DRM, are detailed in Chapter 5.

### **1.3 The Venus Flagship Design Reference Mission**

The Venus flagship Design Reference Mission, optimized to achieve the most high-priority science, is comprised of a highly capable orbiter, two balloons in the clouds, and two landers on different terrains. The orbiter provides telecommunication relay support for a month-long balloon campaign and two five-hour landers and then aerobrakes into a 230-km circular science mapping orbit for a two-year mapping mission. Extremely high-resolution radar and altimetry mapping will explore the surface at resolutions up to two orders of magnitude greater than was achieved with Magellan, opening a new door to studies of comparative geology. While the balloons circumnavigate the planet up to seven times, they continually sample gases and cloud aerosols and measure the solar and thermal radiation within the clouds. The landers perform descent science, obtaining atmospheric measurements in complementary vertical slices and taking images of the surface on the way down. While on the surface, they perform high-fidelity analyses of the elemental and mineralogical content of rocks and soils on and beneath the surface. Panoramic images of the landing sites at an order of magnitude higher resolution than achieved with previous landers provide geologic context for the landing and sampling sites. The mission requires two Atlas V 551 launch vehicles in

the 2020 - 2025 timeframe: one for the orbiter, the other for the in situ vehicles and carrier. The mission, its payload, and the technology development requirements for the DRM are discussed in detail in Chapter 4. The preliminary cost analysis for the DRM gives a range of \$2.7 B to \$3.8 B in FY09.

Clearly, the technological challenges for in situ exploration of Venus are high. The STDT considered mission architectures and payloads whose components and instruments could be at Technical Readiness Level (TRL) 6 or higher by 2015. This ruled out a large number of scientifically promising approaches. Therefore, beyond the DRM, we considered the extra capabilities of a slightly enhanced mission that could be accommodated with the DRM architecture and entirely new capabilities for different architectures that would require a moderate, sustained technology program to achieve extraordinary science return from Venus. Table 1.2 shows how the major open questions defined by the STDT can be addressed by the DRM, by enhancements to the DRM, and by new capabilities for different architectures.

The DRM accomplishes a very wide range of atmospheric, geologic, and geochemical investigations to illuminate how the atmosphere, clouds, surface, and interior interact over many timescales. It does this by using the synergy of simultaneous atmospheric and surface in situ exploration under a very capable mapping orbiter. The total science performance of the DRM is shown in the 4<sup>th</sup> colored column, ‘DRM with synergies.’ The answer to whether Venus ever lost a primary atmosphere through impacts or massive escape will be obtained definitively. Investigations into the structure and evolution of the interior are not as well represented. On the right side, under ‘New Capabilities,’ it is apparent that a seismometry network will be required to answer these important geophysical questions about Venus.

**Table 1.2:** Major Open Questions and How the DRM and Capabilities Beyond Can Address Them.

MAJOR OPEN SCIENTIFIC QUESTIONS ABOUT VENUS	DESIGN REFERENCE MISSION			DRM ENHANCEMENTS				NEW CAPABILITIES				
	Orbiter	Landers	Balloons	DRM with synergies	Orbiter	Landers	Balloons	with synergies	Seismic/ Meteor Stations	Low Alt Balloon	Long Duration Lander	Drop Sondes/ Lidar
<b>VENUS ATMOSPHERE</b> How did Venus evolve to become so different from Earth? Was Venus ever habitable, and for how long? Did Venus lose a primary atmosphere due to impacts or loss to space? What drives Venus' atmospheric superrotation? How do geologic activity and chemical cycles affect the clouds and climate? How are atmospheric gases lost to space?	Yellow	Green	Orange	Green	Yellow	Green	Orange	Green	Yellow	Orange	Green	Orange
<b>VENUS GEOLOGY</b> What is the volcanic and tectonic resurfacing history of Venus? How were the heavily deformed highlands made? How active is Venus geologically? Did Venus ever have plate tectonics and if so, when did it cease? How are geology and climate connected on Venus? What has been the role of water and other volatiles in Venus geology?	Green	Yellow	Green	Green	Green	Yellow	Yellow	Green	Green	Yellow	Green	Yellow
<b>VENUS INTERIOR STRUCTURE</b> Does Venus have Earth-like continents? What are the chemical, physical, and thermal conditions of the interior? How does mantle convection work on Venus? What is the size and physical state of the core? What is the structure of the Venus lithosphere? How have water and other volatiles affected Venus' interior evolution?	Yellow	Green	Orange	Green	Yellow	Green	Orange	Green	Blue	Green	Orange	Green
<b>VENUS GEOCHEMISTRY</b> Was there ever an ocean on Venus, and if so, when and how did it disappear? What caused the resurfacing of Venus over the past billion years? What is the nature of chemical interactions between surface and atmosphere? What are the tectonic forces behind Venus' volcanism? How were the rocks and soils of Venus formed? What do chemical differences of terrains say about the evolution of Venus?	Yellow	Green	Orange	Green	Yellow	Green	Orange	Green	Yellow	Green	Orange	Green

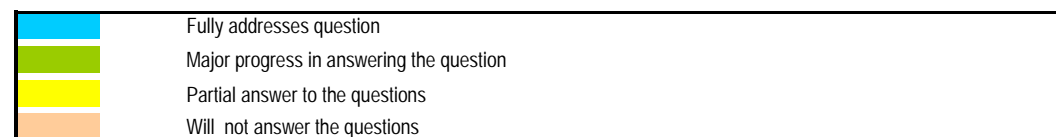


**Table 1.3:** Venus Exploration Technology Development Priorities.

	Technologies for DRM	Comments
1	Surface sample acquisition system at high temperature and pressure conditions	Drilling, sample collection and sample handling are enabling for the Design Reference Mission. Heritage Soviet-derived systems are not available off the shelf, but they demonstrate a feasible approach.
2	Lander technologies for rotating pressure vessel and rugged terrain survivability	Rotating pressure vessel concept is powerful but technologically immature. Tessera and other rugged areas on Venus cannot be reliably accessed unless a properly engineered rugged terrain landing system is provided.
3	Venus-like environmental test chamber	This capability is critical for testing and validation of science measurements as well as for testing of components and systems for their survivability in Venus environment
	New Capabilities	Comments
4	Refrigeration for the Venus surface environment	Almost every long duration (beyond 25 hrs), in situ platform will require some amount of refrigeration to survive. Focus should be on radioisotope-based duplex systems that produce both refrigeration and electrical power.
5	High temperature sensors and electronics, including telecom systems	Refrigeration requirements can be drastically reduced if electronics can operate at elevated temperatures. While a Venus ambient 460°C capability would be most desirable for telecom, data processing/storage, and power electronics, a major reduction in refrigeration loads could be realized already with moderate temperature operation (> 250° C).
	Enhancement to Current DRM Design	Comments
6	Extension of lander life through advanced thermal control	Human intervention during the landers operation on the surface of Venus is not possible unless landers life is extended to at least 24 hrs.

As shown in the middle set of colored columns, enhancements to the DRM that are easily achievable by 2015 with an appropriate technology program can greatly improve the science return of the Venus flagship mission. What is not shown is that these enhancements also reduce risk. The enhanced science possibilities with the DRM architecture, reduced risk, and technology challenges are discussed in Chapter 5.

#### 1.4 Recommended Technology Development

The Venus STDT developed a prioritized set of technological challenges that must be met to bring all instruments and spacecraft systems to a Technological Readiness Level of 6 by 2016. In addition, the STDT studied more advanced technologies that could enable greatly enhanced science and pave the way for an eventual Venus Surface Sample Return (VSSR) mission. Key to enabling a Venus flagship mission is the ability to conduct investigations and tests in Venus simulation chambers. Table 1.3 shows recommended technology development for Venus exploration in priority order.

#### 1.5 Conclusion

A flagship-class mission to Venus is NASA's first opportunity to fly a large mission to another Earth-sized planet with the explicit intention of better understanding our own. A deep understanding of how atmospheric greenhouses work, how volcanic and tectonic processes operate on a planet without plate tectonics, and the fate of oceans on terrestrial planets is within reach. The flagship mission described in this report represents an armada of interconnected platforms to explore the Venus atmosphere and surface in a way that will cast new light on our home world.



## 2 VENUS SCIENCE GOALS AND OBJECTIVES

---

### 2.1 Introduction: Mysteries of Venus

The most prominent planet in the sky's retinue of worlds is one of the most difficult to explore. Shrouded in almost featureless clouds, Mariner 2 detected a drop-off in radio emission towards the limb during its flyby in 1962 (Barath et al., 1964). This was a strong indicator that the emission originated from a very hot surface. Pollack and Sagan (1967) showed that an approximately 100-bar, CO<sub>2</sub>-N<sub>2</sub>, cloudy atmosphere best fit the radiometer data. Current understanding of planet formation in the inner solar system, as well as a similar proximity to the early Sun, strongly suggests that Venus and Earth formed from similar materials (Morbidelli et al., 2000). Currently, one obvious and important exception to their compositional similarity is water. Earth's surface is rich in water, while Venus has none on its surface and nearly none in its atmosphere: a desiccation attributed to loss of H and O to space. The key discovery by Pioneer Venus was the extraordinarily high D/H ratio in the atmosphere, the signature of massive fractionating loss of water (Donahue et al., 1982). How and when this water was lost is key to understanding Venus' evolution, the possible future of the Earth, the evolution of planets around other stars, and the factors that are important for allowing life to take hold on a terrestrial planet.

Venus is an Earth-like planet that experienced a massive runaway greenhouse (Kasting, 1988). Kasting showed that the loss of water probably occurred during a 'moist' greenhouse, with water vapor buffered by a warm ocean, rather than from a steam atmosphere. With a warm ocean and wet interior, it has been suggested that Venus might have had crustal recycling early in its history, an echo of a world with which we are intimately familiar (Sleep, 2000). The dry planet we see today has thick sulfuric acid clouds and no plate tectonics (Solomon et al., 1992). However, volcanic features dominate the Venus landscape, and the planet has been so geologically active that 80% of its history

has been erased (Phillips et al., 1992). The loss of water might be the fundamental reason that Venus is so different from Earth. Without sufficient water in the mantle, an asthenosphere might not develop and the lubricating layer upon which tectonic plate movement depends might be lacking (Kiefer and Hagar, 1991; Grinspoon, 1993).

The Venus atmosphere is more than an impediment to seeing the surface, it is an enigma in itself (Figure 2.1). Sixty five times denser than Earth's, it is more like an ocean than air. A variable photochemical sulfuric acid haze envelopes the outer layers of the clouds, but there is sufficient H<sub>2</sub>SO<sub>4</sub> vapor to produce thick global convective clouds beneath the haze (Esposito et al., 1983). The atmosphere rotates as much as 60 times faster than the solid body, exhibiting wave structures at many spatial scales. How angular momentum is transported in the Venus atmosphere to support the global super-rotating winds is unknown (Gierasch et al., 1997; Schubert, 1983). The gradient in absorbed solar energy from equator to pole is such that heat and momentum flow from poles to equator must occur, although it has never been observed. Storm systems or other eddies in the lower atmosphere might be an important component of Venus' weather. Over each pole, a hemisphere-wide vortex creates mass convergence in polar regions leading to descending air, as seen from Mariner 10 (Limaye and Soumi, 1981; Suomi and Limaye, 1978), Pioneer Venus (Limaye, 1985), Galileo (Peralta et al., 2007), and, recently, from Venus Express (Limaye et al., 2009) (see Figure 2.2).

Except for the spectacular surface images from the Venera missions, little is known of the local geology (Figure 2.3). However, intensive analysis of the Venera 13 and 14 data has yielded important insights into the unique Venus geochemistry, confirming the presence of vast basaltic plains (Surkov et al., 1984). Magellan radar images present a geologically young surface covered with volcanic features ranging from small shields to giant flows to

large volcanic edifices (Saunders et al., 1992). The presence of rift valleys and compressional mountain belts indicate that Venus has been tectonically active. The paucity of impact craters and an average surface age of ~300 - 700 My also points to activity through recent

geologic time (Bullock et al., 1993; McKinnon et al., 1997).

The interaction between the interior, surface, and atmosphere creates a climatic system where all three must be understood to provide insight into the planet as a whole.



**Figure 2.1:** Venus in visible and ultraviolet light as seen from the Mariner 10 flyby in 1974 (Courtesy NASA).

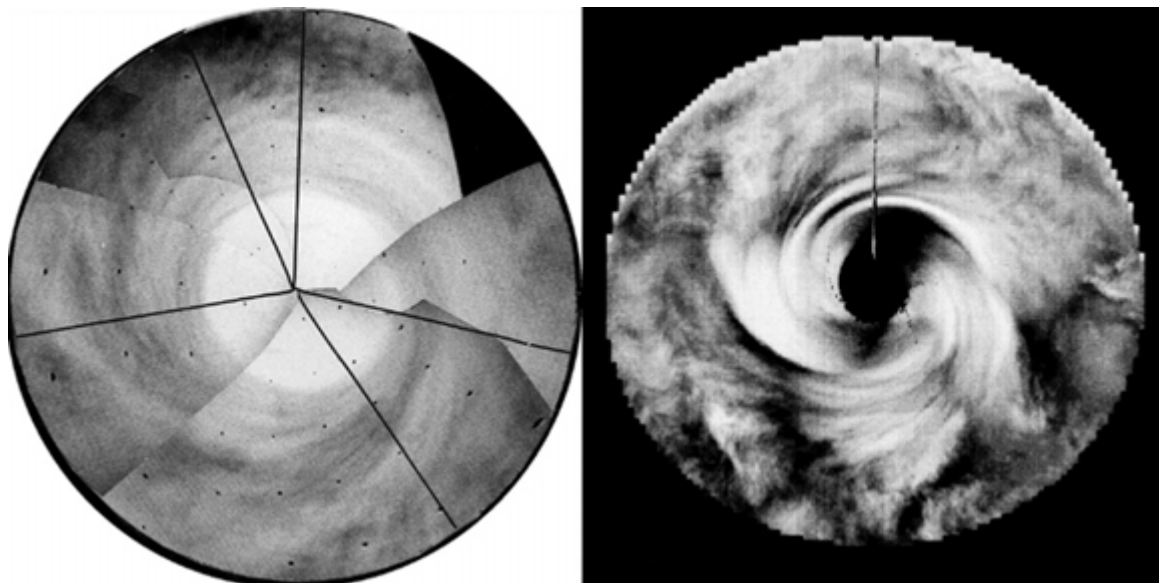


**Figure 2.2:** Southern hemisphere of Venus as seen in a time-averaged composite of Mariner 10 ultraviolet images (Limaye, adapted from Suomi and Limaye, (1978)), and Pioneer Venus OCPP data (Limaye, 1985).

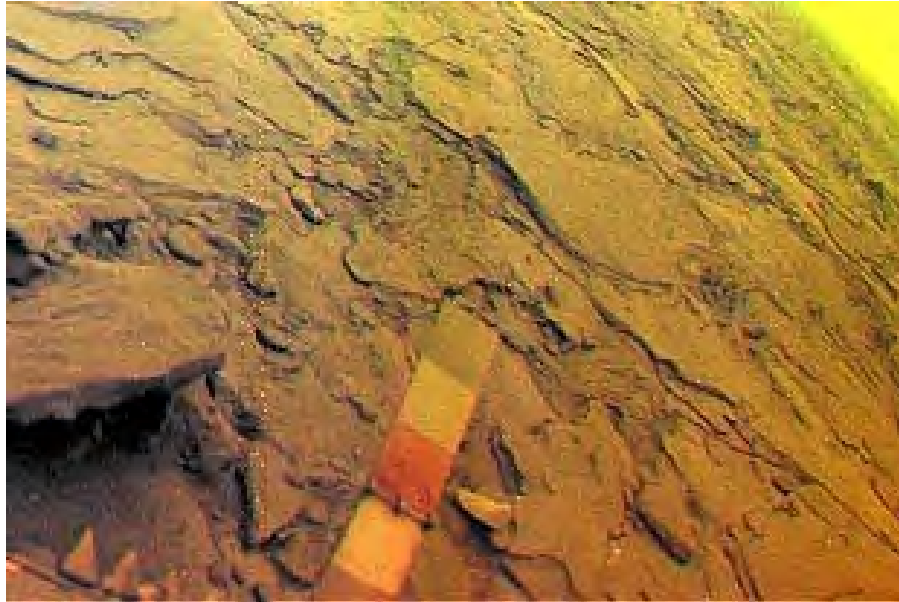


Figure 2.3: The basaltic plain of the Venera 14 landing site. Cm-scale blocks can be seen on the left; thin bedding for at least a few cm of the surface is apparent. The yellow Rayleigh scattered sky can be seen in the upper right.

### 2.1.1 **Venus Flagship Science Traceability**

The results of previous missions and the current Venus Express Mission reveal the complex interactions of the Venus interior, surface, and atmosphere. The array of significant and compelling science questions that would lead to a better understanding of Venus and its environment led NASA's Planetary Science Division in January of 2008 to commission a Science and Technology Definition Team (STDT). The charter of this group was two-fold: (1) formulate science requirements (goals, objectives, investigations,

and measurements) for a flagship-class mission to Venus and (2) generate a technology roadmap to identify both near-term and long-range capabilities that would feed into and lower the risk of a flagship mission. A major result of the STDT's activity is a mission architecture that will provide abundant and revolutionary science advancement. The overarching theme of Venus exploration is to understand our nearest neighbor with the explicit intention of better understanding our own. To this end, we have put forward three major science themes that give rise to specific objectives (Table 2.1).

**Table 2.1:** Driving Science Themes and Objectives for a Venus Flagship Mission.

Science Theme	Science Objective	Science Discipline
What does the Venus greenhouse tell us about climate change?	Understand radiation balance in the atmosphere and the cloud and chemical cycles that affect it	Atmosphere
	Understand how superrotation and the general circulation work	Atmosphere
	Look for evidence of climate change at the surface	Geochemistry
How active is Venus?	Identify evidence of current geologic activity and understand the geologic history	Geology/Geophysics
	Understand how surface/atmosphere interactions affect rock chemistry and climate	Geology/Geophysics
When and where did the water go?	Place constraints on the structure and dynamics of the interior	Geology/Geophysics
	Determine how the early atmosphere evolved	Atmosphere
	Identify chemical and isotopic signs of a past ocean	Geochemistry
	Understand crustal composition differences and look for evidence of continent-like crust	Geochemistry

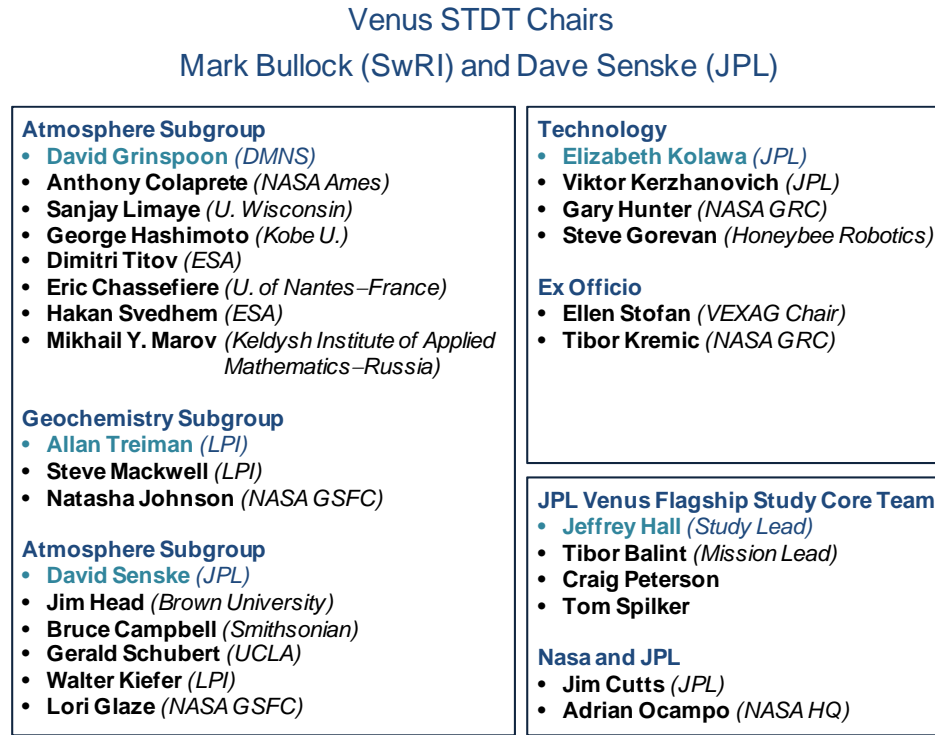


Figure 2.4: The organizational structure of the Venus Science and Technology Definition Team.

The Venus STDT was comprised of planetary scientists and engineers from around the world. More than 100 applications to serve on the team were received; it was, therefore, relatively easy to obtain a scientifically well-balanced team. The JPL flagship study team designed the mission to perform the exploration science prioritized by the science members of the STDT. Lessons learned from former Soviet missions, French space activities, ESA missions, and Japanese plans for exploring Venus were all widely explored by the STDT because there were active participants from each of those organizations. In addition, the STDT worked closely with the Venus Exploration and Analysis Group (VEXAG) to garner community input and serve as a means of communicating results. All Venus STDT products are available on the VEXAG web site at <http://www.lpi.usra.edu/vexag/venusSTDT/>.

The STDT was divided into 4 groups: (1) atmospheric science, (2) geology and geophysics, (3) geochemistry, and (4) technology. The organization chart for the STDT is shown in Figure 2.4.

From a scientific perspective, it was fully recognized that a division by discipline was somewhat arbitrary and that interactions between different processes (e.g., surface geology and the atmosphere) are paramount to understanding Venus. The subgroup work was done to make the task tractable, but a generous amount of time was devoted to communication between the different disciplines.

Guiding the overall process was traceability of the Venus Flagship themes to the high-level science goals identified in the NASA-commissioned “Solar System Decadal Survey” (*New Frontiers in the Solar System: An Integrated Exploration Strategy*, 2003 [National Research Council, 2003]). The Venus STDT also used the NASA 2006 Science Roadmap (NASA, 2006) and the Venus Exploration Analysis Group (VEXAG) report (*Venus Exploration Goals, Objectives, Investigations and Priorities: 2007* [VEXAG, 2007]) as governing documents. Key elements of the overall traceability are provided in Table 2.2.

**Table 2.2:** Traceability of Venus Flagship Science to Major Themes and Documents

Solar System Exploration ("Decadal") Survey	2006 SSE Roadmap and 2007 NASA Science Plan	VEXAG Venus Exploration Goals	Venus Flagship Theme
Learn how the Sun's retinue of planets and minor bodies originated and evolved	How did the Sun's family of planets and minor bodies originate?	How did Venus Originate and Evolve?	What does the Venus Greenhouse tell us about climate change?
Discover how the simple, basic laws of physics and chemistry can lead to the diverse phenomena observed in complex systems	How did the solar system evolve to its current diverse state?	What are the Processes that have and still shape the Planet?	How active is Venus?
Understand how physical and chemical processes determine the main characteristics of solar system bodies and their environments, thereby illuminating the workings of Earth		What does Venus tell us about the fate of Earth's Environment?	
Determine if environments capable of sustaining life exist or have ever existed beyond Earth, what parameters constrain its occurrence, how life developed in the solar system, whether life exists or may have existed beyond Earth, and in what ways life mod	What are the characteristics of the solar system that lead to the Origin of Life?		When and where did the Water go?
	How did Life begin and evolve on Earth and has it evolved elsewhere in the solar System?		
Explore the terrestrial space environment to discover what potential hazards to Earth may exist	What are the hazards and resources in the solar system environment that will affect the extension of human presences in space?	N/A	N/A

Because of the broad community consensus about Venus science priorities through the multi-year VEXAG progress (VEXAG, 2007), the STDT primarily used these findings as a starting point for considering the science that could be done by a flagship mission to Venus. The STDT quickly discovered, however, that defining science requirements for a mission is a vastly different exercise from defining science requirements for Venus exploration in general. As a result, science objectives became focused, redundancies were eliminated, and the most difficult scientific investigations were viewed with greater skepticism. Ultimately, a matrix that maps science objectives and investigations to instruments and spacecraft platforms was assembled. The purpose of the science traceability matrix was to guide the definition of a mission that maximizes the highest priority science.

## 2.2 Exploring Venus to Better Understand the Earth

The history of human exploration, from the original African exodus to the robots dispatched to other planets, has shown that it is the comparisons we make between our home environment and other, alien ones that allow us to understand the world more deeply and to adapt to its changes. Venus is like Earth in many ways: a surface that is geologically young compared to most bodies in the solar system; an environment shaped by active geochemical cycles, clouds, and volcanism; and a climate caused by the interplay of these phenomena. Yet, as we examine the Earth's environmental and climate history, Venus is a world of extremes, not least of which is a runaway CO<sub>2</sub> greenhouse (Figure 2.5).

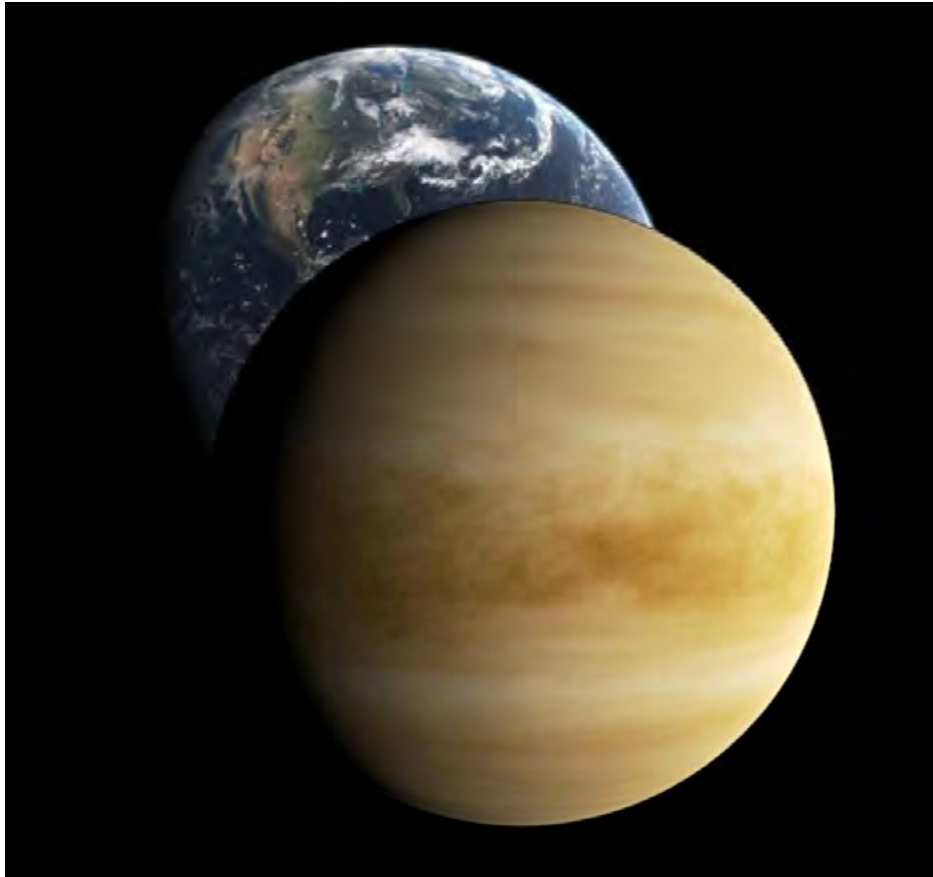


**Figure 2.5:** Venus and Earth, companions in the cosmos that have much to tell us through an examination of their common processes and divergent natures.

The obvious benefit to Earth of additional detailed studies of Venus is in understanding climate change more deeply as we grapple with the uncertain threat of a growing anthropogenic greenhouse (IPCC, 2007). Venus is useful as an extreme case of global warming, both in helping to understand past and current climate processes and changes and as a model for the far future evolution of the Earth's climate under a warming Sun. As extreme as Venus' climate is, its behavior in response to the positive and negative feedbacks that control climate can illuminate poorly understood connections in the Earth's climate system. Simulating the Venus climate using modifications and extensions of terrestrial climate models can help us validate techniques and models, thereby helping to identify assumptions and implicit simplifications in current Earth climate models, which do not apply correctly to more extreme climate regimes.

Venus' thick sulfuric acid clouds might seem impossibly exotic compared with the benign water clouds that float in the Earth's atmosphere. However, several climatically important types of terrestrial clouds have close physical analogs in the Venus clouds; the comparative studies of these clouds can increase the sophistication of our understanding of the important influence of clouds on radiative balance, including microphysics, cloud morphology, dynamics, and cloud coverage on Venus and Earth.

In the isolated, cold air inside the Earth's winter vortex, exotic thin clouds form. These clouds are comprised of sulfuric acid, nitric acid, and chlorine species. These Venus-like clouds are important components in anthropogenic perturbations to Earth's atmospheric chemistry and climate because catalytic reactions on cloud particles further change the atmospheric chemistry. Sulfates in the Earth's stratosphere are enhanced during and after major volcanic eruptions, as a thin, global sulfate aerosol layer remains suspended

for years at a time (Hamill et al., 1977). Sulfate from recent eruptions have lowered global temperatures by 2 – 3 °C for 2 years (Albritton et al., 2001). Much larger eruptions have even greater global effects; for example, Tambora, in 1815, appears to have caused 'the year without a summer' because of a thick, reflective layer that increased the planetary albedo (Coffin and Eldholm, 1994).

Very cold stratospheric aerosols act as catalysts for gas phase reactions. Early attempts to make sense of the chemical and cloud information about Venus led to hypotheses about the role of aerosols in Venus atmospheric chlorine cycles. The Venus thermosphere gets extremely cold at night, and conditions there are not unlike conditions in Earth's nighttime polar atmosphere. A realization that catalytic processes occurring on aerosols in Venus' atmosphere could also occur in Earth's nighttime polar vortex led directly to the appreciation that man-made chlorofluorocarbons could be responsible for the destruction of stratospheric ozone (Molina and Rowland, 1974; Newall, 1980; Rowland, 2006). The first Total Ozone Mapping Spectrometer (TOMS) began monitoring a large, seasonal depression in stratospheric ozone over the South Pole in 1978, extending sometimes to latitudes of 45° (Figure 2.6). If allowed to continue, the effects of increased UV from the attenuated ozone would have had catastrophic effects on crops in the southern hemisphere and in the northern high-latitudes. The study of Venus' atmosphere thus lead to the Montreal protocol, where chlorofluorocarbons were banned and substitutes for their industrial applications developed. Recent work suggests, however, that the chemistry of the "ozone hole" on Earth is still poorly understood (Rowland, 2006). Continuing study of the photochemistry of Cl, O, and S on Venus will similarly lead to further understanding of these reactions on Earth.

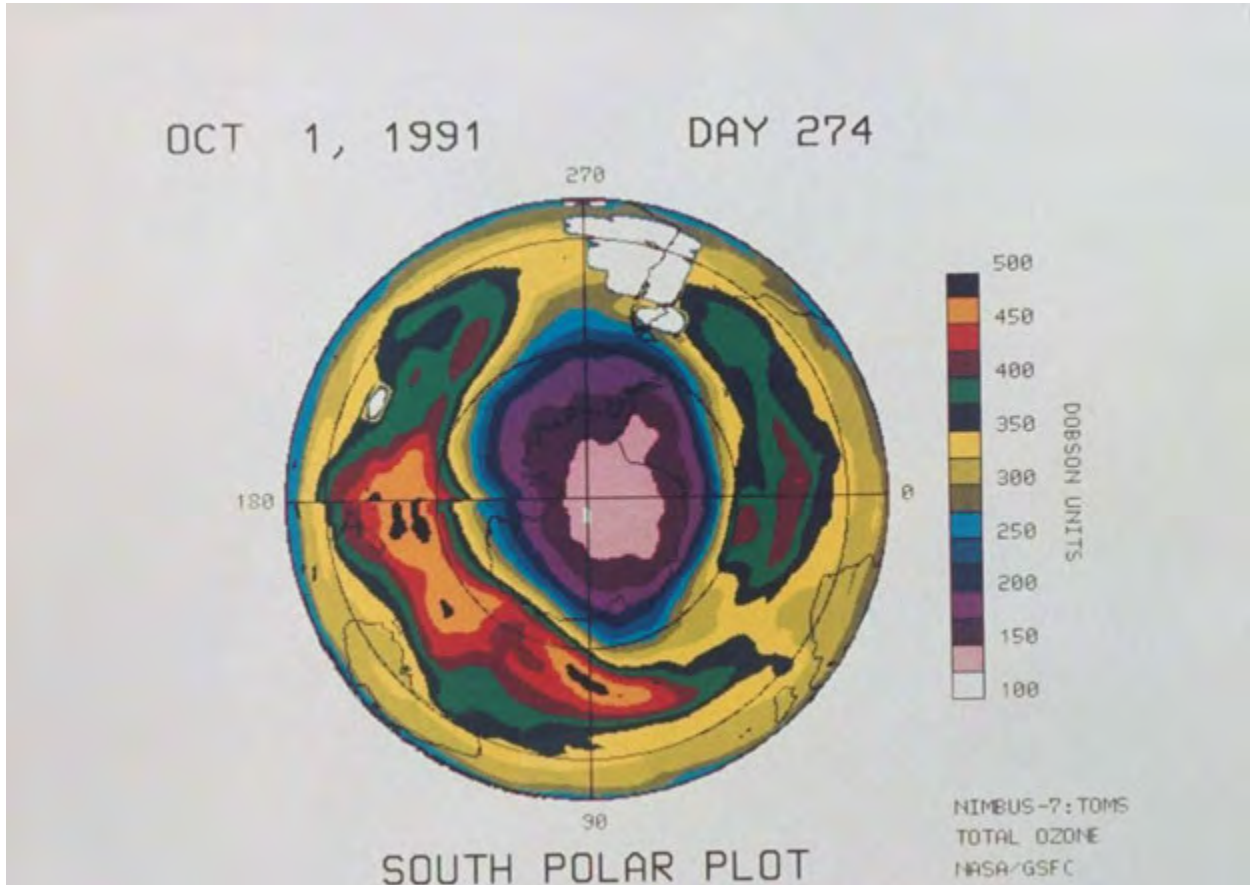


**Figure 2.6:** Total column ozone abundance over the south pole of the Earth during spring. The Total Ozone Mapper (TOM) has monitored ozone for 10 years, illuminating the role that stratospheric temperatures and Cl and F bearing gases play in depleting ozone. Chemical processes thought to operate in the upper atmosphere of Venus were considered for the Earth, leading to an understanding of how CFCs deplete stratospheric ozone and cause health and economic repercussions.

A comparison of the atmospheric dynamics of Venus and Earth is also very useful for refining our understanding of terrestrial dynamics. Explaining the Venus global circulation within the theoretical framework of modeling techniques developed for terrestrial General Circulation Models (GCMs) can contribute to both theoretical understanding and the development of more robust codes. There are some very interesting comparisons between Venus and Earth involving atmospheric angular momentum and exchange with solid planet angular momentum. Angular momentum exchange might be the key for understanding the superrotation on Venus as well as, for example, El Nino Southern Oscillation (ENSO)-connected variations of

Earth's rotation period. Both Venus and Earth have polar vortices; a comparison between the two will deepen the understanding of both.

Space physics is another area where study of Venus can help us to understand important processes on Earth. It will be very fruitful to compare the solar cycle response of the upper atmospheres and exospheric escape fluxes and climates, as well as to characterize the space weather environments and the upper atmospheres.

Venus, with so many strikingly Earth-like qualities in its interior and atmosphere, but lacking an intrinsic magnetic field, might also prove to be a useful analog for Earth during future and past magnetic field reversals.

A flagship mission to Venus will investigate the planet as an interconnected set of processes — a ‘system’ — just as current Earth climate researchers regard the Earth as a ‘system’ (Trenberth, 1992). Comparisons between these fundamentally similar but radically different planetary systems will shed light on Earth science that is not possible in any other way.

### **2.3 Science Background, Goals, and Objectives**

Using the VEXAG report (*Venus Exploration Goals, Objectives, Investigations, and Priorities: 2007* [VEXAG, 2007]), each STDT discipline group compiled a comprehensive set of goals, objectives, and investigations for the exploration of Venus. The detailed science flow, including an evaluation of investigation priority, is provided in Foldout 1. Included in the matrix is a tracking of the VEXAG goals, objectives, and investigations along with the VEXAG priority at the investigation level. Differences in the VEXAG and STDT priorities are due to the need to make choices to formulate a mission relative to overall science priorities. In addition to this science traceability, the STDT evaluated a comprehensive set of measurement techniques needed to perform each investigation, along with a set of mission architecture elements (flown in orbit (o), in the atmosphere (a), or at the surface (l)), and rated them on the following scale: (3) Directly address the science investigation, (2) Major contributor, (1) Minor contributor or supporting observation and (0) Does not address. Using this scoring technique and an assessment of measurement techniques able to make multiple crosscutting observations, the science value of many different mission architectures with many different payloads can be determined.

The STDT concluded that with current instruments and modest technology development a flagship-class mission to the atmosphere and surface of Venus could deeply impact how we see the evolution of terrestrial planets. The remainder of this section provides a detailed discussion, by discipline group, of

the science that could be accomplished by a flagship-class mission to Venus.



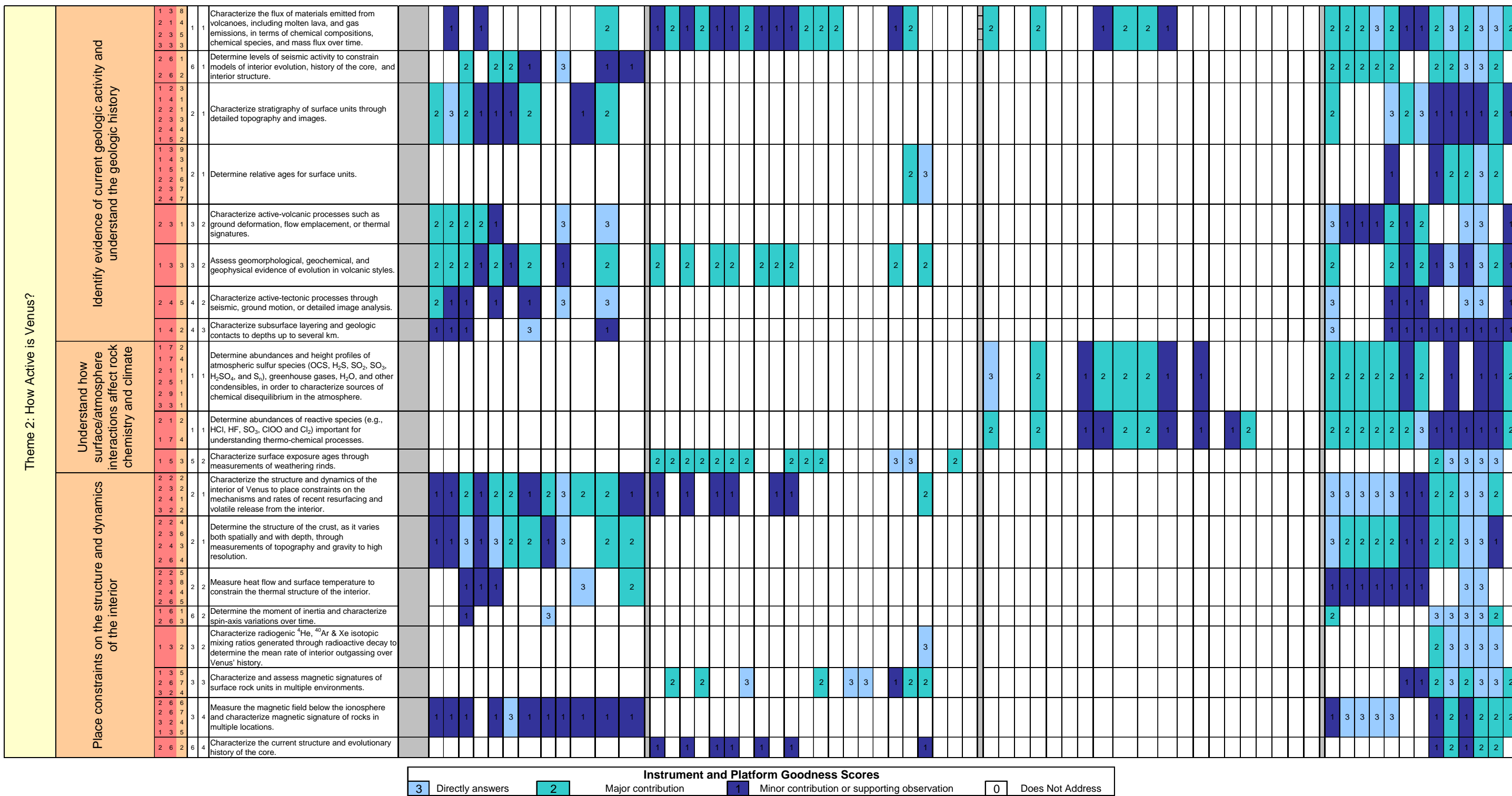
## Instrument and Platform Goodness Scores

### 3 Directly answers

## Major contributions

**1** Minor contribution or supporting observation

0 Does Not Address



2-11  
Final Report of the Venus Science and Technology Definition Team

## Instrument and Platform Goodness Scores

3 Directly answer

### Major contributions

**1** Minor contribution or supporting observation

0 Does Not Address



### 2.3.1 The Venus Atmosphere

#### 2.3.1.1 Present State of Knowledge

The current climate of Venus differs dramatically from that of Earth. The thick, ~92-bar atmosphere is composed of 97% CO<sub>2</sub>, with several trace greenhouse gases, including SO<sub>2</sub>. This gas might be supplied by active volcanism and, through photochemistry and reactions with trace water vapor, supply the 100% global cover of sulfuric acid clouds (Esposito et al., 1997). Although Venus is far drier, with a total water inventory depleted by a factor of 100,000 compared to Earth's, the amount of water vapor in the atmosphere is approximately the same on both worlds. Even at this low abundance, water is an important greenhouse gas. Figure 2.7 shows a schematic of Venus' atmosphere, with its three global

cloud layers and global mean temperature structure.

Previous exploration has revealed that Venus is a planet that has been geologically active enough to resurface nearly the entire planet in the past 1 Gy (McKinnon et al., 1997; Strom et al., 1994). In this regard Venus is uniquely similar to Earth as a terrestrial planet that has erased all direct geomorphologic traces of early bombardment and climatic histories. This suggests a complex history of coupled interactions between the surface, atmosphere, interior, and, possibly, past oceans that have shaped the near-surface environment and the climate history. As on Earth, geologic and atmospheric evolution are tightly linked, and each must be studied to unravel the other (Bullock and Grinspoon, 2001).

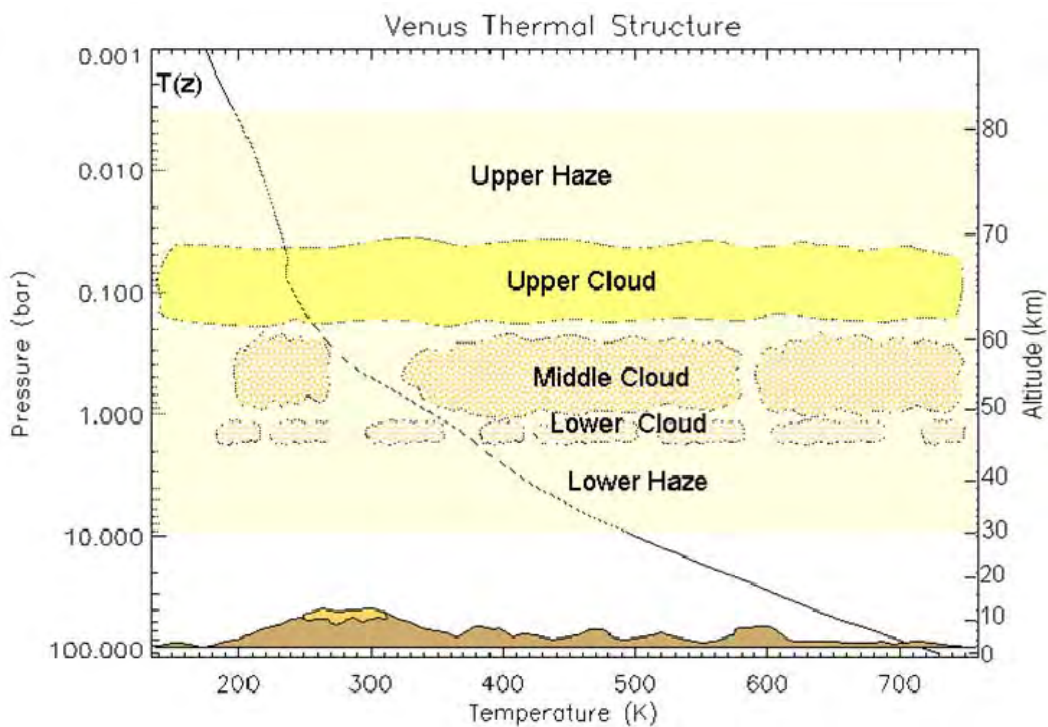


**Figure 2.7:** Globally averaged conditions in the Venus atmosphere. Surface temperatures change little with respect to diurnal or seasonal changes, and the average surface temperature is 735 K. At the surface the pressure is 92 bars. Most of this is CO<sub>2</sub>, but there is also 2.5 bars of N<sub>2</sub>. The 3 cloud decks begin at about 48 km and extend to 68 km. Although the upper cloud is photochemically produced, the middle and lower clouds are convectively dynamic and highly variable. Hazes both above and below the main cloud decks have been observed, also with great variability. Within the middle cloud, conditions are approximately at Standard Temperature and Pressure (STP), although concentrated sulfuric acid aerosols make it a chemically hostile environment (Courtesy D. Crisp).

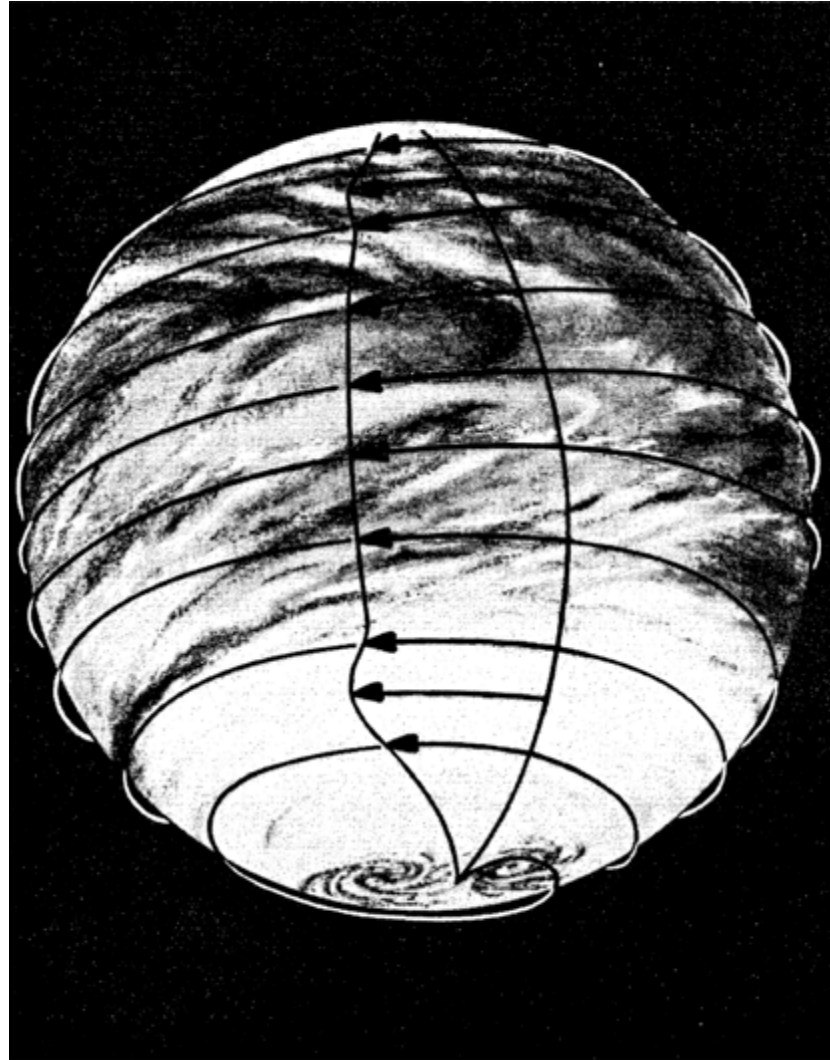


**Figure 2.8:** Venus' cloud top motions from the Mariner 10 flyby, exhibiting a mid-latitude jet, adapted from Schubert, (1983).

#### 2.3.1.1.1 Atmosphere Dynamics

The circulation of the atmosphere of Venus remains a puzzle (Gierasch et al., 1997). Once the slow rotation rate of the planet was discovered, the early expectation of a day side to night side circulation was quickly proven incorrect after the rotation period of the clouds was measured to be 50 to 60 times shorter (Boyer and Guerin, 1969). Tracking of atmospheric entry probes has shown the deep atmosphere to also flow largely from east to west at speeds much greater than the underlying planet, with a weak north-south component (Figure 2.8).

At the cloud tops, 65 - 67 km above the surface, the day side winds have a weaker

poleward component between the equator and  $\sim \pm 60^\circ$  latitudes (peak magnitude of  $\sim 15$  m/s, poleward). Below this depth, all entry probes (which have entered at different latitudes and local times) show that the winds are dominantly zonal; i.e. the east-to-west component is 1 - 2 orders of magnitude stronger than the north-south component. Zonal velocities peak at the cloud tops and decrease monotonically with depth (Kerzhanovich and Marov, 1983; Seiff et al., 1980) (see Figure 2.9). Some Venera landers measured the magnitude of the near surface winds, which appear to be  $\sim 1$  ms<sup>-1</sup> with the direction of this wind not measured.

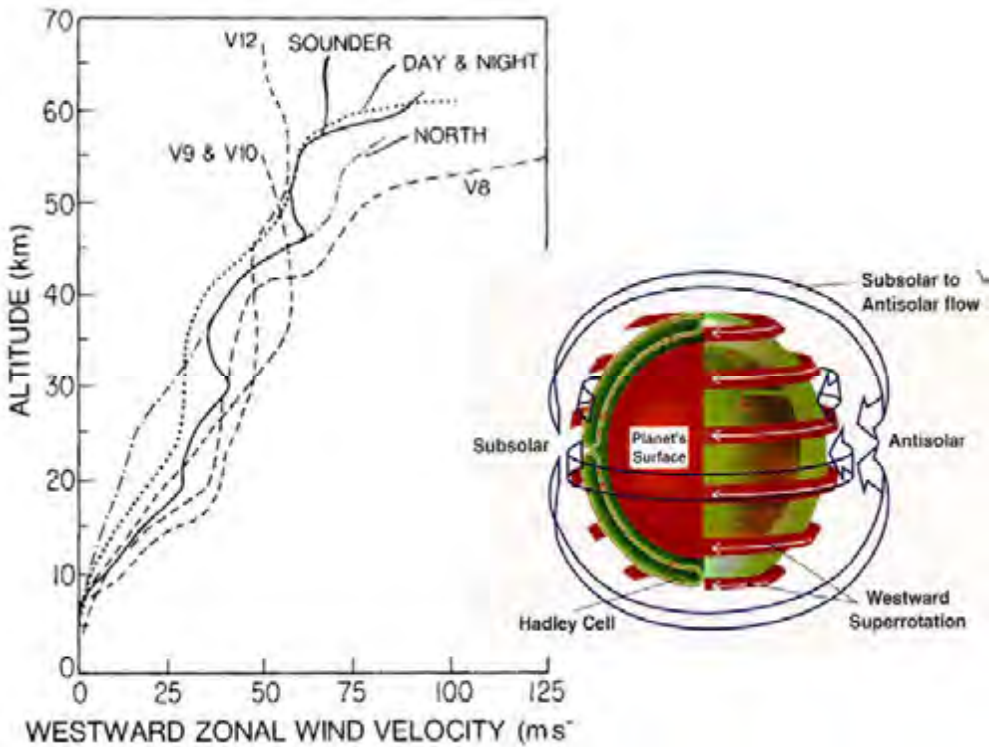


**Figure 2.9:** (left) All probes that have descended into the Venus atmosphere show decreasing zonal velocities with depth. Variations with latitude and time of day were small, although waves are apparent. The diagram on the right is a schematic of the possible general circulation of the atmosphere. The top of the atmosphere is dominated by a solar to anti-solar flow, which grades into a strong zonal flow above the clouds. Hemispheric Hadley cells transport angular momentum upward and warm air poleward, suggesting that superrotation may be sustained by the upward and poleward transport of angular momentum. Corresponding return transport below the clouds from high to low latitudes must also occur, possibly in the form of baroclinic storms or barotropic eddies.

The Visible and Infrared Thermal Imaging Spectrometer (VIRTIS) and Venus Monitoring Camera (VMC) instruments on Venus Express have enabled the monitoring of wind speeds at three different levels of the clouds (Sanchez-Lavega et al., 2008). Venus Express radio occultation-derived temperature profiles of the atmosphere are also enabling a determination of the cyclostrophically balanced flow, which confirms the presence of a mid-latitude jet, as was also found from previous orbiters (Piccialli et al., 2008). Averaged wind profiles in the Venus southern hemisphere within the clouds at 66, 61, and 47 km were derived (Figure 2.10). The 66- and 61-km levels were imaged in reflected light at 380 nm and 980 nm, respectively. The 47-km clouds are seen in silhouette on the nightside, illuminated from

below by 1.74- $\mu\text{m}$  thermal emission. Equatorial zonal winds at the top of the clouds are about 105 m/s. Deeper within the clouds zonal wind speeds are lower, but at all levels are approximately constant from the equator to 45° latitude. Meridional velocities were also derived for the same levels. There is clear evidence for a moderate equator-to-pole flow at the upper cloud level, probably the top of a hemispheric Hadley cell. Deep cloud meridional winds are light, but are equatorward at low latitudes and poleward at mid to high latitudes at the cloud top level. Higher resolution observations than are possible from Venus Express are needed, particularly with hyperspectral imaging, to trace the motion of gases in the deep atmosphere.

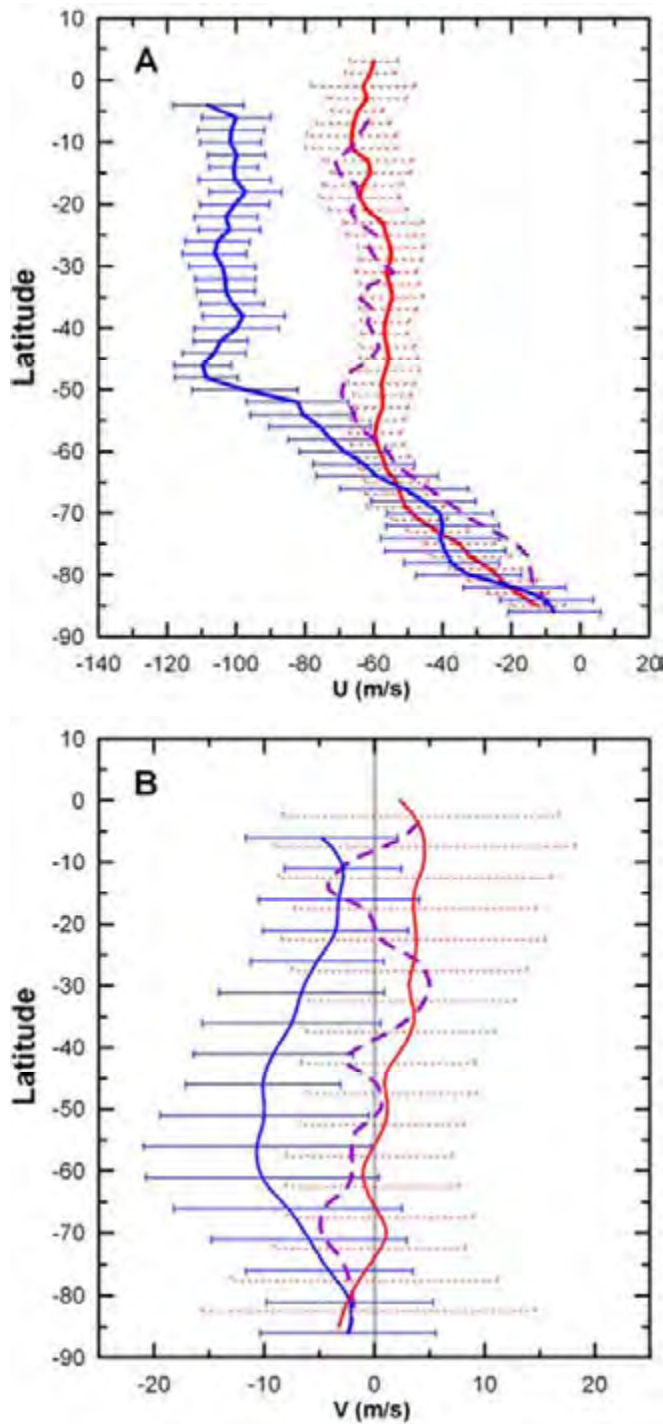


**Figure 2.10:** Averaged wind profiles in Venus' southern hemisphere at cloud level (April 2006 – July 2007) from VIRTIS observations (Sanchez-Lavega et al., 2008). (a) Zonal velocity at 66 km (blue), 61 km (dashed violet), and 47 km (red). Deeper within the clouds zonal speeds are lower, but at all levels is approximately constant from the equator to 45° latitude. (b) Meridional velocities derived for the same levels. There is clear evidence for a moderate equator to pole flow at the upper cloud level, probably the top of a hemispheric Hadley cell. Deep cloud meridional winds are light, but are equatorward at low latitudes and poleward at mid to high latitudes. 66- and 61-km altitudes are seen in reflected light at 380 and 980 nm, respectively. 47 km altitudes are seen at night in emitted thermal radiation at 1.74  $\mu\text{m}$ .

The observations obtained thus far are sparse, and their interpretation requires much caution. Nevertheless, they reveal an atmospheric circulation characterized by peak momentum density that occurs at a level far below the main cloud layer (where the incident solar energy is absorbed). The origin and maintenance of this superrotation presents a puzzle. Recent data from Venus Express indicate that turbulent regions and gravity waves might play an important role in the transfer of momentum (Markiewicz et al., 2007). However, future measurements will be required to understand the magnitudes and the relative importance of mechanisms responsible for momentum transfer between the lower and upper levels of the atmosphere, between the equator and the pole, and between the surface and the atmosphere.

The Earth's atmospheric circulation is forced by the difference in solar energy input between the equator and poles. Venus' atmosphere, too, must move in response to the strong difference in energy input between the equator and poles. The Earth's polar regions radiate less heat to space than the tropics because they are colder. Still, the disparity between energy deposited and energy radiated away drives the general circulation. Because of Venus' thick atmosphere, there is very little difference between the temperature at the poles and the temperature at the equator (less than 10 K) (Seiff et al., 1980). Therefore, the amount of heat radiated to space from the poles and the amount radiated to space from the equator are almost the same (Figure 2.11). There must be vigorous heat transport from equator to poles, driven by their net flux difference. The general circulation must be organized to reduce the equator to pole temperature gradient, so there must be a substantial flow of tropical air to mid-latitudes. Eddies similar to terrestrial baroclinic mid-latitude storms, or barotropic eddies developed

from shear instabilities, might be involved. Determining how the Venus atmosphere simultaneously accomplishes the required meridional transports of heat and angular momentum to maintain its state is a major atmospheric scientific objective for a flagship mission to Venus.

The net cooling at mid latitudes might be enhanced by the generally thinner clouds at these latitudes (Titov et al., 2007). Strong radiative cooling of the deep, high-latitude atmosphere would render the temperature structure strongly subadiabatic; however, this is not observed. To maintain the observed thermal structure in the presence of this high-latitude cooling, adiabatic warming of descending air, such as the descending branch of a Hadley cell, is probably occurring.

Since Venus reflects 80% of incident solar energy, there is less energy input to its climate system than the Earth's. Half of the incident solar energy is absorbed in the upper cloud; half of that is absorbed by an unknown gas or aerosol (Crisp, 1986). Most of the remaining solar energy is deposited in the thick middle and lower clouds, with 2.6% reaching the surface (Crisp and Titov, 1997). Comprised of H<sub>2</sub>SO<sub>4</sub>/H<sub>2</sub>O aerosols, the Venus clouds have a mass loading similar to those of terrestrial cirrus (e.g., 100 mg/m<sup>3</sup>) (Gierasch et al., 1997). They are, however, 10 times greater in vertical extent. While the atmosphere itself is mostly transparent to visible radiation, it is extremely opaque at infrared wavelengths. This is due to pressure-broadened absorption bands of CO<sub>2</sub> and H<sub>2</sub>O, with important contributions from IR scattering in the clouds, SO<sub>2</sub>, CO, and OCS (Pollack et al., 1980). The result is the most powerful greenhouse ever observed; the surface temperature is 500 °C hotter than it would be without an atmosphere, compared with the 33 °C greenhouse warming of Earth.

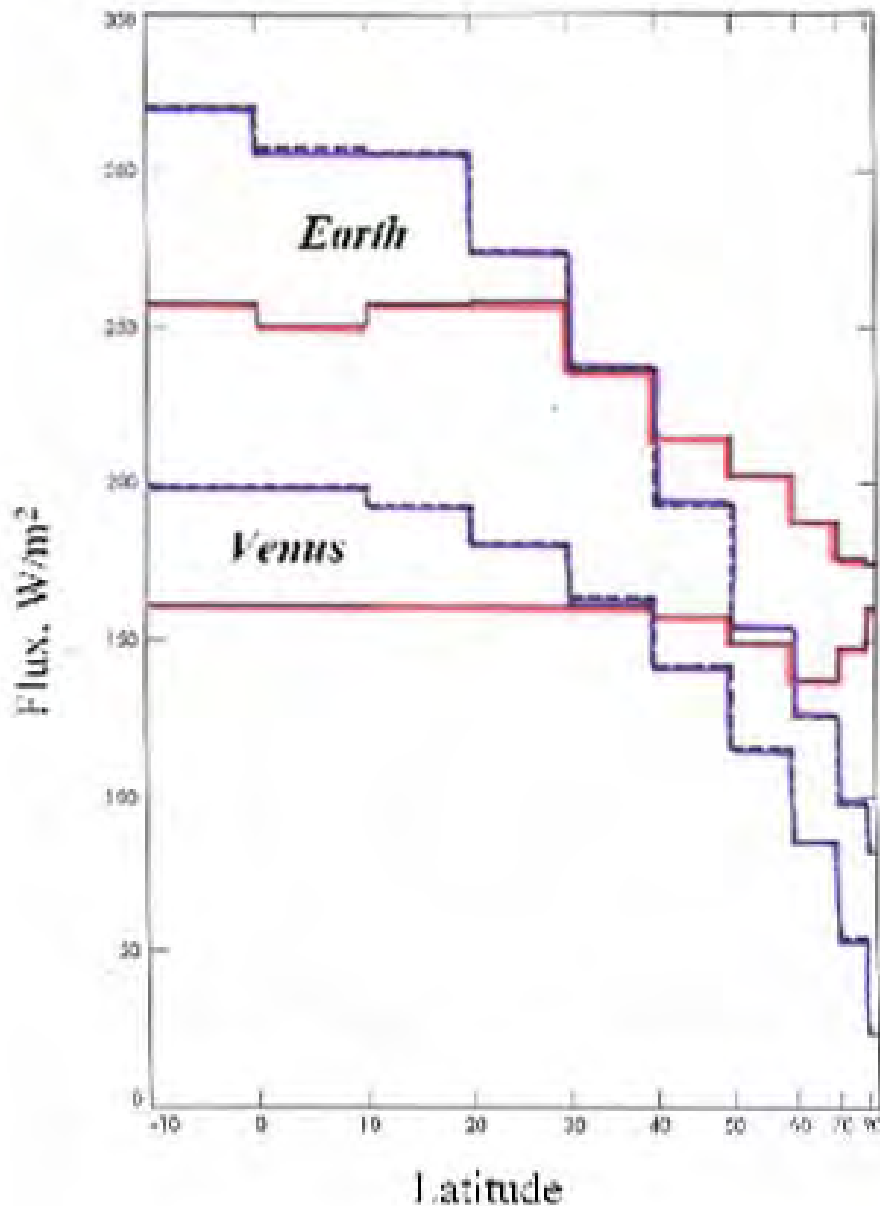


**Figure 2.11:** Solar flux input (blue lines) as a function of latitude for Venus and the Earth. Outgoing thermal flux (red lines) as a function of latitude for Venus and Earth. Because Earth's polar regions are cold, less thermal energy is radiated to space. Venus has an almost uniform temperature with latitude, except for a decrease at the high latitudes of the cold collar. Adapted from Schofield and Taylor, (1982).

The cloud level winds and the morphology evidenced from the ultraviolet images from several missions, including Mariner 10 and Venus Express, as well as the near infrared observations from Venus Express, confirm a hemispheric vortex organization of the circulation centered over the South Pole. While Venus Express cannot observe the

North Hemisphere adequately, Mariner 10 and Pioneer Venus observations of reflected sunlight suggest the presence of a similar hemispheric vortex centered over the Northern rotation pole of Venus. The south pole of Venus from Venus Express is shown in Figure 2.12.

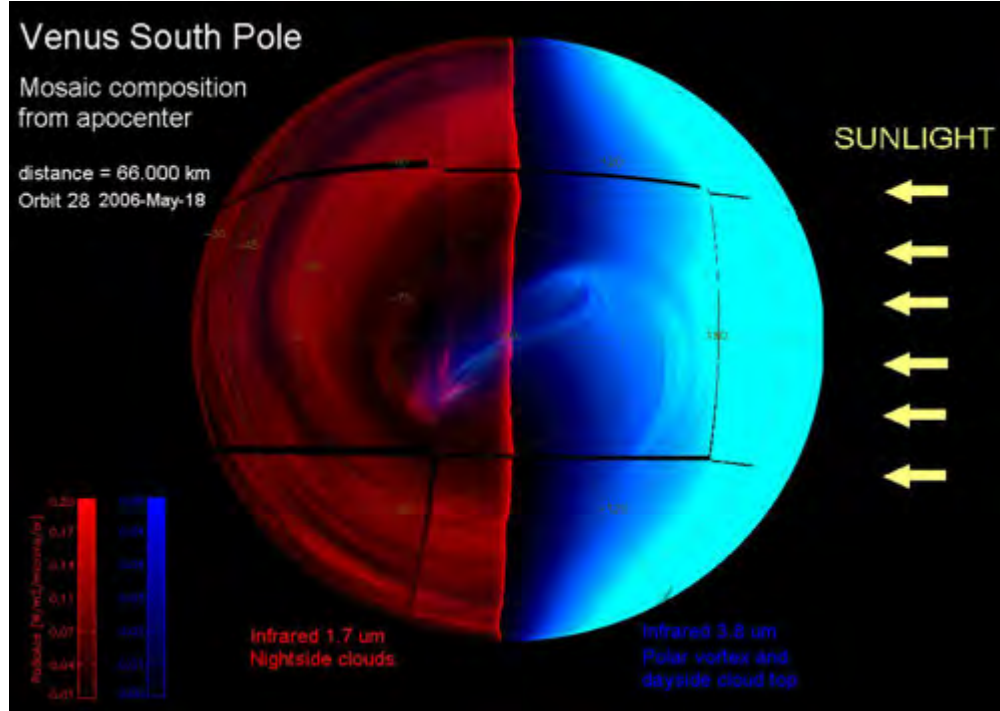


**Figure 2.12:** A view of Venus' south polar vortex and polar dipole seen in reflected sunlight on the dayside (right, in blue), and in emitted heat from the planet on the nightside (left). The vortex structure is deep – from the top of the clouds seen during the day to the bottom of the clouds at night. In the deep night atmosphere, clouds can be seen encircling the vortex. This mosaic was acquired by the VIRTIS instrument on board Venus Express.

The infrared spectral windows, discovered telescopically in 1984 (Allen and Crawford, 1984) and first used near Venus during the fly-by of Galileo (Carlson et al., 1991; Carlson et al., 1993; Carlson and Taylor, 1993; Grinspoon et al., 1993) have been exploited more systematically by Venus Express, providing a dramatically improved capability of studying the atmosphere and surface compared to the earlier missions (see Figure 2.13). The means for investigating a great number of parameters in the atmosphere remotely and in three dimensions, all the way down to the surface, are now available.

How does the vortex organization come about and how long has it existed (Figure 2.14)? More importantly, how deep is this circulation and what are the near-surface winds like? Answers to these questions can come only from systematic observations of winds at multiple levels at widely distributed latitudes and longitudes simultaneously and over an extended period.

The key processes that play a role in the atmospheric circulation that require these measurements are an unambiguous determination of the solar thermal tides and the transfer of angular momentum across latitudes and in the vertical by the longitudinally averaged eddy circulation (Crisp et al., 2003). It is understood that on Venus we cannot afford a flotilla of spacecraft nearly as extensive as the combination of orbiters, radiosondes, aircraft, ships, and ocean buoys used to acquire these observations on Earth; therefore, we will need to rely more on competent numerical models that can realistically simulate the Venus general circulation. However, the validation of such models and their application to fundamental problems of Venus circulation and energy balance would be fundamentally improved through the synergistic, simultaneous observations of vertical profiles, cloud-level properties, and orbital mapping provided by a multi-platform flagship mission.

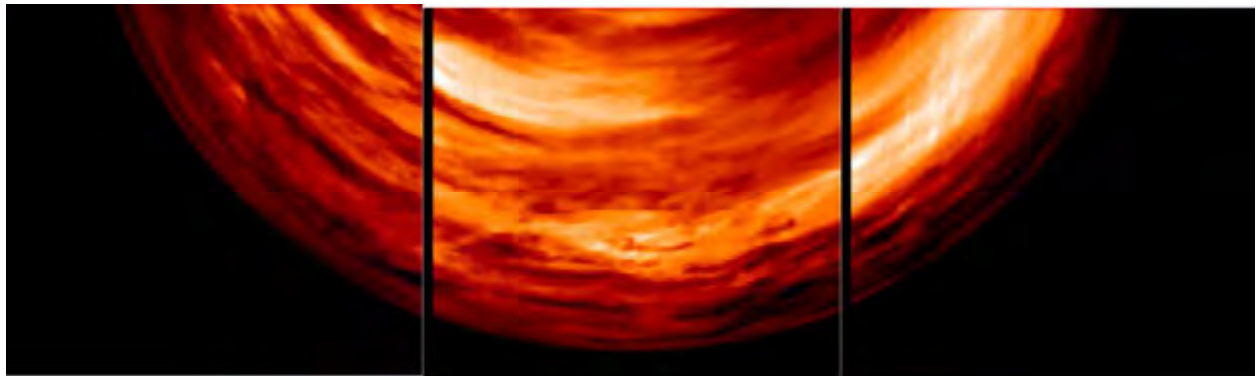


**Figure 2.13:** Composite VIRTIS image of the nightside of Venus taken from a distance of about 65,000 kilometers. The image, taken at a wavelength of  $1.74 \mu\text{m}$ , shows the thermal radiation emitted from about 15 - 20 kilometers altitude. The brighter the color (towards white), the more radiation comes from the surface, so the less cloudy the region.

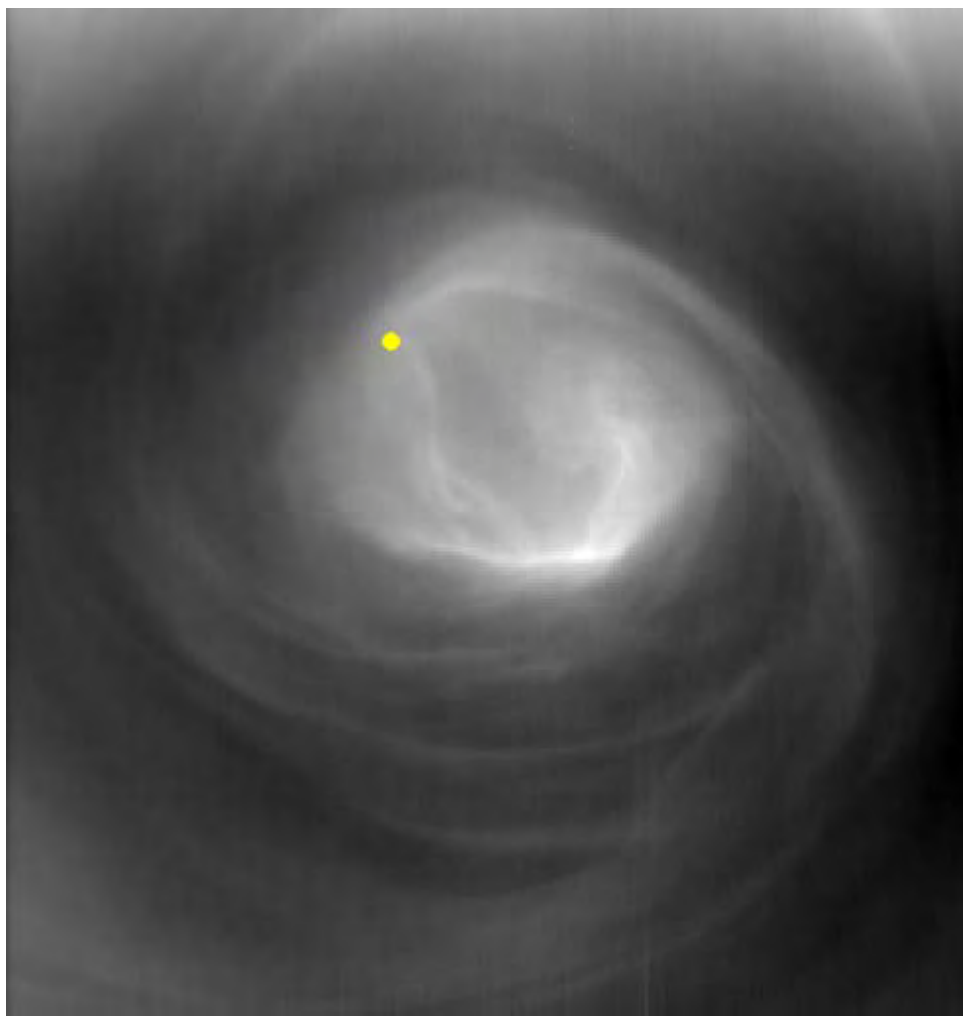


**Figure 2.14:** The Venus south polar vortex as seen by Venus Express' VIRTIS imaging spectrometer at  $5 \mu\text{m}$ . The yellow dot is the south pole of Venus (Piccioni et al., 2007).

### 2.3.1.1.2 Atmospheric Chemistry and Evolution

Much of what we now know about the history of Earth's atmosphere has been inferred from measurements of abundances and isotopic ratios for the noble gases. These gasses are chemically inert and often produced at well-defined rates by the radioactive decay of parent molecules with a range of half-lives that spans most of the history of the planet (Pepin, 1991). The wide range of atomic masses (from  $^2\text{He}$  to  $^{130}\text{Xe}$ ) among the commonest of these gases and the ability to quantify isotopes of each element (typically using mass spectroscopy) make them a convenient yardstick for determining mantle degassing and atmospheric loss rates over time. Thus, measurements of noble gases in the atmosphere of Venus are a powerful tool for tracing Venus' evolution in the same way. A major question is whether Venus ever experienced massive atmospheric blow-off after the development of a primary atmosphere. The heaviest inert gases in Earth's atmosphere (Xe) are mass fractionated relative to chondrites, and radiogenic Xe is highly

depleted on Earth relative to chondrites. Earth has lost most of its Xe, probably due to a very large impact and/or an early era of hydrodynamic escape (Zahnle, 1993). Did the same thing happen to Venus? What are the abundances of the isotopes of Xe in Venus atmosphere? Measuring the ratios of nonradiogenic and radiogenic Xe isotopes will answer these questions (Figure 2.15).

Direct comparisons of the relative abundances of neon, krypton, xenon, argon, and helium and their isotopes between Earth, Mars, and Venus highlight differences in their histories and tell us something about the nature and timing of the events that produced them. For instance, the Pioneer Venus probes discovered that Venus is rich in neon and nonradiogenic argon compared to Earth and Mars, prompting speculation that they might have been brought in during the collision with Venus of a very large comet from the cold outer reaches of the solar system, where substantial quantities of these species can be trapped in water ice as clathrates (Owen et al., 1992).

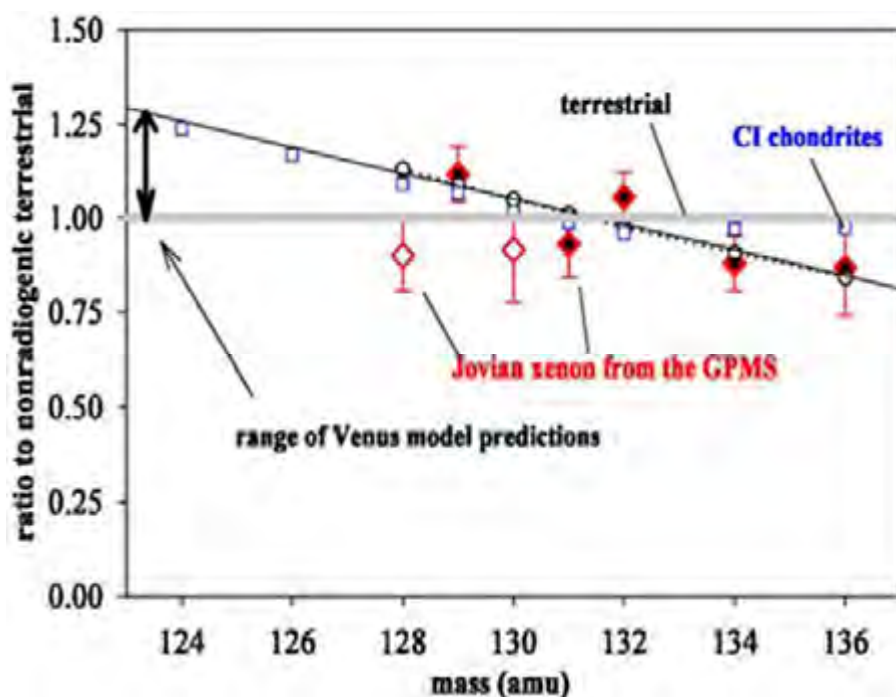


Figure 2.15: The heaviest inert gases in Earth's atmosphere (Xe) are highly depleted and mass fractionated relative to chondrites, which indicates that Earth lost its early primary atmosphere, probably due to hydrodynamic escape or being blown off by a large impact. Is Xe in Venus' atmosphere mass fractionated from early atmospheric blow-off, like the Earth's or is it chondritic, reflecting a primary atmosphere?

The under abundance of radiogenic argon on Venus compared to Earth has often been interpreted as implying that Venus has undergone less outgassing of its interior than has Earth, with important implications for theories of interior and surficial evolution as well as atmospheric evolution. However, Watson et al., (2007) argue that argon compatibility with rock forming minerals must be included in the interpretation of argon ratios on Venus vs. Earth. They further suggest that  $^{40}\text{Ar}$  might accumulate in the atmosphere due to weathering in a hydrologic cycle. What has long been interpreted as implying a difference in total cumulative outgassing might actually say more about the history of an ancient Venus hydrology and evolution of the crust.

How did a planet so remarkably similar to Earth in bulk properties (such as size, mass, and density) and so nearby in the solar system end up with such a radically different surface environment, one where life as we know it could not exist? Was “Earth’s sister planet” always so different? Although, as yet, we have little direct evidence of the earliest environmental conditions on Venus (indeed such evidence has been hard to come by even for our home world), a great deal of circumstantial evidence strongly suggests that these twin worlds started out with essentially similar conditions. As theory of planetary accretion has become more sophisticated, it has become increasingly clear that there is no known mechanism that would segregate initial water inventories between such nearby, similar worlds to the striking degree that their modern-day inventories differ. Most current models suggest that the Earth and Venus have similar chemical compositions and interior structures. However, factors such as the small discrepancy in mean density (after allowing for compressional effects) (Ringwood and Anderson, 1977) and the absence of an internal dynamo (Schubert et al., 1997), as well as discrepancies in the abundances of the noble gases (Pepin, 2006), fuel a lively debate about the extent to which the two planets can be considered to have shared essentially identical origins. The common assumption of identical

origins is also clouded by the possibility of stochastic variations in late accretion history leading to unequal volatile inventories (Morbidelli et al., 2000) or volatile loss and interior processing through catastrophic early impacts (Alemi and Stevens, 2006; Davies, 2008; Zahnle, 2006). Even if we knew the answer to those questions, deriving the path and timescales of Venus’ divergent evolution to its present state would still present numerous challenges. As far as we know, at the time of the origin of life on Earth, Venus and Earth might have had similar environments. Thus, although one of the important goals of future exploration is to confirm and/or refine our understanding of the origin of Venus, our current understanding suggests that the overall evolutionary story of Venus and Earth is one of divergence from similar origins.

The results of previous exploration have provided us with a general theoretical understanding of how this transition likely occurred. The loss rate of water depends strongly on its abundance in the middle atmosphere, as well as the intensity of the solar ultraviolet flux. Models of the process suggest that Venus could have lost an ocean of present-day terrestrial proportions in only a few hundred million years (Kasting, 1988; Kasting et al., 1984). However, such potentially important processes as cloud-albedo feedback in the water-rich early atmosphere have yet to be included in models of early water loss from Venus. The development of such models, in turn, has been hampered by a lack of detailed observations of atmospheric trace abundances and particle compositions in the Venus clouds. Thus, although plausible mechanisms for escape of water have been identified, the timing of this transition from a young, warm and wet Venus to the modern desiccated, hot planet is poorly constrained. We do have several important clues that bracket, but do not tightly define, this timing. The deuterium-to-hydrogen ratio on Venus is enhanced over that on Earth by more than a factor of 100, indicating that most of the atmospheric hydrogen and, presumably,

the water that supplied it, which once existed on the planet, has been lost in fractionating escape processes (Donahue and Hodges, 1992). The uppermost atmosphere of Venus is distinguished from its terrestrial counterpart by the lack of an intrinsic magnetic field, which determines its interaction with the solar wind and the interplanetary magnetic field, controlling the escape of light gases. Hydrogen and oxygen are currently observed to be escaping from the upper atmosphere of Venus through several mechanisms, dominated by non-thermal escape processes. However, extrapolating these loss processes back in time is difficult because the mix of escape processes, fractionation efficiencies, and rates all change over the solar cycle as well as with the structure and composition of the atmosphere, which evolve on much longer timescales. The oxygen produced when H is lost is too massive to escape at any significant rate, according to Jeans' formula, and would remain on the planet, presumably most of it bound chemically within the crust, if thermal escape were the only process available to remove it. However, recent results from the ASPERA instrument on Venus Express show that oxygen is escaping at a rate nearly half that of the hydrogen escape flux, suggesting that large amounts of O could have escaped over time through non-thermal processes (Barabash et al., 2007). So long as liquid water remained available, the formation of carbonates would remove atmospheric carbon dioxide efficiently, as it does on the Earth. Once the surface water was gone, the mixing ratio of water vapor in the upper atmosphere would have fallen sharply and the loss rates of both forms of hydrogen, and the take up of oxygen into minerals, would have begun declining toward the current relatively low levels (Kasting, 1988).

### 2.3.1.2 Open Questions

The most pressing questions regarding the Venus atmosphere can be roughly grouped into those involving the long-term evolution of the planet and those involving the current functioning of the Venus system.

To better understand the evolution of the Venus atmosphere, we must perform investigations to understand how long it has been in its current extreme climate state and how and when it diverged from a possible early Earth-like state. Venus might have been a habitable planet for some of its history; to understand if this was true, however, we need to know how the geologic history related to atmospheric and climate history. Has the rate of geologic activity over the past billion years led to large climate changes? Have these climate changes, in turn, caused changes in tectonic or volcanic activity? Measuring the pattern of noble gas abundances will tell us if it resembles Earth's, and the differences in these patterns reveal important clues about the origin and history of the atmosphere. More specifically, do current argon isotopic ratios constrain the total outgassing history? Is Venus really fundamentally less fully outgassed than Earth? If this is so, we would like to understand the thermal and outgassing history of the planet. What do the Xe isotopes reveal about the origin of the atmosphere and its potential differences from the Earth? What are the implications of the Venus/Earth comparison for the frequency and nature of habitable terrestrial planets throughout the universe?

In addition to these evolutionary questions, there are numerous fundamental open questions concerning the modern atmosphere of Venus: Most generally, it is desirable to understand how the Venus atmosphere is like and unlike the Earth. What are the current sources of atmospheric gases and chemical disequilibrium? Are atmospheric gases out of equilibrium with surface minerals? Are clouds and climate balance supported by active volcanic outgassing? If so, at what rate and how does the atmosphere respond to geologically forced changes in outgassing rate? It is important to understand the nature of the surface/atmosphere chemical cycles on Venus today, how active they are, and, specifically, how sulfur and other volatile elements (Cl, C, O) are transferred between the surface and the above-cloud atmosphere.

Similarly, the composition and lifecycle of cloud particles in the different regions of the global cloud deck should be understood. How do changes and spatial variations in the clouds affect the energy balance of the atmosphere on different spatial scales? Where is solar energy deposited and how is it transported and converted into kinetic energy? Identifying the absorbers of ultraviolet and blue solar radiation is important for understanding the overall energy balance of the planet, as is understanding what energy sources support convection. Understanding what drives and maintains the superrotation, how the general circulation works, and how the polar vortices and waves affect the general circulation are fundamental atmospheric dynamics questions. What is the nature of the thermal tides and observed wave phenomena? What is the source of the lightning-like electrical signals? We must look for their optical counterparts to fully investigate lightning in the Venus environment and measure their frequency, energy, and distribution. Can the generation of lightning be explained through cloud microphysics? What are the chemical effects of these discharges? Understanding the thermal and stability structure of the lowest scale height is fundamental for piecing together a self-consistent picture of the atmospheric dynamics and for estimating how vigorous the mixing is between the surface and lower atmosphere. Similarly, it is important to understand how the upper and lower atmosphere is connected dynamically, energetically, and chemically. What is causing the rapid changes observed in the above-cloud atmosphere and the structure and properties of the upper clouds and hazes? Are they correlated with changes in solar activity or chemical and dynamical processes in the middle atmosphere? We must quantify the loss of elements escaping from Venus today and the isotopic traces they are leaving. Understanding how the solar wind interacts with the upper atmosphere, and how this changes over the solar cycle, will be fundamental to understanding atmospheric loss rates?

The two sets of questions (evolutionary and present-day) are closely linked in that our ability to reconstruct the past evolution of Venus is hindered by limitations in our understanding of the current functioning of the Venus system. Understanding the functioning of modern Venus and, in particular, the interactions between the surface, atmosphere, and interior will also provide the context for us to interpret new data that bears upon the evolutionary divergence between the Earth and Venus.

### **2.3.1.3 Needed Investigations**

To understand the variable above-cloud environment, we must measure the chemical and environmental conditions above the clouds and measure the atmospheric density from the upper atmosphere down to the clouds. To understand the climate balance of Venus, we must measure the radiative balance at several altitudes and spatial locations, as well as measure temperature and motions with sufficient spatial and temporal extent and resolution to derive the three-dimensional thermal structure and motions. Complete vertical measurement from the surface to the cloud-tops of temperature, pressure, and upwelling and downwelling bolometric radiation on the dayside and nightside at two latitudes, combined with global mapping of the thermal infrared and visible radiation, will allow much greater understanding of the climate balance, especially when combined with new understanding of dynamics and cloud structure that could be provided by global mapping of the cloud structure and motions in the near-infrared. In addition to orbital mapping of the atmosphere, cloud-level tracking of at least two balloons that would serve as dynamical tracers while measuring detailed cloud properties in conjunction with local radiative balance would be required. The turbulent and dynamic environment of the lower and middle clouds (48-57 km) is an ideal location to study both the dynamics and chemistry of the Venus atmosphere. Because this region exhibits a weak equator-to-pole flow, balloons inserted at low latitudes would drift poleward as they float with the

predominant east-west winds, thus sampling most longitudes and latitudes of the atmosphere if they lasted a month or more. Such a suite of integrated measurements can best be achieved with a coordinated program of observations from orbital, balloon, and entry-probe platforms.

Measurements of electrical signals and potential correlated optical flashes within the clouds will be required to finally answer the long vexing question of lightning on Venus: both its origin and implications for cloud physics and its effect on the chemistry and equilibrium state of the atmosphere (Russell et al., 2007; Russell et al., 2008). Measuring cloud properties (number densities, particle sizes, and compositions) simultaneously with cloud-level atmospheric abundances will, in addition to shedding important light on radiative balance, also provide new insights into atmospheric chemical cycles and radiative-dynamic feedbacks.

To better understand the evolution of the planet, the abundance of the noble gases and a number of key isotopic ratios need to be determined. Isotopic ratio measurements, especially if they are more accurate than the 10% or so achieved by PV, will allow us to finally distinguish between rival explanations of the observed fractionation patterns (Pepin, 1989; Zahnle, 1993).

New understanding of chemical cycles, dynamics, and surface-atmospheric chemical interactions will be provided by measuring profiles of reactive gases from the clouds to the surface at two locations.

### **2.3.2 Venus Geology**

#### **2.3.2.1 Present State of Knowledge**

Understanding geologic processes and the formation of geologic landforms on Venus will provide insight into terrestrial planet evolution. Shrouded in a blanket of clouds, the surface of Venus has until recently been obscured from

view. The development of radar techniques has provided a means to image the surface and identify geologic features at local to global scales. From the earliest ground-based observations (Campbell and Burns, 1979; Campbell et al., 1976; Goldstein et al., 1978; Pettengill et al., 1967), the surface has been shown to be dramatically different from the heavily cratered smaller terrestrial planets. The paucity of impact structures has suggested a young, potentially active surface (Bullock et al., 1993; McKinnon et al., 1997; Phillips et al., 1992). The orbital Pioneer Venus and Magellan Missions provided a new dimension to understanding Venus by using radar altimetry to generate global topographic maps of Earth's nearest neighbor (Colin, 1980) with a horizontal resolution of 4 - 6 km (Figure 2.16).

The discovery of large, elevated, continent-sized regions suggested that Venus could be geologically more Earth-like than the other terrestrial planets.

The Pioneer Venus and Magellan missions also provided global maps of the Venus gravity field, revealing a distinctly un-Earth-like signature (Figure 2.17).

The strong positive correlation between gravity and topography suggested dynamics in which surface features might be more directly coupled to convection in the interior. Global radio tracking of the orbiting Magellan spacecraft provided refinement of the gravity field with subsequent analyses showing that the upper lithosphere might have some heterogeneities, like the Earth's.

During the same era as the Pioneer Venus Mission, Soviet Venera and Venera-Halley (VEGA) landers provided insight into the surface composition and morphology (Figure 2.18), suggesting the presence of materials similar to terrestrial basalts (Barsukov et al., 1986; Surkov et al., 1984).

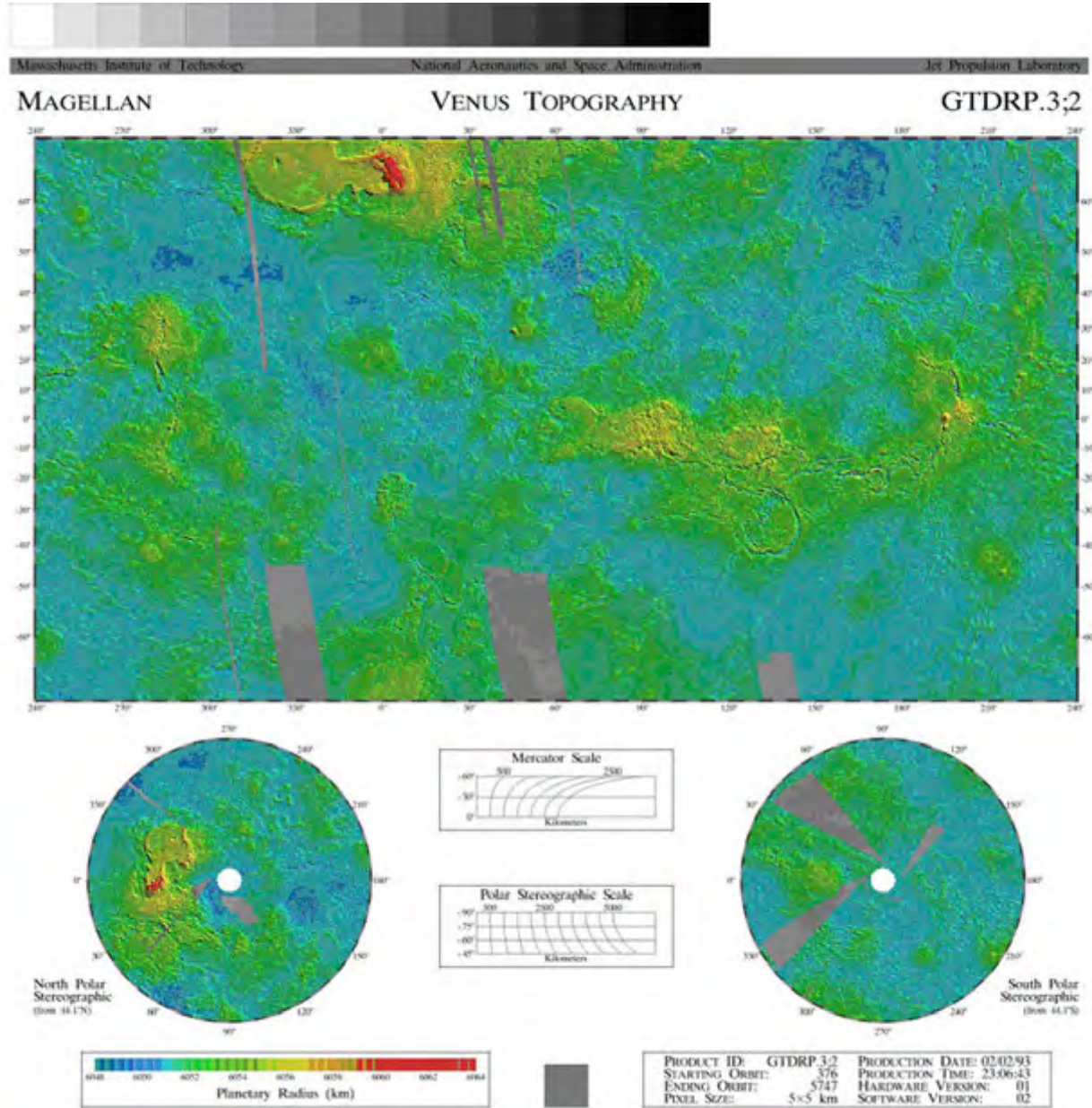


**Figure 2.16:** Magellan Global topography Map of Venus. From a physiographic standpoint, the majority of the surface of Venus is classified as plains. The presence of significant high-standing continent-sized regions has led to the suggestion that evolved crustal materials may be present. Blue regions are plains, highlands are yellow and orange. The highest features on Venus, in Ishtar Terra in the north, are red.

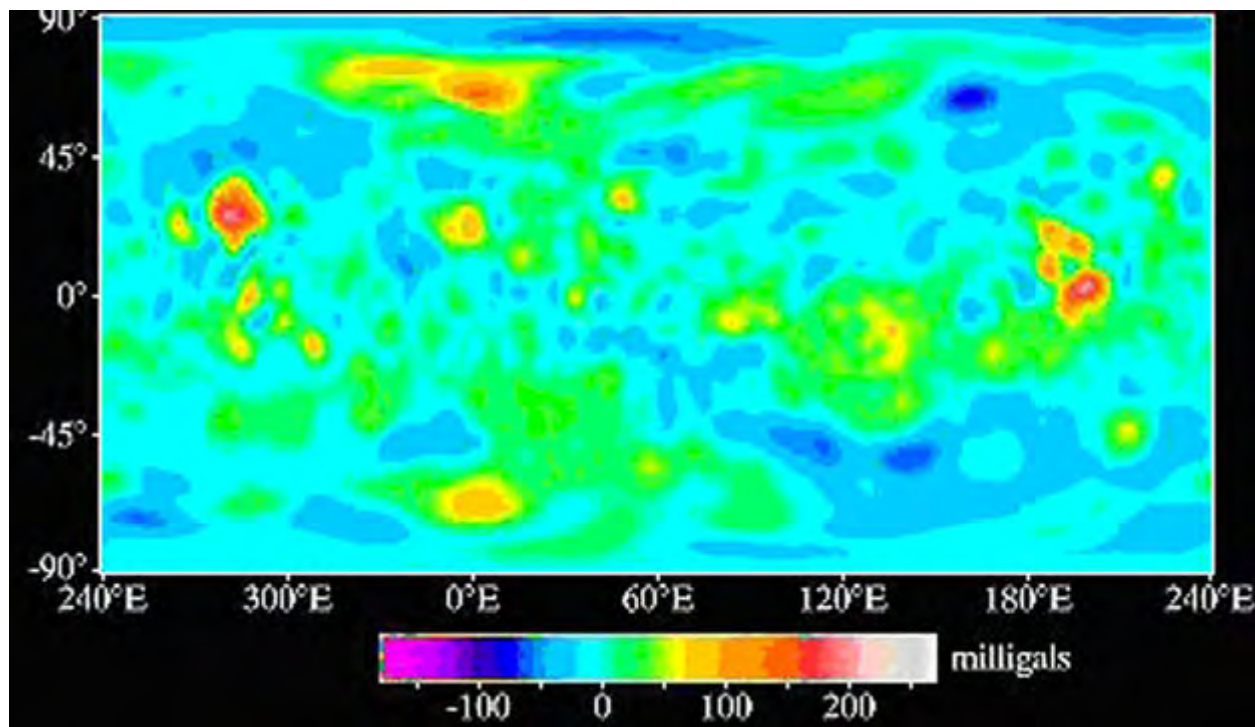
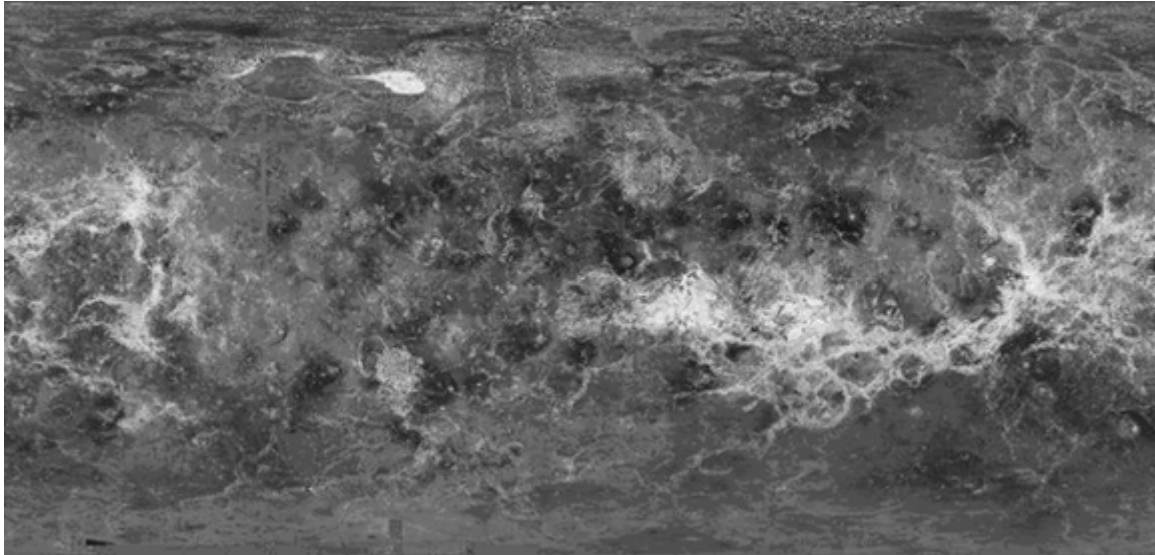


Figure 2.17: Magellan Free-air Gravity Map of Venus. Unlike the Earth, gravity and topography are highly correlated at all wavelengths, suggesting a stronger link between dynamic processes in the subsurface and surface geology on Venus.



Figure 2.18: Venera 14 image of the surface of Venus. Surface morphology and geochemistry suggest that this lander sampled a vast volcanic (basaltic) plain.



**Figure 2.19:** Magellan SAR image of Venus. Although the presence of planet-wide extensional zones, volcanic provinces and compressional mountain belts are reminiscent of features seen on the earth, the lack of plate tectonics suggests that driving force of geologic processes is different than that on the earth.

In the mid-1980s, the orbiting Venera 15/16 provided the first detailed (~1-km scale) Synthetic Aperture Radar (SAR) observations of the north polar region, revealing a landscape of extensive volcanic units and tectonic deformation (Kreslavsky and Basilevsky, 1989). Following up on the discoveries of Venera, the orbiting Magellan SAR mission generated the first global view of Venus at the scale of 100s of meters (Figure 2.19). These data show that geological expression on Venus is diverse and interconnected. Large shield volcanoes with apparently young flows sit at the intersection of huge rift systems, and entire provinces are heavily deformed by compression and extension.

Analysis of the Magellan data reveals many geologic terrains that are quite familiar. From a tectonic perspective, major rift zones indicate regional-scale lithospheric extension resulting in normal faulting, forming structures similar to continental rifts (Figure 2.20a). Collisional tectonics, like that observed along the northern boundary of Ovda Regio, has resulted in regional lithospheric compression and crustal shortening forming ridge belts (Figure 2.20b). Tessera terrain (Figure 2.20c) is characterized by multiple directions of deformation and typically contains elements of both compression and extension.

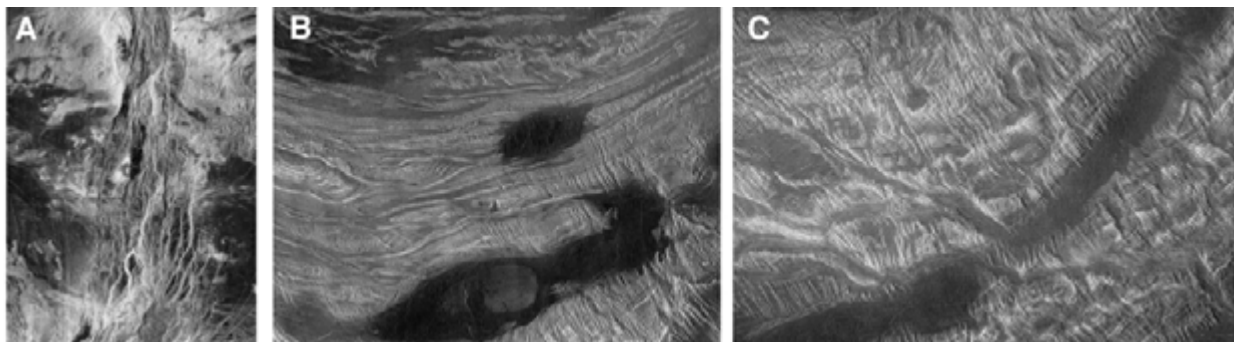


**Figure 2.20:** Tectonic terrains. (a) 600-km section of Devana Chasma, a rift valley located in Beta Regio. (b) Folded mountain belt along the northern edge of Ovda Region indicating N-S trending compression (image 300 x 225 km). (c) Tessera terrain making up the highland of Ovda Regio (image 225 x 150 km).

As these are high, standing, crustal material and are some of the relatively oldest units, it has been suggested that they might represent an evolved, granite-like, crust. Although various tectonic terrains on Venus appear analogous to those associated with terrestrial plate tectonics, the lack of an interconnected network of plate boundaries or regions of subduction leads to the conclusion that plate tectonics is not currently operating.

Volcanic features dominate the surface of Venus, ranging in scale from the limit of the Magellan data to 1000s of km across (Figure 2.21). Regional plains make up more than 80% of the surface and are, presumably, basaltic in composition and interpreted to have been emplaced through widespread lava flooding.

The identification of extensive channel systems suggests that many of these plains are made up of extremely low viscosity ultramafic lavas. Although the majority of the surface is interpreted to be basaltic, localized outcrops of possibly silicic surface rocks have been identified. These “festoon” flows, numbering no more than several, are the first evidence that volcanic rocks on Venus might have a range of compositions. Significant flow fields are often associated with belts of extension and rifting. Like the regional plains, these deposits are interpreted to have been emplaced as low viscosity lavas. Constructional volcanism has produced an array of shields ranging in size from tens to hundreds of kilometers in diameter. In a number of locations (e.g., the Western Eistla Regio), large shields are located along the crest of broad domical rises and often associated with rifts. From a geophysical perspective, these rises have large (100s of km) apparent depth of compensation. Based on both geologic and geophysical information, these rises are

interpreted to be associated with mantle plumes. Finally, global-scale geologic mapping has identified belts of coronae, circular volcanic-tectonic features near the equator. When not associated with belts, coronae are seen all over the planet as individual features. The largest corona, at more than 2000 km in diameter, is Artemis Chasma; speculation is that Artemis Chasma is a site of nascent lithospheric subduction (Schubert and Sandwell, 1995) or an upwelling mantle plume (Hansen, 2002).

With the completion of the Magellan mission in the early 1990s, the exploration of Venus was put on hiatus, except for a brief flyby by Galileo in 1990 (Carlson and Taylor, 1993), until the arrival of Venus Express in April of 2006 (Svedhem et al., 2007). Although the primary objective of the Venus Express mission was to provide data to understand atmospheric processes, new insight into the surface is being achieved by mapping the thermal emission of the surface at 1 micron (Helbert et al., 2008).

Between the questions left unanswered at the end of the Magellan mission and new ones being raised by Venus Express, a renewed scientific vigor has developed to return to Venus to understand the interior, surface, and the interaction between the surface and the atmosphere. In addition, our detailed exploration of Mars and increasing understanding of life in extreme environments compels us to further explore Venus to understand the implications of its evolution for the evolution of Earth and the development of habitable environments. The following subsection discusses fundamental questions still open regarding geology, tectonics, and the link between the surface and the interior.

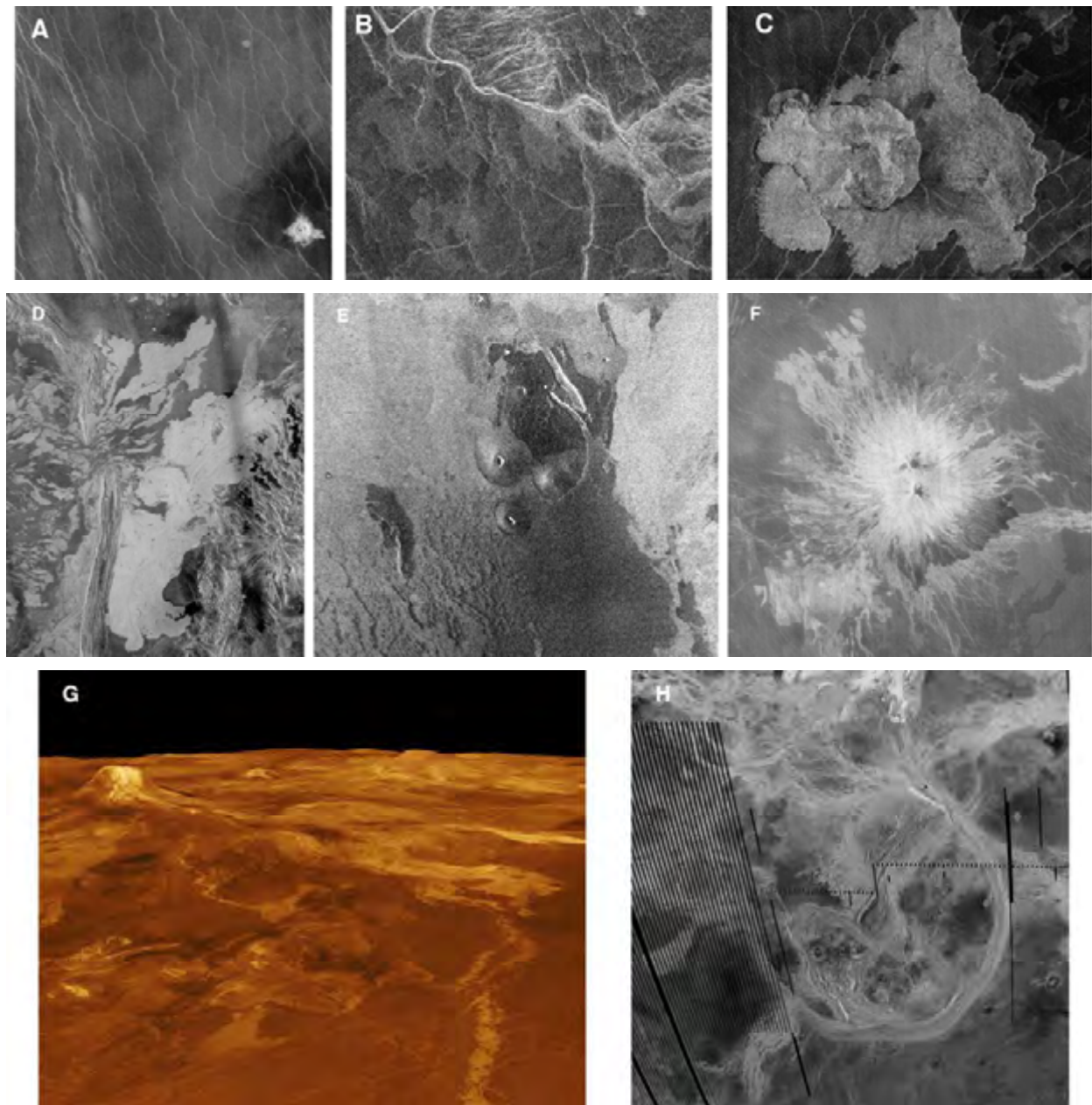


**Figure 2.21:** Volcanic and volcanic-tectonic features on Venus. (a) Regional plains are interpreted to be volcanic in origin and emplaced by widespread lava flooding. The presence of wrinkle ridge indicated broad regional compression. (b) Lava channels 100s of km long indicate some plains forming events were associated with very low viscosity lavas. (c) High viscosity, silicic lava emplacement correspond to “Festoon” flows. (d) Multiple episodes of regional lava flooding are often associated with belts of extension and rifting. (e) Constructional volcanism produces small shields 10s of km in diameter. Volcanoes at this scale are widespread and number in the thousands. (f) Large shields volcanoes (100's of km in diameter) such as Sapas are typically associated with hotspot rises. (g) The 1000 x 1500 km rise of Western Eistla region contains the two shield volcanoes, Gula Mons and Sif Mons. This upland is interpreted to be associated with a mantle plume. (h) The largest corona on Venus is Artemis, a 2000-km diameter volcanic-tectonic structure.

### 2.3.2.2 Open Questions

The surface of a planet is an expression of the evolution of the interior. On Venus, we are limited by the fact that the timing, processes, and mechanisms of geologic activity that alter the planet are a source of considerable debate. A mission that combines orbital reconnaissance with a highly capable surface payload to provide geologic and geochemical information on local to global scales will be vital in reconciling the differences in interpretations of the geologic history of Venus.

The global view of Venus provided by the Magellan Mission has enabled an extraordinary look at the geology of our sister planet; however, the history of geologic processes that have resurfaced is still an active area of investigation (Basilevsky and Head, 1996; Basilevsky and Head, 1998; Basilevsky and Head, 2000a; Basilevsky and Head, 2000b; Ghent and Hansen, 1999; Guest and Stofan, 1999; Hansen, 2000; Hansen et al., 2000; Hansen and Willis, 1996; Head and Basilevsky, 1998; Phillips et al., 1991; Phillips and Hansen, 1998; Stofan et al., 2005). The relatively low number and statistically random distribution of impact craters suggest a good

part of the Venus geologic record has been erased (Figure 2.22).

Few of the impact craters seem to have been superposed by lava or structurally altered due to tectonism (Strom et al., 1994). However, stratigraphic relationships between crater ejecta and endogenic processes are subtle, and stereoscopic analysis of craters from the Magellan radar data show that many appear to have been influenced by low levels of volcanism (Herrick and Sharpton, 2000). An extreme interpretation of this record is that within the past 300 to 1000 My, the lithosphere of Venus underwent a cataclysmic event that erased more than 3 billion years of surface history. Since then, Venus has been collecting impacts, but with little apparent geologic activity. It is difficult to reconcile the stunning sequences of lava flows on the volcanic edifices, massive rift zones devoid of craters, and the evolution of volcanic landforms with a quiescent Venus. On the other extreme, it has been argued that impact craters are so sparse that their spatial randomness could be preserved even as geologic processes continually modify the surface (Phillips et al., 1992).

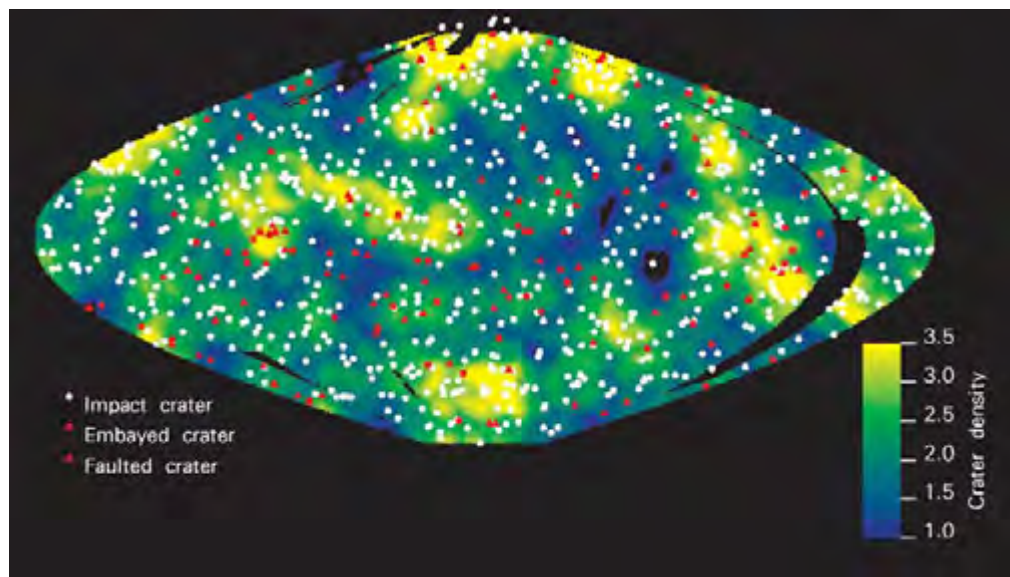


**Figure 2.22:** The impact crater distribution on Venus cannot be distinguished from a random one. With less than 1000 craters, mostly unaffected by volcanic or tectonic processes, this implies that the first 80% of the geologic record was largely erased. An average surface age between 300 and 1000 My was estimated (McKinnon et al., 1997).

Magellan gave us stunning views of the diversity of volcanic, tectonic, and impact processes on the surface. Some geological conclusions from analyses of the Magellan data are:

- Volcanism and tectonism are the most abundant geological processes.
- The styles and abundance of volcanism and tectonism combine attributes of both the Earth (e.g., very heavily tectonically deformed regions such as tessera) and the smaller terrestrial planetary bodies (e.g., vast volcanic plains deformed by wrinkle ridges).
- The distribution of impact craters precludes recently active plate tectonics despite many Earth-like tectonic features (e.g., folded mountain belts).
- Some features (e.g., coronae) are somewhat unique to Venus and might provide important information regarding mantle convection and lithospheric evolution processes.
- The distribution and state of preservation of existing impact craters are consistent with a range of resurfacing models.
- The geological record and sequence of events can be correlated with geophysical data to assess crustal thickness variations and mantle convection patterns.
- The number of impact craters is very small, indicating that the surface geological record is very young (less than 20% of the history of the planet itself).
- 80% of the geological record is no longer obviously preserved in the surface morphology, but might be in the surface rocks.

Despite the detailed look at the surface provided by the Magellan and Venera data, we are left with a range of questions concerning the nature of the surface, its evolution, and its implications for volatile history and interior evolution. For the surface: What is the geochemistry and mineralogy of the different units we see in the Magellan data? What is the origin of layered rocks seen in Venera

panoramas? What formed the mountain belts of Ishtar Terra, which rise up to 11 km about the mean planetary radius (Figure 2.23)? Are the coronae the surface manifestation of mantle plumes? Are the coronae still active? What are the implications of the coronae's morphologic and size diversity? Has resurfacing occurred in brief, global catastrophes, at a steady uniform rate, or by some mixture of these two styles?

Many questions directly relate to the tessera, including whether all tessera formed by the same mechanism(s), how widespread the terrain is, whether tessera form from upwelling or downwelling and their relationship to volcanic rises, and whether the tessera are composed of thickened basaltic crust or a different low-density composition. The current and past rates of volcanic outgassing are unknown, as is an understanding of how volcanoes affected the atmosphere and climate. Even more fundamentally, we need to constrain the role of water in geodynamics and petrogenesis, determine what geodynamical model(s) best account for the observed geology, and determine what happened to the first 80% of the geologic record. Related to this, another important issue in the geologic history of Venus is how the tectonic style might have changed over time. The Earth's surface is broken into a series of plates that migrate over the surface at speeds of up to 10 cm/year. On Venus, by contrast, there is currently little motion of the surface layer, although the underlying mantle must be actively convecting. This condition is known as stagnant lid convection (Solomatov and Moresi, 1996). A significant unknown is whether Venus ever experienced an era of plate tectonics. If so, is there evidence of this recorded on the visible surface (for example, in the highly deformed mountain belts of Ishtar Terra)? If Venus did transition from plate tectonics to stagnant lid convection, when and how did the transition occur? Was this transition related to the global loss of water? Did the transition contribute to the absence of a present-day magnetic dynamo in the core?

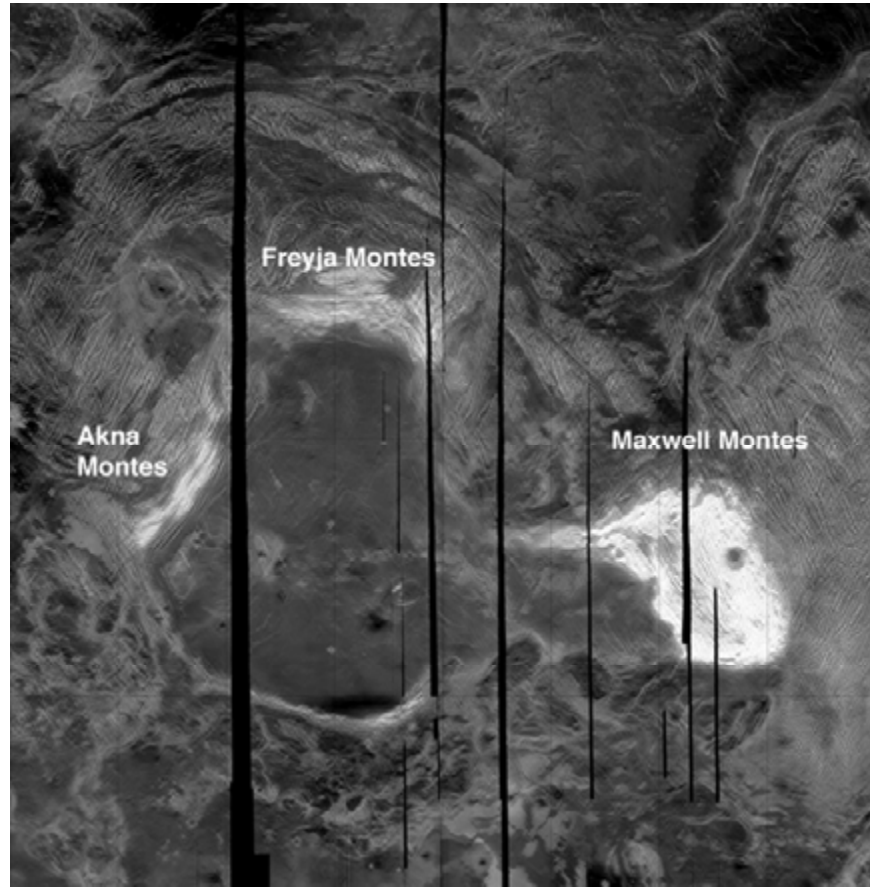


**Figure 2.23:** Magellan SAR image of Ishtar Terra. The high standing volcanic plateau of Lakshmi Planum is surrounded by the compressional mountain belts of Akna, Freyja and Maxwell Montes. Significant lithospheric compression and crustal shortening has occurred. This part of Venus possesses many similarities to terrestrial convergent plate boundaries.

The global view of Venus provided by the Magellan mission has generated much debate as to its geologic history, the evolution of its volatiles, and the nature of its interior. What these views have in common is that geological rates have declined over time, perhaps precipitously or, perhaps, in the more uniform sense of the Earth's heat loss. The discussion on the evolution of Venus is sometimes described as a directional vs. nondirectional scenario:

- Directional Model: (Head and Basilevsky, 1998; Basilevsky and Head, 2002; Collins et al., 1999; Head and Basilevsky, 1998): Regional and global geological mapping reveal that some specific geologic features, units, and structures (e.g., tessera, shield plains, regional plains, wrinkle ridges, etc.)

dominate at different times in history and, thus, form distinctive phases during certain periods of geological history.

- Non-Directional Model: (Addington, 2001; Guest and Stofan, 1999; Hansen, 2000; Stofan et al., 2005): With the possible exception of tessera, geological units and structures occur randomly in space and time. Although there might be local sequences, they are not globally time-correlative.

Just as on Earth (or, perhaps, more so), Venus' geology and climate are interconnected (Bullock and Grinspoon, 2001). The causes and effects of rapid changes in geologic expression can be investigated in unprecedented detail by a capable surface payload and enhanced remote surveying

techniques (Helbert et al., 2008). Intriguingly, the surface and climate systems might be so coupled (Phillips et al., 2001; Solomon et al., 1999) that records of climate change, either in atmospheric or surface isotopes and chemistry, might ultimately elucidate the geologic history of Venus.

To resolve the resurfacing controversy and how it constrains the interior and surface evolution of Venus, it is necessary to determine the stratigraphic relations, geochemistry, mineralogy, and petrology of surface features/terrains, especially tessera. These data, which are the clues to the first 80% of Venus history now obscured by volcanic and tectonic resurfacing, will allow us to constrain the history of volatiles, especially water, on Venus and provide a basis for direct comparison of crustal evolution on Earth and Mars. In addition, isotopic measurements of the composition of the Venus atmosphere and an improved understanding of atmosphere-surface interactions will aid in constraining the outgassing history, in particular current and past volcanic outgassing rates. Higher resolution imaging and topography would allow an improved geological history of the surface to be developed and might allow some time scales, such as regional resurfacing rates, to be constrained. Improved knowledge of the thicknesses, structure of crust and lithosphere, and current seismicity will also constrain the current state of the interior and its evolution and allow our understanding of the formation of Earth-like planets to be better determined.

### 2.3.2.3 Needed Investigations

The overarching objective of any geologic mission to Venus must be to understand the geologic processes and history of Venus. Within the context of this objective, a number of specific questions are put forward:

1. What is the resurfacing history of Venus?
2. If there was a catastrophic resurfacing event, what were the rate and mechanisms of resurfacing and what were the timescales and mechanisms for transitioning to a lower resurfacing rate?

3. If resurfacing has been more uniform in time, what were the characteristic resurfacing dimensions (area resurfaced in a given event, thickness, rate)? What is the global surface composition and how does this correlate with currently defined geologic units?
4. Are there significant volumes of silicic volcanism? Are there significant volumes of sedimentary rocks?
5. How has the style of tectonic deformation changed over time?

In addition to contributions made through geochemistry and atmospheric chemistry, these questions can be addressed through observations of morphology, surface textures, and topography on global, local to regional, and surface (or near surface) scales. Different parts of the puzzle that make up the history of Venus geology can be found at each of these scales. Thus, any hypothesis put forward to explain complex processes, such as global resurfacing, must be consistent with observations across the full spectrum. To address questions regarding the resurfacing history, globally distributed observations are required to evaluate three-dimensional geologic relations. These data include both imaging (SAR) and topographic measurements at a resolution at least an order of magnitude greater than that previously achieved. Information regarding surface composition on a planetary scale can also be used to assess likely provenance of geologic units. Recent orbital IR observations indicate that such an investigation is possible. At more local scales, visible to near IR imaging of the surface from low level aerial or landed platforms can also provide detailed information on surface morphologies and textures. Each of the needed investigations is described in the subsections that follow.

#### 2.3.2.3.1 Global Sampling of Topography

There is a strong need for the investigation of surface structure and morphology of Venus, with high-resolution topography on local to

regional scales. Specific areas of investigation include:

- Assessment of the thickness of lava flows as indicators of rheology and emplacement conditions.
- Evaluation of local slopes in relation to volcanic and aeolian deposits as a guide to processes.
- Mapping the detailed structure in the tesserae as indicator of thermal and tectonic regimes.
- Quantifying crater floor and rim morphology as indicator of crustal properties and infilling.
- Characterization of plains elevation patterns indicative of buried landforms or thermal plumes.
- Determination of the relative timing of plains emplacement and tesserae deformation.
- Assessment of altitude and emissivity behaviors linked with surface-atmosphere interactions.

The detailed surface topography of a planet is essential to understanding the mechanisms and rates of geologic change, the driving forces behind tectonic deformation, and the interaction of the crust and mantle. Measurements of Venus topography by the Magellan mission revealed landform-scale features such as volcanoes, rifts, and tesserae (Figure 2.16), but lacked the fine vertical resolution and dense horizontal sampling to address process-specific questions, such as the thickness of lava flows or fold slopes within the highlands. The STDT concluded that it is a high priority for future Venus exploration to obtain topographic data with dense horizontal sampling and a vertical resolution of 5 m or better to address these issues. Radar systems remain the only means of obtaining high-spatial-resolution altimetry measurements for Venus. The horizontal sampling of these data varies between two practical observing techniques.

In the nadir-looking mode (used by Magellan), a one-antenna radar system

measures the time delay of reflected surface echoes from a series of footprints spaced along the flight path. These footprints can be readily narrowed to about 500-m scale in the along-track direction through Doppler processing, but the cross-track dimension is set by the beam width of the antenna (proportional to the ratio of the antenna size to the transmitted wavelength). Venus atmospheric attenuation limits the practical highest frequency for radar probing, so the likely best cross-track resolution of a profiling altimeter is 3 to 6 km. The vertical resolution is determined by the bandwidth of the radar; achieving 5 m or better ranging accuracy is well within current capabilities. This type of observation would provide a substantial improvement in the detail of topographic profiles over Magellan data, with similarities to the Mars Orbiter Laser Altimeter (MOLA) data for Mars in the along- and across-track horizontal sampling intervals near the equator (Smith et al., 2001).

Much finer detail in topographic data can be obtained with a two-antenna interferometric Synthetic Aperture Radar (InSAR) system (such as used by the Earth-based Shuttle Radar Topography Mission). In one such system, two antennae are separated by 9 m on booms, with one antenna used to transmit the radar signal and both used to receive the reflected echoes. The observing geometry is offset from the nadir by about 35 degrees, allowing for range and Doppler processing that yields radar images from the two received datasets. This image strip parallels the flight path of the spacecraft, and should be 10-km wide to permit overlap with subsequent orbit tracks as Venus rotates. Correlation of the two complex-valued datasets produces interference fringes due to the variations in radar echo path length induced by the surface topography. These phase changes are “unwrapped” to produce a topographic map of the surface and an orthorectified radar image, with a horizontal sampling of approximately 50 m.

This InSAR configuration would likely not detect change at the cm scale, as is done for volcano deformation on Earth. The reason for this is the phase instability of the Venus

atmosphere over short timescales. The dual-antenna radar system will capture the interferometric signature of surface topography, but probably cannot correlate these with later passes to estimate deformation. Repeat-pass radar imaging of major volcanic regions, however, could be used to search for occurrences of lava flow emplacement during the mission, and single-pass observations could be compared with Magellan data to provide a longer timeframe. The discovery of recent lava flows would be of considerable significance as the first volcanic event observed in the inner solar system other than on Earth.

The STDT concluded that an InSAR system could deliver a great deal of high-priority science as part of a Venus flagship payload. The area covered by such “imaging altimetry” would be dictated by the downlink volume, since the data rate for high-resolution, dual-aperture radar imaging is relatively high. Onboard processing might mitigate this concern, but the value of even limited coverage (1 - 5% of Venus) that is possible with current downlink capability and no onboard processing was deemed very high.

#### *2.3.2.3.2 Microwave and IR Observations of Morphology and Composition*

One of the keys to better understanding the history of Venus is to place constraints on the sequence of events by identifying unique geologic units through differences in morphology or possibly composition. To achieve a full understanding of the processes that have shaped the surface of Venus, image data spanning the range from global (100s m/pixel), regional (10s m/pixel) and local (centimeters/pixel) scales are required. By necessity, due to the opaque layer of clouds, radar imaging systems provide the best tool to observe the surface from orbit. Significant advancement in understanding geologic processes on Venus can be achieved by making observations at a spatial scale of one to two orders of magnitude greater than that previously achieved. From an orbital perspective, SAR imaging at a scale of several to tens of meters (when combined with high-

resolution topographic information) will allow a detailed assessment of three-dimensional stratigraphic relations to better discern relative ages. In addition, the finer spatial scale at a high signal to noise should allow for the additional identification of geologic contact boundaries. High-resolution SAR images are a natural by-product of the InSAR system described above. These images would have at least an order of magnitude better resolution than Magellan and could effectively be used to greatly refine definitions of unit boundaries and descriptions and, hence, the series of geologic events.

In addition to microwave observations, the identification of “windows” at infrared wavelengths (1.01 μm, 1.10 μm, and 1.18 μm), from which surface thermal emissions can be observed, provide a new means to examine the surface. Helbert et al. (2008) used Venus Express VIRTIS-M images at 1.01 μm to map much of Venus’ southern hemisphere surface. Radiances from longer wavelength windows from 1 to 3 μm were used to subtract the effects of clouds. Radiances at 1.01 μm for the most part trace altitude-dependent surface temperature. However, intrinsic differences in surface emissivity at 1.01 μm reflect possible compositional differences (Mueller et al., 2008) (Figure 2.24). Using a different algorithm, Arnold et al. (2008) were also able to discern emissivity differences at these wavelengths.

In work using Galileo NIMS spectra, Hashimoto et al. (2008) support these conclusions. They looked at surface emissivity at 1.18 μm and, by subtraction of cloud scattering effects, were able to discern that the lowlands have higher emissivity than the Venus highlands. This is suggestive of felsic highlands, possibly the result of emplacement on the planet when it had oceans, a conclusion also reached by (Mueller et al., 2008). These efforts to map the surface of Venus in the near-1-μm windows represent a unique new way of exploring the planet and its composition. Extrapolations to unique features seen in infrared emissivity can be made throughout the Magellan radar data set,

possibly ushering in a new era of geologic interpretations.

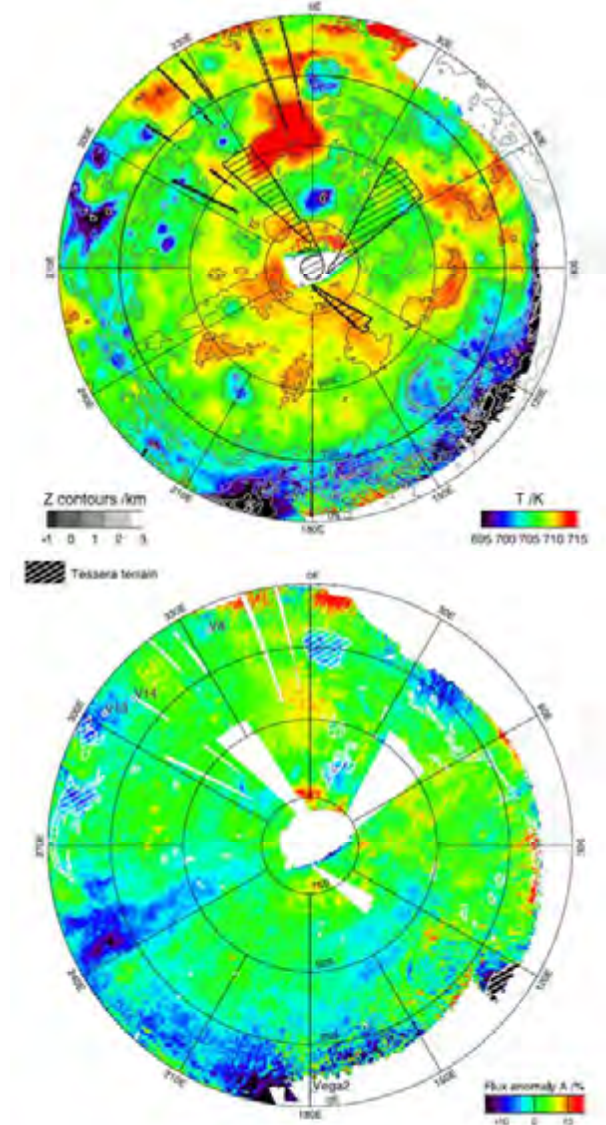


**Figure 2.24:** A new view of Venus. On the left is a map of Venus lower atmosphere and surface temperatures derived from near-IR channels of the VIRTIS instrument. Although emission is correlated with topography as expected, anomalies in the near-IR surface emissivity are apparent on the right. Fluxes from the tessera regions indicate that they are brighter than either the plains or the volcanic rises. This may be due to different compositions or to different weathering histories of the primary rock (Helbert et al., 2008; Mueller et al., 2008).

Although mapping from orbit has obvious advantages (low risk and global coverage and access), there is a strong limitation due to scattering of IR within the Venus clouds. Even

at 1  $\mu\text{m}$ , where there is very little absorption, Rayleigh scattering in the deep atmosphere and conservative scattering within the clouds limits the surface resolution to at best 35 km. The only way to obtain high-quality photogeologic products of Venus is to obtain images from an aerial platform (e.g., descent probe, balloon, or airplane) flying below the clouds.

Descent probes could acquire nested images of their landing sites, as prevailing winds allow the probes to traverse, and IR images from 100 m/pixel (equivalent to Magellan SAR resolution) to as little as 10 cm/pixel would be possible. The opportunities to interpret the geologic structure and history of the observed regions would revolutionize the understanding of the local and regional geology of the Venus surface.

#### 2.3.2.3.3 Visible/NIR Imaging of Surface Textures

A goal of any future imaging mission is to understand the characteristics of the Venus surface at shorter optical wavelengths, in the visible to near-infrared region. Data from the Soviet Venera landers have demonstrated the utility of making observations at the local scale (this has also been shown for Mars from the various landed spacecraft that have operated there). An observational niche that will provide significant advancement in understanding the structure of the Venus surface is the acquisition of regional-scale information during the descent of a landing spacecraft, something that has yet to be achieved. Collecting such data will allow a better correlation and context between surface information and global radar data sets. Since radar information is primarily modulated by surface slopes and roughness, observations at other wavelengths will aid in identifying and mapping contacts between different surface units, while data collected at the surface will facilitate understanding of unit emplacement characteristics and provide context for geochemical analyses of samples.

### 2.3.2.3.4 Science Rationale for Landing Site Selection

Although the results from the Soviet Venera landers suggest that the surfaces that they sampled are primarily basaltic in composition, there is morphologic evidence that suggests a range of rock types might be present. Based on geologic setting, rock types might range from continental-like in nature to those associated with subduction. As such, future measurements should focus on understanding the diversity of rock types on Venus, with implications for crustal recycling. Discussed below are a number of target areas for landed measurements that would most likely provide opportunities to improve the understanding of geologic process on Venus.

- *Tessera* (e.g., Alpha Regio): As discussed previously, it has been suggested that some occurrences of tessera might be composed of low-density, continental-like crust. To investigate this hypothesis, geochemical sampling and optical imaging of a region of tessera is a high priority.
- *Lava Flow fields*: Rocks sampled by the Venera landers show compositions that are similar to terrestrial basalts. Although basaltic plains might generally be representative of Venus, morphologic evidence suggests the presence of more exotic compositions. In areas where lava channels have mechanically eroded the substrate, compositions analogous to carbonatites have been proposed (Kargel et al., 1994). It has also been suggested that broad homogeneous lava flow fields might be analogous to Deccan trap or Snake river plains volcanism and composed of high-Fe/Mg, high-temperature basalts. To provide greater insight into materials that might represent a large part of the Venus crust, it is necessary to determine the chemistry of one or more of these regions.
- *Artemis*: Geological mapping and geophysical modeling of Artemis Corona (2600 km in diameter) suggest a range of possible formation mechanisms, including

incipient subduction (Schubert and Sandwell, 1995) and an upwelling mantle plume (Hansen, 2002). On Earth, igneous rocks from subduction zones and mantle plume hotspots differ significantly in composition. Thus, measurements of rock chemistry in this region could test these alternative formation mechanisms and improve our knowledge of the mantle circulation system. In addition, if Artemis is a site of incipient subduction, then it would be a good candidate for seismic activity, providing a means to better understand the three-dimensional structure of the planet.

- *Regional Plains*: Although the regional plains have previously been sampled, the uncertainties of the measurements are typically large. To provide greater insight into the makeup of “non-exotic” (i.e., typical) surface materials, it would be useful to investigate the chemistry of the rocks that might represent a large part of the Venus crust.

## 2.3.3 Venus Interior Structure

### 2.3.3.1 Present State of Knowledge

To understand Venus at a systems level, it is necessary to have insight into the interaction between the interior, surface, and atmosphere. From a geophysical standpoint, the fundamental objective of a flagship mission is to understand the physical state, structure, and dynamics of the interior of Venus.

Measurements made by the Pioneer Venus Orbiter and by Magellan, primarily of the gravity field (Figure 2.17) and topography (Figure 2.16), provided an important first look at the interior structure of Venus. The gravity field was measured by Doppler tracking, with the effective resolution of the gravity model being strongly dependent on location. In general, resolution is best near the equator ( $30^{\circ}$  N to  $10^{\circ}$  S), where the resolution can be as good as spherical harmonic degree 140 (275 km). Resolution decreases at higher latitudes and is as low as harmonic degree 35 (1100 km) in some places (Konopliv et al., 1999).

Gravity and topography observations indicate that the mean crustal thickness on Venus is 20 - 50 km (Grimm and Hess, 1997) and that the elastic lithosphere is typically 10 – 40-km thick (Barnett et al., 2002; Simons et al., 1997). This range of lithospheric thickness implies that the average mantle heat flux on Venus should be roughly 50 - 70% of that on Earth (Phillips et al., 1997), but considerably higher than present-day Mars. The observation that gravity and topography on Venus are strongly correlated suggests that convective motions in the mantle are strongly coupled to the surface. This is in contrast to the Earth. One consequence of the strong coupling between mantle and lithosphere is that much of the surface topography in some regions of Venus might directly reflect uplift due to mantle convection. Examples include volcanic rises such as Atla Regio and Beta Regio (Smrekar et al., 1997) and coronae (Stofan et al., 1997) (Figure 2.25). In comparison, some topographic highlands, such as Ishtar Terra and tessera, might be dominantly supported isostatically by variations in crustal thickness. The large gravity anomalies at volcanic rises suggest that Venus lacks an Earth-like low viscosity asthenosphere in its upper mantle (Kiefer and Hager, 1991), which might contribute to the apparent absence of plate tectonics on present-day Venus.

Magnetometer measurements show that Venus does not currently have an active magnetic dynamo in its core (Russell et al., 1980). A possible explanation for the current lack of a magnetic field is that stagnant lid convection in the Venus mantle is inefficient and, thus, suppresses core convection and dynamo activity (Nimmo, 2002; Schubert et al., 1997; Stevenson et al., 1983). The physical state of the core is constrained primarily by gravity measurements of the  $k_2$  tidal Love number (Konopliv and Yoder, 1996) and suggests that at least the outer part of the core is liquid; note, however, this interpretation depends on assumptions about core radius and mantle rigidity.

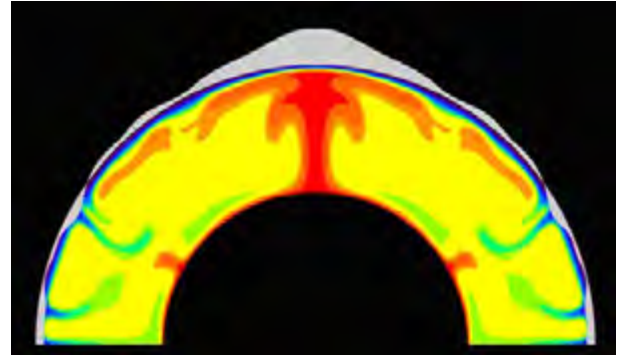


**Figure 2.25:** A numerical simulation of mantle convection on Venus. The hot, upwelling region (red) in the center of the image is an analog of the mantle plumes that may exist under volcanic rises such as Beta Regio. The upwelling flow pushes the surface of the planet up, and cold, sinking material (blue) pulls the surface down. This contributes to the planet's topography and is shown with high vertical exaggeration in gray along the outer surface of the planet in this image. Based on (Kiefer and Kellogg, 1998).

### 2.3.3.2 Open Questions

Spacecraft measurements from prior missions have provided a starting point for understanding the interior of Venus and its coupling to the surface and atmosphere. However, many important questions remain unanswered. A flagship-class mission to Venus could make significant contributions towards answering these questions, including:

1. How tectonically and volcanically active is Venus at present? As discussed previously (Subsection 2.3.2.2), the resurfacing history of Venus is one of the major unsolved problems in Venus geology and geophysics. Seismic measurements would provide a crucial data set for assessing whether Venus is currently active and would be complementary to orbital measurements, such as InSAR topography, and searching for changes in atmospheric SO<sub>2</sub> abundance due to volcanic outgassing. Seismic measurements of venusquakes or of volcanic tremors would provide direct evidence of current tectonic or volcanic activity. Important questions include: What is the size-frequency distribution of

seismicity on Venus? What does this imply about the rate of strain release in the lithosphere? What are the focal mechanisms and the spatial distribution of seismic events? How does this correlate with geologic province, and what does this imply about the origin of different geologic provinces?

2. Does Venus have Earth-like continents?

Although most volcanic structures on Venus appear to be basaltic, several important geologic units, particularly tessera and Ishtar Terra, might be more siliceous (non-basaltic) in composition. Terrestrial experience suggests that siliceous volcanism typically involves water in the melting process. Identifying large volumes of siliceous crust would imply the presence of liquid water at some time in the past history of Venus and, thus, provide important clues about changes in the Venus climate over time. How thick is the crust, and how does this vary laterally across the planet? The average thickness of a planet's crust provides a measure of the time-integrated volcanic activity and is, therefore, an important constraint on models of thermal evolution. Seismic observations can address both questions. Measurements of the seismic wave velocity in the crust will help constrain crustal composition in different parts of the planet. Seismology can also measure crustal thickness using methods such as receiver functions. Making such observations at even one or two locations should significantly reduce the uncertainty in mean crustal thickness obtained from gravity models.

3. What is the chemical composition of the mantle?

Presumably, the Venus mantle is composed of silicate minerals, just as on Earth. However, important details of the composition, such as the proportions of olivine, clinopyroxene, orthopyroxene, and garnet, are likely to be different in some ways. The chemical composition of the

mantle, including volatiles like H<sub>2</sub>O, CO<sub>2</sub>, and S, affects both its rheology and its melting temperature. Measurements of the mantle's seismic velocity will help to constrain the mantle composition and would be complementary to measurements of crustal rock composition made by a Venus lander. In turn, improved knowledge of mantle composition and rheology will permit improved models of both the current style of mantle convection and of the long-term thermal and volcanic history of Venus.

4. At what depths do phase transitions occur in the mantle, and what does this imply about the mantle's thermal state?

An important aspect of the seismic velocity structure in the Earth's mantle is the existence of several major discontinuities in seismic velocity associated with phase changes in the olivine and pyroxene systems. The major discontinuities on Earth occur between 400 and 670 km depth, and the "post-perovskite" phase transition occurs just above the core-mantle boundary. On Venus, the pressure gradient is approximately 10% lower, so phase transitions will occur at slightly greater depth and the post-perovskite transition might not occur at all. An important aspect of these phase transitions is that the transition depth (or pressure) is a function of the mantle's temperature. This serves as a major constraint on the Earth's thermal structure (Helffrich, 2000). Thus, if seismic measurements can constrain the depths at which phase transitions occur in the mantle of Venus, it will be possible to derive new constraints on the temperature structure of Venus' interior.

5. What is the heat flux out of the interior of Venus?

Because heat flux is related to thermal gradient, this question connects to the overall thermal state of Venus. However, heat flux is also a measure of the convective vigor of the mantle and, thus, also relates to questions concerning the

resurfacing history and current activity level of the planet. Current estimates of heat flux on Venus have been determined indirectly via gravity measurements of the elastic lithosphere thickness. Improved measurements of the gravity field, particularly in poorly resolved regions at high latitudes, would contribute to answering this question. Interpretations of gravity observations in terms of heat flux are sensitive to the details of the assumed rheology and, thus, to uncertainties in the composition, such as trace amounts of water. Therefore, direct measurements of heat flux and rock compositions at lander locations are also important.

6. What is the size and physical state of the core? Why is there currently no magnetic dynamo? Was there a dynamo earlier in Venus history? Seismic observations could directly measure the core radius by observing the depth of the seismic velocity discontinuity. They could also measure the physical state of the core (liquid or solid) by determining if S waves are transmitted through the core. Preservation of remnant magnetic fields in crustal rocks is unlikely due to the high surface temperature, but discovery of such signatures would provide important constraints on the thermal evolution of Venus. In particular, it would set a lower bound on the rate of heat loss from the core at the time of dynamo operation and might require that a more efficient mode of mantle convection, such as plate tectonics, operated early in Venus' history.

### **2.3.3.3 Needed Investigations**

#### **2.3.3.3.1 Gravity**

Measurements of Venus' gravity field by means of Doppler tracking of orbiting spacecraft provide important constraints on planetary structure. Improvements in the resolution of the existing gravity model will particularly contribute to our knowledge of the structure of the crust and lithosphere of Venus.

Knowledge of regional variations in crustal thickness helps to constrain the tectonic and volcanic processes that produced geologic units on Venus. Knowledge of variations in lithospheric thickness contributes to our understanding of the thermal evolution of Venus (e.g., Phillips et al., 1997 Simons et al., 1997 Smrekar et al., 1997). In addition, measuring the topography of Venus to an accuracy of a few meters requires that the spacecraft orbit be known with an accuracy of 1 m or better. Experience with Magellan indicates that the required orbit accuracy can be achieved by Doppler tracking of a flagship orbiter. Although either X- or Ka-Band tracking could be used, Ka-Band tracking is desirable because it reduces the effects of solar plasma noise on the tracking data, which reduces the uncertainty in the resulting orbit model. The orbiter should be in a circular, polar orbit to ensure high-resolution Doppler tracking at all latitudes. This is required to avoid significant lateral variations in the quality of the orbital determination and in the accuracy of the resulting topography map. An important goal is that the resulting gravity model has an effective resolution of at least harmonic degree 130 to 150 everywhere on the planet, which corresponds to a spatial resolution of 250 to 300 km. Such a gravity model would be equivalent to the resolution of the Magellan gravity model in the regions that were best resolved.

#### **2.3.3.3.2 Seismology**

Many of the science objectives associated with the interior structure of Venus, including crust, mantle, and core structure, as well as the level of seismic activity, can best be addressed using seismometers. Seismometers are commonly deployed in networks (e.g., Venus Geophysical Network proposed by VEXAG [VEXAG, 2007]). However, important science objectives can be achieved even if just one or two seismometers are deployed. Crustal thickness in the vicinity of a seismometer can be measured using the receiver function method and data from a single seismic station (Ammon, 1991; Yan and Clayton, 2007). Measurement of normal modes constrains the

global seismic velocity structure and, thus, the structure of both the mantle and core (Dahlen and Tromp, 1998; Dziewonski and Anderson, 1981). Finally, observations of seismicity either at an individual seismic station or at several geographically dispersed stations could be used to make an initial assessment of the current seismic activity level on Venus. To be scientifically useful, seismometers should be operated for a period of at least several months.

#### *2.3.3.3.3 Microwave Corner Reflectors*

This experiment is intended to be the radio-wavelength equivalent of the Laser Ranging Retroreflector experiments deployed by the Apollo program on the Moon (Dickey et al., 1994). It is a highly reflective corner reflector that provides a fixed reference point in radar images obtained from orbit or from terrestrial radio telescopes. By tracking the motion of the reflector over time, one can learn a variety of things about the Venus system. One can monitor changes in the planetary rotation rate that are due to angular momentum transfers between the atmosphere and solid body, providing a new window into atmospheric dynamics. In the long term, changes in the pole position with time can be combined with the already measured degree 2 gravity field to measure the moment of inertia. The moment of inertia provides an important constraint on the distribution of mass throughout the planet, such as the size of the core. Similar tracking of the Mars Pathfinder lander (using a radio beacon rather than a corner reflector) was an important contribution to our knowledge of the interior structure of Mars (Folkner et al., 1997).

#### *2.3.3.3.4 Magnetometry*

Venus currently has no internally generated magnetic field. We do not know, however, whether a dynamo was ever active in the past. Measurements of planetary magnetic fields from the balloons and landers would search for remnant magnetism on Venus. Detecting remnant magnetism would place significant constraints on the evolution of the core on Venus. Measurements from the balloons provide a greater geographic coverage, while

measurements close to the surface on the descent probes and landers would be sensitive to smaller magnetized units. When combined with electrometers, the subsurface can be probed with simultaneous measurements of the magnetic and electric fields. This method (magnetellurics) has been used to probe the internal structures of the Earth and Moon and holds promise for determining the depth of the crust, temperature gradient, and the thickness of the lithosphere (Grimm and Delory, 2009).

#### *2.3.3.3.5 Geothermal Heat Flux*

Heat flux is the rate at which a planet loses energy from its interior and is, therefore, an important constraint on its thermal evolution. In general, small planets cool more quickly than large planets and, thus, will have smaller present day heat fluxes. In addition, heat flux will typically vary from place to place on a planet, with geologically young units having higher heat flux than geologically old units. This effect is clearly seen in observations of heat flux on Earth (Pollack et al., 1993). Our existing measurements of heat flux for Venus have all been obtained indirectly from observations of gravity anomalies and topography (Phillips et al., 1997). These results show that heat flux on Venus is somewhat lower than on Earth, with considerable lateral variability. These indirect measurements provide wide geographic coverage and, thus, will continue to be important in understanding the thermal evolution of Venus. However, such measurements are sensitive to assumptions about the mechanical properties of the Venus lithosphere and to uncertainties in the chemical composition, such as trace amounts of water. Thus, direct measurements of the heat flux at lander locations should also be made to serve as calibration points for the global observations.

### **2.3.4 Venus Geochemistry**

#### **2.3.4.1 Present State of Knowledge**

Geochemical investigations include analyses of chemical and structural properties of rocks and other solids at Venus' surface. Specifically, analyses involve assessing

abundances of major, minor, and trace elements; abundances of volatile species (H, C, S) in the solids; and the mineralogy of the surface (i.e., the specific crystalline structures in which the elements are sited). These data can provide crucial constraints on bulk planet composition, core formation, mantle differentiation, crust formation and differentiation, atmosphere evolution, and current atmosphere-surface interactions.

The understanding of Venus' surface composition and properties is very limited compared with the current understanding of other bodies of the inner solar system. The Earth, Moon, and Mars are known from *in situ* investigations, multispectral remote sensing, and samples in hand (including meteorites). Many asteroid types are known from remote sensing and samples in hand (note that more missions are in progress: e.g., Hayabusa and Dawn). Even Mercury's surface is being mapped at high spectral and spatial resolutions by the Messenger spacecraft. In contrast, Venus' surface is known only from limited chemical analyses and *in-situ* imaging at a few sites. These are placed in coarse context by near-global radar imagery, topography, and emittance maps and optical emittance data in the 1- $\mu\text{m}$  wavelength range. Here, we briefly review the available data and discuss gaps in knowledge.

The only data from Venus' surface were acquired by Soviet Venera and VEGA landers

– technological and scientific triumphs – which yielded limited imagery and chemical analyses from seven sites in the low-elevation plains (Abdrakhimov and Basilevsky; Barsukov et al., 1986; Barsukov et al., 1982; Kargel et al., 1993; Surkov et al., 1984). Figure 2.26 shows the remarkable rocky terrain of the Venera 9 landing site.

All other Venera landing sites exhibited flat, broken lava plains with little surface relief. Since plains make up more than 80% of the surface of Venus, the Venera data provide our first look at the broad nature of the geology of the planet. However, it is highly desirable to sample an array of different terrain, including volcanoes, coronae, lava channels, rifts and tessera, to provide a complete geochemical picture.

Although general chemical information was obtained, the Venera and VEGA chemical sensors were relatively insensitive to elements indicative of volatile components and surface-atmosphere interactions, such as S, Cl, C, and H (e.g., Fegley et al., 1992; Kargel et al., 1993). The lack of instrumentation to determine mineralogy (e.g., X-ray diffractometer or Raman spectrometer), restricts the final interpretation as to whether the basalts were glassy or crystalline or whether the minerals were produced by atmosphere-rock reactions (e.g., calcium carbonate and/or sulfate).

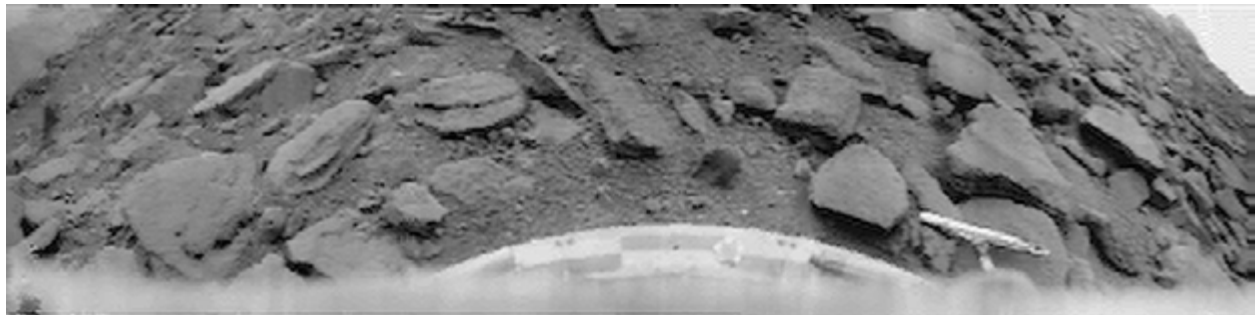


Figure 2.26: Rocky landing site of Venera 9, which was thought to have landed on the edge of a highlands region.

**Table 2.3:** Venus Surface Geochemical Data\*.

	Venera 8	Venera 9	Venera 10	Venera 13	Venera 14	VEGA 1	VEGA 2
K(mass %)	4.0±1.2	0.47±0.08	0.30±0.16	---	---	0.45±0.22	0.40±0.20
U (ppm)	2.2±0.7	0.60±0.16	0.46±0.26	---	---	0.64±0.47	0.68±0.38
Th (ppm)	6.5±2.2	3.65±0.42	0.70±0.34	---	---	1.5±1.2	2.0±1.0
SiO <sub>2</sub> (ppm)	---	---	---	45.1±3.0	48.7±3.6	---	45.6±3.2
TiO <sub>2</sub> (ppm)	---	---	---	1.59±0.45	1.25±0.41	---	0.2±0.1
Al <sub>2</sub> O <sub>3</sub> (ppm)	---	---	---	15.8±3.0	17.9±2.6	---	16±1.8
FeO (ppm)	---	---	---	9.3±2.2	8.8±1.8	---	7.7±1.1
MnO (ppm)	---	---	---	0.2±0.1	0.16±0.08	---	0.14±0.12
MgO (ppm)	---	---	---	11.4±6.2	8.1±3.3	---	11.5±3.7
CaO (ppm)	---	---	---	7.1±0.96	10.3±1.2	---	7.5±0.7
Na <sub>2</sub> O (ppm)	---	---	---	2.0±0.5	2.4±0.4	---	2
K <sub>2</sub> O (ppm)	---	---	---	4.0±0.63	0.2±0.07	---	0.1±0.08
SO <sub>3</sub> (ppm)	---	---	---	1.62±1.0	0.88±0.77	---	4.7±1.5
Cl (ppm)	---	---	---	<0.3	<0.4	---	<0.3

\*Summarized from Lodders and Fegley, (1998)

The geochemical data obtained at seven lowland sites are summarized in Table 2.3 (values at the  $1\sigma$  level). Of the seven sites, chemical data for four only measured K, Th, and U. For three sites, data include most (but not all) major elements of silicate rocks. Only one site includes analyses of K, Th, U, and most major elements (e.g., Fegley et al., 1992). All of these analyses are difficult to interpret because of their low precision by the standards of terrestrial (and MER rover) rock analyses (Treiman, 2007).

Major element analyses from Venera and VEGA are consistent with basaltic rocks (as inferred from radar imagery), comparable to those found on Earth. Within the uncertainty of the data, the parameters FeO, FeO/MnO, and Mg\* (molar Mg/(Mg+Fe)) are comparable to those of the Earth and suggest that the Earth and Venus have mantles of comparable compositions and metallic cores of comparable sizes. These results are quite uncertain because most of the Venera and VEGA analyses of Mg and Mn are only detections at the  $2\sigma$  level. The Venera and VEGA analyses also suggest that Venus' basalts have subchondritic Ca/Al ratios, which might imply an eclogitic mantle source (Treiman, 2007). Eclogite is the mantle-pressure equivalent of basalt, which could suggest a mechanism for transporting crustal basalts to mantle pressures; on Earth,

this occurs via plate tectonic processes, but a mechanism for Venus is not clear.

Venera and VEGA measured abundances of the heat-producing (radioactive) elements K, U, and Th at four sites in the low-elevation plains. At three, abundances are low and comparable to those of average Earth basalts, although one site (Venera 9) analyzed a non-chondritic Th/U ratio (beyond  $2\sigma$  uncertainty). The fourth site (Venera 8) is greatly enriched in these elements, ~25 times that of an average Earth basalt, and rock at the Venera 13 site has a comparable K abundance (no data for U or Th) (Kargel et al., 1993). This variability in abundances of K, U, and Th implies that Venus' mantle and/or crust are heterogeneous and could be an important constraint on tectonic processes (e.g., corona formation).

In addition, the chemical redox indicator (KONTRAST) experiments of Venera and VEGA aimed to constrain the oxidation state of the near-surface atmosphere, a crucial measurement for understanding surface-atmosphere interactions. Unfortunately, the KONTRAST results were and remain ambiguous (Fegley et al., 1997; Florensky et al., 1983).

Atmospheric oxidation state is crucial also in interpreting a Magellan radar finding regarding Venus' surface: specifically, that most high peaks are unusually bright in radar

imagery (i.e., low emissivities) (Pettengill et al., 1982). Generally, the terrain looks similar whether radar-bright or not, which suggests a surface coating or alteration created via a surface-atmosphere interaction. The chemical nature of the low-emissivity material is not known; hypotheses include iron sulfides (low oxidation state), iron oxides, ferro-electric compounds, and semiconductor frost.

Finally, optical emissivity measurements in the 1- $\mu\text{m}$  range from the VIRTIS instrument on the Venus Express spacecraft are beginning to provide additional constraints on surface materials. Venus' atmosphere is transparent enough in this wavelength that the surface can be viewed and imaged from orbit (after removal of atmospheric contributions). Preliminary results show emissivity variations that correlate with the altitude of radar-defined features (Mueller et al., 2008), implying that the surface is being seen and that 1- $\mu\text{m}$  emissivity will provide another set of constraints on surface materials. However, these constraints derive from only two or three wavelengths and can, therefore, provide only limited chemical or mineralogical information.

### 2.3.4.2 Open Questions

The Venera and VEGA landers laid the foundation for addressing more sophisticated geochemical questions. Discussed below are key questions that need to be addressed by any future mission to the surface of Venus.

1. Was there ever an ocean on Venus and, if so, when did it exist and how did it disappear? Was Venus ever habitable? In geochemical terms, these questions require a search for rock compositions affected by, or attainable only with, abundant water. At the scale of individual rocks, many types of materials would unambiguously indicate abundant liquid water, including: sandstone or quartzite; clay-rich rock like shale (Al-enriched), serpentinite (hydrated mantle rock), or rodingite (altered basalt). At the broadest scale, oceans of water should affect magma genesis as they have done on Earth: “No water, no granite; no oceans, no

continents” (Campbell and Taylor, 1983). Venus does have ‘continents’ in the tesserae and in Ishtar Terra (Kaula, 1997), but it is not known whether they are Earth-like ‘granitic’ rock masses or have some other origin; simple geochemical/mineralogic analyses there could immediately show that Venus did once have a water ocean.

2. What caused resurfacing of Venus during the last billion years? Are resurfacing and climate change related? Is Venus still an active planet? Most models of Venus' recent past point to a relatively young surface, completely reworked and resurfaced within the last hundreds of millions of years. This absence of obvious ancient crust has led to geophysical models of periodic catastrophic mantle overturn and crustal disruption (e.g., Strom et al., 1994). Measurement of abundances of heat-producing elements (K, Th, and U) at the surface would help constrain their abundances in Venus' mantle and, thus, the heat production responsible for mantle overturn. Measurement of volatile abundances in fresh basalt at the surface could constrain their pre-eruptive volatile contents and, thus, the atmospheric/climate input from resurfacing (catastrophic or otherwise). The age of Venus' volcanism could be determined directly from geochemical isotopic analyses (though the technical difficulties are daunting) or through investigation of the thicknesses and patterns of weathering ‘rinds’ on rocks, calibrated by laboratory experiments and theoretical studies.
3. What are the nature and extent of present-day chemical reactions between Venus' atmosphere and its surface? Is the composition of the atmosphere buffered by the surface? Because of Venus' high surface temperature, chemical reactions between surface rocks and atmosphere might be so fast and extensive as to partially buffer the atmosphere's composition. This idea was

suggested first for CO<sub>2</sub>, where the mass of the atmosphere was controlled by silicate-carbonate-gas equilibria at the surface (Fegley and Treiman, 1992; Lewis, 1970; Urey, 1952). Current models disfavor CO<sub>2</sub>-buffering, but favor buffering of sulfur gases and oxidation state (Hashimoto and Abe, 1998). To date, these ideas have been tested only through theoretical chemical equilibrium modeling and through limited laboratory experiments. Both are suspect, as the detailed composition of the Venus atmosphere at the surface and the compositions of surface materials, are inadequately known. Even the simplest mineralogical probe at Venus' surface could resolve these question immediately. Another example of atmosphere-surface interactions is the radar-bright (low emissivity) material at many of Venus' high elevations (Pettengill et al., 1988). The radar-brightness is independent of geomorphology but dependent on altitude and latitude, implying that it might be controlled by atmospheric interactions. The nature of those interactions is basically unknown. The local geomorphology in some areas suggests extensive alteration, while the details of the radar emissivity are more consistent with surface coatings. The nature of the coating is unclear; suggested materials include iron sulfide or oxide minerals, Ca-Ti oxides, rare ferro-electric materials, and semiconductor or chalcogenide ‘frosts’ (Brackett et al., 1995; Fegley and Treiman, 1992; Klose et al., 1992; Schaefer and Fegley, 2004; Wood, 1997).

4. What are the tectonic forces behind Venus' volcanism? Can one correlate tectonic settings with magma compositions? The surface of Venus contains many familiar (and some less familiar) volcanic features in tectonic environments similar to Earth's. Based on geomorphologic interpretation, Venus volcanism is primarily basaltic. On Earth, basalts in different tectonic settings

can commonly be distinguished by their geochemistry (e.g., Pearce, 1976; Pearce, 2008; Verma et al., 2006; Vermeesh, 2006; Winchester and Floyd, 1977). By analogy with Earth, one might expect Venus' shield volcanoes to have ‘hot-spot-like’ basalts (i.e., Ocean Island Basalts [OIBs]); basalts associated with rift zones might be alkaline. The extensive plains volcanism might be comparable to that of the large igneous provinces on Earth, where immense volumes of chemically homogeneous basalt were erupted over relatively short durations. The volcanic-tectonic landforms of coronae have no obvious equivalents on Earth, and their origin is a subject of much dispute. Chemical compositions of coronae basalts might help elucidate their origins, but without the benefit of terrestrial analogs. A final interesting, probably volcanic feature are the canali – incised channels that originate in collapse features and that can extend for thousands of kilometers (Komatsu et al., 2001) (Figure 2.21b). These channels have been ascribed to several sorts of fluids: ultrabasic silicate lavas of very high temperature (Gregg and Greeley, 1993); ionic (salt) liquids of relatively low melting temperature (Kargel et al., 1994), or even liquid water in a pre-greenhouse climate (Jones and Pickering, 2003). It remains unclear if any of these models are correct.

#### **2.3.4.3 Needed Investigations**

What specific, investigations can assist in achieving the geochemical objectives of Venus exploration? Two types of measurements are paramount: (1) elemental chemical analyses of rocks (or other solid materials) and (2) mineralogic analyses, determining the crystalline compounds that contain those elements. Measurements of these categories would allow, or allow an approach to, understanding rock compositions, mantle processes that produced surface rocks, planetary-scale processes that produced source

mantles (and by inference, the core and bulk planet compositions), the duration and history of atmosphere-rock interactions, and the temperature, pressure, and intensive chemical parameters of that alteration. Of the many analytic techniques available, gamma-ray spectroscopy, executed so well on the Venera landers (Figure 2.27), has the potential for measuring the bulk elemental composition in the region within 1 m<sup>3</sup> of a lander.

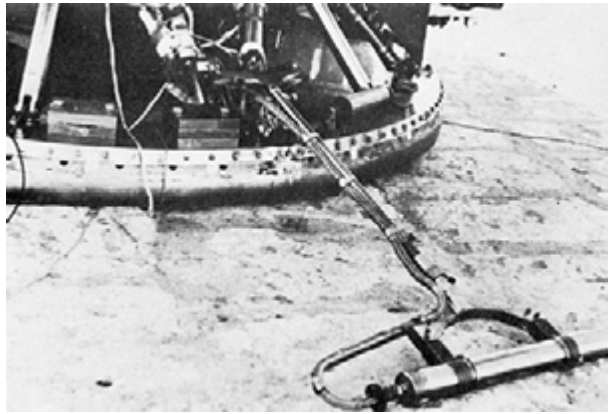


Figure 2.27: Venera 9 gamma ray spectrometer in deployed position. The system was robust enough to obtain K, Th, and U abundances sufficient to classify the surface as comprised of mafic basalts. High K appears in several of the lander gamma ray measurements, presenting a puzzle on the origin of the basalts and a possible role for water in their formation.

X-ray fluorescence spectroscopy, a technique that stimulates inner shell electrons with X-rays and acquires an elemental spectrum of the sample is a precise way of quantifying the elemental composition of the rocks and soils of Venus. Laser Induced Breakdown Spectroscopy (LIBS) can obtain elemental spectra several meters from a lander by illuminating the target with a laser and analyzing the excited gas that is produced. Spectra take only seconds to target and acquire, so a potentially large number of targets could be measured. The Chemcam instrument aboard the Mars Science Laboratory rover (MSL) will use this technique for measuring elemental abundances on Mars. Definitive mineral identification can be achieved by X-ray diffraction, similar to the Chemin instrument on MSL. Raman

spectroscopy on acquired samples or as a near-field remote sensor also holds promise for identifying minerals and weathering layers at the surface.

Other measurements would be valuable as additions to these data (e.g., magnetic properties measurement) or as distinct independent important investigations: e.g. radio-isotopic age dating and measurements of radioisotope initials. The former sort of investigation was judged to be of secondary priority; radioisotope analysis was judged to be too technologically immature for a flagship to Venus in the 2020 - 2025 timeframe.

Geochemical investigations are not independent of site and geology and tectonics: while a single rock from a random spot on a planet (e.g., like a Mars meteorite) can provide a wealth of data, one would not willingly select a random site for geochemical analyses. Many sorts of sites on Venus are interesting, and the exact sites of any flagship mission will depend on orbital dynamic constraints and the availability of communication assets around Venus. However, several types of sites have potential for high science return; among these are Ishtar Terra (the most continent-like province of Venus), tessera highlands (of unknown origin and age), shield volcanoes (in the hopes of leveraging our knowledge of terrestrial volcanoes to those on Venus), and coronae (which would allow testing of the geodynamic models of these unique landforms). This list is not exhaustive, and we envision that a flagship mission's landing sites would be determined by community input, as has been done with the MER and MSL sites.

## 2.4 Venus and Planets Around Other Stars

Over the last 14 years, more than 300 planets have been discovered orbiting other stars. Observational selection has resulted, as of this writing, in an absence of terrestrial planets with masses close to that of Earth among those observed. However, some formation and dynamical models predict a large number of terrestrial planets (Raymond et al., 2006). As far as we know, with the

possible exception of the existence of life on Earth, there is nothing very unusual about our solar system; therefore, discovery and remote sensing of many extrasolar terrestrial planets is widely anticipated. These predictions will soon be testable, as data from the ESA Convection Rotation and planetary Transits (COROT) and NASA Kepler missions begin to reveal the demographics of terrestrial planets in our galaxy and more advanced observational programs make possible the study of the spectra and light curves of such bodies.

Given this expected harvest of terrestrial planet data over the coming decades, the importance of studying these worlds for putting Earth, and life, in context, will be of keen scientific and popular interest. Because of the certainty that knowledge of these planets will be restricted to remote sensing for the foreseeable future, it is vital that we have “ground truth” in the form of terrestrial planet studies that combine remote sensing with *in situ* exploration. Extrasolar terrestrial planets to be observed can be expected to sample a complete suite of evolutionary states representing early, mature, and late phases of planetary history. This increases the importance of comparative studies of the current states and evolutionary histories of Venus, Earth, and Mars. For understanding the possible evolutionary histories of Earth-sized planets, the Venus-Earth comparison represents a unique opportunity.

Exploration of the current terrestrial planets provides us with an increasingly detailed snapshot of planetary evolution at one moment of geological time around a 4.55 billion year old G-type star. In the first billion years of solar system evolution, Venus, Mars and Earth were all very different from their current states, in ways that would be observable through interstellar remote sensing. As we discover and observe extrasolar terrestrial planets, we will see the full range of evolutionary stages and end states. We will undoubtedly see planetary systems of a wide variety of ages, from newly formed systems to “middle aged” systems like our own around stable main-sequence stars, to older planetary

systems around late stage stars. To the extent that we can understand, with some confidence, the likely past and future states of local terrestrial planets, we can expand our knowledge base of terrestrial planet diversity to more than the three examples provided by the current states of these planets.

As our understanding of terrestrial planet evolution has increased, the importance of water as a substance controlling many evolutionary factors has become increasingly clear. This is true of biological evolution, as the presence of liquid water is widely regarded as the key to the possibility of finding “life as we know it” on other worlds (Benner et al., 2004; Pace, 2001). This is also true of geological and climatic evolution. Water is among the most important climatically active atmospheric gases on the terrestrial planets. It is also a controlling variable for tectonic style and geologic processes (Bercovici, 2003), as well as a mediator of surface-atmosphere chemical reactions (Walker et al., 1981). Thus, understanding the sources and sinks for surface water, and characterizing the longevity of oceans and the magnitude of loss mechanisms on terrestrial planets, is paramount for understanding how terrestrial planets in the galaxy evolve. Planets of differing size, composition, and proximity to stars of various stellar types, and the range of physical parameters that facilitate plate tectonics, is key to defining stellar habitable zones.

As we learn through exploration and further modeling to better characterize the evolutionary history of Venus, we will build a context for interpreting observations of extrasolar terrestrial planets. In particular, given the likelihood that Venus and Earth started out with similar surface conditions, and that Venus underwent loss of potentially one or several Earth-sized oceans worth of water, the semi-controlled “experiment” of the apparently divergent histories of Venus and Earth is of particular interest for characterizing the histories and fates of Earth-sized worlds and understanding their dependence on initial

conditions, including stellar type, stellarcentric distance ,and initial volatile abundance.

It is striking that of the three local terrestrial planets two have lost their oceans either to a subsurface cryosphere or to space and one has had liquid oceans for most of its history. It is likely that planetary desiccation in one form or another is common among extrasolar terrestrial planets near the edges of their habitable zones.

On Venus, the very low abundance of water in the atmosphere and crust, combined with volcanism, have led to a sulfur-rich environment (Prinn, 1985). Although this is most obvious in the globally-encircling sulfuric acid cloud layers, there are strong experimental and observational reasons to believe that sulfur gases in the atmosphere interact vigorously with the surface (Bullock and Grinspoon, 2001; Fegley and Prinn, 1989; Prinn, 2001).

The Mars Exploration Rover findings of evidence for aqueous conditions on early Mars have intensified interest in the possible origin and evolution of life there. The evidence suggests that these deposits were formed in a highly acidic and sulfur-rich environment (Squyres et al., 2004; Squyres and Knoll, 2005, Grotzinger et al., 2005). The lack of carbonate deposits of any kind strongly argues for a sulfur-rich, acidic environment as the last of Mars' surface water disappeared (Bullock and Moore, 2007). During this phase, Mars might well have had sulfuric acid clouds sustained by vigorous, sulfur-rich volcanism. A greater understanding of the chemistry of the Venusian atmosphere and clouds and surface/atmosphere interactions might help to characterize the environment of Mars when life might have formed there. In turn, if signs of early life are found on Mars during the upcoming decades of intensive astrobiological exploration planned for that planet, it will strengthen arguments for the plausibility of life in an early and gradually acidifying Venusian environment. Of our two neighboring planets — Venus and Mars — it is not yet known which held on to its surface oceans, and early habitable conditions, for longer.

An understanding of the evolution of the Venusian surface environment is essential for our efforts to contextualize the origin and evolution of life on Earth, and its potential analogs on Mars and terrestrial planets throughout the universe.

## **2.5 Scientific Advancement to be Achieved by a Venus Flagship Mission**

In the nearly 15 years since the conclusion of the Magellan Mission and with new results coming from the Venus Express Mission, significant new hypotheses have been formulated regarding Venus' evolution as a terrestrial planet and its place in the solar system.

Like the Earth, Mars, and Titan, understanding Venus requires information on how the planet operates as a system. That is, to understand the planet as a whole, it is necessary to determine how the interior, surface, and atmosphere all interact. The foundation of the modern study of Venus was put down based on the results of the Magellan mission that was primarily a geologic and geophysical mission and followed by the currently active Venus Express mission. The science objectives discussed here build on the results of these endeavors that provide a framework for this new era of exploration.

The structure, dynamics, and composition of the atmosphere are being observed in great detail by the Venus Express spacecraft. As atmospheric processes are time variable, the need for a long baseline of observations is required. The key to understanding the atmospheric processes is *in situ* chemical sampling and wind measurements. These types of data are needed from the upper atmosphere to the surface. A mission with a complement of two balloons that can each traverse the skies for several weeks measuring the chemistry, temperature, pressure, and winds could acquire many of the important measurements. Two Landers, each instrumented with payloads identical to the balloons, would provide a vertical atmospheric sampling to complement

the balloons and allow all the data sets to be linked.

From a geologic/geophysical perspective, and as has been shown by the missions of the Mars Exploration Program, the ability to make observations at scales that cover several orders of magnitude and three-dimensionally (local at the sub-meter scale to regional at 10s to 100s of meter scales) provides the greatest insight into geologic processes. The Magellan mission has provided a global image context at the 100s of meter scale. With the development of imaging SARs that can provide data at the <10 meter spatial scale with height information derived through interferometric techniques, a major component of a flagship mission should include such a capability. In addition, obtaining three-dimensional global-scale structure provides greater insight into the processes that modify the surface. As such, collecting high-resolution gravity information with global uniform coverage will generate a greater understanding of the linkage between the interior and surface processes.

To fully understand the interaction between the interior, surface, and the atmosphere, chemical (elemental and mineralogical)

analysis of surface materials is required. A mission that incorporates two landers provides the means to target different terrain types (e.g., tessera and a hot spot volcano) to evaluate the greatest diversity of compositions.

The STDT's quantification of the priority and effectiveness of each investigation was used to assess the science value of a wide range of architectures, a process described in Chapter 3 and in Appendix A. Guided by the goal of maximizing the high-priority science return, an architecture with a highly capable orbiter, two balloons, and two landers was chosen: this is the Venus flagship Design Reference Mission (DRM). Table 2.4 traces the science themes to science objectives, to instrument and spacecraft platforms for the Venus DRM.

It is characteristic of exploration that the nature and meaning of discoveries cannot be anticipated. Because Venus and Earth have undergone radically different evolutionary paths with the same laws of physics, a detailed exploration of Venus will tell us more about the complex nature of processes occurring on our planet than can be imagined.

**Table 2.4:** Mapping of Venus Flagship Design Reference Mission Science Objectives to Instruments and Spacecraft Elements.

Science Theme	Science Objective	Instrument Type	Observation Platform
What does the Venus greenhouse tell us about climate change?	Understand radiation balance in the atmosphere and the cloud and chemical cycles that affect it	Vis-NIR Imaging Spectrometer	Orbiter
		Nephelometer	Balloon, Lander (on descent)
		Net Flux Radiometer	Lander (on descent)
	Understand how superrotation and the general circulation work	Sub-millimeter Sounder	Orbiter
		Atmospheric Structure (P/T/winds/accel)	Balloon, Lander (on descent)
		Radio (with USO)	Baloon
	Look for evidence of climate change at the surface	Vis-NIR Camera	Balloon, Lander (on descent)
		Microscopic Imager	Lander
How active is Venus?	Identify evidence of current geologic activity and understand the geologic history	InSAR	Orbiter
	Understand how surface/atmosphere interactions affect rock chemistry and climate	GC/MS	Lander (on descent)
	Place constraints on the structure and dynamics of the interior	Radio (with USO)	Orbiter
		Magnetometer	Orbiter, Balloon, Lander
		Heat Flux Plate	Lander
		Corner Reflector	Lander
When and where did the water go?	Determine how the early atmosphere evolved	GC/MS	Balloon, Lander (on descent)
		Langmuir Probe	Orbiter
		Neutral and Ion Mass Spectrometer (INMS)	Orbiter
	Identify chemical and isotopic signs of a past ocean	XRD/XRF	Lander
		Drill and sample acquisition, transfer and preparation	Lander
	Understand crustal composition differences and look for evidence of continent-like crust	Passive Gamma-ray Detector	Lander



### 3 Choosing the Mission Architecture

The previous chapter describes far more science than can possibly be accomplished in any given flagship mission to Venus. Therefore, it was necessary to take that overarching scientific framework and synthesize a viable flagship mission for the 2020 - 2025 time frame that satisfies the key constraint of not exceeding a total mission cost of \$3 B to \$4 B, while providing the optimal high-priority science return expected. This chapter will describe the process by which the study team achieved this synthesis and selected the mission architecture for the Design Reference Mission (DRM). At the core of this process was an analysis of alternatives that generated numerical ratings for scientific merit, technology developmental difficulty, and mission complexity/cost for a variety of candidate mission architectures. See Appendix A for a complete discussion of the analysis summarized below. The methods and results are also described in detail in Balint (2008b).

#### 3.1 Mission Architectures Analysis of Alternatives

The STDT started from the scientific framework described in Chapter 2. The science subgroups re-organized and, in some cases, consolidated the VEXAG science investigations to create a list of prioritized science investigations. The priorities were characterized as:

1 = Essential to have

2 = Highly desirable

3 = Desirable

4 = Very Good to have

They then analyzed a very wide range of measurement techniques and associated instruments to determine the degree to which these techniques and instruments could satisfy the various investigations using a simple 4-level scale:

3 Directly answers

2 Major contribution

1 Minor contribution or supporting observation

0 Does Not Address

The STDT, supported by the Venus flagship study team at JPL, identified 13 potential spacecraft platforms (Table 3.1), referred to as *architecture elements*, that could, in turn, host the various instruments and measurement techniques and satisfy the desired science investigations.

The architecture elements were:

- Orbital.
- High-level Aerial (> 70 km altitude, above the clouds).
- Mid-level Aerial (52 – 70 km altitude, in the clouds).
- Low-level Aerial (15 – 52 km altitude, below the clouds).
- Near-surface Aerial (< 15 km altitude).
- Single-entry Probe.
- Multiple-entry Probes.
- Short-lived Lander (Single).
- Short-lived Lander (Multiple).
- Long-lived Lander (Single).
- Long-lived Lander (Multiple).
- Surface System with Mobility (surface or aerial).
- Coordinated Atmospheric Platforms.

The science subgroups then rated the ability of the various architecture elements to achieve the desired science investigations using the same method as used for the measurement techniques and instruments. The results of this effort are summarized in Chapter 2, Foldout 1. At this point, it was possible to construct a simple science figure of merit (FOM) for each of the architecture elements by combining the priority of the investigation with the score for the ability of the architecture element to satisfy that investigation. Summing these scores for each of the elements then produced for each element a total science FOM.

**Table 3.1:** Mission Architecture Elements, FOMs, and Cost Estimates.

Architecture Element	Description	Science FOM	Tech. FOM	Cost est.
Orbiter	Self-evident, but can dip into the exosphere for in situ sampling	177	0	\$0.41B
High-Level Aerial	Altitude >70 km, above clouds	169	3	\$0.35B
Mid-Level Aerial	Altitude 52–70 km, in clouds (about the same altitude as the VEGA balloons)	191	3	\$0.30B
Low-Level Aerial	Altitude 15–52 km, below clouds, limited view of surface due to attenuation	176	14	\$1.7B
Near-Surface Aerial	Altitude 0–15 km, NIR imaging of surface is possible, no surface access	170	20	\$3.0B
Single Entry Probe	No surface access, descent science only	136	2	\$0.33B
Multiple Entry Probes	No surface access, descent science only	171	2	\$0.28B
Short-Lived Lander	Single lander, about 5–10 hours lifetime on surface, passive cooling	153	12	\$0.89B
Short-Lived Landers	Multiple landers, about 5–10 hours lifetime on surface, passive cooling	214	12	\$0.70B
Long-Lived Lander	Single lander, days to weeks lifetime, may require active cooling and RPS	223	21	\$3.5B
Long-Lived Landers	Multiple landers, days to weeks lifetime, may require active cooling and RPS, long lived network possible	264	21	\$2.8B
Surface System with Mobility	Active or passive cooling, mobility with surface access at multiple locations (e.g., rover with short traverse or metallic bellows with long traverse)	209	53	\$7.1B
Coordinated Atmospheric Platforms	Large number (e.g., swarm) of in situ elements, with simultaneous measurements	129	21	\$2.8B

The technological difficulty was then assessed in an analogous fashion, where the study team determined the criticality for 15 different technologies for each of the 13 elements while the technology subgroup determined their maturity. The combination of the criticality and the maturity scores created a technology development FOM that then could be used to compare the degree of technology development required for each of the elements. The technologies considered included:

- Pressure vessel.
- Passive thermal control.
- Active cooling.
- High-temperature (HT) electronics platform avionics (command and data handling (CDH), guidance navigation and control (GNC), power modulation and distribution (PMAD), etc.).
- Mid-temperature (MT) electronics platform avionics (CDH, GNC, PMAD, etc.).
- HT actuated mechanisms (robotic arms, mobility, etc).
- HT telecom.

- HT sample acquisition.
- HT energy storage.
- MT energy storage.
- Power generation.
- Solar cells.
- Altitude control.
- Materials and fabrication (balloons, bellows, structures).
- HT health monitoring.

Finally, mission complexity ratings were developed and then translated into predicted mission costs using the rapid cost assessment methodology described in Peterson et al. (2008). This approach can predict relative mission costs between the various architecture elements when the missions are still in their preliminary study phase and not yet fully defined. However, the method is intended for scoping only and does not replace higher-fidelity methods, such as parametric or “grass roots” costing. The accuracy of the rapid cost assessment is estimated at ~10% – 20% for relative costs and ~30% - 40% for absolute costs. The results of these analyses are

presented in Table 3.1 and shown graphically in Figure 3.1.

There are some artifacts from this approach as presented. In considering single versus multiple identical elements it must be borne in mind that it costs more *per element* to develop one lander or probe than it does to develop multiple landers or probes (due to the fact that all design and some test costs can be amortized over the multiple copies). Therefore, the single versions of landers and probes shows a higher

cost than the multiple versions, as these results show the *per element* cost. Also, the costs in Table 3.1 do not include launch vehicles or the science payload costs, which could vary substantially.

At this point, candidate Venus mission architectures can be created by using one or more of the architecture elements described in Table 3.1 and including estimates for associated launch vehicle[s] and the science payload.

**Venus Mission Element Comparison**

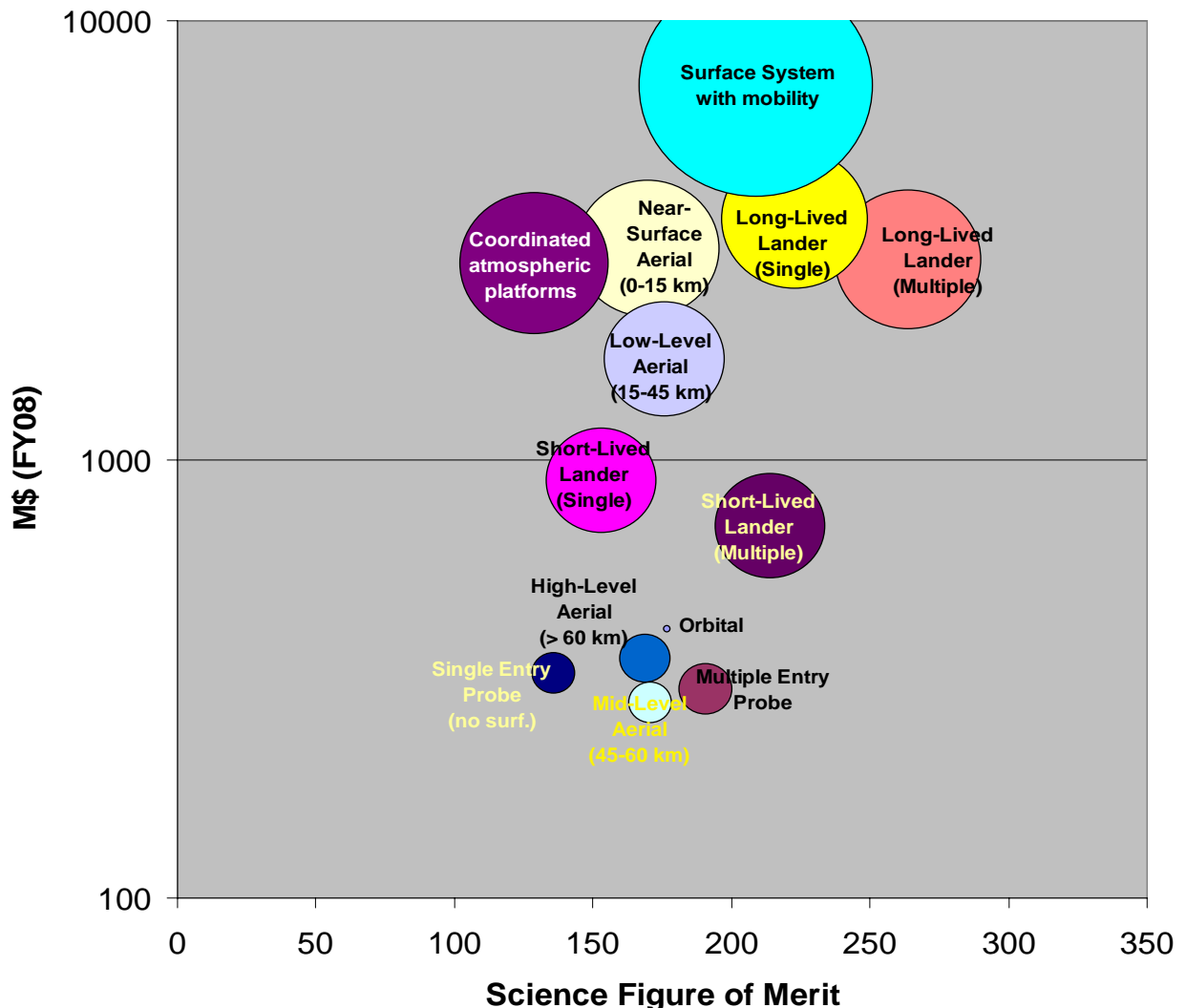


**Figure 3.1:** Venus flagship mission architecture element costs as a function of science figure of merit. The size of each bubble represents the relative technology development challenge necessary to fly each element.

To date, a significant number of Venus missions have either flown or been proposed using mission architectures that included orbiters (Magellan), probes (Pioneer-Venus), balloons (VEGA), and short-lived landers (Venera). While the mission architecture elements of these past missions are similar to those of the Venus Design Reference Mission, there will be major differences in the science instrument payloads and, hence, the kinds of science questions that can be addressed. The technological readiness of these previously used platforms is clearly high and results in low technology development ratings in the Venus flagship trade study. The opposite is true for platforms not previously used,

particularly those involving long durations in the high-temperature regions of the lower atmosphere and on the surface.

The STDT and the JPL Venus flagship study team synthesized 17 mission architectures that spanned a large part of the design space to determine those that would most likely fit within the assumed cost cap of a Venus Flagship mission and achieve the highest-priority science. Science figures of merit and total mission cost estimates were compiled for all of these architectures using the methodology described above. The options are listed in Table 3.2, and the results are plotted in Figure 3.2.

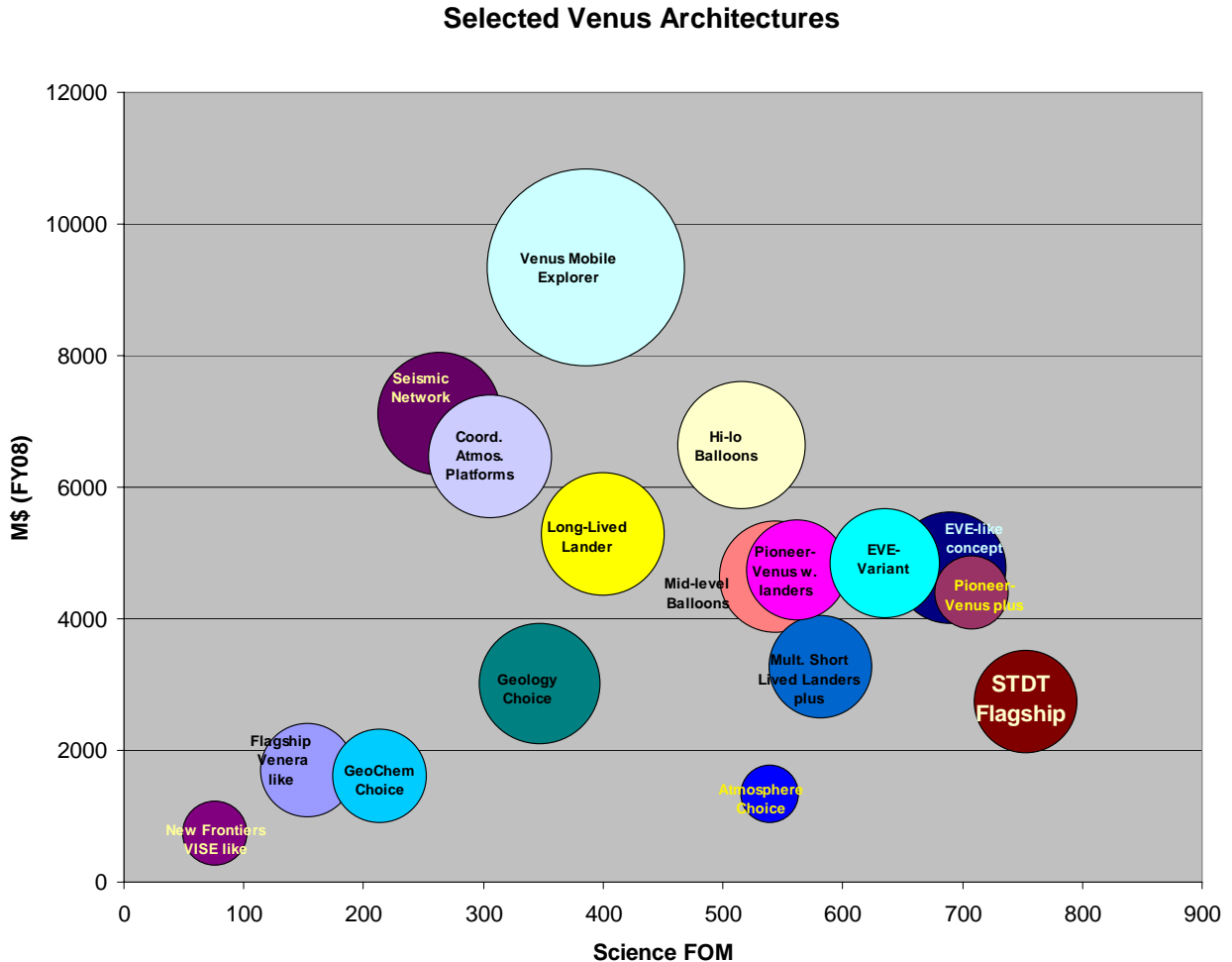


**Figure 3.2:** Venus flagship mission architecture costs as a function of science figure of merit. The size of each bubble represents the level of technological development necessary to fly each mission type.

**Table 3.2:** Mission Architectures Descriptions.

Mission	Science FOM	Tech. FOM	Components		
Flagship Venera like	153	12	Flyby	Short lived lander	
Venus Mobile Explorer	386	53	Orbiter	Surface System w. mobility	
Pioneer-Venus plus	708	8	Orbiter	Multiple (4) Entry Probes	1 High Level Balloon
Seismic Network	264	21	Flyby	Long-lived multiple landers (4)	1 Mid-level Balloon
Hi-lo Balloons	516	23	Orbiter	High-Level Aerial (> 60 km)	Near-Surface Aerial (0-15 km)
Mid-level Balloons	544	17	Orbiter	Mid-Level Aerial (45-60 km)	Low-Level Aerial (15-45 km)
Mult. Short Lived Landers plus	582	15	Orbiter	Short-Lived Lander (4)	Mid-Level Aerial (45-60 km)
Coord. Atmos. Platforms	306	21	Orbiter	Multiple (4) coord. Platforms	
EVE-like concept	690	18	Orbiter	Short-Lived Lander (Single)	High-Level Aerial (> 60 km) Mid-Level Aerial (45-60 km)
Pioneer-Venus w. landers	562	14	Orbiter	Multiple (4) Entry Probes	Short-Lived Lander (Multiple)
Long-Lived Lander	400	21	Orbiter	Long-Lived Lander (Single)	
EVE-Variant	635	17	Orbiter	Short-Lived Lander (Single)	High-Level Aerial (> 60 km) Single Entry Probe (no surf.)
New Frontiers VISE like	77	6	Flyby	Short lived lander	
STD T Flagship DRM	753	15	Orbiter	2 Mid-Level Aerial (52-70 km)	Short-Lived Lander (2)
Geology Choice	347	20	Orbiter	Near-Surface Aerial (0-15 km)	
Atmosphere Choice	539	5	Orbiter	2 Mid-Level Aerial (52-70 km)	Multiple (2) Entry Probes
GeoChem Choice	214	12	Flyby	Short-Lived Lander (2)	

**Table 3.3:** Potential Flagship Mission Architectures, FOMs, and Costs.

Recommended by	Mission architecture concept	Science FOM	Tech. FOM	Cost est.
<b>Mission architecture choices by STDT Science Subgroups</b>				
Geology Subgroup	Multi-element architecture with 1 orbiter; and 1 near surface aerial platform	347	20	\$3.0B
Atmospheric Subgroup	Multi-element architecture with 1 orbiter; 2 mid-level aerial platforms; and 2 entry probes	539	5	\$1.3B
Geochemistry Subgroup	Multi-element architecture with 1 flyby; and 1 short lived lander	214	12	\$1.6B
<b>STDT recommended mission architecture for detailed Flagship study</b>				
Full STDT	Multi-element architecture with 1 orbiter; 2 mid-level aerial platforms; and 2 short lived landers (could include long lived elements)	753	15	\$2.7B

Each of the three STDT science subgroups, (i.e., geology and geophysics, atmosphere, and geochemistry) had its preferred mission architecture included in the group of 17 that maximized the scientific return for its own subgroup. A fourth was jointly proposed by the STDT that represented a balanced compromise across the science subgroups. This balance was achieved when it was determined that, if properly instrumented, the landers could provide much of the same science as entry probes (in addition to their landed science), while balloon-based measurements would complement the landed science. The science and technology FOMs and estimated costs for these four architectures are shown in Table 3.3. The STDT found that single-element architectures, such as a near-surface mobility platform alone, cannot address as many key science questions for Venus and, thus, were not selected for the DRM.

It is evident from Table 3.3 that the STDT-recommended multi-element mission architecture has the highest science FOM and provides flexibility for payload accommodation on the various mission architecture elements. This allows for scalability in response to mission cost cap changes and readily lends itself to international collaboration because partners can take responsibility for different elements that are highly independent. In addition, this architecture supports synergies between the different platforms through continuous

simultaneous science measurements, an advantage not afforded by individual missions that make measurements at different locations and altitudes many years apart. Furthermore, the various mission elements could be flown alone as competed Discovery and/or New Frontiers missions, which would allow enabling science investigations to be performed before a Venus flagship mission is flown.

To summarize, the *recommended architecture* includes: a highly capable *orbiter* with a design lifetime of up to 4 years; *two cloud-level super-pressure balloons* floating at a constant altitude between 52 and 70 km, each with a design lifetime of 1 month; and *two landers* that would perform science measurements during atmospheric descent and subsequent to landing. The baseline architecture calls for short-lived landers because most of the critical landed science can be carried out during the expected 5-hour lander lifetime. The 5-hour minimum lander lifetime was determined on the basis of the following considerations:

1. The Soviet Venera and VEGA landers provide a proof-of-concept example that lander lifetimes as short as 1 hour can still enable surface sample acquisition and analysis.
2. The geochemistry subgroup of the STDT estimated that the XRD/XRF instrument requires 2 hours of measurement on each of the two samples to obtain adequate results.

3. The engineering team determined that a 1-hour duration would be sufficient to reach a depth of 10 cm (specified in the 2003 Decadal Survey as requirement for sampling National Research Council, 2003) given the available power.
4. Analysis of passive thermal management techniques based on insulation and phase change heat sink materials indicated that a 5-hour lifetime was achievable despite being over twice as long as the longest duration seen on the Soviet program (Venera 13 - 127 minutes, Abdrakhimov and Basilevsky, 2002). However, a lander lifetime of significantly longer than 5 hours would require new technology developments for passive thermal management (see Subsection 5.2.2) or active refrigeration (see Subsection 5.4.2.1).

However, two instruments that are not included in the recommended architecture — a long-lived seismometer and a long-lived meteorology station — would significantly enhance the science return. Their exclusion was primarily a result of the technological challenge and cost constraints, objections that would go away once the requisite technology development program were executed. Subsection 5.4.1.2.3 discusses the seismometry and meteorology options in detail.

## 3.2 Design Reference Mission Trades

There are many different options for implementing the recommended architecture. The study team performed a number of trade studies that explored the key aspects of this parameter space and used the results to choose a specific approach for the DRM. This section will describe the results of that process, considering in turn the following:

- Science instrument selection.
- Major mission architecture trades (telecom, orbits, launch vehicles).
- In situ vehicle trades (entry vehicle, balloon, lander).

### 3.2.1 Selection of the Science Instruments

The first and most crucial task was the selection of the science instruments for each of the elements in the architecture. While this is only a notional selection (as actual instrument selection would be the result of a competitive process for the actual mission), for the sake of developing a realistic DRM for the chosen architecture, it was necessary to be as specific as possible in defining this science planning payload.

Although some potential science instruments were automatically excluded by the choice of the DRM mission architecture (e.g., seismometers are not very useful on short missions), there was still a need to make choices and synthesize a planning payload that was consistent with the overall mass, power, and cost budgets. The study team made provisional instrument selections at a workshop and then refined those selections as the details of the mass, power, and cost budgets evolved during formulation of the DRM. Preliminary payloads were selected on the basis of the highest priority science investigations, while recognizing that limitations in cost, mass, and power (particularly for the in situ elements) existed. The notional payloads for the three mission architecture elements (orbiter, balloons, and landers) are provided in Table 3.4.

An iterative verification step was then performed by re-computing the science FOM for the selected mission architecture after removing those science investigations that could not be addressed using the selected instruments. The science FOM did not change, indicating that the instruments selected for the notional payload represented a good match for this mission architecture. Had there been a change, it would have been necessary to revisit the instrument selection to try and identify a payload that had a smaller impact on the science FOM.

**Table 3.4:** Notional Payload For The Orbiter, Two Balloons, and Two Landers. (Note that, with the exception of the nephelometer and net flux radiometer, all of the descent phase instruments for the landers are also used during the landed phase.)

Orbiter	2 Balloons	2 Landers	
Lifetime (4 years)	(1 month)	Descent Phase (1–1.5 hour)	Landed Phase (5 hours)
InSAR — Interferometric Synthetic Aperture Radar	ASI — Atmospheric Science Instrument (pressure, temperature, wind velocity)	ASI	Microscopic imager
Vis-NIR Imaging Spectrometer	GC/MS — Gas Chromatograph/Mass Spectrometer	Vis-NIR Cameras with spot spectrometry	XRD/XRF
Neutral Ion Mass Spectrometer	Nephelometer	GC/MS	Heat Flux Plate
Sub-mm Sounder	Vis-NIR camera	Magnetometer	Passive Gamma Ray Detector
Magnetometer	Magnetometer	Net Flux Radiometer	Sample acquisition, transfer, and preparation
Langmuir Probe	Radio tracking	Nephelometer	Drill to ~10 cm
Radio Subsystem (USO — Ultra Stable Oscillator)			Microwave corner reflector

**Table 3.5:** Summary of Key Mission Trades (Selected in **BOLD**).

TRADES	OPTIONS		
Data return from in situ elements – lander & balloon	Orbital relay	Flyby relay	Direct-to-Earth (DTE)
<b>Orbit Design</b>	Circular	Elliptical	<b>Elliptical then Circular</b>
Launch Vehicles	Single	Double	Triple
Element Allocation between Vehicles	<b>Orbiter on Launch vehicle 1 (LV1)</b> <b>Balloons/Lander on launch vehicle 2 (LV2)</b>		

### 3.2.2 Major Architectural Trades

The study team analyzed the following mission design trades before settling on a specific concept for the DRM:

- Use (or not) of the orbiter as a telecom relay for in situ assets.
- Power source for the balloons.
- Targeting of one or two locations for entry of the balloons.
- Targeting of one or two landing sites for the landers.
- The number of entry vehicles.
- The number of carriers.
- The number of launch vehicles.

The results of these trades then bounded the selection of trajectories and orbits for the mission. The architecture trades are

summarized in Table 3.5 and discussed in detail below.

#### 3.2.2.1 Telecom Trades

The options here are direct-to-Earth communications, relay through a flyby stage delivering the probes, and relay through an orbiter. The study team concluded that an orbiter serving as a telecommunications relay was essential for the in situ assets in order to:

1. Return a meaningful amount of data.
2. Reduce their telecom power requirements.
3. Provide relay capability for the entire 1-month operating lifetime of the balloons.

Direct-to-Earth (DTE) communications from the in situ elements are insufficient for several reasons. The telecom data rate is impacted, among other factors, by the separation distance, telecom power, antenna size and design, and atmospheric attenuation.

The largest obstacle to achieve a sufficiently high data rate is the range, which scales as one over distance squared. This already favors relay telecom. Atmospheric attenuation means that high frequencies (X- or Ka-Band) are not usable; consequently, lower frequencies (S-Band) must be used. A key problem is that the landers will generate a lot of data in a short amount of time, particularly given the imaging investigations during descent and on the surface. To return the full data from the landers direct-to-Earth before the landers expire, a massive, high-power telecom system would be required, with a corresponding increase in power requirements and thermal management, greatly increasing the lander mass. The study team deemed this a much worse design choice than using a nearby telecom relay. The much lower data rates from the balloons are more conducive to DTE communications; however, the power requirements are very significant, particularly if the Venus-to-Earth distance is not near its 0.3 AU minimum. Once the choice was made to provide a telecom relay for the landers, the STDT determine to use the same relay for the balloons, thereby achieving high-value data returns. An orbiter becomes the only feasible relay platform given the 1-month lifetimes of the balloons and the inability of a flyby spacecraft to remain visible for more than a few hours.

### 3.2.2.2 Orbit Trades

Given the selection of an orbital relay, there are implications for the choice of orbit. The orbiter needs to be in an orbit that allows it to view the landing sites for the entire duration of the landed missions. Analysis showed that highly elliptical (Molniya-like) orbits at Venus were needed to provide 5 or more hours of visibility for each of the landing sites. However, a low-circular or near-circular orbit is needed for the orbital science objectives, particularly the radar mapping investigation. Hence, a single orbit will not meet both the telecom relay requirements and the science

requirements. The preferred option is to divide the orbiter mission into two distinct operational phases: Phase 1 in which the orbiter is essentially dedicated to the telecom relay function and performs little or no science; and Phase 2, in which the orbiter is dedicated to taking science measurements and no longer performs a telecom relay function. Since the transfer from elliptical to circular can be implemented with aerobraking, there is a substantial propulsion advantage to implementing the in situ mission first. A detailed explanation of this operational scenario and the achievable telecom data rates is provided in Chapter 4.

### 3.2.2.3 Launch Vehicles

Once this operational approach was selected, it immediately led to the key design decision of the number of launch vehicles to be used. If a single launch vehicle is used, then all elements must go into orbit first because the orbiter must already be in place and serving as a telecom relay prior to atmospheric entry of the landers and balloons. However, the propellant requirements for this are very large given the approximately 1700-m/s  $\Delta V$  orbit insertion maneuver (see Table 4.33). No single launch vehicle is currently capable of sending that much mass ( $\sim 10,000$  kg) to Venus; this option was, therefore, discarded by the study team.

With a minimum of two launch vehicles, the orbiter can be sent separately and arrive at Venus in advance of the in situ elements, allowing for ample time to prepare for its telecom relay functions. The choice then becomes how many launch vehicles to use for the in situ elements. The most straightforward approach is to use a single launch vehicle and carrier spacecraft, as long as it is compatible with the launch mass capability available, packaging considerations, targeting requirements, and operational support. It was also found that two Atlas V-551 launch vehicles could deliver more mass to Venus than a single Delta IV-H, at lower total cost. In

addition, the two launch vehicle options would allow for programmatic flexibility, in case one of the launches needed to be descoped for budgetary reasons. As described in Chapter 4, a viable one-launch vehicle solution for the in situ elements exists; hence, the study team adopted this approach. A comprehensive second-tier trade study was then conducted on potential interplanetary trajectories for the two spacecraft; the details of this study are described in Chapter 4.

### **3.2.3 In Situ Vehicle Trades**

Some of the trades described below are common to the balloon and lander elements or deal with the way the balloon and lander are integrated. Other trades are specific to the balloon or the lander.

#### **3.2.3.1 Common Trades**

##### **3.2.3.1.1 Entry Mode**

A direct entry from the interplanetary trajectory was selected to avoid the high cost of propellant for getting into orbit, an approach consistent with the targeting requirements needed to land on the specified landing sites. This approach does involve higher g-loads during entry, which impacts the feasibility of certain power system options for the entry vehicles; these factors, however, are overridden by the performance advantages.

##### **3.2.3.1.2 Element Allocation between the Entry Vehicles**

The prime options considered here were to put the four in situ elements in four separate entry vehicles or to pair a lander and a balloon in two aeroshells. This second option not only minimized the number of aeroshells, but meant that a single aeroshell and entry system design

would meet the full mission requirements. The key issue here was whether or not the targeting objectives could be achieved.

There was a clear consensus on the STDT that the two landers needed to target geologically different landing sites. As it turned out, the reachable sites for a given launch opportunity are somewhat restricted, as will be shown in Chapter 4. Nevertheless, it was possible to target the two highest-priority terrain types — namely, the tessera and the lava flow fields — in both the 2021 and 2022 launch opportunities. In contrast to the landers, there are no target longitude requirements on the balloons because they are expected to fly for a month, circumnavigating the planet multiple times and flying over all longitudes and many latitudes; however, entry at different locations would ensure that the balloons would follow different paths around the planet, increasing their coverage of the atmosphere. This balloon flexibility allows for the possibility of packaging a balloon and a lander inside the same entry vehicle, achieving cost and systems engineering simplifications by having only two identical entry vehicles (each with one balloon and one lander) instead of three or four entry vehicles, each with either a balloon or lander (or two balloons in one, and one each for the landers). The team adopted this approach, much like the Soviet VEGA mission did in 1985 for the same reasons.

Finally, a direct entry from the interplanetary trajectory was selected to avoid the high cost of propellant for getting into orbit, an approach consistent with the targeting requirement needed to land on the specified landing sites.

**Table 3.6:** Summary of Common Balloon/Lander Trades (Selected in **BOLD**).

TRADES	OPTIONS		
Entry mode	From orbit	Direct entry	
Element allocation between Entry Vehicles	4 separate EVs	<b>Balloon/lander in EV1</b> <b>Balloon/lander in EV2</b>	2 balloons in EV1 2 landers in EV2
Package of balloon and lander in entry vehicle		Lander inverted	Lander in landed orientation

**Table 3.7:** Summary of Balloon Trades (Selected in **BOLD**)

TRADES	OPTIONS			
Balloon Design	Montgolfiere balloon	<b>Superpressure light gas balloon</b>	Zero pressure light gas balloon	Phase change fluid cycling balloon
Power system	Radioisotope	Primary batteries	Solar plus secondary batteries	

### 3.2.3.1.3 *Packaging of the Lander and Balloon Vehicle*

Once the decision had been made to package a lander and a balloon in one entry vehicle, packaging strategies were considered. Based on the lander configuration (described in detail in Chapter 4), it was clear that the minimum required packing volume and minimum corresponding heat shield area and mass was achieved if the lander orientation was inverted with respect to the balloon and gondola. Placing the lander beneath the balloon also meant that the lander would not interfere with balloon inflation, since it could be released once the heat shield and backshell were ejected.

### 3.2.3.2 **Balloon Trades**

Table 3.7 summarizes the balloon trades.

#### 3.2.3.2.1 *Balloon Design*

There are four basic balloon designs that were examined for use on the DRM: Montgolfiere (hot air) balloon; a light-gas, superpressure balloon; a light-gas, zero-pressure balloon; and a phase-change, buoyancy-fluid, altitude-cycling balloon. The requirement for one month of lifetime precludes use of zero-pressure balloons because the transition from day to night as the balloon drifts around the planet would cause a substantial loss of buoyancy due to the loss of solar heating, causing the balloon to descend into the hot lower atmosphere and be destroyed. The common terrestrial strategy of dropping ballast to compensate for this loss of buoyancy can be used on Venus; however, like on Earth, this approach is limited to 1 or 2 transitions, which would result in only 5 to 10 days of lifetime on Venus. The Montgolfiere balloon is also precluded by the 30-day

lifetime requirement. Tens of kilowatts of heat power are needed for buoyancy at Venus, which is impractical for radioisotope sources on any time scale or chemical sources for more than 30 days. This leaves solar-heated Montgolfiere balloons as the only option, a configuration that does not meet the 30-day requirement because the balloon spends half the time in darkness.

The phase-change, altitude-cycling balloon is one in which the buoyancy-generating fluid inside the balloon changes phase from a gas to a liquid when the balloon ascends to a colder altitude at Venus. This condensation reduces the overall buoyancy, causing the balloon to change from ascent to descent. As the balloon descends into warmer atmosphere, the buoyancy fluid evaporates again, increasing the buoyancy and causing the balloon to arrest its descent and start rising once more. The net result is a balloon that continually cycles across a range of altitudes that can be specified with the right choice of fluids and attendant balloon design. Despite successful demonstration experiments of this concept in the Earth's atmosphere (Nock et al, 1995) the altitude-cycling balloon technology remains relatively immature. This lack of technical maturity led the study team to reject this design for the DRM despite the scientific advantages of being able to make repeated atmospheric measurements across a range of altitudes. This decision should be revisited in the future if the phase-change, altitude-cycling balloon technology becomes sufficiently mature.

With these three balloon options rejected, the only viable option becomes the light-gas superpressure balloon, the same choice that was made for the Soviet VEGA mission in

1985. Superpressure balloons are stable in altitude across the entire range of solar heating levels, which makes them ideal for a long-duration flight of the kind required in the DRM. The technology is mature, with thousands of superpressure balloons flown on Earth over the years, in addition to the two VEGA balloon flown on Venus.

### **3.2.3.2.2 Balloon Power System**

The study team performed power system trades for the balloon to determine the best approach for a 1-month mission, evaluating the impact of selection of batteries, solar cells, or an RPS. The team arrived at the following findings:

1. Primary batteries are the simplest approach and one that can satisfy the main science objectives for the balloon.
2. Solar power has three problems:
  - a. Protecting the solar cells from the sulfuric acid droplets in the clouds (achievable, but with some technology or engineering development required).
  - b. As the balloons drift pole-ward, the solar incidence angle reduces to the point that the power generated rapidly drops (a real issue for extended durations, since the current understanding of the Venusian winds show that the balloons will likely end up at high latitudes).
  - c. A solar power system will still need secondary batteries to support operations when the balloon is on the dark side of Venus. The associated power and power-switching system would require additional mass.
3. While use of RPS power would allow for increased balloon lifetime, increased returned data volume, and improved uplink data rate, any ASRG or MMRTG would have to be modified to work in the Venusian atmosphere and would also need to be protected from the acid, with a possible loss in efficiency and power output that cannot currently be quantified without more

detailed analysis of the required RPS design changes. Use of an RPS would also increase the complexity (and possibly size) of the aeroshell and cruise stage to manage the thermal loads and might create center-of-gravity (CG) issues during entry. Use of an ASRG also restricts the entry flight path angle to reduce the entry g-loads to tolerable values, reducing the space of possible trajectories and insertion sites. RPS and launch approval costs would also be a substantial increase to the overall mission costs. It should be noted, however, that there could be dedicated balloon mission architectures, potentially in the Discovery or New Frontiers mission classes, where an ASRG-enabled aerostat, with its continuous sampling and telecom over a 1-month lifetime, could provide significant science return over a battery-operated mission once technical and architecture challenges with entry g-loads and mitigation of the corrosive atmosphere are addressed. An MMRTG would provide the same amount of power as an ASRG, but it would be significantly larger (in both volume and mass) and would require 4 times more  $^{238}\text{Pu}$  and more complex accommodation inside the aeroshell. Therefore, MMRTGs would be less desirable for the balloons. Further details on the benefits of an RPS to enhance the balloon mission are provided in Chapter 5.

The above discussion on the potential use of an ASRG or an MMRTG is only valid for a cloud level balloon mission element. For surface or near-surface mission architecture elements, the development of a new Venus-specific RPS is required. This development would need to address operation in the high temperature and pressure environment. Such a new RPS would likely be coupled with active cooling for the payload.

**Table 3.8:** Summary of Lander Trades (Selected in **BOLD**)

TRADES	OPTIONS		
Lander terminal descent system		Parachute	Drag Plate
Thermal Control System	Liquid - Vapor PCM	Solid - Liquid PCM	Active refrigeration
Power system	Solar	Primary Batteries	Radioisotope Power

### 3.2.3.3 Lander Trades

Table 3.8 summarizes the lander trades.

#### 3.2.3.3.1 Lander Terminal Descent System

A cruciform (or cross) parachute was selected over a rigid drag plates for three reasons:

1. Inclusion of a rigid drag plate makes it more difficult to efficiently pack the lander in the aeroshell. The Russian Venera landers used a drag plate configuration, where the spherical aeroshell was better suited to accommodate it than doing so on the flight qualified U.S. aeroshell designs considered for the Venus DRM.
2. Unlike a parachute, which could be deployed late in the descent to reduce the landing impact while minimizing descent time, use of a drag plate would have provided a constant deceleration during descent, requiring either a longer descent period (and a corresponding shorter landed period due to the heat saturation of the lander) or a higher impact velocity.
3. Descent imaging of the surface requires a stable platform to minimize image smear; cruciform (or cross) parachutes provide smaller oscillation amplitudes and rates than rigid drag plates by moving the center of gravity higher up. The parachute will have to be released before the lander touches down to eliminate the possibility of the parachute draping over the lander. However, the extreme density of the Venusian atmosphere near the surface allows the landing impact to be easily attenuated with a simple crush pad.

#### 3.2.3.3.2 Lander Thermal Control

All thermal control options will use insulation to minimize the heat leak into the

lander. The options considered here were: the use of passive systems using the thermal capacity of the lander only; a phase change material (PCM) employing a solid-to-liquid phase change; and a PCM employing a liquid to vapor phase change material and an active refrigeration system. For reasons of technical maturity the approach using the solid-to-liquid PCM was adopted for the DRM and consistent with a 5-hour duration landed mission, although technology investments in the other approaches were identified as enabling for extended life.

#### 3.2.3.3.3 Lander Power System

The above discussion on the use of an ASRG or an MMRTG is only valid for a cloud level balloon mission element. For surface or near-surface mission elements, the development of a new Venus surface-specific RPS is required. This development would have to address operation in the high temperature and pressure environment. Such a new RPS would likely be coupled with active cooling for the payload. However, for the limited mission duration here, the use of primary batteries is a satisfactory solution. Power for the extended lifetime elements is a separate issue and is addressed in Chapter 5.

## 3.3 Design Reference Mission Synopsis

The results of these key design decisions transformed the high-level mission architecture recommended by the STDT into a Design Reference Mission suitable for further design and analysis. In summary, the proposed mission point design includes two launches. The study baselined launches in 2021, ~6 months apart; note however, that backup launch options are available every 19 months

(in 2022 and 2024) due to orbital phasing between Venus and Earth. Each of the two Atlas V-551 launch vehicles can deliver up to ~5500 kg mass to Venus. The carrier spacecraft with two Venus entry systems, each accommodating a balloon and a lander, would be launched in late April 2021 on a Type IV trajectory and arrive at Venus, after a 456-days cruise, in late July 2022. The two aeroshells would be released from the carrier 20 and 10 days before arrival, targeting their predetermined entry and landing sites on the dayside of Venus. This was required by the science investigations (to allow for imaging during descent and after landing).

During the flyby, the carrier spacecraft would be equipped to provide a limited backup telecom support for the landers and balloons, and additional confirmation that the entries were successful.

The orbiter would be launched in late October 2021 on a Type II trajectory and would arrive at Venus in early April 2022, following a 159-day cruise. This earlier arrival would provide sufficient time for the orbiter to set up a 300-km × 40,000-km elliptic orbit, with the apoapsis optimized for up to ~5 – 6 hours of continuous visibility of the *in situ* elements (as a function of their landing location). The entry systems would be staged to enter Venus ~13 hours apart, allowing the orbiter to communicate with one balloon/lander pair at a time in two consecutive orbits.

Following atmospheric entry, the separation, descent and then inflation of the balloon and the descent and landing for the lander would follow steps and timelines similar to those of the historic Russian VEGA missions. The balloons could deploy in approximately 15 – 20 minutes and begin operating. The landers would take ~1 – 1.5 hours to descend and would perform descent science. This would be followed by surface operations, while communicating the data to the orbiter. After completing *in situ* science

support, the orbiter would aerobrake to circularize its orbit at ~230 km and begin its own 2-year science mapping phase.

The details of the Design Reference Mission and second-level trade studies are described in Chapter 4.

## 4 DESIGN REFERENCE MISSION

---

### 4.1 Introduction

This chapter describes a Design Reference Mission (DRM) that implements the preferred Venus flagship mission architecture developed in Chapter 3. All elements, including new technology developments required for the DRM, are covered here. The DRM is a pre-Phase A level of design that merges inputs from two primary sources:

1. The JPL Venus Flagship Study Engineering Team.
2. JPL's Advanced Projects Design Team, also known at Team X.

The main purpose of the DRM is to quantify the resources needed to implement the Venus flagship investigation via the recommended mission architecture. Of particular interest are the required launch mass, the data volumes, and the total mission cost. The DRM described here is not intended to be the final choice of Venus flagship mission; instead, it is simply an example mission concept that both achieves a very large fraction of the science objectives and provides sufficient engineering definition for first-order estimates of the needed resources. The level of detail for this DRM is uneven, with some elements having received significant design and analysis work (e.g., mission design) and other elements not advanced beyond the rough concept stage (e.g., the lander). The report will provide details where available and note otherwise where significant detailed work has not yet been done.

A mass margin of 43% has been applied to the current best estimates (CBE) of the mass of all spacecraft systems. This has been allocated between a subsystem level contingency for each mission element with the percentage determined by the maturity of that element and an overall system contingency. The DRM was treated as an in-house JPL build mission to allow use of JPL schedule and cost estimating models.

### 4.2 Design Reference Mission Summary

The DRM uses a dual-launch approach to get the orbiter and in situ vehicles to Venus. The launches occur approximately six months apart in 2021, with backup launch options available every 19 months (in 2022 and 2024) due to orbital phasing between Venus and Earth. Each of the two Atlas V-551 launch vehicles will deliver approximately 5500 kg to Venus. The carrier spacecraft with two Venus entry vehicles will launch first, in late April 2021, on a Type IV trajectory, arriving at Venus in July 2022 after a 456 day cruise. The two entry vehicles are identical, each accommodating a cloud-level balloon and a short duration lander. The orbiter will launch in late October 2021 on a Type II trajectory and will arrive at Venus in early April 2022 following a 159-day cruise. This fast trajectory means that the orbiter arrives first at Venus despite launching second from Earth. The orbiter uses chemical propulsion to enter into a 300-km × 40,000-km near-polar elliptical orbit, an orbit optimized to provide telecommunications relay coverage for both entry vehicles. The orbiter remains in this telecom orbit until the end of the one-month balloon mission, after which it transitions to a 230-km altitude circular orbit through use of aerobraking over a 6-month period. This low circular orbit is optimized for the synthetic aperture radar instrument (InSAR) that will map the planet over a 2-year main mission phase, with an option for an additional 2 years.

The two entry vehicles will arrive at Venus 13 hours apart (one orbital period) to enable the orbiter to serve as a telecom relay for only one balloon and lander pair at a time. One lander will be targeted for Alpha Regio, a tessera region at 27° S, 3° E; the other lander will be targeted for a region of lava flow fields at 47° S, 7° E. Landings will occur in daylight to enable imaging during atmospheric descent and while on the surface. The balloon and lander will separate at a 56-km altitude, after which the lander will descend to the ground in

1 hour under a 2.5-m diameter parachute. The balloon will execute an aerial deployment and inflation sequence very similar to that employed by the Soviet VEGA balloons in 1985. The sequence consists of a low-speed parachute-arrested descent with the balloon first deployed from a storage container and then inflated with helium from high-pressure tanks over a 5-minute period. The parachutes will be constructed from high-temperature compatible, sulfuric acid resistant fiberglass material. The 7.1-m diameter, helium-filled spherical superpressure balloon is designed to fly at a 55.5-km altitude and carry a 108-kg payload that includes science instruments, spacecraft subsystems, and all mass margins and contingencies. The nominal balloon flight lifetime is 1 month, sufficient to enable each balloon to circumnavigate Venus five or more times. It is expected that the meridional winds will move the balloons poleward to provide a large range of latitudinal coverage.

Each lander is designed for a 5-hour lifetime after reaching the surface. The landers consists of an insulated pressure vessel that houses most of the science instruments and spacecraft systems, plus a landing system and other externally mounted components. Lander lifetime will be limited by heating of the electronic payload inside the pressure vessel that will eventually surpass the ability of the passive thermal control system to absorb. While on the surface, the lander will acquire and analyze two rock samples obtained by a

drill: one from the weathered surface rock and one from a presumably unweathered depth of 10 cm. Images of the surface and numerous other scientific measurements will be taken; the data will be radioed to the orbiter before the end of the 5-hour mission.

A planning payload for the DRM was selected by the STDT based on the highest priority science objectives and measurements with preference given to instruments where there was flight heritage. This planning payload is summarized in Table 4.1 with a breakdown provided for which instruments are on which platform. Note that there is some commonality of instruments between the platforms, namely the nephelometer, the magnetometer and the GCMS used on the balloons and landers. One very high priority instrument not included in the planning payload was a seismometer on the lander. This was excluded from the DRM for reasons of low technical maturity, the same reasons why it features prominently in the discussion of and recommendations for new technology in Chapter 5.

Further details on the instrument planning payload, the mission design, and the spacecraft are presented in Sections 4.3, 4.4, and 4.5, respectively. Planetary protection issues are briefly described in Section 4.6. A discussion of open issues and trades is presented in Section 4.7. The new technology requirements for the DRM are presented in Section 4.8.

**Table 4.1:** Science Planning Payload for the DRM.

Orbiter	2 Balloons	2 Landers	
Lifetime (4 years)	(1 month)	Descent Phase (1hour) and Landed Phase	Landed Phase (5hours)
InSAR — Interferometric Synthetic Aperture Radar	ASI — Atmospheric Science Instrument (p; T; wind; acceleration)	ASI	Microscopic imager
Vis-NIR Imaging Spectrometer	GC/MS — Gas Chromatograph / Mass Spectrometer (long life)	Vis-NIR Cameras with spot spectrometry	XRD / XRF
Neutral Ion Mass Spectrometer	Nephelometer	GC / MS	Heat Flux Plate
Sub-mm Sounder	Vis-NIR camera	Magnetometer	Passive Gamma Ray Detector
Magnetometer	Magnetometer	Net Flux Radiometer	Sample acquisition, transfer, and preparation
Langmuir Probe	Radio tracking	(Nephelometer)	Drill to ~10 cm
Radio Subsystem (USO — Ultra Stable Oscillator)			

### 4.3 Science Payload Description

The selection of science instruments for the planning payload was a joint effort by the Science and Technology Definition Team (STDT) and the engineering team. Through the selection process, the teams attempted to capture the vast majority of the science objectives without exceeding the expected mass and cost constraints for the mission. Brief descriptions of the selected instruments and their science context are presented below, grouped by platform: orbiter, balloon and lander. Wherever possible, mass, power, size, cost, and data rate metrics were estimated from currently developed or flight heritage instruments that were judged to be good proxies for this mission. This approach is reasonable because the engineering design of the balloon gondola and the lander generally provide protective enclosures that isolate the science instruments from the harsh Venusian environment. Consequently, this enabled widespread use of instrument proxies that were originally designed for other environments. Exceptions primarily consist of the lander sample acquisition system, atmospheric structure sensors (e.g., temperature, wind), and a few others that directly interface with the environment, as will be noted below.

It should be noted that for the actual mission, the instruments will be selected via a competitive process. Therefore, the instruments listed below are primarily used as an “existence proof” that it is possible to satisfy the science objectives within the available payload mass and power allocations.

#### 4.3.1 Orbiter Instruments

Table 4.2 provides a summary of the orbiter instruments, along with their mass, power, heritage (if any), and information source. Figure 4.1 illustrates the orbiter configuration and the Interferometric Synthetic Aperture Radar (InSAR) placement on the orbiter.

##### 4.3.1.1 Orbiter Visible-Near Infrared (Vis-NIR) Imaging Spectrometer

The Visible Near Infrared (Vis-NIR) Imaging Spectrometer will provide images of various cloud layers and potentially the Venus surface, depending on the particular frequencies used. The measurement requirements for the Vis-NIR are listed in Table 4.3. Similar instruments have been flown previously and would likely require little or no technology development for use on the orbiter. Note that the 0.2 km/pixel resolution is achievable for cloud top observations, but the resolution for deep atmosphere and surface observations will be much worse due to scattering.

**Table 4.2:** Orbiter Instruments.

Instrument	Mass (kg)	Power (W)	Source or proxy
Vis-NIR Imaging Spectrometer	33.1	44	MRO CRISM
InSAR	157	1,900*	JPL in-house studies.
Submillimeter Sounder	19.9	59	Rosetta
Ultra-Stable Oscillator (USO)	1	5	MRO
Magnetometer (incl. boom)	4.4	2	Messenger
Langmuir Probe	0.5	1	Rosetta
Neutral Ion Mass Spectrometer	13.2	25	Cassini

\* InSAR max power is 2.9 kW (imaging mode); nominal power is 1.9 kW (DEM mode)

**Table 4.3:** Vis-NIR Measurement Requirements.

Imaging	
Resolution	2,000 $\lambda/\Delta\lambda$ , spectral. 0.2 km/pixel spatial for “Spot” views, 10 km/pixel for global views
Frequency of measurement	once per minute (depending on mapping strategy)
Range of measurement	0.25 to 4.0 $\mu\text{m}$ , in selectable wavelength ranges
NIR/IR	
Resolution – NIR/IR	5,000 $\lambda/\Delta\lambda$ spectral, <1 km spatial
Frequency of measurement	once per minute (depending on mapping strategy)
Range of measurement	0.8 to 25 $\mu\text{m}$

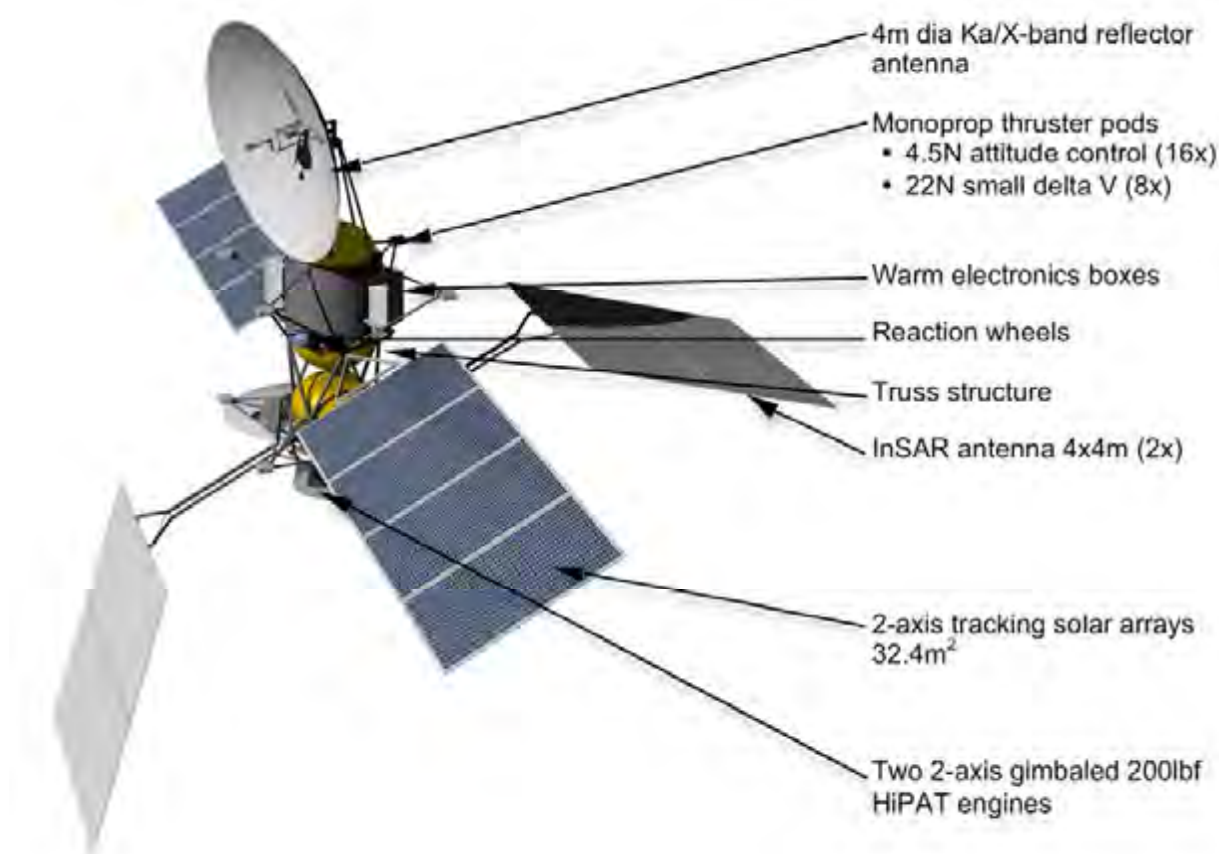


Figure 4.1: Orbiter in deployed configuration (artist's rendering).

This remote sensing instrument will produce image cubes of high spatial and spectral resolution in the visible and near infrared. It is in the same class of instrument as VIRTIS on Venus Express, NIMS on Galileo and VIMS on Cassini and CRISM on MRO (CRISM, 2009). It will allow mapping and monitoring of several variable gas species as well as cloud structures at many altitudes and a range of other variable atmospheric phenomena, such as oxygen airglow, which are diagnostic of chemical and dynamical cycles (see Figure 4.2). The instrument data rate (after CRISM) is estimated to be 30 Mb/s.

In the primary mapping mode, image cubes will be taken from orbit approximately once every minute. More intensive and specifically targeted campaigns will be necessary to perform limb measurements and to search for certain variable phenomena, such as lightning.

This instrument will allow us to determine abundances, spatial distribution, and temporal

variations of many atmospheric species. Of particular interest are the sulfur species — OCS, H<sub>2</sub>S, SO<sub>2</sub>, and Sn — throughout the atmosphere, including in the cloud-forming region (Pollack et al., 1993). We will also measure other reactive species important for understanding thermo-chemical processes (e.g., HCl, HF, SO<sub>3</sub>), measure greenhouse gases such as H<sub>2</sub>O and other condensables, and in general, characterize sources of chemical disequilibrium in the atmosphere. Through mapping the spatial and temporal variation of radiatively active species beneath the clouds, this instrument will potentially help to characterize gas emissions from volcanoes and, thereby, potentially contributing to important breakthroughs in understanding current geological activity and its connection with atmospheric chemistry and climate. The instrument will also be optimized for studying variations and movements in the global cloud deck.

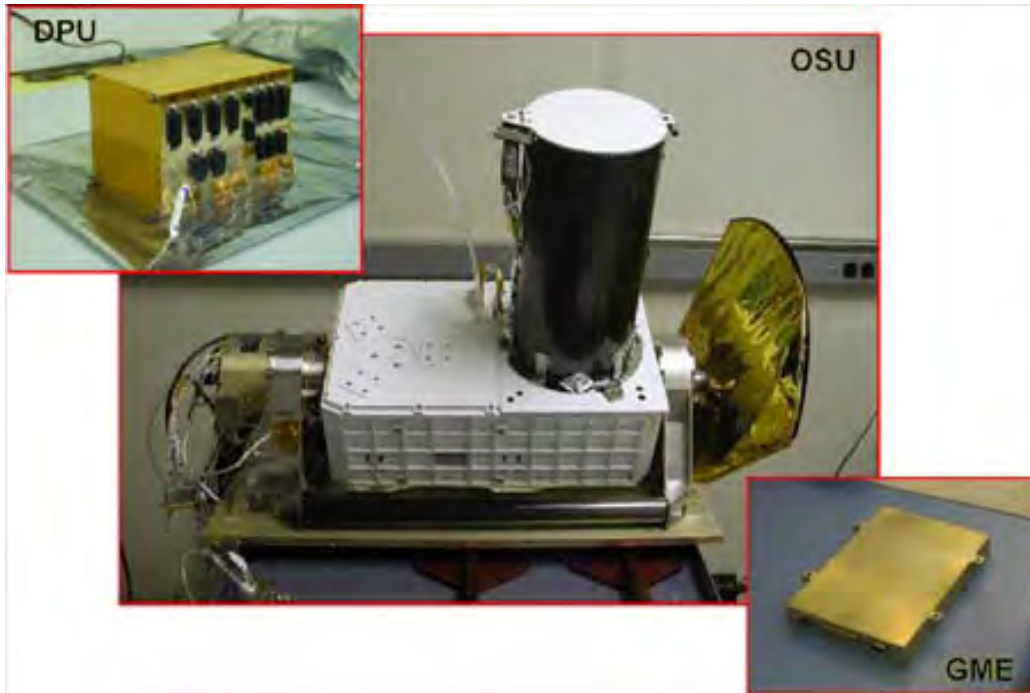


**Figure 4.2:** Image of the CRISM instrument, showing the Optical Sensor Unit (OSU), Gimbal Motor Electronics (GME), and the Data Processing Unit (DPU) (CRISM, 2009).

Infrared observations, especially in the optical “window regions” at 1.7 and 2.3  $\mu\text{m}$ , will track structures and motions in the middle cloud region. Through comparisons of spectra in these different window regions, we can also determine the size, distribution, and shapes of cloud aerosols (Grinspoon et al., 1993). Taken together, these measurements of gas abundances and cloud variability will lead to major advances in understanding the climate and radiative balance of Venus. Additionally, the Vis-NIR imaging spectrometer will have channels optimized for mapping the nightside surface emission of Venus. Using 3 windows around 1  $\mu\text{m}$  that contain emission coming from the surface, it will be possible to obtain wavelength ratios that can place important constraints on surface composition (Helbert et al., 2008; Mueller et al., 2008). These data might be of great importance for determining relative ages of surface types and might provide some constraints on the existence of evolved compositions, such as andesites, on the surface (Hashimoto et al., 2008) and, hence, the history of water on Venus.

#### 4.3.1.2 Orbiter Interferometric Synthetic Aperture Radar (InSAR)

InSAR provides comprehensive measurements of the topology and topography of the Venusian surface. Table 4.4 provides a summary of the InSAR measurement requirements and instrument characteristics. Several notes below the table explain some of the assumptions regarding the measurements.

The Magellan mission provided a revolution in understanding the regional distribution of terrains and the global-scale three-dimensional geology of Venus (Saunders et al., 1992; Solomon and Head, 1991). To make the next advancement in knowledge, understanding processes at the local scale is required. To accomplish this, it is necessary to make observations at spatial scales of at least an order of magnitude greater than previously attained. As conceived here, the InSAR system will have the capability to operate in an interferometric mode to produce high-resolution topographic information at a posting of 50 m/pixel and as a standalone imager to extremely high-resolution data of local areas at 6 m/pixel.

**Table 4.4:** InSAR Measurements and Characteristics.

Mode	Posts (m)	Hght Acc (m)	Looks	Data Rate (Mb/s)	BW (MHz)	PW (μs)	Duty Cycle (kW)	DC Power (kW)	Ping-pong	PRF (Hz)
DEM	50	<4	72	1(100)	12.5	40	23	1.9	No	6,100
Imaging	6	N/A	4	100 (260)	50	60	33	2.9	N/A	5,500

Notes:

1. The DEM mode requires onboard processing to achieve data rates indicated. The raw data rates, e.g. (100), are for 84 BAQ. Assume 32 bits/post +10%. For imaging an 82 BAQ (block adaptive quantization) could be used to reduce the data rate to 130 Mb/s. On board range compression could reduce the “raw” data rate to about 100 Mb/s.
2. Height accuracy (Hght Acc) is calculated for single-side look only (90% or  $1.6\sigma$ ), an additional, opposite side look over the same area will improve this value by a factor of 1.4.
3. The look angle for all calculations is 30°. Some variation is possible for targets of opportunity. The swath in all cases is 10 km.

The concept proposed here is comprised of two 4-m × 4-m antennas that are separated by 9 m on booms, with one antenna used to transmit the radar signal and both used to receive the reflected echoes (Figure 4.1). The observing geometry from the 230-km circular polar orbit is offset from the nadir by about 30 – 35 degrees, allowing for range and Doppler processing that yields radar images from the two received datasets. The image strip parallels the flight path of the spacecraft and is approximately 10 km wide to permit overlap with subsequent orbit tracks as Venus slowly rotates. Correlation of the two complex-valued datasets produces interference fringes due to the variations in radar echo path length induced by the surface topography. These phase changes are “unwrapped” to produce a topographic map of the surface and an ortho-rectified radar image. At a resolution of 50 m per pixel, it requires  $1.8 \times 10^{11}$  pixels to cover the entire planet, or  $7.2 \times 10^{14}$  bits at approximately 4,000 bits per pixel. The DRM is designed to return  $3 \times 10^{14}$  bits of InSAR data over the course of the mission, allowing for approximately 40% of the planet to be mapped at this resolution and correspondingly less at higher resolutions.

The InSAR instrument requires pointing control, knowledge, and stability of 150 arcsec ( $3\sigma$ ), 50 arcsec ( $3\sigma$ ), and 1000 arcsec/sec ( $3\sigma$ ), respectively. Other requirements of this instrument on the mission architecture, systems, and operations will be addressed in

follow up studies.

#### 4.3.1.3 Orbiter Submillimeter Sounder

The Submillimeter Sounder provides for the characterization of wind, atmospheric temperature, and some atmospheric composition. Table 4.5 shows the measurement requirements for the sounder. While submillimeter sounders have been flown for other applications, it is likely that design modifications would be required to adapt them for use at Venus. The technology readiness level (TRL) of this instrument is, therefore, estimated to be 4.

The thermal emission of Venus in the submillimeter range contains a wealth of information about physical properties and chemical composition of the atmosphere in the 60- to 140-km altitude range. The atmospheric dynamics of Venus can be constrained by temperature and (Doppler) wind measurements in both nadir and limb mode. Nadir observations provide a larger latitudinal coverage, while the limb observations are more sensitive to winds, especially in the upper atmosphere. Temperature and wind speed accuracies of about 1 – 2 K and 5 m/s, respectively, can be achieved. Carbon monoxide lines would typically be used for this purpose, providing at the same time the 3-D distribution of this important gas in Venus’ atmosphere. Simultaneously, at least one other atmospheric species (e.g., water vapor and its isotopes) could be monitored.

**Table 4.5:** Submillimeter Sounder Measurement Requirements.

Frequency of measurement	Continuous
Range of measurement	Top of atmosphere to cloud deck (60 to 140 km)
Sensitivity	Winds, temperature, various molecules
Accuracy	Winds to $\pm 25$ cm/s

The 3-D determination of other chemically important species like SO, SO<sub>2</sub>, ClO, HCl, OCS, hydrogen radicals, etc., will be performed in limb mode, which will have up to 50 times higher sensitivity compared to nadir mode. Transition between nadir and limb modes requires the spacecraft to rotate between nadir pointed and limb pointed orientations. Thanks to recent developments in submillimeter technology (for the Herschel Space Observatory [ESA, 2009]), observations of both dedicated spectral lines and the broadband submillimeter survey for new molecules are a possibility. Large parts of these bands are not accessible from Earth-based observations, and Herschel will not be able to observe Venus, since it is too near to the Sun. The exact design of a submillimeter instrument can be adapted to the needs of the mission in terms of complementarity to other instruments in the payload. While the vertical resolution of the submillimeter observations will always be a little better than a scale height in Venus' atmosphere, the horizontal resolution can

range from a few kilometers to a few 100 km. Based on the current technology, submillimeter bands between approximately 300 and 1200 GHz are feasible. The mass of the instrument is expected to range between 10 and 20 kg, and the power consumption between 30 and 60 W.

#### **4.3.1.4 Orbiter Radio Science Subsystem (Ultra-Stable Oscillator)**

Precise tracking of the orbiter's location is enabled by the addition of an ultra-stable oscillator (USO) to its telecom subsystem. This enables measurement of the Venus gravity field. It also uses occultation measurements to determine atmospheric density profiles. Table 4.6 provides the requirements for the gravity field measurements. Table 4.7 shows the requirements for occultation measurements. USOs are readily available, and the techniques for these kinds of measurements are fully mature; therefore, no technology development is required.

**Table 4.6:** Gravity Field Measurement Requirements.

Requirements on Telecom System	Dual X and Ka-Band; Two way tracking
Requirements on orbit determination and Knowledge	Orbit reconstruction to 1 meter (vertical) and 10 m (horizontal) accuracy.
Spatial Resolution	Spatial resolution < 300 km necessary (at least to spherical harmonic degree 120)
Coverage	Global

**Table 4.7:** Atmospheric Occultation Measurement Requirements.

Vertical resolution (this is determined by sampling interval, based on S/N)	100 m desired
Frequency of measurement	Every occultation pass whether to Earth or to another orbiter around Venus
Range of measurement	Top of atmosphere to surface (minimum attenuation altitude)
Sensitivity	Stability of USO needs to be < 1 part in $10^{15}$
Accuracy	$\pm 0.5$ K in temperature

With the addition of a USO, the radio subsystem will be useful for occultation measurements yielding high vertical resolution profiles of the density and temperature of the atmosphere in the range of 35 km to 90 km and of the ionospheric electron density above 100 km. In addition, bi-static radar measurements can be carried out, with the spacecraft acting as a transmitter and a ground station on the Earth acting as the receiver. These measurements will give dielectric properties and roughness of the surface, and might be complementary to the data from the InSAR. Data on the gravity field and gravity field anomalies of Venus can be derived from accurate tracking of the orbit. A fundamental goal of any future mission to Venus is to expand the understanding of the relation between the surface geology and interior processes. As discussed in Chapter 2, data collected from the tracking of the Pioneer Venus and Magellan spacecraft provide a useful data set to understand general planetary structure and major interior processes

(Konopliv et al. [1999]). Because the resolution of these data varies across the planet, improving on this gravity field data set is of high priority with the goal of achieving uniform coverage for the high-degree and order spherical harmonics (see Figure 4.3). Gravity data will be obtained through Doppler tracking of the orbiter at either X- or Ka-Band. Ka-Band tracking is desirable because it reduces the effects of solar plasma noise on the tracking data. Knowledge of the spacecraft orbit to 5-m accuracy is required to achieve a gravity field measurement of approximately spherical harmonic degree 130 to 150, which corresponds to a spatial resolution of 250- to 300-km. The resulting gravity model will also be useful for geophysical modeling. Ideally, the orbiter will be in a circular orbit to ensure high-resolution Doppler tracking at all latitudes. The most important parameter of the USO is its phase noise, which shall be  $<2 \times 10^{-13}$  over 10 s to achieve the above-mentioned objectives.

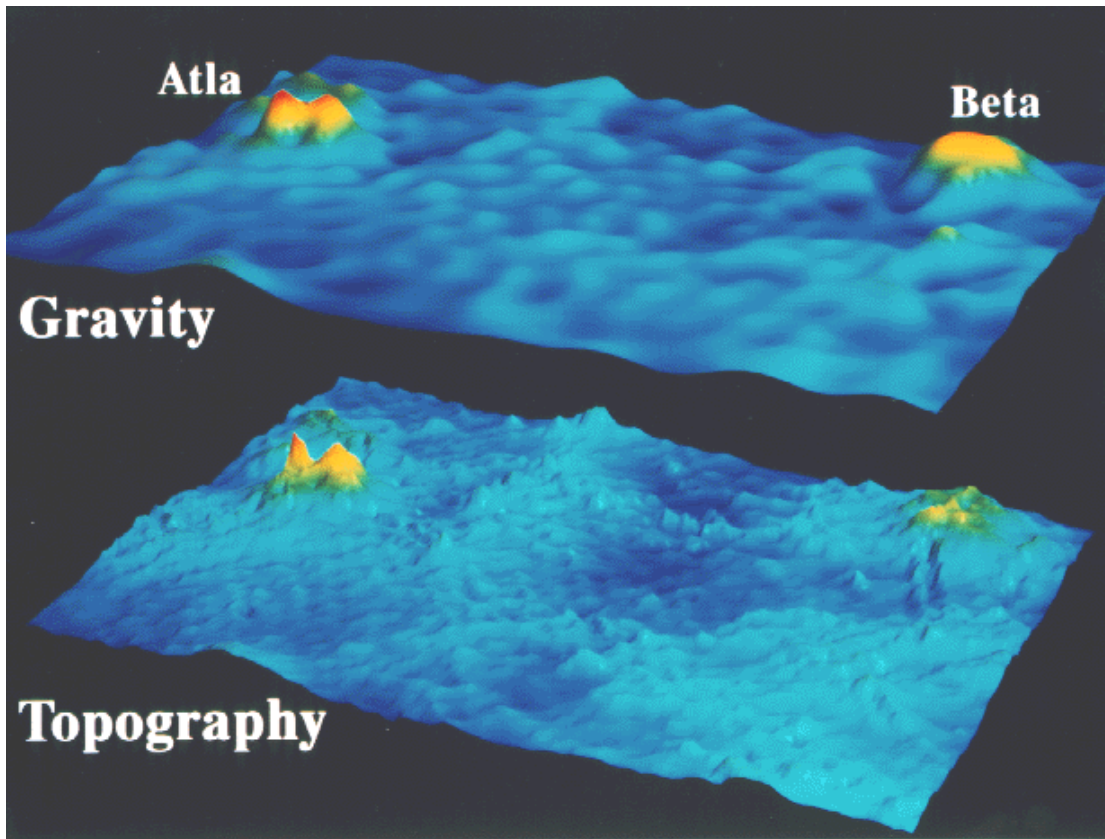


Figure 4.3: Gravity data from Magellan (JPL, 2009).

Occultation measurements can only be performed when the geometry of the orbital plane and the position of Earth and Venus are such that occultations of the radio signal do occur. This takes place in seasons; for a polar orbit, typically two to three such seasons occur in one Earth year. One season allows measurements to be taken at all latitudes, but only for a limited range of local solar times. Data from many seasons need to be considered for a good coverage in local solar time. Normally, the occultations take place close to the planet. Measurements can be taken during the occultation ingress, egress, or both, where one is covering the northern hemisphere and the other is covering the southern hemisphere. Typically, measurements can be taken at intervals of two days to allow operation by other instruments in the intermediate orbits. The duration of an occultation season is typically two months. The best performance is achieved when the Earth-Venus distance is small.

Bi-static measurements can be done at any time; however, best performance is achieved when the distance S/C-Venus and the distance Venus-Earth is at its minimum. Due to the slow rotation of Venus, opportunities for observing specific features on the planet at good observing conditions are sparse and

should be given priority when they occur (see Figure 4.4). Gravity field measurements can be done close to pericenter only, but at any time of the year independently of any seasons. Again, the slow rotation rate of the planet limits the opportunities for observing specific features on the planet.

All radio science activities require the spacecraft antenna to point in specific directions. Simultaneous observations by other instruments is facilitated by gimbaling the 4-m-diameter main antenna on the spacecraft.

#### 4.3.1.5 Orbiter Magnetometer

The magnetometer determines the magnetic field of Venus and requires an accuracy of a few nano-Tesla. Numerous high-precision magnetometers have been flown that can provide the required resolution (Fimmel et al., 1983). The magnetometer will have to be boom mounted to avoid any magnetic fields generated by other orbiter systems.

#### 4.3.1.6 Orbiter Langmuir Probe

The Langmuir Probe determines the electron temperature, density, and potential around the orbiter. There are several heritage versions of Langmuir Probes (Fimmel et al., 1983); therefore, no technology development should be required.

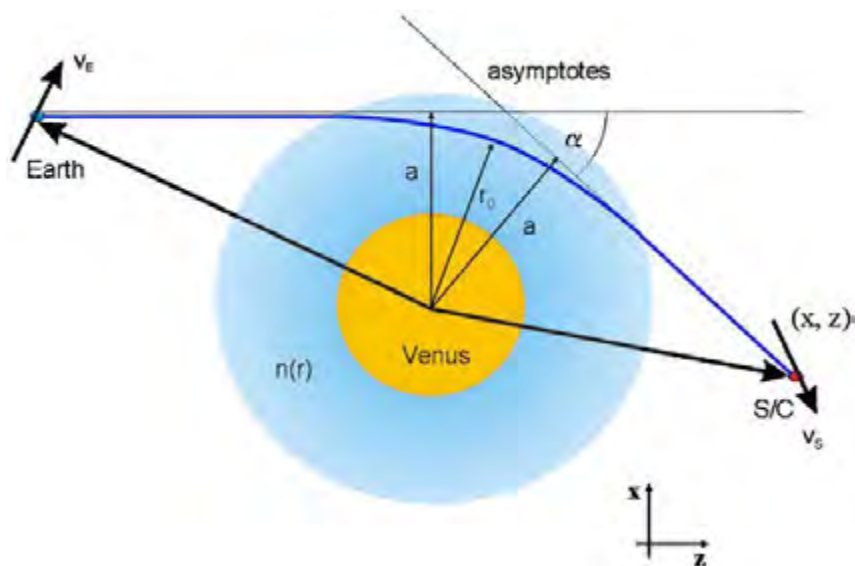


**Figure 4.4:** Ray bending in the Venus atmosphere. Ray path closest approach distance to and deflection angle are related to the impact parameters  $a$  (asymptote closest approach distance) and index of refraction  $n(r)$ . The  $(x,z)$  coordinate system is a planetocentric coordinate system (Hausler et al., 2006).

#### 4.3.1.7 Orbiter Neutral and Ion Mass Spectrometer (NIMS)

The Neutral and Ion Mass Spectrometer (NIMS) will characterize the neutral and ionized elements in the upper atmosphere and will determine the effect of the solar wind on the upper atmosphere. The measurement requirements for the NIMS are listed in Table 4.8. There are several heritage versions of NIMS (e.g., Cassini INMS, Waite et al, 2004); therefore, no technology development should

be required.

#### 4.3.2 Balloon Instruments

Table 4.9 provides a summary of the balloon instruments, along with their mass, power, heritage, and source of the performance metrics. Figure 4.5 illustrates the balloon gondola and payload. The balloon data collection strategy and data volume estimate are discussed in Subsection 4.3.4.2.

**Table 4.8:** NIMS Measurement Requirements.

Resolution	0.1 AMU
Accuracy	O,C,N,H,He absolute fluxes to $\pm 15\%$ . Relative fluxes to $\pm 2.5\%$
Constraints	For as much of a solar cycle (11 years) as possible

**Table 4.9:** Balloon Instruments.

Instrument	Mass (kg)	Power (W)	Source or Proxy
Gas Chromatograph Mass Spectrometer	11	40	Huygens, VCAM
Thermocouple, Anemometer, Pressure Transducer, Accelerometer	2	3.2	MVACS, ATMIS
Radio Tracking	0	0	-
Net Flux Radiometer	2.3	4.6	Galileo Probe
Magnetometer	1	2	JPL internal studies
Nephelometer	0.5	1.2	Pioneer Venus
Lighting Detector	0.5	0.5	FAST
TOTAL	17.3	51.5	

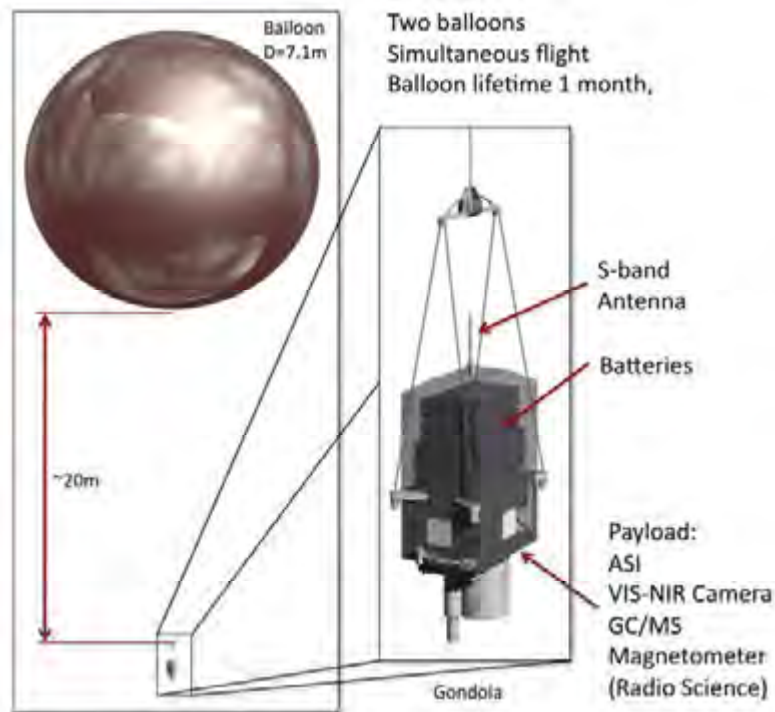


**Figure 4.5:** Balloon instruments.

**Table 4.10:** Balloon GCMS Measurement Requirements.

Resolution	0.1 AMU
Number of spectra per mission	He = 15, other noble gases = 75, CO = 75, sulfur compounds = 200 including two 3 hour campaigns with a spectrum acquired every 20 minutes
Range of measurement	1 - 150 AMU
Sensitivity	0.1 ppb Xe, Kr
Accuracy	Abundance and isotope ratios of He, Ne, Ar, Kr, Xe to $\pm 5\%$ . Abundance and isotope ratios of H, O, N, S, C to $\pm 10\%$ . N <sub>2</sub> , H <sub>2</sub> S, OCS, HF, O <sub>2</sub> and other gases to $\pm 10\%$ . Volcanogenic gases H <sub>2</sub> O, SO <sub>2</sub> , HCl, CO to $\pm 1\%$

#### 4.3.2.1 Balloon Gas Chromatograph Mass Spectrometer (GCMS)

The GCMS is used during the balloon mission to measure the atmospheric composition along the horizontal wind-driven balloon path. This instrument is essential for measuring the concentrations of the noble gases and their isotope ratios. In addition, the GCMS will provide ground truth for trace gas compositions that also can be obtained from orbital remote sensing instruments (for example, by the submillimeter sounder). Table 4.10 provides the key measurement characteristics of the GCMS. The instrument metrics are predictions on what will be achievable in the 2021 time frame given past performance and ongoing improvements in GCMS technology. Some technology development for the gas inlets might be required to deal with the sulfuric acid aerosols in the clouds.

#### 4.3.2.2 Balloon Meteorology or ASI (Temperature Sensor, Anemometer, Pressure Transducer, Accelerometer)

The Meteorology or Atmospheric Science Instrument (ASI) instruments will characterize the gross atmospheric properties, including temperature, pressure, and wind speeds and direction (using both an anemometer and accelerometer to provide complimentary measurements). Table 4.11 provides the measurement requirements for these instruments. These instruments will require mounting on a 1-m mast or arm to avoid local

effects from the gondola. All of these instruments have substantial flight heritage; therefore, no technology development is anticipated.

ASI consists of sensors designed to characterize the atmospheric structure, including the basic state variables of density, pressure, temperature and wind. ASI measurements characterize the atmosphere and, in doing so, constrain the atmospheric radiative balance (from temperature), dynamics, including waves (e.g., gravity) and turbulence (e.g., convection), and regions in which volatiles (e.g., clouds) impact the lapse rate via heating/cooling.

#### 4.3.2.3 Balloon Net Flux Radiometer

To understand the climate balance of Venus, it is crucial to simultaneously measure upwelling and downwelling radiation to high accuracy across a broad range of visible and infrared wavelengths over as wide a range of solar angles as possible. For these measurements, the DRM payload includes net flux radiometers in the balloon payload.

This instrument will measure upwelling and downwelling radiation from 0.2- to 25- $\mu\text{m}$  wavelengths, with a signal-to-noise ratio of greater than 200 from 0.2 to 3  $\mu\text{m}$  and greater than 100 from 3 to 25  $\mu\text{m}$ . The corresponding accuracy is within less than 5% from 0.2 to 3  $\mu\text{m}$  and less than 10% from 3 to 25  $\mu\text{m}$ . The instrument will require eleven look angles, from nadir to zenith. The instrument data rate is estimated to be 256 bits/sec.

**Table 4.11:** Balloon Meteorology Measurement Requirements.

Temperature Sensor	
Resolution	0.1 K
Frequency of measurement	5 minute cycles where 1 measurement taken every 10 s. Acquire 100 hours worth of observations in 5 minute blocks over the course of the mission.
Range of measurement	180 K – 350 K
Sensitivity	0.1 K
Accuracy	$\pm 0.5$ K
Constraints	Operates in H <sub>2</sub> SO <sub>4</sub> /H <sub>2</sub> O aerosol environment (pH = -2)
Pressure Sensor	
Resolution	0.1 mbar
Frequency of measurement	5 minute cycles where 1 measurement taken every 10 s. Acquire 100 hours worth of observations in 5 minute blocks over the course of the mission.
Range of measurement	250 – 2500 mbar
Sensitivity	0.1 mbar
Accuracy	1 mbar
Constraints	Operates in H <sub>2</sub> SO <sub>4</sub> /H <sub>2</sub> O aerosol environment (pH = -2)
Anemometer / Accelerometer on Balloon	
Frequency of measurement	5 minute cycles where 1 measurement taken every 10 s. Acquire 100 hours worth of observations in 5 minute blocks over the course of the mission.
Range of measurement	1 – 100 m/sec
Accuracy	$\pm 10$ cm/s between v = 1 – 10 m/sec; $\pm 100$ cm/s between v = 10 – 100 m/sec Wind direction $\pm 20^\circ$
Constraints	Operates in H <sub>2</sub> SO <sub>4</sub> /H <sub>2</sub> O aerosol environment

During the balloon mission, measurements will be made at least once every 30 minutes. This instrument will contribute important data toward the ultimate goals of measuring the deposition of solar energy globally and determining radiative balance, including cloud and greenhouse-gas opacities over wavelength and solar deposition and thermal emission as a function of latitude and longitude. With several circumnavigations and, therefore, high precision measurements over several diurnal cycles, we will be able to use models to fill in a much more comprehensive view of the complete radiative balance of the atmosphere.

Therefore, the balloon Net Flux Radiometer will characterize the radiative profile during its 30-day operating lifetime, circumnavigating the planet several times. Table 4.12 provides the measurement requirements for the Net Flux Radiometer. There is some heritage in Net Flux Radiometer design, which is considered in the DRM. However, new designs are being developed and proposed that would provide more look angles than achieved with previously flown instruments; these new designs could be considered if required by science. The current technology readiness of these new designs is TRL 4/5.

**Table 4.12:** Balloon Net Flux Radiometer Measurement Requirements.

Resolution	11 look angles from nadir to zenith
Frequency of measurement	Every 30 minutes
Range of measurement	Two channels, 0.2 to 3 $\mu$ m and 0.8 to 25 $\mu$ m
Sensitivity	SN >200 from 0.2 to 3 $\mu$ m, SN >100 for 8 to 25 $\mu$ m
Accuracy	<5% from 0.2 to 3 $\mu$ m, <10% for 8 to 25 $\mu$ m
Constraints	Operates in H <sub>2</sub> SO <sub>4</sub> /H <sub>2</sub> O aerosol environment

**Table 4.13:** Balloon Radio Tracking Measurement Requirements.

Resolution	0.01 m/s
Frequency of measurement	Every hour on the visible side, on average every 3 hr on backside via the orbiter.
Accuracy	<0.1 m/s in velocity and 200 - 500 m in position

#### 4.3.2.4 Balloon Radio Subsystem (Ultra-Stable Oscillator)

Precise tracking of the balloon trajectories is enabled by use of a two-way Doppler system, sufficiently stable oscillator (SSO), and Very Long Baseline Interferometer (VLBI) measurements. This will allow determination of the wind speed and direction affecting the position of the balloons. Measurement requirements are listed in Table 4.13. No technology development will be required, as USOs are readily available with the required precision.

#### 4.3.2.5 Balloon Magnetometer

The balloon magnetometer determines Venus' magnetic field and requires accuracy to a few nano-Tesla. While numerous high-precision magnetometers have been flown that can provide the high resolution required, the mass constraints on the gondola will likely require some modification. For example, lightweight designs have been flown as part of the Free Flying Magnetometer program, which provides a technology readiness of TRL 6. The magnetometer will be boom mounted to avoid magnetic fields generated by other balloon systems.

#### 4.3.2.6 Balloon Nephelometer

The balloon nephelometer will characterize the aerosol and cloud particulate properties of the atmosphere and some limited composition. Table 4.14 provides the measurement requirements for the nephelometer. There is some heritage in nephelometer design,

although new designs are being developed and proposed that would provide higher accuracy and, possibly, eliminate the need for an external mirror assembly. The technology readiness of the new designs is TRL 4/5.

#### 4.3.2.7 Balloon Lightning Detector

There are several potential approaches to a lightning detector, including broadband radio receivers and simple microphones designed to pick up either the electromagnetic or acoustic effects of lightning. Mass and power constraints will likely drive the selection of a specific approach for the balloon and determine the instrument sensitivity. There are numerous high-heritage solutions; therefore, no significant technology development is anticipated.

### 4.3.3 Lander Instruments

Table 4.15 provides a summary of the lander instruments, along with their mass, power, heritage (if any), and source of the data. Figure 4.6 shows an artist's concept of the lander on the surface of Venus.



Figure 4.6: Artist's concept of lander on the surface.

**Table 4.14:** Balloon Nephelometer Measurement Requirements.

Frequency of measurement	Every 15 minutes
Range of measurement	Particle size range 0.1 to 50 $\mu\text{m}$
Sensitivity	Polarizing nephelometer can do composition
Accuracy	Size and number densities to $\pm 10\%$ . Aerosol constituents to $\pm 15\%$ .
Constraints	Operates in $\text{H}_2\text{SO}_4/\text{H}_2\text{O}$ aerosol environment

**Table 4.15: Lander Instruments.**

Instrument	Mass (kg)	Power (W)	Source or Proxy
Gas Chromatograph Mass Spectrometer	11	40	Next-gen Huygens, JPL VCAM
X-ray Diffraction and Fluorescence	12	50	MSL CheMin
Microscopic Imager	0.3	6.8	MER MI
ASI: Thermocouple, Anemometer, Pressure Transducer, Accelerometer	2	3.2	MVACS, ATMIS
Lander Spectroscopic Imaging System (Descent Camera)	0.5	1	MER engineering cameras
Panoramic camera	0.5	1	MER engineering cameras
Drill camera	0.5	1	MER engineering cameras
Intrinsic Gamma Rays	1.5	4.1	MSL (mass / power)
Magnetometer	10	2	Messenger (mass / power)
Nephelometer	0.5	1.2	Pioneer-Venus
Net Flux Radiometer	2.3	4.6	Galileo Probe
Surface Corner Reflector	5	0	None
Heat Flux Plate	0.5	1	JPL/SwRI internal study
Drill and Sample Handling System	35	120	MSL drill analog
<b>TOTAL</b>	<b>81.6</b>	<b>201</b>	

Figures 4.7, 4.8, 4.12, 4.15, 4.17, and 4.18 show the location of various lander instruments and the drill system. The lander instrument data collection strategy and data volume estimates are discussed in Subsection 4.3.4.1.

It can be seen that most of the instruments are located inside the protective pressure vessel and either make observations through

windows (e.g., the imaging cameras) or on samples brought inside (e.g., XRD/XRF, GCMS). The interior of the pressure vessel is kept at Earth-like pressure and temperature conditions, a circumstance that enables the use of instruments originally designed for the much less harsh environments of Earth and Mars and greatly reducing the technology development requirements.

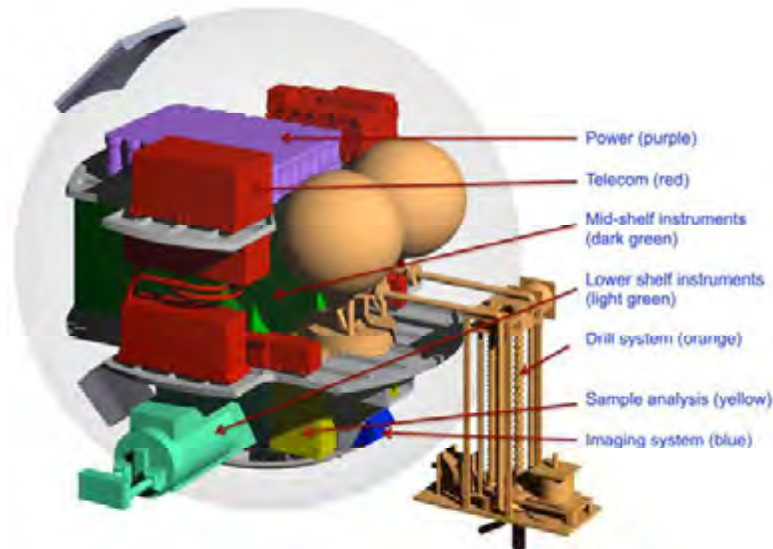


Figure 4.7: Lander instruments and drill system overview.

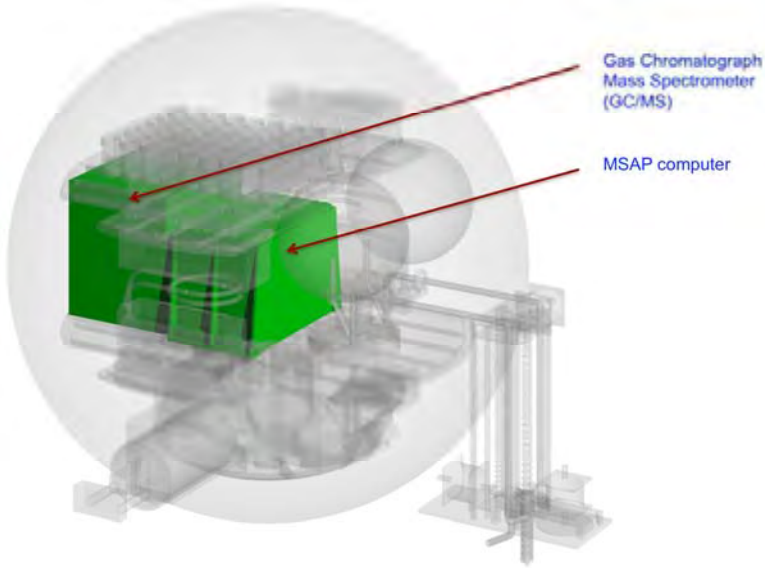


Figure 4.8: Selected lander instruments (GCMS).

#### 4.3.3.1 Lander Gas Chromatograph Mass Spectrometer (GCMS)

This GCMS (see Figure 4.8) is used during the lander's descent to measure the atmospheric composition along the vertical descent path to the surface. While on the surface it will also accept pyrolyzed samples from the drill system. Table 4.16 provides the key measurement characteristics of the GCMS during descent. Table 4.17 shows the key measurement characteristics of the GCMS

after landing. The instrument metrics shown are predictions of what will be achievable by the time the DRM is launched in 2021. Note that this instrument will be housed inside a pressure vessel and therefore protected from the Venusian environment during its operational lifetime. Also, the study team adopted the simplifying assumption that the same GCMS instrument could be used for both the lander and the balloon, hence the commonality of performance metrics.

**Table 4.16:** Descent GCMS Measurement Requirements.

Resolution	0.1 AMU
Frequency of measurement	Approximately every 5 km during descent
Range of measurement	1 - 150 AMU
Sensitivity	0.1 ppb Xe, Kr
Accuracy	Abundance and isotope ratios of He, Ne, Ar, Kr, Xe to $\pm 5\%$ . Abundance and isotope ratios of H, O, N, S, C to $\pm 10\%$ . N <sub>2</sub> , H <sub>2</sub> S, OCS, HF, O <sub>2</sub> and other gases to $\pm 10\%$ . Volcanogenic gases H <sub>2</sub> O, SO <sub>2</sub> , HCl, CO to $\pm 1\%$

**Table 4.17:** Landed GCMS Measurement Requirements.

Resolution	0.1 AMU
Frequency of measurement	Atmospheric sample every 15 minutes, plus two pyrolyzed surface samples.
Range of measurement	1 - 150 AMU
Sensitivity	Pyrolyze surface samples and quantify products to $\pm 10\%$
Accuracy	Abundance and isotope ratios of He, Ne, Ar, Kr, Xe to $\pm 5\%$ . Abundance and isotope ratios of H, O, N, S, C to $\pm 10\%$ . N <sub>2</sub> , H <sub>2</sub> S, OCS, HF, O <sub>2</sub> and other gases to $\pm 10\%$ . Volcanogenic gases H <sub>2</sub> O, SO <sub>2</sub> , HCl, CO to $\pm 1\%$



**Figure 4.9:** CheMin III prototype. Left: 3-D model showing internal components of the CCD camera (left to right: muffin fan, radiator, evacuated chamber holding Thermo-Electric Cooler [TEC], CCD, sample chamber and X-ray tube). Center: Prototype with 114-mm Debye-Scherrer camera for scale. Right: Sample holder with piezoelectric vibration system (Sarrazin et al., 2005).

#### 4.3.3.2 Lander X-Ray Diffraction and X-Ray Fluorescence (XRD/XRF)

In the DRM payload, science goals related to the mineralogy of the Venus surface are addressed primarily through X-ray diffraction (XRD), which is implemented in a combined XRD/X-ray fluorescence system. A system like this, the CheMin instrument (Vaniman et al., 1998), is on the manifest of the MSL Mars rover, has been implemented for terrestrial use, and has been proposed for lunar landed missions (Figure 4.9). The XRF portion of the CheMin-type design was descoped early from its MSL implementation, so it is not accounted for in the MSL design and is not reflected in Figure 4.9.

##### 4.3.3.2.1 X-ray Diffraction

X-ray diffraction is the standard reference method for identifying minerals and quantifying mineral proportions in mixtures and can provide important constraints on the chemical compositions of the minerals. The objective of XRD analysis in the DRM is to determine the minerals present at the surface: specifically, the chemical compounds in which the surface elements are held. Identification of the minerals (with chemical composition obtained via other instruments) is crucial for understanding the nature of the materials at the Venus surface, its thermal and chemical histories, and the extent and nature of surface-atmosphere interactions.

X-ray diffraction (as baselined here) operates by directing a collimated beam of monochromatic X-rays at a multigranular sample. Some of the incident X-rays are diffracted by the sample; that is, scattered at distinct angles from the incident beam, with the angles determined by the repeat distances between atoms (or planes of atoms) in the crystalline mineral (e.g., Suryanarayana and Norton, 1998). In the baseline instrument, based on CheMin (Vaniman et al., 1998), diffracted X-rays are seen in transmission geometry and detected by a cooled CCD camera/detector (Figure 4.10).

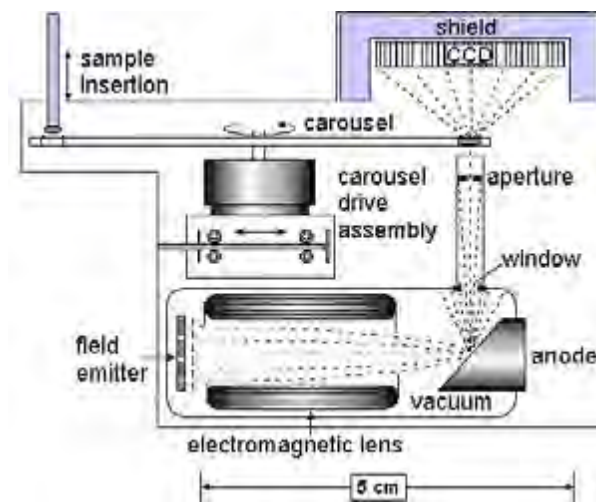


**Figure 4.10:** Schematic of the flight CHEMIN instrument (NASA-CheMin, 2009).

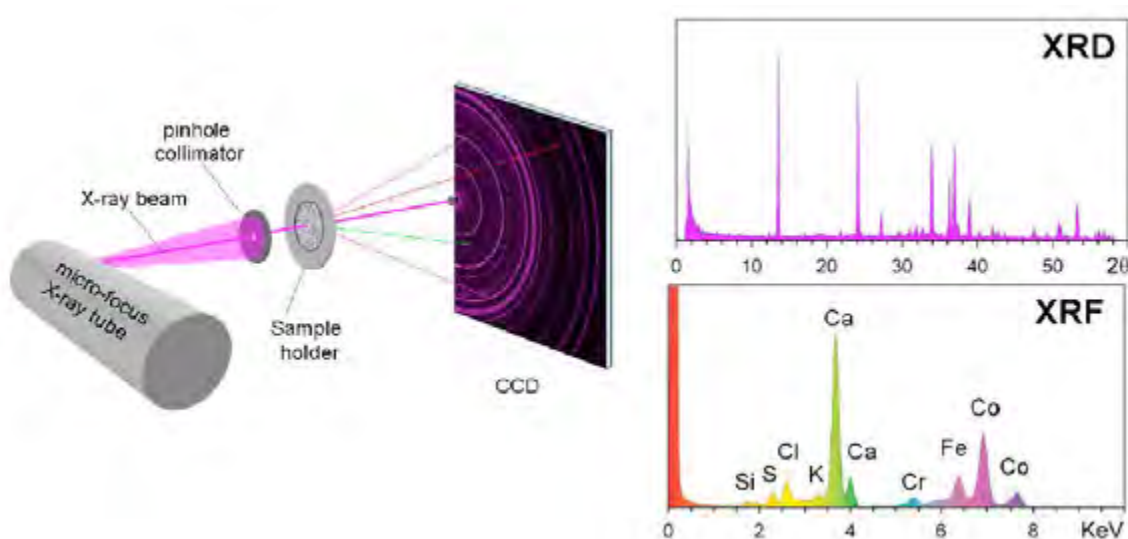


**Figure 4.11:** Geometry of the original CheMin XRD/XRF instrument. (a) (left) overall geometry of CheMin; (b) (above right) XRD  $2\theta$  plot obtained by summing diffracted photons from the characteristic line of the X-ray source [colored magenta in Figure 4.11(a)]; (c) (below right) X-ray fluorescence spectrum obtained by summing all of the X-ray photons detected by the CCD [XRF photons from the sample shown schematically in green and red] (Sarrazin et al., 2005).

Because the grains in the sample are at random orientations (forced in the CheMin design by controlled vibrations), the diffracted X-rays describe circles around the center of the transmitted beam, with each circle at the characteristic diffraction angle for the given mineral and planes of atoms (Figure 4.11).

As implemented in CheMin, the X-ray camera/detector collects many successive images of short exposure times, so that few camera pixels are hit by more than one X-ray during an exposure frame. The multiple frames can be uplinked as collected or processed on board to sort out X-rays of other energies that arise either from the source or from X-ray fluorescence of the sample.

Based on the CheMin implementation, these XRD analyses require that a few 10 of milligrams of powdered sample be delivered into the instrument, inside the pressure vessel. The grain in the sample would ideally be between  $\sim 50$  and  $\sim 100$   $\mu\text{m}$  in longest dimension. In turn, this requires a sample drill, or scoop and grinding system, a sieve system, and a sample delivery system. The X-ray tube requires high-voltage ( $\sim 10$  kV), which is maintained by the instrument and contained within it. The CCD detector must be cooled,

which requires power and a heat-rejection capability.

In operation, XRD analysis is simultaneous with XRF analysis (see below) and must follow sample acquisition. Thus, XRD analysis must follow these operations: landing, documentary imagery of sampling site, deployment of the sampling device, acquisition of a sample (e.g., drilling or scoop), sieving of sample, and delivery of the sample to the analysis cell. While an XRD/XRF analysis is in progress, other operations are not impeded (assuming available power), including acquisition and preparation of another sample. Following an analysis, another cell would be moved to the analytical position and another sample could be transferred for XRD/XRF analysis.

Mission planning data for the XRD (and XRF) system are based on the CheMin instrument on MSL (NASA-CheMin, 2009), with total data volume for two full analyses of 125 Mbit. As implemented on MSL, each high-precision XRD pattern would take  $\sim 10$  hours; note, however, that this duration can be reduced with a brighter X-ray source. For example, the configuration used in the DRM

assumed an approximately 2-hours measurement for each of the two samples.

If the DRM had time in excess of the nominal five hours and sufficient power and cooling, XRD/XRF analyses could be repeated. The limiting instrument resource would be sample analysis cells. In the CheMin design, cells are arranged in pairs so that a single pair would suffice for the nominal DRM. Additional analyses would require more than a single pair of cells.

Determination of the mineralogy of the surface and near-surface materials is traceable to many of the VEXAG Goals and Objectives (VEXAG, 2007), as detailed in Chapter 2 of this report. The highest-level VEXAG (2007) goals that specifically call out the determination of Venus mineralogy include: Goal 1, Objective 2 (Map the mineralogy and surface composition on a planetary scale), Investigations 1, 2, and 3; Goal 1, Objective 3 (Characterize the history of volatiles in the interior, surface, and atmosphere), Investigation 4; Goal 2, Objective 2 (Investigate the resurfacing history and the role of tectonism, volcanism, impacts, erosion, and weathering), Investigation 3; and Goal 3, Objective 1 (Search for fossil evidence of past climate change in the surface and atmospheric composition), Investigations 1 and 2.

#### 4.3.3.2.2 X-ray Fluorescence

In the DRM payload, science goals related to the chemical composition of the Venus surface are addressed primarily through X-ray fluorescence (XRF) analysis, which is implemented in a combined XRF/XRD system. A system like this, the CheMin instrument, was originally on the manifest of the MSL Mars rover (but was descoped), has been implemented for terrestrial use and has been proposed for lunar landed missions.

X-ray fluorescence is a standard analytical method used extensively on Earth and in planetary probes to the Moon and Mars. The Viking landers had XRF analyzers (Clark et al., 1977), and XRF is a portion of the APXS analyses (the ‘X’ part) in the Lunar Surveyor, the Mars Pathfinder, MER, and the MSL lander spacecraft (Wänke et al., 2001; Gellert

et al., 2004) payloads. X-ray fluorescence analysis starts with a beam of X-rays impinging on the target sample (Beckhoff et al., 2006). Some of those incident X-rays will eject inner shell electrons from atoms of the target; outer shell electrons will drop to those inner shells and release X-rays characteristic of the element and the electron transition. Most of the fluoresced X-rays would be K-shell emissions (K-shell is the lowest energy state of an atom), corresponding to electrons dropping from P to S shells. The number of fluoresced X-rays for a given element is directly proportional to the concentration of those atoms in the sample, with corrections for efficiency of electron ejection, efficiency of K-shell emission compared to other de-excitation modes, and absorption of X-rays by the sample, any needed windows, and the X-ray detector. Together, these effects mean that XRF precision is proportional to element abundance (i.e., it is most useful for major and minor elements and less useful for trace elements) and that XRF precision is lower for elements of low atomic number (softer X-rays) and increases with atomic number (limited eventually by the energy of the incident X-rays). In the original CheMin implementation (Vaniman et al. 1998), fluoresced X-rays are detected by a dedicated PIN diode in reflection geometry and by the CCD sensor for diffracted X-rays (transmission geometry) (Figure 4.11).

Based on the original planned CheMin implementation, these XRF analyses require that a few 10 of milligrams of powdered sample be delivered into the instrument, inside the pressure vessel. The grain in the sample would ideally be between ~50 and ~100  $\mu\text{m}$  in longest dimension. In turn, this requires a sample drill or scoop and grinding system, a sieve system, and a sample delivery system. The X-ray tube requires high-voltage (~10 kV), which is maintained by the instrument and contained within it. The CCD detector must be cooled, which requires power and a heat-rejection capability.

In operation, XRF analysis would be simultaneous with XRD analysis (see above) and must follow sample acquisition. Thus,

XRD analysis must follow these operations: landing, documentary imagery of sampling site, deployment of the sampling device, acquisition of a sample (e.g., drilling or scoop), sieving of sample, and delivery of the sample to the analysis cell. While an XRF/XRD analysis is in progress, other operations are not impeded (assuming available power), including acquisition and preparation of another sample. Following an analysis, another cell would be moved to the analytical position and another sample could be transferred for XRF/XRD analysis.

Mission planning data for the XRF (and XRD) system are based on the CheMin instrument. As implemented on MSL, each high-precision XRF analysis would take ~10 hours; note, however that this duration could be reduced with a brighter X-ray source. Consequently, in the current DRM design the XRF measurement is assumed to take about 2 hours of analysis for each of the two samples.

If the DRM lifetime on the surface could be extended beyond the baselined five hours by providing sufficient power and cooling, XRF/XRD analyses could be repeated. The limiting instrument resource would be sample analysis cells. In the CheMin design, cells are arranged in pairs so that a single pair would suffice for the nominal DRM. Additional analyses would require more than a single pair of cells.

Determination of the chemical compositions of surface and near-surface materials is traceable to many of the VEXAG Goals and Objectives (VEXAG 2007), as detailed in Chapter 2 of this report. The highest-level VEXAG (2007) goals that specifically call out chemical composition include: Goal 1, Objective 2 (Map the mineralogy and surface composition on a planetary scale), Investigation 1; Goal 2, Objective 2 (Investigate the resurfacing history and the

role of tectonism, volcanism, impacts, erosion, and weathering), Investigation 3; Goal 2, Objective 3 (Determine the chronology of volcanic activity and outgassing), Investigation 4; and Goal 2, Objective 4 (Determine the chronology of tectonic activity), Investigation 6.

The X-ray Diffraction and Fluorescence (XRD/XRF) instrument provides identification and quantification of minerals in geologic materials (e.g., basalts, evaporites, soils). Table 4.18 provides the key measurement requirements for the XRD/XRF. Current XRD/XRF designs, such as that used for the Mars Science Lander (MSL) CheMin (Chemistry and Mineralogy) instrument might, if successful, be adequate for this DRM instrument (see Figure 4.12), eliminating the need for further technology development. Alternative designs are currently at a technology readiness of TRL 4.

#### **4.3.3.3 Lander Microscopic Imager**

The microscopic imager sits in front of the XRD/XRF and provides visual imagery of the samples brought in for analysis. The MER microscopic imager provides adequate resolution and served as the basis for the lander imager (see Figure 4.12).

#### **4.3.3.4 Lander Atmospheric Science Instrument (ASI)**

ASI consists of sensors designed to characterize the gross atmospheric properties and structure, including the basic state variables of density, pressure, temperature, and wind speed and direction (using both an anemometer and an accelerometer to provide complimentary measurements). Sensors include atmospheric temperature sensors (e.g., thermocouples) and pressure sensors (e.g., piezoelectric or diaphragm sensors), and an anemometer.

**Table 4.18: XRD/XRF Measurement Requirements.**

Duration	~120 minutes per sample.
Fluorescence	Per sample, ~100 X-ray energy spectra (~1,024 ch x 8 bit)
Diffraction	Per sample, ~100 X-ray diffractograms (3,000 x 3,000 x 8 bit)

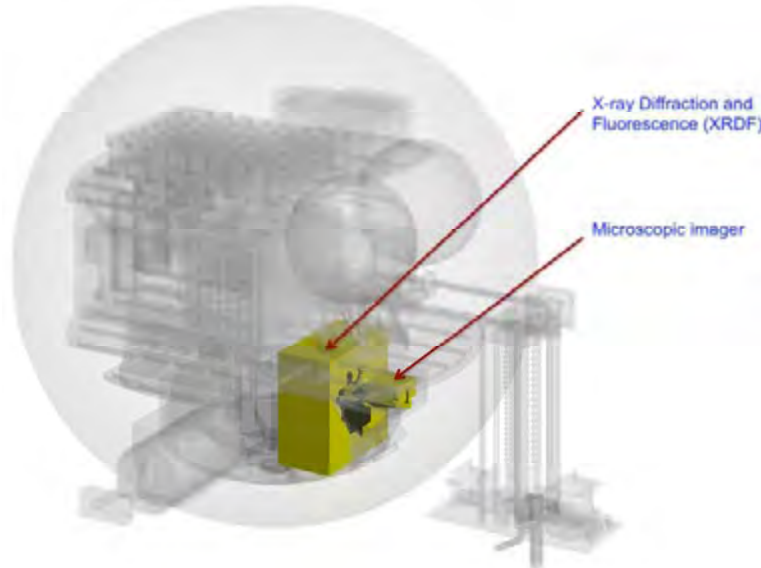


Figure 4.12: Selected lander instruments (XRD/XRF and microscopic imager).

The approximate observing plan is to measure the temperature, pressure, and wind every 0.1 seconds during descent and every 10 seconds for the duration of the 5-hour landed mission.

Table 4.19 provides the measurement

requirements for these instruments. These instruments will require mounting on a 1-m mast or arm to avoid local effects from the lander. All of these instruments have substantial flight heritage; therefore, no technology development is anticipated.

**Table 4.19: Lander Meteorology Measurement Requirements.**

Temperature Sensor	
Resolution	0.1 K
Frequency of measurement	Every 0.1 s during descent, every 10 s after landing
Range of measurement	150 K – 760 K
Sensitivity	0.1 K
Accuracy	$\pm 0.5$ K
Constraints	Operates in $H_2SO_4/H_2O$ aerosol environment
Pressure Sensor	
Resolution	0.01 mbar (at 100 mbar); 1 mbar (at 95 bar)
Frequency of measurement	Every 0.1 s during descent, every 10 s after landing
Range of measurement	0 mb to 95 bar
Accuracy	0.1 mbar (at 100 mbar); 25 mbar (at 95 bar)
Constraints	Operates in $H_2SO_4/H_2O$ aerosol environment
Anemometer / Accelerometer	
Frequency of measurement	Every 0.1 s during descent, every 10 s after landing
Range of measurement	1 – 100 m/s during descent, 0.1 – 10 m/sec landed
Accuracy	$\pm 10$ cm/s. Wind direction $\pm 20^\circ$ .
Constraints	Operates in $H_2SO_4/H_2O$ aerosol environment

#### 4.3.3.5 Lander Cameras (Descent, Panoramic, and Drill Context)

The Venus DRM science measurement requirements dictate the inclusion of three different cameras in the landers. The applicable measurement requirements are

listed in Table 4.20. The Venus environment and the lander pressure vessel design place engineering constraints on the design of the lander cameras; these are summarized in Table 4.21.

**Table 4.20:** Lander Camera Measurement Requirements

Descent camera
Pixel footprint of $\leq 1$ m from 1 km altitude.
Field of view $>25^\circ$ ( $>36^\circ$ preferred).
Nadir viewing.
Spectral band centered at $1.01 \pm 0.005 \mu\text{m}$ ; bandpass $0.04 \mu\text{m}$ .
Additional discrete bandpass filters along edge of detector array (<5% of array width) at wavelengths of $0.55 \mu\text{m}$ (0.09- $\mu\text{m}$ bandpass), $0.66 \mu\text{m}$ (0.06- $\mu\text{m}$ bandpass), $0.77 \mu\text{m}$ (0.03- $\mu\text{m}$ bandpass), and $0.87 \mu\text{m}$ (0.04- $\mu\text{m}$ bandpass) for unresolved band spectrometry (spatial resolution can be degraded by up to 20x from that in $1.01\text{-}\mu\text{m}$ band). Also include a linearly variable spectral filter spanning the range between $0.5$ and $1.1 \mu\text{m}$ along the edge of the detector array. Response rates in these bands (and for the peaks across the linearly variable filter response) made comparable (within a factor of 2) to that in the main $1.01\text{-}\mu\text{m}$ band.
Maximum exposure time limited to keep image smear $<1$ pixel at maximum expected lander angular swing rate.
SNR $>100$ for maximum allowed exposure to scene with radiance $0.4 \text{ W/m}^2/\mu\text{m}/\text{sr}$ .
$[(\text{max-min}) / \text{noise}] / \text{noise}$ (where noise = rss combination of read noise + photon shot noise + dark current noise) $>/=40$ for a scene contrast of $0.04$ ( $(\text{max-min})/(\text{max+min})$ ) assuming the maximum signal is derived using the maximum allowed exposure time and a scene radiance of $50 \text{ W/m}^2/\mu\text{m}/\text{sr}$ , or the maximum signal = $1/2$ full well, whichever is smaller.
Image acquisition at least as often as one every 12 sec.
Nested images providing stereo overlap.
Collect $\sim 15$ images on descent and return $\sim 5$ immediately (during descent); the remainder can be stored in a low priority queue to be returned with panorama during surface operations.
Onboard autonomous method of assessing image quality to select the $\sim 5$ best descent images to return initially.
Surface cameras
Obtain images of potential drilling sites.
Obtain panoramic images of the landing site surroundings.
IFOV $\leq 1$ mrad.
FOV $\geq 60^\circ$ .
Signal-to-noise ratio $\geq 100$ .
Filter wheel for panoramic camera only ( $\geq 5$ filters; spectral bands 100-nm wide centered at $1.0$ , $0.85$ , $0.75$ , and $0.65 \mu\text{m}$ plus clear).

**Table 4.21:** Environmental and Pressure Vessel Design Constraints for the Lander Cameras.

Environment
Outside pressure vessel: <1 bar to 92 bar pressure and $30^\circ\text{C}$ to $462^\circ\text{C}$ temperature
Inside pressure vessel: <1 bar pressure and $30^\circ\text{C}$ temperature
Minimize window diameters
Total overall length from outer window surface to focal plane between 7 and 15 cm
Panoramic camera filter wheel must be at least 7 cm behind outer window surface; more, if possible.
Minimize mass
Minimize exposure time for descent camera to freeze motion

#### 4.3.3.5.1 Descent and Surface Imaging — Science Rationale

Currently, no synoptic regional imaging exists of the surface of Venus at visible to near infrared wavelengths. A substantial new view of the geology of Venus can be obtained with the successful acquisition of image data from a lander while it descends to the surface, something not done on any prior Venus mission. Such data can be used to make correlations with SAR images and identify additional or clarify units and unit boundaries to determine stratigraphic relations. The discovery of atmospheric “windows” at  $\sim 1.01\text{ }\mu\text{m}$  suggests that it should be possible to obtain surface images during the descent of a landed asset. To achieve the best science, the system should have a pixel footprint of  $\leq 1\text{ m}$  from a 1-km altitude, a spectral band centered at  $1.01\text{ }\mu\text{m}$  with a bandpass of  $0.04\text{ }\mu\text{m}$  and a field of view greater than  $25^\circ$ . Once on the surface, panoramic imaging with a second camera will enable geologic investigations to assess lander-scale geologic processes and potential variability in rock types. To best achieve the desired science, the imager requires a field of view of  $\geq 60^\circ$ . Key mineral spectral signatures are centered at  $1.0$ ,  $0.85$ ,  $0.75$ , and  $0.65\text{ }\mu\text{m}$ . In addition, a clear, broadband filter should be included for morphologic studies.

The notional descent camera uses a Teledyne HyViSI hybrid silicon detector coupled to their TCM6604A read-out integrated circuit (ROIC). (Bai et al., 2004; Simms et al., 2007). This device employs a thick silicon membrane to enhance its quantum efficiency (QE) at  $1\text{ }\mu\text{m}$ . Its  $27\text{-}\mu\text{m}$  pixels yield a high response rate and large fullwell to facilitate meeting the SNR requirement with short exposure times. The array size is  $640 \times 480$  pixels. A possible alternative detector would be a Sensors Unlimited InGaAs  $640 \times 512$  array of  $25\text{-}\mu\text{m}$  pixels, which also provides high QE at  $1\text{ }\mu\text{m}$  and large fullwells;

however, its response does not extend below about  $0.7\text{ }\mu\text{m}$ . The optics operate at f/2 for high signal rates. Their 2.8-cm focal length provides an IFOV of  $0.96\text{ mrad}$  and a FOV of  $35^\circ \times 26.5^\circ$ . Imaging performance is optimized at  $1\text{ }\mu\text{m}$ ; the spot size expands to nearly  $200\text{ }\mu\text{m}$  in the shorter wavelengths of the filters placed at the edge of the array. Spectral filters are mounted directly on top of the detector array. The optics include a pair of vacuum-spaced windows as their outer elements to withstand the external pressure and temperature. Heat-rejection coatings are applied to the surfaces on either side of the vacuum gap. The diameter of the outside window is 3.4 cm. The entire descent camera is mounted viewing in the nadir direction. The distance from the outside window face to the focal plane is 11.5 cm. A layout of the optics with ray tracing is shown in Figure 4.13.

First-order modeling of radiative transfer in the Venus atmosphere and the camera spectral response indicates that for a surface albedo of 0.1 and contrast of 0.3, adequate contrast SNR ( $\geq 40$ ) can be achieved at  $1.08\text{ }\mu\text{m}$  at altitudes up to about 16 km for a  $20^\circ$  solar zenith angle for an exposure time of 2 ms (Crisp, 1996; Meadows and Crisp, 1996; Campbell and Shepard, 1997; Campbell et al., 1998; Moroz, 2002). This exposure time would limit the smear to 1 pixel for a lander descent instability (swing) of 20%. While detailed modeling of the lander descent instability has not been completed, this assessment gives reasonable confidence that good quality descent imaging can be obtained up to substantial altitudes. Increasing the solar zenith angle to  $70^\circ$  reduces the maximum possible imaging altitude to about 2 km. Therefore, entries near midday are preferred for descent imaging. Note that the identified landing locations for the two DRM landers are at less optimal locations: that is, closer to the terminator line of Venus.

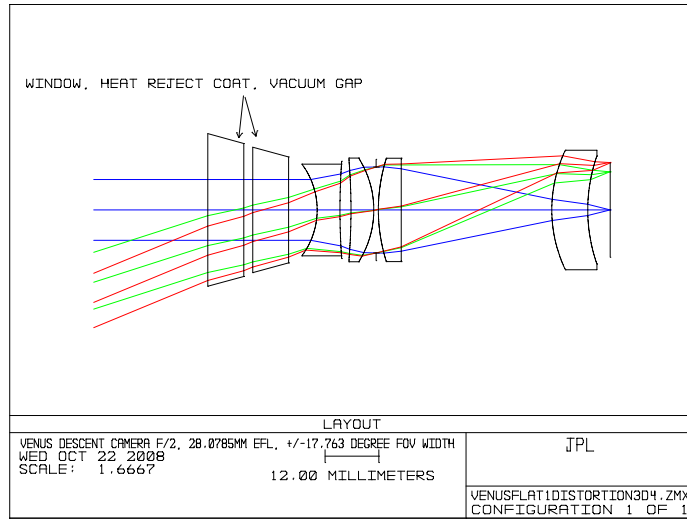


**Figure 4.13:** Optical design for the notional descent camera. (It meets the science requirements and the volume constraints.)

The two notional surface cameras – that is, the panoramic and drill context cameras – are designed to be identical except for the inclusion of a filter wheel in the panoramic imager. Both use a  $1024^2$  frame transfer CCD detector. The E2V CCD47-20 device with  $13\text{-}\mu\text{m}$  pixels is baselined. Other devices from other manufacturers are available, but have slightly larger pixel sizes. The optics operate at f/13 to provide diffraction-limited performance at minimum size. They are based on the MER HAZCAM optics design. (Maki et al., 2003) Their 1.3-cm focal length provides an IFOV of 1 mrad and a FOV of  $60^\circ \times 60^\circ$ . Imaging

performance is good across the 0.6- to  $1\text{-}\mu\text{m}$  spectral range. The optics again include a pair of vacuum-spaced, heat-rejection-coated windows as their outer elements to withstand the external pressure and temperature. The outside window diameter is 11.2 cm. The focal plane is located 10.6 cm inside of the pressure vessel external surface, allowing room for the filter wheel to be placed just in front of the focal plane while still clearing the inside surface of the insulation. Figure 4.14 shows the optical layout. The filter wheel is based on the heritage design from the MER Pancam (Bell et al., 2003).

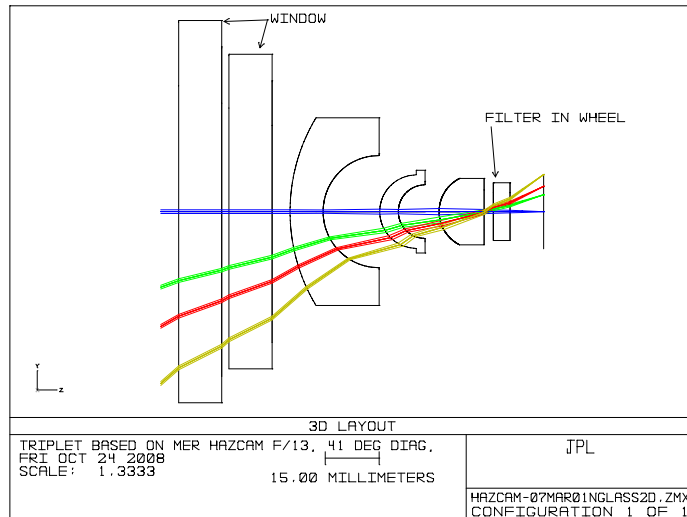


**Figure 4.14:** Optical design for the notional surface cameras. (It meets the science requirements and the volume constraints.)

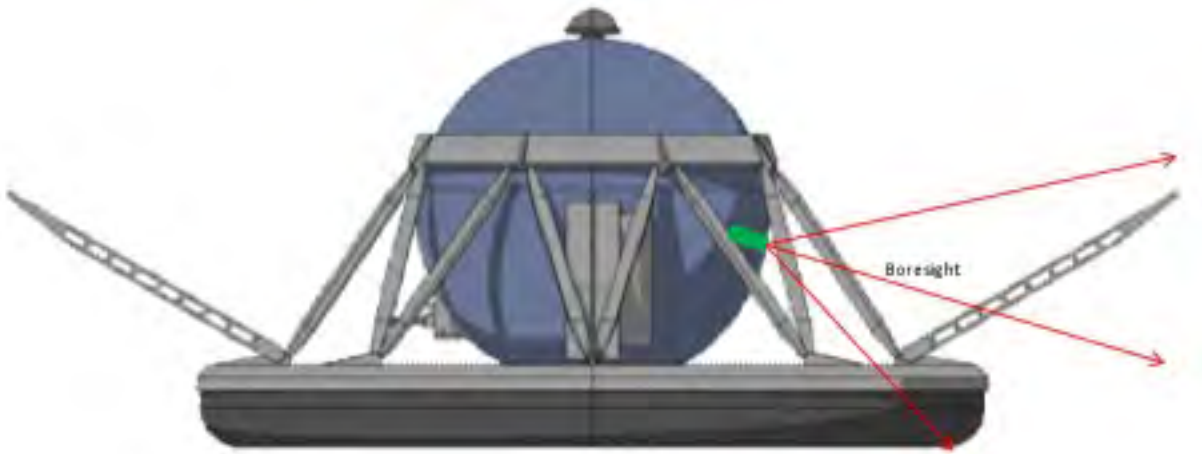


**Figure 4.15:** Panoramic camera views from the base of the lander to 15° above the horizon.  
(Rotation of the pressure vessel provides 360° of azimuth coverage.)

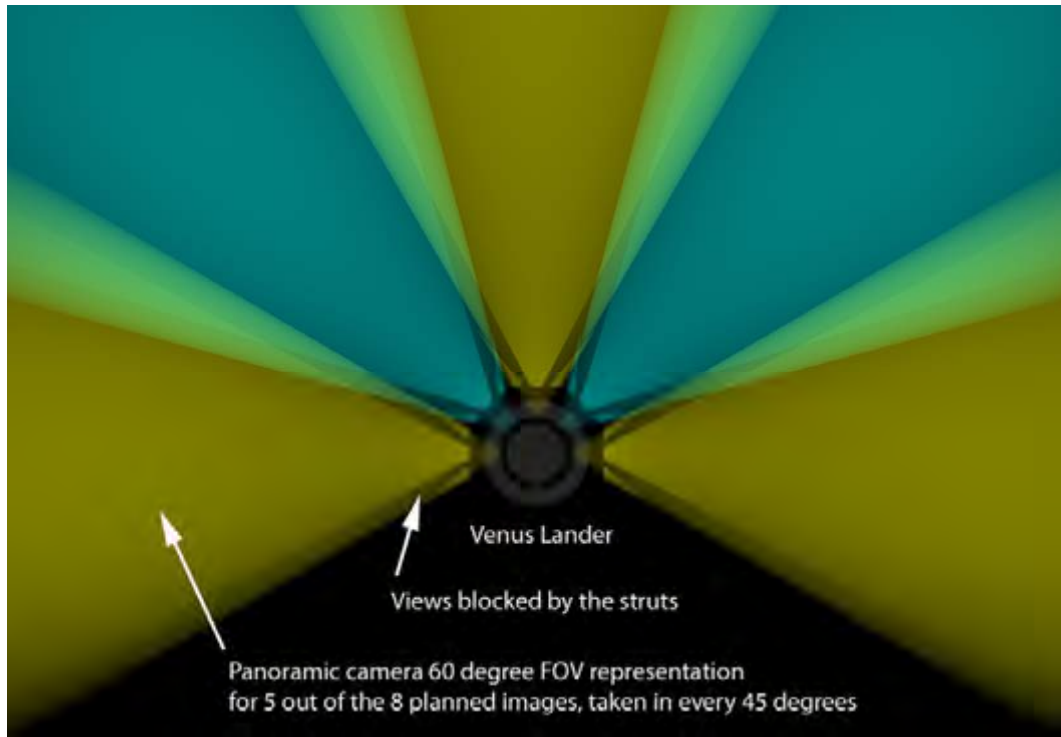


**Figure 4.16:** Simulation of panoramic camera views for 5 out of 8 images.

The panoramic camera is mounted in the lower half of the pressure vessel about 0.15 m below the centerline. To minimize the amount of insulation that must be removed to accommodate the camera, the axis of symmetry of the primary optics and detector is oriented radially. The boresight points downward about 15° below horizontal (Figure 4.15). The FOV, thus, extends from 45° below

to 15° above the horizon. The closest edge of the FOV will include the edge of the lander's impact ring. Rotation of the entire pressure vessel about its vertical axis provides the 360° azimuthal panoramic views (8 positions per panorama, limited by data volume). The FOV will be somewhat obscured by the struts supporting the rotation ring of the pressure vessel, as shown in Figure 4.16. In this

simulation the views of the panoramic camera are shown for 5 out of the 8 planned images. By acquiring panoramic images with sufficient side-to-side overlap, the effect of the obscuration from the struts can be minimized and excellent stereo information can be obtained. The size of the blocked out areas could be reduced by keeping the struts as narrow as possible, and by taking more than 8 images, which would produce more overlap, but would also increase the data volume. The camera will be in focus for object distances from 1 m to infinity. The option of placing the camera in the upper half of the pressure vessel to avoid having to view between the struts was investigated; however, the only configurations that oriented the boresight toward the surface involved having to remove large amounts of insulation or place the entire camera outside the protection of the pressure vessel. Therefore, these alternative camera placement options were rejected.

The drill site camera is mounted in the lower half of the pressure vessel viewing the area just beneath the drill at an angle roughly  $45^\circ$  from vertical (Figure 4.17). No filter wheel is included; however, a flat optical element is substituted at the filter position to limit the spectral passband and retain the focal plane position, so that the same optical design can be used as for the panoramic camera. The drill site camera focus is optimized at an object range of 0.4 m and provides in-focus imaging

for object ranges between 0.2 and 0.8 m. Although the drill site camera is mounted below the pressure vessel and its imaging targets will be shaded by the impact ring and the drill housing assembly, sufficient illumination from scattered sunlight should allow adequate imaging.

The camera head electronics for all three cameras are shared and are based on MER camera heritage (Maki et al., 2003). Encoding is to 14 bits per pixel. The camera electronics include a 2-frame storage buffer. Only one camera will be used at a time. The data interface to the lander C&DH system is RS-422. Data are transferred at a rate of 500 kb/s. The electronics box dimensions are  $8 \times 7 \times 4$  cm. The electronics box should be placed in close proximity to all three cameras; therefore, the cameras should all be located in the same sector of the pressure vessel sphere to minimize the length of the wires carrying the weak analog signals from the detectors to the shared ADC. The detectors and the electronics all operate at the nominal  $30^\circ\text{C}$  temperature of the interior of the pressure vessel. The cameras depend on the lander for conditioned power and for all data storage and onboard data processing. Processing algorithms will include lossless and lossy data compressions and an autonomous method of assessing image quality to select the ~5 best descent images to return initially.

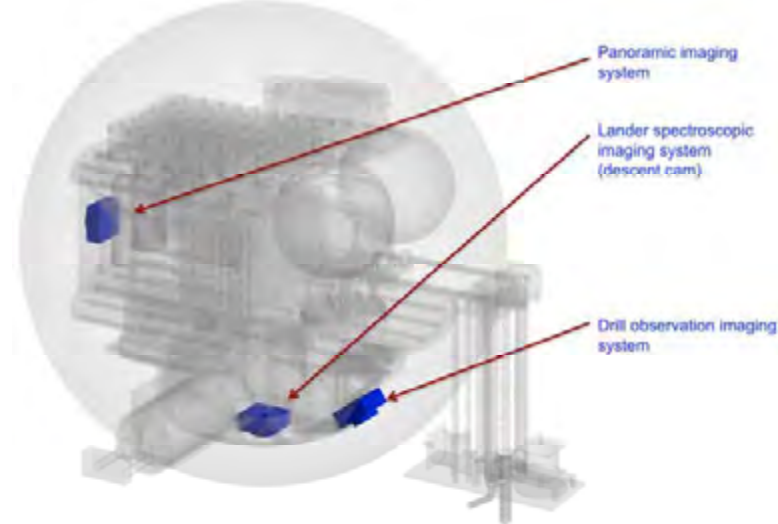


Figure 4.17: The drill site camera observes all potential drilling areas.

**Table 4.22:** Performance Parameters and Resource Requirements for the Lander Cameras.

Parameter	Descent Camera	Panoramic Surface Camera	Drill-site Surface Camera	Electronics Box
IFOV (mrad)	1	1	1	
FOV (°)	$35 \times 26$	$60 \times 60$	$60 \times 60$	
Array size	$640 \times 480$	$1,024 \times 1024$	$1,024 \times 1024$	
Focal length (cm)	2.7	1.3	1.3	
f/#	f/2	f/13	f/13	
Spectral bands ( $\mu\text{m}$ )	$1.08 \pm 0.02$ plus Vis non-imaging filters at edge of array	100-nm wide bands centered at 1.0, 0.85, 0.75, and 0.65 $\mu\text{m}$ plus clear	Visible panchromatic	
Nominal exposure time (ms)	2	50 – 3,000 depending on filter	50	
Window diameter (cm)	3.4	11.2	11.2	
Mass (kg)	0.5	1.1	1.0	0.15
Power (W)				0.75

In addition, an autonomous drilling site selection algorithm must be implemented. This algorithm will involve using drill camera images to determine the areas accessible by the drill, run science signature filters to find areas that have specific characteristics (this will involve relatively simple image processing operations such as image masking, image filtering, edge detection, and region segmentation), extract high-science-value regions, and prioritize the regions to be drilled according to science value and drill positioning uncertainty. Lander autonomy for drill location selection is further discussed in Subsection 4.5.5.10. Table 4.22 summarizes the performance parameters and the resource requirements for the lander cameras. As can be seen from the table, lander camera performance meets all science requirements with modest resource requirements.

#### 4.3.3.6 Lander Intrinsic Gamma Rays

In the DRM payload, a passive gamma-ray spectrometer (PGS) system is used to detect abundances of the naturally radioactive elements K, U, and Th. These elements are the most important active sources of heat in a planet, and thus provide critical constraints on planetary geophysics. These elements are also critical in geochemistry in constraining the bulk composition of the planet, igneous fractionation processes, and possibly aqueous fractionations.

Gamma-ray spectrometry is a standard analytical method on Earth for a variety of major and trace elements (Gilmore 2008). The method detects radioactive, gamma-ray emissions, which are either intrinsic (natural radioactivity) or induced by a high-energy particle fluence (e.g., protons or neutrons, as instrumental neutron activation analysis). For Venus, those gamma-rays are only from naturally radioactive elements. (Cosmic rays and other energetic radiation from the interplanetary environment do not penetrate Venus' atmosphere and so will not induce gamma radiation at the surface.) Gamma rays emitted from the sample impinge on a detector material, which is affected by the gamma ray in a detectable manner. The three major detection modalities are: optical scintillation / luminescence (production of a photon of optical wavelengths); semiconductor conductance (production of a conduction-band electron in a semiconductor material); and heat (production of heat in inelastic scattering or absorption of the gamma ray). The Venera and VEGA landers on Venus used the first modality (optical luminescence); the gamma-ray spectrometer (GRS) instrument on the MRO orbiter around Mars uses the second modality (electron liberation in a Ge detector); the third modality is under development in terrestrial laboratories.

**Table 4.23:** Intrinsic Gamma Ray Measurement Requirements.

Duration	Minimum 2 hours (from Venera/VEGA), otherwise, as long as possible.
Resolution	Single spectrum of ~ 5000 channels and 16 or 32 bits.

In operation, a PGS detector system ‘looks out’ of the pressure-temperature vessel through the pressure vessel that is relatively transparent to the gamma-rays generated on the Venus surface. Thus, a PGS analysis represents a distance-weighted average of compositions within the field of view and within a few centimeters of the surface. In this sense, a PGS measurement may not correspond entirely to an XRF analysis — both methods can detect K-shell emission, but may give different abundances if they access different materials. However, scene-averaged abundances of heat producing elements are very relevant for geophysical studies. The Venera and VEGA PGS systems collected data for the mission life on a single field of view; to obtain analyses on more than one area would involve moving the detector.

The accuracy of a PGS analysis depends on the number of gamma rays detected, which depends on analysis duration, detector efficiency, and detector volume. Analysis durations are comparable for the Venera, VEGA, and DRM missions (limited by thermal load on the lander). GRS detector volume in the DRM is constrained by the size of the lander, and cannot be significantly larger than that in the Venera and VEGA mission. In detector efficiency, the new scintillator material LaBr<sub>3</sub>:Ce appears to be several times more efficient than the NaI(Tl) material used by Venera and VEGA (Milbrath et al., 2006). Thus, we can reasonably expect PGS analyses on the DRM to be a moderate improvement over those of Venera and VEGA. Resource requirements for the PGS system are based on the instrument planned for.

If the DRM had time in excess of the nominal five hours, and sufficient power and cooling, PGS analysis could be extended. The quality of the analysis — the precision and detection limits for abundances of K, Th, and U — would improve with counting statistics.

Thus, an analysis for 10 hours (as opposed to the DRMs five hours) would give analyses for these elements with detection limits and uncertainties improved by a factor of 1.4.

Determination of the abundances of K, Th, and U in surface and near-surface materials addresses many of the VEXAG Goals and Objectives (VEXAG 2007), as detailed in Chapter 2 of this report. All of the goals and objectives listed above under X-ray Fluorescence are also addressed (at some level) by PGS analyses. In addition, one can cite from the VEXAG (2007) goals that include internal structure, thermal structure, and thermal evolution, including: Goal 1, Objective 2 (Map the mineralogy and surface composition on a planetary scale), Investigations 2 and 5; and Goal 2, Objective 6 (Determine the history of and current state of interior evolution of Venus).

The lander Intrinsic Gamma Ray instrument is based on the MSL Radiation Assessment Detector (RAD) (MSL RAD 2009) instrument which is capable of identifying neutrons, gamma rays, protons, and alpha particles (subatomic fragments consisting of 2 protons and 2 neutrons, identical to helium nuclei), and will identify heavy ions up to iron.

#### 4.3.3.7 Lander Magnetometer

The lander magnetometer determines Venus’ local magnetic field and requires an accuracy of a few nano-Tesla. While numerous high-precision magnetometers have been flown that can provide the high resolution required, the temperature extremes on the lander will likely require some modification. Note that more lightweight designs that have been flown as part of the Free-flying Magnetometer program might be applicable and would provide a technology readiness level of 6. The magnetometer will have to be boom mounted to avoid any magnetic fields generated by other lander systems and encased in phase-change material

to maintain a temperature within acceptable limits during descent and for a few minutes after landing. The mass estimate of 10 kg shown in Table 4.15 includes the boom structure and phase-change material.

#### 4.3.3.8 Lander Nephelometer

The lander nephelometer will characterize the aerosol and cloud particulate properties of the atmosphere and some limited composition. Table 4.24 provides the measurement requirements for the nephelometer. There is some heritage in nephelometer design, although new designs are being developed and proposed that would provide higher accuracy and possibly eliminate the need for an external mirror assembly. The current technology readiness of the new designs is TRL 4/5 (see Figure 4.18).

#### 4.3.3.9 Lander Net Flux Radiometer

The lander net flux radiometer (NFR) will characterize the radiative profile during descent and landing. Table 4.25 provides the measurement requirements for the net flux radiometer. There is some heritage in net flux radiometer design, although new designs are being developed and proposed that would provide more look angles than previously flown instruments. The current technology readiness of the new designs is TRL 4/5.

To understand the climate balance of Venus, it is crucial to simultaneously measure upwelling and downwelling radiation to high accuracy across a broad range of visible and infrared wavelengths along multiple altitude profiles. For these measurements, the DRM payload includes net-flux radiometers in the descent phase payload of the surface landers.

**Table 4.24:** Lander Nephelometer Measurement Requirements.

Frequency of measurement	Every 1 km between 40 and 70 km
Range of measurement	Particle size range 0.1 to 50 $\mu\text{m}$
Sensitivity	Polarizing nephelometer can do composition
Accuracy	Size and number densities to $\pm 10\%$ . Aerosol constituents to $\pm 15\%$ .
Constraints	Operates in $\text{H}_2\text{SO}_4/\text{H}_2\text{O}$ aerosol environment ( $\text{pH} = -2$ )

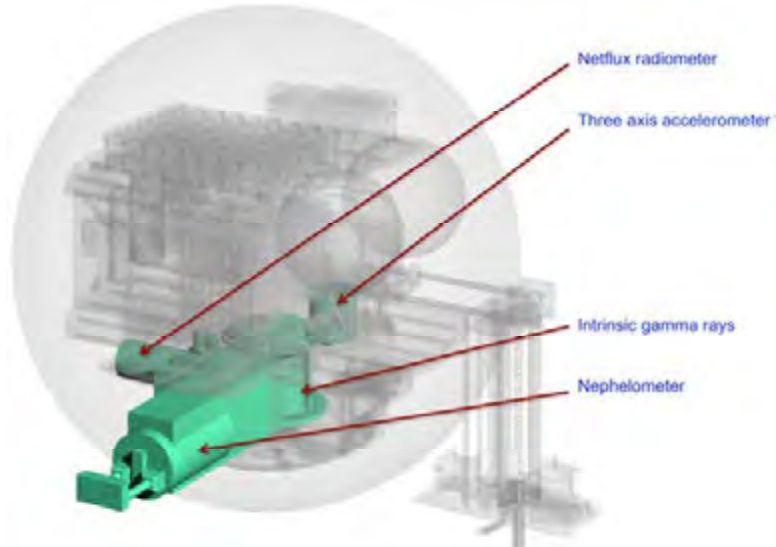


**Figure 4.18:** Selected lander instruments (radiometer, accelerometer, gamma ray, and nephelometer).

**Table 4.25:** Lander Net Flux Radiometer Measurement Requirements.

Resolution	11 look angles, from nadir to zenith
Frequency of measurement	Every 1 km or better during descent
Range of measurement	0.2 to 3 $\mu\text{m}$ and 0.8 to 25 $\mu\text{m}$
Sensitivity	SN > 200 from 0.2 to 3 $\mu\text{m}$ , SN > 100 for 3 to 25 $\mu\text{m}$
Accuracy	<5% from 0.2 to 3 $\mu\text{m}$ , < 10% for 3 to 25 $\mu\text{m}$
Constraints	Operates in $\text{H}_2\text{SO}_4/\text{H}_2\text{O}$ aerosol environment

This instrument will measure upwelling and downwelling radiation from 0.2 to 25  $\mu\text{m}$  with a signal-to-noise ratio of greater than 200 from 0.2 to 3  $\mu\text{m}$  and greater than SNR 100 from 3 to 25  $\mu\text{m}$  and an accuracy within less than 5% from 0.2 to 3  $\mu\text{m}$  and less than 10% from 3 to 25  $\mu\text{m}$ . The instrument will require eleven look angles, from nadir to zenith. During descent, measurements will be made at least once per kilometer.

This instrument will contribute important data toward the ultimate goals of measuring the deposition of solar energy globally and determining radiative balance, including cloud and greenhouse-gas opacities over wavelength and solar deposition and thermal emission as a function of altitude, latitude, and longitude. With two altitude traces of high-precision measurements, we will be able to use models to fill in a much more comprehensive view of the complete radiative balance of the atmosphere.

#### 4.3.3.10 Surface Corner Reflector

The main purpose of the surface corner reflector is to provide a precise determination of the lander's position on the surface via reflected radio waves from the orbiter. Once known, the lander's position becomes a known reference point that can be carefully tracked over time to yield information on the change in Venus' pole position. Note that the corner reflector is not required for the operation of the InSAR instrument on the orbiter.

The design for the surface corner reflector is notional at this time. Analysis shows that a device on the order of 0.5 m across is required to reflect a sufficiently strong signal. This size

is not too much smaller than the size of the pressure vessel, suggesting that some type of deployable reflector will be required to satisfy packaging constraints on the lander and entry vehicle. For purposes of the DRM, a mass of 5 kg has been allocated for the reflector in lieu of a detailed design that will be generated in subsequent studies.

#### 4.3.3.11 Heat Flux Plate

Of fundamental importance for understanding the structure of the lithosphere is the determination of the geothermal heat flux. On Earth, this has been an important series of measurements from the deepest continental cratons to newly formed crust at mid-ocean ridges. Typically, a series of thermometers is embedded several meters into bedrock and allowed to come to thermal equilibrium. The temperature gradient thus directly measured is used to determine the geothermal temperature gradient and, along with rock thermal properties, the geothermal heat flux.

On Venus, a different approach is necessary because of the large heat flux from the atmosphere and because embedding a probe several meters into the surface is impractical. Venus has one advantage over Earth: diurnal and annual temperature variations are small or non-existent (Seiff, 1983). As a result, heat flux coming out of the ground might be measured directly by placing a partially insulating plate on the surface, allowing it to reach thermal equilibrium, and then measuring the temperature difference that develops across the plate.



**Figure 4.19:** Cross section of the flux plate. The yellow material is a 1-cm thick low conductivity material, the red slab is a 1-mm thick copper plate, and the blue is high conductivity, conformable material with a thickness of 1 - 2 cm.

Such a heat flux plate should be small so that it can reach thermal equilibrium in an hour or two, but should be designed so that good thermal contact can be made with the surface, reducing edge effects. A low-thermal-conductivity square plate, 10 cm on a side and 1-cm thick, with a carbon nanotube underside skirt of 1- to 2-cm thickness (Baratunde et al., 2007) would develop a temperature difference of a few 10s of milliKelvin for a reasonable range of geothermal heat fluxes (Figure 4.19). Using thermocouples in a bridge arrangement, such precision is easily achievable. The plate needs to be deployed on a flat surface, but is somewhat robust with respect to surface roughness on scales of 1 - 3 cm. A temperature difference measurement of  $\pm 1$  milliKelvin would enable the determination of geothermal heat flux to  $\pm 5$  mW, sufficient to distinguish between major hypotheses of the formation of the Venus lithosphere.

#### **4.3.4 Data Taking Scenario and Data Volumes**

The short lifetimes and limited electrical energy of the lander and balloon gondola constitute serious constraints on the data acquisition and downlink strategy for their respective science instruments. Quantitative data taking scenarios devised for the DRM yield a self-consistent design with properly matched data volumes, downlink capability, and electrical power resources.

##### **4.3.4.1 Lander**

The data rate and telecom system design are controlled mostly by the requirements of imaging and XRD/XRF after landing. With the current point design (see Subsection 4.5.1.7) the lander-orbiter telecom link can support 64 kb/s for the lander at a latitude of  $-25^\circ$  and 128 kb/s for the lander at a latitude of  $-47^\circ$ .

During the one-hour descent, the ASI operates at a rate of 10 samples per second while the other atmospheric instruments (GCMS, Nephelometer, NFR) operate at a rate of one sample per second to get adequate vertical resolution. The descent imager takes one  $1024 \times 1024$  pixel image every 10 s. Each image is reduced to  $512 \times 512$  pixels, compressed by factor of 8 and transmitted in real time to the orbiter. Fifteen original, lossless  $1024 \times 1024$  pixel images are stored for transmission during descent and after landing. With the descent rate of approximately 7 m/s the highest resolution at the last image is approximately 10 cm per pixel. Like the Huygens probe, the Venus lander will be designed to rotate during descent to provide off-axis views of the surface. For wind measurements the orbiter extracts and records Doppler data from continuous lander-orbiter telecom operation.

Table 4.26 shows the lander instrument data and power budget for the DRM.

**Table 4.26:** Lander Instruments Power and Data Budget.

Instrument	Data per cycle, kbit	Power, W	Cycle duration, min	Energy fm bat per cycle w/cont, W*h	Sample rate, s		Cycles per mission / Duty cycle	Total operation time, h	Energy/mission, W*h	Data volume during descent, Mbit	Total data volume, Mbit	Required battery mass, kg	Transmission time required, min
					Descent	Surface							
GCMS	2.00	41	1/60	0.019	1	60	3,900	3.0	205	7.20	7.8	0.63	2.031
XRDF	72,000	50	120.0	143		7,200	2	5.0	300		144	1.62	37.500
Microscopic imager	8,389	1	1	0.03			4		0.07		34	0.000	8.738
ASI	0.25	2	1/60	0.0010	0.1	10	37,800	2.0	7	9.00	9.45	0.02	2.461
Descent camera	2,150	1.00	1.00	0.03			15	1.0	0.25	32.3		0.001	8.400
Panoramic camera	293,601	1	5	0.15		3 hrs	2		0.17		587	0.001	152.917
Drill camera	58,720	1	5	0.15			1	0.08	0.08		59	0.000	15.292
Real-time image transmission	459		1/6		1/6		360	1.00		165.2	165		43.008
Intrinsic gamma-ray spectrometer	1,000	4		6.00				5.0	30.00		1	0.092	
Magnetometer	0.064	5	1/6	0.02	1	10	5,400	2.0	17	0.23	0.35	0.05	0.090
NFR	0.192	5	1/10	0.01	1	60	3,600	2.0	17	0.69	0.69	0.05	0.180
Nephelometer	0.08	5	1/60	0.00	1	60	5,400	2.0	17	0.29	0.43	0.05	0.113
Surface corner reflector	None												
Heat flux plate	0.048	2	1	0.06		600	30	5.0	1.9		0.0014	0.01	0.000
Drilling	10	100	30	77.38			2	1.0	155		0.02	0.48	0.005
Housekeeping	1.00	2	1/6	0.01	10	10	2,160	6.0	22	0.36	2	0.07	0.563
Telecom		270	1	6.35			360	6.0	2,287			7.02	
CD&H		10	1	0.30			360	6.0	108			0.33	
<b>TOTALS</b>									2,885.0	215.2	1010.5	11.6	271.3

After landing, atmospheric instruments continue to operate with a 10-s sampling interval. The pressure vessel rotates around its vertical axis to 8 positions  $45^\circ$  apart to enable panoramic images. At each position, the  $60^\circ$  FOV panoramic camera takes three  $1024 \times 1024$  pixel images through different color filters while the drill camera takes one  $1024 \times 1024$  pixels image. The overlap between images is  $15^\circ$  and can be used for stereo processing and to filter out the view-obstructing landing struts, which connect the pressure vessel to the lander's crash pad. Drill camera images are processed on board to find the optimal location for drilling (see Subsection 4.5.5.10). The panoramic imaging cycle repeats after 3 hours to search for possible changes. XRD/XRF will get 2 spectra of the surface samples. Four photomicrographs of the samples will be transmitted.

Table 4.26 gives details of the 1 Gbit total data volume from each lander. The data volume capacity of the telecom system is 1.38 Gbit, providing a 38% margin that can be used for enhanced science data return or redundant transmission of high-priority data.

#### 4.3.4.2 Balloon

The average data rate for the balloon-orbiter link is over 500 b/s, when the orbiter range is less than 30,000 km and the elevation angle is more than  $20^\circ$ . Figure 4.20 shows visibility periods and possible periods of data transmission during the 30-day balloon mission.

Proper conditions for the 500 b/s data rate exist for several hours on practically every orbit. The telecom system assumption — that S-Band capability will be unavailable at 70-m DSN antennas (or their equivalent) by 2021 — implies that no data can be transmitted in the direct-to-Earth (DTE) link from the balloon. Therefore, the DTE carrier link in the DRM is

limited to use as a science tool for Doppler and VLBI wind tracking only. Subsection 4.5.4.5 gives more details of the telecom subsystem.

The DRM specifies only primary batteries on the balloon as the energy source. The design's 22-kg battery provides sufficient electrical energy to power scientifically rich instrument operations and data return that meet the investigation requirements. Trade studies, which considered science priorities, yielded the data volume and electrical energy budget shown in Table 4.27.

The GCMS instrument is the second most energy-consuming device on the gondola (after the transmitter), but produces a relatively low data volume. On the other hand, the Venus Atmospheric Structure Instrument (VASI) produces a large data volume with only moderate energy consumption. Therefore, the major trades are between number of GCMS spectra, DTE transmission for wind tracking and VASI sampling that generates data to be transmitted to the orbiter. The scenario shown in Table 4.27 provides a total of 385 GCMS spectra (including 15 spectra of Helium isotopes and 75 spectra of noble gases), 101 hours of VASI sampling at a rate of 10 samples/min in 5 minute blocks, 30-min magnetometer and net flux radiometer sampling, 360 hours monitoring of acoustic and lightning events, and recording of some acoustic and lightning waveforms.

The balloon transmission strategy is to operate for 7-minute sessions out of the hour when the balloon is on the visible side. This will typically allow for multiple communications sessions during each 13-hour orbit. (See also Subsection 4.5.4.5 for additional details.) The balloon science return will consist of a total of 20.5 Mbit of science data and 55 hours of wind tracking.

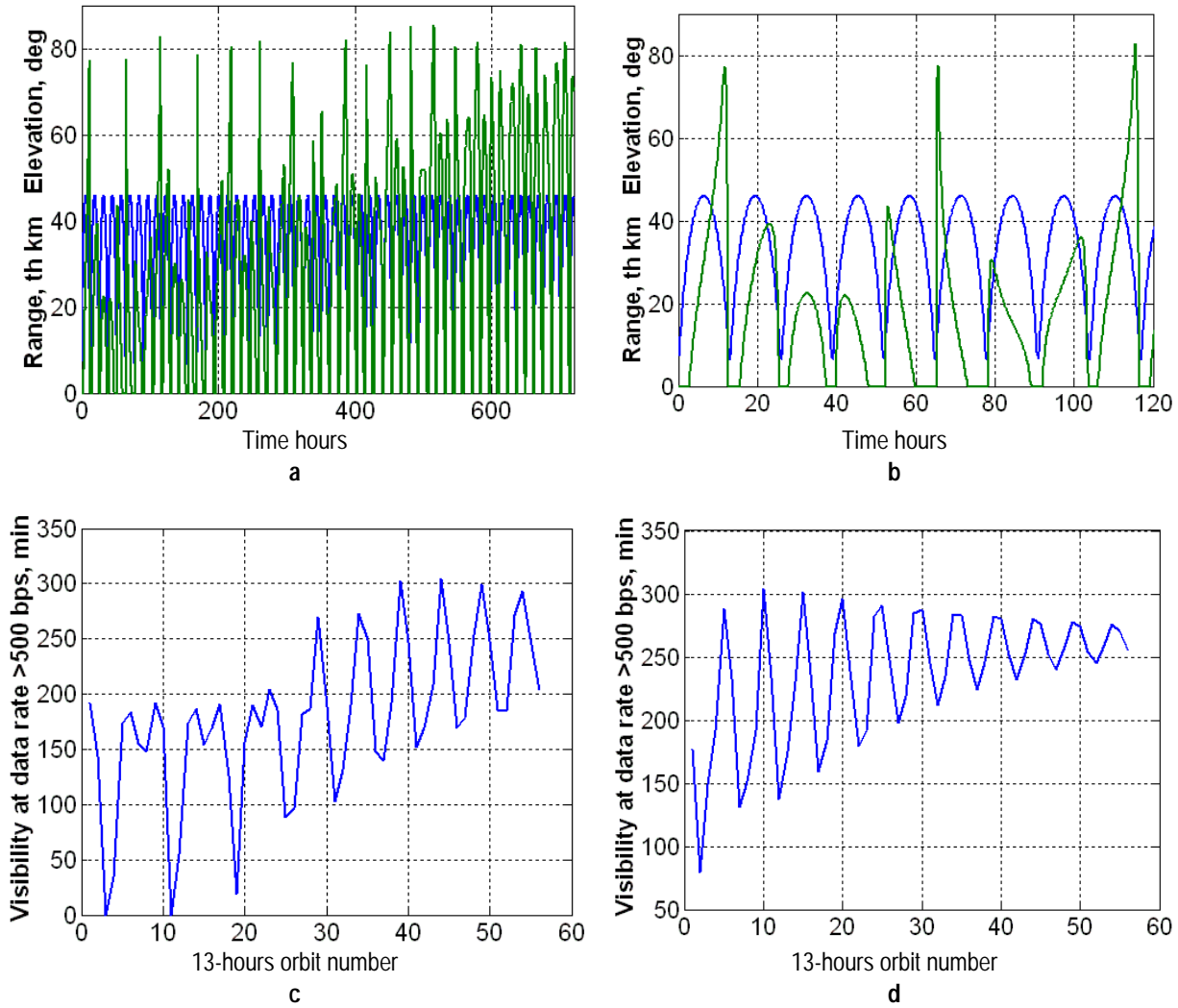


**Figure 4.20:** Balloon-orbiter visibility periods (a, b) and possible periods of data transmission (c, d) during 30-days balloon mission. a, b: orbiter range (blue) and elevation angle (green), balloon insertion at  $-25^\circ$ ; a: during the whole 30-days mission; b: during the first five days; c: balloon insertion at  $-25^\circ$ ; d: balloon insertion at  $-47^\circ$ .

**Table 4.27:** Balloon Instruments Power and Data Budget.

	Data per cycle, kbit	Average power, W	Cycle duration, min	Energy per cycle w/cont and DC efficiency, W*h	Cycles per mission	Operation time/mission, h	Energy/mission, W*h	Data/mission, kbit	Battery mass, kg	Orbiter relay transmission time, h
GCMS/ He	6	31.7	60	52.78	15	15	792	90	2.28	0.05
GCMS / N	6	18.8	13	6.81	75	16	510	450	1.47	0.25
GCMS / C	6	23.6	7	4.58	75	9	344	450	0.99	0.25
GCMS / S	3	23.6	7	4.58	200	23	917	600	2.64	0.33
ASI+Nephelometer	14.8	2	5	0.28	1,210	101	336	17,908	0.97	9.95
NFR	0.176	3	1	0.08	1,440	24	120	253	0.35	0.14
Magnetometer	0.064	2	1	0.06	1,440	120	240	92	0.69	0.05
Li/Log	0.2	0.4	60	0.69	360	360	246.9	72	0.71	0.04
LI/WF	2.5				30	360		75		0.04
MIC/Log	0.2		60		360	360		72		0.04
MIC/WF	10				60	360		600		0.33
Engineering	0.20		60			720		144		0.08
TX DTE		35	7	5.87	360	42	2,113		6.09	
TX to Orbiter		35	7	5.87	111	13	651		1.88	
RX		15	1	0.36	1,440	24	517		1.49	
CD&H		6	1	0.18		120	720		2.07	
CD&H / sleep		0.22	1	0.012		600	132		0.38	
<b>TOTALS</b>							<b>7,639</b>	<b>20,807</b>	<b>22.0</b>	<b>11.56</b>

## 4.4 Mission Design and Trajectories

### 4.4.1 Overview

The Venus DRM consists of one orbiter and two entry vehicles, each of which contains a lander and a balloon. As described in Chapter 3, a dual-launch configuration was selected for the DRM consisting of two Atlas 551 launch vehicles to Venus. One launch vehicle will deliver the orbiter on a Type II trajectory to Venus, while the other launch vehicle will send the two entry vehicles mounted on a carrier stage on a Type IV trajectory. The orbiter launch mass is 5306 kg and the carrier launch mass (with the entry vehicles) is 5578 kg.

The orbiter will arrive at Venus first, with sufficient time for checkout and phasing maneuvers before the landers and balloons arrive 3.5 months later. The orbiter is designed with two functions. First, it will act as a telecommunication relay to transmit data to/from both the landers and balloons to Earth.

The landers are designed for a 1-hour atmospheric descent and then 5 hours of operation on the surface. The balloons and their payloads are designed to operate for one month. Once the landers and balloons have completed their missions, the orbiter will transition from its telecom relay phase to perform its second function during the orbital science phase with a 2-year primary mission.

### 4.4.2 Trajectories and Launch Vehicle

The trajectory selection was based on minimizing launch energy and arrival velocity plus ensuring a 21-day launch period for each payload. The mission timeframe is 2020 to 2025 (see Section 3.3), with an emphasis on the first available launches in 2021. Table 4.28 summarizes the possible trajectory transfer options to Venus in the desired mission timeframe, with values listed for the midpoint of a 21-day launch period. The selected 2021 Type II and Type IV launches are highlighted in yellow.

**Table 4.28:** 2020 Through 2025 Earth/Venus Launch Opportunities.

Opportunity	Type	Est. Launch Date	Est. Arrive Date	Flight Time (days)	min c3 (km <sup>2</sup> /s <sup>2</sup> )	DLA (deg)	VHP (km/s)	Entry Velocity (km/s)	Atlas V-551 Approx Injected Mass (kg)
2020	I	3/13/2020	7/3/2020	112	11.4	-2.005	6.030	11.9	
	II	3/27/2020	9/15/2020	172	9.0	38.085	5.730	11.7	
2021	I	10/24/2021	2/27/2022	106	13.1	10.074	5.380	11.6	
	II	10/29/2021	4/6/2022	159	7.8	-26.143	4.760	11.3	5450
2021	"+III"	5/16/2021	6/16/2022	396	12.6	-14.573	5.432	11.6	
	"-III"	5/10/2021	6/15/2022	401	12.7	-16.593	5.257	11.5	
	"-IV"	4/30/2021	7/30/2022	456	6.8	22.463	4.546	11.2	5580
2023	I	5/27/2023	9/22/2023	118	11.6	-16.480	4.050	11.0	
	I	5/18/2023	10/24/2023	159	6.1	15.017	3.910	11.0	5590
2022	"+III"	12/24/2022	1/30/2024	403	9.2	10.849	3.659	10.9	
	"-III"	12/8/2022	2/13/2024	433	6.7	-5.476	3.386	10.8	
	"-IV"	11/29/2022	2/13/2024	441	7.1	-4.682	3.445	10.8	5580
2024	I	12/26/2024	5/9/2025	134	7.0	-0.490	3.800	10.9	
	II	11/30/2024	5/10/2025	161	9.8	8.130	3.200	10.7	5000
2024	"+III"	7/13/2024	8/22/2025	404	7.8	-10.269	4.679	11.3	
	"-III"	6/18/2024	8/29/2025	437	5.8	2.006	3.684	10.9	
	"-IV"	6/2/2024	8/29/2025	453	6.6	6.374	3.895	11.0	5400

The trajectories shaded in yellow are the ones selected for the Design Reference Mission.

The Type II and Type IV trajectory transfers are shown in Figures 4.21 and 4.22. The Type II trajectory has a flight time of about 160 days and travels approximately a half revolution around the Sun. The Type IV trajectory travels approximately one-and-a-half revolutions around the Sun, with a flight time of approximately 450 days. Following the staggered arrival, that results from the dual-launch combined with the Type II and Type IV trajectory options, the orbiter would perform

its Venus Orbit Insertion (VOI) maneuver at Venus approximately 3.5 months before arrival of the landers and balloons. This provides sufficient time for in-orbit checkout of the orbiter's subsystems and instruments and the performance of phasing maneuvers, optimized for telecom support for the in situ elements. The range from Venus to Earth at the time of the landers arrival is approximately 230,000,000 km (or ~1.5 AU).

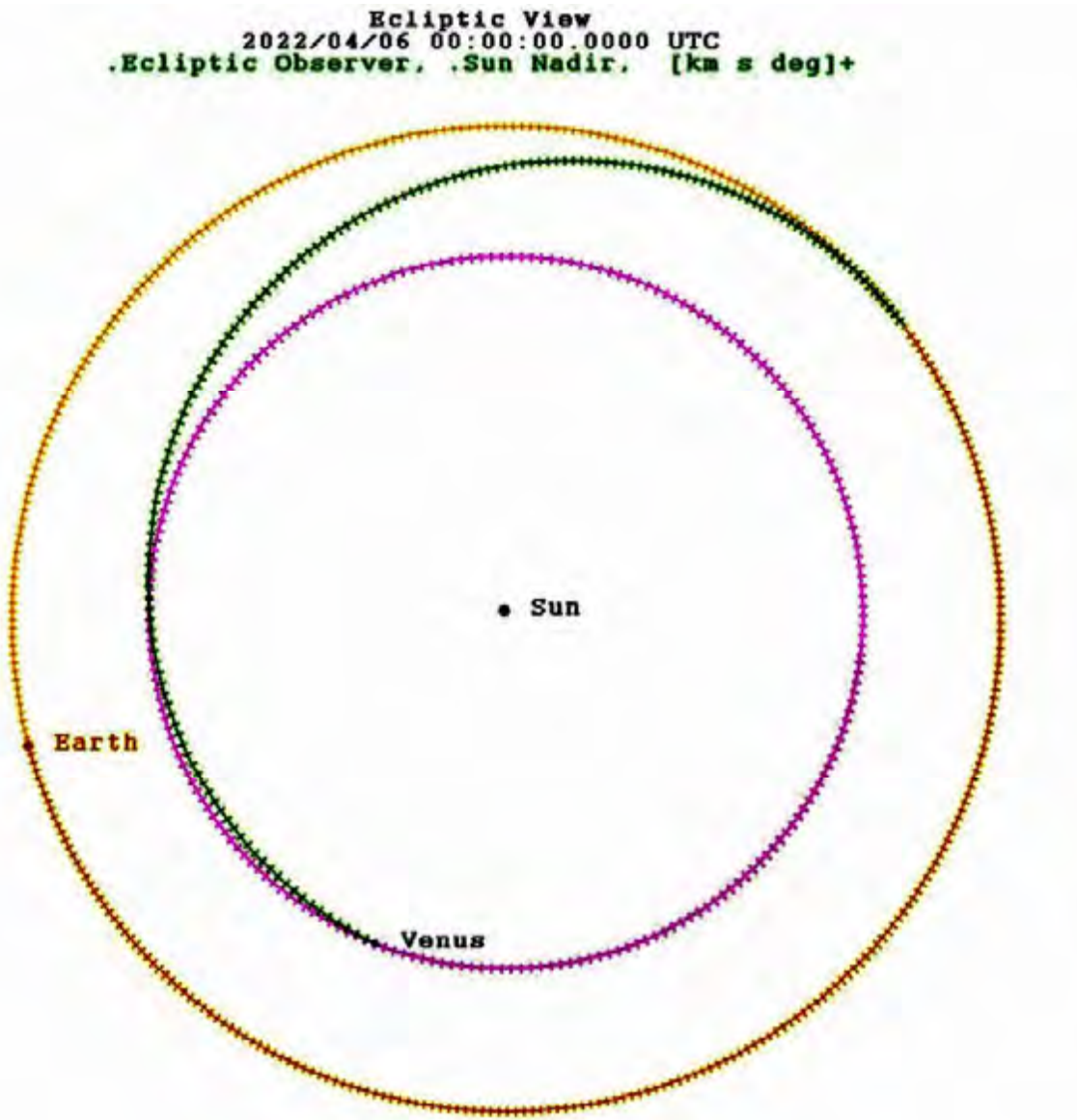


Figure 4.21: 2021 Type II Earth/Venus trajectory.

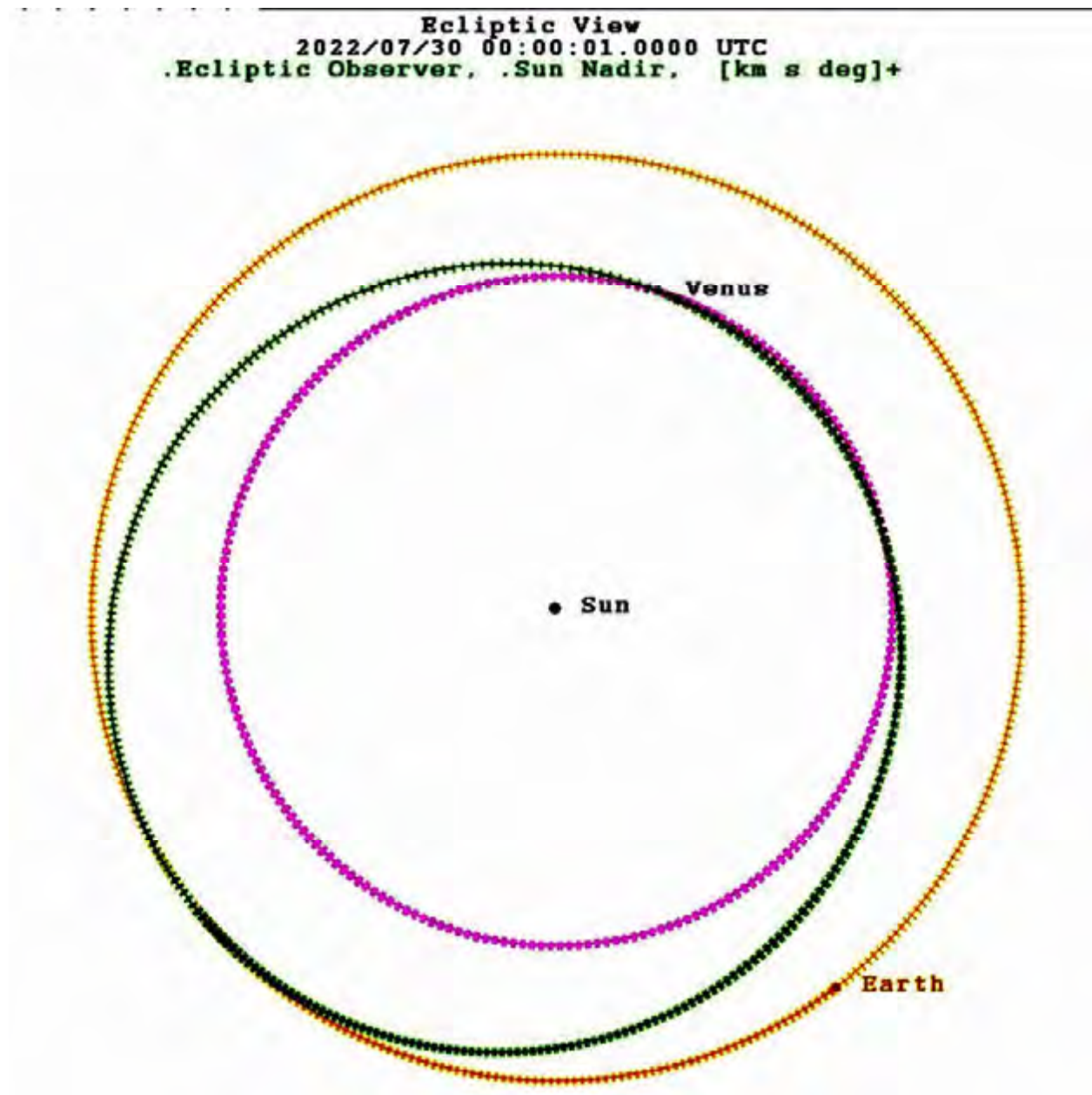


Figure 4.22: 2021 Type IV Earth/Venus trajectory.

Both spacecraft will be launched from the Cape Canaveral Air Force Station in Florida. The two launch vehicles are selected based on the required mass to be delivered to Venus, which is also affected by the chosen trajectory. The allowable injection mass for the Atlas V 551 L/V is a function of the C<sub>3</sub> value and in Figures 4.23 and 4.24 is plotted over the 21-day launch period for both the 2021 Type II

and Type IV launches. This launch period is required by mission design in order to account for launch uncertainties, such as the weather. Since the launch time is optimized for a midpoint, the required C<sub>3</sub> increases at the beginning and end of the window, while the delivered mass decreases. However, the change is less than 1.5%; this change is accounted for in the mission design.

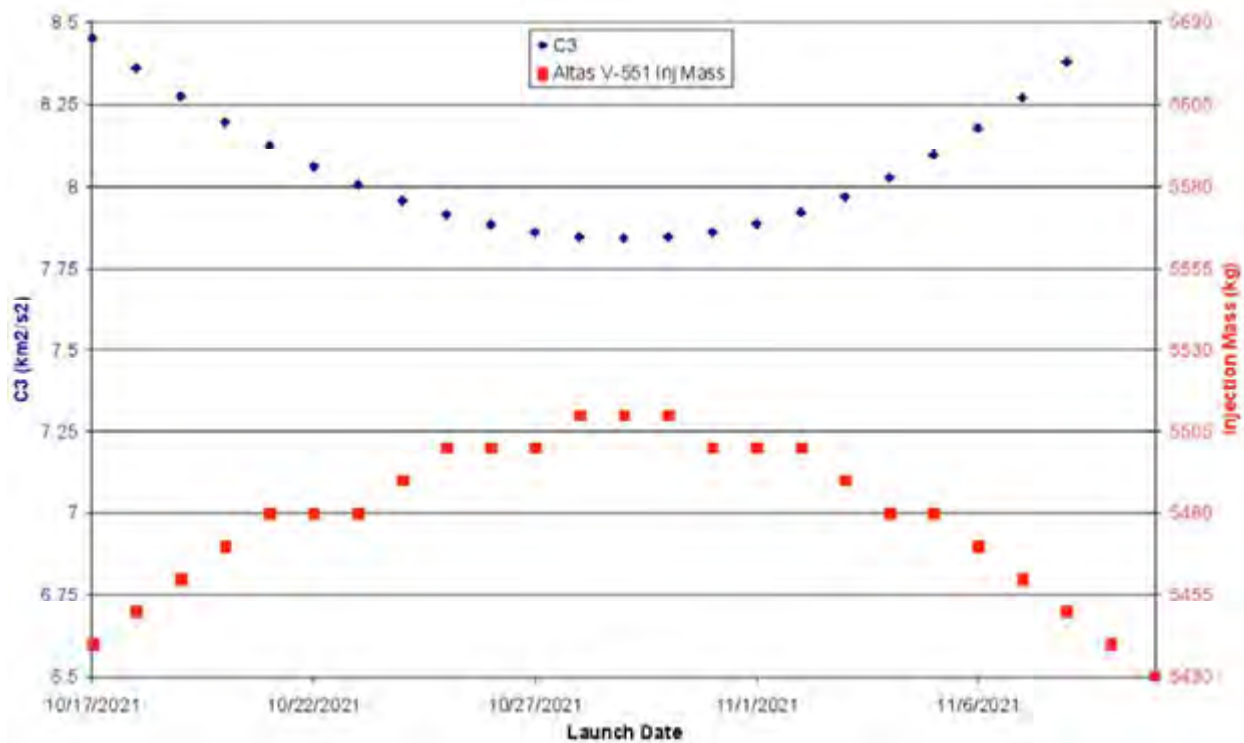


Figure 4.23: C3 and injection mass vs. launch date for 2021 Type II launch period.

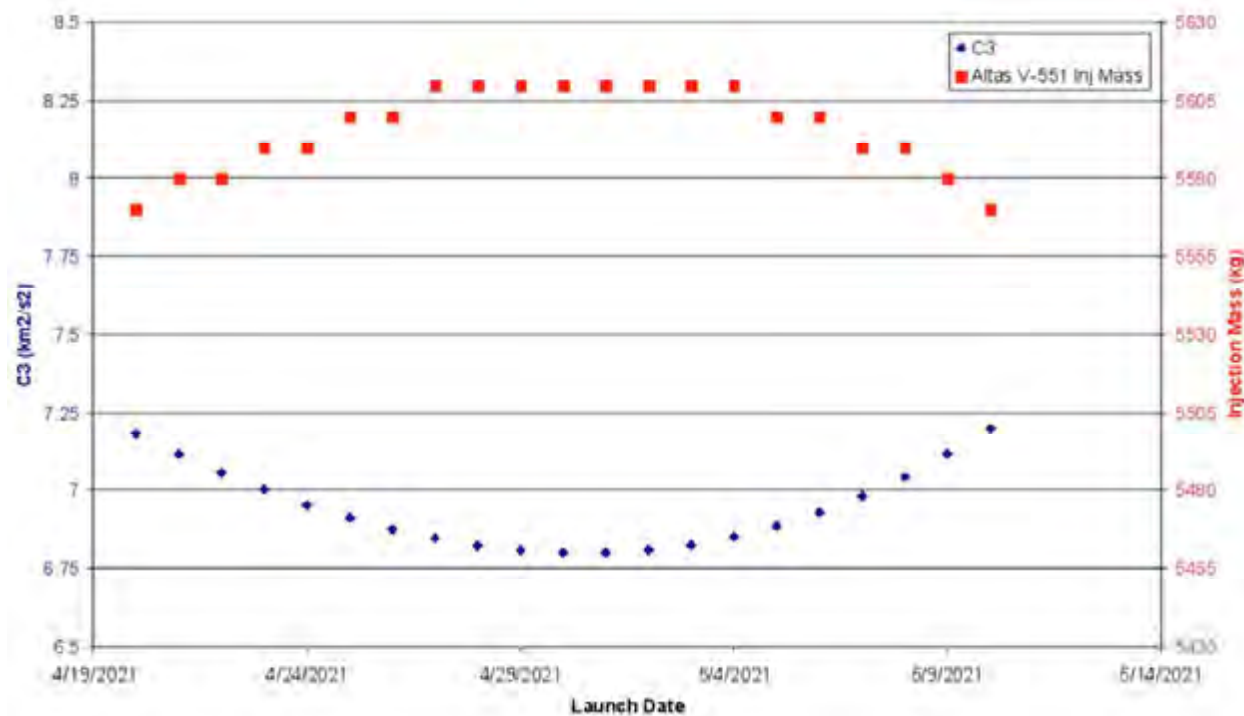


Figure 4.24: C3 and injection mass vs. launch date for 2021 Type IV launch period.

#### **4.4.3 Orbit Design and Landing Sites**

There are many constraints and requirements that must be satisfied to enable the orbiter to perform telecom relay functions for the two landers and two balloons. These include:

- The orbiter must be above  $15^\circ$  elevation from the landers for at least 8 hours to cover the entire lander descent and on-surface operations time period.
- The landers must be in view of the Sun (above  $\sim 20^\circ$  elevation) for imaging illumination.
- Entry flight path angles (EFPA) for the landers are calculated to be between a steep  $-40^\circ$  and a shallow  $-7.5^\circ$ . A steep EFPA would result in a Pioneer-Venus like entry, with high atmospheric entry heating rates and high g-loads. Entry with a shallow EFPA could accommodate a significantly lower heating rate, allowing for lighter TPS materials and low g-loads. Low g-loads could support RPSs on the in situ elements, although not used in the current DRM. Instead, in this design, the STDT selected landing locations driven by science objectives. These locations are accessible through entry trajectories with shallow EFPA. These EFPA also include an approximately  $1.5^\circ$  margin for targeting and atmospheric uncertainties. This margin is added to avoid skip out for the shallow EFPA cases and to provide an entry heating upper bound for the steep EFPA case.
- The allowable landing zone (bounded by shallow and steep entry flight path angles, latitudinal access, and the terminator for daytime landing), vary across the 21-day launch period; therefore, landing site selection must work for any launch date.
- The carrier must serve as an emergency telecom relay backup if the orbiter fails; therefore, the carrier also must have adequate visibility of the landing sites and sufficiently close distance during its flyby of Venus. Noted that this backup telecom capability is covering only the time period for the lander descent and surface operations, up to 6 hours, with a reduced data rate and volume. In addition, this backup capability will require the two entry systems to enter Venus simultaneously for an optimized close-range flyby distance. Consequently, the backup relay telecom results in a redesigned flyby trajectory, simultaneous entry and telecom coverage of the two landers, and lower data volumes and data rates, compared to the nominal configuration with staggered entry and telecom from both the balloon and the lander one entry at a time.
- For the nominal telecom, adaptive data rates (ADR) will be utilized. The relay telecom option will use a fixed data rate optimized for range. Both of these scenarios will be pre-programmed; in the case of orbiter failure, ground operation will make the decision to change the operational scenario to the backup relay telecom case. A fixed telecom data rate capability for the backup relay was chosen for its robustness, while accepting a lower data rate and volume. This backup scenario is not a mission design driver, but should be studied further in future assessments.

Trade studies based on these requirements and constraints resulted in the selection of an elliptical polar orbit for the telecom relay phase of the orbiter, with a periapsis altitude of 300 km, an apoapsis altitude of 40,000 km with an inclination of  $88.8^\circ$ . Figure 4.25 shows the incoming orbiter trajectory as well as the initial orbit. The orbiter must perform a large propulsive Venus Orbit Insertion (VOI) maneuver of approximately 1,800 m/s upon arrival at Venus.

The carrier's incoming trajectory was analyzed in conjunction with the orbiter design. Figure 4.26 shows the allowable landing site region that satisfies all of the constraints listed above. Given this area, the STDT identified two specific landing sites in different terrains for the DRM.

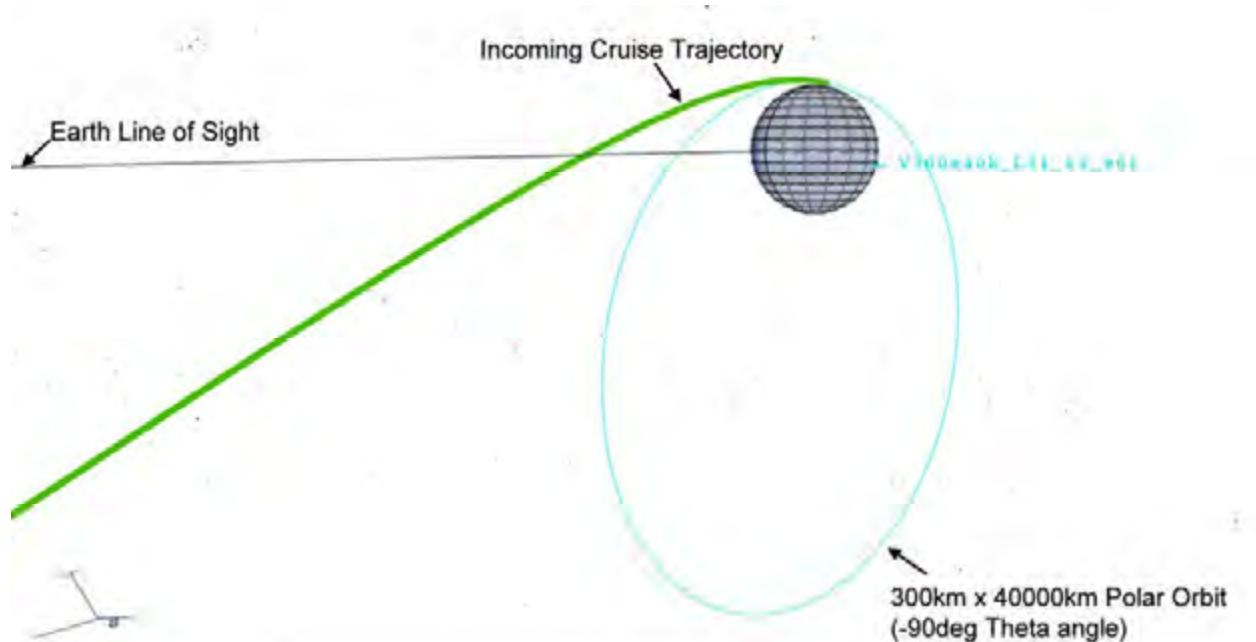


Figure 4.25: Incoming orbiter trajectory and post-VOI orbit.

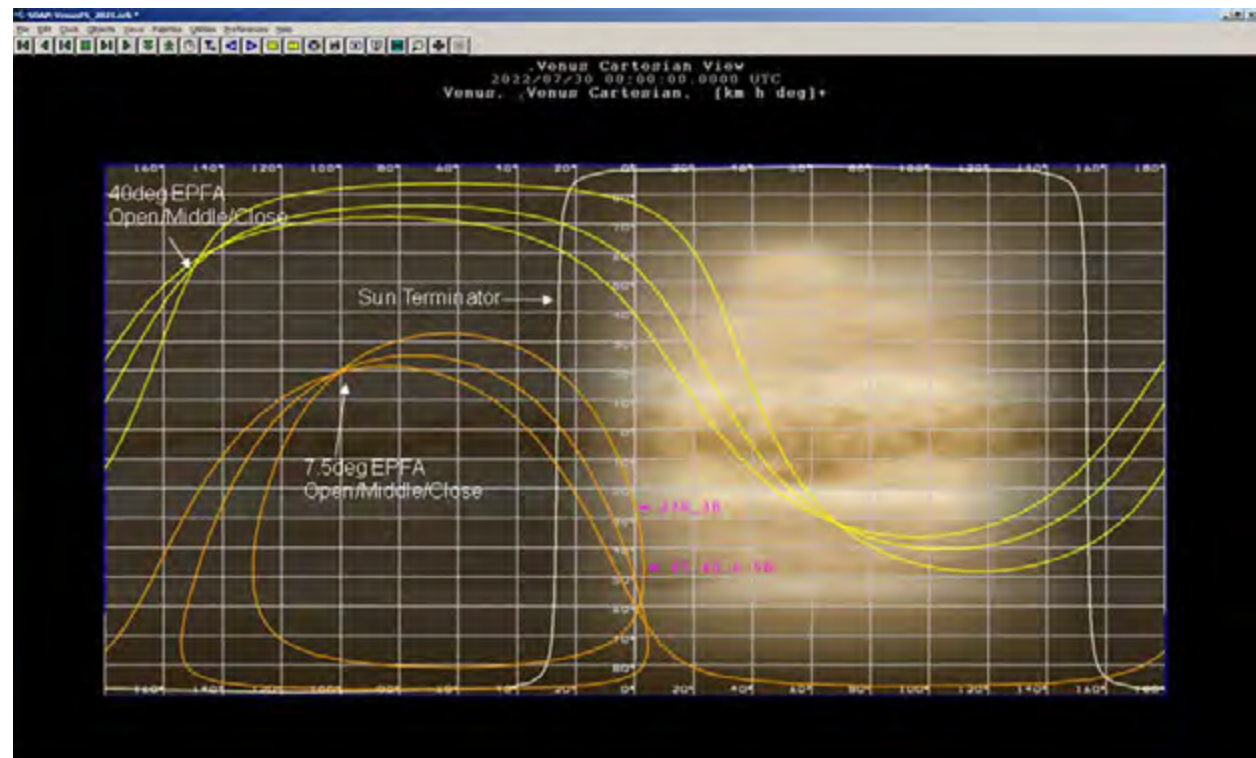


Figure 4.26: Landing area accessible from the 2021 launch opportunity. The orange lines denote the minimum flight path angle limits over the launch period and the yellow lines denote the maximum flight path angle limits based on entry deceleration. The DRM landing sites are noted with the pink latitude and longitude coordinates.

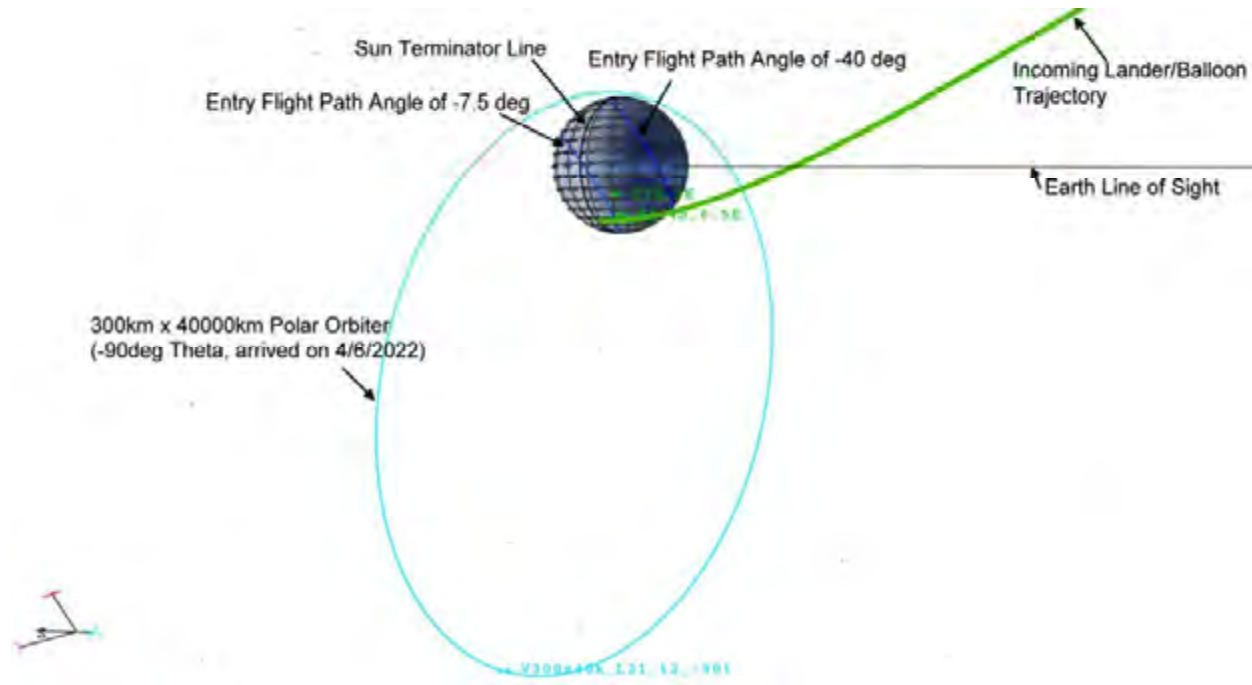


Figure 4.27: Incoming lander trajectory and orbiter.

These sites are 27° S, 3° E (Alpha Regio) and 47.4° S, 6.5° E (Lava Flow Fields). The science drivers for these landing sites are further discussed in Chapter 2.

Figure 4.27 shows the incoming lander trajectory and the orbiter at the time of arrival. Staggering the lander entries by one orbit revolution (13 hours) simplifies the telecom relay task (for example, antenna pointing) by having only one lander transmit at a time.

The carrier timeline during approach requires the release of the first and second entry vehicle 20 days and 10 days prior to arrival, with a re-targeting maneuver in between. The carrier will then perform another divert maneuver to target the required flyby trajectory.

Figure 4.28 shows the elevation angles from the two selected landing locations to the orbiter. Both have elevation angles above 15° for 8 hours or more, ensuring good telemetry coverage. Figure 4.29 shows the Sun elevation angles from the two selected landing locations. Both sites are in view of the Sun upon arrival, with elevation angles above 20° for several hours after arrival. Figure 4.29 also shows the Earth elevation angles from the two selected landing locations. Unfortunately there is not good visibility to the Earth for the two landers upon arrival. Only landing sites with high entry flight path angles (closer to the Earth line of sight) would be in view of the Earth upon arrival.

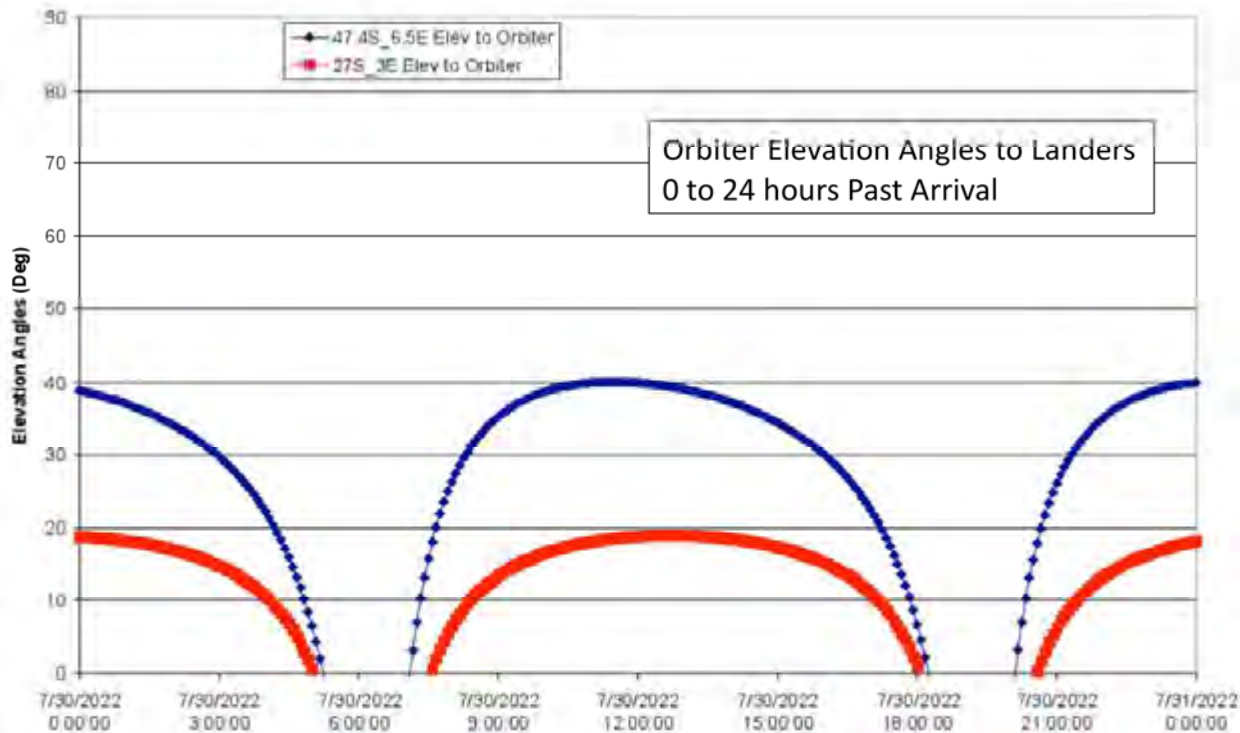


Figure 4.28: Orbiter elevation angles to lander upon arrival.

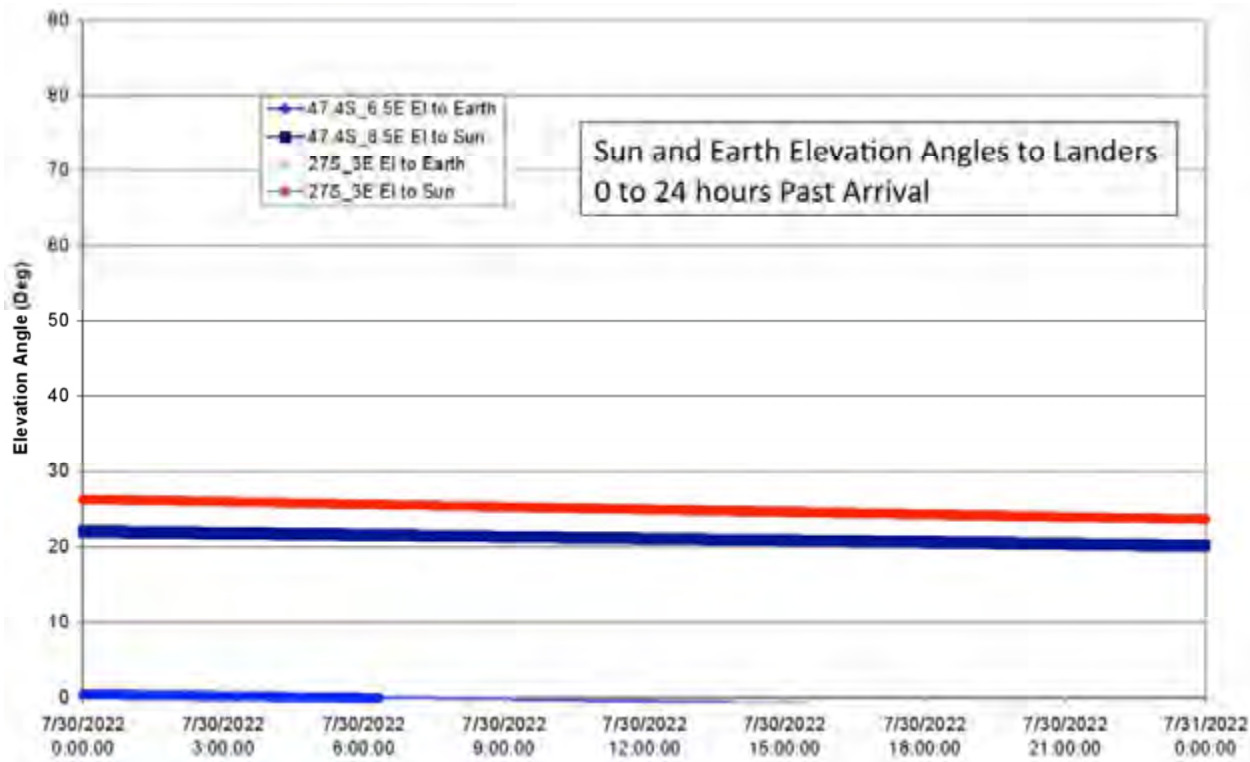


Figure 4.29: Earth and Sun elevation angles to lander upon arrival.

**Table 4.29:** Orbit Maintenance  $\Delta V$  vs. Altitude

Orbital Altitude	Maintenance $\Delta V$
200 km	~130 m/s per year
220 km	~37.5 m/s per year
230 km	~21 m/s per year
250 km	~7 m/s per year

#### 4.4.4 Orbiter Science Mission Design

The orbiter telecom relay mission phase ends 30 days after carrier arrival, at which point the balloons will have exhausted their electrical power supply and ceased transmission. The orbiter will then transition to a 230-km altitude circular orbit as required for the orbital science phase of the mission. Done propulsively, this transition would require about 2 km/s  $\Delta V$ . Therefore, the DRM will minimize propellant consumption by using aerobraking. The study team did not do a detailed design of the aerobraking phase of the mission but, instead, relied on the Magellan experience to indicate feasibility of this approach. For planning purposes, aerobraking was assumed to be executed over a 6-month period in four sub-phases: Walk-in, Main phase, Walk-out, and Transition. The Walk-in phase takes about two weeks and consists of numerous small maneuvers that lower the periapsis altitude from 300 km into the atmosphere with drag effects first detectable at about 140 km. The Main phase will last about three months and accomplishes the majority of the apoapsis reduction with atmospheric drag. During the Main phase, maneuvers will be executed to maximize aerodynamic drag, while ensuring a sufficiently low heating rate on the spacecraft during the atmospheric passes. During the Walk-out phase, the rate of aerobraking slows to maintain a 2-day orbit lifetime in case of a safing event. This phase lasts about one week. Over the course of the next few weeks, the Transition phase establishes the desired orbit for the orbital science phase.

Once in the final science orbit, the orbiter begins a 2-year primary orbital science mission. The 230-km circular polar orbit at 88° inclination requires 168 m/s of  $\Delta V$  per year for orbit maintenance. The 168 m/s is required to

maintain the orbital altitude in the presence of Venus' upper atmosphere. The 168 m/s is the sum total of 4 years' worth of maintenance maneuvers, amounting to about 42 m/s per year. Team X assumed that the orbiter was in a “polar” orbit: this could be 90° or 88° inclination. The solar activity level starts high during the proposed mission, meaning that maintenance maneuvers must be performed more frequently than later in the mission. The 42 m/s per year is an expected average  $\Delta V$  cost in the presence of the anticipated atmospheric density at 225-km altitude.

For example, the orbit maintenance  $\Delta V$  requirement associated with atmospheric drag is demonstrated in Table 4.29 using an assumed area of 20 m<sup>2</sup>, C<sub>d</sub> of 2, and mass of 1500 kg. The “Maintenance  $\Delta V$ ” is computed using the assumptions that (a) it does not account for the gradual decrease in mass from propellant usage and (b) the orbit precision is maintained very tightly.

#### 4.4.5 Mission Options

An analysis was performed to examine an alternate mission architecture consisting of nearly simultaneous launches of the two vehicles. This Side-by-Side Launch strategy sends both the orbiter and the carrier to Venus on Type II trajectories, with a minimum of 1 week between launches. The results showed that it was possible, but at the price of a slightly higher C<sub>3</sub> that would reduce the total launch injection mass capacity by about 250 kg (~4.5%). An additional drawback is that the orbiter arrives only 1.5 to 2 weeks before the carrier; an aggressive strategy in terms of ensuring that the orbiter is ready for the telecom relay phase. The combination of these two factors made this option less favorable and to be considered only as the backup option. Note, however, that the main benefit of the Side-by-Side launches is that the Venus-Earth

distance upon arrival is significantly less than that of the DRM approach (~120,000,000 km vs. 230,000,000 km, or 1.5 AU vs. 0.8 AU) and, therefore, allows for higher telecom rates from orbiter to Earth and improved prospects for direct-to-Earth telecom from the balloons during their missions.

The other significant mission alternative studied involved the next launch opportunity after the one chosen for the DRM. This 2023/2024 Type II and Type IV launch opportunity was shown to be feasible with comparable performance metrics. The main difference is that the allowable landing area moves from the southern to the northern hemisphere.

#### **4.4.6 Mission Timeline Details**

This subsection describes the DRM mission timeline in more detail. The mission architecture storyboard, shown in Figures 4.30a and 4.30b, consists of six key steps. Figure 4.30a shows the interplanetary trajectories and the mission phases associated with the two launches. Figure 4.30b provides a storyboard for the entry, descent, and landing phase (EDI) and Entry, Descent, and Landing (EDL) phases of the in situ elements.

- *Step 1:* The carrier S/C is launched first, on April 30, 2021, on an Atlas V 551 launch vehicle on a Type IV trajectory to Venus.
- *Step 2:* The orbiter S/C is launched second, on October 29, 2021, on an Atlas V 551 launch vehicle on a Type II trajectory to Venus. Although launched second, the orbiter will arrive first at Venus.
- *Step 3:* Following a 159-day cruise, the orbiter arrives at Venus on April 6, 2022. The orbiter then performs a large burn for the Venus Orbit Insertion (VOI) maneuver. The resulting highly eccentric 300 km × 40,000 km orbit was selected to provide telecom relay support for the in situ elements (balloons and landers) during their short lifetimes.
- *Step 4:* After 436 days of cruise, 20 days before the carrier flies by Venus, the entry system release sequence begins with release

of the first of the spin-stabilized entry vehicles. The carrier performs a small re-targeting maneuver and then releases the second entry system 10 days after the first (and 10 days before entry). The carrier's final re-targeting maneuver adjusts its Venus flyby timing and geometry to provide backup telecom support for the in situ elements.

- *Step 5:* The first of the two entry systems enters Venus's atmosphere and steps through the EDI phases for the balloon and the EDI phase of the lander. One orbiter revolution (13 hours) later, the second entry system enters Venus's atmosphere and repeats this entry and deployment sequence. The orbiter communicates with only one lander at a time (greatly simplifying orbiter antenna pointing requirements). The EDI and EDL steps are discussed below and illustrated in Figure 4.30b.

- *Step 5a:* The entry system carries a balloon and a lander.
- *Step 5b:* Its aeroshell protects the in situ elements from entry heating and aerodynamic forces until decelerating sufficiently to allow deploying a drogue parachute with mortar.
- *Step 5c:* The drogue further decelerates the system, which separates into two parts: the balloon and its gondola, helium inflation system, and main parachute; and the lander, with its main parachute. The backshell release operation will pull out the balloon main parachute, and the balloon flight train in turns pulls out the lander parachute. The balloon's flight train will descend at 5 m/s; the lander's flight train will descend at 7.5 m/s: this helps ensure proper spatial separation between the two systems. The balloon main parachute ensures that aerodynamic pressure on the balloon is within tolerable limits during the deployment and inflation process. The balloon will be released from its storage container at approximately 56-km altitude.

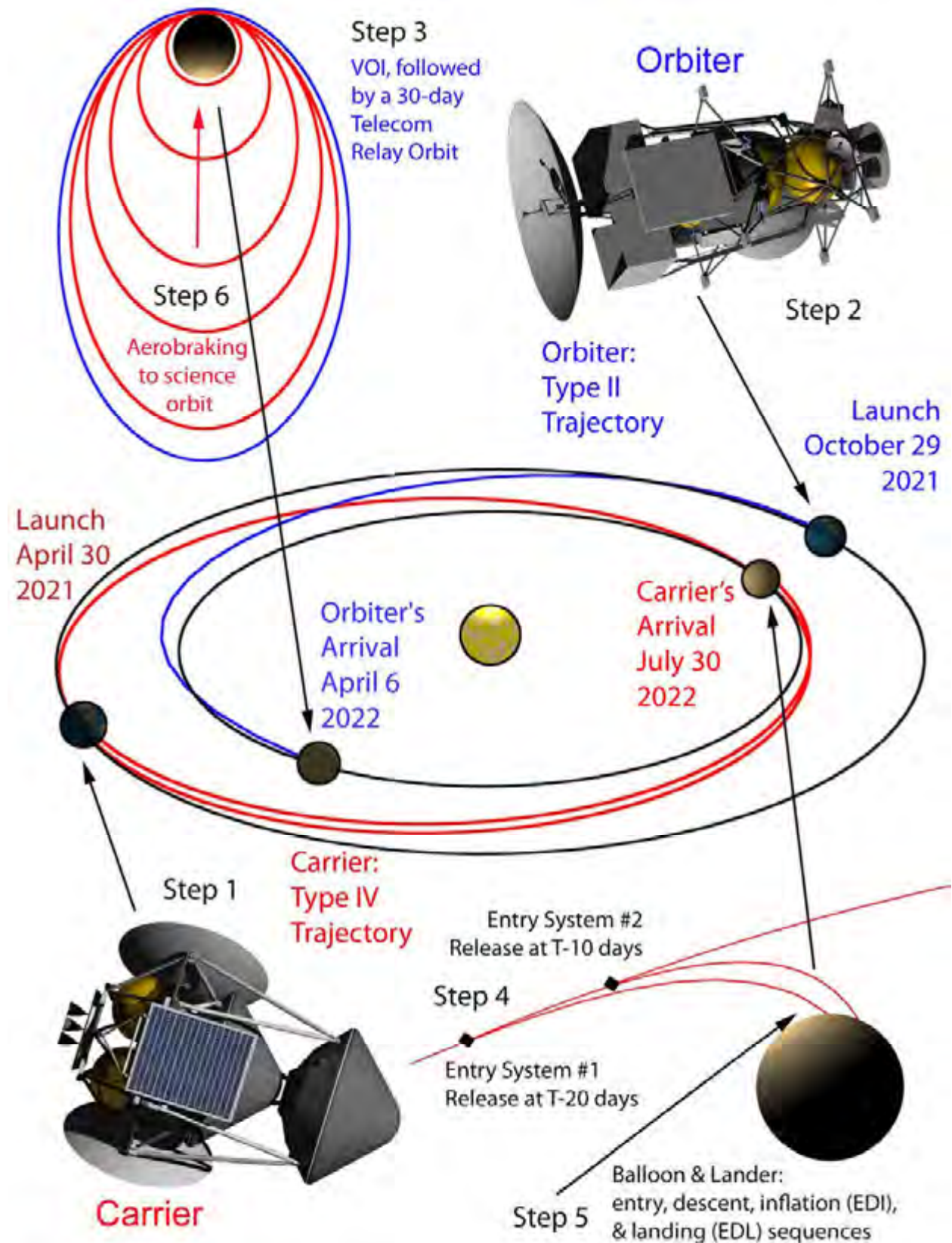


Figure 4.30a: Storyboard for the interplanetary trajectory phase of the Venus DRM.

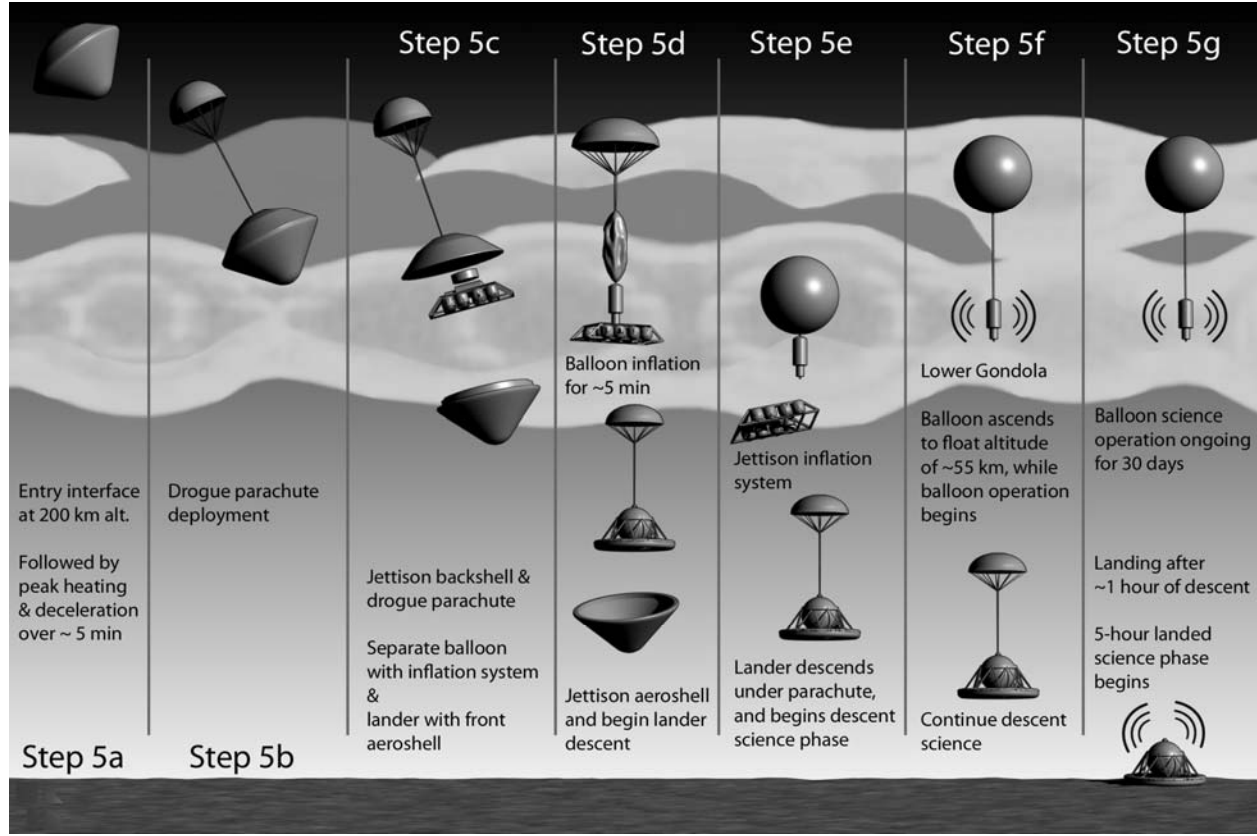


Figure 4.30b: Storyboard for the EDI and EDL phases of the in situ elements.

- *Step 5d:* Valves will be opened soon thereafter to begin the flow of helium gas into the balloon through a flexible pipe that connects to the high-pressure tanks. The balloon will be fully inflating in 5 minutes, at which time it will be ~1 km below its nominal 55.5-km equilibrium altitude.
- *Step 5e:* The helium inflation system will then be jettisoned, and the balloon, now fully buoyant, rises to the equilibrium altitude and begins its one-month science mission. During this time, the lander continues its descent to the surface, taking measurements along the way. The jettisoned helium tanks from the balloon will not hit the lander on the way down because they have very different ballistic coefficients and, therefore, adequate lateral separation will occur given the approximately 6 minute time delay between the separation events.
- *Step 5f:* Once the balloon is fully inflated and the helium tanks are jettisoned, the balloon ascends to its 55.5-km nominal float altitude while the cord connecting the balloon to the gondola is extended. The aerostat then begins its science operations phase.
- *Step 5g:* The lander will reach the ground after 1 hour of descent, followed by its 5-hour surface science operations phase. The collected science data is relayed to the orbiter throughout. The surface operation phase, including the drill location selection, sample acquisition, and analysis, is discussed in Subsections 4.5.5.9 and 4.5.5.10.
- *Step 6:* Once the in situ relay telecom support phase is completed, the orbiter performs an aerobraking maneuver over a 6-month period that reduces the orbit from

300 km × 40,000 km to a 230-km circular orbit for 2 years of orbiter science operations that complete the prime mission. The orbiter carries sufficient propellant for a 2-year extended mission after the prime mission. The baseline architecture includes only the short lived lander that operates on the surface for about 5 hours and the balloon that operates for ~1 month, requiring telecom support from the orbiter. For an extended surface mission beyond the baseline, a long-lived element could operate on the surface over a Venus-day of 243 Earth days. (This would not affect the baseline balloon lifetime.) In this case, the orbiter would stay on its elliptic telecom relay orbit and initiate its aerobraking maneuver once this data relay function is no longer required. Such an extended surface mission phase would increase the overall mission lifetime by 243 days and delay the orbiter science phase by the same duration. It would also impact mission cost to account for the additional operational costs. Since the orbiter science phase is baselined for only 2 years, this extension due to the long-lived in situ element, could still be accommodated within the additional 2 years, supported by the propellant margin.

Further details on the timeline are provided in Figure 4.31.

## 4.5 Vehicle Descriptions for Mission Elements

This section provides detailed descriptions of all spacecraft elements of the DRM, grouped in subsections for the orbiter, carrier, entry vehicle, balloon, and lander. Additional information is provided at the end on the other associated mission architecture elements, including mission operations, ground data system, and programmatic.

The DRM uses the JPL Team X design approach of adding a 43% contingency on the current best estimate (CBE) mass. In the mass tables presented later in this section, some mass contingency is added directly to specific spacecraft elements and then a lump sum

“system” contingency is added at the end to make the overall total contingency equal 43% of the CBE.

### 4.5.1 Orbiter

#### 4.5.1.1 Overview

As discussed in Section 4.4, the orbiter will be launched on a fast Type II trajectory approximately 6 months after the carrier launch. After inserting into a highly eccentric Molniya-like orbit (300 km × 40,000 km) with a 13-hour period, the orbiter will have sufficient time for spacecraft checks before the arrival of the in situ elements (balloons and landers) ~3.5 months later. In the first phase of the mission, the orbiter spacecraft provides telecom relay support between the in situ elements and Earth. The planned 1-month lifetime of the balloons defines the duration of this mission phase. Aerobraking over a period of 6 months achieves the transition from this telecom orbit to a low circular (230 km) orbit for the second phase: namely, for the orbiter science investigations. While it is expected that the specified 2-year primary science mission will accomplish all of the required orbital science objectives, the propellant reserves will accommodate an additional 2 years of extended mission if the decision is made to do so.

The orbiter design is driven primarily by the large power system, the radar instrument, and the mission design that includes vastly different orbits for telecom relay and science. Specifically, the size of the InSAR instrument is not only a significant mass driver, but it also demands high power. Data storage requirements (C&DH) and thermal design also influence the power system design. Solar panels must be sized accordingly, and designed for the high solar flux at Venus orbit. The propellant mass is sized for the large 1,800-m/s Venus Orbit Insertion (VOI) maneuver (that includes 5% gravity loss and further contingency) and for additional propellant needed for aerobraking and science orbit maintenance. The orbiter ΔV requirements are listed in Subsection 4.5.1.5, Table 4.31.

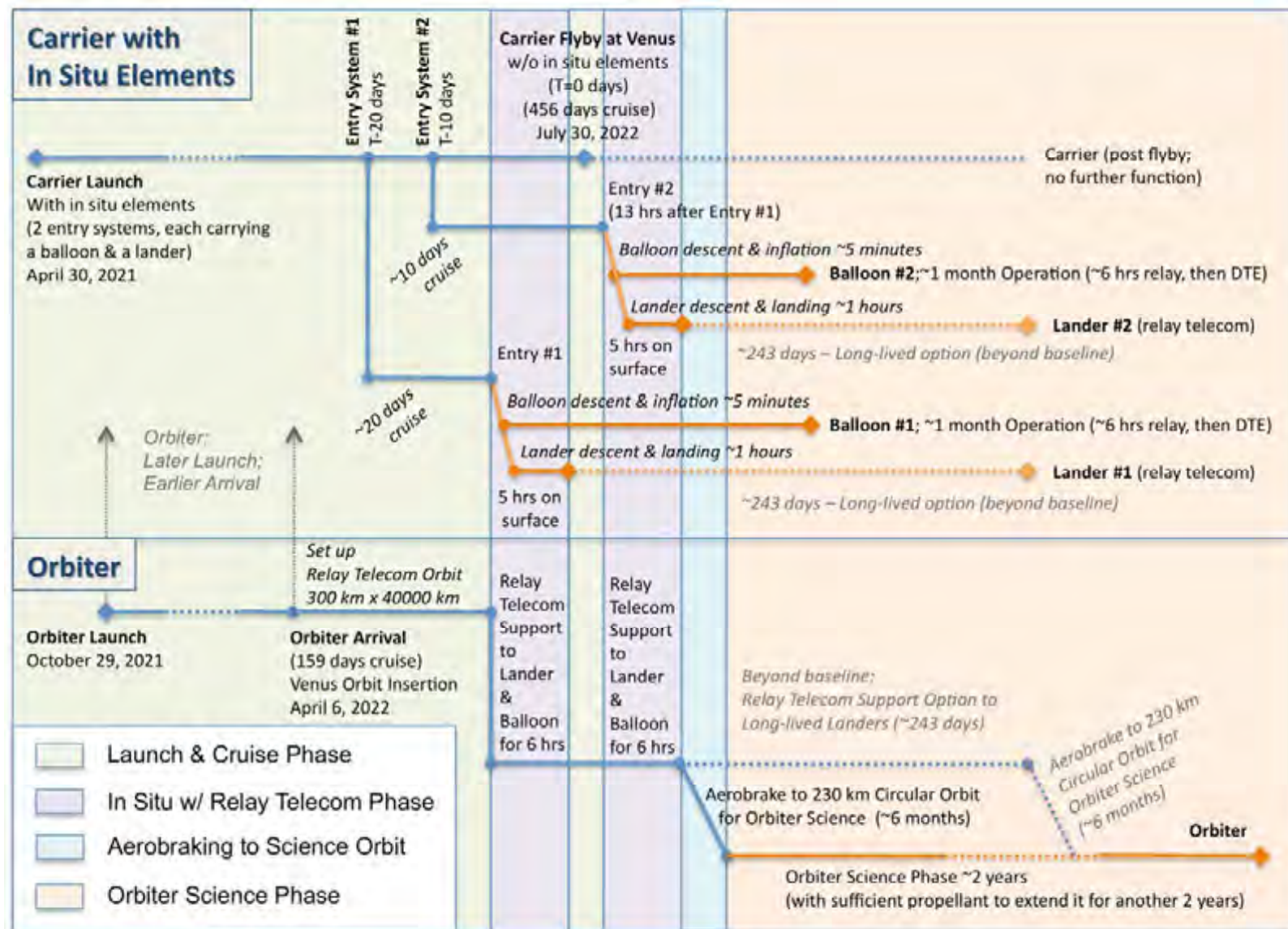


Figure 4.31: Detailed timeline for the Venus DRM.

**Table 4.30:** Orbiter Mass Summary.

Element	CBE Mass (kg)	Cont. (%)	CBE+Cont. (kg)
<b>Payload on Orbiter</b>			
Vis-NIR Imaging Spectrometer	33.1	20	39.7
InSAR	157.0	30	204.1
Submillimeter Sounder	19.9	20	23.9
Magnetometer	4.4	20	5.3
Langmuir Probe	0.5	20	0.6
Neutral Ion Mass Spectrometer	13.2	20	15.8
Radio Subsystem	1.0	0	1.0
<b>Payload total</b>	<b>229.1</b>	<b>26.8</b>	<b>290.4</b>
<b>Spacecraft bus</b>			
Attitude control	62.0	19	74.0
C&DH	36.9	30	48.0
Power	210.7	30	274.0
Bi-Prop System	233.8	27	296.0
Structures and Mechanisms	426.6	30	554.6
S/C-Side Adapter	38.2	30	49.6
Cabling	93.5	30	121.6
Telecom	145.6	15	167.2
Thermal	114.6	30	148.9
<b>Bus Total Mass</b>	<b>1362.0</b>	<b>27.3</b>	<b>1733.8</b>
<b>System Level Contingency</b>			<b>251.1</b>
Bus + Payload Dry mass	1591.1	27.2	2275
Propellant and Pressurant			3030.4
<b>Spacecraft CBE + Contingency (Wet)</b>			<b>5306</b>
Launch Vehicle Capability		Atlas V 551	5450
Launch Vehicle Margin		2.6%	144

NOTE: Total contingency is  $(290.4 - 229.1) + (1733.8 - 1362.0) + 251.1 = 684.2$  or 43% of the 1591 kg dry S/C CBE mass.

From these, the resulting wet and dry launch masses are 5306 kg and 2024 kg, respectively, including subsystem heritage contingency. The design margin is 43% on dry mass. The launch vehicle capability is 5510 kg, providing an additional 204 kg (3.7%) launch vehicle margin. The power system, using solar panels, will provide 9868 W EOL at Venus and would include 2 secondary batteries with a storage capacity of 12096 Wh. The payload would include seven instruments: specifically, an InSAR; a Vis-NIR imaging spectrometer; a neutral ion mass spectrometer; a submillimeter sounder; an ultra-stable oscillator (uso); a magnetometer; and a Langmuir probe. Details on the orbiter instruments are given in Subsection 4.3.1. A summary of the orbiter mass allocation is shown in Table 4.30. The

power allocation for the orbiter, including the instruments, is provided in Subsection 4.5.1.4.

#### 4.5.1.2 Orbiter Attitude Control System (ACS)

The pointing stability of the orbiter is driven by the bounding conditions between the telecom relay from: (a) the in situ elements and the orbiter; (b) the orbiter and Earth; and (c) orbiter pointing for InSAR measurements during the science orbit period, requiring an accuracy up to 1 arcsec/sec. In addition, the solar arrays will use two 2-axis gimbals for pointing. The large 4-m X/Ka-Band high gain antenna (HGA) will be attached to the bus via a 2-DOF gimbal mechanism and requires a pointing control of 108 arcsec ( $3\sigma$ ) for telecom back to Earth. The InSAR instrument requires pointing control, knowledge, and stability of

150 arcsec ( $3\sigma$ ), 50 arcsec ( $3\sigma$ ), and 1000 arcsec/sec ( $3\sigma$ ), respectively. Orbiter pointing control, knowledge, and stability was designed to 108 arcsec ( $3\sigma$ ), 50 arcsec ( $3\sigma$ ), and 1000 arcsec/sec ( $3\sigma$ ), based on the HGA and InSAR requirements and those of the other orbiter science instruments. The design also allows for a maximum of 2 slews within the mission duration, although it was not a design-driving requirement.

A design trade study led to the conclusion that reaction wheels were the preferred low-mass option for achieving this level of attitude control compared to thruster-only control. Consequently, the orbiter will employ 3-axis stabilization with reaction wheels for fine pointing and thrusters to unload the wheels. A redundant set of four Honeywell HR14 reaction wheels will be set up in a pyramid configuration, with a 53-Nms momentum storage capacity. The inertial stellar attitude determination for the spacecraft bus is achieved using two Galileo AA-SRT star trackers with accuracy within  $\pm 3.0$  arcsec (Pitch/Yaw) at  $3\sigma$  and  $\pm 30$  arcsec (Roll) at  $3\sigma$ . For a redundant Inertial Measurement Unit (IMU), 2 Honeywell MIMU YG9666B gyros were considered, with a low 0.005%/hr bias stability, which can propagate attitude for long intervals (e.g., hours). Safing operations and attitude re-initialization is supported with 16 inexpensive and high-flight-heritage Adcole Coarse Sun sensors, providing  $2\pi$  steradians coverage. Proper calibration of the InSAR system might require a metrology system to precisely measure the distance and orientation of the two antennas. Such a system was included in the DRM using the aircraft-borne JPL GeoSAR system as a proxy, scaled down to two cameras and two lasers (as compared to 8 and 5 for GeoSAR).

The current ACS design will employ a test bed that includes a full set of reaction wheels, one star tracker, and one IMU. The test bed would also include a full set of spares and redundant hardware. ACS hardware components (e.g., the star trackers and the metrology system) and algorithms have high space flight heritage and would only require

minimal technology development before the technology cutoff date. The ACS hardware and algorithms, therefore, represent low risk.

#### **4.5.1.3 Orbiter Command and Data Handling**

The Command and Data Handling (C&DH) system is designed with dual-string redundancy and a cold spare, with a design lifetime of  $\sim 4$  years, including a 1-year cruise. The main driver for C&DH is the InSAR instrument, requiring onboard storage for as much as  $\sim 1.4$  Tbits of data that could be collected over a single orbit, assuming an uncompressed data rate of 260 Mb/s in continuous InSAR operating mode. Overall, the C&DH system must be compatible with the objective of delivering  $\sim 300$  Tbits of data to Earth over 2 years of science operations.

The C&DH core functions are performed using the JPL in-house flight computer system known as MSAP (Multi-Mission System Architecture Platform). For planning purposes on the DRM, the non-volatile memory (NVM) card and solid-state recorders (SSR) were assumed to use off-the-shelf components from SEAKR Engineering Inc. New development requirements include a Mission Unique Card (MUC), in the form of a compact PCI (cPCI) 6U card, providing high-speed interface to the SSR. A modified MSAP Telecommunications Interface (MTIF) will boost downlink data rate to 15 Mb/s. The system would also include two instrument digital electronics cards, co-located in the C&DH chassis, while interfacing with the C&DH system through cPCI.

Each of the two strings consists of the following MSAP components: (a) one Space Flight Computer (SFC) cPCI board, containing a RAD750 processor that runs up to a clock rate of 132 MHz, a 256-KB non-volatile EEPROM memory for storing the initial boot-loader program, and a 128-MB DRAM for software code execution, heap storage, etc.; (b) one SEAKR 96 GBytes Flash Memory Card (FMC) cPCI board; (c) one MTIF cPCI board, which provides an interface to the telecom S-Band Transponder, and a MID-STD-1553B Bus Controller interface; (d) one PPC cPCI

board, providing power to all cPCI boards; and (e) one MREU board, providing a MID-STD-1553B Remote Terminal (RT) interface over 120 Analog Channels and Discrete I/Os, and including an internal power supply and a collection of spacecraft engineering telemetry. All of the components would be housed in a single chassis. The solid-state recorder is designed with a SEAKR 1.6 Tbits model, which is shared between the two strings and is internally redundant. SEAKR 1.6 Tbits model can achieve a data transfer rate of 2 Gb/s.

#### 4.5.1.4 Orbiter Power System

The power system consists of solar arrays, secondary batteries, and supporting power electronics. Power system sizing is primarily driven by the second phase of the mission; that is, during the orbiter's science orbit using InSAR while communicating the multi-terabyte amount of data at high data rates when Earth is at a maximum distance of 1.72 AU.

The 32-m<sup>2</sup> rigid and deployable solar panels are mounted in a dual-wing configuration, producing 9868 W at EOL. For enhanced front-side radiation, 25% of the available cell area is devoted to Optical Solar Reflectors (OSR). Heating of the solar panels is the largest risk item for the Venus orbiter. Heating can occur from three sources: (1) solar flux, (2) reflected IR from the planet, and (3) atmospheric heating during the aerobraking phase. The design must maintain acceptable temperatures; thus, the cell packing factor is reduced from 90% to ~70%. To mitigate the high heat flux induced thermal warping and the related interconnected fatigue at Venus orbit, the solar panels employ a carbon rib-reinforced carbon facesheet design. This design should prevent warping during transitions between night and day orbit phase passes.

Two secondary batteries are included in the design. These batteries have a power storage capacity of 12096 W-hr, assuming 40% DOD. The batteries are sized to support the orbiter during the 38.5 minutes eclipses, when the orbiter is on its 230-km circular 91.5 minutes period orbit. They might be also used if the

power needs to be augmented during high-power operating modes (e.g., Topo Radar Science mode with telecom).

In addition to the power generation and storage elements, the baseline design includes a typical 28-V DC electrical bus. While it is beyond the scope of a pre-Phase A design, it is conceivable that the high power requirement for the instruments may require a bus redesign to higher voltage levels (e.g., 48V, 75V, or 100V), in order to deliver the required power without excessive amperage levels.

From an operational point of view, eight distinct power modes were identified, covering all relevant operating modes foreseen for all mission phases between launch and science operations. The power modes are:

- Mode 1: Earth Telecom: 1336 W.
- Mode 2: Topo Radar Science mode with Telecom: 4937 W.
- Mode 3: Topo Radar Science mode without Telecom: 4354 W.
- Mode 4: Safe mode: 1767 W.
- Mode 5: Cruise phase: 1756 W.
- Mode 6: Trajectory Correction Maneuver (TCM): 1644 W.
- Mode 7: Relay Telecom mode in support of the in situ elements: 1741 W.
- Mode 8: Instrument phasing low power mode: 1358 W.

#### 4.5.1.5 Orbiter Propulsion System

The propulsion system on the orbiter is used during Venus Orbit Insertion (VOI), aerobraking maneuvers, orbit maintenance, and momentum wheel unloading and is designed with expendables for a 5 years of operation (i.e., 1 year cruise, 2 years science, and 2 years extended mission).

The assumption is that a precursor flagship mission, such as one of the proposed Outer Planet Flagship Missions (OPFM) to either Titan or Europa, will space qualify the “Bang-Bang” pressure control hardware, software, and electronics. The use of one of the two 900-N gimbled, dual-mode, HiPAT main engines is assumed for the 1.15-hour Venus

Orbit Insertion. The two-engine design is based on Cassini heritage. Future trade studies should assess whether a single or dual main engine configuration is needed to meet throughput, performance, and reliability needs for the Venus DRM in light of the Outer Planets Flagship Mission designs using a single main engine. The fuel and oxidizer are pressurized separately, using a single 48.9" ID titanium tank with titanium PMD for each (with ETS-8 heritage). Smaller thrusters are also used during other mission phases. For momentum wheel unloading, safe mode turns, attitude control, and for small  $\Delta V$  requirements sixteen 4.5-N monopropellant thrusters will be employed. For slightly larger  $\Delta V$  needs, eight 22-N monopropellant thrusters can be used.

The  $\Delta V$  requirements for the orbiter are shown in Table 4.31.

#### 4.5.1.6 Orbiter Structures and Mechanisms

The orbiter structure consists of a strut truss built around propellant tanks, consisting of aluminum, titanium, and composite materials. In the stowed configuration, the spacecraft will fit in an Atlas V 5-m medium fairing (Figure 4.32). The mass estimate for the orbiter structure and mechanisms is 554.6 kg, considering a 30% contingency (see Table 4.32). When deployed, the InSAR reflector arrays will be canted 45 degrees from each other, separated 9 m apart, with the entire system canted 30 degrees from nadir. Each reflector array is fed by an X-Band phased array feed. The 4-m diameter Ka/X-Band antenna can be pointed in both axes, and solar arrays can track the Sun in one axis (Figure 4.1).

**Table 4.31:**  $\Delta V$  Requirements for the Orbiter

Item	$\Delta V$ requirement
<b>Cruise and Approach:</b>	
Launch:	0
TCM1:	40 m/s
TCM2:	10 m/s
TCM3:	5 m/s
TCM4:	5 m/s
<b>Orbit Insertion:</b>	
VOI (Impulsive): (300 x 40,000 km orbit)	1710 m/s
VOI (gravity losses): (-5% gravity losses due to the 1.1-hour burn arc)	85.5 m/s
VOI Fault Recovery: (mid-burn interruption/restart)	20 m/s
<b>Lander Relay:</b>	
Orbit Phasing: (conservative)	20 m/s
<b>Aerobraking:</b>	
Walk-in: (14.6 m/s + contingency, to drop periapse to 140 km)	20 m/s
Main Phase: (bring orbit down to 140 x 230 km)	100 m/s
Walk-out: (17.4 m/s + contingency: 230x230 km orbit)	27 m/s
Pop-up contingency: (in case the orbiter has to perform an emergency pop-up maneuver for any reason)	20 m/s
Additional contingency:	30 m/s
<b>Primary science:</b>	
Orbit Trim Maneuvers - maintain a 230 km altitude; maneuvers performed about once a month for 4 years.	: 168 m/s
<b>End-of-Mission:</b>	
Final: (passive descent into Venus' atmosphere)	0
Total DV:	2260.5 m/s

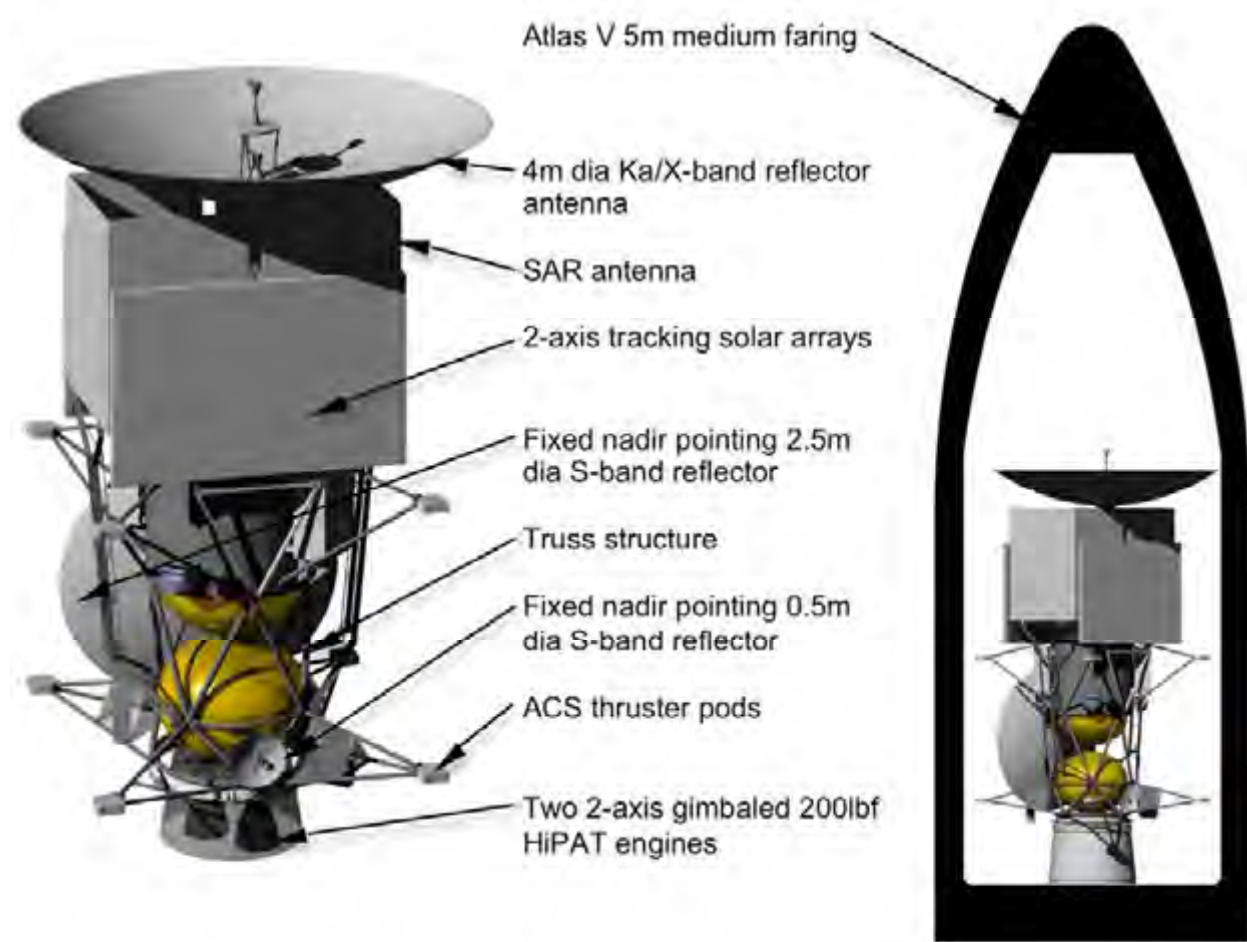


Figure 4.32: Orbiter in stowed configuration (left) and inside fairing (right).

**Table 4.32:** Mass Breakdown for Orbiter Structure and Mechanisms.

Element	Units	Mass (kg)
Primary Structure	1	333.5
Secondary Structure	1	29.7
Instrument Mounts	1	23.8
Solar Array Structure	2	53.8
Solar Array Drive Assemblies 2-axis per array	2	18.2
Solar Array Latch/Release + Booms	2	19.2
Antenna Gimbal Assemblies 2-axis per antenna	1	11.7
Main Engine Gimbal	2	14.8
InSAR Launch Restraint	2	2.0
Main Engine Boom	2	4.1
Integration Hardware	1	23.3
Balance Mass 3-axis	1	20.4
<b>TOTAL (less S/C-side adapter)</b>		<b>554.6</b>
Adapter, Spacecraft side	1	49.6
Cabling Harness	1	121.6

#### 4.5.1.7 Orbiter Telecom System

Based on science and mission requirements, the orbiter telecom subsystem must provide:

1. High downlink rates for science data during the orbiter science phase.
2. Store-and-forward relay services for Venus in situ elements (landers, balloons).
3. Reliable, low-rate engineering command and telemetry links for critical events (launch, VOI) and safemode.

Thirty-four-meter DSN antennas will be used during normal operations, with 70-m (or equivalent) antennas assumed available only for safemode and critical events.

The orbiter telecom subsystem consists of an X-Band and Ka-Band system for communicating with the Earth and an S-band system for relay with in situ assets. Block diagrams of the orbiter X/Ka-Band and S-Band systems are shown in Figure 4.33 and Figure 4.34, respectively.

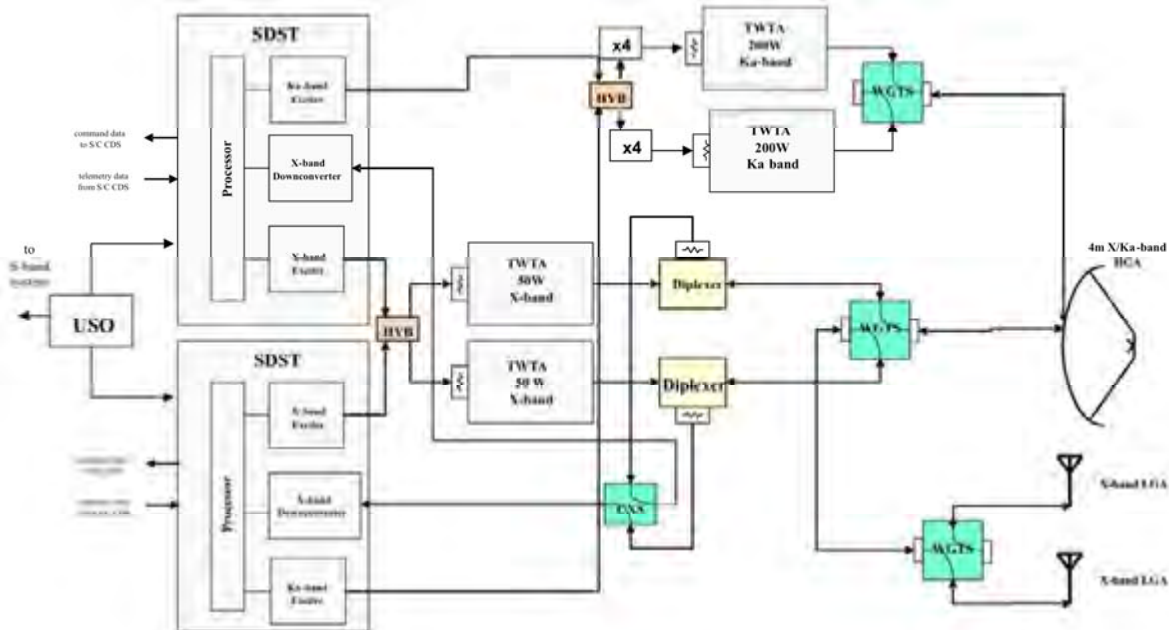


Figure 4.33: Block diagram of the orbiter's X/Ka-Band system.

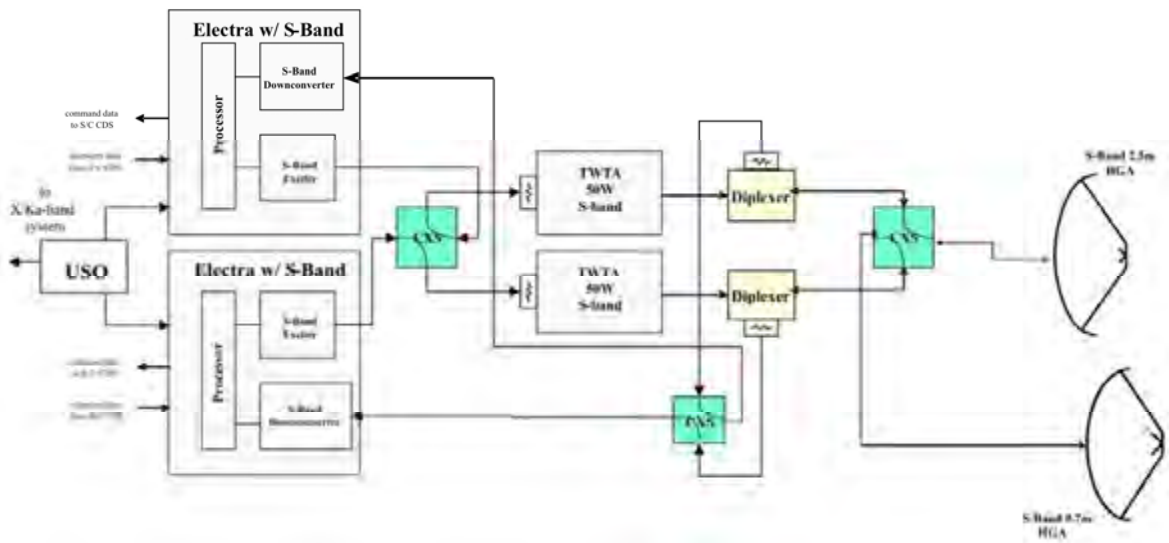


Figure 4.34: Block diagram of the orbiter's S-Band system.

Significant features of the telecom design include the following:

- Redundant cross-strapped X/Ka-Band Small Deep Space Transponders (SDSTs).
- Redundant cross-strapped S-Band Electra transceivers.
- One Ultra-Stable Oscillator (USO) for radio science.
- Redundant cross-strapped 200 W Ka-Band traveling wave-tube amplifiers (TWTAs).
- Redundant cross-strapped 100-W X-Band TWTAs.
- Redundant cross-strapped 50 W S-Band TWTAs.
- One 4-m, dual-feed X/Ka-Band, articulated high gain antenna (HGA).
- One 2.5-m S-Band fixed HGA.
- One 0.7-m S-Band fixed HGA.
- Two X-Band low-gain antennas (LGAs).

The orbiter-Earth communications design is primarily driven by the extremely high rate requirement of the InSAR instrument, which produces data at rates ranging from 100 to 260 Mb/s (uncompressed) and 1 to 100 Mb/s (compressed). To maximize the science downlink rate, Ka-Band was selected because it offers better link performance than X-Band assuming equivalent telecom hardware and 34-m DSN tracking. An X-Band system is also included for uplink commanding and for high- and low-rate communications during cruise, safemode, and critical events. During the orbiter science phase, the primary data link is the Ka-Band although, in principle, X-Band downlink can be used simultaneously with Ka-Band to enhance science return and/or serve as an operational backup to Ka-Band. For example, the X-Band downlink could be used when bad weather is expected at the ground tracking station or if there are hardware failures that affect the Ka-Band system or the

ability to point the HGA accurately. These options can be considered in future studies.

Design control tables (DCTs) containing the representative link performance for the orbiter are shown in Tables 4.33, 4.34, 4.35, and 4.36. At the maximum Earth-Venus range of 1.72 AU, the Ka-Band system with a 4-m HGA and a 200-W TWTA supports a downlink rate of nearly 15 Mb/s, assuming availability of high-rate LDPC coding. HGA boresight pointing accuracy of 0.5 mrad or better is achieved with a closed-loop pointing system using two star trackers mounted directly to the HGA structure. The X-Band system can support a downlink rate of nearly 1.5 Mb/s (with Turbo coding) or 1.3 Mb/s (with LDPC coding). Figure 4.35 shows the HGA data rate profile for up to a 4-year science mission, assuming LDPC coding with a maximum data rate of 75 Mb/s. (Note that this maximum data rate is not utilized in the baseline design, as the orbiter C&DH configuration only supports data rates up to 15 Mb/s.) For safemode communications, 10 b/s on the LGA is supportable up to 45-deg off point to a 34-m and 75-deg off boresight to a 70-m (or equivalent). Further trades can be performed to improve the safemode link capability (e.g., higher X-Band TWTA power, broader beam LGAs, or more LGAs).

A summary of cumulative downlink data volume, assuming 8 hours of DSN tracking per day, is shown in Table 4.37. Even if we consider only the minimum supportable data rate of ~15 Mb/s with a Ka-only downlink, the orbiter returns more than 300 Terabits (Tbits) in the first 2 years. Using actual supportable Ka-Band data rates, the orbiter could return nearly 800 Tbits. Table 4.37 also illustrates that using X-Band simultaneously with Ka-Band can significantly enhance data return with rates over 10 Mb/s when the Earth-Venus range is 0.65 AU or less.

**Table 4.33:** Orbiter Science Downlink, 200-W Ka-Band,  
4-m HGA, 0.5-mrad Pointing Error, 34-m DSN.

200.0 W TWTA					
Ka-Band HGA, 4 m antenna diameter, 0.03° (0.5 mrad) off-point		2.573E+08		Range, km	
DSN 34 m station /Configuration: X/Ka RCP		1.7200		Range, AU	
Canberra/20 deg. elevation/90% CD Weather (Year Average)		0.24		OWLT, hrs	
Hot body noise = 3 K		20		SEP, deg	
2-way coherent		20		Elev Angle, deg	
Tlm channel/ LDPC AR4JA ( $n=16,384$ , $k=8,192$ )/ FER=10 <sup>-6</sup>					
Link Parameter	Unit	Design Value	Ka 32000	RF band Freq, MHz	
<i>TRANSMITTER PARAMETERS</i>					
1 S/C RF Power Output	dBm	53.01	200	Xmtr Pwr (W), EOL	
2 Total Circuit Loss	dB	-1.50			
3 Antenna Gain (on boresight)	dBi	59.95	0.16	3 dB Beamwidth	
4 Ant Pointing Loss	dB	-0.37	HGA	S/C Antenna	
5 EIRP (1+2+3+4)	dBm	111.10			
<i>PATH PARAMETERS</i>					
6 Space Loss	dB	-290.76			
7 Atmospheric Attn	dB	-1.16	90 Year Average	Weather % Distribution Type	
<i>RECEIVER PARAMETERS</i>					
8 DSN Antenna Gain	dBi	78.78		Canberra: 34mBWG, DSS34	
9 Ant Pointing Loss	dB	-0.10	n/a	LNA Selection	
10 Polarization Loss	dB	-0.04	X/Ka RCP	DSS Config	
<i>TOTAL POWER SUMMARY</i>					
11 Total Rcvd Pwr (Pt) (5+6+7+8+9+10)	dBm	-102.18	2	WAY	
12 Noise Spec Dens	dBm/Hz	-178.98			
System Noise Temp	K	91.06			
Vacuum, zenith	K	21.33			
Elevation	K	1.47			
Atmosphere	K	64.94			
Hot Body Noise	K	3.32	(from Venus)		
13 Received Pt/No	dB-Hz	<b>76.80</b>			
<i>CARRIER PERFORMANCE</i>					
14 Tlm Carrier Supp	dB	-15.21	TRUE	TLM ON?	
15 Rng Carrier Supp	dB	0.00	0	RNG MI?	
16 DOR Carrier Supp	dB	0.00	FALSE	DOR ON?	
17 Received Pc/No (13+14+15+16)	dB-Hz	61.60			
18 Carrier Loop Bandwidth, Bl	dB-Hz	4.77	3	Carrier Bl, Hz	
19 Phase Noise Variance	rad <sup>2</sup>	0.0004			
Thermal Noise Contribution	rad <sup>2</sup>	0.0000			
Transmitter Noise Contribution	rad <sup>2</sup>	0.0004			
Solar Noise Contribution	rad <sup>2</sup>	0.0000			
19a Loop SNR	dB	33.48			
20 Required Carrier Loop SNR	dB	10.00			
21 Carrier Margin	dB	23.48			
<i>TELEMETRY PERFORMANCE</i>					
22 Tlm Data Supp	dB	-0.13	80	tlm MI, deg	
23 Rng Data Supp	dB	0.00	0	peak mg MI, deg	
24 DOR Data Supp	dB	0.00			
25 Pd/No (13+22+23+24)	dB-Hz	76.67			
26 Data Rate	dB	71.64	14576961	data bit rate, bps	
27 System Demodulation Losses	dB	-1.00		(Estimated loss for high rate LDPC)	
28 Baseline Eb/No (25-26+27)	dB	4.03			
29 Output Eb/No (required to close all loops)	dB	1.00			
29a Performance margin (30-31)	dB	3.03		AR4JA LDPC (n=16,384, k=8,192); FER = 10 <sup>-6</sup>	

**Table 4.34:** Orbiter Science Downlink, 50-W X-Band, 4-m HGA, 0.5-mrad Pointing Error, 34-m DSN.

50.0 W TWTA					
X-Band HGA, 4 m antenna diameter, 0.03° off-point		2.573E+08		Range, km	
DSN 34 m station /Configuration: X/Ka diplexed RCP		1.7200		Range, AU	
Canberra/20 deg. elevation/90% CD Weather (Year Average)		0.24		OWLT, hrs	
Hot body noise = 0 K					
2-way coherent		20		SEP, deg	
Tlm channel/ (Turbo ½, 8920 bit frame)/FER=10 <sup>-4</sup>		20		Elev Angle, deg	
Link Parameter	Unit	Design Value	X 8420	RF band Freq, MHz	
<i>TRANSMITTER PARAMETERS</i>					
1 S/C RF Power Output	dBm	46.99	50	<i>Xmtr Pwr (W), EOL</i>	
2 Total Circuit Loss	dB	-1.50			
3 Antenna Gain (on boresight)	dBi	48.36	0.62	<i>3 dB Beamwidth</i>	
4 Ant Pointing Loss	dB	-0.03	HGA	<i>S/C Antenna</i>	
5 EIRP (1+2+3+4)	dBm	93.82			
<i>PATH PARAMETERS</i>					
6 Space Loss	dB	-279.16			
7 Atmospheric Attn	dB	-0.17	90 Year Average	<i>Weather % Distribution Type</i>	
<i>RECEIVER PARAMETERS</i>					
8 DSN Antenna Gain	dBi	68.25		<i>Canberra: 34mBWG, DSS34</i>	
9 Ant Pointing Loss	dB	-0.10	n/a	<i>LNA Selection</i>	
10 Polarization Loss	dB	-0.03	X/Ka diplexed RCP	<i>DSS Config</i>	
<i>TOTAL POWER SUMMARY</i>					
11 Total Rcvd Pwr (Pt) (5+6+7+8+9+10)	dBm	-117.42	2	<i>WAY</i>	
12 Noise Spec Dens	dBm/Hz	-183.70			
System Noise Temp	K	30.46			
Vacuum, zenith	K	18.97			
Elevation	K	0.49			
Atmosphere	K	10.63			
Hot Body Noise	K	0.37		<i>(from Venus)</i>	
13 Received Pt/No	dB-Hz	66.28			
<i>CARRIER PERFORMANCE</i>					
14 Tlm Carrier Supp	dB	-15.21	TRUE	<i>TLM ON?</i>	
15 Rng Carrier Supp	dB	0.00	0	<i>RNG MI?</i>	
16 DOR Carrier Supp	dB	0.00	FALSE	<i>DOR ON?</i>	
17 Received P <sub>c</sub> /N <sub>o</sub> (13+14+15+16)	dB-Hz	51.07			
18 Carrier Loop Bandwidth, Bl	dB-Hz	4.77	3	<i>Carrier Bl, Hz</i>	
19 Phase Noise Variance	rad <sup>2</sup>	0.0001			
Thermal Noise Contribution	rad <sup>2</sup>	0.0000			
Transmitter Noise Contribution	rad <sup>2</sup>	0.0000			
Solar Noise Contribution	rad <sup>2</sup>	0.0000			
19a Loop SNR	dB	42.64			
20 Required Carrier Loop SNR	dB	10.00			
21 Carrier Margin	dB	32.64			
<i>TELEMETRY PERFORMANCE</i>					
22 Tlm Data Supp	dB	-0.13	80	<i>tlm MI, deg</i>	
23 Rng Data Supp	dB	0.00	0	<i>peak mg MI, deg</i>	
24 DOR Data Supp	dB	0.00			
25 P <sub>d</sub> /N <sub>o</sub> (13+22+23+24)	dB-Hz	66.14			
26 Data Rate	dB	61.73	1489672	<i>data bit rate, bps</i>	
27 System Demodulation Losses	dB	-0.30			
28 Baseline Eb/N <sub>o</sub> (25-26+27)	dB	4.11			
29 Output Eb/N <sub>o</sub> (required to close all loops)	dB	1.00		<i>Turbo ½, 8920; FER=10<sup>-4</sup></i>	
29a Performance margin (30-31)	dB	3.11			

**Table 4.35:** Orbiter Safemode, 50-W X-Band, LGA, 45° Pointing Error, 34-m DSN.

50.0 W TWTA							
X-Band LGA, 45.0° off-point				2.573E+08	Range, km		
DSN 34 m station /Configuration: X/Ka diplexed RCP				1.7200	Range, AU		
Canberra/20 deg. elevation/90% CD Weather (Year Average)				0.24	OWLT, hrs		
Hot body noise = 0 K							
1 way				20	SEP, deg		
Tlm channel/ (Turbo ½, 1784 bit frame)/FER=10 <sup>-4</sup>				20	Elev Angle, deg		
Link Parameter	Unit	DesignValue	X 8420	RF band Freq, MHz			
<b>TRANSMITTER PARAMETERS</b>							
1 S/C RF Power Output	dBm	46.99	50	Xmtr Pwr (W), EOL			
2 Total Circuit Loss	dB	-2.50					
3 Antenna Gain (on boresight)	dBi	9.10	45.00	Boresight Angle, Deg			
4 Ant Pointing Loss	dB	-5.10	LGA	S/C Antenna			
5 EIRP (1+2+3+4)	dBm	48.49					
<b>PATH PARAMETERS</b>							
6 Space Loss	dB	-279.16					
7 Atmospheric Attn	dB	-0.17	90 Year Average	Weather % Distribution Type			
<b>RECEIVER PARAMETERS</b>							
8 DSN Antenna Gain	dBi	68.25	Canberra: 34mBWG, DSS34				
9 Ant Pointing Loss	dB	-0.10	n/a	LNA Selection			
10 Polarization Loss	dB	-0.07	X/Ka diplexed RCP	DSS Config			
<b>TOTAL POWER SUMMARY</b>							
11 Total Rcvd Pwr (Pt) (5+6+7+8+9+10)	dBm	-162.79	1	WAY			
12 Noise Spec Dens	dBm/Hz	-183.75					
System Noise Temp	K	30.09					
Vacuum, zenith	K	18.97					
Elevation	K	0.49					
Atmosphere	K	10.63					
Hot Body Noise	K	0.00	0				
13 Received Pt/No	dB-Hz	20.96					
<b>CARRIER PERFORMANCE</b>							
14 Tlm Carrier Supp	dB	-3.01	TRUE	TLM ON?			
15 Rng Carrier Supp	dB	0.00	0	RNG MI?			
16 DOR Carrier Supp	dB	0.00	FALSE	DOR ON?			
17 Received P <sub>c</sub> /No (13+14+15+16)	dB-Hz	17.95					
18 Carrier Loop Bandwidth, Bl	dB-Hz	4.77	3	Carrier Bl, Hz			
19 Phase Noise Variance	rad <sup>2</sup>	0.0498					
Thermal Noise Contribution	rad <sup>2</sup>	0.0481					
Transmitter Noise Contribution	rad <sup>2</sup>	0.0017					
Solar Noise Contribution	rad <sup>2</sup>	0.0000					
19a Loop SNR	dB	13.02					
20 Required Carrier Loop SNR	dB	10.00					
21 Carrier Margin	dB	3.02					
<b>TELEMETRY PERFORMANCE</b>							
22 Tlm Data Supp	dB	-0.13	45	tlm MI, deg			
23 Rng Data Supp	dB	0.00	0	peak rng MI, deg			
24 DOR Data Supp	dB	0.00					
25 Pd/No (13+22+23+24)	dB-Hz	17.95					
26 Data Rate	dB	12.36	17	data bit rate, bps			
27 Radio Loss	dB	-0.46					
28 SubCarrier Demod. Loss	dB	-0.21					
29 Symbol Sync. Loss	dB	-0.25					
30 Baseline Eb/No (25-26+27+28+29)	dB	4.67					
31 Output Eb/No (required to close all loops)	dB	1.50					
31a Performance margin (30-31)	dB	3.17					

**Table 4.36:** Orbiter Safemode, 50-W X-Band, LGA, 75° Pointing Error, 70-m DSN.

50.0 W TWTA					
X-Band LGA, 75.0° off-point			2.573E+08	Range, km	
DSN 70 m station /Configuration: X/X			1.7200	Range, AU	
Canberra/20 deg. elevation/90% CD Weather (Year Average)			0.24	OWLT, hrs	
Hot body noise = 0 K					
1 way			20	SEP, deg	
Tlm channel/ (Turbo ½, 1784 bit frame)/FER=10 <sup>-4</sup>			20	Elev Angle, deg	
Link Parameter	Unit	Design Value	X 8420	RF band Freq, MHz	
<i>TRANSMITTER PARAMETERS</i>					
1 S/C RF Power Output	dBm	46.99	50	Xmtr Pwr (W), EOL	
2 Total Circuit Loss	dB	-2.50			
3 Antenna Gain (on boresight)	dBi	9.10	75.00	Boresight Angle, Deg	
4 Ant Pointing Loss	dB	-12.10	LGA	S/C Antenna	
5 EIRP (1+2+3+4)	dBm	41.49			
<i>PATH PARAMETERS</i>					
6 Space Loss	dB	-279.16			
7 Atmospheric Attn	dB	-0.17	90 Year Average	Weather % Distribution Type	
<i>RECEIVER PARAMETERS</i>					
8 DSN Antenna Gain	dBi	74.49		Canberra: 70m, DSS43	
9 Ant Pointing Loss	dB	-0.10	n/a	LNA Selection	
10 Polarization Loss	dB	-0.08	X/Ka diplexed RCP	DSS Config	
<i>TOTAL POWER SUMMARY</i>					
11 Total Rcvd Pwr (Pt) (5+6+7+8+9+10)	dBm	-163.53	1	WAY	
12 Noise Spec Dens	dBm/Hz	-184.29			
System Noise Temp	K	27.00			
Vacuum, zenith	K	12.09			
Elevation	K	1.67			
Atmosphere	K	13.25			
Hot Body Noise	K	0.00	0		
13 Received Pt/No	dB-Hz	20.76			
<i>CARRIER PERFORMANCE</i>					
14 Tlm Carrier Supp	dB	-2.72	TRUE	TLM ON?	
15 Rng Carrier Supp	dB	0.00	0	RNG MI?	
16 DOR Carrier Supp	dB	0.00	FALSE	DOR ON?	
17 Received P/N (13+14+15+16)	dB-Hz	18.04			
18 Carrier Loop Bandwidth, Bl	dB-Hz	4.77	3	Carrier Bl, Hz	
19 Phase Noise Variance	rad <sup>2</sup>	0.0488			
Thermal Noise Contribution	rad <sup>2</sup>	0.0471			
Transmitter Noise Contribution	rad <sup>2</sup>	0.0017			
Solar Noise Contribution	rad <sup>2</sup>	0.0000			
19a Loop SNR	dB	13.11			
20 Required Carrier Loop SNR	dB	10.00			
21 Carrier Margin	dB	3.11			
<i>TELEMETRY PERFORMANCE</i>					
22 Tlm Data Supp	dB	-3.32	43	tlm MI, deg	
23 Rng Data Supp	dB	0.00	0	peak rng MI, deg	
24 DOR Data Supp	dB	0.00			
25 Pd/No (13+22+23+24)	dB-Hz	17.43			
26 Data Rate	dB	11.76	15	data bit rate, bps	
27 Radio Loss	dB	-0.47			
28 SubCarrier Demod. Loss	dB	-0.21			
29 Symbol Sync. Loss	dB	-0.26			
30 Baseline Eb/No (25-26+27+28+29)	dB	4.73			
31 Output Eb/No (required to close all loops)	dB	1.50			
31a Performance margin (30-31)	dB	3.23			

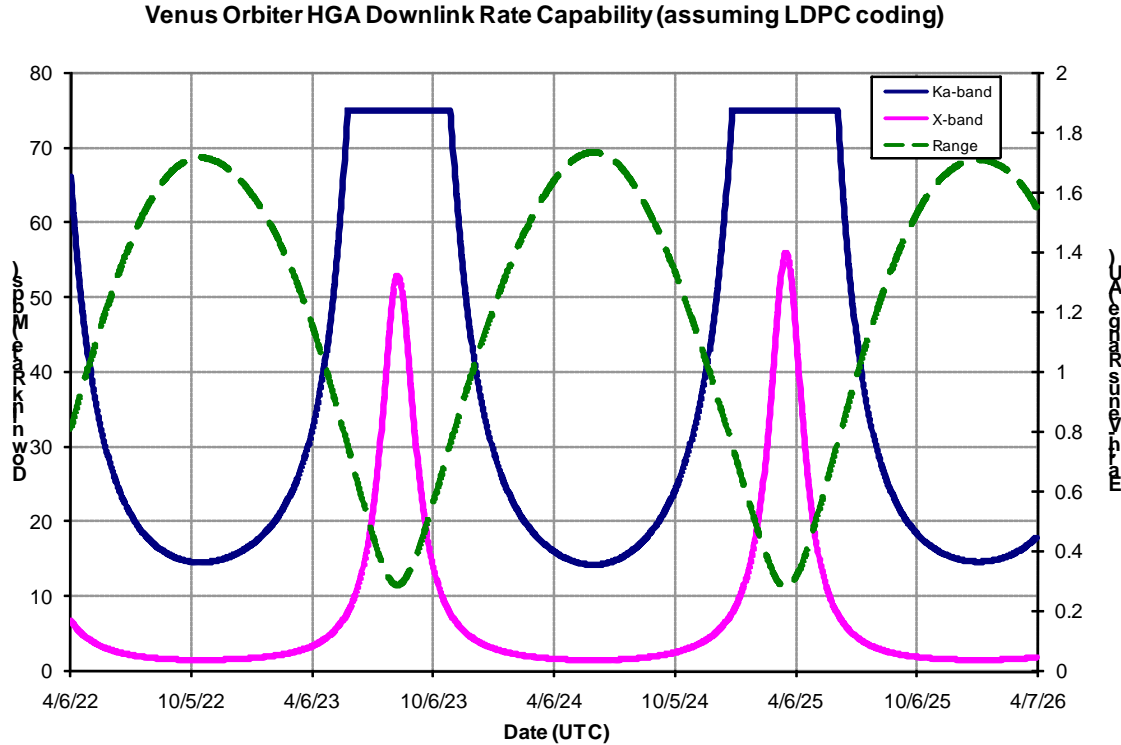


Figure 4.35: Orbiter HGA downlink rate capability vs. range over 4 years. The figure also shows the Earth-Venus range, impacting the telecom data rate.

**Table 4.37:** Orbiter Cumulative Downlink Data Volume in Terabits.

	Assuming rate capability at max range			Assuming actual data rate capability		
	Ka only (Tbits)	X only (Tbits)	Ka + X (Tbits)	Ka only (Tbits)	X only (Tbits)	Ka + X (Tbits)
After 1 year	153.2	15.7	168.9	238.5	24.4	262.8
After 2 years	306.5	31.3	337.8	792.0	160.4	952.3
After 3 years	459.7	47.0	506.7	1189.2	261.9	1451.1
After 4 years	612.9	62.6	675.6	1529.6	320.6	1850.2

The orbiter relay design is driven by the requirement to provide communications support to various in situ elements at Venus. These in situ elements consist of two landers and two balloons. The current design assumes the orbiter will nominally communicate with one in situ element at a time, except for Entry/Descent/Inflation/Landing, when the orbiter may receive data simultaneously from a balloon and a lander if the redundant relay radio is also powered on. Specifically, following the separation of the lander and the balloon from the entry system, the larger S-Band HGA would receive the higher data volume and data rate from the lander, while the smaller S-Band HGA would communicate

with the balloon. S-Band was chosen because it was successfully used by the Pioneer-Venus probes and the Venera/VEGA landers and because it offers small atmospheric losses through the thick Venusian atmosphere. X-Band atmospheric losses are approximately 10 dB worse. Electra radios were selected on the basis of development and flight heritage, as well as their capability for using the Proximity-1 Protocol with adaptive data rates. The protocol requires a 2-way link to operate (the forward link is for acknowledgement and control messages), but provides reliable, error- and gap-free data transmission. The adaptive data rate strategy uses the protocol to autonomously command and coordinate data

rate changes based on the actual measured signal-to-noise ratio. Use of adaptive data rates maximizes the data volume returned by optimizing the data rate profile subject to actual link conditions (rather than predicted performance based on worst case geometry) and protects against loss of data due to unmodeled losses or fades. Orbiter relay performance is discussed in Subsection 4.5.5.7.

#### **4.5.1.8 Orbiter Thermal System**

The Venus environment for an orbiter imposes external thermal inputs of approximately twice those at the Earth. This includes a significant contribution from the planet itself due to reflection and emission from the clouds. Nevertheless, standard spacecraft thermal control hardware will suffice for the DRM orbiter. This includes MLI blankets or white paint (with low solar absorptance and high IR emittance) on external surfaces, thermal louvers, electric heaters, temperature sensors and a feedback control system to maintain the desired internal temperature.

### **4.5.2 Carrier**

#### **4.5.2.1 Overview**

As discussed in Section 4.2, the Carrier spacecraft is designed to deliver the in situ elements of the Venus DRM and will be launched on a Type IV trajectory to Venus using an Atlas V-551 launch vehicle (see Figure 4.36). The carrier will deliver two entry systems, each carrying a cloud-level balloon and a short-lived lander, which are further discussed in Subsections 4.5.3, 4.5.4, and 4.5.5, respectively. As seen in Figure 4.36, a stacked configuration has been used for purposes of the DRM. This facilitates the spin-up of the entry vehicles prior to release by having a common axis of rotation; however, this approach suffers from the risk of not being able to release the second vehicle if the first one itself fails to release. The complexities of this approach will need to be explored in detail during future studies, and alternate configurations should be considered and compared to this original design.

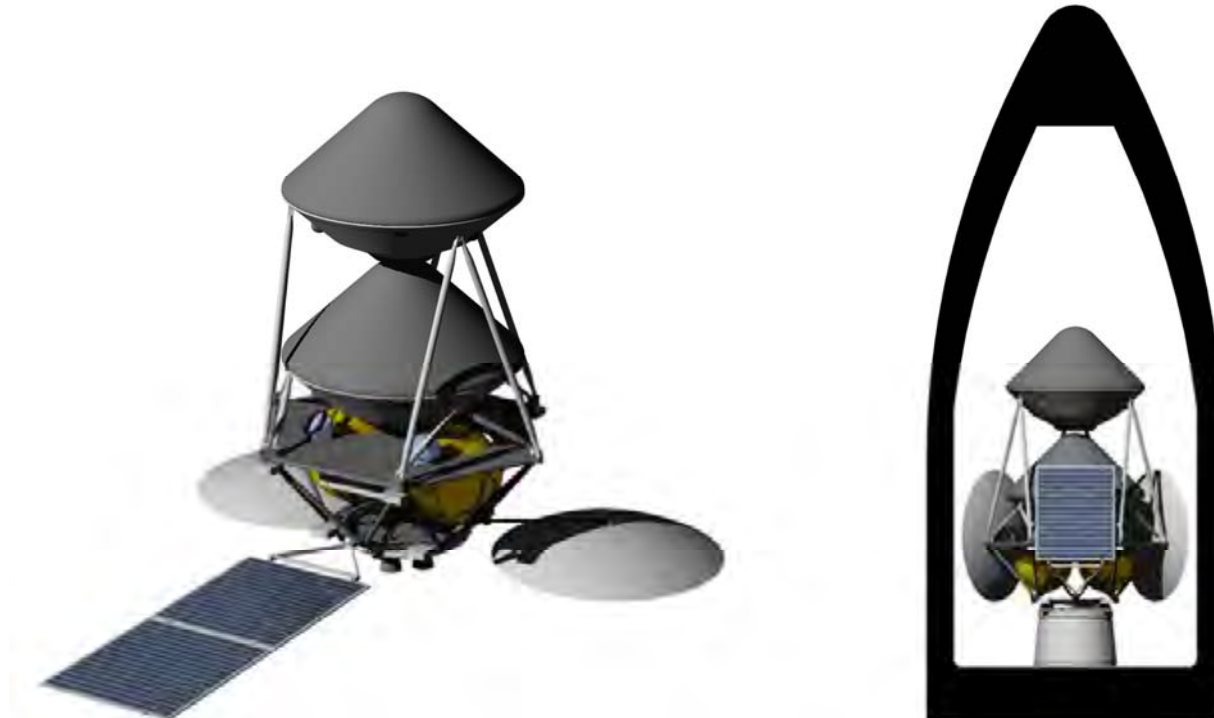


Figure 4.36: Carrier with 2 entry systems (left) and inside the fairing (right).

**Table 4.38:** Carrier Mass Summary.

Parameter	CBE Mass (kg)	Cont. (%)	CBE+Cont. (kg)
Two Entry Systems		-	3938
Carrier Bus:			
Altitude Control	41.0	11	45.7
C&DH	16.3	30	21.2
Power	43.5	30	56.5
Mono-Prop	106.2	4	110.8
Structure and Mechanisms	419.2	30	544.9
S/C-Side Adapter	18.3	30	23.8
Cabling	40.1	30	52.1
Telecom	55.0	12	61.5
Thermal	41.6	25	52.1
<b>Carrier Bus Only Total Mass</b>	<b>781.1</b>	<b>24</b>	<b>968.7</b>
System Contingency			148.3
<b>Carrier Bus Total Dry Mass w/ Cont.</b>			<b>1117</b>
Hydrazine Propellant			523
<b>Carrier Bus Total Wet Mass w/ Cont.</b>			<b>1640</b>
<b>Bus + Entry System Wet Mass w/ Cont.</b>			<b>5578</b>
Launch Vehicle Capability		Atlas V 551	5580
Launch Vehicle Margin		0%	2

Note: Total contingency is  $(968.7 - 781.1) + 148.3 = 335.9$  or 43% of the 781.1 kg Bus Total CBE Mass.

The carrier is designed to be a dual-string spacecraft consistent with the redundancy requirements of a flagship mission. The carrier mass summary is shown in Table 4.38. The carrier features 32 kg (1%) margin on allowable launch mass, on top of the 43% margin on the current best estimate dry mass.

The carrier lifetime was set to 15 months, which includes 14 months of cruise and 1 month for science operations. Since the main purposes of the carrier are to deliver the in situ elements to Venus and to provide backup telecom support from the in situ elements upon entry and over the lifetime of the landers (up to 6 hours), operations beyond this timeframe are not required.

Key design drivers for the carrier include structures, power, and telecom. Specifically, support structures are required for secure delivery and release of the two entry systems. The solar panels, which provide power during the long cruise phase in the inner solar system between Earth and Venus, have to be high solar flux tolerant. The telecom relay should provide backup support to the in situ elements during nominal operations when primary data

is relayed to the orbiter from the balloons and landers or during a backup scenario if the orbiter fails or the primary relay is not available. In this case, this backup relay through the carrier would be used to collect the highest possible data volume from the landers. These scenarios are discussed in Subsection 4.5.2.7.

#### 4.5.2.2 Carrier Attitude Control

The main design requirement for the carrier is derived from loose pointing to Earth of the X-Band antenna with a  $0.5^\circ$  control; that translates to 1800 arcsec at  $3\sigma$  per axis. The design includes reaction wheels, start trackers, gyros, Sun sensors, solar array gimbal control, and supporting electronics.

The carrier is 3-axis stabilized and uses reaction wheels for fine pointing. The redundant set of 4 reaction wheels are set in a pyramid configuration and are periodically desaturated using thrusters. In the current design, Honeywell HR14 Nom type reaction wheels (with 53 Nms momentum storage capacity) were considered. The spacecraft bus employs redundant (2) precision start trackers

for stellar inertial attitude determination. These Galileo AA-STR star trackers provide accuracy within  $\pm 3.0$  arcsec (P/Y),  $3\sigma$  and  $\pm 30$  arcsec (Roll),  $3\sigma$ . The spacecraft bus also includes a redundant inertial measurement unit. These redundant gyros—or inertial measurement units—have low bias stability that can propagate attitude for long intervals (e.g., hours). Specifically, two Honeywell MIMU YG9666B provide  $0.005^\circ/\text{hr}$  bias stability. Cheap and high flight heritage Sun sensors are used to support Safing operations and attitude re-initialization. Sixteen Adcole Coarse Sun sensors provide  $2 \pi$  steradian coverage (i.e., hemisphere above Earth). Solar array pointing is achieved with a solar array gimbal control Unit. The ACS baseline configuration includes a redundant set of MOOG 2-channel Electronics Control Units. The design uses a test bed approach, that includes a full set of reaction wheels, one star tracker, and one IMU for cost saving. The design also includes a full set of spares and a full set of redundant hardware. Note that the current carrier ACS design is more stringent than necessary to fulfill its pointing requirements; future studies will address this issue in more detail. Furthermore, in future studies, mission trades should be also reassessed for an optimum ACS operating mode. In the current design, the carrier is predominantly 3-axis stabilized, driven by relay telecom pointing requirements during Venus flyby. For the release of the two entry systems, the carrier spins up subsequently, then returns to a 3-axis stabilized mode. Other trades could include a predominantly spin stabilized carrier that becomes 3-axis stabilized during the relay telecom phase only, or a 3-axis stabilized carrier with spin tables for entry system release. The former was considered more complex from an operating point of view, while the latter was rejected due to implementation complexity and cost using multiple spin tables and targeting requirements.

#### 4.5.2.3 Carrier Command and Data Handling

The main C&DH subsystem uses MSAP architecture and is designed to allow for telecom relay support between the in situ elements and Earth. Under nominal conditions, the primary telecom relay would be performed through the orbiter, while the carrier would play a secondary role. In the case of an orbiter failure, however, the carrier could be used to receive data from the landers, store it onboard, and relay it back to Earth at a later time. For this, the carrier is designed to store  $\sim 4$  Gbits of data.

#### 4.5.2.4 Carrier Power System

The carrier is powered by solar arrays with a total area of  $4.4 \text{ m}^2$  in a hybrid configuration with two 50-AH lithium-ion secondary batteries.

The power system is sized based on the highest power requirement during the telecom mode (see Mode 1 below), combined with the maximum distance of 1 AU between the Sun and the carrier during the cruise. While the design is only notional, it also accounts for a minimal off-pointing ( $12^\circ$ ).

These solar arrays are gimbaled with one degree of freedom and sized to provide continuous power during the telecom mode, as discussed below.

The size requirement of the secondary batteries could increase further if the solar arrays are off-pointing during the telecom support to the in situ elements.

The solar panels are gimbaled with one degree of freedom, while a second degree of freedom is provided by the spacecraft rotating about the high-gain antenna's pointing axis. The cosine losses were not assessed in the design.

From an operational point of view, four distinct power modes were identified for the carrier, covering all relevant operating modes foreseen between launch and post flyby. These are:

- Mode 1: Telecom mode: 526 W (describing the telecom link between the carrier and Earth).

- Mode 2: Cruise mode: 398 W (supporting the carrier during the cruise phase).
- Mode 3: Separation mode: 399 W (addressing the power requirement during the separation of the two entry systems).
- Mode 4: Telecom relay mode: 426 W (providing power to the telecom system during communications between the carrier and the in situ elements).

#### 4.5.2.5 Carrier Propulsion System

The propulsion system is used to support the 3-axis cruise phase, spinning operations for the release of the two entry systems, and desaturating the momentum wheels.

For most of the 456 days of cruise, the carrier is 3-axis stabilized, which requires periodic unloading of the momentum wheels. For this and for turns and safe holds, sixteen 4.5-N thrusters will be used. During the releases of the entry systems, four 22-N thrusters are utilized for fast spin up and spin down. Finally, for significant velocity change ( $\Delta V$ ) requirements during trajectory correction maneuvers (TCM) and probe targeting, four 267-N thrusters will be employed. (Redundant pairs are included to bracket the center of gravity (CG) before and after probe release.) This design includes blow-down monopropellant propulsion, two conventional titanium-diaphragm-type propellant tanks with Gamma Ray Observatory (GRO) heritage.

The baseline  $\Delta V$  budget includes accommodations for cruise and approach phases, including 4 TCMs; for the two lander deployments, diverting maneuvers, and cleaning up; and final maneuvers at the end of mission, totaling 376 m/s. The  $\Delta V$  requirements for the carrier is shown in Table 4.39.

#### 4.5.2.6 Carrier Structures and Mechanisms

The carrier structure consists of two entry vehicles, each supported by three sets of carbon fiber composite bipods. In the stowed configuration, the spacecraft will fit in an Atlas V 5-m short fairing (Figure 4.36). The mass estimate for carrier structure and

mechanisms is 544.9 kg, as detailed in Table 4.40.

**Table 4.39:**  $\Delta V$  Requirements for the Carrier.

Item	$\Delta V$ requirement
<b>Cruise and Approach:</b>	
Launch:	0
TCM1:	40 m/s
TCM2:	10 m/s
TCM3:	5 m/s
TCM4:	5 m/s
<b>Lander 1 Deployment:</b>	
Deployment:	0
Divert Maneuver: (Transfer onto Lander 2's trajectory)	126 m/s
Clean-up maneuver:	5 m/s
<b>Lander 2 Deployment:</b>	
Deployment: 0	
Divert Maneuver: (Transfer onto the flyby trajectory)	180 m/s
Clean-up maneuver:	5 m/s
End-of-Mission:	0
<b>Total Carrier <math>\Delta V</math> for the Baseline:</b>	<b>376 m/s</b>

**Table 4.40:** Mass Breakdown for Carrier Structure and Mechanisms.

Element	Units	Mass (kg)
Primary Structure	1	462.6
Secondary Structure	1	8.9
Entry System Latch / Release System	6	15.6
Solar Array Structure	1	8.0
Solar Array Drive Assemblies 1-axis per array	1	6.1
Solar Array Latch/Release + Booms	4	1.3
Integration Hardware	1	32.4
Balance Mass 3-axis	1	10.0
<b>TOTAL (less S/C-side adapter)</b>		<b>544.9</b>
Adapter, Spacecraft-side	1	23.8
Cabling Harness	1	52.1

After the deployment of the solar array, three bipod struts release entry vehicle 1, followed by the release of entry vehicle 2. Finally, the two 2.5-m high-gain antennas deploy into their fixed position to complete the flyby configuration of the Carrier (see Figure 4.37).

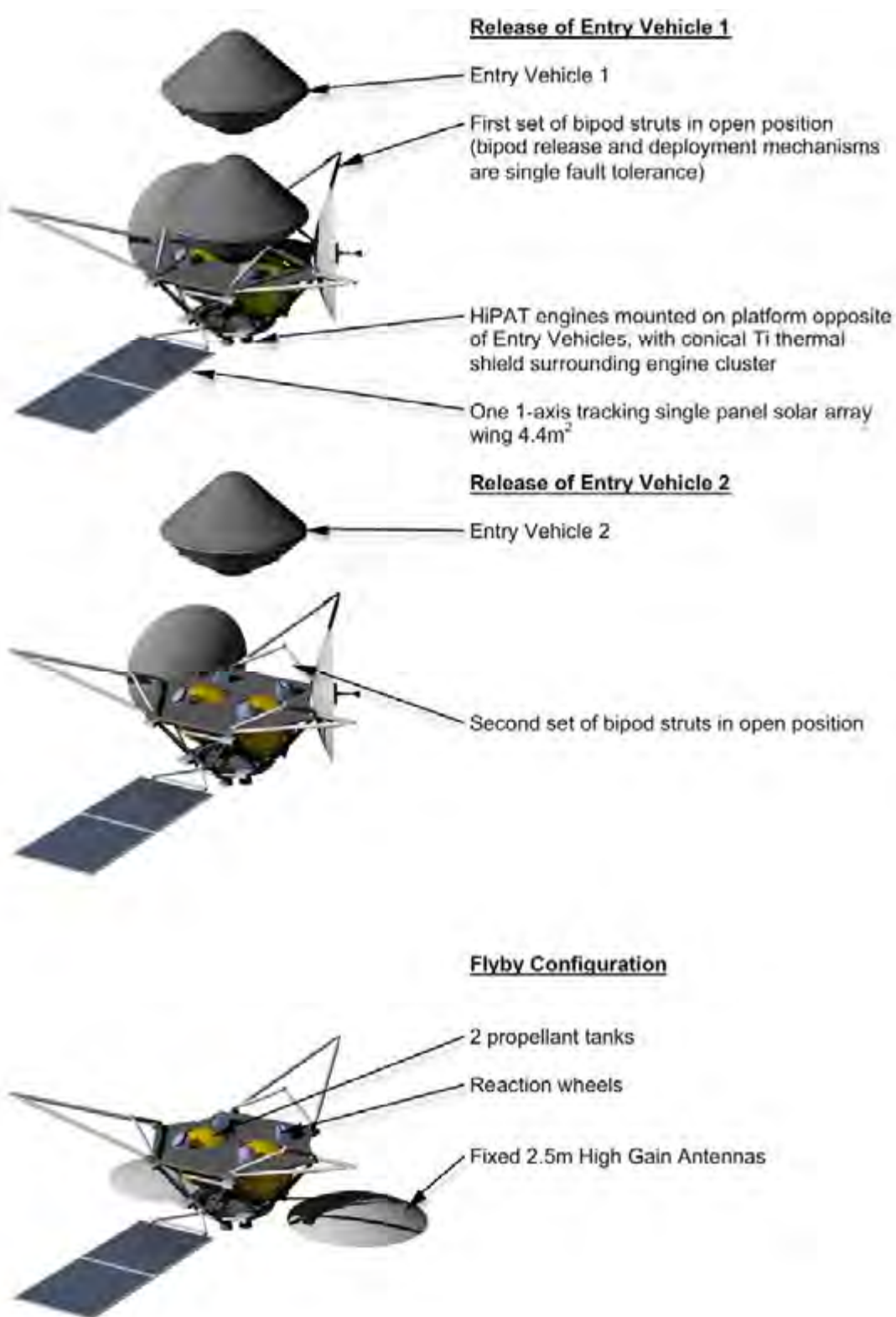


Figure 4.37: Carrier deployment sequence: Release of entry vehicle 1 (top). Release of entry vehicle 2 (middle). Deployment of fixed antennas in flyby configuration (bottom) (artist's rendering).

#### 4.5.2.7 Carrier Telecom System

The primary purposes of the carrier spacecraft are to deliver the in situ elements to Venus and to provide backup relay support to the landers (and/or balloons if they are in the HGA field of view). Based on science and mission requirements, the carrier telecom subsystem must be able to provide: 1) store-and-forward relay services for Venus in situ elements (landers, balloons) as a backup to the orbiter and 2) reliable high- and low-rate engineering command and telemetry links during cruise, science playback, critical events (launch, lander release), and safemode. Thirty-four-meter DSN antennas will be used during normal operations, with 70-m (or equivalent) antennas assumed available only for safemode and critical events.

The carrier telecom subsystem consists of its own X-Band system for communicating

with the Earth and an S-Band receive only system for communicating with in situ assets. A block diagram of the carrier X-Band and S-Band systems is shown in Figure 4.38. Significant features of the telecom design include the following:

- Redundant, cross-strapped X-Band Small Deep Space Transponders (SDSTs).
- Two S-Band Electra transceivers.
- One Ultra-Stable Oscillator (USO) for radio science.
- Redundant, cross-strapped, 50-W, X-Band traveling wave-tube amplifiers (TWTAs).
- One 2.5-m, dual-feed S/X-Band fixed high-gain antenna (HGA).
- One 2.5-m S-Band fixed HGA.
- Two X-Band low-gain antennas (LGAs).

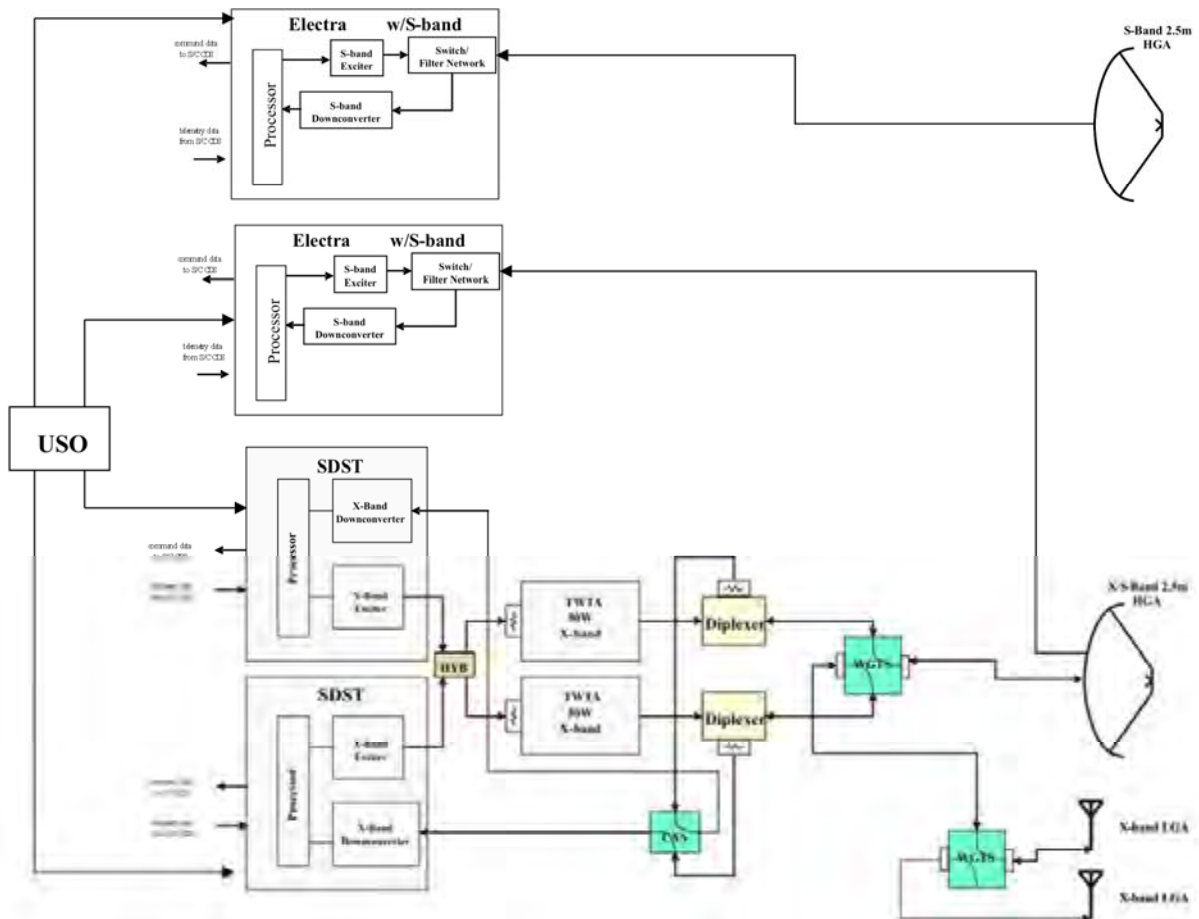


Figure 4.38: Carrier telecom X- and S-Band system.

Unlike the orbiter, the carrier-Earth communications design is not driven by an extremely high downlink rate requirement, which makes X-Band a logical choice. The X-Band system supports uplink commanding, as well as high- and low-rate communications during cruise, science playback, critical events, and safemode. The carrier and orbiter have similar X-Band systems, except the carrier has a 2.5-m fixed HGA instead of a 4-m articulated HGA.

A design control table (DCT) containing representative link performance for the carrier HGA is shown in Table 4.41. The HGA can support 500-kb/s downlink at the maximum Earth-Venus range of 1.72 AU. The carrier safemode performance is the same as the orbiter because the designs are equivalent.

The carrier can provide receive-only (i.e., no adaptive data rates) relay support for up to two in-situ elements simultaneously, provided they are located near each other and are within the beam of one of the two 2.5-m HGAs. The availability of the orbiter for relay support determines which in-situ elements the carrier will track, as well as the strategy for pointing the carriers fixed HGAs.

In the nominal relay scenario, the orbiter provides primary relay support for all of the in-situ elements. Since the carrier is a flyby vehicle, it can provide backup, receive-only support for one lander and/or one balloon. Since the orbiter-lander link uses the Proximity-1 communications protocol to automatically adjust the lander transmission rate in response to changing link conditions, the actual lander transmission rate might be different from the predicted rate (or rate profile) that will be sequenced into the carrier. In the best case, the lander transmit rate profile matches that sequenced in the carrier and the carrier receives a redundant set of data. The carrier misses any data that is not transmitted at the rate it is expecting, but it can still collect Doppler data. For balloon tracking, the double-sided 3-dB beamwidth of the 2.5-m carrier HGA is  $3.6^\circ$ , which is much narrower than  $13^\circ$  beamwidth of the 0.7-m orbiter HGA. If the

balloon is close enough to the boresight of the selected HGA, the carrier could get Doppler and/or telemetry from the balloon.

In the anomalous relay scenario, the orbiter is unavailable to provide relay support to the in-situ elements. It was assumed that orbiter unavailability, due to system or mission failure, would be known during the cruise phase of the carrier spacecraft, allowing sufficient time to re-adjust the operations to the backup scenario. (Future studies should address a backup scenario, where orbiter failure occurs close to Venus flyby, thus not allowing operating scenario changes by humans-in-the-loop.) In this situation, the landers will be retargeted to land at the same time, and will transmit simultaneously to the carrier as it flies by. The flyby trajectory would be also adjusted for an optimized closer flyby distance to facilitate the telecom between the landers and the carrier. It is assumed that the landing sites and carrier pointing strategy are selected such that each lander is within  $2^\circ$  of the HGA boresight that is tracking it. This implies an additional 3 dB of pointing loss compared to the nominal relay scenario, reducing data rates by a factor of 2. Because the carrier does not have S-band transmission capability, it cannot use the adaptive data rate technique, and must rely on sequenced (predicted) lander data rate changes. The sequenced data rate profile will likely be conservative, with additional margin carried to protect against uncertainty in lander tilt and telecom modeling. Lander relay performance is discussed in Subsection 4.5.5.7. While the primary focus of the backup scenario is to obtain the science data from the landers, once that is completed, the carrier will attempt to obtain data from the two balloons. This sequence is driven by the short lifetime of the landers in the extreme near-surface Venus environment, while the balloons will operate at an Earth-line ambient environment. Since the balloons are designed for a significantly longer lifetime, the data collected during the landers' operations will be stored on the gondolas then relayed to the carrier.

**Table 4.41:** Carrier Downlink, 50-W X-Band, 2.5-m HGA, 3-mrad Pointing Error, 34-m DSN.

50.0 W TWTA				X 8420	RF Band Freq., MHz
X-band HGA, 2.5 m antenna diameter, 0.17° off-point DSN 34 m station / Configuration: X/Ka diplexed RCP Canberra / 20 deg. Elevation / 90% CD Weather (Year Average) Hot body noise = 0 K Two-way coherent Tlm Channel / (Turbo 1 / 2, 8920 bit frame) / FER = $10^4$				2.573E+08 1.7200 0.24	Range, km Range, AU OWLT, hr
				20 20	SEP, deg Elev Angle, deg
				X 8420	RF Band Freq., MHz
Link Parameter	Unit	Design Value			
<b>TRANSMITTER PARAMETERS</b>					
1 S/C RF Power Output	dBm	46.99	50	Xmtr Pwr (W), EOL	
2 Total Circuit Loss	dB	-1.50			
3 Antenna Gain (on boresight)	dBi	44.28	1.0	3 dB Beamwidth	
4 Ant Pointing Loss	dB	-0.36	HGA	S/C Antenna	
5 EIRP (1 + 2 + 3 + 4)	dBm	89.41			
<b>PATH PARAMETERS</b>					
6 Space Loss	dB	-279.16			
7 Atmospheric Atten	dB	-0.17	90	Weather %	
<b>RECEIVER PARAMETERS</b>					
8 DSN Antenna Gain	dBi	68.25		Canberra: 34 m BWG, DSS34	
9 Ant Pointing Loss	dB	-0.10	N/A	LNA Selection	
10 Polarization Loss	dB	-0.03	X/Ka Diplexed RCP	DSS Config	
<b>TOTAL POWER SUMMARY</b>					
11 Total Rcvd Pwr (Pt) (5 + 6 + 7 + 8 + 9 + 10)	dB, dBm/Hz	-121.83 -183.75	2	WAY	
12 Noise Spec Dens					
System Noise Temp	K	30.09			
Vacuum, zenith	K	18.97			
Elevation	K	0.49			
Atmosphere	K	10.63			
Hot Body Noise	K	0.00	0		
13 Received Pt/No	Db-Hz	<b>61.92</b>			
<b>CARRIER PERFORMANCE</b>					
14 Tlm Carrier Supp	dB	-15.21	TRUE	<i>TLM ON?</i>	
15 Rng Carrier Supp	dB	0.00	0	<i>RNG MI?</i>	
16 DOR Carrier Supp	dB	0.00	FALSE	<i>DOR ON?</i>	
17 Received Pd/No (13 + 142 + 15 + 16)	dB-Hz	47.71			
18 Carrier Loop Bandwidth, BL	dB-Hz	4.77	3	<i>Carrier BL, Hz</i>	
19 Phase Noise Variance	rad <sup>2</sup>	0.0001			
Thermal Noise Contribution	rad <sup>2</sup>	0.0001			
Transmitter Noise Contribution	rad <sup>2</sup>	0.0001			
Solar Noise Contribution	rad <sup>2</sup>	0.0000			
19a Loop SNR	dB	38.33			
20 Required Carrier Loop SNR	dB	10.00			
21 Carrier Margin	dB	28.33			
<b>TELEMETRY PERFORMANCE</b>					
22 Tlm Data Supp	dB	-0.13	80	<i>tlm, MI, deg</i>	
23 Rng Data Supp	dB	0.00	0	<i>peak rng MI, deg</i>	
24 DOR Data Supp	dB	0.00			
25 Pd/No (13 + 22 + 23 + 24)	dB-Hz	61.78			
26 Data Rate	dB	57.37	545678	<i>data bit rate, bps</i>	
27 System Demodulation Losses	dB	-0.30			
28 Baseline Eb/No (25 + 26 + 27)	dB	4.11			
29 Output Eb/No (required to close all loops)	dB	1.00			
29A Performance margin (30-31)	dB	3.11			

It is expected that the data volume from this backup relay scenario would be significantly lower than that from the nominal case, and should be optimized in future assessments.

#### 4.5.2.8 Carrier Thermal Control System (TCS)

The carrier TCS maintains all equipment within flight-required temperature ranges for all mission phases and carrier attitudes. The maximum power consumption in the carrier is 312 W. This heat is removed passively through radiators that are pointed away from Venus and the Sun during the entire mission. Passive louvers on the radiator surfaces control component temperatures during variations in component power dissipation. The area of the radiators is estimated to be 0.8 m<sup>2</sup>. Survival heaters are installed on the carrier to protect electronics in the event the spacecraft must endure a safing mode. The propellant tanks

and lines are maintained within Allowable Flight Temperature (AFT) limits using film heaters and thermostats and are blanketed with Multi-Layer Insulation (MLI). The outer layer of all MLI blankets is Beta Cloth to provide micrometeoroid protection. The high solar flux at Venus requires careful design of MLI blanket construction, especially the selection of outer blanket layers, to minimize solar absorptance.

#### 4.5.3 Entry Vehicle

##### 4.5.3.1 Overview

The DRM includes 2 identical entry vehicles, each carrying a lander and a balloon with a gondola. The aeroshell is a standard 45-degree sphere cone similar in shape to the Pioneer-Venus aeroshells. A cross section of the aeroshell and its internal components are shown in Figure 4.39.

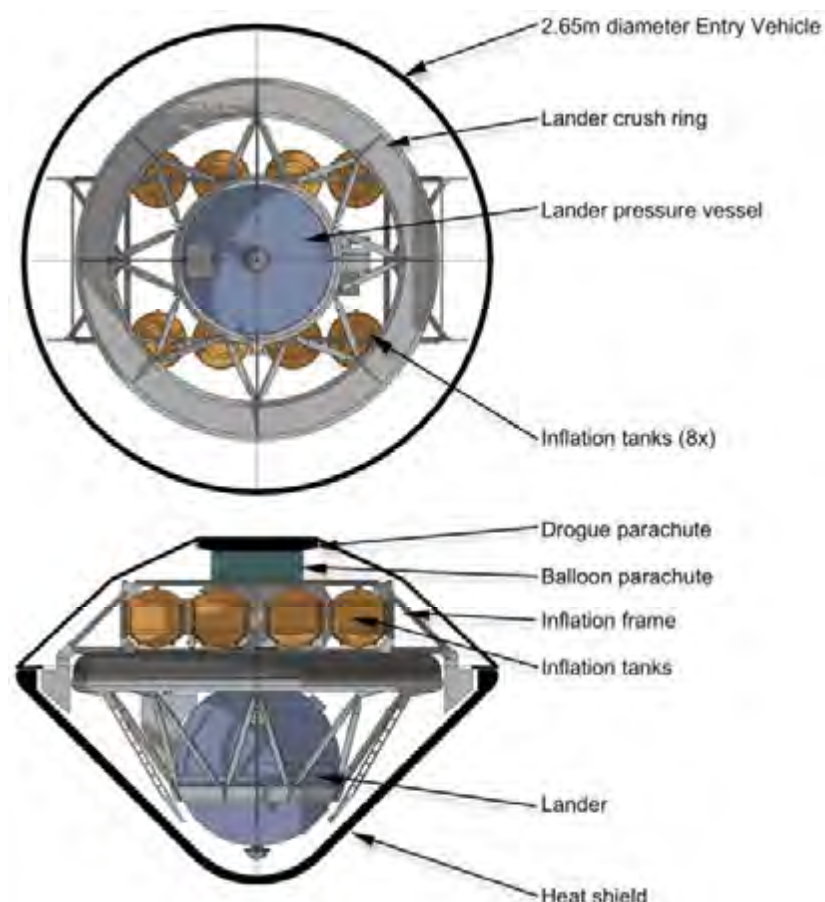


Figure 4.39: Entry vehicle sectional views, top (above), and side (below) (artist's rendering).

**Table 4.42:** Entry Vehicle Mass Summary.

Parameter	CBE Mass (kg)	Cont. (%)	CBE+Cont. (kg)
Balloon	162.5	0	162.5
Lander	686.3	0	686.3
Carried Elements Total	848.7	0	848.7
<b>Entry System Bus</b>			
Attitude Control	0.3	10	0.3
Command and Data Handling	0.8	30	1.0
Power	2.6	30	3.4
Helium Inflation System	98.1	30	127.1
Structures and Mechanisms	213.0	30	276.9
S/C-Side Adapter	12.6	30	16.3
Cabling	28.5	30	37.1
Telecom	0.5	21	0.6
Thermal	426.4	2	436.7
<b>Bus Total Mass</b>	<b>782.7</b>	<b>15</b>	<b>899.4</b>
<b>Bus + Carried Elements Mass</b>	<b>1631.4</b>		<b>1748.1</b>
Additional System Contingency			219.9
<b>Entry System Total CBE + Cont.</b>			<b>1968</b>
Residual Helium			1.3
<b>Entry System Total CBE + Cont. Wet</b>			<b>1969</b>

Notes: (1) Total contingency is (1748.1-1631.4) + 219.9 = 336.6 kg, or 43% of 782.7 kg Bus Total CBE Mass.

(2) The fully margined aeroshell TPS mass is carried under the Thermal line.

The entry vehicle mass is estimated to be 1969 kg, which includes a total margin of 43% on the current best estimate. The entry system mass summary is presented in Table 4.42. The entry systems are powered by thermal batteries (see Subsection 4.5.3.4). They are spin stabilized after release from the carrier during the 10- and 20-day cruises. The entry systems are not carrying science instruments in the current DRM, although an instrumented aeroshell with temperature, heat flux, and recession sensors could provide valuable information on atmospheric entry physics and the heat shield material response. The key design drivers include the size of the entry vehicle needed to house the internal components and the mass of the thermal protection system (TPS) and related structures needed to protect the payload from the harsh entry environment. The size of the aeroshell is a significant mass driver, especially if the science driven entry and landing locations result in high entry-flight path angles and, thus, high entry heating and g-loads (see

Subsections 4.4.3 and 4.5.3.9). The current configuration shows a first order accommodation of the in situ elements inside the aeroshell. For this, the center of gravity requirement of  $X_{cg}/D < 0.4$  is not yet satisfied. In future studies the design will be optimized to reduce  $X_{cg}/D$  from the current value of ~0.46 to below 0.4.

#### 4.5.3.2 Entry Vehicle Attitude Control

The two entry systems will be released from the carrier at 20 and 10 days before arrival. The entry systems are phased to enter the atmosphere 13 hours apart, which correspond to the orbital period of the orbiter during this relay telecom support phase. The entry systems are spin stabilized at 10 RPM once they are released from the carrier; which is similar to the spin rate of the Galileo probe. Note, however, that recent work in this area indicated that for Venus entry, 2 RPM would be sufficient; this will be reassessed in future studies. The atmospheric entry sequence is triggered with a g-switch; the follow up

sequences are timed from there on, including the deployment of the drogue chute, the backshell, and the main chute. The rest of the sequence includes separation of the heat shield, balloon deployment, inflation, and main chute separation, and a similar sequence for the lander, as discussed in Subsection 4.4.6.

#### **4.5.3.3 Entry Vehicle Command and Data Handling**

The entry vehicles do not require their own C&DH system. Instead, following separation from the carrier they will use the C&DH system on the balloon for sequencing the pyro device rings and other events up to the main parachute deployment and balloon and lander separation.

#### **4.5.3.4 Entry Vehicle Power System**

Following atmospheric entry, the power system on the entry vehicle must support the separation events of the backshell, heat shield, lander, inflation system, and gondola. Therefore, in the design, the inflation system and the pyro activation hardware (such as the firing box) are accounted for on the entry vehicle. For this, on each entry vehicle the design includes two thermal batteries with a mass of 0.76 kg. These batteries power the Pyro Firing Unit on the entry system with an internal, dual-redundant firing card with a mass of 1.1 kg.

#### **4.5.3.5 Entry Vehicle Propulsion System**

The entry system does not have its own propulsion system. Once it is released from the carrier spacecraft, it will cruise in a spin-stabilized mode until atmospheric entry, which is further discussed in Subsection 4.5.3.9.

#### **4.5.3.6 Entry Vehicle Structures and Mechanisms**

The entry vehicle consists of a backshell and a 45-degree sphere-cone heat shield covered in carbon-phenolic ablative material (Figure 4.40). The maximum diameter of the aeroshell is 2.65 m. CAD modeling confirms that this is large enough to contain all internal components. The mass estimate for the entry vehicle structure and mechanisms (without the

in situ elements) is 276.9 kg, including a 30% subsystem mass contingency (see Table 4.43). Each entry vehicle will contain one balloon and one lander, with the balloon and inflation system packed under the backshell and the lander fitted inverted into the 45-degree heat shield (see Figure 4.40). This inverted orientation is used because the shape of the lander fits naturally into the 45-degree sphere-cone geometry, while it does not fit well otherwise. This inverted orientation requires a turnover event during balloon and lander separation so that the lander is oriented with the crushpad pointed downwards at landing. The system to accomplish this turnover event has not been designed in detail; notionally, however, it is expected that a tether connecting the top of the lander to the bottom of the balloon inflation system will be used to exert a transient force that will rotate the lander into the correct orientation, after which the rope will be cut with a pyrotechnical cutter. In this scenario, the balloon parachute ultimately exerts the force that rotates the lander. Once the cutter fires, the balloon and lander separate and the lander parachute deploys.

#### **4.5.3.7 Vehicle Telecom System**

The entry vehicle will have an S-Band, low-gain antenna located either on the backshell or accessible through an RF transparent window on the backshell. This antenna is connected to the lander telecom system and is used for any relay communication that occurs during the period from carrier separation through entry and, subsequently, backshell separation. During the 10 to 20 days between separation to atmospheric entry, the entry system will be in a silent cruise mode, with very low standby power to the subsystems. The batteries on the lander are sized to provide periodic low-data-volume critical-event data during this pre-entry cruise phase. The rear-facing LGA is needed because the lander LGA is forward-facing, which is in the direction of peak heating and plasma flow during entry, and therefore, more susceptible to communications blackout.

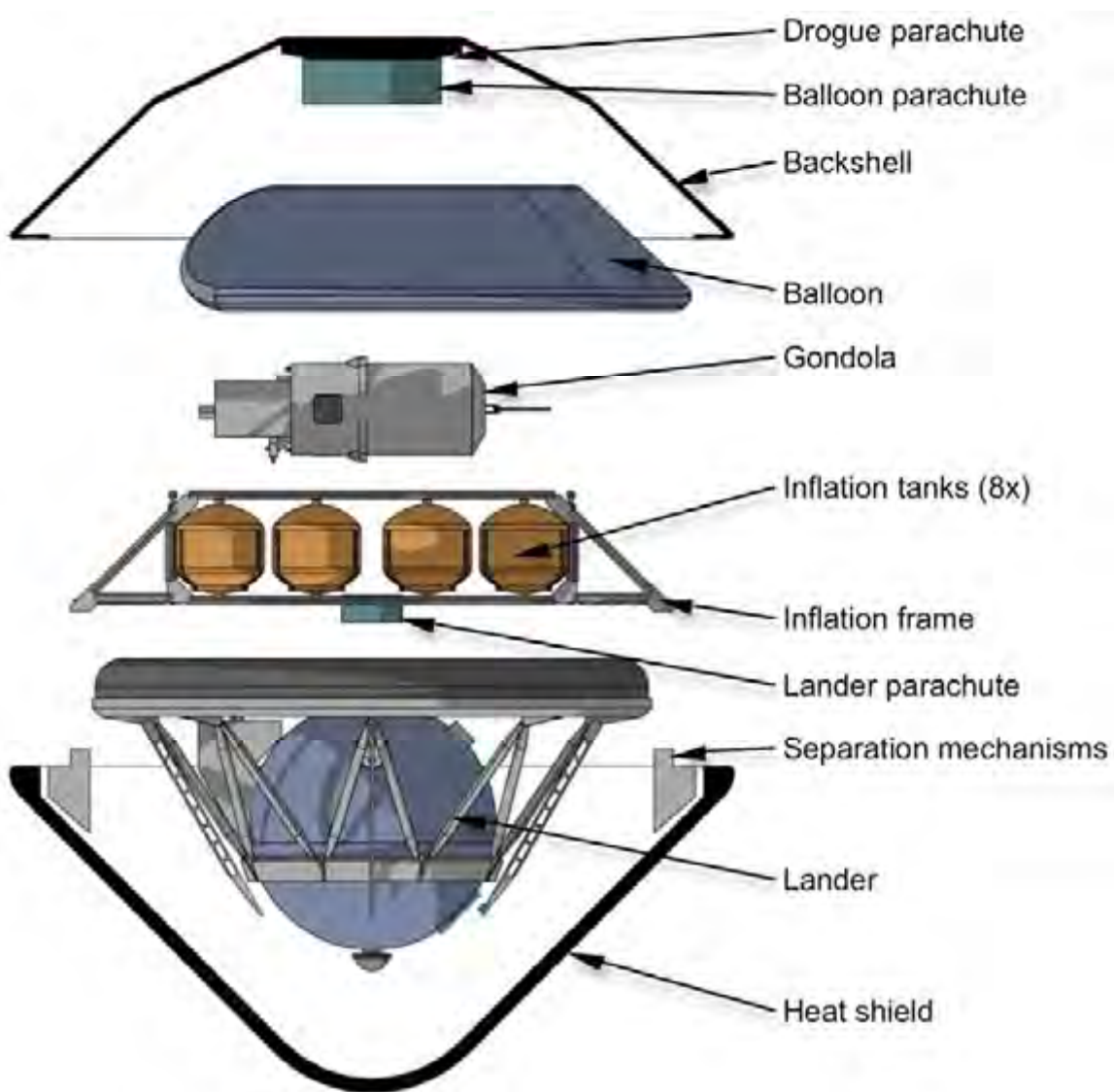


Figure 4.40: Entry vehicle exploded view showing in situ elements (artist's rendering).

**Table 4.43:** Mass Breakdown for Entry Vehicle Structure and Mechanisms.

Element	Units	Mass (kg)
Primary Structure	1	143.0
Secondary Structure	1	78.0
Parachute	1	26.0
Drogue parachute (includes mortar and canister)	1	7.8
Integration Hardware	1	9.1
Balance Mass	1	13.0
<b>TOTAL (less SC-side adapter)</b>		<b>276.9</b>
Adapter, Spacecraft-side	1	16.3
Cabling Harness	1	37.1

#### 4.5.3.8 Entry Vehicle Thermal System

The Entry System aeroshell utilizes a carbon-phenolic (CP) Thermal Protection System (TPS) to absorb and remove the aerothermal heating from atmospheric entry. CP was selected due to heritage considerations on the Pioneer-Venus and Galileo probes and the high dynamic pressure encountered during atmospheric entry. No other available TPS material could handle the peak entry conditions encountered. Although, in theory, it would be possible to develop a new TPS material for this mission, the cost of such a development effort would need to be traded against the potential mass savings. Specifically, one of the assumed ground rules of the study was to minimize the number of technology development efforts that would be required. It was determined that the mission could be performed with a heritage material. There is little doubt that a TPS development program could result in a lower-mass solution, but at significant cost. NASA Ames could fully support a technology development program to develop a range of new TPS materials for this and other mission proposals; it was suggested, however, that, ideally, this work should be undertaken within a technology program and not necessarily within a mission proposal. This is particularly true in the current case where, as stated, an optimized TPS would be an enhancing, rather than enabling, technology.

The testing limitation is a significant concern that is not detailed here, but should be addressed in future studies. One of the primary reasons to employ a heritage material is that the performance limits of this material are well beyond the current entry conditions. However, the possibility that a new or modified facility might be required for qualification of the TPS should be considered. Note that the argument of heritage is always contentious. It is clear that the current proposal cannot claim direct heritage at the aeroshell level to Pioneer-Venus or Galileo. However, the claim is being made at the TPS material level. Heritage rayon precursor materials exist at Ames and can be employed to either (1) develop CP material for

this mission using the same materials and processes employed for P-V and Galileo or (2) use the heritage rayon to demonstrate equivalent performance of a new CP material manufactured with contemporary constituents and processes. NASA Ames has stockpiled significant quantities of heritage rayon for the Mars Sample Return entry vehicle. This material could be converted to heritage CP (with process and constituents traceable to PVLP CP) for a flagship mission or it could be used to verify the “in-family” performance of CP material currently being manufactured for rocket nozzles using contemporary materials. NASA ARC has sufficient heritage rayon in hand today to build limited size and numbers of heat shield.

The internal components of the aeroshell will not heat up significantly during the brief transient event because of the thermal isolation of the lander and the balloon payloads within the aeroshell. The interior of the aeroshell has a single layer aluminized Kapton blanket to reduce the radiation loss from the interior to space. This will reduce the amount of heating required by the lander and the balloon payload during cruise to maintain all equipment above their lower AFT limits in the non-operational state.

Although the aeroshell is shaded from the Sun during cruise, the backshell is painted with a white paint to minimize solar loads on the structure, which could potentially overheat the payload elements within. Strategically placed film heaters and thermostats within the aeroshell keep the payload temperatures above their lower non-operating temperature limits.

#### 4.5.3.9 Entry Vehicle Entry Descent and Landing (EDL)

The atmospheric entry design for the DRM follows the same procedures and shares many of the same metrics as that for the Pioneer-Venus mission. The EDL sequence is schematically illustrated in Figure 4.30b in Subsection 4.4.6. Trajectory simulations were performed using the estimated entry interface speed of ~11.2 km/s to quantify the altitude, velocity and acceleration profiles versus time. The altitude versus time plot for the DRM is

shown in Figure 4.41. This data was then used as input to a TPS sizing analysis performed by the aerothermodynamics branch at NASA ARC. The analysis indicates that the maximum stagnation-point heating rate will be  $2850 \text{ W/cm}^2$  based on the calculated ballistic coefficient of  $348.8 \text{ kg/m}^2$ . The expected entry environment can be well tolerated through use of carbon-phenolic thermal protection material, as was done for Pioneer-Venus. The sizing calculation resulted in a 29.6-mm thick layer of carbon-phenolic, which includes all of the margins typically used on NASA entry systems. This results in a total TPS mass of 323 kg.

In comparison, the Pioneer-Venus Large probe (PVLP) had 16 mm of TPS at the stagnation point (margined), which is less than calculated for the Venus DRM. In TPS sizing, peak heat flux and stagnation pressure select the TPS material type, while total heat load determines the TPS thickness. The proposed vehicle enters the Venusian atmosphere with a shallow EFPA relative to PVLP. Consequently, the current vehicle has a significantly higher heat load and larger TPS

thickness. Approximate factors for flank turbulent heating, based on estimates provided by NASA ARC aerothermal experts, were employed to arrive at the final margined TPS thickness, as reported. Peak turbulent flank heating rates on the current design are predicted to be within the Pioneer-Venus experience and within the  $7\text{-kW/cm}^2$  testing limit of current facilities. The primary difference between P-V and VDRM is that with the smaller entry flight path angle and longer trajectory time during entry the total flank heat load encountered by the VDRM entry system will be much higher than that for the PVLP. (It should be noted that the scope of the current study was not sufficient to baseline high-fidelity Navier-Stokes and shock-layer radiation analyses, as would be required. However, assuming a flank heating of about 3 times the stagnation point convective heating rate is a good rule of thumb for Venus entries. It is recommended that further quantification of the aerothermal environments encountered would need to be part of any additional work on this concept.)

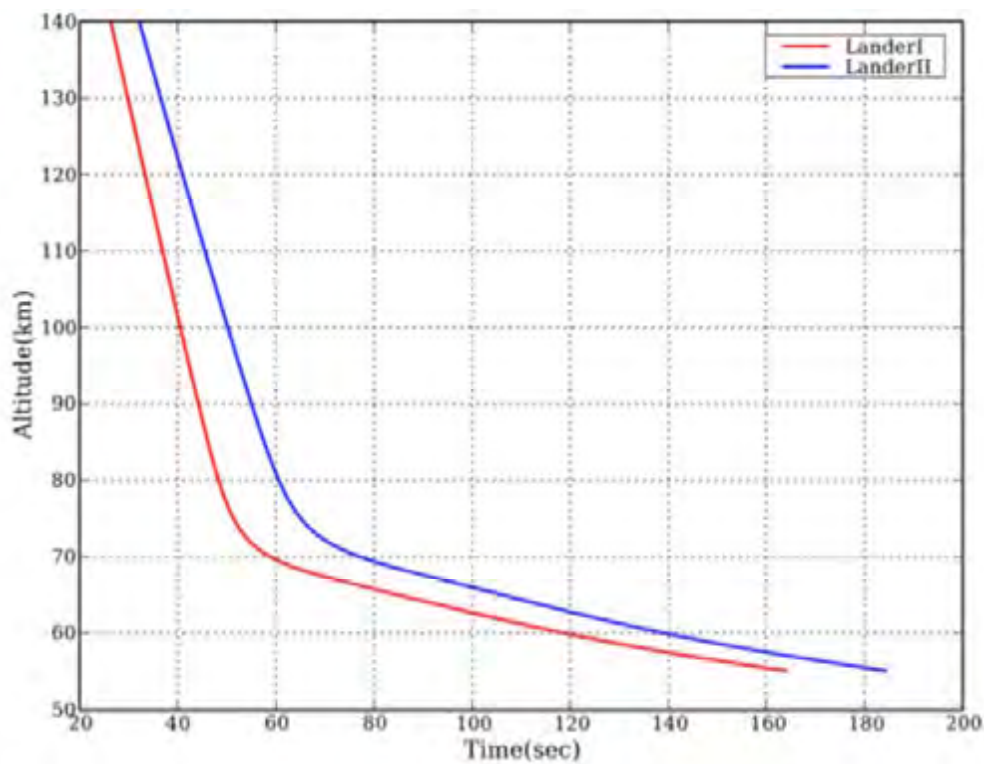


Figure 4.41: Nominal atmospheric entry plot.

No attempt was made to tailor the TPS thickness based on the distributed aerothermal environment; such work was beyond the scope of the current study. A direct comparison of PVLP to the current design is given in Table 4.44.

**Table 4.44:** Comparison of Entry Conditions and Design Between PVLP and DRM

	PVLP	DRM
Diameter, m	1.42	2.65
Entry Mass, kg	316.5	2,020
Ballistic Coef, kg/m <sup>2</sup>	186	349
EFPS [intertial], deg	-31.8	-13.8
Entry Velocity [intertial], km/s	11.6	11.1
Entry Altitude, km	138	220
Time to M=0.82, s	26.6	106
Stag. Point Max Conv. Heat Flux, W/cm <sup>2</sup>	2,321	1,210
Stag. Point Max Rad. Heat Flux, W/cm <sup>2</sup>	2,463	1,393
Stag. Point Max Tot. Heat Flux, W/cm <sup>2</sup>	4,690	2,571
Peak Stag. Press, atm	10	6
Peak Gs	288	97
Stag. Point Heat Load, J/cm <sup>2</sup>	13,135	20,620
Zero Margin Stag. Point TPS Thickness, cm	0.78	1.32

The final TPS mass reported above is only an initial estimate that resulted from a single-day Team-X session. Consequently, there was insufficient time to optimize the design; instead, the focus was on finding a convergent design solution, with the understanding that further refinements and optimization should be performed in the future.

To enable Venus missions, including the VDRM, TPS material and TPS testing experts studied strategies to utilize existing facilities capabilities combined with analysis as an approach to verify the performance of heritage CP as well as establish a qualification program that will result in no critical behavior of the as manufactured CP for future missions, like the VDRM. These were outlined and presented to the larger Probe Community at the 6<sup>th</sup> International Planetary Probe Workshop (IPPW6) (Venkatapathy et al., 2008) and referred here as an approach that could balance the risk, cost, and schedule.

Since the atmosphere of Venus is dense enough to be insensitive to small timing

variations during the EDL sequence, a g-switch is used to initiate timer operations for the atmospheric deployment, inflation, and landing operations. The peak entry g-load is calculated to be 123 g for the first entry system, with an EFPA of -15°, and 92 g for the second entry system, with an EFPA of -12°. Following a 56-s deceleration to a subsonic velocity of Mach<0.6, a mortar-deployed drogue parachute opens to further decelerate the entry system. This sequence is detailed in Subsection 4.4.6.

The trade-offs over which entry option would be executed were considered too detailed for inclusion in this study. Actually, peak shoulder heating is an entropy swallowing effect and, beyond a certain critical size, is not significantly affected by heat shield diameter. Shoulder heating is not a problem for fully dense CP, as the estimated levels are well within the proven performance envelope of the material.

The NASA ARC experts consulted for this study did consider EFPA variation of +/-1 deg as part of quick analysis to see the changes in heat load; this was taken into account in estimating the mass via margin.

#### 4.5.4 Balloons

##### 4.5.4.1 Overview

The Design Reference Mission (DRM) includes two balloons that will fly at a 55.5-km altitude for one month. These are single string designs based on the presumption that redundancy is provided by having duplicate balloons and payloads. The balloons are identical: each carries the same set of science instruments as part of the payload module (also known as the gondola). The balloons will take measurements of the Venusian atmosphere and clouds and relay the collected data to the orbiter on an occasional basis during their one-month lifetime. The 55.5-km flight altitude is suitable to meeting the science measurement objectives while providing a moderate temperature environment (30 °C) that allows for the use of existing balloon materials of construction. The balloons are expected to drift poleward due to the prevailing winds and end up in the polar

vortex by the end of the 30-day mission. This will provide substantial latitudinal coverage for the balloon science investigations. This subsection will describe the details of the balloon and gondola designs selected for the DRM.

The balloon is a spherical superpressure balloon filled with helium. This type of balloon is stable in altitude to atmospheric turbulence and diurnal solar flux variations without the need for active control through ballasting and gas venting. Superpressure balloons are, therefore, well-suited to the long duration mission requirement of 1 month at Venus. The DRM has adopted the particular Venus balloon design recently developed by JPL, ILC Dover, and NASA Wallops (Hall et al., 2008a, 2008b), suitably scaled up in size to accommodate the desired DRM payload mass. A prototype balloon is shown in Figure 4.42. The current DRM mass breakdown is shown in Table 4.45. The DRM requires a 7.1-m diameter balloon, as compared to the 5.5-m

size prototyped by the JPL-led team. This 30% diameter increase results in a 30% increase in the predicted tensile stress on the balloon material, which is tolerable given the predicted structural safety margin of 3 for the existing prototype balloon. This gives confidence that the larger size required by the DRM can be accommodated, although validation experiments will be required to confirm this.

The balloon subsystem is comprised of three elements: the balloon itself, the gondola that houses the scientific instruments and their support systems, and a 20-m long tether that structurally connects the balloon and gondola. As seen in Table 4.45, the estimated total floating dry mass is 149.6 kg, of which 45.0 kg (43%) is contingency mass on top of the current best estimate dry mass of 104.6 kg. The addition of 12.9 kg of helium brings the total floating wet mass to 162.5 kg. The balloon is 7.1 m in diameter, which is sufficient to float the entire 162.5-kg floating mass at a 55.5-km altitude at Venus.

**Table 4.45:** Balloon Mass Summary.

Element	CBE Mass (kg)	Cont. (%)	CBE+Cont (kg)
Science payload			
GC/MS	11.0	30	14.3
ASI	2.0	30	2.6
NFR	2.3	30	3.0
Mag	1.0	30	1.3
Neph	0.5	30	0.7
Lighting det.	0.5	30	0.7
Total Science payload	17.3	0	22.5
Balloon and Gondola Platform			
C&DH	3.1	30	4.0
Power	29.2	30	38
Structures	47.3	24	58.8
Cabling	2.9	50	4.4
Telecom	3.7	14	4.2
Thermal	1.1	28	1.4
Balloon and Gondola Platform Dry Mass	87.3	27	110.8
Balloon, Gondola and Science Total Dry Mass	104.6	27	133.3
System Contingency			16.3
Subsystem Total Dry Mass w/ Cont.			149.6
Helium			12.9
<b>TOTAL Balloon System Mass w/ Cont.</b>			<b>162.5</b>

Note: Total contingency is  $(133.3 - 104.6) + 16.3 = 45$  kg or 43% of the 104.6 kg balloon system CBE mass.



Figure 4.42: Prototype Venus balloon (Hall et al., 2008a).

The balloon will be aerially deployed and inflated in the atmosphere after entry. This process is briefly described in Subsection 4.4.6 (Figure 4.30b) and mimics that used by the Soviet VEGA balloons in 1985. The sequence will be autonomous and ends when the discharged helium inflation tanks are jettisoned and the fully inflated balloon starts floating.

#### **4.5.4.2 Balloon Command and Data Handling**

The gondola command and data handling unit is a Mac-100 device from Magellan/Bristol. This single-string system uses the UTMC radiation-hardened 80C196 microprocessor with a watchdog timer, a hardware-based critical command decoder, and a temperature controlled crystal oscillator. The mass of this device is 3 kg. The device consumes 7 W of power and can store up to 12 Mbits of data in RAM. This data storage equals 41% of the expected total data volume of 29 Mbits collected over the 30-day mission. To minimize power consumption during this time, the C&DH system is substantially duty-cycled with a very low power sleep mode used when not taking scientific measurements or communicating with the orbiter. An event clock module is used to sequence the duty-cycling and is based on a Dallas/Maxim DS1558 watchdog real time clock/calendar. This event clock module will have a mass of 200 grams and will consume approximately 220 mW of power.

The balloon cannot control its trajectory; therefore, the only flexibility is in the timing of the data acquisition and transmission events. The balloon will arrive at Venus with a pre-programmed data collection sequence for the full 30-day mission. This can be modified during the mission by uploading a new command sequence. The transmission strategy is only notional at this point: the timing of visibility between the balloon and the orbiter is uncertain due to the wind variability; hence, some kind of handshaking scheme is required to notify the balloon when the orbiter is in view. The design of that system will need to be done in follow-on studies.

#### **4.5.4.3 Balloon Power System**

The DRM utilizes an all-primary battery approach for the balloon gondola. While limited in total electrical energy, this approach avoids the complication of developing sulfuric acid resistant solar panels, while still achieving the desired science goals. A total of 220 SAFT LSH-20 lithium-thionyl chloride (Li-SOCl<sub>2</sub>) cells are used, arranged in 20 strings of 11 cells each. Each cell can provide 13 amp-hours of current at 3.67 Volts for an energy of 47.7 Watt-hours. Therefore, the total energy capacity of the 220 cell unit is 10.5 kW-hours. The total mass of all cells is 22.0 kg. Power electronics will be required for battery depassivation, load switching, and power conversion. This can be implemented on four 3U form factor electronics cards with an estimated mass of 1.6 kg. The mass of the battery enclosure and support structure is estimated to be 5.25 kg.

From an operational point of view, three distinct power modes were identified for the balloons, covering all relevant in situ operating modes. These power modes are:

- Mode 1: In situ science: 128 W.
- Mode 2: In situ telecom: 79 W.
- Mode 3: Sleep mode for science and telecom: 220 mW (during this quasi-sleep mode the C&DH system will require power for an event clock module).

Use of solar array with rechargeable batteries in combination with primary batteries might significantly increase data return. Further study is required to estimate an optimum combination and sulfuric acid protection issues.

#### **4.5.4.4 Balloon Structures and Mechanisms**

The balloon structure consists of three main components: the balloon, the gondola, and the inflation system (see Figures 4.43 and 4.44). The balloon consists of a fabric-based laminate material and metal end fittings. The balloon structure consists of aluminum, titanium, and composite materials.

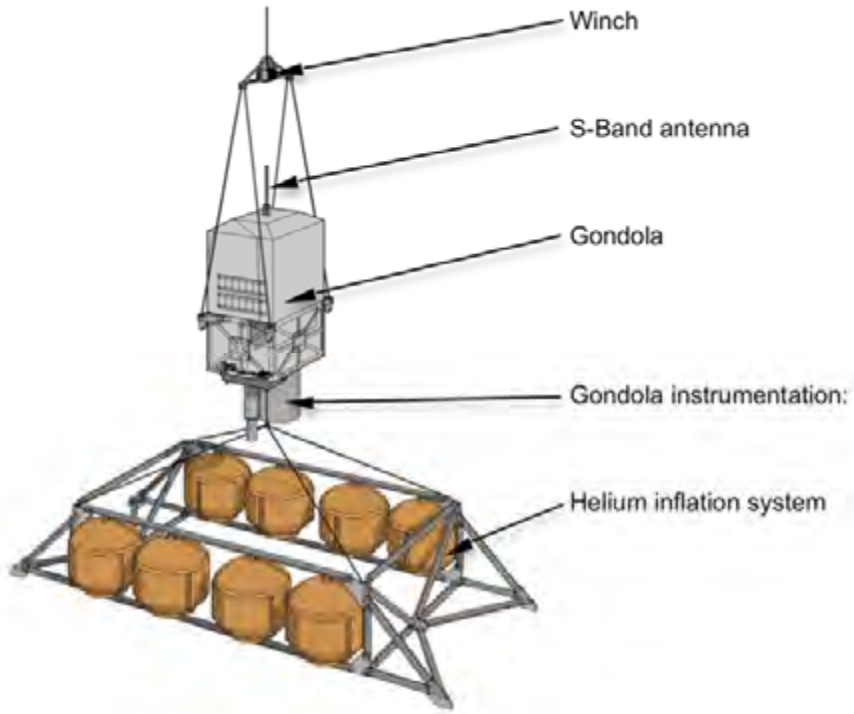


Figure 4.43: Balloon gondola attached to helium inflation system frame (artist's rendering).

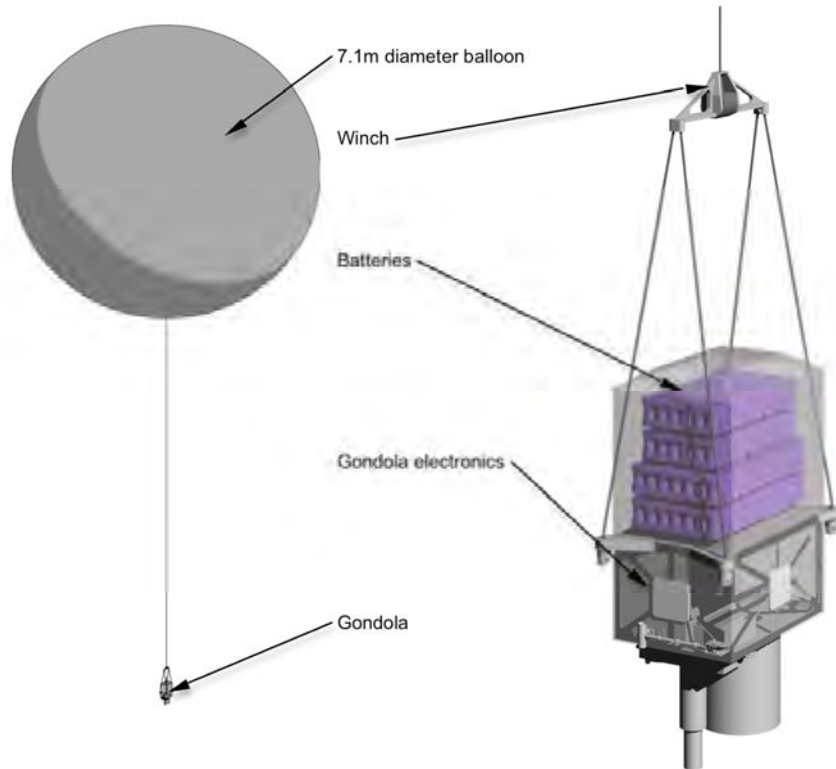


Figure 4.44: In situ balloon deployed (left) and gondola (right) (artist's rendering).

**Table 4.46:** Mass Breakdown for Balloon Structure and Mechanisms.

Element	Units	Mass (kg)
Primary Structure	1	10.4
Secondary Structure	1	3.9
Environment Protection	1	0.4
Tether	1	0.4
Teflon Coating	1	0.1
Gondola Deployment Device	1	1.2
Balloon	1	38.2
Balloon metal end fittings	1	2.3
Integration Hardware	1	0.7
TOTAL (less S/C-side adapter)		57.6
Cabling Harness	1	4.8

The mass estimate for the balloon structure and mechanisms is 57.6 kg, including a 30% subsystem mass contingency (see Table 4.46).

After the balloon system separates from the entry vehicle, the inflation system (Figure 4.43) inflates the balloon and is jettisoned.

The balloon material is a high-strength, sulfuric-acid-resistant laminate developed by JPL, ILC Dover, and NASA-Wallops (Hall et al., 2008). Figure 4.45 shows a schematic diagram of this material comprised of the following elements:

- An outer layer of 25-μm thick Teflon film for acid resistance.
- The inside surface of the Teflon is metalized with 30 nm of aluminum to provide a highly reflective surface for visible light, thereby minimizing the solar heating at Venus.
- The next layer in is a 25-μm thick metalized Mylar film for helium gas retention.

- The Mylar is, in turn, bonded to a Vectran fabric that provides the high strength needed to withstand the internal pressurization.
- Finally, the innermost layer is an aliphatic urethane coating that bonds to the Vectran fabric and provides a good surface on which to bond the internal gore-to-gore structural tape.

This laminate has an areal density of 173 g/m<sup>2</sup>. Structural tapes are used on the inside and outside surfaces to connect the 16 flat gores into a nominally spherical shape. A second Teflon cover tape is laid down on top of the outside structural tape to provide the required sulfuric acid resistance. A sulfuric acid resistant adhesive developed by ILC Dover is used to bond this cover tape on to the Teflon surface of the gore, providing complete acid protection.

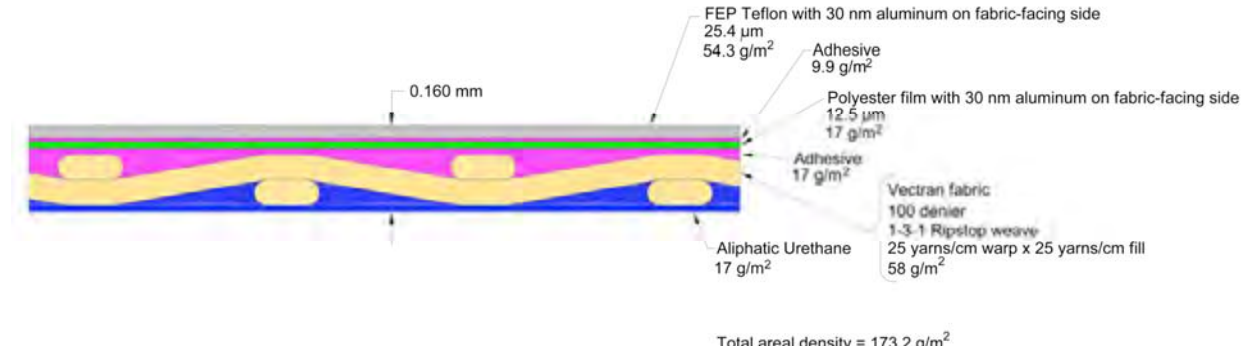


Figure 4.45: Balloon laminate material.

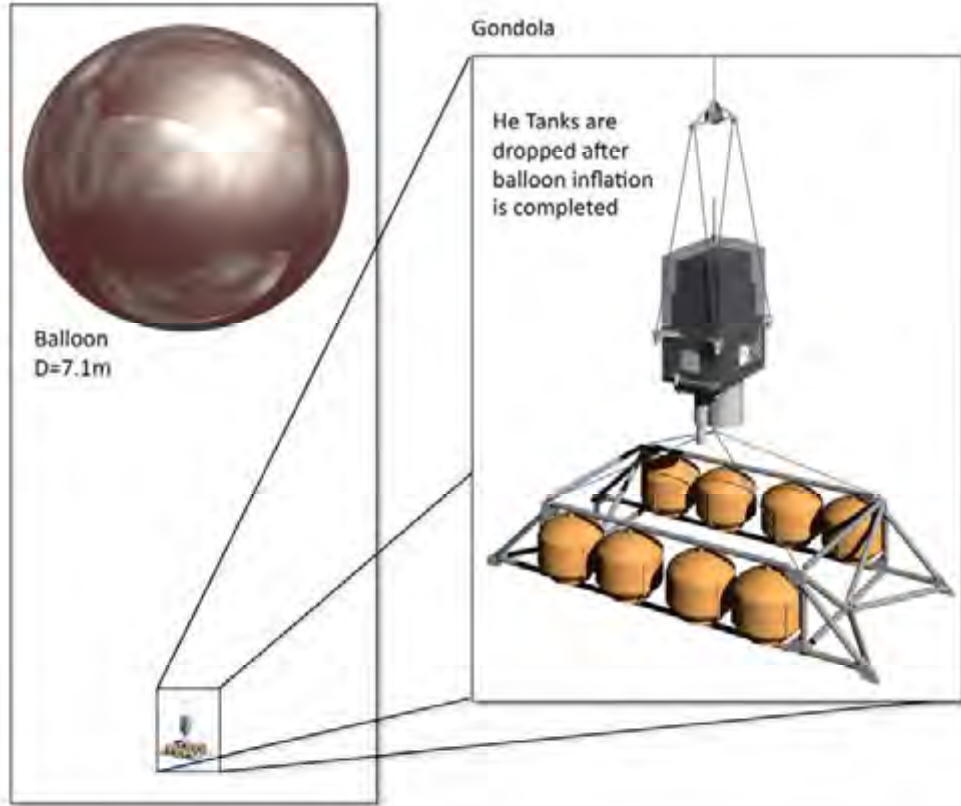


Figure 4.46: Venus balloon helium tank support structure.

The JPL, ILC Dover, and NASA-Wallops team have constructed two 5.5-m diameter prototypes of this balloon and conducted extensive laboratory tests on the balloon material and both prototypes (Hall et al., 2008, 2009). The balloon is, therefore, considered to be a mature technology at TRL 6.

A CAD model of the gondola is presented in Figures 4.5 and 4.44. The gondola structure is a vented box built from aluminum struts and face sheets. The outer surfaces of the box are coated with Teflon to provide sulfuric acid resistance. Venting is accomplished through a 25-mm tube that contains a sulfuric acid filter. This allows ambient atmosphere to flow into and out of the gondola, thereby equalizing the pressure during altitude changes without bringing sulfuric acid droplets inside. Individual components inside the gondola are mounted on horizontal decks, as shown in Figure 4.5. The support structure is sized to accommodate the maximum entry deceleration load of 400 g, well in excess of the expected

value of 123 g for the first entry system, with an EFPA of -15° and 92 g for the second entry system with an EFPA of -12°.

During the initial deployment and inflation of the balloon, the gondola is mechanically connected to the helium tank support structure (Figure 4.46). There is a 4-m long flexible hose connecting the Helium tanks and gondola to the bottom of the balloon; therefore, during the inflation sequence, the balloon-to-tank separation distance will be less than 4 m. However, after inflation it is necessary to greatly increase the separation distance between the balloon and gondola because the metalized balloon will interfere with radio communications. A descent rate limiter mechanism is used to accomplish this separation process in a controlled manner. This mechanism unspools the tether at a speed of 0.2 m/s after inflation of the balloon, increasing the balloon to gondola separation distance from 4 m to 20 m in 80 seconds.

#### 4.5.4.5 Balloon Telecom System

Based on science and mission requirements, the balloon telecom subsystem must be able to support: 1) low-rate engineering command and telemetry links via the orbiter or carrier and 2) carrier-only (Doppler) links to the ground. Thirty-four-meter DSN antennas will be used during normal operations. If 70-m antennas (or equivalent S-Band capability [although this is not planned]) are available, low-rate, direct-to-Earth communications might be possible.

The S-Band telecom systems on the balloons are identical. A block diagram of the balloon S-Band system is shown in Figure 4.47. Significant features of the telecom design include the following:

- One S-Band L3 CXS-610 transponder with diplexer, modified to accept input from a Sufficiently Stable Oscillator (SSO).
- One SSO for radio science.
- One S-Band low-gain antenna (LGA).

The telecom system is located on the gondola, which is suspended 20 m below the

balloon. Because the balloon has metal coated films, there will be a conical exclusion zone within 10° of zenith, where the link will not close because transmission is blocked by the balloon. During operations, communications sessions will be planned to avoid communicating in geometries where the balloon blocks the signal.

A design control table (DCT) containing representative link performance for the balloon-to-orbiter telemetry link during the 30-day balloon science phase is shown in Table 4.47. During operations, short 7-minute communications sessions once per hour will be scheduled when the range is 30,000 km or less. The link can support 500 b/s. Additional 7-minute communication sessions will be scheduled when the Earth is in view, such that the ground network will track the RF carrier signal to obtain additional Doppler and VLBI data. Balloon commanding will be performed by relay through the orbiter and nominally consists of short sequences to configure upcoming communications sessions.

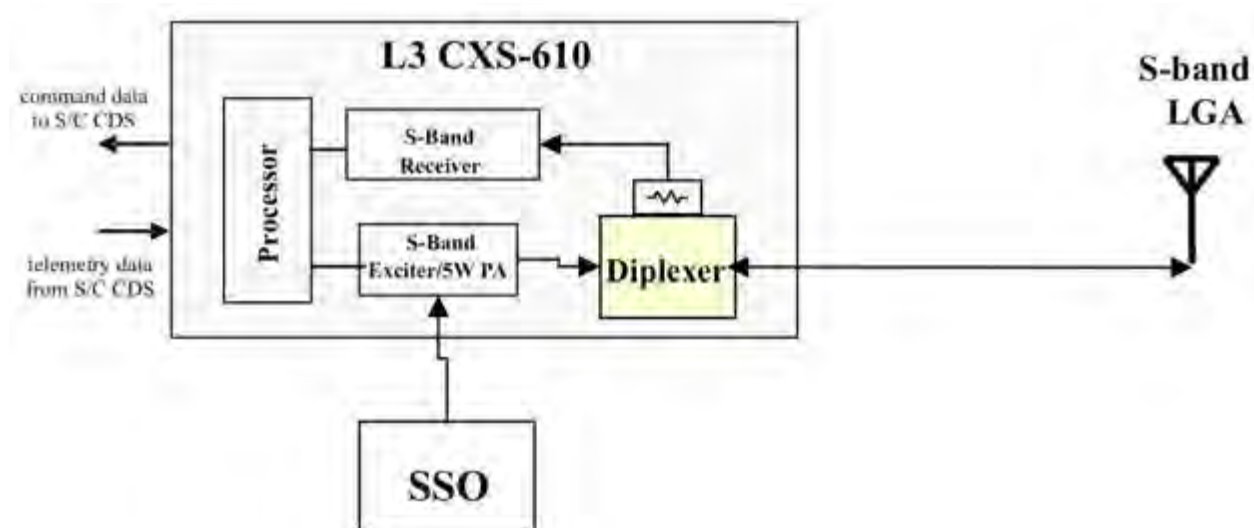


Figure 4.47: Block diagram of the balloon's telecom S-Band system.

**Table 4.47:** Balloon-to-Orbiter Relay Link.

Link Parameter	Units	Design Value	Notes
<b>TRANSMITTER PARAMETERS</b>			
1. Balloon Transmitter Power	dBm	36.99	5 W
2. Balloon Circuit Loss	dB	-1.7	
3. Balloon Antenna Gain	dBi	1	LGA (HPBW 140 or 180 deg)
4. EIRP	dBm	36.29	
<b>PATH PARAMETERS</b>			
5. Atmospheric Attenuation	dB	0.00	Balloon will not see any
6. Space Loss	dB	-188.43	30,000 km
<b>RECEIVER PARAMETERS</b>			
7. Orbiter Antenna Gain	dBi	21.15	0.7-m HGA
8. Orbiter Circuit Loss	dB	-2.3	
9. Orbiter Pointing Loss	dB	-3.15	7.3-deg error (= full-planet coverage at 30,000 km)
<b>TOTAL POWER SUMMARY</b>			
10. Total Received Power	dBm	-136.44	
11. System Noise Temperature	K	730.63	2.5-dB noise figure; 650 K Venus S-band hot body noise at antenna
12. Noise Spectral Density	dBm/Hz	-169.96	
13. Received Pt/No	dB-Hz	33.52	
<b>TELEMETRY PERFORMANCE</b>			
14. Telemetry Data Suppression	dB	-0.44	Telemetry mod index 72 deg
15. Total Data Power	dBm	-136.88	
16. Received Pd/No	dB-Hz	33.08	
17. Data Rate	dB-Hz	26.99	500 bps
18. Demodulation Loss	dB	0	
19. Eb/No	dB-Hz	6.09	
20. Threshold Eb/No	dB-Hz	3	RS + (7, 1/2); RS decode on the ground
21. Performance Margin	dB	3.09	

#### 4.5.4.6 Balloon Thermal System

The balloon and its payload will be maintained within allowable non-operating temperature limits during cruise to Venus by means of controlling the aeroshell temperature, which includes the balloon and lander elements. The aeroshell is passively controlled with thermal coatings and MLI blanketing. Thermostatically controlled film heaters are used as a safeguard measure within the aeroshell structure to maintain temperatures above the lower non-operating temperature limits of all the elements within. The duration of entry of the balloon in the upper atmosphere is short enough for the aeroshells thermal inertia to absorb entry heating; therefore, no thermal control system is necessary to maintain the payload below the upper

operating temperature limits. Furthermore, the deployment and separation events occur in a benign thermal environment such that the balloon and the payload will be maintained within the operating temperature limits without the need for a thermal control system. The float environmental conditions are fairly constant and uniform and at benign temperatures. Consequently, no thermal control is required for the balloon envelope or the payload for the duration of the mission.

#### 4.5.4.7 Balloon Operations

The balloons are passive vehicles that inherently track a constant density altitude and move with the winds. Therefore, the only command and control requirements pertain to the data acquisition and transmission operations. The notional plan is for the data

acquisition sequence to be preprogrammed for the entire 30-day balloon mission, with the option of having the capability to upload modified sequences if necessary. Data collection will be front loaded to provide a basic science return early in the mission. The science instruments will subsequently be duty-cycled as time goes on to stretch out the primary battery power supply. Data relay through the orbiter cannot be entirely pre-programmed because of the uncertainty in the wind-driven balloon trajectory around the planet and the resultant line-of-sight periods between the balloon and orbiter. Therefore, some form of telecom hand-shaking will be required so that the balloon knows when the orbiter is in view and able to receive data. At an average transmission rate of 500 bits/sec and a total data volume of 20.5 Mbits (Subsection 4.3.4.2), this requires 41,000 seconds of balloon-to-orbiter data transmission over the 30-day mission, which is only 1.6% of the total available time. Although the details of this process were not designed in this study, a 1.6% duty cycle is so low that a feasible solution should exist.

## **4.5.5 Lander**

### **4.5.5.1 Overview**

The two identical landers are designed to accommodate 10 science instruments, plus a surface corner reflector and a drill-based sample acquisition and handling system. The DRM lander design is roughly patterned off the Soviet Venera and VEGA landers, although relatively little detailed mechanical and thermal design work has been done to date. The past Soviet successes indicate the feasibility of this approach for a Venus lander design, but the specific resource metrics (mass, power, volume) estimated here are clearly uncertain given the lack of specific detailed design work for the DRM.

These landers are single-string designs where redundancy is provided by having duplicate landers. Some of the instruments are used during atmospheric descent only, while others are used on the surface. Most of the instruments and subsystems are housed inside a pressure vessel, where the temperature is passively controlled using insulation and phase change material. The expected lifetime of the lander is 5 hours on the surface, approximately twice that of the longest-lived Soviet lander from the Venera program. (The Venera 13 lander survived for 127 minutes on the surface.). The pressure vessel includes three types of penetrations, which constitute a significant fraction of the total heat leakage from the environment. These are: (a) windows for imagers; (b) feedthroughs for data and power wires and sensors; and (c) tubes for the sample acquisition system and the pressure sensor. The drill and sample acquisition system are rigidly mounted outside of the pressure vessel. Surface access to a range of autonomously accessible locations is achieved using a rotating pressure vessel and onboard processing. Sampling and drilling operations are further discussed in Subsection 4.5.5.9. The lander mass summary is shown in Table 4.48.

### **4.5.5.2 Attitude Control System**

The lander descends through the atmosphere under a parachute, which will provide attitude stability in the correct crush-pad down orientation. However, accelerometers will be incorporated to help reconstruct the descent trajectory and determine the lander's orientation once on the ground. Three Allied Signal QA3000-020 navigation-grade accelerometers will be used. These devices have a resolution of 0.1  $\mu\text{g}$  and a range of  $\pm 25 \text{ g}$ . These accelerometers have high flight heritage: this type has been used on the Mars Observer, Delta II launch vehicles, and the Mars Pathfinder.

**Table 4.48:** Lander Mass Summary.

Element	CBE Mass (kg)	Cont. (%)	CBE+Cont. (kg)
<b>Lander payload</b>			
Gas Chromatograph Mass Spectrometer	11.0	30	14.3
X-ray Diffraction and Fluorescence	12.0	30	15.6
Microscopic Imager	0.3	30	0.4
Thermocouple, Anemometer, Pressure Transducer, Accelerometer	2.0	30	2.6
Lander Spectroscopic Imaging System (Descent Camera)	0.5	30	0.7
Panoramic camera	0.5	30	0.7
Drill camera	0.5	30	0.7
Intrinsic Gamma Rays	1.5	30	2.0
Magnetometer	10.0	30	13.0
Nephelometer	0.5	30	0.7
Net Flux Radiometer	2.3	30	3.0
Surface Corner Reflector	5.0	30	6.5
Heat Flux Plate	0.5	30	0.7
Drill and Sample Handling System	35.0	30	45.5
<b>Payload Mass Total</b>	<b>81.6</b>	<b>30</b>	<b>106.2</b>
<b>Lander Bus</b>			
Altitude Control	0.2	10	0.3
C&DH	10.7	30	13.9
Power	18.6	30	24.2
Structures and Mechanisms	219.0	30	284.7
Cabling Harness	25.6	30	33.3
Telecom	8.5	18	10.0
Thermal	116.7	30	151.4
<b>Bus Total Mass</b>	<b>399.3</b>	<b>30</b>	<b>517.8</b>
<b>Lander Bus + Payload</b>	<b>480.9</b>	<b>30</b>	<b>623.9</b>
System Contingency			62.1
<b>Lander Bus + Payload /w all contingency</b>			<b>686</b>

NOTE: Total contingency is  $(623.9 - 480.9) + 62.1 = 205.1 \text{ kg}$  or ~43% of the 480.9 kg Lander Bus + Payload CBE mass.

#### 4.5.5.3 Lander Command and Data Handling

The lander's single-string-designed C&DH subsystem must support a 6-hour mission at Venus, including the 1-hour descent phase. The main C&DH subsystem uses the JPL MSAP architecture. The lander includes a Motor Interface Card, which will be adapted for the drill. The lander will operate in a completely autonomous mode due to the short duration of its mission. This includes the data acquisition, the data transmission sequence, and the landing sequences.

#### 4.5.5.4 Lander Power System

The two landers must operate during the 1-hour descent and for ~5 hours on the surface. This short operation can be supported with internal power storage: namely, with primary batteries, which would provide a simple, low-risk, and cost-effective solution, with significant design heritage. Note that solar panels would not work at Venus surface conditions and internal power generation in the form of a radioisotope power system (RPS) would be too expensive to develop and not required for this short duration. The use of

RPSs on longer surface missions is discussed in Section 5.4.

As the lander descends to the surface, the outside temperature increases to  $\sim 460$  °C, while the temperature inside the pressure vessel is mitigated by phase-change materials. This temperature is relevant to keep the batteries (and electronics, which also contribute to the heat input) within a desired operating temperature range. The design goal is then to keep the batteries at an internal temperature off  $\sim 55$  °C.

The lander batteries consist of 126 SAFT LSH-20 lithium-thionyl chloride cells (the same cells used on the balloons) arranged as 14 parallel strings of 9 cells each. The total battery cell mass is estimated at 12.6 kg, not including a housing and support structure mass of 15.6 kg. The nominal capacity of a cell is 13 AH at 3.67 V, translating to 47.7 W-hr each. Therefore, the nominal battery capacity for each lander is 6.01 kWh for 126 cells (not-derated). A 6-hour mission is short enough to require derating of the voltage and capacity. For this case, the cell capacity is 9.5 Ah at  $\sim 2$  amps and 3.35 V at a corresponding cell temperature of 55 °C. From this, the derated battery energy for the 9 cells 4.0 Ah. This compares quite closely to the 4.1-kWh requirement shown.

The power system also includes lander power electronics, with a mass of 1.6 kg, with 3U form factor electronics slices (0.4 kg CBE each). These support (a) the battery depassivation circuit and telemetry circuits; (b) load switching; (c) power conversion; and (d) pyro firing. (The pyro functions are required during the lander deployments, making the lander power electronics more expensive than that for the balloon/gondola.)

From an operational point of view, two distinct power modes were identified for the lander, covering all relevant in situ operating modes. These modes are:

- Mode 1: Descent with telecom: 492 W (during this time the lander would perform

descent science measurements and communicate the data to the orbiter).

- Mode 2: Surface Operations with telecom: 729 W (during this time the lander would perform its science measurements, including sample acquisitions and handling, and communicate the data to the orbiter).

Due to the short lifetime of the lander, it is expected that the science measurements, data processing, and telecom are working continuously. Therefore, no other operating modes were identified for science or telecom only or for standby mode.

#### **4.5.5.5 Lander Descent and Landing**

Following atmospheric entry by the entry system and separation between the balloon and the lander, the lander will descend to the surface on a small parachute. This was the approach successfully used on Venera 8, although subsequent Soviet landers did use fixed drag plates. The need to do descent imaging on the DRM lander motivates the use of a small parachute to provide a more stable platform than can be achieved with a drag plate. In particular, the fixed drag devices used on Venera 13 and Venera 14 experienced angular rates up to 60°/sec, which are prohibitive for the descent imaging. The cruciform parachute (or other stable parachute-like disk-band gap) typically have swinging amplitude of only 2 to 5 degrees with a period of 5 to 10 sec (depending on the length of the suspension lines) that yields an angular rate of  $<7$  °/sec, which is 3 times less than maximum swinging rate for non-smeared descent images. The parachute will be a 2.5-m diameter cruciform (or cross) fiberglass parachute that will be sized to enable a 1-hour atmospheric descent and provide a landing speed of  $\sim 7.5$  m/s. Fiberglass is tolerant of both sulfuric acid and the 460 °C temperatures found on the Venusian surface. The impact of landing will be absorbed by an annular crush-pad, as shown in Figure 4.48. Further details on the EDL process are given in Subsections 4.4.6 and 4.5.3.9.

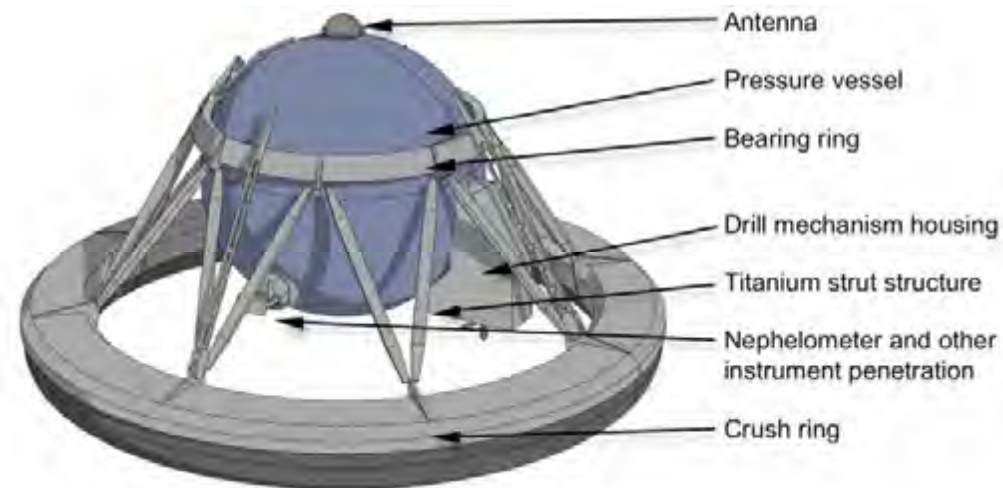


Figure 4.48: Lander configuration (artist's rendering).

#### 4.5.5.6 Lander Structures and Mechanisms

The lander consists of a spherical pressure vessel hung on a bearing ring supported by a truss and crush ring. The pressure vessel is titanium, with 5-cm thick thermal insulation on the exterior. The truss and upper section of the crush ring are also titanium, with crushable honeycomb material below (Figure 4.48). This design features the novel functionality of a rotating pressure vessel, enabled by the bearing ring and driven by a high-temperature motor mounted on the outside. The purpose of the rotation is two-fold: first, it provides a simple way of moving the drill to a good drilling site (see also Subsection 4.5.5.10) without using a robotic arm with articulated joints; second, the rotation allows for simple, high-quality panoramic images to be obtained using one camera looking out through one window. High-temperature-compatible dry lubricants will be used on the bearings, which only have to tolerate 2 or 3 very low speed (0.2-rpm) rotations during the mission lifetime.

After separation from the aeroshell, the lander descends under a small diameter parachute and lands at an estimated speed of 7.5 m/s. The impact is absorbed by a ring-shaped crush pad, which is similar to the approach used on the Venera and VEGA missions. The notional design shown in

Figure 4.49 includes outriggers that are deployed at the moment of landing to help accommodate slopes that might otherwise pose a tip-over hazard. However, there are a number of issues with this lander concept that were not addressed in the DRM, including tolerance to landing on rocks that might impact and damage the pressure vessel and the possible draping of the small parachute over the lander immediately after landing. These problems and others will need to be addressed on follow-on studies that perform a more detailed and comprehensive design of the overall lander system.

The configuration of instruments inside the lander is shown in Figure 4.7. The mass estimate for the lander structure and mechanisms is 284.7 kg, as detailed in Table 4.49.

#### 4.5.5.7 Lander Telecom System

Based on science and mission requirements, the lander telecom subsystem must be able to support: 1) medium-data-rate engineering telemetry links via the orbiter and 2) low- to medium-data-rate engineering telemetry links via the carrier (in case the orbiter is not available). In the nominal relay scenario, the orbiter will be the prime relay asset and the landings will be staggered such that the orbiter only needs to communicate with one lander at a time.

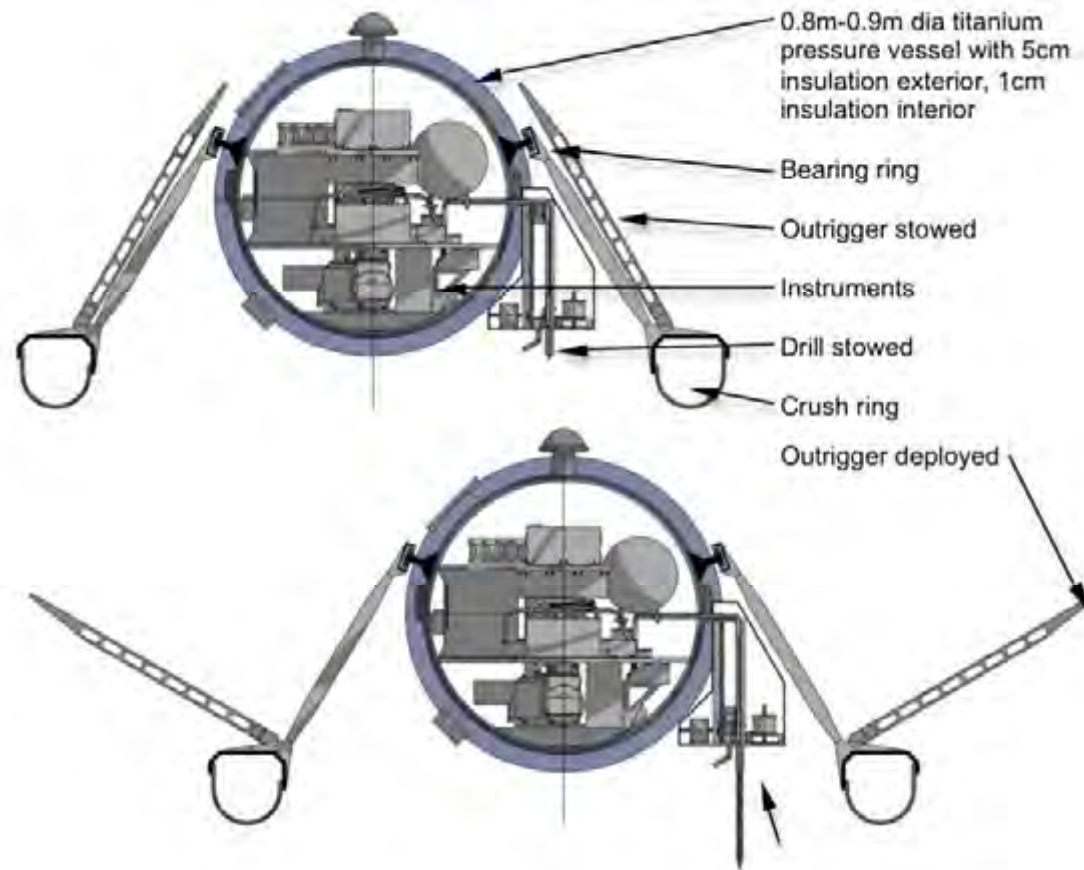


Figure 4.49: Lander design: stowed (above), and with drill and outriggers deployed (below) (artist's rendering).

**Table 4.49:** Mass Breakdown for Lander Structure and Mechanisms.

Element	Units	Mass (kg)
Primary Structure	1	104.0
Lander Release System	4	5.2
Crush-plate / legs	1	117.0
Internal Mounting Structure	1	26.0
Outriggers (including hinges)	4	5.2
Pressure Vessel Bearing	1	6.5
Pressure Vessel Bearing Ring	1	3.9
Outrigger Launch Restraint	4	1.3
Parachute	1	7.8
Parachute Canister	1	2.6
Integrated Hardware	1	3.9
Balance Mass	1	1.3
<b>TOTAL (less S/C-side adapter)</b>		<b>284.7</b>
Cabling Harness	1	33.3

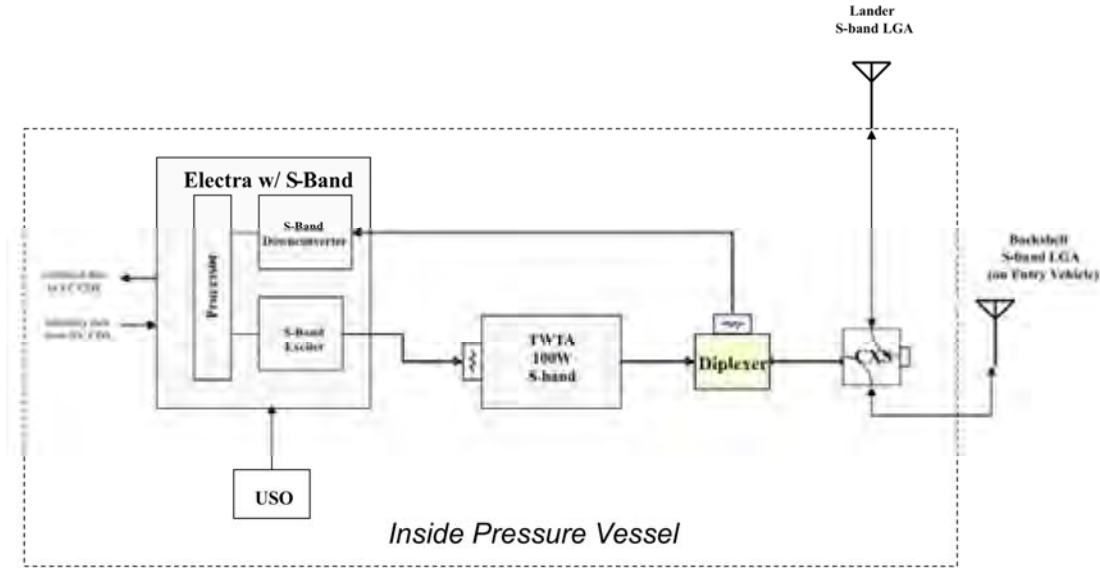


Figure 4.50: Block diagram of the lander's S-Band system.

The S-Band telecom systems on the landers are identical. Except for the LGA, the telecom subsystem is located within the pressure vessel to protect it from the Venusian environment. A block diagram of the lander S-Band system is shown in Figure 4.50. Significant features of the telecom design include the following:

- One S-Band Electra transceiver.
- One Ultra-Stable Oscillator (USO) for radio science.
- One 100-W S-Band traveling wave-tube amplifier (TWTA).
- One S-Band low-gain antenna (LGA).

An average information bit rate of 40 kb/s is sufficient to return the science data collected during the six-hour prime mission (a one-hour descent and five hours at the surface). Assuming no tilt, an LGA with 140° half-power beamwidth, and 3-dB design margin, the lander at the Alpha Regio site (where the maximum carrier elevation is 20°) can support 64 kb/s. The lander at the Lava Flows site, where the maximum carrier elevation is 40°, can support at least 128 kb/s. Plots showing the supportable data rate and 5-hour cumulative data volumes for each landing site over a 24-hour period are shown in Figures 4.51 and 4.52, respectively. It is assumed that orbiter phasing will be adjusted to coincide with periods of maximum cumulative data

volume for each lander. If the phasing cannot be adjusted to optimize coverage for both landers, priority can go to the Alpha Regio lander because there is more margin with the lander at the Lava Flows site.

If the orbiter is not available to support relay, the landers will be re-targeted to landing sites near each other. The carrier will be diverted to fly by the landing sites and track the landers simultaneously in a listen-only mode. Since the carrier will be in listen-only mode and not using adaptive data rates, additional margin might be needed to account for the possibility of adverse landing tilts, which will reduce the supportable data rates. Furthermore, it is assumed that the new landing sites are close enough together that they remain within 2° of the boresight of the body-fixed carrier HGAs that are communicating with each lander. The effect of this degraded pointing is an additional 3 dB of loss. From a geometric perspective, because the carrier will fly by the sites instead of going into orbit, it is likely that the elevation profile will be more favorable, with communication closer to the LGA boresight (where gain is higher), although the range profile might be worse to allow the carrier to remain in view for six hours. Further study is needed to better quantify telecom performance in the absence of orbiter relay support.

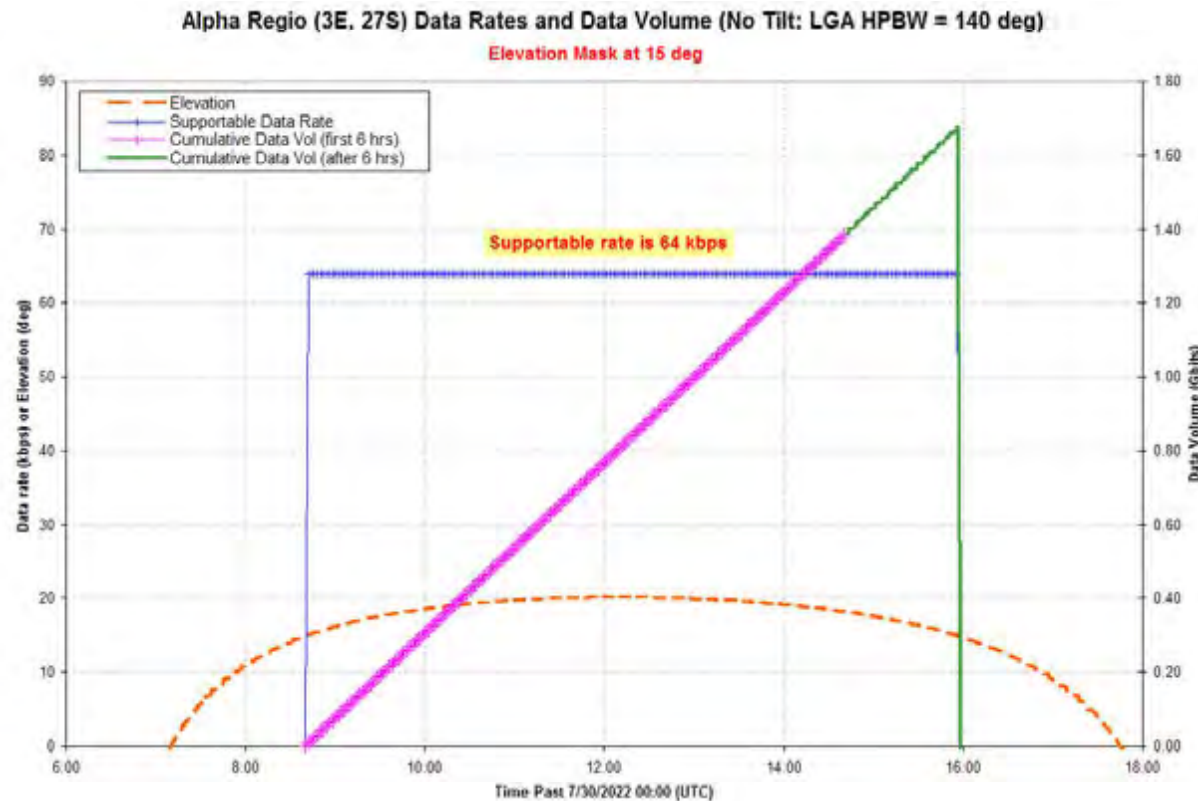


Figure 4.51: Lander-to-orbiter data rate and 5-hour cumulative data volume for Alpha Regio site.

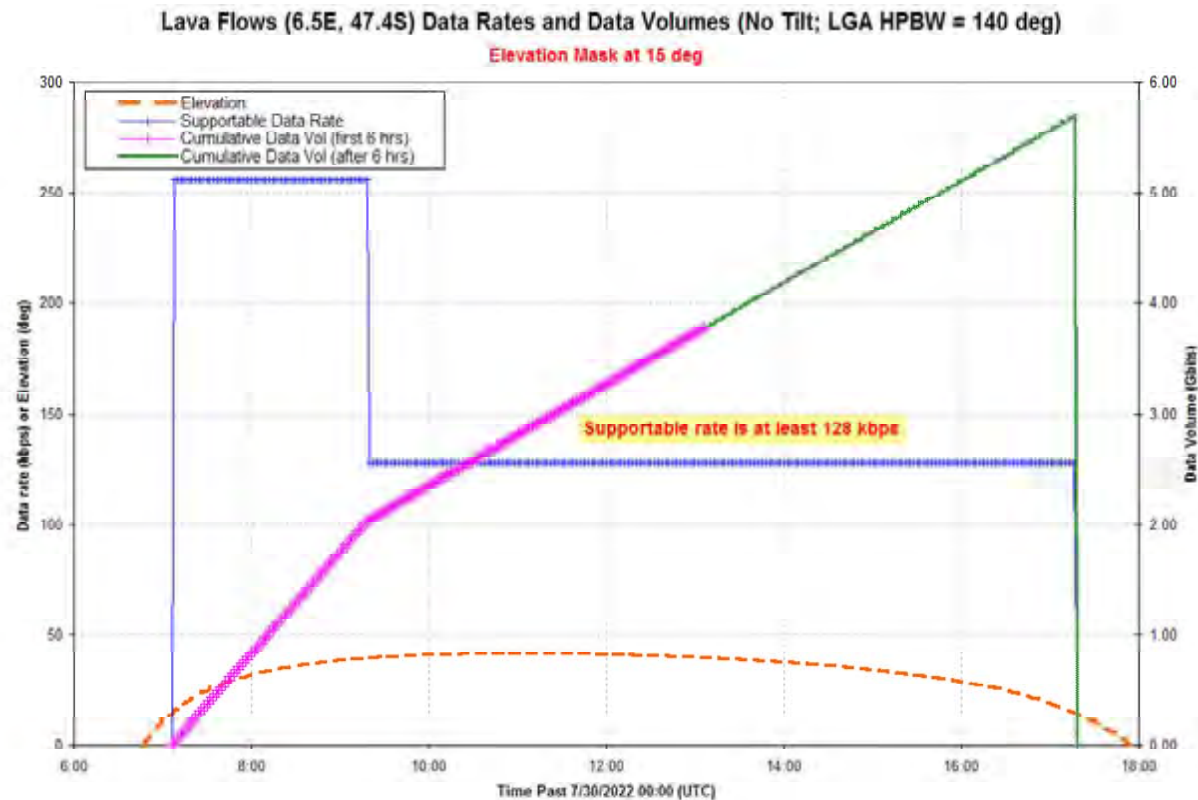


Figure 4.52: Lander-to-orbiter data rate and 5-hour cumulative data volume for lava flows site.

#### 4.5.5.8 Lander Thermal System

The lander thermal control approach is designed to meet a mission duration of approximately 5 hours on the surface, in addition to the 1-hour descent. The approach is entirely passive, making it simple and robust. Typical component upper qualification temperatures are at 75 °C which is 20 °C above the allowable flight temperature limit of 55 °C. The lower qualification temperature is -35 °C, which is 15 °C lower than the allowable flight temperature limit of -20 °C, which would most likely be encountered during cruise. The batteries have non-operating temperature limits of -40 °C to +10 °C and operating temperature limits of -10 °C to +60 °C. Key design features minimize radiative, conductive, and convective heat transfer through the pressure shell to the internal components and use thermal energy storage within the shell to maintain functionality for the mission.

1. **Exterior insulation**, 5 cm thick, with a thermal conductivity of 0.05 W/mK, made of porous silica is used to reduce heat transfer into the structural shell. This insulation is available from several manufacturers and goes by the trade names of Microtherm, Min-K, and Zircal. There are some differences between insulation from the different vendors, but any of them should work. In general the design of the exterior insulation would require the insulation to be fabricated into blocks that would then be cemented to the outer surface of the shell using a sodium silicate adhesive. A thin exterior skin of titanium is used as a retainer to hold the insulation in place during entry and landing.
2. **Interior insulation**, 1-cm thick, is the same material as that used on the exterior. It is

used to reduce heat transfer to the backfill gas within the lander. An interior skin is also used to keep the insulation in place.

3. **The lander is backfilled** with carbon dioxide to limit conductive and convective heat transfer through the internal atmosphere. The interior pressure can be within 5 to 800 Torr (~0.007 atm to ~1 atm) and maintain adequate thermal and pressure conditions within the lander. (Further studies should address the mission impact of a suitable XRD/XRF sub-compartment design, which maintains the pressure at the lower end of this range to support XRF spectra measurements of the light elements, such as Na, Mg and Al.)
4. **Phase Change Material (PCM)** is used to absorb thermal energy generated by the electronics within the lander and the heat leaked in through the pressure vessel walls. Lithium nitrate trihydrate has the highest energy absorption density exhibiting a solid to liquid phase transition. This material was successfully used by the Soviets on the Venera landers. Approximately 35 kg of this material is required for the DRM.

The lander TCS design was developed using a simple thermal math model (TMM). The TMM is based on insulation data, PCM capacity data and empirical correlations for thermal convective coefficients. Figure 4.53 shows temperature as a function of time for the payload electronics, structural shell and insulation demonstrating the payload is below the AFT limit of 55 °C at 5 hours of surface operation. The thermal response of the lander during descent through the atmosphere is shown in the first hour of the figure. The landed mission begins at the one hour mark.

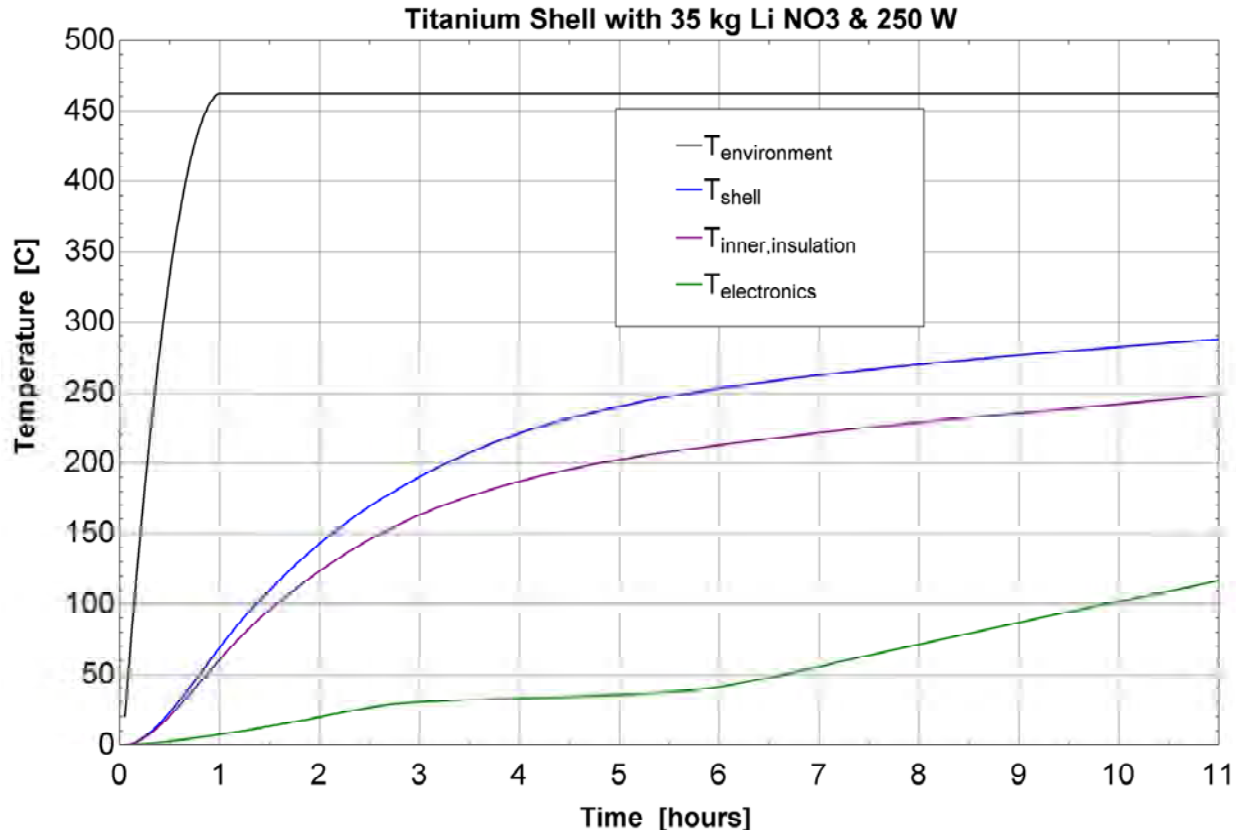


Figure 4.53: Thermal model results of Venus lander. The internal payload temperature is the green line.

The thermal model assumes there are 3 window penetrations in the shell for cameras. The diameter of each window is 3.4 cm for the Descent camera and 11.2-cm diameter for the Panoramic camera and the Drill Site camera. For thermal modeling purposes, 20% IR transmission through the windows is assumed as an upper bound case. Around each window there is a Titanium frame that is assumed to be un-insulated, which is a conservative assumption. Each frame has a cross-section of 0.5-cm outer diameter around the window with a penetration length of 6 cm. There are 15 cable penetrations modeled as copper conductors 0.3-cm diameter by 30-cm long, which conduct heat from the exterior ambient temperature to the payload temperature.

The power dissipation in the lander is assumed to be 400 watts continuous. The interior of the lander is backfilled with CO<sub>2</sub> gas at low pressure (e.g., in the range of 5 to 800 Torr), therefore the thermal model

accounts for gas conduction and convection between the inner insulation surface and the payload. It is also assumed that the interior of the lander will be at 0 °C at the beginning of descent into the atmosphere. A heat flow diagram shown in Figure 4.54 gives an indication of the heat loads and their associated paths at the end of the mission time, 5 hours on the surface. At the beginning of the surface mission, the heat loads are higher because the temperature difference between the lander and the environment are greater.

Interpretation of the heat flow diagram is as follows. On the left side of the figure is the temperature of the ambient environment, 462 °C, which is also the same temperature as the exterior surface of the insulation. There is 585 W of heat conducting through the insulation at 5 hours on the surface. There is also a total of 292 W of heat conducting through the titanium window frames, which are connected to the pressure vessel shell.

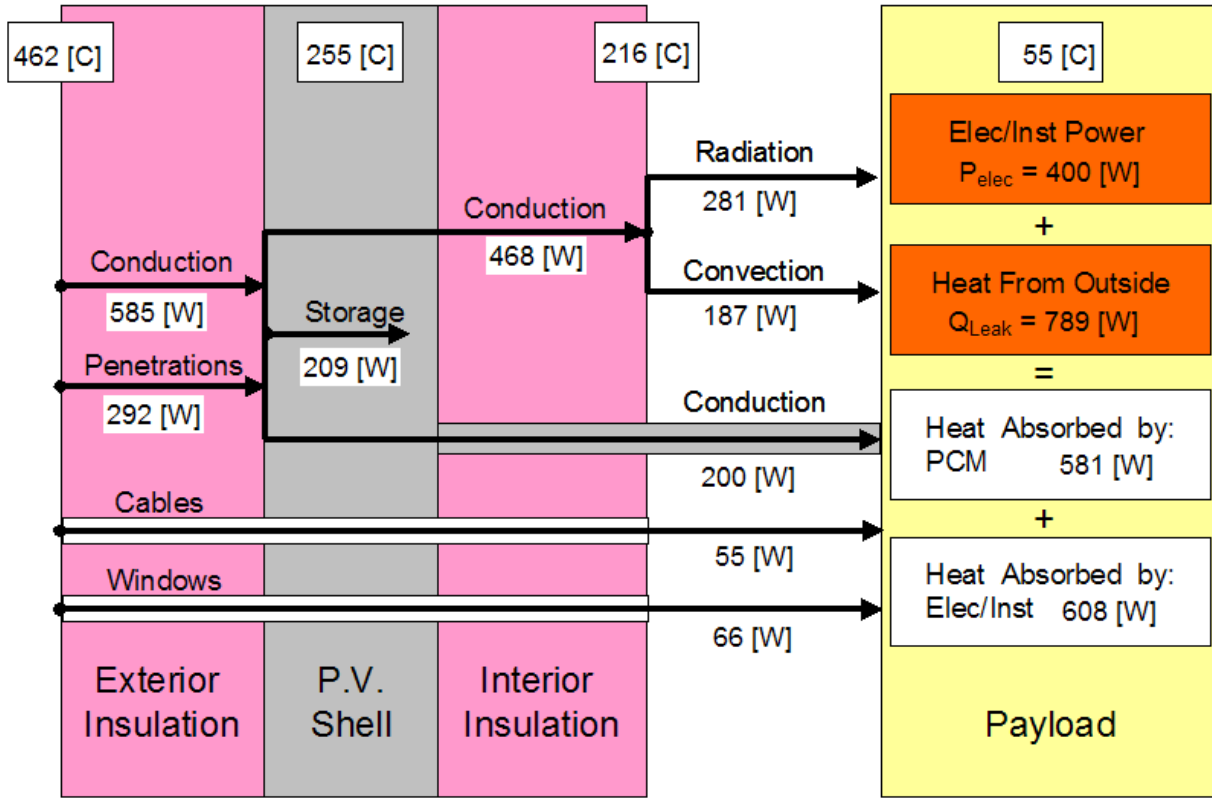


Figure 4.54: Heat flow diagram of the lander at end of mission.

Some of this heat (209 W) is stored thermally in the shell; the rest is conducted through the interior insulation (468 W) or through the structural mounts (200 W) between the shell and the equipment shelves. Heat is transferred from the surface of the inner insulation by radiation (281 W) and by convection (187 W) to the payload electronics, instruments and Phase Change Material. The cable and the window heat loads are 55 W and 66 W respectively. The payload and the PCM receive heat from the external sources and must also absorb the self-generated heat load of 400 W.

#### 4.5.5.9 Lander Sample Acquisition System

The sample acquisition and handling system is a complex element crucial to the success of the lander mission. For purposes of the DRM, we adopted a basic approach that mimics that used on the Soviet Venera and VEGA missions after considering other options that are described in Table 4.50. The design of this

system is clearly notional at this time and there are significant technology development requirements that are discussed later in Subsection 4.8.1.

The high temperatures of the Venus surface make it likely that heterogeneous reactions between the atmosphere and surface minerals have been extensive. The depth of the weathered layer is unknown, since there are very few experimental or theoretical limits on the nature of these processes. However, Venera images of the surface show that plates of basalt with a thickness of a few cm are detached from the bedrock, indicating some kind of horizon that may be the result of either thermal processes (such as cooling of the lava as it was emplaced) or a difference in chemistry at this depth. For this reason, the Decadal Survey (National Research Council, 2003) specified that samples should be acquired at the surface and at 10 cm below the surface.

**Table 4.50:** Sampling Technology Comparison.

Sample Acquisition Technologies	Sample Description	Comments
Ultrasonic Drill/Corer	Powder/Core	Low Power, Low Preload, Long Time Duration
Gravity Drop Harpoon	Powder/Regolith	Low Power, Short Time Duration, Low Autonomy
Brush Wheel Sampler	Regolith/Soil/Sand	Low Power, Low Autonomy, Works well on surfaces with loose Material
Scoop	Regolith/Soil/Sand	High Power, High Autonomy, Works well on surfaces hard and soft surfaces, Long Time Duration
Rotary Drill/Corer	Powder/Core	High Autonomy, Short Time Duration with High Preload and High Power
Rotary Percussive Drill/Corer	Powder/Core	Low Power, Low Autonomy, Short Time Duration, Additional Complexity with Percussive capability
Pneumatic Sampling	Regolith/Soil/Sand	Picks up loose material from surface (often created by a separate drill), low power, low autonomy, requires a dense atmosphere

*Note: Selected approach highlighted in yellow.*

Comparison of the chemistry and mineralogy of samples between the surface and at depth will place very important constraints on the nature of surface/atmosphere interactions. Therefore, the DRM adopted as a requirement that the lander sample acquisition system will acquire samples from the immediate surface and at 10-cm depth for analysis by the XRD/XRF instrument and microscopic camera.

The selection of a rotary drilling system for generating samples on the Venus lander is based on (a) the sampling requirements for the science, (b) the short duration mission time, (c) the need for high autonomy, (d) physical characteristics of the lander, (e) low risk, and (f) Russian Heritage. The three science instruments that require samples are the XRD/XRF, the GCMS (via a pyrolyzer) and the Microscopic Imager. These instruments require about 1 cm<sup>3</sup> of powder each from a weathered surface layer and from presumably harder, unweathered rock that is expected to be found at an approximate depth of 2 to 10 cm. This requires a sampling tool, such as a rotary drill, that can travel relatively long distances (i.e., 10+ cm). Since the short mission duration does not provide adequate time to put a human operations team in-the-loop for the sampling process, this requires the sample acquisition system to have a significant degree of autonomy, as discussed in Subsection 4.5.5.10. The lander will be in excess of 600 kg and

provide a stable base to attach a rotary drill as well support the necessary high preload.

Table 4.50 shows potential sample acquisition technologies for the DRM that have been either tested in R&D field experiments or in actual flight missions. Based on the Technology Readiness Level, science requirements, short mission duration, high level of required autonomous operation and Russian heritage, a Soviet-style rotary drill combined with a pneumatic vacuum sampling system was chosen for the DRM (shaded in yellow). The rotary drill will provide the science instruments with a powder sample from a hard material and it is one of the lowest-complexity sampling tools that can be utilized at high levels of autonomous operations. A rotary drill has the capability to sample at a wide range of depths and, as stated before, the lander mass provides a large preload. With a high power draw over a short mission duration, a rotary drill can generate the required sample within the shortest period of time to maximize the time for the science instruments to analyze the sample. The pneumatic vacuum sample transfer system minimizes complexity and optimally utilizes the environmental conditions on the Venusian surface. The Russians successfully demonstrated rotary drilling and vacuum sample transfer on the Venusian surface with their Venera 13, Venera 14, and VEGA 2 landers back in the early 1980s by acquiring 3–6 cm<sup>3</sup> of sample.

The rotary drill for the Venus lander will have 3 high-temperature actuators external to the pressure vessel, which will be used for applying preload by (a) translating the drill stem, (b) rotating the drill bit, and (c) switching the sample distribution path. The drill will translate via a lead screw type mechanism with shafts used for guiding the linear motion. This mechanism will turn rotational motor input into translation motion. The lead screw will provide high translational force with a low required input torque. The drill bit will be rotated using a motor and an appropriate gear ratio that will be sized to cut into a range of materials that could be encountered on the Venusian surface. The sample distribution path system will guide and deliver the surface samples from two required depths (surface and 2 – 10 cm) to the sample transfer and handling system, and discard any unwanted material in between.

The sample transfer and handling system will utilize two metal tubes, leading to a rotary sample tray inside the pressure vessel and to the GCMS pyrolyzer. The rotary sample tray would shift the samples to both the XRD/XRF and the Microscopic Imager for analysis. The two samples, from the two depths (one each),

will be carried inside using two low pressure (near vacuum) tanks, that will use the pressure differential between them and the Venusian atmosphere at the surface to suck the sample into the pressure vessel, allowing it to fall into the rotary sample tray using gravitational forces. The two tanks will be used only for one sampling event each. This would preclude the lander from having insufficient suction force for the second sample. The two-tank method will also eliminate the need for opening and closing the vacuum tanks autonomously in real time and any sensing capabilities associated with such an operation.

The drill and the sample acquisition assembly would be permanently mounted on the pressure vessel, which would also include appropriate tabular penetrations to get the samples to the instruments (see Figure 4.55). This design could further simplify both the mechanisms and the drilling operations. However, in order to access the best drilling location the pressure vessel itself will be rotated in a full circle, while onboard autonomous processing would allow to select the best drilling location from this accessible 3 – 3.5-m long circular strip. This will be further discussed in Subsection 4.5.5.10.

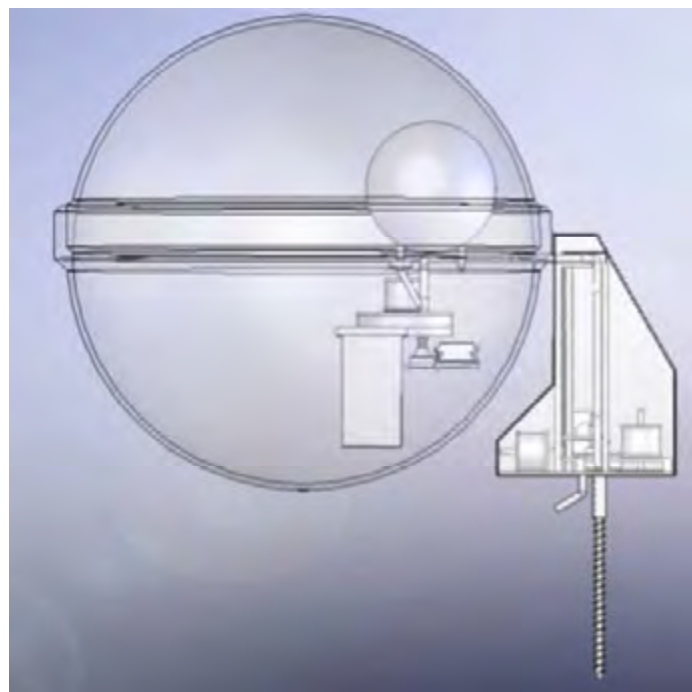


Figure 4.55: Sample acquisition system with deployed drill.

The mass estimate of the sample acquisition and handling system is 35 kg CBE. The best proxies to compare functionality and size are the Russian Venera and MSL sample acquisition systems. The mass of the Russian Venera drilling system was 26 kg and the current best estimate for the drill and sample handling system on MSL is 30 kg. The additional mass in this DRM design is to account for the second low-pressure tank and to provide additional margin. Finally, the DRM used the VEGA power draw number of 90 W to size the lander power system required to support the drilling operations.

Subsection 4.8.1 discusses the technological status and development needs for the drilling and sample handling system.

#### **4.5.5.10 Lander Autonomy for Drill Location Selection**

Drill sample acquisition and processing is considered to be a high-value science goal for the Venus Flagship Mission. In the current plan, two drill samples will be acquired during the surface operations. Selection of appropriate drilling sites is important to ensure that high-value samples are acquired. Drilling in a sandy area, for example, would not provide the desired science return. The short, 5-hour lander lifetime is insufficient to allow for humans-in-the-loop interaction, including selection of the drilling location. Therefore, an analysis was performed to investigate the possibility of performing autonomous drill site selection by the Venus lander.

Specifically, following a 1-hour descent, the lander must perform sample acquisition from two different depths at a scientifically relevant location. The 5-hour lifetime of the lander precludes humans-in-the-loop selection of the drilling site. Instead, it will be selected autonomously onboard by using surface images and feature recognition algorithms to identify good and bad drilling locations accessible by the lander. Several images will be taken using the drill camera to survey the drill-accessible area. A pre-computed image

mask will be used to extract the image regions accessible to the drill system. These regions will be further processed using science signature filters to dismiss low science value areas (such as sand) and select target areas of potentially high science value. Edge detection and region segmentation algorithms will be used to verify that cracks are avoided and that the surface areas of high-value targets are large enough to ensure that the drill can be successfully directed to and penetrate the target sites (see Figure 4.56). The final candidate target sites can be ranked based on their science signature metrics and probability of successful drilling. Assuming a MER-class processor, a conservative estimate of onboard processing time suggests that ~3 – 5 drill targets will be identified within 3 to 10 minutes. As a concept demonstration, this autonomous drilling site selection process was successfully simulated using example images taken by the Russian Venera 9 and Venera 14 landers. The process steps are illustrated in Figure 4.56.

#### **4.5.6 Mission Operations**

A detailed mission operations plan for the DRM has not been completed, although some preliminary aspects are outlined in the Ground System description in the next subsection. The mission architecture description, timelines and data taking scenarios described elsewhere in this report do provide the context and some of the requirements for designing the mission operations in a future study.

#### **4.5.7 Ground Systems**

The ground system is designed to support maximal data return from the mission's two landers, two balloons and orbiter (including science through the Radio Subsystem). The quantity of science data collected by these elements, most notably the InSAR instrument, required a design with at least one 8-hour pass per day, even though there are no data latency requirements on the system.

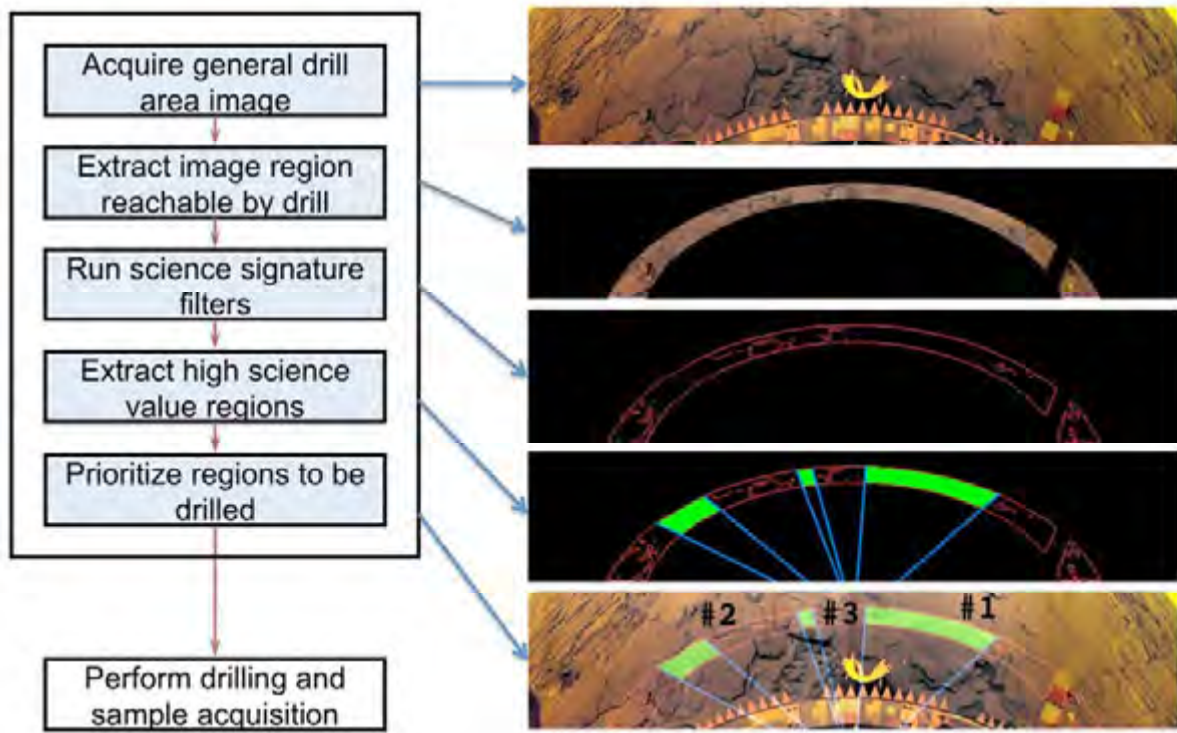


Figure 4.56: Process diagram with examples for autonomous drill location selection.

During the telecom relay phase the available downlink time will vary between 5 and 8 hours due to orbital geometry and occultation timing. Based on this, the allowed average of 7 hours of downlink will be scheduled. The downlink pass is baselined with normal quality (95%), and normal continuity, though depending on the link this could degrade further due to atmospheric effects. The occultation timing presents some potential operations complexity, but enables passes selected to maximize data return. These passes will return science, engineering and housekeeping data, and potentially daily table updates and minor sequence updates. Weekly primary command passes will also be scheduled. DSN 70-m antennas, VLBA (Very Long Base Array) in North America and EVN (European VLBI

Network) will track the balloons. The received signal will be digitally recorded for post-processing data demodulation, Doppler and VLBI measurements of the velocity and balloon position.

For orbital science operations, the science return is dependent on the Venus–Earth distance with potential data rates varying between 15 Mb/s and 75 Mb/s between the extremes of 1.7 and 0.3 AU. (Note that the orbiter's C&DH system used in the current DRM supports data rates up to 15 Mb/s, while the telecom system would be capable to support data rates up to the 75 Mb/s limits. Further studies are expected to optimize the design to take advantage of these higher data rates.) Occultation then controls pass availability (see Table 4.51).

**Table 4.51:** Data Return Volume from Orbiter to Earth.

Parameter	Distance (0.3 AU)	Distance (1.7 AU)
Occultation (0% of orbit)	1.5 Tbits/day	300 Gbits/day
Occultation (40% of orbit)	900 Gbits/day	180 Gbits/day

**Table 4.52:** Ground Segment DSN Operations.

Name (description)	Antenna Size (meters)	Service Year (year)	Hours per Track (hr)	Tracks per Week (# tracks)	Weeks Required (# weeks)	Pre- & Post-Config. (hr)	Total Time Reqd. (hr)
Launch and Operations	34BWG	2021	8	21	2	42	378
Launch and Operations	34BWG	2021	8	14	2	28	252
Cruise–Cruise	34BWG	2021	8	1	15	15	135
Cruise–approach hvy	34BWG	2021	8	21	3	63	567
DDOR	70	2021	1	4	3	24	36
Cruise–approach lt	34BWG	2021	8	14	3	42	378
DDOR	70	2021	1	3	3	18	27
Orbit insertion	34BWG	2021	8	21	1	21	189
DDOR	70	2021	8	21	4	168	840
Set-Up Relay and Telecom Orbit	34BWG	2021	8	3	4	12	108
Set-Up Relay and Telecom Orbit	34BWG	2021	8	7	11	77	693
Aerobraking	34BWG	2021	8	14	20	280	2520
Initial Science Operations—Cruise	34BWG	2021	8	7	26	182	1638
Routine Science Operations—DT	34BWG	2021	8	7	80	560	5040

These numbers assume 7% overhead and 15% margin. This design is intended to maximize the quantity of data downlinked, even so, at maximum distance, if maximum occultation geometry occurs simultaneously, downlink capabilities limited to the order of 180 Gbits per day could be seen and could last for a period of weeks. Due to the limitations discussed above, it is conservative to assume that at least 180 Gbits/day could be maintained throughout the 2-year orbiter science phase, which translates to over 130 Tbits of data.

Notable design features include use of the existing AMMOS system (with standard adaptations for command and telemetry dictionaries) and the use of MPCS in conjunction with MSAP on the spacecraft. The design uses a 15 Mb/s Ka-Band return link for Science data and a 0.5 kb/s X-Band forward and return link for commanding, engineering, health, and housekeeping. This system will also support emergency communications. The DSN 34-m Beam Wave Guide (BWG) will be used for all tracking. The DSN 70-m will be used for Doppler. The use of existing multi-mission ground system software and processes that adapt multi-mission ground system is assumed (see Table 4.52).

## 4.6 Planetary Protection Considerations

Several past studies of planetary protection issues have concluded that the surface environment of Venus presents a negligible chance of either forward or back contamination and that the cloud environment presents such a slight chance of contamination that it does not require any special precautions in mission planning (Space Sciences Board, 1970; Space Sciences Board, 1972).

In 2005, in light of advances in astrobiology, including the discovery of extremophile organisms, new ideas about the possible viability of cloud-based life on Venus (for example (Schulze-Makuch et al., 2004)), and the prospect of a new generation of Venus spacecraft, NASA’s Office of Planetary Protection asked the Space Studies Board’s Committee on Origin and Evolution of Life (COEL) to provide advice on planetary protection concerns related to missions to and from Venus. A Task Group on Planetary Protection Requirements for Venus Missions was formed and heard expert testimony at several meetings. The Task Group concluded that no significant risk of forward contamination exists in either landing on the

surface of Venus or exposing spacecraft to the Venusian clouds, and recommended that the previous COSPAR Category II planetary protection classification of Venus be retained (Space Studies Board, 2006). Category II includes missions to those bodies where there is “significant interest relative to the process of chemical evolution and the origin of life, but where there is only a remote chance that contamination carried by a spacecraft could jeopardize future exploration.” For category II bodies, the legal requirements are only for simple documentation. This required documentation includes a short planetary protection plan, primarily to outline intended or potential impact targets; brief pre-launch and post-launch analyses detailing impact strategies; and a post-encounter and end-of-mission report providing the location of inadvertent impact, if such an event occurs.

For planetary protection concerns, the relevant question is ultimately not the probability of any habitable niche existing on present day Venus, but the likelihood of such a niche, if it does exist, possessing physical

conditions which overlap the conditions under which terrestrial organisms can survive, grow and reproduce. The judgment of the ad hoc Task Group was that the chance of such overlap is too slight to significantly impact planning for future Venus missions. This history is reviewed, and the rationale behind these studies discussed in more detail by Grinspoon and Bullock, (2007).

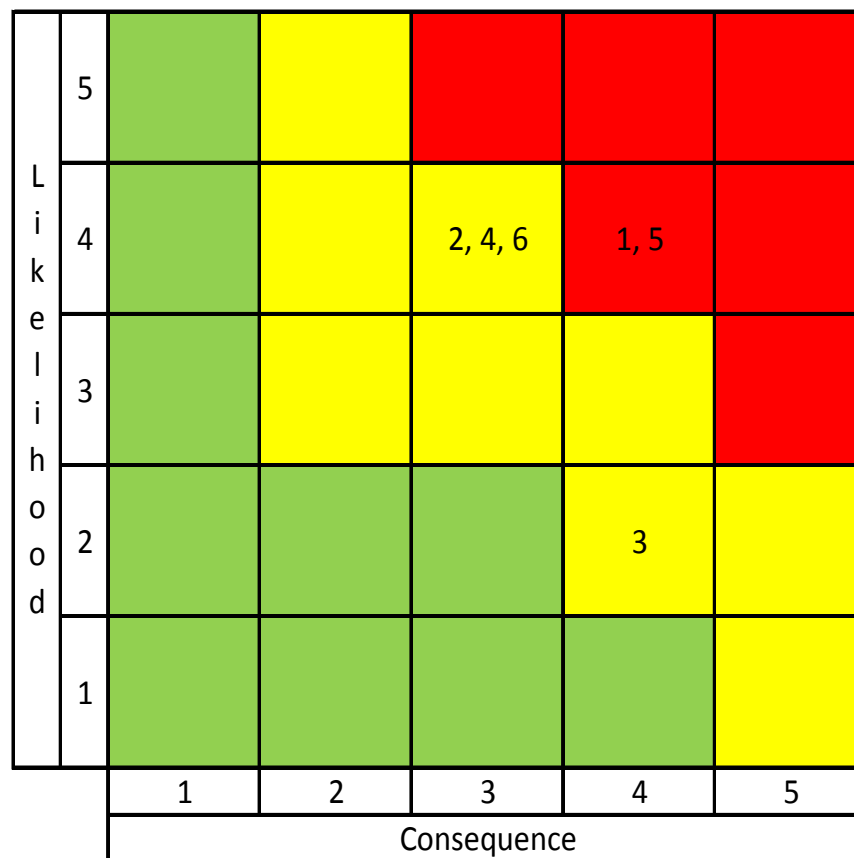
#### 4.7 Open Issues and Identified Risks

The Venus flagship DRM is at an early stage of development and therefore has a number of areas where further design and analysis work is required. Table 4.53 summarizes the key open issues and known risks that should be addressed in the future to mature this Design Reference Mission concept. The top six are listed as Numbers 1 - 6 in the table and are plotted in Figure 4.57 on a standard  $5 \times 5$  matrix of consequence versus likelihood. Options for enhancing or substantially changing the DRM with development and introduction of new technologies will be discussed in Chapter 5.

**Table 4.53: DRM Open Issues and Risks.**

No.	Name	Description	Consequence
1	Sample Acquisition and Handling System	Current DRM design is notional, not detailed. Soviet Venera and VEGA experience proves feasibility of approach, but implementation details must be worked out.	Resource allocations (mass, power, \$) may grow significantly. There are potential schedule impacts too.
2	Mass estimate at limit of launch vehicle capability	Further mass growth will require a much more expensive launch vehicle (e.g., Delta IV-H) since the largest Atlas V is already baselined.	Substantial increase in mission cost or else mission descopes that eliminate valuable science return.
3	Orbiter failure	Current dual launch architecture reduces value of in situ payload if orbiter fails to perform its telecom relay function. Alternatives to dual launch architecture can be reconsidered.	Loss of the orbiter will significantly reduce data return from in situ assets.
4	Rotating Pressure Vessel	Current DRM design is notional, not detailed. This is a new technology that requires development.	Resource allocations (mass, power, \$) may grow significantly. There are potential schedule impacts too.
5	Landing System for Rough Terrain	Current DRM design is notional, not detailed.	Resource allocations (mass, power, \$), may grow significantly. There are potential schedule impacts too.
6	Multi-element systems engineering and architecture robustness	The multi-element architecture is complex and few design and system engineering details have been worked out to date.	Mass and cost estimates may grow significantly.

No.	Name	Description	Consequence
7	Lander Telecom Elevation Limits	It is uncertain what the real elevation angle limit is for good telecom from lander to orbiter. Rough terrain may also tilt the lander in an unfavorable direction.	Some good landing sites may become disqualified if the angular restriction becomes more pronounced.
8	InSAR Development	The DRM radar instrument design is preliminary.	Resource allocations (mass, power, \$, transmitted data) may grow significantly. There are potential schedule impacts too.
9	V&V for Venus Surface Environment	Lander will require significant environmental testing at Venus surface conditions. Estimated costs for this may be low.	Lander V&V costs may grow substantially. There are potential schedule impacts too.
10	Mission trades for different launch opportunities.	Different launch opportunities will provide access to different landing regions on Venus. The robustness of the scientific investigations to these changes needs to be investigated and quantified.	Possible reductions in science return for some launch opportunities.
11	Proximity communications	The multi-element architecture requires multiple telecom relays from in situ vehicles to orbiter and then back to Earth. The design of this system remains at a very early stage and may not capture all of the costs.	Potential cost growth to make this system work properly. There are potential schedule impacts too.
12	Data rate for balloon	The data rate for the balloon, 500 b/s, may be too low relative to reasonable science goals with respect to sample frequency.	Some atmospheric science investigations may not fulfill desired science goals.
13	Aerobraking	Aerobraking design details not yet worked out.	May take longer than the 6 months allocated and/or require more spacecraft mass.
14	Solar power for balloon payload	Future study should look at use of solar power to replace or augment current primary battery design for balloon gondola.	May enable a significant increase in balloon science data and/or balloon flight lifetime.
15	Surface corner reflector	No detailed design yet. The large size of this structure (~0.5 m) may require a deployable device.	Mass and cost estimates may grow significantly.
16	Heat flux plate instrument	Technically immature for Venusian environment.	Mass and cost estimates may grow significantly.
17	X-ray tubes for XRD/XRF instrument	Carbon nanotube-based technology for X-ray tubes can significantly reduce mass and power requirements.	Potential mass and power savings.
18	Gamma ray detector	Updated design and prototype validation from Venera era required.	Mass and cost estimates may grow significantly.
19	Balloon deployment and inflation system	DRM requires a larger balloon and hence more helium than VEGA. This larger system has not yet been validated.	Mass and cost estimates may grow if validation experiments reveal significant problems.
20	Parachute draping over the lander	Must develop a system to prevent the parachute from draping over the lander after reaching the surface.	Parachute may interfere with lander science operations.



	Consequence of Occurrence	
Level	Mission Risk Levels Definitions	
5	Mission failure	
4	Significant reduction in mission return	
3	Moderate reduction in mission return	
2	Small reduction in mission return	
1	Minimal (or no) impact on mission	
	Implementation Risk Level Definitions	
5	Overrun budget and contingency, cannot meet launch with current resources	
4	Consume all contingency, budget, or schedule	
3	Significant reduction of contingency or launch slack	
2	Small reduction of contingency or launch slack	
1	Minimal reduction of contingency or launch slack	

	Likelihood of Occurrence	
Level	Likelihood	Level Definition
5	Very High	> 70%: Almost certain
4	High	> 50%: More likely than not
3	Moderate	> 30%: Significant likelihood
2	Low	> 1%: Unlikely
1	Very Low	< 1%: Very unlikely

Figure 4.57: 5 x 5 Matrix for top 6 Risks.

## 4.8 New Technology Requirements for the DRM

The Design Reference Mission manages to provide an outstanding science return with a mission architecture that requires limited development of new technologies. The surface sample acquisition and handling system, the rotating pressure vessel, and the rugged terrain landing systems are the key areas where technology development is clearly needed for the platforms. In addition, there are technology needs for some of the in situ instruments. Details on these areas will be discussed in the remainder of this section.

In addition, there are a set of technologies that can either enhance the current DRM or enable different and more ambitious alternate architectures. Those technologies and their science drivers will be discussed in Chapter 5.

### 4.8.1 Surface Sample Acquisition System

The Design Reference Mission baselined a rotary drill sample collection system patterned off the successful Soviet Venera and VEGA missions in the [1970s and] 1980s. The Venera drill could reach the surface 400 mm beneath its initial position and could drill to a 30 mm depth (i.e less than the 10 cm requirement for the DRM). Although the Soviet drills were tested on harder rocks, on Venus it appears that they actually encountered softer material like weathered basalt or perhaps compact ashy material for which they drilled the full 30 mm in less than 2 minutes. DRM sample system designers will need to calibrate the set of lessons that can be learned from the successful Venera and VEGA drilling systems. Although no such system exists today, the performance metrics of the Soviet system applied at least to regolith, fragments and porous rock targets correspond in many respects to those required for the DRM and therefore it can, as a first approximation, serve as both the conceptual basis for the DRM and the basis for estimating the mass and power that eventually will be required to implement the capability. Implementation therefore involves a two-step process: first, to recover, in some sense, the

Soviet technology by designing and building new systems based on modern components and then measuring the performance of those designs with extensive testing under Venusian surface conditions. Second, there may be a need to engineer functional capabilities that the Soviet systems did not have in order to achieve the specific DRM requirement to robustly drill up to 10 cm deep in basaltic rock. Those additional functional capabilities are likely to include some combination of longer drill times, higher energy efficiency (energy per unit depth drilled) and feedback control.

Attempts at soil analysis at the Venus surface with the onboard sampling system started with Venera 11 and 12, but proved unsuccessful due to failed pressure seals. The sampling systems of Venera 13, 14 and VEGA 1, 2 were improved and, with the exception of VEGA 1, successfully performed their sampling and sample distribution tasks. The unexplained electrical shock to the VEGA 1 spacecraft prematurely initiated the deployment and operation of the drill system at 18-km altitude, instead of at touchdown. The Russian sampling systems (including support hardware) were about 26 kg, and consumed up to 90 W of peak power. The total length of the drill stem was about 40 cm, with a core diameter of about 16 mm. There was sufficient travel in the drill stroke to reach a surface (about 30 cm) and drill for 3 cm. The system was capable of functioning at 500 °C and consisted of a drill-based sampling assembly, a soil feed mechanism, a gas generator assembly for pyrotechnic devices, and a vacuum chamber (Figure 4.58). The system provided for straightforward, open loop, auger flight transport of sample cuttings to a vacuum based instrument chamber located inside the pressure vessel. The whole process of collection and analysis of the sample took a few minutes. This level of successful system implementation was only possible by extensive testing conducted under conditions designed to simulate the Venus environment (development took 2 - 3 years).

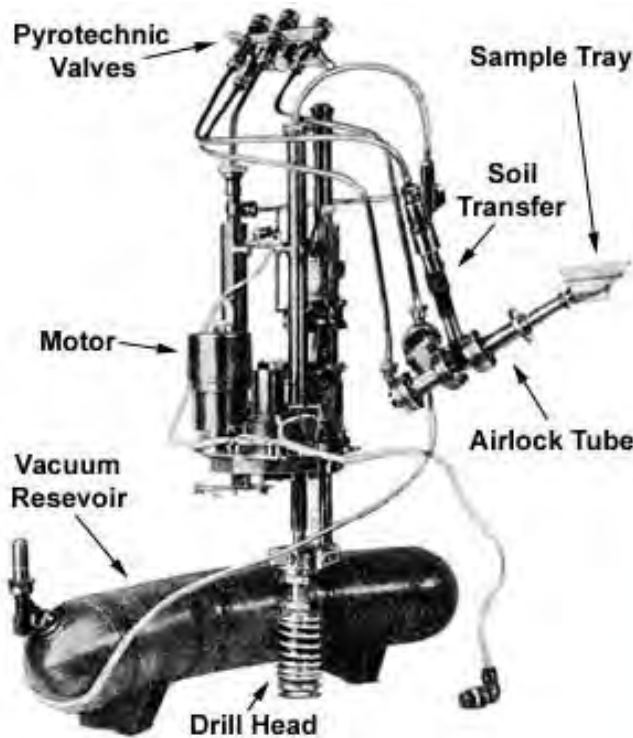


Figure 4.58: The Venera 13 and Venera 14 sample collection system.

The Venera telemetry showed that surface was reached by lowering drill by ~115 mm and was bored for 30 mm.

Compositional analysis of the drilled material is consistent with basaltic rock. the DRM requirement of getting below the weathered rock layer to a depth of perhaps 10 cm represents an extension most likely beyond that demonstrated on the past Soviet missions. It is not impossible that this goal can be achieved by relatively small modifications of the Russian design (increase operation time from 2 to 10 min, higher power etc).

The specific components required for the DRM sample acquisition system will now be described.

#### 4.8.1.1 High Temperature Electric Motors

High temperature (HT) motors will be needed for the DRM sample acquisition system, especially for the high-duty-cycle motor actuating the drill shaft drive train. This motor shaft will likely see a higher number of revolutions, under load, than all other surface actuators combined. This central motor needs to withstand the internal heating from its power input in addition to the ambient

temperatures of operation. An attempt should be taken to acquire Russian HT motors used for the Venera/VEGA drill. Two years ago, a survey of electric motors available anywhere in the world revealed a maximum high-temperature of operation at 270°C ambient. Today, for the purpose of supporting a landed Venus mission drilling operation, a switch-reluctance electric motor has been shown to run indefinitely, drilling into chalks with no gear reduction at Venus temperatures (Ji, 2008). In addition, a brushless DC motor (Figure 4.59) is not far behind in development and a switched reluctance motor has demonstrated operation at 500 °C while a high temperature bearing-less motor is under development (Morrison et al., 2003.). These types of electric motors, however, will require more testing and iterative development to optimize their mass and volume and their performance profiles. This long development process must be accomplished before these motors can be full up integrated into drilling system prototypes capable of being tested in simulated Venus environments.



Figure 4.59: High-temperature DC motor (Honeybee).

#### 4.8.1.2 Resolvers and Encoders

The Venera/VEGA drills were heavy and strong. Zacny et al (2008) gives a VEGA system mass of 26 kg; however, there is some uncertainty as to whether other additional heavy and dedicated deployment mechanisms were also employed to articulate the drill from the stowed position to placement on a surface target. The drills successfully operated in an open loop fashion and delivered samples to the instruments consisting of some combination of soil, rock cuttings and fragments resulting from the drilling process. The actual drill depth was 30 mm, which was sufficient for the purpose of obtaining samples from very weak or porous rock and relatively homogeneous regolith which might include very small rock fragments. It is likely though not necessary, that the 10-cm depths required by the DRM will require the robustness afforded only by feedback control on the drill system. The feedback addresses jamming difficulties associated with varying chip removal rates and weight on bit issues that arise when drilling deep (2 to 10 cm) into strong and varying rock or into regolith that contain small rocks bigger than half the diameter of the drill stem. Recent experience with the Mars MER and Phoenix missions, and the MSL rock drill development demonstrate the utility of sophisticated drilling algorithms that can accommodate a wide range of rock and regolith physical properties and reliably achieve the desired drill depths. The set of physical challenges not only refers to a

wide range of rock strengths and encountering small rocks in regolith targets, but also to very difficult rock drilling problems, such as engagement of the drill bit at an uneven or highly sloped rock surface or drilling through a hard spot in a soft rock or drilling into a crack in a hardened regolith target. For these drilling algorithms to work, the development of high-temperature resolvers (or encoders) that provide actuator output position knowledge will be required so as to foster the development of servo-controlled, fully autonomous drilling systems. Motor current sensing, sensor electronics, force and torque sensors, motor drivers, and motor electronics will all be required for high-temperature drilling systems and algorithms. Conventional encoders will not function at Venus surface temperatures, and magnetic fields associated with resolver operations will drift with elevated temperatures. This drift over time at high temperatures is not yet well understood. New types of high-temperature resolvers are under development; however, the comprehensive development, characterization, and testing of high-temperature resolvers composed of new materials packaged in sampler prototypes, and drilling into strong basalts at Venus surface conditions, will be required to implement feedback control on a Venus drilling system. Though basic boring can be accomplished without feedback, the feedback system will increase probability of achieving of 10 cm depth in rock.

#### 4.8.1.3 Lubrication, Bearings and other High Temperature Drive Train Elements

Conventional bearings will not function for very long at Venus temperatures. Bearings made of silicon carbide and races made of Stellite (a specialty steel) have been demonstrated to operate for relatively long time periods at Venus temperatures; however, the frictional profiles and operational lifetimes of these materials remain uncertain. Employing dry lubricants, such as tungsten disulfide, on gear components has been shown to work for short periods on bearings and spur gears at Venus surface temperatures; however,

much more research and development is required to analyze the wear performance of tungsten disulphide on planetary gears and other drive train elements under stress, such as harmonic drives. Additionally, aerospace suppliers such as General Magnaplate, Inc. claim proprietary coatings that will enable long-duration electromechanical component operations at Venus temperatures. These coatings should be investigated and tested as candidates leading to the development of longer-lasting, high-temperature drive trains. Drill system support and positional/surface placement mechanisms might benefit from the development of a high-temperature brake. A high-temperature brake might not be too difficult to envision, but almost nothing is currently known about how any frictional brake might perform in the Venus surface environment.

#### **4.8.1.4 Drill Bits Tailored for work at Venus**

On Mars, sharp diamond-cutting elements (employed on the Rock Abrasion Tool) wear at rates that are significantly lower than when operated in the Earth's environment on rocks of similar strength. The mechanism responsible for this unusual mechanical behavior is not well understood, but might be related to the lack of moisture on Mars. Although there is some high temperature boring at Earth for geothermal wells, we know even less about how drill bits of any material will perform when cutting into regolith or strong rock at high temperatures and surrounded by a supercritical carbon dioxide atmosphere at Venus. A very significant research and development and chamber-testing program will be required to produce reliable and efficient long-lasting drill bits.

#### **4.8.1.5 Vacuum/Low Pressure Tanks Sample Transfer Technology**

The Soviet sample transfer system was based on gas transport of rock pieces and shavings from the drill to an internal chamber driven by the high atmospheric pressure on the surface. It is a conceptually simple approach and worked reliably on the Venera and VEGA

missions. Nevertheless, it will be necessary to develop, build a prototype, and conduct extensive testing to validate a robust design for the Venus flagship mission.

#### **4.8.1.6 Prototype & Algorithm Development**

Drills (Figure 4.60), support mechanisms, sample processing, and distribution and contingency sampling elements outfitted with high-temperature motors, resolvers, bearings, lubricants, brakes, and high-temperature drive trains will need to be designed, built, and extensively tested in a terrestrial setting as well as inside a Venus chamber at pressure and temperature. This prototype testing must include extensive strong rock and regolith drilling (at relevant temperatures and pressures) so as to fully characterize the complex systems reaction produced by the environment and drilling loads generated from a wide range of targets. Time and funding should be provided to iterate designs of multiple drill system prototypes so as to optimize the incremental benefits of the extended and comprehensive testing. Prototype testing should proceed beyond just the drill subsystem to development of drill testing that simulates drilling from the drill mounting and articulation hardware and from a lander or lander mockup. Finally, prototypes of primary and support hardware in the sampling chain, including analytical instruments, should be integrated together to allow for end-to-end tests in a Venus-simulated environment. This end-to-end testing means autonomous drilling into a variety of targets from a lander (or high-fidelity lander mockup), transferring acquired samples to a sample processor (if needed), and moving the (processed) samples from the high-pressure environment to the low-pressure instrument-staging area where the samples are provided precisely to working versions of the analytical instrumentation and measurements taken. Along this hardware-based development path, drilling algorithms matched to the drill, its motors, drill bits, the environment, and a range of targets must be developed and refined during the end-to-end testing program.



Figure 4.60: High-temperature drill.

#### 4.8.1.7 Development Plan

High-temperature motor development in support of a Venus mission is underway and approaching TRL 6 for switch reluctance motors and TRL 5 for brushless DC motors. However, the development of reliable actuators capable of operating under load at Venus surface temperatures and pressures will be crucial to the acquisition and distribution to instruments of high-quality samples. Also, high-temperature actuators will be enabling (for rock drilling and for other electromechanical mission elements operating at 700+ Kelvin). The development of high-temperature motors for a flagship-class mission to Venus must achieve a very comprehensive TRL 6, far in excess of the current development status, so as to be suitable for insertion into the design of a flight system. This development profile should be front loaded so that all the design issues and difficulties are put to rest early and so that multiple drill prototypes can be designed and tested in the near term, long before the mission launch date. For lubricants, bearings, electromechanical drive train components,

brakes, and resolvers, the comprehensive development of high-temperature (and pressure) versions of all these elements are as crucial as the development of high-temperature actuators because all these additional elements are needed to develop full-up, high-performing drilling systems and sample transport elements, such as carousels and transport tubes. Developmental work in the Venus mission context has only just begun in the area of resolvers and bearings. Almost no work has been performed on high-temperature lubricants and key drive-train components, such as planetary gear heads and harmonic drives. Only one lubricant has been significantly tested at Venus temperatures. Other candidate lubricants (and coatings) will need to be evaluated in the drive train and bearing context at Venus temperatures and pressures. This component R&D effort should also be front loaded to allow for the development of full-up systems for testing and iterative designing purposes. The vacuum-based sample-transfer technology might be developed somewhat independently of the drilling prototype, as its interface can probably be defined well enough for later add on and

integration. Drill system redundancy or the development and testing of a contingency sampling system should begin shortly after the development of the 1<sup>st</sup> primary drill prototypes and when the instrument payload has been well defined. All elements of a future Venus sample acquisition, processing, and distribution system will need long development tracks, which then leads sequentially to the long development and testing of full drilling prototypes (along with prototypes of any articulating mount and the sample-transport subsystems). Beginning this development as soon as possible will leave the greatest possible time margin for completion of these difficult tasks (many of them sequential in nature); beginning development in the near term might lend a great deal of benefit along the way to precursor Discovery and New Frontiers missions.

### **4.8.2 Rotating Pressure Vessel**

A novel feature proposed in the Design Reference Mission is a rotating pressure vessel. As described in Subsection 4.5.5, a rotating pressure vessel on the lander provides two major advantages: first, it enables the otherwise fixed drill system to access an extended area around the lander, thereby improving the ability to collect samples from desirable rocks. Second, it simplifies the process of obtaining panoramic images. A single camera looking out through a single window can be used because the pressure vessel can be simply rotated between successive images of the panorama. Having just one window for the imaging system also serves to significantly reduce the heat leak into the lander interior.

The DRM design for the rotating pressure vessel is at a conceptual level, and no known prototyping activity has yet occurred. Therefore, the rotating pressure vessel requires technology development in which the requirements are related to those for drilling and actuation systems.

The system essentially operates at Venus surface temperatures, driven by an electric motor and gear box that provides low rotation speeds (1 revolution per minute). Motor,

bearing and lubrication technology used by drills will in principle suffice for rotating the pressure vessel, albeit customized for its loads and rotation speed. Prototypes will need to be constructed and tested for the Venusian surface environment to validate the chosen design. This validation will need to include testing for the high entry vehicle deceleration rates that will load the pressure vessel bearing to a very large extent.

### **4.8.3 Rugged Terrain Landing System**

The Design Reference Mission consists of two landers that will be targeted to different landing locations on Venus. One of those locations is specified to be in a tessera region, which is expected to be more rugged than the relatively flat plains on which the Venera and VEGA vehicles landed. This poses a significant challenge to design of the lander so that it can tolerate this kind of rugged terrain. There are three potentially severe adverse consequences that must be avoided:

- Landing on a rock that impacts the bottom of the lander in such a way as to cause damage to the pressure vessel or other externally mounted equipment.
- Landing on such a steep slope that it causes the lander to tip over.
- Landing on such a steep slope that the telecommunications antenna is unable to establish an adequate data link.

The DRM did not address the technology challenges of this requirement in any significant way. Notional outriggers are shown in the CAD models (e.g., Figure 4.49) that could address the tip over concern, but there are no other design features to prevent rock impact damage or telecommunications interruptions from high slopes. This is an area that simply was not analyzed during the study but is nevertheless crucial to accomplishing the DRM. This is a prime candidate for follow-on study and technology development.

### **4.8.4 Instruments**

#### **4.8.4.1 Venus Heat Flux Plate**

The requirement is to measure heat flow on Venus with an accuracy of  $\pm 5 \text{ mW/m}^2$ . Ultra-

tall Carbon nanotubes (CNTs) in the height range of 10 mm to 25 mm are being considered to establish tight thermal contact between heat flux plate and the rough surfaces of Venusian rocks. CNTs are high thermal conductivity material that when grown to lengths of 1 to 2 cm on heat flux plates serve the purpose of extremely conformal material to ensure good contact with uneven rock surface. A joint JPL-Caltech team has developed a process to grow 10 to 25 mm tall CNTs on different substrates (Figure 4.61). Further technology development is needed to achieve - (i) reproducible ultra-tall CNT growth on large area substrates, (ii) enhanced adhesion of CNTs to the substrates, (iii) increased compliance property of CNTs to achieve conformability to surfaces with roughness on the order of 1 to 2 cm. Growing CNTs either on smaller substrates and then tiling them to create large area heat flux plates or directly growing them on large area substrates is an important problem to be solved. Enhanced adhesion to the plate surface is important to ensure non-flaking of CNTs during measurement so that there is no perturbation of heat flow from the Venus surface to the heat flux plate. CNTs are expected to function well in the Venusian atmosphere of supercritical CO<sub>2</sub> and high temperature.



Figure 4.61: 10-mm tall thick block of CNTs on a silicon substrate.

#### 4.8.4.2 CNT X-ray Tubes for XRD/XRF Instrument on Venus

An electron source is the most basic component of a variety of diagnostic, analytical and imaging techniques and most often is the primary reason for the instrument's bulkiness and high power requirements (because of the presently prevalent thermionic emitters). X-ray diffraction/X-ray fluorescence (XRD/XRF) instruments for definitive mineralogy on Venus can greatly benefit from CNT field emitters. JPL has developed an architecture of multiwalled carbon nanotube (MWNT) bundles (see Figure 62) that has delivered the highest reported current densities at low electric fields ( $\sim 10 - 15 \text{ A/cm}^2$  at  $\sim 5$  to  $10 \text{ V}/\mu\text{m}$  over  $100\text{-}\mu\text{m}$  diameter area). Based on this architecture, application specific electron sources have been developed for miniature X-ray tubes (see Figure 4.63) that operate at lower acceleration voltages (10 to 20 kV with Cu or Co-target), and are capable of increased photon flux ( $10^7$  to  $10^{12} \text{ Photons/s}$ ) that allow faster data collection rates (limited only by the detector speed) on the order of minutes as opposed to hours. CNT emitter based X-ray tubes weigh less than 50 g and together with a custom-designed high-voltage power supply can weigh less than 1 kg, and can have significant impact on sensitivity, resolution, and power consumption of XRD/XRF instruments.

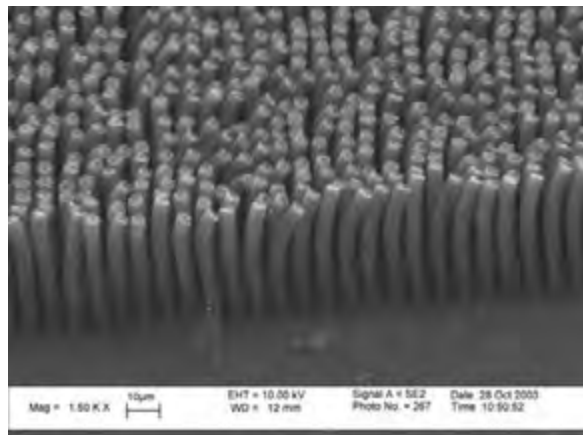
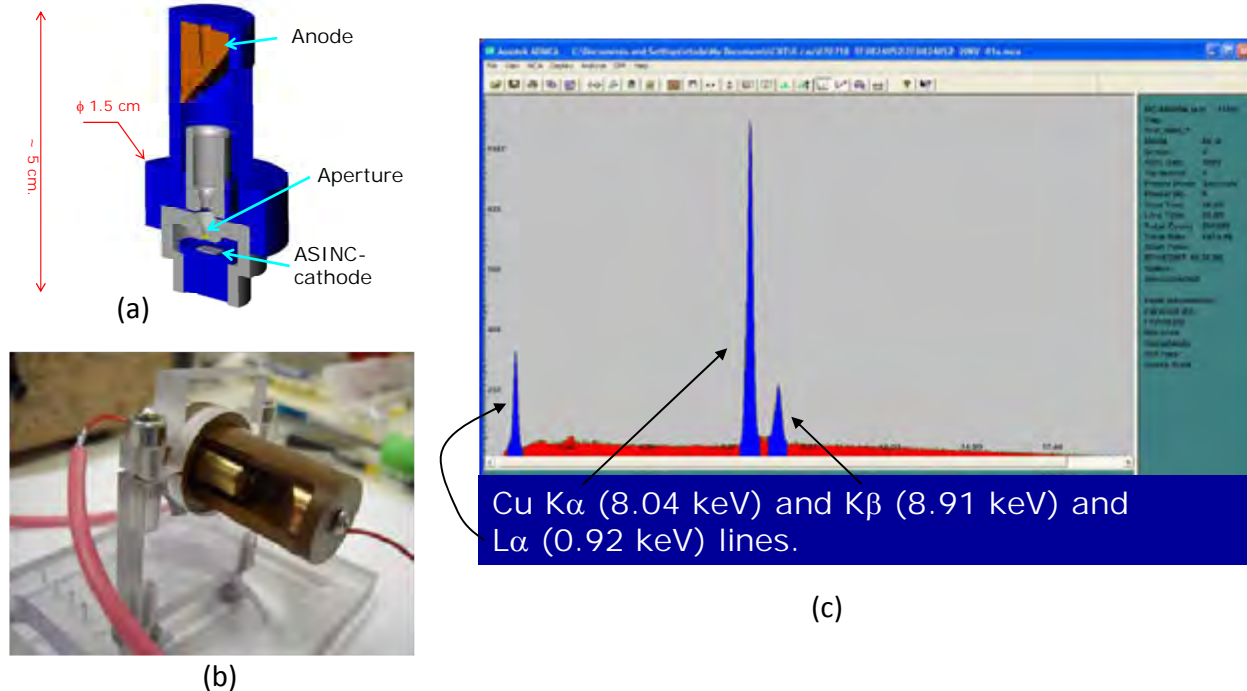


Figure 4.62: Ordered arrays of CNT bundles with specific array parameters that enable high current density emission.



**Figure 4.63:** X-ray tube details: (a) Exploded drawing of the copper X-ray tube using ASINC. (b) Photograph of the copper X-ray tube as fabricated. (c) Preliminary Cu X-ray spectrum that was generated using this ASINC X-ray tube.

While basic CNT X-ray tube concept has been demonstrated, technology development is still needed to transition this development into a usable X-ray tube that has capability to focus X-ray beam to spot size of 50- to 100- $\mu\text{m}$  diameter. Integrating the CNT X-ray tube with collimators is a challenge. Producing an X-ray tube that is ready for integration with an XRD/XRF instrument needs a stand-alone vacuum packaged component that has beam position and beam energy tenability. The beam tailoring optics that can be monolithically integrated with CNT electron emitters needs to be designed such that photon flux on the order of  $10^{12}$  to  $10^{14}/\text{s}$  can be produced from a small area source (100- to 200- $\mu\text{m}$  diameter). X-ray production efficiency exponentially decreases as the acceleration voltage is decreased. Hence the current density from the CNT source needs to be increased correspondingly to maintain the necessary photon flux. This optimization, while easily explained in theory, needs careful designing of the CNT array source to keep the electrostatic screening effect to a minimum. Even here, enhanced adhesion of CNT arrays to the substrate is necessary to withstand high

field operation. This will be a common development between the heat flux plate and the XRD/XRF instrument.

#### 4.9 Mission Cost Estimate

The cost for the Venus flagship Design Reference Mission is estimated to be in the range of \$2.7 B to \$3.8 B. This was determined on the basis of two analyses: first, the cost-complexity methodology of Peterson et al (2008), and second, the cost model approach used by JPL's Team X with reserve levels determined by a cost risk sub-factor analysis. Assumptions underlying this estimate include:

- The spacecraft are designed and built at JPL using commercially available components.
- The technology cutoff date is 2016.
- 24-month duration for Phases A and B, 52 month duration for Phases C and D.
- The overall mission is rated as Class A, as is the orbiter.
- The landers and balloons are single-string designs on the presumption that using two

units of each in the mission provides the necessary level of redundancy.

- No contributed hardware from foreign partners.
- Pre-Phase A technology development funding at the level of ~ 3% of the total mission cost.

## 5 MISSION AND PAYLOAD ENHANCEMENTS FOR EXTRAORDINARY SCIENCE RETURN

---

### 5.1 Background: Path to a Venus Surface Sample Return Mission

The Venus Design Reference Mission optimizes the use of heritage technologies and mission architecture to provide considerable scientific return with low to moderate risk, while minimizing requirements for new technologies. To accomplish this, the surface science of the Design Reference Mission is completed within a short, five-hour period, and *in situ* cloud level balloon atmospheric experiments are designed to last a month. The Design Reference Mission is based on instruments and subsystems that are already at a Technology Readiness Level (TRL) of 6 or are expected to be developed to a TRL of 6 by 2015 with appropriate investments in new technology as described in Chapter 4.

However, enhancements to the DRM that would require only modest technology development could yield large dividends in science return. Landers able to survive long enough for commanded operations; new power sources for long lived balloons are described in Sections 5.2 and 5.3, respectively. The added science value and lowering of risk that these enhancements could achieve make them high-priority near-term technology investments.

In addition there are numerous scientific investigations that can yield extraordinary science return for understanding the Venus environmental and planetary system that are not included in the current Design Reference Mission. Generally speaking, these supplementary, or alternate, science investigations require a significant amount of new technology development, a key reason they were not included in the DRM. There are multiple pathways that could transform the current DRM into a different flagship mission that incorporates one or more of the supplementary science investigations that are described in this chapter. One or more missions to Venus before the flagship could accomplish some of the science objectives of

the current DRM requiring adjustment in the payload or architecture. The development of new technologies to perform new science investigations and make them significantly less expensive and less risky is discussed in Section 5.4. The highest priority science investigation alternatives for further refinement of the Venus flagship mission design given the likelihood of future changes, and the associated technology development are also described.

One of the highest priority science objectives of the Venus community is to develop an understanding of the structure and dynamics of the interior of the planet. This priority is reflected in the VEXAG document (VEXAG, 2007) as well as in the high level ‘open questions’ matrix in Chapter 1. Fundamental questions such as the thickness of the thermal lithosphere, the behavior of the mantle, the current rate of internal activity, and the nature of Venus’ nonmagnetic core must be addressed in order to understand Venus’ unique geologic history. Some volcanic and tectonic features are familiar, and some are not. Comparisons with partially understood geology on Earth will increase our understanding of these processes in ways that could not be done by studying the Earth’s geologic record alone. Direct seismic measurements will be enormously useful in addressing these questions making seismometry one of the highest priority alternative investigations. Considerable detail on the science and technological development of seismometers for Venus is given in Subsection 5.4.1.2.

The successes of the Mars exploration program have shown the crucial importance of exploring geologically diverse terrains *in situ* (Squyres et al., 2006). At Venus, this motivates the use of long duration and/or mobile exploration platforms that can access those diverse terrains and survive long enough for extensive scientific investigations. Although the DRM includes a pair of mid-

altitude balloons, access to the deep atmosphere and near surface regions will require a different kind of balloon along with new supporting subsystems that can enable extended high temperature operation. Long duration landers, described in Subsection 5.4.1.3, can also support these alternate science investigations, following in the footsteps of the Mars exploration paradigm. A low-altitude balloon platform that can traverse and image the surface for extended durations is discussed in Subsection 5.4.1.4. A far better understanding of Venus atmospheric chemistry and dynamics would be obtained by multiple dropsondes and a cloud lidar instrument, described in Subsection 5.4.3.4. Global mapping at extremely high resolution from an orbiter would enable huge advances in understanding Venus' geologic history and is also possible, especially with very high data rates for data transmission afforded by optical communications (Subsection 5.4.4). The technologies to fly these missions are on the path towards an NRC Decadal Survey-recommended Venus Surface Sample Return (VSSR) mission, and would build on the scientific discoveries and technology advances achieved by a Venus flagship mission.

Recommended technology development for the Venus flagship, in priority order, is presented in Section 5.5.

Appendix B describes additional advanced in situ exploration concepts such as rovers, airplanes, and solar cells. These concepts, although significantly beyond the DRM concept, were investigated as part of the STDT activities.

## 5.2 Enhancements to the Landed Mission

### 5.2.1 *In-situ* Science at the Venus Surface

The analytic abilities of an autonomous vehicle are restricted, primarily because investigations cannot be directed by scientists observing the landing site. The ability to select target rocks and soils for excavation and analysis, and to base measurement decisions on new data, requires moderately extended lander lifetimes on the order of 24 hours or

more. Selection of targets for geochemical, mineralogical, and elemental analyses would provide a much greater chance for obtaining a good understanding of how the atmosphere and surface interact, and the nature of geologic processes that shaped the surface of Venus.

An assessed trade between potentially significant science benefits and technical risk to the landed portion resulted in the nominal surface lifetime of five hours of the DRM. A potentially significant science and technical risk to the landed portion of the Design Reference Mission is the required operation time of five hours. While based on previous Venus missions (the longest of which lasted 127 minutes (Marov and Grinspoon, 1998), this approach assumes smooth, autonomous operation from landing until the end of the five hour span. Limiting features of this approach include:

- No margin for system delays or malfunctions. The data collected in the five hour span is the total delivered by the lander's science payload, regardless of whatever technical difficulties may occur or any unexpected features of the landing site are encountered.
- Human-in-the-loop interactions are impossible due to time constraints and the speed of light. Mission science could not be optimized by either adjustments to equipment or measuring procedures.
- Time averaging or repetition of data is limited to that which occurs in the five hour span. Extended monitoring of conditions on the Venus surface or repeating measurements with a full range of instruments available on the lander is most likely not possible.

All landed Mars missions have shown the extraordinary adaptive surface exploration that can be done if the exploration is commanded by scientists and engineers based on the previous data (Squyres et al., 2004a; Squyres et al., 2004b). Discoveries can lead to new targeted investigations that would not be possible with autonomous or preprogrammed spacecraft. For the Venus flagship DRM, the

risk of not achieving the scientifically most valuable science would be reduced if it were possible to have the science team pick drill locations based on the initial photographic survey of the landing area. Mission risk can also be reduced if the mission team can interact with the lander and help troubleshoot any problems that arise. As a recent example, operations during the Phoenix mission showed how techniques were developed to solve a sampling problem, and then applied to the spacecraft's operation (Smith, 2008).

### **5.2.2 Extended Surface Life Landers**

A Venus surface mission on the order of 5 hours or less precludes the possibility of having a ‘human in the loop’ for directing a Venus Lander to focus on specific targets of scientific interest. A desirable goal on the order of 24 hours of surface operations would permit at least a limited form of human interaction with the spacecraft during the mission. A passive thermal architecture to achieve this lifetime performance appears to be within the realm of possibility but it will require technology development. There are a number of ideas in the literature that describe a ‘long-life’ architecture (Buggy, 2009; Seghi, 2007). These generally involve the use of a phase change material such as lithium nitrate trihydrate ( $\text{LiNO}_3 \cdot 3\text{H}_2\text{O}$ ) to absorb thermal energy generated by electronics inside the pressure vessel and a water evaporative cooling system to absorb the energy coming from the Venus environment.

A water-based heat absorption system can take advantage of the solid to liquid phase change and the liquid to vapor phase change. Getting rid of the water vapor presents challenges. Venting the vapor to the atmosphere is one solution. At Venus surface atmospheric pressure, water evaporates at approximately 305 °C so it can't be used to keep conventional electronics cool. However, it could be used to keep the outer boundary of the vessel at a lower temperature than the ambient environment. This would significantly

reduce the heat flow into the pressure vessel until the water runs out. A Small Business Innovation Research (SBIR)-sponsored program has developed a thermal architecture based on venting the water vapor to the atmosphere and their model shows lifetimes on the order of 20 to 28 hours are possible (Seghi, 2007). The pressure vessel contains the science instruments, electronics, batteries and  $\text{LiNO}_3$  Phase Change Material (PCM) modules, creating an earth-like environment inside. The vessel is surrounded by insulation layers which are either an aerogel or a porous silica product. Within the insulation layers there is a wick structure that contains water that can initially be frozen during transit from Earth to Venus. As the water absorbs environmental heating it maintains a layer within the insulation below 305 °C.

The advantage of such a thermal system is greatly enhanced if it can house electronics and telecommunication hardware that can function at higher temperatures than spacecraft typically operate, namely above 75 °C. With the highest available specification for conventional electronics of 125 °C, lander lifetime could be improved. This is particularly true with technologies that can withstand 300 °C (Subsection 5.4.2.8), for which lander lifetimes much longer than 24 hours become possible.

An analysis was conducted to illustrate the parameters associated with a boiling water and lithium nitrate PCM system. The results shown in Figure 5.1 are for a design with a 90 cm diameter titanium pressure vessel, 50 kg of water, 45 kg of Lithium Nitrate PCM, 110 kg of porous silica insulation, 100 kg electronics/science payload, 21 kg of battery. With average power dissipation for a 24 hour mission at 210 Watts, the depth of discharge of the batteries reaches 80%. The temperature of the internal payload starts at -15 °C at atmospheric entry and reaches 61 °C at 20 hours and 88 °C at 24 hours.

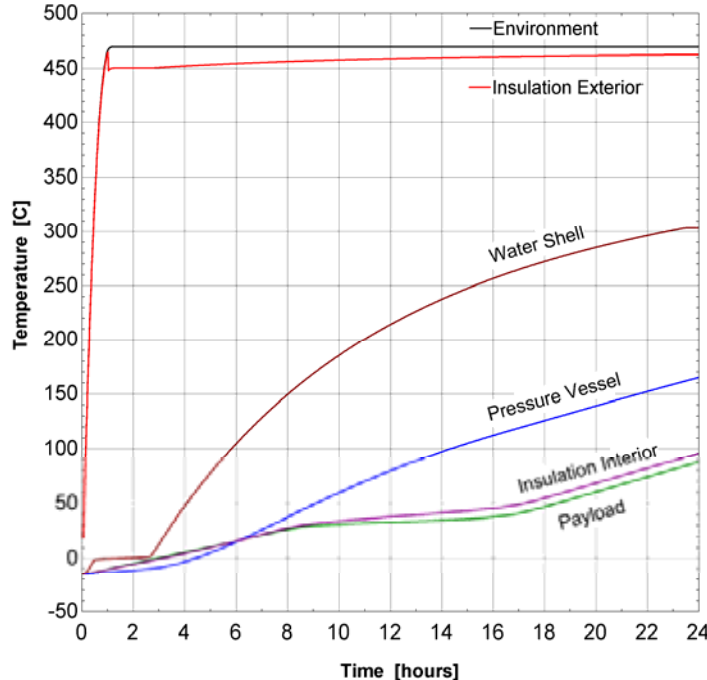


**Figure 5.1:** Temperatures from a thermal model of a Venus lander utilizing water vapor and LiNO<sub>3</sub> phase change material passive cooling. The interior of the vessel can maintain temperatures below 100 °C for up to 24 hours.

Another cooling technology that involves evaporating water using heat generated by the electronics and shell parasitic loads absorbs the vapor with a water-getter such as Lithium metal. This takes advantage of the high heat of vaporization of water which is about 2400 kJ/kg at 1 bar pressure. The water vapor exiting the electronics could be used to absorb additional parasitic heat from a radiation shield inside the shell. The water vapor is then piped to an exterior vessel containing a lithium metal matrix. A highly exothermic reaction takes place forming LiOH (liquid) and a low density LiH powder as well as Li<sub>2</sub>O powder. This system can potentially remove 3 to 4 times more energy per unit mass than the best PCM technology. This includes the mass of the lithium in addition to the water. This technique has never been proven in testing.

Yet another means by which the heat storage capacity of the pressure shell could be increased could use an enclosed layer of lithium. Lithium has the highest specific heat of any solid (nearly twice that of beryllium), melts at 180 °C and has a heat of fusion (432

kJ/kg) exceeding that of water at (333 kJ/kg). Its low density (530 kg/m<sup>3</sup>), however, can create volume concerns. As with the water shell design, the lithium shell is contained within the insulation layer exterior to the pressure vessel. The insulation design has an exterior layer to reduce heat flow to the lithium shell, a middle layer to reduce heat flow between the lithium shell and the pressure vessel and finally an interior layer that reduces heat flow from the pressure vessel to the payload. The specific design point to produce the results shown in Figure 5.2 includes a 90 cm diameter titanium pressure vessel, 50 kg of lithium, 45 kg of lithium nitrate PCM, 110 kg of porous silica insulation, 100 kg electronics/science payload, 21 kg of battery. With average power dissipation for a 24 hour mission at 210 Watts, the depth of discharge of the batteries reaches 80%. The temperature of the internal payload starts at -15 °C at atmospheric entry and reaches 64 °C at 20 hours and 90 °C at 24 hours. The thermal performance is comparable to the water shell design.

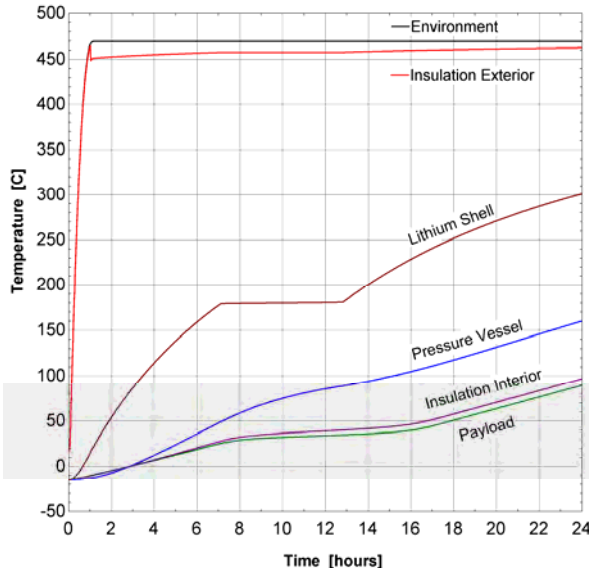
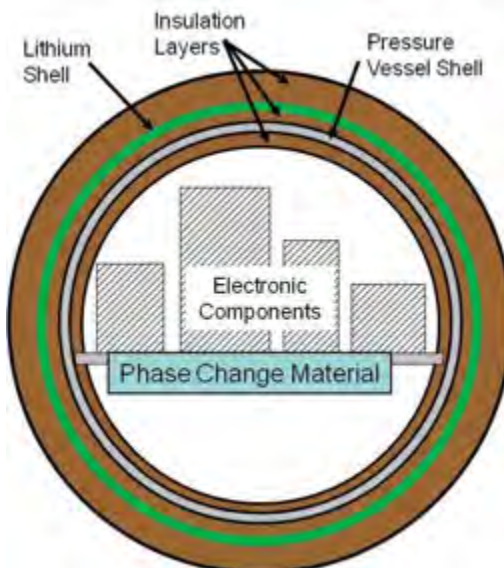


Figure 5.2: Temperatures from a thermal model of a Venus lander utilizing solid-liquid lithium phase change material shell liner for passive cooling. The interior of the vessel can maintain temperatures below 100 °C for up to 24 hours.



### 5.3 Enhancements to the Balloon Mission

#### 5.3.1 In-situ Atmospheric Science at Venus

Balloons are probably the most scientifically capable platforms for deep and extended in situ investigations of atmospheric circulation and chemistry, for exploring the Venus greenhouse effect, and for understanding how the clouds form. Very long duration balloons could circumnavigate the planet multiple times, probing the winds and sampling the gases and clouds to build up a picture of the atmosphere of Venus unobtainable in any other way.

At 55 km, the north-south winds are light but mostly poleward. Therefore as the balloons circle the planet in the prevailing east-west flow, they will drift poleward. With balloon missions of several months, equatorial and high-latitude winds could be determined directly, and chemistry variations with latitude would be sampled. Long duration balloons might eventually reach the polar vortices and be swept downward towards the poles, obtaining dynamical and chemical measurements until they were destroyed. Communications and data rate are crucial issues for these kinds of investigations, as is power. Extended balloon missions with much

greater data volume are possible within the DRM architecture. Science investigations of the Venus greenhouse, atmospheric chemical cycles and clouds, and the atmospheric superrotation are much more likely to succeed with enhanced balloon mission capability.

#### 5.3.2 Enhanced Mid-Altitude Balloons

The Venus DRM includes two mid-cloud balloons, operating at an altitude of ~55 km. The collected data is communicated to the orbiter during their 30-day lifetime, while circumnavigating Venus multiple times and slowly drifting from the entry locations towards the polar regions. The limited storage capacity of its 22 kg of primary battery based power system requires cycling between periodic science measurements, telecom, and sleep mode to save energy.

In a recent mission concept study, performed under NASA's Discovery and Scout Mission Capabilities Expansion (DSMCE) program, a similar balloon configuration was described with comparable science objectives, but utilizing an Advanced Stirling Radioisotope Generator (ASRG) as the power source, instead of using primary batteries (Baines and Balint, 2009). This concept is a good example of a potential enhancement to the balloon elements of the

Venus DRM, while also highlighting the mission impact of using ASRGs.

The ASRG enhances the balloon mission by allowing for long-term (>30 days) continuous in situ operation, limited only by the lifetime of the super-pressure balloon. This in turn enables continuous measurement coverage of spatially and temporarily varying atmospheric waves, convection, reactive species, and cloud aerosols. In particular, the ASRG provides power under nighttime and low-Sun conditions at high latitudes. It enables complete, long-term, longitudinal time-of-day studies of dynamical and chemical processes near the pole.

The Nuclear Polar VALOR concept was designed to communicate direct-to-Earth (DTE), because the Discovery mission cost cap would not allow for a telecom orbiter. In comparison, the Venus DRM would use an orbiter relay, which would support about 3 to 6 times higher data rates than DTE telecom (depending on the Venus-Earth range), assuming the same 5 W RF telecom power.

The Venus DRM balloons would perform periodic measurements while duty cycling between the various instruments, carrying out 7 minutes of data transmission to the orbiter and 55 hours of wind tracking. This would provide a total science data volume of 20.5 Mbits from one balloon. In comparison, an ASRG-enabled balloon could perform continuous science measurements and telecom (when visible to Earth or to the orbiter if available). Consequently, it could transmit about 135 Mbits of data directly to Earth, which is about 7 times more than that from the Venus DRM balloons. Transmitting to an orbiter, this data volume could be increased by at least 3 fold, making the overall data return from a single balloon as high as ~400 Mbits, and from two balloons ~800 Mbits. This is ~20 times higher than that from the DRM balloon configuration. This increased data capability could support additional high data volume instruments on the balloon, such as imagers or radars, and the addition of drop sondes, which are discussed further in Subsection 5.4.3.4.

Besides the significant science benefits, potential use of ASRGs on a mid-altitude balloon mission would also introduce programmatic, mission architecture and technical complexities. Potential technical obstacles to accommodating the ASRG technology are three-fold. First, the g-load tolerance limit (30g) of the ASRG requires a shallow Entry Flight Path Angle (EFPA), and possibly entry from orbit. This is also a function of the allowable EFPA margin, and should be studied in the future. Second, the ASRG requires a dedicated thermal design for cruise phase inside the aeroshell to remove its excess/waste heat. These will be addressed below.

From a programmatic point of view, ASRGs are significantly more expensive than primary batteries. This additional impact to the mission cost due to ASRG unit cost, launch approval, accommodation and design changes to the spacecraft to implement the power system, however, might not have as big an impact on a flagship mission as it would on a Discovery mission, where the mission cost cap is limiting.

The mission architecture would also require a redesign, primarily driven by the g-load tolerance of the ASRG. The ASRG's 30g limit necessitates a shallow EFPA, which in turn limits the reachable landing locations from one launch opportunity to another. This could also force the carrier spacecraft to get into an appropriately low orbit and release the entry systems from there, consequently lowering the entry g-loads experienced by the entry systems. This could significantly increase the cost of the mission, and would result in a second orbiter instead of a flyby carrier and a separate science/telecom orbiter. Details of the various trajectory options and their impact on the mission architecture are further discussed in the Nuclear Polar VALOR study report (Baines and Balint, 2009).

The technology impact of using ASRGs on a balloon mission includes operational issues through all mission phases from Earth storage and integration on the launch pad and launch, through cruise, entry, descent, and inflation

(EDI), and to in situ operations, as addressed below:

- Earth storage duration could be up to about 3 years, and is expected to have virtually no impact on the mission. The ASRGs would be stored at a Department of Energy (DoE) facility and delivered to the Cape before launch.
- The aeroshell and spacecraft designs would have to account for easy integration of the ASRG on the launch pad, including connecting up the thermal management system. During launch, the vibration environment needs to be within an ASRG-specific allowable range.
- The cruise phase includes the interplanetary trajectory from Earth to Venus, during which the gondola's ASRG is housed inside the entry system (aeroshell) with the lander. Inside the aeroshell the ASRG requires a thermal design that removes its waste heat. This can be achieved with heat pipes or a fluid loop (which could be similar to the MSL design). The radiated and conducted waste heat must be also isolated from the payloads of the gondola and the lander.
- During the atmospheric entry phase, the ASRG experiences entry g-loads as a function of the entry velocity and the EFPA. A suitable mission design must ensure that the g-load does not exceed the 30g limit of the ASRG design. This necessitates new trajectories with shallow EFPAAs, but with sufficient margins to avoid skip-out. In comparison, the Pioneer-Venus probes with a steep 40° EFPA experienced g-loads in the 300 – 400g range, over 10 times higher than can be tolerated by an ASRG.
- During EDI, the atmospheric entry heating reduces the efficiency of the backshell radiators. Therefore, the aeroshell must have sufficient thermal inertia to absorb the excess heat from the ASRG until the parachute opens and the aeroshell separates. From that point on, the ASRG would operate inside the Venus atmosphere, where

convection, conduction, and radiation heat-transfer mechanisms will apply.

- During in situ operations the balloon floats at 55 km altitude, where the temperature and pressure conditions of the predominantly CO<sub>2</sub> atmosphere are ~30 °C and ~0.5 bar, respectively. Since the ASRG is designed for vacuum and Mars surface operation, this would result in a backflow through the ASRG's pressure relief device. Therefore, the mission design should properly address the mission impact of the ASRG performance characteristics. Specifically, the ASRG has an inlet through the pressure relief device, which would be open to the Venus environment, so that, upon entry the inner workings of the ASRG inside the housing would be pressurized with atmospheric gases up to the 0.5-bar ambient pressure. This would likely result in some performance degradation. To protect the ASRG from reactive trace gases and aerosols in the Venus environment, the inlet pipe would need to be fitted with (1) a fine-mesh (1-μm-diameter holes or smaller) Teflon getter that blocks sulfuric acid aerosols, and (2) a carbonate-based inner getter that absorbs all acidic components. The 1 μm-diameter fine-mesh Teflon getter — which also would be needed to protect the GC/MS — has been well tested at JPL under the pressure/temperature and aerosol size distribution conditions of Venus flight. It has been shown to be 100% effective at blocking all aerosols with radii greater than 0.50 μm over a simulated 1-week flight, corresponding to the flight of the non-ASRG-powered VALOR mission proposed for Discovery in 2006. This blocking radius includes virtually all Venus mode 2 sulfuric acid droplets, which have been determined to have a mean radius of  $1.05 \pm 0.10 \mu\text{m}$ , with an effective variance of just  $0.07 \pm 0.01 \mu\text{m}$  (Hansen and Houvenier, 1974). For added protection during its longer, month-long flight, the ASRG inlet pipe may be

fitted with a finer mesh, with holes as small as 0.25  $\mu\text{m}$ . Further investigations might be required to see if there are any seals or valves that might directly interface with the outside atmosphere, and could be damaged and thus expose internal ASRG components.

Much larger data volumes and extended balloon missions that can travel to the polar regions would greatly reduce the risk of not acquiring a complete enough dataset to understand the Venus greenhouse, atmospheric chemical cycles, and the atmospheric superrotation. A second option for the balloons capability enhancement would be to use a solar photovoltaic panels for power generation. Since balloons would travel to the polar regions, the solar cells option is far less attractive as compared to the use of the ASRGs.

## 5.4 Mission Architecture Enhancements

### 5.4.1 Surface Exploration

#### 5.4.1.1 Enhanced In-situ Science at the Venus Surface

A highly capable long-lived lander (months or longer) on Venus would be mankind's first extended outpost on a planet with an extreme greenhouse effect. A lander that could survive for long enough to track the weather and obtain a range of seismic events, would also be able to more thoroughly explore its nearby environment. The lander could also serve as a relay station for science data being gathered by *in situ* instruments such as the seismic/meteorological planetary network. Being able to drill to depths of up to a meter and to acquire soil and rock samples at a variety of locations would greatly enhance the ability to provide the crucial information of how pristine Venus rocks reacted with the atmosphere.

The illusion of static volcanic plains from the Venera lander images obscures the fact that visually, the surface of Venus undergoes vast changes. Night and day with intense scattering by the thick atmosphere will change the scene dramatically, perhaps even altering

the illumination of the landscape and lander workspace. Other changes, such as particles lofted by the winds, and even the changing appearance of the lander and sampled sites, would provide significant insights into the dynamic nature of Venus' surface.

#### 5.4.1.2 Seismometer and Meteorological Planetary Network

Seismology and meteorology are two investigations that require long-lifetime measurements on the surface, and hence cannot be fully accomplished in a short duration surface mission. How active is Venus? Are there Venus quakes? How deep are the basaltic plains and what is beneath them? It is important to recognize that significant science can be accomplished with just one seismometer on the surface of Venus, while the broader goal of understanding the interior structure will require several seismic stations around the planet. For example, crustal thickness in the vicinity of a seismometer can be measured using the receiver function method and data from a single seismic station (Amman, 1991; Yan and Clayton, 2007). A broader and more complete picture of Venus' interior, the dynamics of the mantle, and the nature of the lithosphere will require a network of at least four seismometers spaced around the planet. Based on terrestrial seismicity, such a network operating for one Earth year would probably be sufficient to meet these science goals.

Surface meteorological measurements were acquired at diverse locations on Venus by the Venera landers (Marov et al., 1973). Pressure, temperature and wind speeds for a few minutes at each location have been invaluable for understanding this exotic environment. Beyond that, however, the dynamics of Venus atmosphere is not understood, mostly because we know very little about the weather in the lowest 3 atmospheric scale heights (99% of the atmosphere's mass). From the cloud layers up to about 100 km, there is a clear and consistent poleward flow, probably the poleward branches of two hemispheric Hadley cells (Gierasch, 1975). Therefore, a strong poleward to equator flow must exist below the clouds.

On Earth, baroclinic eddies perform this function as the familiar mid-latitude winter storm fronts. Pressure changes herald the passing of these eddies, as they do on Mars. Do analogous processes occur on Venus? If not, what is the nature of the poles to equator flow? Could barotropic instabilities be responsible, as they seem to be for Venus' mid-latitude jets? Measurements at multiple geographical locations and surface altitudes are necessary to begin to answer these questions. Optimum scientific benefit could be achieved from extended operations for one Venus solar, or 117 Earth days.

Fundamentally, a seismometer measures the three vector components of the displacement field as a function of time due to the passage of seismic waves. There presently exists a range of seismometer and geophones of various sensitivities that can operate at room temperature or could be adapted for planetary missions of moderate or cold temperatures (Lay and Wallace, 1995; Lognonne, 2005; Mocquet, 1999). Existing seismometers can generally be divided into three categories:

- Short-period (SP) seismometers and geophones measuring signals from approximately 0.1 to 100 Hz. – generally using variable inductor or variable capacitive mass-spring designs.
- Broadband sensors (BB) having a flat response proportional to ground velocity from approximately 0.01 to 50 Hz. These sensors generally have higher power requirements than SP sensors.
- Very broadband seismometers (VBB) measure frequencies from below 0.001 Hz to approximately 10 Hz. These designs have generally been satisfied with multiple sensors used to achieve these very broad ranges.

For understanding the near surface weather of Venus, meteorological stations that measure temperature, pressure and wind should be made for as long as possible. Optimum science benefit could be achieved from extended operations for one Venus solar day or 117 Earth days. Along with winds, pressure

measurements track the passage of baroclinic or barotropic instabilities (storms). Ultra Stable Oscillator-enabled measurements of winds do not apply once on the surface and alternate anemometry must be employed, such as hot-wire, momentum, sonic, or pressure techniques. However, advances in pressure and temperature sensors that function reliably and accurately at Venus surface ambient temperatures and pressures suggest that development for a Venus mission would be easily possible with the appropriate development effort.

#### *5.4.1.2.1 Venus Seismometry and Surface Meteorology Science Objectives*

The objectives of the seismology experiment are to characterize the current activity of Venus and to probe the interior structure of the planet. The meteorology measurements can help improve the understanding of the surface environment and the dynamics of the Venus atmosphere. The specific combined objectives of the seismology/meteorology network experiment include:

- Provide measurements of the size-frequency distribution of seismic events and characterize the internal structure of Venus (crust, mantle, and core) by measuring the P and S wave seismic velocities as a function of depth in the planet.
- Improve understanding of the surface meteorology and atmospheric conditions on Venus with measurements such as temperature, wind speed and direction, and pressure to determine long-term trends.
- Provide correlation between observed planetary events and changes in weather conditions. Variations in meteorological/atmospheric conditions could be compared with the baseline data taken from short-lived measurements such as a lander meteorological station and atmospheric composition with the mass spectrometer.

#### *5.4.1.2.2 Scientific Advances from Venus Seismometry and Meteorology Stations*

The low frequency end of the seismic spectrum involves the normal modes of the global oscillations of Venus. Such seismic waves have very long wavelengths and thus will effectively sample the structure of all of Venus. On Earth, normal modes are an important part of the determination of seismic velocity models (Dziewonski and Anderson, 1981). Because different minerals have different seismic velocities, the measured velocity structure of the planet will place bounds on the chemical composition. The transition from the rocky mantle to the metallic core is marked by a major discontinuity in seismic velocity. The physical state of the core (liquid or solid) can be determined from the S wave velocity (shear waves do not transmit through liquids). Another important advantage of normal modes is that low frequency data place low demand on data storage and uplink capabilities. The higher frequency end of the spectrum is the subject of body wave seismology. The relatively short wavelengths of body waves provide higher resolution details of planetary structure, such as crustal thickness or mantle velocity discontinuities associated with mineral phase changes. On Earth, typically two different types of sensors are used in a given seismometer to provide measurements over the entire frequency range (Lay and Wallace, 1995).

Crustal thickness is a measure of the time-integrated volcanic eruption rate, and thus is a high priority measurement objective. Moreover, observations at even a single seismic station could be used to make an initial assessment of the current seismic activity level on Venus. A more elaborate mission concept is the Venus Geophysical Network concept involving at least 4 seismic stations operating on the surface of Venus for at least one Earth year, while a less ambitious approach can have one to four seismometers operate for at least a half Venus solar day (117 Earth days).

It is highly desirable that seismic measurements be made on the surface of Venus for extended durations that are equivalent in sensitivity and resolution to those performed on the Earth. The operational requirements for Venus environments include ~500 °C operation and ~90 bars for durations from 117 Earth days to 1 Earth year. Given the current state of technology development and depending on the mission architecture, such measurements may not be feasible. Rather, measuring at least a subset of the seismic frequency range would be desirable, with significant science benefits.

If the seismology experiment is a part of a refrigerated spacecraft with a radioisotope power source coupled with cooling, then it may be possible to achieve the full range of target measurement requirements. However, if the experiment is performed at ambient surface temperatures using high temperature electronics and high temperature power sources or/and high temperature batteries, then some performance trade-offs may be necessary.

Atmospheric superrotation may be forced by angular momentum exchanges with the surface, although the mechanisms of upward transfer of angular momentum within the atmosphere are not understood. Meteorological stations that can weather data at two locations simultaneously over one Venus solar day would provide extremely important information on the dynamics of the near-surface atmosphere. The specific goals of the meteorology experiment, in addition to providing wind speed and direction and atmospheric temperature and pressure, are to determine the vertical and horizontal structure at the base of the local atmospheric boundary layer, and to observe changes at the locations with time. Both short term, local pressure waves, such as baroclinic eddies and long term regional, weather pattern variations may exist (Schubert, 1983).

#### *5.4.1.2.3 Technology for Venus Seismometry and Meteorology*

The options to technologically realize a seismometer and meteorological network on

the surface of Venus and secure its long-term operation from 117 days to 1 year include:

- Use a refrigerated pressure vessel to be able to operate a network in mild thermal environment enabling the use conventional, space rated components. Issues associated with measurement interfaces to the ambient surface and environment would have to be addressed.
- Use components that can fully and reliably operate in Venus surface environment without thermal control including high temperature sensors, high temperature electronics and telecom system, and high temperature power sources and batteries.
- The development of a hybrid system using both refrigeration and environmentally hardened components. The use of high temperature components would enable the optimization of the refrigeration system to minimize its power and mass, and refrigeration can protect components that can't operate at Venus surface temperature and pressure.

The technology development needed for Venus refrigeration system is described in Subsection 5.4.2.1. The state of the art and technology development needs for high temperature components are described in Subsection 5.4.2.

#### *5.4.1.2.3.1 Seismometry Technology*

A seismometer measures the three vector components of the displacement field as a function of time due to the passage of seismic waves. The principal measurement requirements for seismometers are:

- Measurement Frequency Range: On Earth, the longest period seismic normal mode,  ${}_0S_2$ , has a period of 3233 seconds (Dziewonski and Anderson, 1981). Because Venus has a smaller radius, the fundamental normal mode period will be somewhat shorter than on Earth. This implies a minimum measurement frequency of 0.3 mHz. At the high frequency end, measurements up to at least 10-30 Hz are

important (Lay and Wallace, 1995). As with seismometers used on Earth, covering the full frequency range is likely to require two distinct sensors. For the long period sensor, measuring just the vertical component is sufficient. For the short period sensor, measuring all three vector components of the wave field is necessary.

- Amplitude Sensitivity: A desirable goal is for the minimum amplitude sensitivity to be in the range  $10^{-8}$  to  $10^{-9} \text{ m sec}^{-2} \text{ Hz}^{-1/2}$ , which is similar to the goal for the ESA ExoMars seismology package being designed for use on Mars (Lognonne, 2005; Mocquet, 1999). In order to measure the full range of possible signals from the smallest measurable amplitude to the largest likely event, 24 bit digitization (or its analog equivalent) of the amplitude time series is necessary.
- Duration of Observations: Because seismic events occur randomly in time, the seismology experiment would benefit from the longest possible observation interval. For an initial seismic experiment, an observation period of at least a few months is necessary. If a seismometer is coupled with a meteorology station on a long-lived lander, a minimum observation period of 117 Earth days (or 1 Venus solar day) is a reasonable target. Ideally, seismic measurements would be recorded continuously during that time.

There is currently a technical void with respect to seismometers and geophones which can exceed an operating temperature of 260 °C. The primary barrier to the development of such high temperature seismometers is the lack of available materials which can be used to fabricate a sensor structure capable of exhibiting the appropriately sensitivity to seismic events and surviving high-temperature conditions. For example, standard geophones use a variation on Linear Variable Displacement Transformers (LVDT) with multiple coils and ferrite materials. The operation of these ferrite

materials at higher temperatures is limited, because they demagnetize. Thus, these geophones cannot operate at higher temperatures due in part to the limitations in the LVDT technology. Further, coupling of a basic sensor to mechanical mechanisms such as springs is also necessary to make a seismic measurement. It is important to note that the materials used to make any proposed sensor type need to be inherently high-temperature tolerant and capable of operation at Venus temperatures and pressures.

Multiple approaches exist to solving the problem of producing high-temperature seismometers. One straightforward approach would be to fabricate a simple geophone measuring the higher frequency range of seismic events between 1 - 30 Hz (Shearer, 1999). A high temperature version of the geophone could measure a change in the inductance of high temperature variable inductor coils (Inproxtechnology, 2009). As in a geophone, a moving mass then results in a change in the frequency of an oscillator. An advantage of this approach is that the basic measurement creates a frequency modulating (FM) transmitter whose rate of frequency change is proportional to the rate of change of acceleration at the sensor. In effect, by taking a measurement and creating a frequency, digitization is achieved at the source whose value can be used to activate an oscillator. This approach is viable using presently available high temperature sensors and circuitry, and is potentially capable of providing significant Venus seismometry data in the higher frequency range. A higher frequency geophone is considered reasonably achievable with existing sensor technology. Packaging and robustness issues would need to be addressed. The development of a seismic instrument, which measures across the complete frequency range, is a significant technical challenge for a longer term development. Given on-going advancements in high temperature MEMS technology, such a broad range measurement device is achievable; the corresponding electronics and

communication technologies for a more complex system would be very challenging.

The opposite end of the complexity spectrum is to attempt to reproduce a high temperature version of the seismic sensors proposed for Mars in the Netlander instrument (Lognonné et al., 2000). This would involve not only the development of high temperature Micro-Electro-Mechanical Systems (MEMS) based accelerometers (Okojie et al., 2002), but also more complex circuitry including memory and the data handling to support the instrument. While such an approach would provide a complete spectrum of seismic information, the remaining technical challenges are very significant and equal to developing high temperature semiconductors to the capability of silicon-based technology. In other words, a more complex high temperature seismic instrument would require great development efforts or a hybrid system with a power source and refrigeration system for long-lived operation.

The preceding discussion outlines the very large option space of choices for a seismometry investigation at Venus. Detailed trade studies will be required to determine the best system-level approach for a flagship mission. A key consideration is the data volume generated by the seismometer. For a seismometer in which all three vector components of the wave field are measured with 24 bit digitization at frequencies up to 30 Hz (requiring sampling at 60 Hz), the required data rate is approximately 4.5 kbits per second. This high data rate would require substantial power and telecom assets to relay data back to Earth over extended periods of time. More limited investigations at either lower sampling frequencies or shorter durations can be considered as an alternative scenario, at the cost of reduced science utility. A second key consideration is the operating temperature of the seismometers and associated system components. It may be possible to build systems that operate at Venus surface temperatures and thereby avoid the need for active refrigeration; however, such systems will need to include data storage and handling

functionality unless gaps can be tolerated in the data due to a temporary lack of telecom availability when either the orbital relay or the Earth is not visible from the seismometer. These trades, and many others, will need to be analyzed to yield viable scenarios and accordingly, guide the technology development priorities for seismometry investigations at Venus.

#### *5.4.1.2.3.2 Meteorology*

Obtaining an understanding of the day-to-day Venus ground ambient metrology/atmospheric conditions, using a high temperature weather station, requires a basic measurement system that includes temperature, wind flow and pressure. Variations in these fundamental weather data would greatly improve understanding of the dynamics of the deep atmosphere and assist in the correlation with data from other measurements such as the InSAR or seismometer. Some general specifications for such sensors include: 1) operation at 500 °C, 2) measure pressure of  $92 \pm 0.1$  bars with 10 Hz to 100 mHz frequency response 3) measure temperature from 450 – 500 °C with 1 °C resolution, 4) measure wind speeds from 0.3 to 1.0 m/s with 0.03 m/s resolution, and 5) measure gas species variations with time.

#### **5.4.1.3 Long-Lived Landers**

The introduction of a Long-Lived Lander into the Flagship mission would have many of the same advantages of the Extended Surface Life Landers, but magnified significantly by the wide range of opportunities afforded by this platform. By Long-Lived, the concept is to have a refrigerated Lander system with a near full complement of Lander capabilities operating not for a day, but potentially months on the Venus surface. The technology development related long term power and refrigeration needed to enable a Long-Live Lander is discussed in section 5.4.2.1 and 5.4.2.2

#### *5.4.1.3.1 Scientific Objectives of a Long-Lived Lander*

The scientific objectives of a lander operating at the surface of Venus for months

or longer are to:

- Sample multiple sites and multiple depths, including rocks and soils, for a complete survey of the elemental composition, mineralogy, and chemistry of the landing site.
- Acquire long-duration observations of time-varying phenomena such as seismicity, temperature, pressure, and winds, and lighting.
- Decrease mission risk and optimize science return by providing extended duration missions with complete instrument operation for extended periods of time. Long-term active cooling provides the ability to monitor a wide range of environmental and seismic events on the Venus surface and compare these results over extended periods of time.
- Provide the capability with added time to have ‘human-in-the-loop’ enhancement and control of experiments. This allows optimization of the choice of sampling sites and much richer set of analyses based on what has been learned previously.

#### *5.4.1.3.2 Scientific Advances from a Long-Lived Lander*

An example of the advantages of a long-lived lander can be found in geochemistry investigations and the addition of humans in the loop. In a long-duration mission, having ‘humans in the loop’ would directly address one of the major targets of Venus geochemical investigations: diversity of surface materials, which is a high priority science objective of the VEXAG (2007) goals and objectives (VEXAG, 2007). A landed spacecraft will have access to surface materials with a range of physical properties and chemical compositions, each of which would help address a particular goal, objective, or unknown about Venus. Without human intervention, a Venus lander will have to rely on either a pre-programmed sampling routine, or machine vision algorithms. While feasible within the Design Reference Mission and scientifically valuable, both of these

approaches have implementation risks and they might miss valuable science opportunities that human operators would recognize and exploit.

The DRM specified use of machine vision techniques to evaluate the scene and select the drilling location that was deemed most valuable through pre-programmed criteria. Machine vision is a huge advance over rigid pre-programming, but comes nowhere close to the value added of having scientists make the sampling decisions. For Venus, probably the biggest limitation is that we do not really know how the landing scene may appear. Since the machine vision techniques for the Flagship mission will have to be trained on existing images such as Venera/VEGA images and Mars surface images there is the possibility that if the scene attributes at the Venus Flagship landing sites are quite different than anything experienced previously then the right drilling locations will not be specified by the machine vision algorithms.

Having humans in the decision-making loop, selecting samples to be analyzed and types of analyses, would allow crucial targets to be identified, prioritized, selected, and analyzed. This type of decision-making structure has long heritage, starting with the Apollo lunar explorations, currently with the MER lander missions on Mars, and is baselined for the MSL Mars mission. With human decision-making in a Venus landed mission, one could be assured of identifying representative samples of local surface materials, and of identifying unusual materials to satisfy the VEXAG goals related to surface diversity. If a long-lived lander is flown to Venus, an expanded sampling system could be implemented to further optimize the scientific return.

Physically, Venus surface materials seen by the Venera and VEGA landers include massive rocks, platy materials that might represent lava flow tops or weathering rinds, sand in amongst these rocks, and dust lifted by the landers' impacts (Garvin, 1981) (Figure 5.3). Each of these materials holds clues to the evolution of

Venus' surface. Bulk rock analysis can provide information about the interior and past history of Venus, including its planetary accretion, differentiation to core and mantle, and formation of its crust (including possibly the effects of water). Analysis of the platy materials, if related to weathering, will provide information about surface-atmosphere interactions and how climate may be affected by surface chemistry. Sand-sized material and dust contain information about impact cratering and wind regimes.

Beyond geology, the data retrieved by a long-lived lander would not be limited by the five hour window, but would be time resolved and track changing conditions on the planet over a Venus day. Data acquisition could be repeated multiple times to verify consistency and accuracy. The time component of the surface environment on Venus (the ‘weather’) is currently unknown; a long-duration station could give us a baseline to understand the pressure and temperature variations over time scales ranging from hours to weeks, confirming or questioning our current understanding of the surface environment. The lander could also serve as a relay station for information being gathered by *in situ* instruments such as a seismic/ meteorological network.

The long-lived lander data could also be correlated with that being taken by an orbiter or balloons; for the first time measurements at three separate levels could be compared improving the understanding of Venus conditions beyond what would be contributed by the orbiter, balloon, or lander independently. For example, if the presence of volcanic activity is noted by the seismic network, the relative effect of this activity could be tracked by the lander instruments, noted in the mid-atmosphere by the balloons, and the overall planetary effects tracked by the orbiter. This approach strongly optimizes the three-level approach of the mission, if data are taken for extended times to allow such three-level comparisons.



Figure 5.3: Venera 13 image showing slab-like lava with soil and pebbles interspersed between slabs. The horizon can be seen on the left, with a small hill on the right edge of the horizon.

#### 5.4.1.4 Low Altitude Balloons

The introduction of low level mobile systems, such as low altitude balloons, can add enormous scientific capability, and potentially public excitement, to Venus exploration. The only locations where we can actually see what the surface of Venus looks like at visible wavelengths are the spectacular, but static, images from the Venera Landers (Abdrakhimov and Basilevsky, 2002; Garvin et al., 1984; Kargel et al., 1993). The only geologic context we have for Venus is provided by the global Magellan radar image dataset. In order to establish a chronology of events and to interpret the geologic history of Venus, geologists must be able to see contacts between geologic units, stratigraphic relationships, and structure.

Much like the geology seen from an airplane during a flight on Earth, aerial perspectives of the planet Venus can yield a unique understanding of the planetary geology. A low-level balloon which traverses at an altitude low enough to view the surface provides an effective way of surveying the regional geology of Venus. Using prevailing winds, horizontal traverses of thousands of kilometers are possible. Balloon altitude control techniques can also be used to perform vertical traverses through the atmosphere and

thereby acquire atmospheric vertical profile information at multiple locations. An extremely capable balloon that could touch down, retrieve a sample, and then retreat to cooler levels could analyze sample chemistry, mineralogy, and elemental abundance at diverse locations. Airplane-based observations of the Venus surface can complement these balloon missions at different altitudes and with an increased level of directional control.

An extension of the mid-altitude balloon concept that is part of the Design Reference Mission is one in which balloons float at low altitudes and includes periodic descent to the surface. An important key to understanding atmospheric processes and perhaps the evolution of Venus resides in the lower 20 km of the atmospheric column, where nearly 80% of the atmospheric mass exists. Measurements of variabilities in trace atmospheric species during a low-level traverse would be extremely important for gaining a deeper understanding of surface atmosphere chemical interactions. Also, the transport of angular momentum is thought to be accomplished by eddies and circulation whose size, motions and longevity are poorly understood. Length of day variations, detected by the microwave corner reflector, may show angular momentum exchanges between the surface and

atmosphere that contribute to the atmospheric superrotation. The determination of winds in the lowest scale height of the atmosphere would place these angular momentum measurements in context.

Finally, low-altitude balloon traverses are an ideal way to do geological photoreconnaissance of the Venus surface. By obtaining visible images of the surface across thousands of km, it would be possible to observe diverse lithologies and their relative positions in the geologic sequence. By extrapolating these results to the global Magellan radar datasets, a new and potentially revolutionary understanding of the geologic history of Venus would be possible.

These exciting investigations can be well addressed by different kinds of low altitude balloons which target the lower atmosphere and may include altitude control functionality all the way to the planetary surface. The use of such low altitude balloons would allow the ability to explore the atmosphere in three dimensions over time, allow surface exploration, and intensively investigate lower atmosphere properties and chemical processes.

#### *5.4.1.4.1 Scientific Objectives of a Low Altitude Balloon*

The scientific goals of the low altitude balloon platform and its combined instrument package are to acquire:

- Multispectral imaging of surface at a resolution of 1 – 10 m, where there is a gap between radar images at 75-m resolution, and Venera landed images at cm-scales. These data will elucidate the relationship between large and small-scale morphologies, look for lateral variations in lithology, and quantify block sizes.
- Multiple surface analyses over different lithologies and chemical compositions correlated to those lithologies.
- Extended traverse sampling, enabling the definition and correlation of large-scale geologic units.

- Monitoring of compositional and physical variations in atmosphere with altitude and latitude.
- Variable resolution and high resolution imagery in regional context—essentially enabling geotraverses with ground truth.

#### *5.4.1.4.2 Scientific Advances from a Low Altitude Venus Balloon*

Low altitude balloons are a telerobotic science platform that can fly and navigate in a dynamic 3-dimensional atmospheric environment, thus enabling the global *in situ* exploration of planetary atmospheres and surfaces (Gilmore et al., 2005). One approach is the use of aerobots with altitude control which employs reversible-fluid changes to permit repeated excursions in altitude. The essential physics and thermodynamics of reversible-fluid altitude control have been demonstrated in a series of altitude-control experiments conducted in the Earth's atmosphere (Cutts et al., 1996). A possible instrument package for such a balloon system includes a visible/near-infrared multispectral imaging system as well as an X-ray fluorescence detector mounted within a flexible snake that could hang from the balloon and measure major and minor surface element composition.

An approach to such a mission, including possible exploration sites, has been described in the literature (Gilmore et al., 2005). A low altitude balloon could circumnavigate Venus and remain stable at low altitudes for hours of observations. Dives to the surface could produce multispectral stereo imaging at up to cm-scale resolution. Meter-scale imaging spanning 10s of km can be directed to boundaries between geologic units of interest. Technology such as an XRF instrument mounted on a ‘snake’ (a rope-like extension from the balloon’s gondola, which would periodically come in contact with the surface to perform *in situ* measurements. Surface access can be maximized by utilizing local winds due to slope effects (Gilmore et al., 2005).

Since the surface of Venus is never visible through the cloud layer, one mission for a low altitude balloon on Venus is to fly at an altitude below the clouds where the surface can be viewed (Landis et al., 2003). Modeling of radiative transfer in the Venus atmosphere and the camera spectral response indicates that adequate contrast can be achieved looking at the surface in near-infrared wavelengths at altitudes up to about 16 km with a 20-deg solar zenith angle (Bullock and Grinspoon, 2002). Lower altitudes allow better contrast and wider spectral range. 16 km corresponds to a temperature of about 340 °C, at a pressure of 31 bars and an atmospheric density of 26 kg/m<sup>3</sup>. If the mission is chosen at a location where the surface is 3 km above the average, the temperature decreases to 315 °C.

#### *5.4.1.4.3 Technology Development Requirements for Low-Altitude Balloons*

The great advantage of the cloud-level balloon proposed for the Design Reference Mission is that the 30 °C temperature at that altitude (55 km) allows the use of available polymer balloon materials, albeit arranged in a novel laminate. Balloons for enhanced or alternate mission concepts will need to tolerate much higher temperatures at lower altitudes (~460 °C near the surface). The balloon materials, design concepts and technology needs for these different missions will be described below. More details can be found in the NASA Extreme Environments Technologies Report (Kolawa et al., 2007).

The technology required to implement a lower altitude (< 50 km) Venus balloon is not mature and faces four main challenges:

- Available polymer balloon materials and adhesives do not work at the 460 °C surface temperatures. The lowest allowable altitude is in the range of 8 - 15 km (350 - 400 °C) at which Kapton film balloons can survive. Polybenzooxazol (PBO) film balloons have the potential to tolerate surface temperatures, but their technological development remains incomplete.

- Most scientific instruments cannot tolerate high temperatures. Therefore, long duration flights in the lower Venus atmosphere will require some form of refrigeration to remove the heat leaking in from the environment.
- Electrical power is difficult to obtain below the Venus clouds since the solar flux is much reduced and the operating temperature of solar panels is very high compared to terrestrial or standard spacecraft environments.
- The balloon's suspended payload is significantly mass limited. Therefore, the payload and internal power source needs to be both capable and light.

In response to these challenges, a number of balloon designs and mission concepts have been developed, each targeted at a different set of science objectives. The three most prominent of these concepts will now be described.

A proposed Venus Surface Sample Return (VSSR) mission would require a balloon to lift the sample from the surface, carrying an ascent vehicle (a rocket) to a rocket at an altitude of approximately 60 km. This rocket would then fire to take the sample into Venus orbit from which it would rendezvous with a spacecraft for the journey back to Earth. Without a balloon, the sample has to be rocket-launched from the surface and the aerodynamic drag penalty from the high density Venus atmosphere is prohibitive. In this application, therefore, the balloon must traverse the entire range of altitudes and temperatures that correspond to these altitudes (from 0 to 60 km). Currently, no known balloon material is capable of doing so. The most promising solution to this problem was described by Kerzhanovich et al., (2005) where a multi-balloon system is used with two balloons. A metal balloon is used first to lift the sample from the surface to an altitude of approximately 10 km, after which the helium is transferred to a second balloon made from Teflon-coated Kapton film, which carries the payload and metal balloon to the rocket launch

altitude. Figure 5.4 from Kerzhanovich et al., (2005) illustrates the concept. A thin metal balloon works at Venus because the very high atmospheric density generates very large amounts of buoyancy per unit volume. (Note that the buoyancy results from the mass difference of the balloon displaced CO<sub>2</sub> volume of the atmosphere, and the combined mass of the balloon, its fill He gas, and the payload.) Figure 5.5 shows a proof-of-concept metal bellows balloon that was successfully tested at the Jet Propulsion Laboratory for inflation and leakage at 460 °C. The second Kapton balloon is required because at higher altitudes the atmospheric density decreases to the point that a metal balloon cannot generate enough buoyancy to float itself much less a payload.

If a large altitude traverse is not required, then a metal balloon alone will suffice for a near surface mission. The Venus Mobile Explorer mission concept (Kolawa et al., 2007; NASA, 2006; VEXAG, 2007) is based on the premise that a metal balloon can fly at an altitude of up to 5 km, performing aerial reconnaissance over long ground tracks and potentially doing other scientific investigations. Passive thermal control could suffice for a mission duration of several hours. Active refrigeration coupled with radioisotope-generated electrical power could enable a mission of very long duration, limited only by the leakage of helium buoyancy gas from the metal balloon.

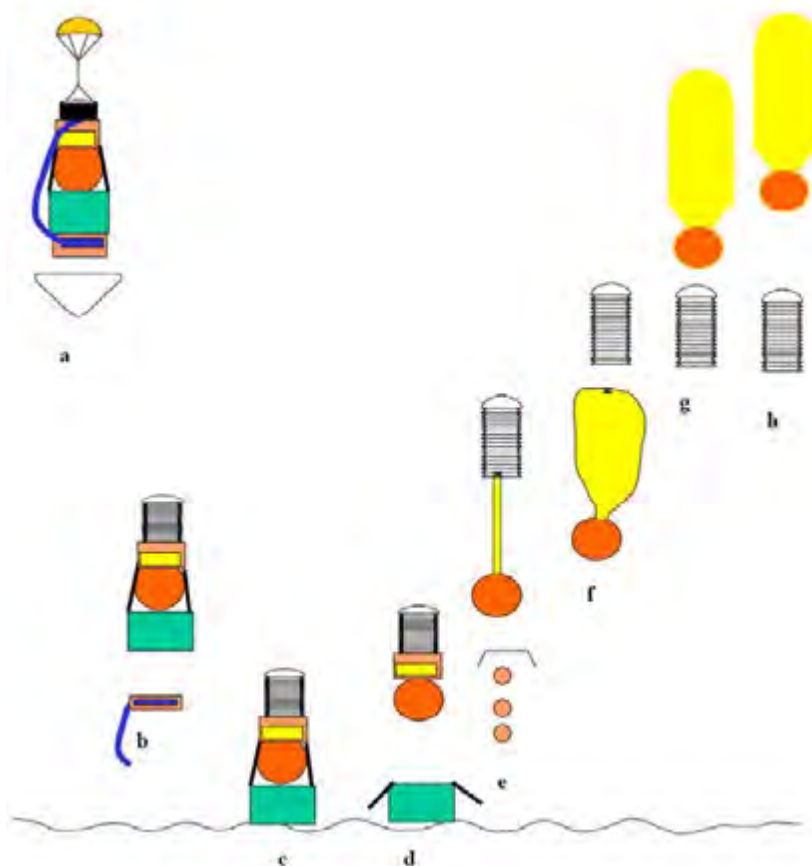


**Figure 5.4:** VSSR two-balloon mission concept. a - aeroshell separation, b – Low altitude balloon (LAB) inflation and Inflation system release, c – surface operations, d – launch, e – deployment of High Altitude Balloon (HAB), release HAB container, f – inflation of HAB and LAB separation, g – HAB ascent to cruise altitude, h – HAB at cruise altitude (Kerzhanovich et al., 2005).



**Figure 5.5:** Proof of concept metallic bellows, tested at JPL.

Although the principle of the Venus metal balloon has been demonstrated in the laboratory, there are significant technical challenges in the areas of deployment and inflation, optimization for low mass, altitude control, and validation of leak-free operation. More advanced concepts might also require significant onboard autonomy functionality for flight controls, hazard detection and avoidance and science data collection.

The other major concept for a high temperature Venus balloon mission is the altitude cycling balloon (Chassefiere et al., 2008; Nock et al., 1995). For this concept, the balloon is filled with a buoyancy fluid that changes phase from a liquid to a gas depending on the balloon altitude (temperature). When flown in the troposphere, a stable cycling occurs as follows: as the balloon rises, it gets colder and the buoyancy gas starts to condense. This condensation reduces the overall buoyancy until the weight of the balloon and payload can no longer be supported and the balloon starts to descend. As it descends, the buoyancy fluid starts to

evaporate and the overall lift increases until the descent is arrested and the balloon starts to rise again. For Venus, the likely buoyancy fluid is a mixture of helium and water, with the water undergoing the phase change during flight. Large altitude excursions from 60 to 0 km at Venus can be created by collecting the condensed liquid into a reservoir and delaying its re-evaporation (Bachelder et al., 1999). However, the lack of a single balloon material that can span that entire altitude range is an obstacle, and may limit the cycling balloon to a minimum altitude of approximately 10 km.

Repeated traverses through a large altitude range provide a unique opportunity for scientific investigations of the Venus atmosphere. However, there is an additional major benefit of this concept and that is thermal management of the payload. Every time the balloon ascends to its maximum altitude, it enters a cold environment that allows for cooling of the payload. This provides a mechanism for removing the payload heat that accumulates during each low altitude excursion and, if a proper balance can

be achieved, it could avoid the need for an active refrigeration system.

The Venus cycling balloon can be characterized as having low technical maturity with outstanding challenges in the areas of heat exchanger design, balloon materials for the entire altitude range (if near surface operation is required) and validation and verification of the thermodynamic performance at Venus. The technology challenges are significantly less severe for mission scenarios that restrict altitude cycling to the middle and upper atmosphere only.

### **5.4.2 Technologies for Exploring the Surface of Venus**

#### **5.4.2.1 Refrigeration**

The ability to actively refrigerate instruments and electronics fundamentally changes the nature of any long-lived mission, including landers, low altitude platforms, or independent in situ instruments. Such a refrigeration system has two main components: a power source and a refrigeration machine that uses the power source to pump heat from the payload back out into the environment. The radioisotope power is the only realistic long-lived power source for the surface of Venus. Typically an RPS system would be used to jointly power the electronic components of the payload as well as the refrigeration system.

The options for an active Venus refrigeration system are briefly summarized in Table 5.1. The most mature and highest efficiency options for Venus are the Stirling refrigeration systems. These require either an electrical power input or directly pneumatic coupling with a Stirling heat engine in what is known as duplex operation. Long life operation in Stirling machines is achieved through the absence of sliding mechanical parts. Indeed, life tests of Stirling converters for the ASRG program have accumulated in excess of 4 years of operation and are still going (Lewandowski et al., 2008).

No Stirling machines have yet been built and tested for the Venus surface environment. However, many Stirling heat engines and refrigerators have been built and used for both terrestrial and space applications. This experience provides confidence that this technology can be successfully extrapolated to the Venus refrigerator application with sufficient technology development resources. There are two main aspects to that extrapolation: first, the Stirling machines must be adapted for Venus environmental temperatures; second, a duplex Stirling machine must be produced that integrates the heat engine and refrigerator functions into an integrated, high efficiency device.

**Table 5.1: A Brief Review of Venus Cooling Options (Landis, 2006).**

Approach	Characteristics
Thermoelectric	Inefficient at Venus temperature ratios (<1% of Carnot)
Reverse Brayton	High speed turbomachinery as is currently operating on Hubble Space Telescope, but less efficient than Stirling cycle
Free-Piston Stirling	Rotating or free piston linear configurations are possible Cryocooler currently operating on NASA spacecraft (25% of Carnot)
Free-Displacer Stirling	Novel concept being developed under SBIR activities [Sun Power SBIR contract,]. Hybrid between free-piston and thermo-acoustic Stirling (22% of Carnot)
Thermo-Acoustic Stirling	Eliminates the need for a displacer Many are currently operating on NASA/DOD/NOAA spacecraft (17% of Carnot)
Multi-stage Rankine/Brayton	High speed turbomachinery, high temperature motors Requires staging integrated into design (not yet developed)
Mixed Refrigerant Cycle	Terrestrial systems commonly used for natural gas liquefaction. High temperature Venus systems require different refrigerants, early development work in progress

There are some examples of duplex Stirling machines that were built for terrestrial refrigeration applications (Penswitch, 1994). However, those devices were rather exploratory in nature and not close to the high efficiency, long-life machines required for commercial or space applications. In contrast, a lot of work has been done on Stirling heat engines for electricity production and considerable technical maturity has been obtained. Recent work on Stirling cycle power converters for the ASRG program describes long-lived performance at hot end temperatures of 650 and 850° C with Carnot efficiencies of approximately 40% (Lewandowski, 2008), while other tests report 55% Carnot efficiencies with converters working at a hot end temperature of 850° C (Shaltens, 2007). This level of performance is suitable for a Venus power application, although higher hot end operating temperatures approaching as much as 1200° C are preferred because they would yield a higher specific power and hence lower mass device.

Stirling refrigerators have been built for both terrestrial and space applications. In particular, long-lived, space-based cryocoolers have been in operation for many years, and they operate at comparable or greater temperature ratios than are required for Venus refrigeration (Wierzchos and Ascaso, 2002). However, these cryocoolers are typically small devices that pump just a few Watts of heat from very low temperatures, 55 to 80 K. The thermodynamic efficiency of these cryocoolers tend to be in the range of 10 - 15%, although, like most other types of refrigerators, larger Stirling devices show better efficiencies due to the proportionally reduced effects of parasitic heating, so that 20% to 25% efficiencies

become possible (Radebaugh 2000). Adaptation of this cryocooler technology to the Venus surface temperature environment will require a significant re-design to accommodate the much higher 460° C heat rejection temperature.

A trade study was conducted to quantify the size of refrigerator required for typical Venus surface applications. It dramatically illustrates that the use of multistage refrigeration will greatly reduce the amount of plutonium required to power the system. In this context, multistage refers to multiple refrigerators that operate in series such that the heat rejected by one refrigerator is collected and pumped to a higher temperature by the next one. Figure 5.6 illustrates a 2-stage design in which the two refrigerators work from a common Stirling power source. In this example, 700 W of heat is entering the lander from the environment and an additional 400 W of electrical energy is being dissipated as heat energy by the payload. The first stage cooler pumps the heat entering the payload up to the intermediate temperature of 250° C, from where the second stage cooler pumps this heat out to the environment, along with the waste heat from operation of the first stage cooler and the incoming heat leak from the environment through the insulation, for a total of 3000 W. Use of multiple stages allows for the environmental heat to be intercepted and removed at a higher temperature than the 30° C payload, providing major improvements in thermodynamic efficiency. Table 5.2 shows how this improved thermodynamic efficiency translates into greatly reduced requirements for plutonium, measured in general purpose heat sources (GPHS) modules, which are the building blocks of the RPSs (A GPHS module houses ~0.5 kg of  $^{238}\text{Pu}$ ).

**Table 5.2:** GPHSs Required for Lander and Lander Subset Cooling.

Heating and Cooling Load	# Cooling Stages	# GPHS Required
Case 1: Complete Lander (400 W Heating/700 W Cooling)	1	94
	2	72
	3	54
Case 2: Lander Subset (100W Heating/700 W Cooling)	1	65
	2	31
	3	17

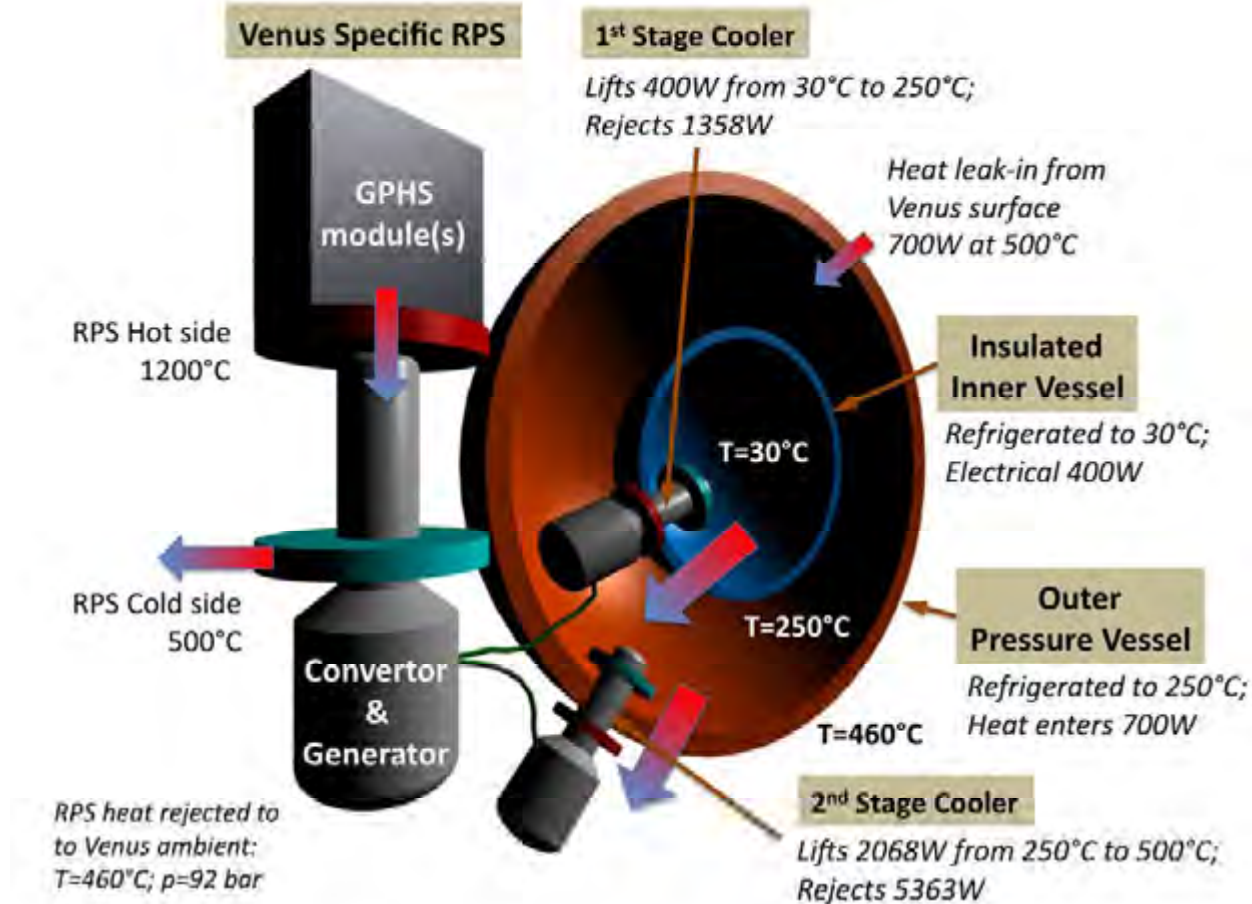


Figure 5.6: Thermodynamic Two Stage System for both Power Generation and Cooling on the Venus surface for a Lander. By staging the cooling, the power requirements drop considerably.

The GPHS savings as the number of Cooling Stages increases and required number of units for two cases: Case 1. Cooling of a complete Lander system assuming 400 W of electrical power dissipation at 30 °C and 700 W of environmental cooling; and Case 2 Cooling of a subset of the Lander system assuming 100 W of electrical power at 30 °C and 700 W of environmental cooling (Power at 55% , Cooler at 30% of Carnot, Respectively, 1200 °C Hot-end)

Two cases are shown in the Table 5.2. In Case 1, the cooling of a complete lander - similar to that in the DRM is considered. The number GPHS modules necessary to provide the required cooling for a two-stage refrigerator is 72, and for a three-stage refrigerator is 54. These are comparable numbers to that of the planned 2020 Outer Planets Flagship mission for which a total of

approximately ~40 GPHS modules is planned (that is, when using 5 MMRTGs) (Dudzinski 2008). In Case 2, reduced heat dissipation from the payload is considered to illustrate the benefits of using lower power electronics or for having a reduced set in science instruments. The reduction in GPHS modules is substantial. Even further reductions in GPHS modules can be achieved by improving the thermal insulation to reduce the heat leak, or by using high temperature electronics to raise the payload temperature. Finally, it should be noted that this analysis makes some aggressive assumptions about the achievable performance of the Venus machine, particularly a refrigerator efficiency of 30% of Carnot and a heat engine hot end temperature of 1200° C, both of which are beyond what has been demonstrated in any kind of experimental device to date. Alternate assumptions based on

a less capable Venus refrigerator will lead to a correspondingly larger number of GPHS modules.

In summary, there is considerable technical maturity in the field of Stirling heat engines and refrigerators that can serve as the foundation for development of refrigerators for Venus. However, substantial technological development is still required given the extreme temperature environment of the Venus surface. The most significant technical challenges are:

- To combine a Stirling heat engine and refrigerator into a long-lived duplex machine with at least two stages of cooling.
- To achieve a high thermodynamic efficiency that will keep the GPHS module (or  $^{238}\text{Pu}$ ) requirements at a manageable and affordable amount.
- To create a complete system design with the multi-stage refrigerator integrated into the Venus platform (lander, rover, balloon). Surface and near-surface payload compartments are typically spherical pressure vessels of minimum diameter to limit the environmental heat leak. Integration of a two-stage Stirling-based refrigerator into this architecture is a challenge given the need to preserve the thermal insulating properties of the original pressure vessel.
- To address issues arising from the potential electromagnetic or mechanical vibration byproducts of the Stirling-converter-based power source and refrigerator that could interfere with scientific instruments. In particular, there is a concern that the mechanical vibration of the machine could interfere with seismometry measurements if the Stirling converter is not physically decoupled from the seismometer.

#### 5.4.2.2 Radioisotope Power Systems

In contrast to photovoltaic power, radioisotope power systems are capable of providing substantial power levels (hundreds of Watts) at all altitudes. The 87 year half life of plutonium-238 makes an RPS an effectively

unlimited source of electrical energy for virtually any conceivable Venus exploration mission. Table 5.3 describes the properties and relative advantages of the main RPS options along with some non-RPS options for contrast.

NASA is currently developing two types of Radioisotope Power Systems (Mason, 2006, Balint 2007). Both systems convert the radioisotopic decay heat of Plutonium-238 to electricity, using either static or dynamic methods. The Multi-Mission Radioisotope Thermoelectric Generator (MMRTG) is utilizing the Seebeck effect of static thermocouples for heat-to-electric power conversion, and incorporates flight heritage elements from the General Purpose Heat Source Radioisotope Thermoelectric Generator (GPHS-RTG). The Advanced Stirling Radioisotope Generator (ASRG) uses a dynamic Stirling convertor to generate power that is not yet space qualified in an RPS; note however, that Stirling-cycle convertors have been successfully employed in space-based cryocoolers. Therefore, technology development is required to migrate cryocooler-based Stirling technology to the power generation application operating in the Venus near surface environment (Balint, 2006). The technological status of existing Stirling conversion based power sources is described in Hyder (2000), Landis 2007, Mellot 2004, Landis and Mellot 2007, Schreiber 2006, Lewandowski 2008, Schreiber 2000.

The ASRG works as follows. Heat is supplied to the convertor from a General Purpose Heat Source (GPHS) module producing thermal power from plutonium ( $^{238}\text{Pu}$ ). The heat input to a convertor results in a hot-end operating temperature. Heat is rejected from the cold end of the convertor. The Stirling closed-cycle system, using Helium as the working fluid, converts the heat from a GPHS module into reciprocating motion with a linear alternator resulting in an AC electrical power output. An AC/DC convertor in the Stirling convertor controller converts the AC power to DC.

**Table 5.3:** Long-Term Powers Sources (500 We & 1200W heat lifted for 117 day mission).

Approach	Properties
Radioisotope Thermoelectric	Efficiency ~3% on Venus ( $T_{hot}=850^{\circ}C$ , $T_{cold}=500^{\circ}C$ ) Difficult to couple with efficient active cooling Demonstrated in space, and will be used on Mars (MSL) Thermoelectric (Chmielewski 1989, Wong 2004) conversion approaches are possible
Radioisotope Brayton/Rankine	Requires high speed turbomachinery Speed reduction for mechanical coolers (Mason, 2006)
Radioisotope Free-Piston Stirling	Overall efficiency ~17% on Venus ( $T_{hot}=850^{\circ}C$ , $T_{cold}=500^{\circ}C$ ) Duplex system couples engine with active cooling (Schreiber 2006, Shaltens 2006)
Radioisotope Thermo-Acoustic Stirling	Overall efficiency ~13% on Venus, ( $T_{hot}=850^{\circ}C$ , $T_{cold}=500^{\circ}C$ ) Duplex system couples engine with active cooling (Abelson et al. 2005) Eliminate displacer with some reduction in performance. (Schreiber, 2006)
Solar Array	Efficiency of known photovoltaics is near zero at Venus surface temperatures at standard optical frequencies. (Landis, 2008)
Battery	Secondary batteries require charging (Harrison and Chapman, 2008) Primary batteries limit mission duration (Kolawa et al., 2007; Cutts et al., 2007 ; Balint et al., 2007)
Microwave beamed power	Station in atmosphere produces solar power; power is transmitted to surface by microwaves Not demonstrated in Venus environment Very low technology maturity, with many technical questions need to be answered; not yet considered a viable option

With proper masses, spring rates and damping (dynamic/acoustic tuning), the convertor will resonate as a Free-Piston, Free-Displacer, or Thermo-Acoustic Stirling Thermodynamic Cycle Convertor.

RPSs based on direct thermoelectric conversion (i.e., the MMRTG) can easily exceed their 14 years design lifetime, due in part to the use of well-known materials, rigorous component testing, and a Pu-238 heat source with an 87.7-year half-life. A major motivation for considering the use of a RPS on NASA missions is their ability to produce continuous, reliable electrical power in remote and often severe environments, with no reliance on sunlight. Some past NASA missions to the outer planets could not have been performed without RPS, and some spacecraft continue to operate far beyond their original expectation due in large part to the long life RPS.

Since dynamic conversion is about four times more efficient than static conversion, the ASRG requires about the quarter of the  $^{238}\text{Pu}$  compared to the MMRTG, while generating the same amount of electric power and

rejecting proportionately less waste heat. Excess heat can be either a benefit or a shortcoming depending on the mission in question. For example, the Mars Science Laboratory rover, to be launched in 2011, will use a single MMRTG. On the surface of Mars it will utilize the waste heat to keep the Warm Electronic Box (WEB) at a desired temperature during the cold nights. Although this excess heat is desirable on the surface, during the cruise phase – while bottled up inside the aeroshell – it needs to be removed and rejected to space. Therefore, MMRTG enabled missions require more capable cooling systems during the cruise phase inside an aeroshell than the ones using ASRGs, since the former requires 4 times more  $^{238}\text{Pu}$  than the latter. This would be particularly important to a future mission to Titan considering 5 RPSs to be carried inside an aeroshell (as indicated by Titan Explorer mission studied in 2007 as the Outer Planet Flagship Mission Phase 1), where the generated heat would be ~10000 W(t) with MMRTGs and ~2500W(t) with ASRGs.

The excess heat of an RPS on a long-lived Venus in situ exploration platform would have undesirable impacts on both of the above discussed mission phases. During the cruise phase the in situ elements would be inside an aeroshell, requiring removal of the waste heat. Near or on the surface of Venus the high temperature of the environment would reduce the temperature difference between the hot and cold sides of the RPS, and with it the efficiency of the power conversion process. For these reasons a long-lived Venus surface mission would likely consider a dynamic power conversion based RPS.

It should be noted that today's RPSs under development are not designed to operate in the Venus environment on or near the surface, although ASRGs could operate satisfactorily in the cloud level at 55-km altitude, where the pressure and temperature conditions are Earth-like (Balint et al., 2008). Near the surface, RPSs must tolerate high pressure, temperature, and corrosion, and for most considered mission architectures a Venus specific RPS will likely need to be coupled with active refrigeration (Balint et al., 2008; Balint, 2006), as discussed in Subsection 5.4.2.1.

Stirling RPS systems designed for Venus applications have been proposed since the 1990s (Dochat, 1992). Stirling hot-end material (MarM-247) is being developed in the Advanced Stirling Converter / Advanced Stirling Radioisotope Generator (ASRG) project to operate for 17 years at 850° C (Lewandowski et al.) for the next generation of ASRGs, beyond the current 650° C design. A single (previous generation) Stirling convertor has been operated in 2005 over 300 hours with a 850 °C hot-end temperature and 90 °C cold-end temperature with 38% efficiency and 88 W power output with heat input equivalent to 1 GPHS (and 114 W power output with unlimited heat input). While impressive, these are not yet Venus environmental temperatures. To be truly validated in the Venus surface environment, the cold end temperature has to be raised from 90 °C to 480 °C, with an expected decrease in overall thermodynamic conversion efficiency. An increase in

conversion efficiency could be achieved by increasing the hot end temperature beyond 850 °C to as much as 1200 °C. However, this will require further development for the hot-end material. Maturation for flight application is on-going: A 7 - 8 W/kg, 17-year life (i.e., 3 years storage + 14 years operations) ASRG is slated for potential use on the Discovery-13 Mission in the 2013/2014 timeframe.

For Venus missions of less than 1 year, the current Venus hot end material, MarM-247, may be suitable for temperatures of up to as high as 977 °C and, with the addition of a protective coating, up to as high as 1077 °C. Nevertheless, proper testing will be required to quantify the actual maximum temperature with the existing materials of construction. For even higher temperatures, a different class of material would be required. NASA GRC conducted initial development of advanced materials (refractory metal alloys and ceramics) specifically for high-temperature Stirling applications. Although not fully mature at the present time, these advanced materials have the capability of operating at temperatures in the range of 1100 to 1200 °C. Tradeoffs of maximum operating temperature versus required development and risk need to be investigated in terms of long-term thermal stability, outgassing, and synergistic effects, for example, the combined effects of radiation, temperature, and aging time.

Identifying the appropriate size for the RPS is also an important issue, in light of science goals and exploration objectives. Static landers, for example, may require more power than aerial platforms, but they are less mass and volume constrained. Aerial platforms, such as the Venus Mobile Explorer concept (NASA, 2006), traverses using a metallic bellows system, limiting the suspended mass for the gondola, which accommodates the power and refrigeration systems. Therefore, future RPS technology development for a Venus RPS with active refrigeration should reflect science drivers and related mission architectures.

NASA's Radioisotope Power Systems under development – i.e., MMRTG and ASRG

– use Pu-238 housed in General Purpose Heat Source (GPHS) modules. Plutonium availability was identified as a key issue for enabling future NASA missions in all mission classes, namely for Flagship, New Frontiers and Discovery class missions. In response, NASA and the US Department of Energy is assessing plutonium needs for future NASA missions and making necessary steps to allocate a sufficient inventory to enable these missions (Dudzinski, 2008). For the near future the primary driver is the next Outer Planet Flagship Mission to Europa, planned for a 2020 launch with the potential for 5 RPSs on the orbiter. Additional plutonium need may arise from Discovery and New Frontiers missions, but at a significantly smaller scale using one or two RPSs each. A potential long-lived Venus Flagship mission could contribute to further demands on the plutonium inventory. Therefore, future mission studies on alternative Venus mission architectures should assess plutonium needs and work with NASA HQ to be included in Pu<sup>238</sup> production and allocation plans.

#### 5.4.2.3 High Temperature Energy Storage

Venus exploration missions pose significant challenges for energy storage systems. Many concepts for Venus surface missions (landers and seismic/meteorological stations) require mass- and volume-efficient energy storage systems that can operate at temperatures as high as 480 °C. Venus atmospheric exploration missions (aerial platforms, atmospheric probes) likewise require energy storage systems that can operate at 50 to 480 °C, depending on the altitudes. Operation of the batteries and fuel cells at high temperatures presents a number of technical challenges, including: (a) Stability of electrode materials at elevated temperatures; (b) Electrolyte stability and undesirable side reactions such as electrolyte oxidation at the cathode and reduction at the anode; (c) Corrosion of the current collectors and the seals; (d) Increased electrolyte vapor pressure; (e) Stability and compatibility of the separator materials at elevated temperatures; (e) Safety issues due to high reactivity of the electrode materials with

electrolyte, separator; and (f) Hardware issues arising from CTE mismatch [Kolawa et al., 2007 – EE tech report].

In the US, over the past five decades, several high-temperature energy storage technologies have been developed by and for NASA, the Department of Energy (DoE), and the Department of Defense (DoD) and as a result several battery chemistries operating above 400 °C were created and qualified. The development was virtually stopped in 1995, due to the emergence of interest in Li-Ion batteries, offering high performance at 25 °C. Further details on high temperature energy storage can be found in Kolawa et al. (2007) and Mondt et al. (2004). High temperature batteries that are under development and offer a promise for Venus missions can be classified into two groups: a) Thermal Batteries; and b) High-Temperature Rechargeable Batteries. Thermal batteries were developed by DOD and DOE for use in weapons and missiles. These are primary batteries and are activated thermally before use. A signal from an external source initiates the ignition of pyrotechnic materials (heat pellets) within the battery. This ignition in turn results in a melting of the electrolyte and the battery produces electrical power for a relatively short period of time. Thermal batteries contain an alkali or alkaline earth metal anode, a molten salt electrolyte, a transitional metal salt cathode, and a heat source (usually positioned between the cells). Lithium alloys are the most commonly used anode materials in the thermal batteries, though magnesium metal and calcium are also used. Transition metal sulfides (FeS<sub>2</sub>, CoS<sub>2</sub>) are presently used as the cathode materials in the present-day versions of the thermal batteries, although calcium chromate, potassium dichromate, potassium chromate, lead chromate, and metal oxides have also been used. A eutectic mixture of lithium chloride and potassium chloride is often used as the molten salt electrolyte in these batteries. Current state of the art thermal batteries have specific energy of about 45 Wh/kg.

Significant work was carried out in the 1970s and 1980s on the development of high-temperature (300 to 600 °C) rechargeable batteries. DOE and several contractors examined high-temperature rechargeable batteries for over 30 years for electric vehicle and load leveling applications. These systems include: a) LiAl–FeS<sub>2</sub>, b) Na–S, and c) Na-metall chloride. Although these batteries were designed as rechargeable versions, they can function in the primary battery mode as well. Some of the important characteristics of the three high-temperature rechargeable batteries are given in the Table 5.4.

#### 5.4.2.3.1 Lithium–Metal Sulfide (LiAl–FeS<sub>2</sub>) Batteries

This is a molten salt rechargeable battery and was developed primarily at Argonne National Laboratory in the early 1970s for vehicular propulsion. These batteries use a lithium alloy anode such as Li–Al, FeS<sub>2</sub> cathode, and a molten salt electrolyte, LiCl+KCl. Other metal sulfides, such as nickel and cobalt, may offer higher performance for some niche applications.

#### 5.4.2.3.2 Sodium–Sulfur (Na–S) Batteries

This system was the first high-temperature battery that was widely studied and well developed. Development was initiated in the beginning by the observation that sodium beta alumina ceramic permits rapid mobility of sodium ions. The Na–S battery is a solid electrolyte type that employs a molten sodium

anode, a solid beta alumina electrolyte/separator, and a molten sulfur cathode. This system has good cycle life but is plagued by the fragile nature of the ceramic separator and safety issues upon separator failure. Na/S<sub>2</sub> batteries for terrestrial application are available at specific energy of 220 W·hr/kg, and specific energy of over 300 W·hr/kg is predicted for space batteries. This technology was also space qualified on space shuttle flight STS-87, in November 1997, which might be relevant during the cruise operation, but not for high-T operation on the surface of Venus (Figure 5.7). The two companies that currently produce sodium-sulfur batteries are doing so at similar specific energy.

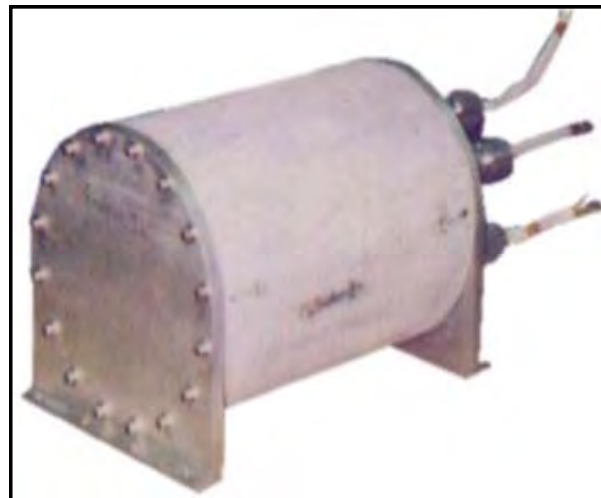


Figure 5.7: Sodium Sulfur battery flown on the STS-87 Space Shuttle demonstration.

**Table 5.4:** State of the art high temperature secondary batteries.

Characteristic	LiAl–FeS <sub>2</sub>	Na–NiCl <sub>2</sub>	Na–S
Operating temperatures (°C)	400 – 475	220 – 500	290 – 450
Open circuit voltage (V)	1.73	2.58	2.08
Discharge voltage range (V)	1.2 – 1.8	2.1 – 2.5	1.7 – 2.0
Theoretical specific energy (Wh/kg)	490	800	755
Specific energy for batteries (Wh/kg)	Near 100	90 – 130	80 – 220
Energy density for batteries (Wh/l)	Near 150	70 – 130	90 – 150
Cycle life (cycles)	>1,000	>1,000	2,000
Energy efficiency (%)	80	80	80

#### 5.4.2.3.3 Sodium–Metal Chloride ( $\text{Na}-\text{MCl}_2$ , $\text{M}=\text{Ni}, \text{Fe}$ ) Batteries

This battery, pioneered in the 1980s by the Beta R&D Company and known as the “ZEBRA” (Zero Emission Battery Research Activities) battery, is an offshoot of sodium-sulfur, with the sulfur cathode replaced with nickel or iron chlorides in contact with a tetrachloroaluminate melt for improved safety.

The modified thermal batteries are projected to have specific energy of about 200 Wh/kg and could operate at temperatures up to 500° C. The modifications required include: removal of the heat pellets, removal of the activation squib, thermal design changes (removal of the insulation materials), use of advanced molten salt electrolytes to achieve operation in the desired temperature range, cell hardware and seal designs, and increase of electrode thickness. The major issues that need to be addressed before rechargeable batteries could be considered for Venus missions include: adapting cell and battery designs for space applications, ensuring the stability of seals and terminals, minimize the corrosion of current collectors at high temperatures, determine the effects of zero gravity upon performance, improving the safety, and optimizing the electrolyte composition to improve conductivity and reliability.

The current development work on high temperature batteries has included assessment of alternate anode and cathode materials as well as new electrolytes based on solid as well as molten salt electrolytes. Based on one or more of these advanced anode and cathode materials and a solid-state or molten salt electrolyte, it is possible to develop high-temperature primary and rechargeable batteries with an energy density far exceeding the LiAl/FeS<sub>2</sub> system. Although actual battery hardware has not yet been developed with most of these advanced materials, the laboratory results to date have been quite promising. These batteries are expected to offer significant advantages over existing elevated temperature batteries in terms of simpler design and operation as well as increased energy density.

Sandia National Laboratories has developed a high temperature primary battery that can operate at temperatures up to 250° C. Also, JPL recently reported a primary battery that could operate up to 450° C. These two battery systems are based on fluoride ion-based, solid-state electrolytes. The major limitation of these batteries is that they can only operate at very low discharge rates. Further development work on these systems is expected to make them attractive for future Venus surface missions.

Other energy storage technologies are possible that can provide power densities beyond 220 W-hr/kg at high temperatures. For example, electrochemical cells which use carbon dioxide exclusively at the cathode for use in environments where carbon dioxide is abundant was proposed by Hagedorn (1993) and described by others (Mondt, 2004; Kolawa, 2007). This technology could allow high specific energy density estimated to be over 1 KW-hr/kg. Currently this technology is at a very low maturity level and would need development.

#### 5.4.2.4 High Temperature Sensors

A range of sensors applicable to Venus missions have been and continue to be developed for a variety of target applications, including high temperature aerospace and industrial applications. Sensor development includes high-temperature positioners, accelerometers, pressure sensors, thin film sensors, and chemical sensors (Waite et al., 2006). Each of these sensor types will be briefly described in the following subsections. Examples of high temperature sensors of relevance to Venus missions, including the concept of a Venus Integrated Weather Sensor (VIWS) System are discussed in details in references (Hunter, 2007).

##### 5.4.2.4.1 Pressure Sensors

Conventional Si-based pressure sensors are temperature limited while devices such as SiC-based pressure sensors have a much wider operating temperature range. Progress has been made in both SiC pressure sensor micromachining and packaging (Okojie, 2006). The resulting sensors have

demonstrated the capability to withstand high temperatures with improved reliability and operation up to 600 °C (Okojie, 2001). These SiC-based pressure sensors were demonstrated to operate for over 130 hours at 600 °C, with a projected 5,000 hours at 500 °C and have been demonstrated multiple times in engine environments at pressures up to 500 psi. This mature technology has been transferred to industry and is presently being commercialized

([http://www.sti.nasa.gov/tto/Spinoff2008/ip\\_2.html](http://www.sti.nasa.gov/tto/Spinoff2008/ip_2.html)). A commercial advantage of this product is that the sensors are less complex than current, similar sensors thus reducing the likelihood of performance failure. Further, high temperature operation (600° C) of separate discrete SiC pressure sensors and anemometers has been previously demonstrated. Research efforts are geared towards integrating three functionalities in a MEMS structure: a pressure sensor, an anemometer, and a temperature differential sensor (Okojie, 2003).

GaN-based pressure and temperature sensors have been recently explored for

extreme environments, and prototype GaN sensors have been demonstrated (Son, 2005; Liu, 2006; Ni, 2007). GaN sensor technologies can offer several unique capabilities although, at the present time, they are not as mature as SiC sensors. GaN microsensors developed to date are based on  $\text{Al}_x\text{Ga}_{1-x}\text{N}/\text{GaN}$  heterostructure devices. The major advantages of  $\text{Al}_x\text{Ga}_{1-x}\text{N}/\text{GaN}$  sensors are robustness in wide ranges of temperature and pressure (a few K to >800 K, 0 to >10 Kbar) high sensitivity, and the reliable and reproducible sensor fabrication (Guhel, 2002). Different from Si or SiC devices, an  $\text{Al}_x\text{Ga}_{1-x}\text{N}/\text{GaN}$  heterostructure sensor requires neither a specific doping profile within the layer sequence to form a polarization sheet charge, nor any implantation or high-temperature annealing steps to form the source and drain contact regions. Also,  $\text{Al}_x\text{Ga}_{1-x}\text{N}/\text{GaN}$  sensors are planar thin film devices deposited on a rugged and electrically insulating sapphire substrate which makes the processing of multi-sensor arrays and their metal interconnection simple, mechanically stable, and straight forward.

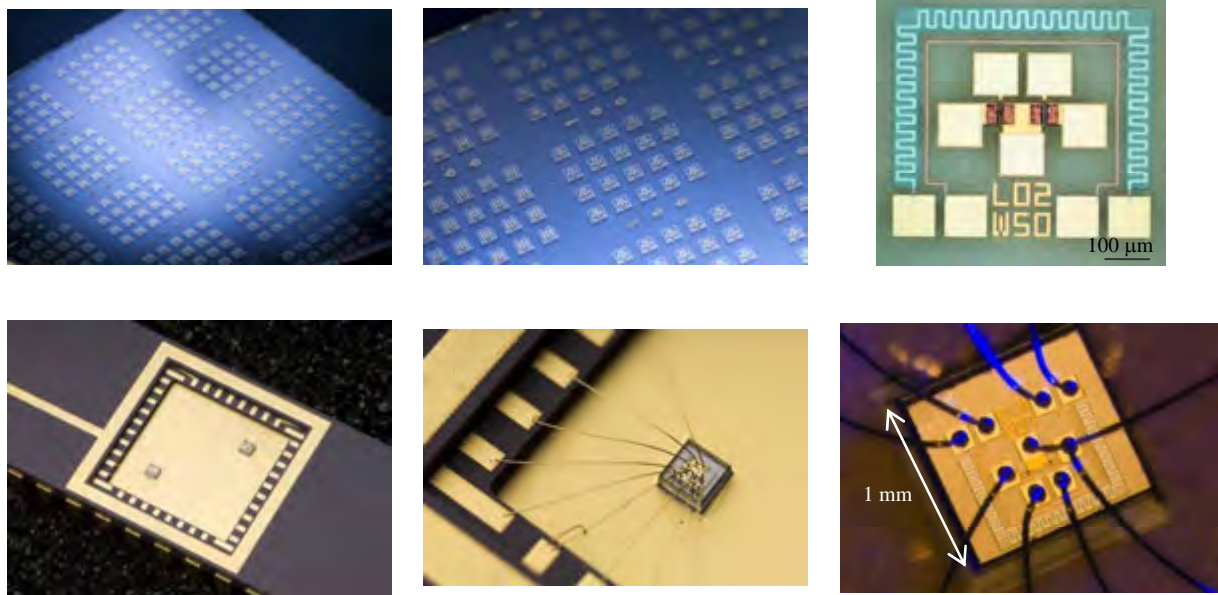


**Figure 5.8:** Pictures of GaN HEMT micro CWA sensors. Top row: wafer-level GaN HEMT chemical sensors fabricated on a SiC substrate. Bottom row: GaN HEMT sensor chip packaged on a ceramic dip socket using Au wire-bonding.

The recent results obtained at JPL with prototype GaN HFET sensors indicate that the GaN sensor will be suitable for pressure sensing of about 100 bar with the accuracy of 0.1 mbar. The results acquired with the prototype sensor also indicate that the GaN sensor held at a fixed strain may be useful to measure temperature differences of as little as 0.1 K in the range of 50 K to > 800 K.

#### 5.4.2.4.2 Physical Sensors

High temperature physical sensors, including those for strain, temperature, heat flux, and surface flow, are required for surface measurements in propulsion system research at temperatures up to 1100 °C (Wrbanek, 2006). This technology has a long history of test stand implementation in a variety of environments, typically at temperatures well beyond those necessary for Venus. These sensors are microfabricated and have been placed at variety of high temperature materials and complex surfaces. Measurement requirements for these sensors are usually as simple as voltage or current. A multifunctional sensor, such as that already demonstrated at 700 °C and patented, could integrate into one "smart" sensor, resulting in the design of individual gauges that measure strain magnitudes and direction, heat flux, surface temperature, and flow speed and direction (Lei, 1999). Thus, in one sensor system, a range of physical parameters regarding the environment can be measured under Venus relevant conditions. Integration of this technology to applications such as the Crew Exploration Vehicle heat shield interface seals and in-situ monitoring of the Stirling engine is on-going with long-term demonstration of sensors at temperature above 800° C planned in 2009.

#### 5.4.2.4.3 Chemical Sensors

The development of MEMS-based chemical microsensors to measure emissions in high temperature, harsh environments has been on-going for engine emission monitoring applications (Hunter, 2006). The fundamental approach used by this technology is that each sensor is designed to be selective to the chemical species of interest intending to

provide direct measurement of the chemical species predominately without the need for, e.g., pattern recognition hardware or extensive processing in order to interpret the results. Sensors composed of Schottky diodes, electrochemical cells, and resistors composed of a variety of harsh environment materials are used to detect a range of species with sensor operating temperatures ranging from 500 – 700 °C. Engine testing is underway for a High Temperature Electronic Nose system to detect species such as nitrogen oxides ( $\text{NO}_x$ ), oxygen ( $\text{O}_2$ ), carbon dioxide, and hydrocarbons ( $\text{C}_x\text{H}_y$ ) with the detection of other species available at Venus temperatures and above (Navair, 2007). A commercial manufacturer is leading this project in association with the aeronautic engine manufacturers, the Navy, and NASA. The planned result of this program in 2009 is a validated, commercial sensor system for use in jet engine test stands. Other species of interest for Venus application, such as sulfur dioxide ( $\text{SO}_2$ ), can also be detected but are at an earlier stage of development.

GaN-based micro chemical sensors have been recently developed for *in situ* chemical species detection and monitoring in extreme environments (Schlwig, 2002; Son, 2007; Kang, 2004). Electrical signals characteristic of chemical analytes ( $\text{H}_2$ ,  $\text{CO}$ ,  $\text{NO}$ ,  $\text{NO}_2$ , acetylene, etc.) have been measured with GaN HEMT (high electron mobility transistor) sensors at the sensor temperatures as high as 400° C (Fig. 5.8). For operations at higher temperatures (>500° C), GaN MOS (metal oxide semiconductor) HEMT sensors would be necessary in order to avoid the burn-out of Schottky gate electrode and prevent high gate-leakage current.

High sensitivity detection has been reported with gate electrode designs and optimization of  $\text{Al}_x\text{Ga}_{1-x}\text{N}/\text{GaN}$  epitaxial structures (Son, 2008). With the sensing mechanism based on "modification of surface polarization charges by chemical species adsorbing on the gate electrodes", GaN HEMT sensors are most sensitive to the chemical species with strong dipole moments. High selectivity detection of organophosphate compounds compared to

common organic solvents has been reported. High sensitivity detection of caustic gases (HCl, Cl<sub>2</sub> & NH<sub>3</sub>), which is not possible with Si-based sensors, has been recently demonstrated with GaN HEMT sensors, indicating reliable operation of GaN micro chemical sensors in caustic environments such as in Venus.

#### **5.4.2.5 High Temperature Electronics**

Currently available electronic systems for Venus missions would depend predominantly on silicon-based Very Large Scale Integrated (VLSI) CMOS circuits which need to be maintained through passive or active cooling in an Earth-like environment. These VLSI CMOS circuits are typically available on bulk Si CMOS technology and are rated to operate up to 125° C. Selective number of Si CMOS components are also available commercially (for example from Honeywell [www.honeywell.com/sites/portal?smap=aerospace&page=Hi](http://www.honeywell.com/sites/portal?smap=aerospace&page=Hi) (Ohme, 2004; Ohme, 2006)) in High Temperature Silicon-On-Insulator CMOS (HTCMOS). These components include microcontroller (83C31), static random access memory (32k ×8 SRAM), analog multiplexer, crystal clock, linear regulator, operational amplifier and are able to operate at temperatures as high as 300° C. At temperatures above 300°C only discrete wide bandgap semiconductor devices (diodes and transistors) are available that are fabricated using Silicon Carbide (SiC) (Neudeck, 2000; Neudeck, 2002), Gallium Nitride (GaN) (Daumuller, 1999; Wurfl, 2000) or Gallium Arsenide (GaAs) semiconductors (Wilson 1995). Commercial versions of these transistors are generally not optimized for operation at 500°C for extended period of time. For example, Cree Inc. has conducted

accelerated life tests using a maximum junction temperature of 410 °C on their SiC MESFET (Ward, 2005) and reported failures after 730 hours. Life testing of small signal SiC JFET transistors from Semisouth Laboratories at 500° C at JPL showed time dependent degradation of device characteristics within the first 10 hours of evaluation (Chen, 2008).

Development and optimization of SiC devices for high temperature operation is producing exciting results in favor of using SiC technology as the choice for implementing 500 °C integrated electronics. In 2007, NASA Glenn Research Center (GRC) successfully fabricated and operated a small scale integrated high temperature SiC circuits over thousands of hours at 500 °C (Neudeck, 2008; Spry, 2008, <http://www.nasa.gov/externalflash/yir2k7/circuit.html>). In support of the NASA Aeronautics program, GRC has produced a 500 °C SiC based differential amplifier, an inverting amplifier, a NOR gate, and NOT gate. Figure 5.9 shows an overview of the on-going electronics development. These are complete devices including packaging and interconnects with the device operating in the ambient 500 °C conditions for thousands of hours, the NAND gate operating solo, and the NOT and NOR gates operating in a cascaded configuration to prove interconnected circuit capabilities at temperature. The devices are fabricated from commercially available (Cree Inc.) single-crystal wafers of SiC and capable of further miniaturization. The current level of complexity of the SiC electronics is parallel to that available in the Mercury era (early 1960s) and circuits of increasing levels of complexity are currently being designed and fabricated.

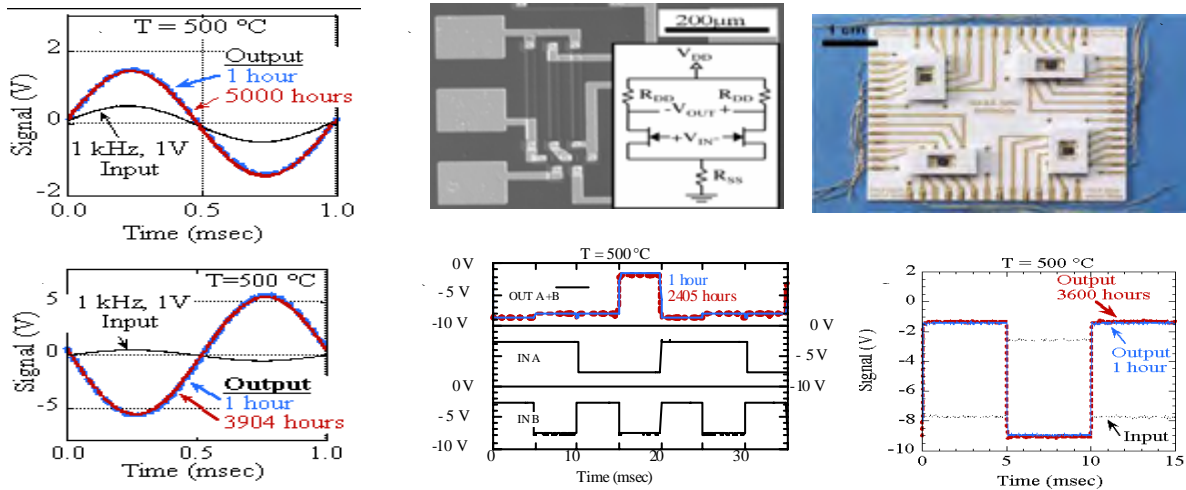


**Figure 5.9:** A sampling of the high temperature electronics available. a) Differential Amplifier IC output at 5000 hours and 500 °C, b) Picture of Differential Amplifier IC and Schematic, c) High temperature packaging for SiC electronics, d) Inverting Amplifier IC, e) NOR logic gate, f) NOT logic gate. All components have demonstrated long-term operation at 500 °C.

An alternative approach to solid-state devices are vacuum transistors, well-suited for extreme temperatures because they require high internal temperatures (700 – 800 °C) in order to operate. These thermionic vacuum devices (Figure 5.10) are capable of long-term operation at 500 °C (McCluskey, 1996; DelCastillo, 2007), with negligible degradation.

They are low-noise, linear devices, with electrical performance parameters that are virtually independent of temperature. Vacuum triodes exhibit excellent stability as a function of temperature from room temperature to 500 °C. These same devices demonstrate excellent stability as a function of time at 500 °C for 48 hours. Hence, high-temperature circuits made with vacuum transistors do not need elaborate circuitry to compensate for variation of transistor performance with temperature. Recently JPL demonstrated an extremely small vacuum transistor made with Carbon Nano Tube (CNT) that operated at 700 °C. JPL has used this device to fabricate a 700 °C inverse majority logic gates in a very small footprint (0.05 mm by 0.05 mm) (Manohara, 2008; Manohara, 2009). The low-noise, temperature-insensitive properties of the vacuum tube transistors including the CNT

based versions make them ideally suited for telecommunications applications.

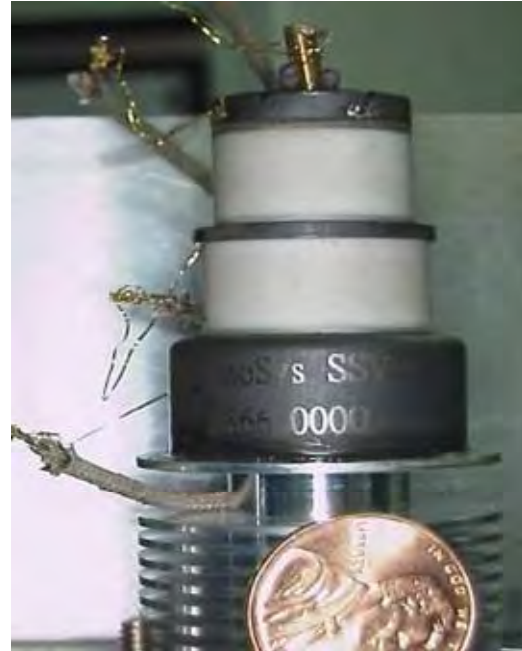


**Figure 5.10:** High temperature vacuum triode including heater, cathode, grid, and anode.

The CNT based version of the vacuum devices in particular seems to show promise in significantly reducing the power size and mass of electronic system. However, careful design and improvement of the device packaging (vacuum enclosure) and materials are required

to enable operation at 500 °C (Delcastillo, 2008) and 92 bar pressure.

With respect to passive devices, high temperature resistors, such as ruthenium oxide, have shown stable resistance to 500 °C (temperature coefficient of resistance) and following extended exposure at 500 °C. Unfortunately, capacitors have proven to be significantly more challenging. General-purpose ceramic capacitors, often tend to exhibit wide variations in capacitance with increases in temperature, particularly due to changes in the dielectric constant. Temperature compensating capacitors, such as NP0, exhibit a predictable temperature coefficient of capacitance; however, increasing temperatures above 400 °C significantly increases leakage currents, making it difficult for the capacitor to hold a charge. Experimental capacitors based on high Curie temperature ferroelectrics have exhibited excellent behavior at the desired temperature, but their capacitance can vary significantly with temperature. Various experimental capacitors are currently under development at certain companies, such as TRS Technologies, and universities, such as Auburn University and the University of Houston (Johnson, 2007; Delcastillo, 2006).

Due to the high temperatures of the Venus ambient environment, issues such as the degradation of materials with temperature, stresses resulting from coefficient of thermal expansion (CTE) mismatch, and creep become significant (Delcastillo, 2006; Chen, 2008). At Venus temperatures, polymers for printed circuit boards and adhesives are no longer an option due to degradation. Ceramic substrates, such as alumina or aluminum nitride, can be used for high temperature hybrid circuits, but it is critical that the substrates are designed using high temperature trace materials. Die attach materials need to have a melting temperatures that are only slightly greater than the target environment to avoid exposing the device to further temperature extremes. One method that Auburn University has developed to minimize the stresses related to processing, while maintaining sufficient interfacial

strength, is to rely on interdiffusion of metal layers (Au-Sn-Au) to reach a target composition. Finally, wirebond material selection must take into account die metallization and substrate metallization to minimize the formation of brittle intermetallics. An excellent overview of high temperature micropackaging technologies is given by Chen (2004).

Electronics operating at 300 °C will greatly reduce the mass of the cooling system needed for Venus missions. However, the available menu of commercial 300 °C circuits is barely adequate for building a 300 °C electronic instrument. A larger and more sophisticated menu of ICs capable of operating at this temperature will enhance our ability to design sophisticated systems. Also the significant leakage current of these circuits at 300 °C is a major power drain that limits the battery life. High temperature circuits fabricated on advanced ultra thin SOI CMOS technology can have an order of magnitude lower leakage current which will minimize this problem.

The amount of data processing in high temperature environments depends on complexity of the instruments involved and the overall mission architecture. ASIC operational amplifiers together with simple logic functions would be sufficient for long-term pressure or temperature measurements. The more advanced the instrument or the operating system, the more advanced the electronics need to be. For example, a long life Venus seismometer with Netlander-like capabilities will need analog sensor interface electronics, a high resolution data converter, a high density microcontroller and a megabyte memory operating at high temperature.

The formation of high temperature memory would be necessary if it is chosen to maximize the data return of in-situ data systems. That is, while continuous data transmission can provide data while the transmitter is in sight of the orbiter, high temperature data storage is necessary if it is determined than no data can be lost from planetary in-situ devices. The prospects of high temperature data storage using current SiC technology (even the most

advanced) are daunting. This in part is due to the fact that metal-oxide-semiconductor (MOS) circuits commonly available in silicon and central to present memory storage are not available in SiC or in other high temperature semiconductor technologies (Neudeck, 2002).

High temperature motors and actuators will need high temperature power electronics for drive and control of actuators as well as for precision analog electronics for interface with sensors (i.e., position sensors). None of the above circuits are currently available. Also, the lack of complementary transistors makes it extremely difficult to realize the circuit power reduction achieved in Si based CMOS technologies in wide-bandgap semiconductors. Significant work has been done, for example, on high power SiC devices or high temperature SiC transistors, but not on devices that are both high temperature and high power (Neudeck, 2000). Absence of complementary devices seems to also impact both traditional and CNT based versions of thermionic vacuum devices.

Two approaches are suggested regarding the advancement of high temperature electronics and data processing. The first is to use the simpler circuits presently available in SiC to create state machines and control devices which can be used for Venus applications. A fundamental point related to electronics and communication development at 500 °C is that due to the low maturity of SiC electronic materials, a direct transfer of Si based approaches to SiC is problematic. For example, at present, no high precision DC operational amplifiers or large-scale digital integrated circuits are possible in SiC or in other high-temperature semiconductor technologies. Nonetheless, using design approaches present in the earlier days of Si electronics reminiscent of what was used to enable the Apollo missions, significant progress can be made. For years, valid seismic measurements were made with simpler electronics technology. As noted above, what are available are analog amplifiers and logic gates configured from SiC that have been demonstrated at 500 °C for thousands of hours.

Such components can be used to first condition the signal from the sensor, convert it into an oscillatory signal, and transmit that signal thus providing the functionality of a seismometer without complex electronics. A simplistic approach to circuit design can provide a basic operational system, but maturation of existing high temperature electronics, such as those demonstrated in SiC, for Venus instrument and applications is necessary.

Second, the maturation of high temperature electronics using a variety approaches to the comparable maturity of silicon is highly desirable. For example, significant advances are feasible both using commercial SiC technology and advancing the basic SiC materials themselves (Powell, 2008). These developments would have to be of the complete system; not only of the electronic materials themselves but device contacts, interfaces, packaging, and related communication technology.

Further, a standard methodology for testing and assessing the reliability of high temperature circuits for Venus application needs to be developed. This methodology needs to establish procedures for accelerated life tests that factor in both the upper operating limits temperature of the electronic devices and the specifics of Venus environment such as its atmospheric chemistry and pressure.

#### **5.4.2.6 High Temperature Telecommunications**

Only limited work has been done in developing long range, high power, and high temperature transmitters for Venus applications. Absence of high frequency passive and active RF components seems to be a major issue limiting the progress in this area. In the recent search for high temperature RF semiconductors for building a high temperature solid-state transmitter, Softronics Inc could identify only two high frequency (2 GHz) high power (10 W and 60 W) SiC transistors offered by Cree Inc. (Sternowski, 2008). The transistor used in the circuit retained 40% of its room temperature gain at a junction temperature of 275° C (Figure 5.11 a,

b), which corresponds to an ambient temperature of approximately 200° C. The decreased conductance of these transistors at high temperature translates to significant inefficiencies for the transmitter. Softronics' solution for RF passives was to use copper-on two sides of the ceramic substrate to make capacitors and RF transmission lines. High inefficiency of high-temperature RF circuits translates to additional rise in junction temperature, which will require elaborate thermal management. Softronics final recommendation for a high temperature SiC transmitter was to us an array of low power SiC RF amplifiers together with passive power combiners to help relieve the need for elaborate thermal management.

An alternative to solid-state transmitters was demonstrated by Innosys using a mechanical resonant cavity based oscillator. This type of

device does not use any semiconductor elements and are heavy but seem to offer stable power-temperature performance at 500° C (McCluskey 1998, Sadwick, 2005).

Short-range, low-power, high-temperature transmitters are at an early stage of maturity. For example, a Cree SiC transistor was used to build an oscillator shown in Figure 5.11(c) with an integrated antenna that operates at an ambient temperature through 275 °C at 1 GHz (Schwartz, 2005).

Also recently a high temperature (400 °C) pressure sensor integrated with a 30 MHz oscillator/transmitter based on a commercial Cree Inc. SiC MESFET transistor has been demonstrated (Wang, 2005). Other work has shown a loop antenna integrated within the oscillator enabled the wireless transmission of the pressure to distances of 1 m.

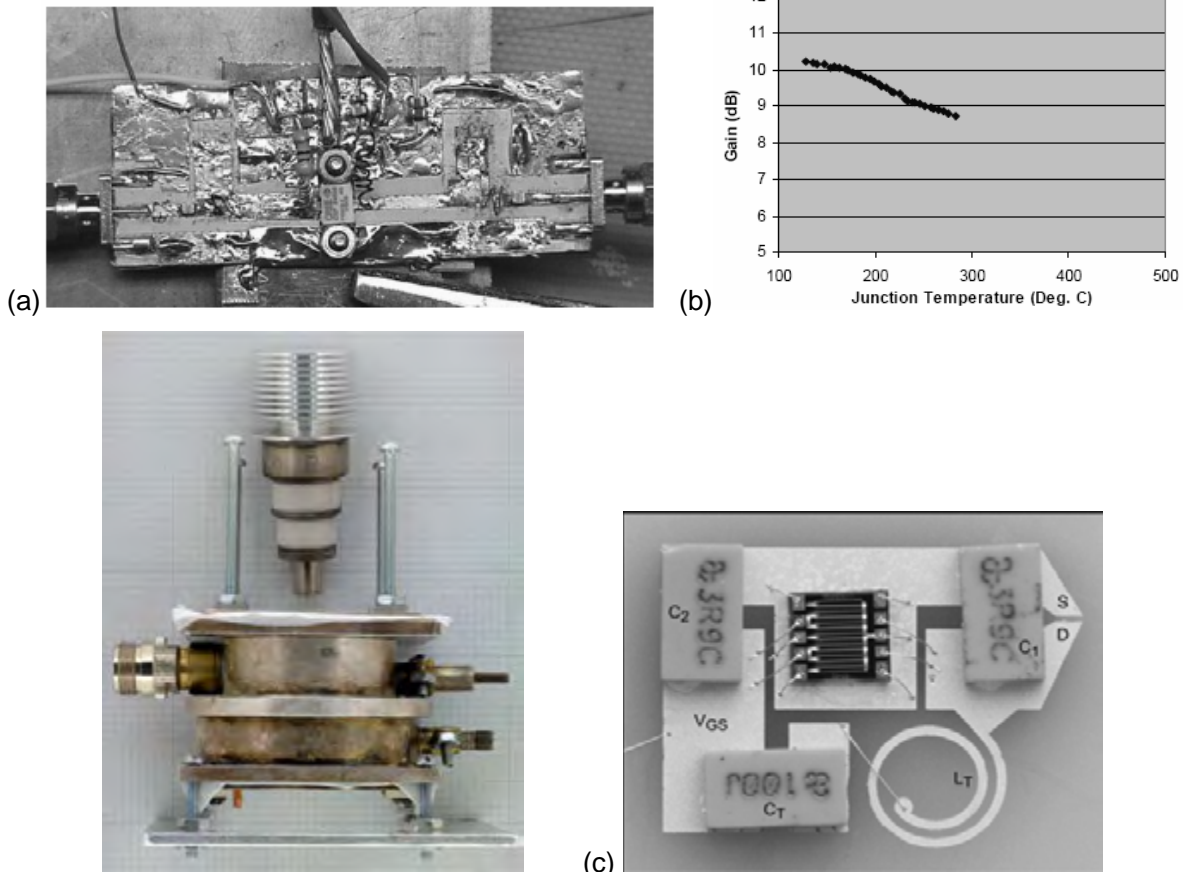


**Figure 5.11:** (a) High Temperature SiC RF Amplifier prototyped by Softronics. (b) RF amplifier gain as function of temperature. (c) High temperature oscillator comprised of SiC MESFET, ceramic chip capacitors, and a spiral inductor.

Further, an oscillator based on the same Cree SiC MESFET with an output power of 4.9 dBm (3 mW) at 453 MHz and 475 °C was demonstrated, but no antenna was integrated with the oscillator (Schwartz, 2005). Overall, the commercial Cree SiC MESFET would be significantly challenged as-is to provide viable operation on Venus. High temperature transistors/circuits/packaging technology has been used to demonstrate simple capacitor-transistor based oscillators using N (negatively doped) channel junction field effect transistors (JFETs) (LEW, 18256-1 Patent Application). These oscillators can be used for building long life high temperature wireless systems for frequencies less than 100 MHz.

It should be noted that SiC components could operate at 500 °C and 1 GHz for extended periods of time using alternate circuit designs and advanced packaging/contact technology (Gao, 1994). For example, computer simulations of the theoretical RF frequency/gain/ temperature performance benefits of a SiC/SiC heteropolytype junction clearly indicate that 6H-SiC/3C-SiC heterojunction bipolar transistors (HBT) should enable RF amplification up to 5 GHz at 500 °C. However, such an approach would entail considerably more development than a simple oscillator circuit.

GaN based transistors are also expected to have good RF performance at high temperatures because of their wide bandgap. However, sufficient data to evaluate this claim is not yet available. AlGaN/GaN transistors grown on sapphire have been shown to have irreversible damage to the material structure at a junction temperature of 600 °C (Daumiller, 1999). In a more recent reliability analysis, AlGaN/GaN transistors grown on SiC have been shown to have a projected Mean Time to Failure of less than 1 hour (Jimenez, 2006). Again, the failure mechanism is degradation of the material structure; however, unlike SiC, the basic operation of GaN structures for long periods has not yet demonstrated.

Preliminary results in high temperature communication technology described above are only providing a limited proof of concept that long life, high temperature communication systems can be made for Venus missions. Based on the current state of the art and the mission requirements, further development of high temperature transmitters and corresponding RF components for this purpose are required. These developments are central to any high temperature instrument or sensors system designed to operate in Venus environment.

Significant improvements to RF components are achievable but would require concentrated development. For example, although MHz frequency transmission is viable, the SiC transistors developed by NASA GRC and used for 500 °C demonstrating circuits of Figure 5.11(c) will have to be completely redesigned to improve their RF properties and their operating frequency to several GHz. At the current time, this appears to be the most viable option for improved transmitter performance. In addition, the passive components required to construct oscillators and amplifiers must be developed to the same level of reliability. Lastly, packaging of the circuits is required. While on-going development in the Aeronautics program will help, it will not be a complete solution to Venus specific problems.

In parallel, the same type of development is necessary for other promising types of transmitter technologies. Vacuum tubes or GaN semiconductor technologies can either provide an alternative to or complement existing SiC technologies. For example, a vacuum tube system might allow different design options in fabricating the Lander-Orbiter transmitter system. Combinations of SiC-GaN semiconductor material systems are already being explored for their advantages in communication applications (Neudeck, 2007; Dziewonski, 1997). The technologies needed for exploring the surface of Venus are summarized in Table 5.5.

**Table 5.5:** Summary of Technologies for Surface Exploration of Venus.

Capability	Requirements	State of the art (TRL level)	Development focus
Refrigeration	<ul style="list-style-type: none"> <li>- long life in Venus environment (months)</li> <li>- high efficiency</li> <li>- capable of ~3kW total heat rejection</li> <li>- suitable for integration with lander and low altitude balloon pressure vessels</li> <li>- minimized mechanical vibration</li> </ul>	TRL~3  <ul style="list-style-type: none"> <li>- high temperature operation not demonstrated at the system level</li> </ul>	<ul style="list-style-type: none"> <li>- Stirling machines need to be adopted for Venus environment</li> <li>- duplex Stirling machine must be produced that integrates the heat engine and refrigerator functions into a high efficiency and high reliability device.</li> </ul>
High-temperature power system	<ul style="list-style-type: none"> <li>- long life in Venus environment</li> <li>- high conversion efficiency</li> <li>- low mass</li> </ul>	TRL~3  <ul style="list-style-type: none"> <li>- demonstrated single Stirling converter for 300 hours operation with a 850 °C hot-end temperature and 90°C cold-end, 38% efficiency and 88 W power output with heat input equivalent to 1 GPHS.</li> </ul>	<ul style="list-style-type: none"> <li>- cold end operation needs to be raised from 90 °C to 480 °C with high conversion efficiency preserved</li> <li>- material testing, system development and validation for reliable operation in Venus surface environment.</li> </ul>
High-temperature energy storage	<ul style="list-style-type: none"> <li>- long life in Venus environment (117 days min.)</li> <li>- high specific energy - rechargeable and primary batteries</li> </ul>	TRL 4  <ul style="list-style-type: none"> <li>- demonstrated LiAl-FeS<sub>2</sub>, Na-S, and Na-metal chloride secondary batteries with specific energy in the 100-200 Wh/kg range</li> </ul>	<ul style="list-style-type: none"> <li>- adapt cell and battery designs for space applications</li> <li>- stability of seals and terminals</li> <li>- minimize the corrosion of current collectors at high temperatures</li> <li>- optimize the electrolyte composition to improve performance and reliability</li> </ul>
High-temperature sensors	<ul style="list-style-type: none"> <li>- long life in Venus environment (117 days min.)</li> <li>Seismometers:<ul style="list-style-type: none"> <li>- 0.3 mHz to 10 Hz frequency range</li> <li>- 10<sup>-8</sup> to 10<sup>-9</sup> msec<sup>-2</sup>Hz<sup>-1/2</sup> amplitude sensitivity</li> </ul></li> <li>Other sensors:<ul style="list-style-type: none"> <li>- pressure, temperature, wind speed, gas species variation in time</li> </ul></li> </ul>	TRL 2-6  <ul style="list-style-type: none"> <li>- geophones operating up to 260 °C</li> <li>- high-temperature pressure, temperature, and anemometers used on Venera/VEGA and Pioneer</li> </ul>	<ul style="list-style-type: none"> <li>- high-temperature MEMS technology for seismometers</li> <li>- SiC and GaN high temperature sensors</li> </ul>
High-temperature electronics (500 °C)	<ul style="list-style-type: none"> <li>- long life at Venus environment (117 days min.)</li> <li>- data acquisition, processing, and storage capability</li> <li>- power management</li> </ul>	TRL 2-3  <ul style="list-style-type: none"> <li>- limited integrated circuit capability demonstrated</li> <li>- limited electronics packaging</li> <li>- data storage, ADC, power converters, and other needed components never demonstrated</li> </ul>	<ul style="list-style-type: none"> <li>- SiC-based electronics</li> <li>- GaN-based and miniaturized vacuum electronics</li> <li>- high-temperature electronic packaging, passive components</li> <li>- reliability, long life</li> </ul>

Capability	Requirements	State of the art (TRL level)	Development focus
Medium-temperature electronics (300 °C)	- low power dissipation at 300 °C - long life and reliability	TRL 4 <ul style="list-style-type: none"><li>- medium temperature components developed for automotive and oil drilling industry</li></ul>	<ul style="list-style-type: none"><li>- HTSOICMOS electronic components</li><li>- low power</li><li>- test, validation, and reliability</li></ul>
High-temperature telecom	- long life at Venus environment (117 days min.) - high data rate (~4.5 kbs)	TRL 2 <ul style="list-style-type: none"><li>- demonstrated 2 GHz operation at 275 °C using SiC</li><li>- SiC and vacuum tube based oscillator demonstrated at ~500 °C</li></ul>	<ul style="list-style-type: none"><li>- SiC based RF components for transmitters</li><li>- miniaturized vacuum tube technology for power amplifiers</li><li>- SiC based RF components for transmitters</li></ul>

### 5.4.3 Atmospheric Exploration

#### 5.4.3.1 Enhanced Venus Atmospheric Science

Previous measurements of the atmospheric dynamics and wind velocity profiles on Venus revealed a complex structure dependent on both altitude and latitude (Schubert et al., 1980). This complexity is shown in Figure 5.12 summarizing the results of multiple missions. There is also significant variation in temperature with altitude ranging from 473 °C on the day-side surface to -173 °C exospheric temperature on the night-side. The dominant circulation of the atmosphere above the lowest one or two scale heights is a zonal retrograde motion with 100 m/s winds at 60-km altitude. There is also a superrotation of the atmosphere at altitudes of 150 km and above. Low latitude height profiles of the zonal wind have alternating layers of high and low shear. Meridional winds below 60 km vary in speed from a few to about 10 m/s; the winds are poleward at the cloud tops. At cloud level, solar heating combines with the zonal

circulation to produce a cloud top polar vortex. Eddies in the form of convective cells, small-scale gravity waves, and planetary scale waves are found throughout the atmosphere. Eddies, as well as mean meridional circulations, may be important in the transport of energy and momentum. Venus' atmospheric circulation is not steady despite the planet's small obliquity and nearly circular orbit (Schubert et al., 1980).

As described in Chapter 2, significant questions remain regarding the Venus atmosphere and its unique properties. While the Design Reference Mission will address a number of these questions, simultaneous, multiple atmospheric probes, which would be vital for gaining a global snapshot of the Venus atmosphere system, are not part of the mission. This enhancement addresses those questions by the use of multiple entry probes inserted into different locations in the atmosphere and simultaneously providing data on local conditions.

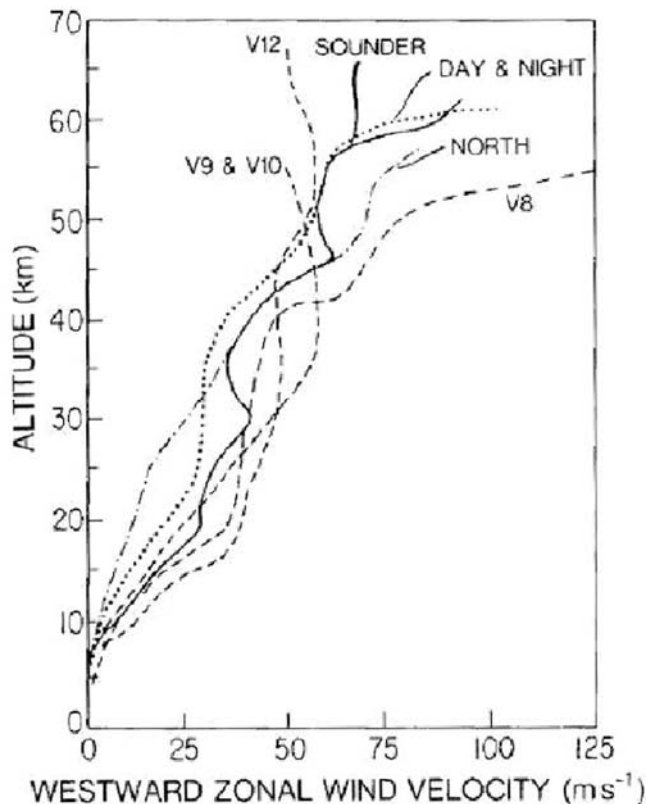


**Figure 5.12:** Wind velocity profile measured by Pioneer Venus: Day, Night, and Sounder probes are compared to those measured by Venera 8,9,10, and 12 (V8, V9, V10, and V12). The winds flow from east to west at all altitude and latitudes where measurements exist (Schubert et al, 1980).

#### 5.4.3.2 Scientific Objectives for Venus Atmospheric Science beyond the DRM

The goal of enhanced atmospheric science return complements the Design Reference Mission objectives in order to gain a better understand of the dynamics of the Venus atmosphere. These enhancements can be achieved with dropsondes or radar reflection tracking of balloons. Specific goals include:

- Take a “snapshot” of the atmospheric dynamics and velocity profiles with multiple probes simultaneously entering the atmosphere at many different local times and at many different latitudes, in contrast to previous investigations in which entry probes have surveyed at most four different latitudes and local times simultaneously.
- Provide improved information on the circulation of the atmosphere of Venus by

simultaneous measurements at multiple locations and insight on momentum transfer within the atmosphere between the lower levels and the upper levels and at various locations across the planet.

- Complement the wind velocity and direction data with temperature and chemical species information to further characterize the atmosphere.
- Correlate data from this simultaneous multi-element investigation with that of the Design Reference mission.

#### 5.4.3.3 Scientific Advancements from Enhanced Venus Atmosphere Investigations

Overall, the wind velocity profiles in Figure 5.12 show considerable spatial and temporal variation, but currently available observations are not sufficient to know to what extent such

variations are random and chaotic, and to what extent they are variable with latitude and solar zenith angle (SZA) in a predictable way. Many dynamical, radiative and chemical phenomena, several of which may be coupled, are suggested by current data to possibly vary with SZA, but current measurements are not adequate to resolve these spatio-temporal correlations and patterns, which may be essential for understanding the global dynamics, radiative balance and atmospheric chemical cycles of Venus. For example, thermally driven atmospheric tides are forced by the motion of the subsolar point across the upper cloud, where most of the sunlight is absorbed. These tides are apparent in Pioneer Venus and Venus Express infrared temperature retrievals, but the height resolution is not sufficient to define the vertical structure throughout the atmosphere (Schubert, 1983). There are two major approaches to investigate these atmospheric phenomena: Cloud LIDAR and dropsondes.

#### 5.4.3.4 Atmospheric Drop Sondes

An architectural enhancement would be a suite of from 6 to 24 identical instrumented dropsondes to be deployed in the atmosphere simultaneously at widely dispersed locations (Crisp et al., 2003; Lorenz, 2008). It would be most valuable to simultaneously cover a range of solar zenith angles and latitudes. In particular, there has never been a Venus atmospheric entry probe between noon and midnight and this range of solar zenith angle would fill in significant gaps in our knowledge. Similarly, no probe has entered poleward of  $\sim 60^\circ$  N and  $32^\circ$  S latitudes. Although such dropsondes provide only a snapshot of the atmosphere at a time, the simultaneity of multiple of them at globally distributed locations will provide very valuable information about the spatial variations in state of the Venus atmosphere which has not been possible to date on a global scale. Many dynamical, radiative and chemical phenomena, several of which may be coupled, are suggested by current data to possibly vary with solar zenith angle, but current measurements are not adequate to resolve

these spatio-temporal variations and patterns, which may be essential for understanding the global dynamics, radiative balance and atmospheric chemical cycles of Venus and transport of angular momentum and trace species. For example, thermally driven atmospheric tides are forced by the motion of the subsolar point across the upper cloud, where most of the sunlight is absorbed (Gierasch et al., 1997). These tides are apparent in Pioneer Venus and Venus Express infrared temperature retrievals and cloud level winds, but the height resolution is not sufficient to define the vertical structure throughout the atmosphere. In particular, the amplitudes and phases of the diurnal and semi-diurnal tidal components are not well determined. These are crucial for evaluating the role of the thermal tides in transporting momentum in the Venus atmosphere, which so far can be only inferred from inadequate numerical models or the limited observations which do not cover the day and night hemispheres at the same level.

These dropsondes would not only measure wind speed and direction, but also temperature and atmospheric gas abundances. This full array of data would be provided at multiple entry locations, altitudes, all at the same time. This enhancement to the Design Reference Mission would provide, for the first time, these data by deploying this suite of dropsondes and establishing a communication network which simultaneously feeds information back to the orbiter. This approach depends on capable instrument suite, power, and communication systems.

Such a suite of dropsondes equipped with net-flux radiometers would provide crucial information on variations of down-welling and up-welling radiation as a function of altitude, latitude and solar zenith angle, which would provide much-needed input for the next generation of General Circulation Models which would accurately simulate the response of the atmosphere to solar radiation. In concert with the tracking data this would allow a much more sophisticated reconstruction of the atmospheric superrotation, and other major

dynamical phenomena such as the lower atmosphere Hadley circulation, than cannot be achieved on the basis of present data.

Another advantage to this platform would be simultaneous measurements of chemical abundances profiles at several dispersed locations. For example, the CO to COS ratio is known to vary with latitude and serves as a tracer of the global Hadley circulation (Yung and Liang, 2008). At present it is not known if the photochemically driven cycle of these short to medium lived species results in measurable abundance variations with solar zenith angle. Such a measurement would greatly enhance our ability to understand coupled chemistry, radiation and dynamics. Likewise, other reactive species, including water vapor, several compounds of sulfur and halogens are likely to vary spatially, reflecting global processes.

Finally, if they were equipped with cameras, dropsondes could perform descent imaging at a wide variety of diverse locations. Those that entered on the night side would not be at a disadvantage, as images in emitted near-Infrared wavelengths at around 1 micron would actually have superior signal to noise (Moroz, 2002).

An approach which entails a simpler probe mechanism, but more extensive orbiter design, is to drop less complicated dropsonde devices but keep track of their location through Doppler radio and/or radar reflection tracking. Through Doppler radio and/or radar reflection tracking, dropsondes could measure wind velocity profiles from the cloud deck to the surface. A handful of previous velocity profiles have been obtained from VLBI or Doppler tracking from Earth and show considerable spatial and temporal variation.

High precision tracking of latitudinally distributed dropsondes from orbit and/or Earth is essential to determine or even get an indication of the direction of the zonal or east-west flow near the surface of Venus to answer the fundamental question of the exchange of angular momentum between the surface and the atmosphere. So far, on a few surface probes have provided estimates of the wind

speed near surface (1 meter height above the local topography) but no indication of the direction. If, as the prevailing observations from the entry probes at low to high latitudes suggest, the near surface flow is also in the same sense as the direction of the rotation of the solid planet, then the question is whether the ambient flow in polar latitudes is in the opposite direction to maintain a no net-exchange of momentum between the atmosphere and the solid planet. Any momentum exchange should be evident in the length of day variations and any confirmation of such momentum exchange is crucial for understanding the peculiar spin-state of Venus and perhaps its history.

In this manner, dropsondes could measure wind velocity profiles from the cloud deck to the surface. The added complexity of this enhancement would be concentrated in the orbiter rather than in the dropsondes; it is the orbiter that would then need a method of continuous transponding, and receiving the reflected signal back in a manner that would allow an understanding of the various dropsonde positions and velocity. The amount of mass per dropsonde would be less since each is a passive device (perhaps as simple as a corner reflector or small metalized balloon). However, given the reduced mass and complexity of the dropsondes, many more of them could be employed for the mission. This could allow the multiple dropsonde experiments to be performed to determine variations over time or in correlation with events or conditions observed by other elements of the mission such as the balloons.

Such an array of dropsondes would provide information not achievable by a small number of entry probes or orbital observations. In essence, the introduction of an array of simultaneous dropsondes into the Venus atmosphere would be a way to watch the dynamics and complexity of the Venus atmosphere unfold in near real-time. Like other enhancements to the Design Reference Mission, these components would provide an added exploratory nature to the mission; riding the winds from the high atmosphere to low;

being exposed to environments ranging from sulfuric acid clouds to high temperature; traversing the planet on hurricane-like winds and down to the extreme high pressure lower atmosphere. This enhancement provides not only new scientific data, but also demonstrates a new method of achieving planetary atmospheric data.

#### *5.4.3.4.1 Technologies for Drop Sondes/Probes*

Drop sondes or probes would have to survive for a short period of time in a wide variety of environments (increasing temperature and pressure, corrosive sulfuric acid clouds, supercritical carbon dioxide) as they descend to the surface. Depending on the sondes or probes payload and duration of operation, the combination of different design architectures and technologies will be needed to achieve the desired life and performance. If the science investigation includes descent imaging, a combination of passive thermal control and conventional space electronics and telecom can be used. The penalty would be a relatively high probe mass. In order to reduce the probe mass by minimizing thermal control requirements the moderate temperature SOI electronics could be used for data processing and communication. For probes with simple payloads (temperature, pressure and other basic sensors), high temperature sensors, electronics, and batteries can be used providing system survivability as the drop sondes or probes approach the surface and higher temperatures and pressures. The benefit of this approach would be a significant mass reduction and longer life (limited by battery life).

The communication infrastructure for such a multi-component probe system would have to take into account the labeling and identification of the signals and data from each sonde or probe. The orbiter would then have to adequately transmit that information with timestamp back to Earth.

#### **5.4.3.5 Cloud Lidar**

Earth based telescopic observations of Venus in reflected sunlight have shown that the global cloud cover undergoes significant

albedo variations. Pioneer Venus Orbiter Cloud Photo Polarimeter (OCPP), (Kawabata et al., 1980; Sato et al., 1996) and now imaging observations from the Venus Monitoring Camera (VMC) on Venus Express observations continue to reveal such variations, notably in high latitudes (Markiewicz et al., 2007; Moissl et al., 2008). While the OCPP observations suggested that the polar brightness variations were due to varying amounts of haze, other causes have not been fully explored (Sato et al., 1996). Combined VMC and VIRTIS observations from Venus Express suggest a varying cloud top height (unit optical depth) from equator to pole, peaking at the latitude of the polar collar, with the range being about 7 km. The observations suggest some degree of variability as well (Ignatiev et al., 2009).

Further, the cloud top altitude in polar regions, at the core of the Venus vortex centered over the pole, is seen to be controlled by dynamical instability. This is seen very dramatically in the infrared observations from VIRTIS and OIR. By enabling observations of the variations of the cloud top in polar latitudes, there is a potential for learning more about the Venus vortex and the dynamical processes. This is particularly important because it is possible to learn much about the dynamical processes from morphology and the structure of the cloud cover given the challenges in systematic, temporal observations of the dynamical state of the Venus atmosphere for a thorough understanding of the superrotation of the deep atmosphere.

A multi-wavelength LIDAR instrument is capable of measuring more precisely the cloud topography from orbit with much greater precision. The ability to detect clouds has been demonstrated by the MOLA instrument at Mars (Neumann et al., 2003). The MESSENGER mission to Mercury also attempted to detect a reflection from the Venus clouds during its fly-by in June 2006. Unfortunately the laser wavelength of 1032 nm used by the instrument is very poorly suited for the Venus atmosphere. Nevertheless,

MESSENGER observations are suggestive of a return from Venus at the closest altitude where the experiment was attempted (Zuber et al., 2008). LIDAR at other wavelengths are expected to be better capable to determine the cloud topography. More importantly, multiple LIDAR wavelengths would enable learning more about the cloud microphysics on a global scale at altitudes not accessible to entry probe or balloon borne observations, and should be pursued.

#### **5.4.4 Orbiter Science Enhancements**

##### **5.4.4.1 Enhanced Science Investigations from Orbit**

NASA's planetary exploration experience has shown that with each order of magnitude increase in instrument fidelity, new answers, new questions, and a radically deeper understanding of the planet ensues. In order to develop the kind of informative geologic maps for Venus that we have for Earth and Mars, many orders of magnitude in image quality will be necessary. In the Design Reference Mission detailed in Chapter 4, a high-resolution imaging radar or dual-antenna interferometric terrain mapping system is highly constrained by the available downlink rate. With no onboard processing, a dual antenna 6 m baseline imaging radar produces about 260 Mbps, and the conceptual 50-m topography mapper produces about 100 Mbps. Onboard processing techniques may well improve to the point where a much more limited dataset (e.g., focused images or phase difference maps) could be downlinked, but this type of processing precludes almost any additional compensation for platform motion errors or other systematic effects. The most robust solution for increasing the area of Venus mapped by such radars is to increase the downlink volume available.

##### **5.4.4.2 Global and Targeted Ultra-Fine Resolution Radar Mapping**

The total area of Venus is about  $4.6 \times 10^{14}$  m<sup>2</sup>. A rough estimate is that a complete, 6-m resolution image map of the planet would require 1.8 Pbits of raw downlinked data, and a global 50-m resolution DEM would require

0.7 Pbits. Either global map will require about 1800 hours of total instrument operation, distributed appropriately over the course of at least one Venus rotation cycle. Even finer radar image resolution (down to the 1 - 2 meter scale) can be achieved for targeted locations through well demonstrated spotlight-mode synthetic aperture techniques, which require the spacecraft to track a particular location on the ground for periods of order 10 seconds. The data rate for such observations would be similar to that of the 6-m imaging mode, but with more limited total area covered (perhaps a few percent of the surface). Such imaging and topographic datasets would reveal Venus in unprecedented detail, far exceeding our knowledge of any other planetary surface.

The scientific objectives of global and targeted ultra-fine resolution mapping of Venus are to:

- Provide an unprecedented understanding of the Venus surface by fine resolution mapping of the Venus surface.
- Provide detailed landing site information for future Venus lander exploration and Venus Surface Sample Return (VSSR).
- Correlate other flagship mission data such as those obtained by the balloon surveys.

##### **5.4.4.3 Optical Telecommunications**

A very high resolution radar system produces such high data volumes that the chief technological problem is bandwidth. Optical telecommunication is one solution to this problem. The Venus Laser Transceiver (VLT) option is an optical transceiver for Venus orbiter to Earth telecommunications to achieve a greater than 10X data volume return compared to Ka-band communications. The VLT is based upon the 50-cm aperture Mars Laser Optical Transceiver to be flown during a pre-2020 pathfinder mission. The NASA SOMD directorate Space Communications and Navigation (SCaN) Architecture Definition Document (ADD) calls for optical communications pathfinder demonstrations with data return rates of at least 100 Mb/s at 1 AU by 2020, and calls for an operational

capability to support mission sets in the 2025+ timeframe.

The operations concept assumes (a) on-board spacecraft storage sufficient for the projected worst case periods of communications outages, nominally solar conjunctions, (b) a low inclination circular Venus orbit, and (c) an Earth ground station availability of 80%, although orbital optical receivers could also contribute to increased data volume capability. For data volume modeling, we presume an overlap of line-of-sight spacecraft visibility and Earth station availability to allow a nominal eight hours per day of communications. Data transmitted to Earth should be maintained in on-board storage until receipt is confirmed by return optical or conventional RF acknowledgement.

The flight system comprises a 50-cm aperture optical head containing transmit/receive optics and an optical uplink detector assembly, a low-frequency vibrations

isolation platform, and a non-vibration isolated electronics box containing the laser transmitter and digital flight processor. The VLT transmits 10 W at 1550 nm, and has redundant transmit lasers. Table 5.6 summarizes the primary characteristics of the VLT. The VLT system assumes that the spacecraft provides coarse pointing of the terminal within a  $\pm 5$ -milliradian dead band. Figure 5.13 is a conceptual drawing of the optical head and Figure 5.14 is a functional block diagram of the major transceiver subsystems.

An Earth ground based system with receive stations of 10 m effective aperture is assumed. With a requirement that the optical receive stations be located at least 1 km above mean sea level, 80% availability can be met by four ground stations. Availability of orbital optical receiver platforms is also envisioned for the 2025+ timeframe, but the equivalent aperture would be less than a 5-m ground station.

**Table 5.6:** VLT Summary Specifications.

Parameter	Value	Condition
Aperture	50 cm	Survives direct sun pointing
Laser Transmitter	10W; 1550 nm	Redundant 10W lasers
Peak Data Rate	1.2 Gb/s	100 ps PPM16, 1/2 rate code
Vibration Isolation	Passive >1 Hz; Active <1 Hz	"Disturbance Free Platform"
Pointing /Acquisition/ Tracking	Beacon Assisted	
Terminal Mass	123 kg	includes 30% contingency
Terminal Power	243 W	includes 30% contingency

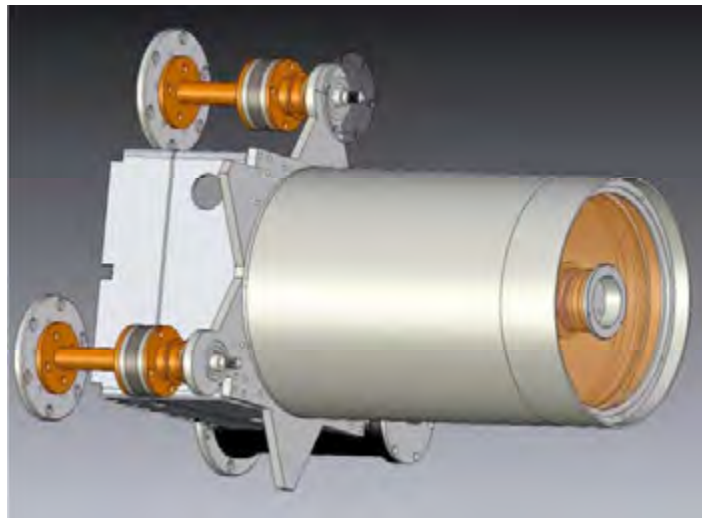


Figure 5.13: VLT Optical Head Concept Drawing.

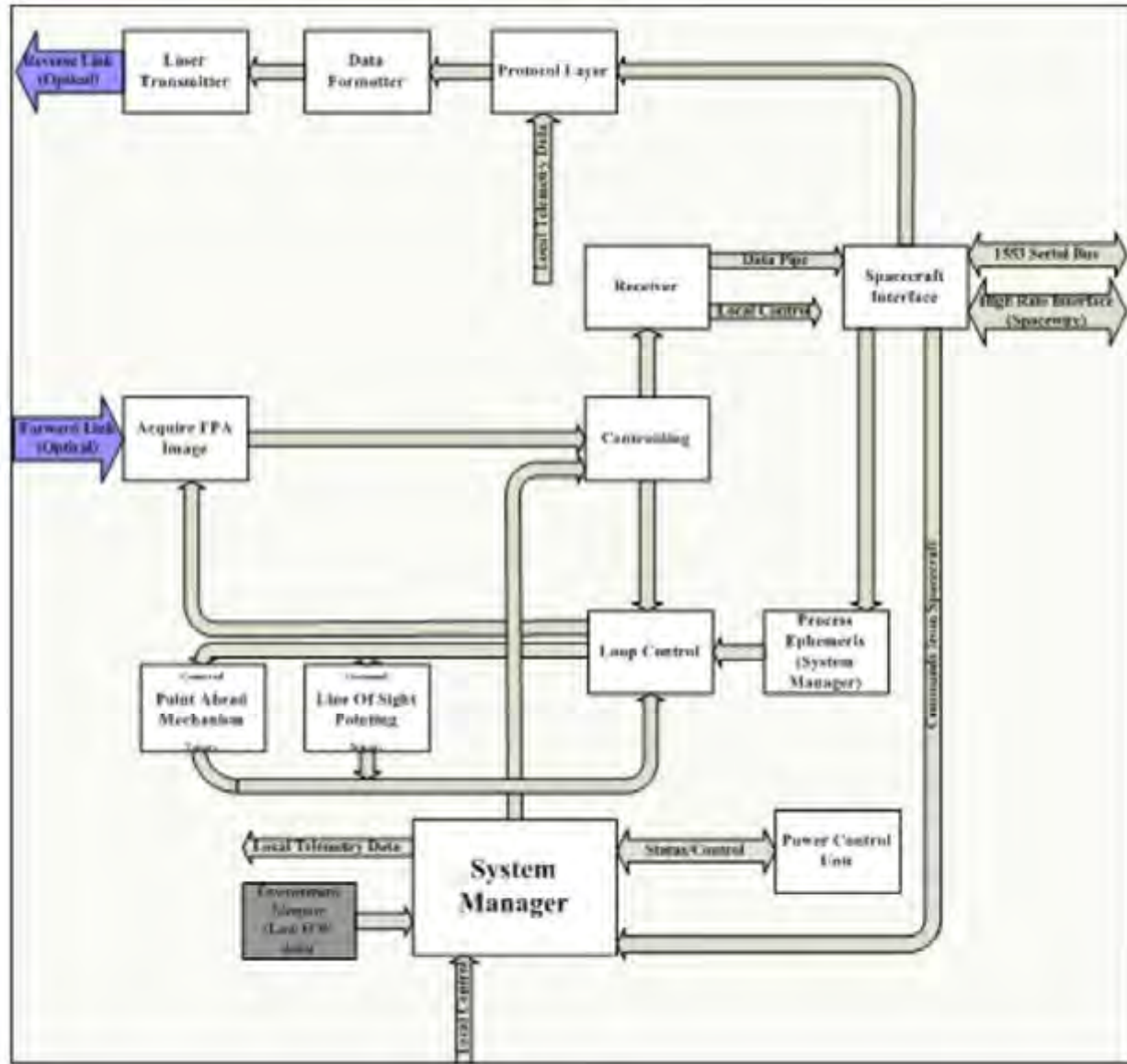


Figure 5.14: VLT Major Functional Subsystems.

**Table 5.7:** VLT Link Specifications and Data Volume.

Parameter	Value	Condition
Downlink Wavelength	1550 nm	nominal
Downlink Laser Average Power	10 W	Single polarization state
Transmitter Aperture	50 cm	
Transmitter Optical Loss	-1.9 db	
Pointing Loss	-0.6 dB	
Modulation	PPM16 .. 64	Plus 6.25% inter-symbol guard time
Modulation Bandwidth	10 GHz	= 100 ps PPM slot width
Data Encoding	SCPPM	0.7 dB gap to capacity
Code Rate	0.5	
Nominal Atmospheric Transmittance	87 %	90th percentile
Nominal Sky Radiance	$10^{-2} \text{ W m}^{-2} \text{ sr}^{-1} \text{ nm}^{-1}$	90th percentile
Nominal Atmospheric Coherence Length	5 cm	
Earth Receiver Aperture	10 m	Or equivalent aperture
Downlink Bandpass	0.3 nm	= 39 GHz
Receiver Optical Loss	-5.5 dB	
Digital Implementation Loss	-2 dB	
Detection Efficiency	45%	SNSPD detector
Detector Jitter Loss	-1 dB	SNSPD detector
Maximum Data Rate	1.2 Gb/s	
Nominal Data Rate	440 Mb/s	
Nominal Link Margin	3 dB	
Data volume	4.6 Petabits / year	8 hr/day downlink

The achievable data volume can be estimated assuming 8 hours/day operations. Atmospheric transmittance and sky radiance at 1550 nm is representative for a station at 2.3 km altitude, such as the Table Mountain Facility (TMF). A 90th percentile radiance of  $10^{-2} \text{ W m}^{-2} \text{ sr}^{-1} \text{ nm}^{-1}$  is used for data volume calculations. Table 5.7 summarizes link performance and data volume calculations.

## 5.5 Recommended Technology Priorities

The criticality and maturity of all technologies required for the Design Reference Mission (Chapter 4) and for mission and payload enhancements described in this chapter are summarized in Table 5.8. The technologies listed in the table are ranked based on their mission criticality and their maturity.

The mission criticality factor is defined in four categories, increasing from 0 to 3, as:

- **Criticality 3:** Technology is considered essential, where the mission can't be

implemented without this technology. No alternative solution known at this time, and the technology is classified as 'must have.'

- **Criticality 2:** Technology will significantly enhance mission performance, survivability etc.; and/or reduce mass, power etc. This category is classified as desirable.
- **Criticality 1:** Technology will add some capabilities to the mission, and classified as useful.
- **Criticality 0:** Technology will not add capabilities for the mission, and therefore classified as not needed.

The technology maturity is correlated in relation to NASA Technology Readiness Levels (TRL), but it is defined in terms of maturity in relevant Venus environment in a scale of 1 to 3, as:

- **Maturity 3:** System prototype tested and validated in a Venus relevant environment (TRL 6 - 9).

**Table 5.8:** Technology criticality and maturity for Venus mission options.

Technology	Orbiter		Cloud-level aerial (52-70 km)		Short lived lander (few hours)		Enhanced life lander (~24 hours)		Seismic/Meteorological Network		Near surface aerial (0.1-15km)		Long-lived lander (months)		Atmospheric probes and sondes	
	C	M	C	M	C	M	C	M	C	M	C	M	C	M	C	M
Pressure vessel (chapter 4)	0		0		3	3	3	2	3	2	3	1	3	2	0	
Passive thermal control (chapter 4 and 5)	0		0		3	3	3	1	0		0		0		3	3
HT Surface Sample Acquisition System (chapter 4)	0		0		3	1	3	1	0		0		3	1	0	
Rugged Terrain Landing (chapter 4)	0		0		3	3	3	3	0		0		3	1	0	
Venus Specific Radioisotope Power System (chapter 5)	0		0		0		0		3	1	0		3	1	0	
Refrigeration (chapter 5)	0		0		0		0		3	1	3	1	3	1	0	
HT Electronics (~500C) (chapter 5)	0		0		0		0		3	1	1	1	1	1	1	1
MT Electronics (~300C) (chapter 5)	0		0		0		0		0		1	2	1	2	1	2
HT Telecom (chapter 5)	0		0		0		0		3	1	0		1	1	1	1
High Temperature Meteorological Sensors (chapter 5)	0		0		0		0		3	2	0		3	2	3	2
High Temperature Seismic Sensors (chapter 5)	0		0		0		0		3	1	0		3	1	0	
HT Energy Storage (chapter 5)	0		0		0		0		3	1	0		1	1	1	1
Materials and Fabrication (Balloon, Bellows, Structures) (chapter 5)	0		3	3	0		0		0		3	1	0		0	

C - Criticality

- Maturity 2:** Critical system components proven in a Venus relevant environment (TRL 4 - 5).
- Maturity 1:** Demonstrated feasibility, basic physics shown to be sound (TRL 1 - 3).

The color code used in the table depends on the combination of technology criticality for a particular platform and technology readiness level. For example, cases of high criticality but very low maturity for certain technologies are marked red. Cases of high maturity are marked green as well as cases of low criticality regardless of maturity. Transition cases of technologies at medium criticality or high criticality and medium maturity are marked yellow. The color code is described below:

		MATURITY		
		1	2	3
CRITICALITY	1	1,1	1,2	1,3
	2	2,1	2,2	2,3
	3	3,1	3,2	3,3

The Venus Design Reference Mission design is based on a science-driven architecture that distributes science measurements on three platforms, namely on an orbiter, on two cloud level balloons and on two short lived landers. Since all of these platforms have been successfully used in the past for Venus exploration missions, this resulted in a very conservative approach to

accomplish the mission's science goals. Consequently, the DRM mission points to an architecture that maximizes the use of heritage technologies and, in turn, minimizes the number of new technologies required for the implementation of this mission. The new technology that would require extensive development is a multiple sample acquisition and processing system that can operate under Venus surface conditions. The high temperature motors and actuators developed for sample acquisition system can be used for the pressure vessel rotation mechanism. The rugged terrain landing system needs to be developed in order to reliably access Tessera and other rugged areas on Venus. The pressure vessel, passive thermal control, and insulation for the short-lived lander (5 hrs) as well as technologies for mid altitude balloons are considered to be mature. The capability to test and validate scientific measurements and to assess the survivability of all exposed sensors/instruments and lander components in Venus-like environment is critical to the mission success.

The extended scope mission concepts, described in this chapter, include low altitude aerial mobility platforms capable of operating and surviving at the Venus near-surface environment; long-lived landers; descent probes and drop sondes for atmospheric research; as well as a multi-element architecture in the form of a long-lived seismic network.

The near-surface aerial mobility platforms will require the development and testing of materials for the lightweight pressure vessel as well as for a high temperature balloon system, likely in the form of metallic bellows. A suitable, low mass refrigeration system is critical for this mission concept. High and medium temperature electronics could provide significant benefits by reducing the temperature lift requirements on the refrigeration system.

Long-lived landers require similar critical technologies as low altitude balloons but include also design solutions for safe landing.

Long life (months or longer) will require new designs for pressure vessel potentially using new materials (e.g., beryllium or honeycomb structure based light weight designs). These static landers would also require a long-lived power source, such as a Venus-specific RPS coupled with a refrigeration system. In addition, landers will require mechanical systems for robotic arms with integrated high temperature sample acquisition in order to acquire samples at different locations around the lander. In particular, with proper system design medium temperature electronics could be decrease thermal load if the relevant circuit technology is available.

Depending on a selected architecture and mission design seismic and meteorological networks may operate in Venus environment for extended periods of time with or without refrigeration. If the second option is chosen, the networks will require a broader range of high temperature components. Although detailed performance requirements for these components will depend on the details of the selected architectures as well as on the science data acquisition scenarios, the general list of technologies will include high temperature sensors, power generation and storage, electronics for data acquisition and storage, power distribution and telecom. Depending on the selected architecture, maturing these technologies to the level where they can be used for Venus missions will require extensive trade study, detailed planning and a sizable and long term investment in technology development.

The recommended technology development priorities for Venus exploration are summarized in Table 5.9. It should be also noted that the development priorities listed in Table 5.9 reflect technology needs for the DRM and the extended life mission architectures documented in this report. However, this priority list is robust enough to account for potential future changes to the DRM architecture in response to potential future precursor New Frontiers or Discovery missions

**Table 5.9:** Venus Technology Development Priorities

	<b>Technologies for DRM</b>	<b>Comments</b>
1	Surface sample acquisition system at high temperature and pressure conditions	Drilling, sample collection and sample handling are enabling for the Design Reference Mission. Heritage Soviet-derived systems are not available off the shelf, but they demonstrate a feasible approach.
2	Lander technologies for rotating pressure vessel and rugged terrain survivability	Rotating pressure vessel concept is powerful but technologically immature. Tessera and other rugged areas on Venus cannot be reliably accessed unless a properly engineered rugged terrain landing system is provided.
3	Venus-like environmental test chamber	This capability is critical for testing and validation of science measurements as well as for testing of components and systems for their survivability in Venus environment
<b>New capabilities</b>		<b>Comments</b>
4	Refrigeration for the Venus surface environment	Almost every long duration (beyond 25 hrs), in situ platform will require some amount of refrigeration to survive. Focus should be on radioisotope-based duplex systems that produce both refrigeration and electrical power.
5	High temperature sensors and electronics, including telecom systems	Refrigeration requirements can be drastically reduced if electronics can operate at elevated temperatures. While a Venus ambient 460 °C capability would be most desirable for telecom, data processing/storage, and power electronics, a major reduction in refrigeration loads could be realized already with moderate temperature operation (>250 °C).
<b>Enhancement to current DRM design</b>		<b>Comments</b>
6	Extension of lander life through advanced thermal control	Human intervention during the lander operation on the surface of Venus is not possible unless lander life is extended to at least 24 hrs.



## 6 SUMMARY AND CONCLUSIONS

---

Venus was the first planet visited by spacecraft from Earth. Mariner 2, NASA's first interplanetary craft, established that Earth's sister planet has a radically different climate. Russian, American, and European craft have subsequently shown that Venus has a diverse and relatively young surface suffused with volcanic features and a dynamic atmosphere shaped by climate feedbacks. These investigations point toward a planetary history characterized by divergence from a more Earth-like past. Yet our current data sets are inadequate for confirming and refining this narrative of dramatic global change. No spacecraft has conducted in situ observations of Venus since the VEGA balloons in 1986. No American spacecraft has been launched to Venus since Magellan in 1989. In the intervening decades, instrumental capabilities have improved dramatically; these improvements will allow us to definitively address some of the biggest mysteries presented by Venus. Over this same time span, we have successfully explored Mars and the outer solar system and have discovered abundant planets around other stars. These advances have created a context where a flagship Mission to Venus can add immensely to our general understanding of solar system evolution and to our specific understanding of Earth-like planets. Most importantly, since the late 1980s, the need to understand the mechanisms of planetary change has been recognized to be a crucial societal priority.

The Venus Science and Technology Definition Team (STDT) reviewed the open science questions concerning Venus and defined the science objectives and investigations for a flagship mission in the 2020 to 2025 timeframe. After evaluating a wide range of mission architectures, the STDT concluded that a flagship consisting of one capable orbiter, 2 month-long balloon flights, and 2 5-hour landers (see Figure 6.1) exploring different parts of the planet will return the highest priority science at the lowest cost and risk.



**Figure 6.1:** (left) One of the Venus flagship landers on a lava flow at the end of its mission (artist: Tibor Balint). (right) Venus, Earth's would-be twin of the solar system, has undergone a radically different atmospheric and geologic evolution from Earth's. What can it teach us about our home world?

This became the Design Reference Mission (DRM), which was studied in detail by JPL's Venus flagship study team and Team X. The DRM accomplishes the science objectives defined by the Venus STDT within the predefined design constraints. Technology challenges for this mission are modest, but require a targeted technology development

plan, starting immediately, to achieve TRL of 6 for all instruments and subsystems in the 2015 time frame for the dual launches of an orbiter and an in situ package in 2021.

In addition, the STDT found that several very-high-priority science investigations are not technologically ready, but could be with the appropriate investments. In many cases, these technologies are on the critical path to an eventual Venus Surface Sample Return mission. The highest science priority beyond the Design Reference Mission would be placing a seismometer/meteorological network on Venus that operates for at least one solar day (117 Earth days). The second priority is to develop passive thermal systems that allow a lander to operate at the surface of Venus for 24 hours or more. Beyond that, the capability to fly low in Venus' thick, hot atmosphere and survey the surface is a very high science priority. In the first and third of these cases, high-temperature electronic systems and active nuclear-powered refrigeration and power systems would have to be developed.

A program of research and technology development, culminating in a simultaneous, in-depth, multi-platform investigation of Venus with modern instrumentation promises to teach us a great deal that is relevant to the continued well being of our nation, our planet, and our biosphere.

## **6.1 Acknowledgements and Notes**

- i. The research described in this report was carried out at the Jet Propulsion Laboratory, California Institute of Technology, under a contract with the National Aeronautics and Space Administration.
- ii. The cost information contained in this document is of a budgetary and planning nature and is intended for informational purposes only. It does not constitute a commitment on the part of JPL and Caltech.
- iii. Copyright 2009. All rights reserved.

## 7 References

---

- Abdrakhimov, A. M., Basilevsky, A. T. "Geology of the Venera and VEGA landing-site regions." *Solar System Research* **36**, 136-159. 2002.
- Abelson, R. D., Balint, T. S., Evans, M., Schriener, T., Shirley, J. H., Spilker, T. R. "Extending exploration with advanced radioisotope power systems." Technical Report JPL D-28903, PP-266 0333, National Aeronautical and Space Administration, Washington, DC. October 2005.
- Addington, E. A. "A stratigraphic study of small volcano clusters on Venus." *Icarus* **149**, 16-36, 2001.
- Albritton, D. L., et al. "Climate change 2001: The scientific basis, summary for policymakers, A report of Working Group I of the intergovernmental panel on climate change." IPCC, pp. 20. 2001.
- Alemi, A., Stevens, D. E. "Why Venus has no moon." Vol. B.A.A.S. **38**, pp. 491. 2006.
- Allen, D. A., Crawford, J. W. "Cloud structure on the dark side of Venus." *Nature* **307**, 222-224. 1984.
- Amman, C. J., "The Isolation of Receiver Effects from Teleseismic P Waveforms." *Bull. Seism. Soc. Am.* **81**, 2504-2510. 1991.
- Arnold, G., Haus, R., Kappel, D., Drossart, P., Piccioni, G. "Venus surface data extraction from VIRTIS/Venus Express measurements: Estimation of a quantitative approach." *Journal of Geophysical Research-Planets* **113**. 2008.
- Bachelder, A., Nock, K. T., Heun, M. K., Balaran, J., Hall, J., Jones, J. A., Kerzhanovich, V. V., McGee, D. P., Stofan, E., Wu, J. J., Yavrouian, A. "Venus geoscience aerobot study (VEGAS)." AIAA Paper 99-3856. 1999.
- Bai, Y., et al. "Large Format Hybrid Visible Silicon Focal Plane Arrays for Space- and Ground-based Astronomy." Proc. of SPIE, Vol. 5499. 2004.
- Baines, K. H., Balint, T. S. "Nuclear Polar VALOR (Venus Atmospheric Long-duration Observatory for in situ Research)." National Aeronautics and Space Administration, Discovery and Scout Mission Capabilities Expansion (DSMCE) Program, Proposal # N7-DSMCE07-0014. 2009.
- Baines, K. H., Balint, T. S., Hall, J., Kerzhanovich, V., Howe, S., Wallace, M., Baker, C., Pauken, M., Allen, G. "Nuclear Polar VALOR: An ASRG-Enabled Venus Balloon Mission Concept." AGU Fall Meeting, Paper number: P33A-1439, December 15-19. 2008.
- Balint, T. S., Cutts, J. A., Kwok, J. H. "Overview of flagship class Venus mission architectures." 6th International Planetary Probe Workshop. 2008.
- Balint, T. S. "Radioisotope Power Systems in Support of NASA's Planetary Exploration Plans." Presented at the Science Council Meeting of the Center for Space Nuclear Research, Idaho Falls. April 18, 2007.

- Balint, T. S., Cutts, J. A., Kolawa, E. A., Kwok, J. H. "Mitigating extreme environments for long-lived Venus in-situ missions." European Geosciences Union (EGU) General Assembly, Vienna, Austria, 13–18. April 2008.
- Balint, T. S., Kolawa, E. A., Cutts, J. A. "Mitigating extreme environments for in-situ Venus and Jupiter missions." Journal of British Interplanetary Society, JBIS, Vol. 60, No. 7 pp.238-248, July 2007.
- Balint, T. S., Kwok, J. H., Kolawa, E. A., Cutts, J. A., Senske, D. A. "Mission architecture and technology options for a flagship class Venus in-situ mission." 59th International Astronautical Congress, A3. Space Exploration Symposium, Session 6. Solar System Exploration, Glasgow, Scotland, IAC-08.A3.6.9, September 29–October 3 (14 pages and Interactive Presentation). 2008.
- Barabash, S., Fedorov, A., Sauvaud, J. J., Lundin, R., Russell, C. T., Futaana, Y., Zhang, T. L., Andersson, H., Brinkfeldt, K., Grigoriev, A., Holmstrom, M., Yamauchi, M., Asamura, K., Baumjohann, W., Lammer, H., Coates, A. J., Kataria, D. O., Linder, D. R., Curtis, C. C., Hsieh, K. C., Sandel, B. R., Grande, M., Gunell, H., Koskinen, H. E. J., Kallio, E., Riihela, P., Sales, T., Schmidt, W., Kozyra, J., Krupp, N., Franz, M., Woch, J., Luhmann, J., McKenna-Lawlor, S., Mazelle, C., Thocaven, J. J., Orsini, S., Cerulli-Irelli, R., Mura, M., Milillo, M., Maggi, M., Roelof, E., Brandt, P., Szego, K., Winningham, J. D., Frahm, R. A., Scherrer, J., Sharber, J. R., Wurz, P., Bochsler, P. "The loss of ions from Venus through the plasma wake." Nature **450**, 650-653. 2008.
- Barath, F. T., Barrett, A. H., Copeland, J., Jones, D. E., Lilley, A. E. "Symposium on radar and radiometric observations of Venus during the 1962 conjunction: Mariner 2 microwave radiometer experiment and results." Astronomical Journal **69**, 49. 1964.
- Baratunde, A. C., Xu, X., Fisher, T. S. "Increased real contact in thermal interfaces: A carbon nanotube/foil material." Applied Physics Letters **90**, 093513. 2007.
- Barnett, D. N., Nimmo, F., McKenzie, D. "Flexure of Venusian lithosphere measured from residual topography and gravity." Journal of Geophysical Research **107**, 2-1-2-21. 2002.
- Barsukov, V. L., Surkov, Y. A., Dimitriev, L. V., Khodakovskiy, I. L. "Geochemical studies on Venus with the landers from the VEGA 1 and VEGA 2 probes." Geochemistry International. **23**, 53-65. 1986.
- Barsukov, V. L., Volkov, V. P., Khodakovskiy, I. L. "The Crust of Venus: Theoretical Models of Chemical and Mineral Composition." Proceedings of the 13th Lunar and Planetary Science Conference, Vol. 87. Journal of Geophysical Research, Houston, pp A3-A9. 1982.
- Basilevsky, A. T., Head, J. W. "Evidence for rapid and widespread emplacement of volcanic plains on Venus: Stratigraphic studies in the Baltis Vallis region." Geophysical Research Letters **23**, 1497-1500. 1996.
- Basilevsky, A. T., Head, J. W. "The geologic history of Venus: A stratigraphic view." Journal of Geophysical Research **103**, 8531-8544. 1998.
- Basilevsky, A. T., Head, J. W. "Geologic units on Venus: Evidence for their global correlation." Planetary and Space Science **48**, 75-111. 2000a

- Basilevsky, A. T., Head, J. W. "Rifts and large volcanoes on Venus: Global assessment of their age relations with regional plains." *Journal of Geophysical Research* **105**, 24,583-24,612. 2000b.
- Basilevsky, A. T., Head, J. W. "On rates and styles of late volcanism and rifting on Venus." *Journal of Geophysical Research* **107**, 8-1-8-17. 2002.
- Beckhoff, B., Kanngieber, B., Langhoff, N., Wedell, R., Wolff, H. *Handbook of practical X-Ray Fluorescence Analysis*. Springer. 2006.
- Bell, J. F., et al. "Mars Exploration Rover Athena Panoramic Camera (Pancam) investigation." *JGR* v. 108, no. E12. 2003.
- Benner, S. A., Ricardo, A., Carrigan, M. A. "Is there a common chemical model for life in the universe?" *Current Opinion in Chemical Biology* **8**, 672-689. 2004.
- Bercovici, D. "The generation of plate tectonics from mantle convection." *Earth and Planetary Science Letters* **205**, 107-121. 2003.
- Board, S. S., "Assessment of planetary protection requirements for Venus missions." Report of a Study by the Space Studies Board of the National Research Council, National Academy of Sciences, Washington, DC. 2006.
- Board, S. S. "Review of planetary quarantine policy." ad hoc Committee for Review of Planetary Quarantine Policy, Space Science Board of the National Research Council, National Academy of Sciences, Washington, DC, pp. 3-4. 1972.
- Board, S. S. "Venus: Strategy for exploration." Report of a study by the Space Science Board of the National Research Council, National Academy of Sciences, Washington, DC, pp. 12-13. 1970.
- Boyer, C., P., G. "Etude de la rotation rétrograde, en 4 jours, de la couche extérieure nuageuse de Vénus." *Icarus* **11**, 338-355. 1969.
- Brackett, R. A., Fegley, B., Arvidson, R. E. "Volatile transport on Venus and implications for surface geochemistry and geology." *Journal of Geophysical Research* **100**, 1553-1563. 1995.
- Bugby, D. "Novel architecture for a long-life lightweight Venus lander." Space Propulsion and Energy Sciences International Forum, Huntsville, Alabama. February 24–26. 2009.
- Bullock, M. A., Grinspoon, D. H. "The recent evolution of climate on Venus." *Icarus* **150**, 19-37. 2001.
- Bullock, M. A., Grinspoon, D. H. "Climate change on Venus and future spacecraft mission priorities." COSPAR, Vol. Abstract COSPAR02-A-02662, Houston, Texas. 2002.
- Bullock, M. A., Grinspoon, D. H., Head, J. W. "Venus resurfacing rates: Constraints provided by 3-D Monte Carlo simulations." *Geophysical Research Letters* **20**, 2147-2150. 1993.
- Bullock, M. A., Moore, H. J. "Atmospheric conditions on early Mars and the missing layered carbonates." *Geophysical Research Letters* **43**, L19201, doi:10.1029/2007GL030688. 2007.

- Bullock, M. A., Senske, D. A., Balint, T. S., Campbell, B. A., Chassefiere, E., Colaprete, A., Cutts, J. A., Gorevan, S., Grinspoon, D. H., Hall, J., Hartford, W., Hashimoto, G. L., Head, J. W., Hunter, G., Johnson, N., Kiefer, W. S., Kolawa, E. A., Kremic, T., Kwok, J., Limaye, S. S., Mackwell, S. J., Marov, M. Y., Ocampo, A., Schubert, G., Stofan, E. R., Svedhem, H., Titov, D. V., Treiman, A. H. "NASA's Venus science and technology definition team: A flagship mission to Venus." *B.A.A.S.* **40**, 32.08. 2008.
- Campbell, B., Greeley, R., Stofan, E. R., Gaskell, R., Shepard, M. K., Klaasen, K. "Imaging the surface of Venus: feasibility of drop-probe photography," *LPSC XXIX*, 1998.
- Campbell, B. and M. K. Shepard. "Effect of Venus surface illumination on photographic image texture," *GRL* **24**, 6, 731-734, March 15, 1997.
- Campbell, D. B. and B. A. Burns. "Venus - Further evidence of impact cratering and tectonic activity from radar observations." *Science* **204**, 1424-1427. 1979.
- Campbell, D. B., Dyce, R. B., Pettengill, G. H. "New radar image of Venus." *Science* **193**, 1123-1124. 1976.
- Campbell, I. H., Taylor, S. R. "No water, no granites—No oceans, no continents." *Geophysical Research Letters* **10**, 1061-1064. 1983.
- Carlson, R. W., Baines, K. H., Encrernaz, T., Taylor, F. W., Drossart, P., Kamp, L. W., Pollack, J. B., Lellouch, E., Collard, A. D., Calcutt, S. B., Grinspoon, D. H., Weissman, P. R., Smythe, W. D., Ocampo, A. C., Danielson, G. E., Fanale, F. P., Johnson, T. V., Kieffer, H. H., Matson, D. L., McCord, T. B., Soderblom, L. A. "Galileo infrared imaging spectrometer measurements at Venus." *Science* **253**, 1541-1548. 1991.
- Carlson, R. W., Kamp, L. W., Baines, K. H., Pollack, J. B., Grinspoon, D. H., Encrernaz, T., Drossart, P., Lellouch, E., Bezard, B. "Variations in Venus cloud particle properties: A new view of Venus's cloud morphology as observed by the Galileo near-infrared mapping spectrometer." *Planetary and Space Science* **41**, 477-486. 1993.
- Carlson, R. W., Taylor, F. W. "The Galileo encounter with Venus: Results from the Near-Infrared Mapping Spectrometer." *Planetary and Space Science* **41**, 475-476. 1993.
- Chassefiere, E., Koralev, O., Imamura, T., Baines, K. H., Wilson, C. F., Titov, D., Aplin, K. L., Balint, T., Blamont, J. E., Cochrane, C. G., Ferencz, C., Ferri, F., Gerasimov, M., Leitner, J. J., Lopez-Moreno, J. J., Marty, B., Martynov, M., Pogrebenko, S. V., Rodin, A., Whiteway, J. A., Zasova, L., Michaud, J., Bertrand, R., Charbonnier, J. M., Team, E. "European Venus Explorer (EVE): An in situ mission to Venus." *Experimental Astronomy*.
- Chen, L. "Survey report of current status of high temperature microdevices packaging." NEPP OAI/NASA GRC. 2004.
- Chen, Y., Castillo, L., Aranki, N., Assad, C., Mazzola, M., Mojarradi, M., Kolawa, E. "Reliability assessment of high temperature electronics and packaging technology for Venus missions." *Digests of IEEE 2008 International Reliability Physics Symposium IRPS*. pp 641-642. 2008.

- Chmielewski, A. "RTGs for space exploration at the end of the 20th Century." 24th Intersociety Energy Conversion Engineering Conference, Washington DC, paper IECEC-899237 vol. 2 715-720. August 6–11, 1989.
- Clark, B. C., Castro, A. J., Rowe, C. D., Baird, A. K., Rose, H. J., Toulmin, P., Christian, R. P., Kelliher, W. C., Keil, K., Huss, G. R. "The Viking X-ray fluorescence experiment—Analytical methods and early results." *Journal of Geophysical Research* **82**, 4577-4594. 1977.
- Coffin, M. F. and O. Eldholm. "Large igneous provinces: Crustal structure, dimension, and external consequences. *Reviews of Geophysics* **32**, 1-36. 1994.
- Colin, L. "The Pioneer Venus Program." *Journal of Geophysical Research* **85**, 7575-7598. 1980.
- Collins, G. C., Head, J. W., Basilevsky, A. T., Ivanov, M. A. "Evidence for rapid regional plains emplacement on Venus from the population of volcanically embayed craters." *Journal of Geophysical Research* **104**, 24121-24139. 1999.
- Colozza, A. "Evaluation of Solar Powered Flight on Venus." 2nd International Energy Conversion Engineering Conference, Providence, RI, paper AIAA-2004-5558. August 16–19, 2004.
- CRISM Website 2009, <http://crism.jhuapl.edu/instrument/>
- Crisp, D. "Radiative forcing of the Venus mesosphere I. Solar fluxes and heating rates." *Icarus* **67**, 484-514. 1986.
- Crisp, D., Allen, M. A., Anicich, V. G., Arvidson, R. E., Atreya, S. K., Baines, K. H., Banerdt, W. B., Bjoraker, G. L., Bouger, S. W., Campbell, B. A., Carlson, R. W., Chin, G., Chutjian, A., Clancy, R. T., Clark, B. C., Cravens, T. E., del Genio, A. D., Esposito, L. W., Fegley, B., Flasar, M., Fox, J. L., Giersch, P. J., Goody, R. M., Grinspoon, D. H., Gulkis, S. L., Hansen, V. L., Herrick, R. R., Huestis, D. L., Hunten, D. M., Janssen, M. A., Jenkins, J. E., Johnson, C. L., Keating, G. M., Kliore, A. J., Limaye, S. S., Luhmann, J. G., Lunine, J. I., Mahaffy, P., McGovern, P. J., Meadows, V. S., Mills, F. P., Niemann, H. B., Owen, T. C., Oyama, K. I., Pepin, R. O., Plaut, J. J., Reuter, D. C., Richards, M. I., Russell, C. T., Saunders, R. S., Slanger, T. G., Smrekar, S. E., Stevenson, D. J., Titov, D. V., Ustinov, E. A., Young, R. E., Yung, Y. L. "Divergent evolution among Earth-like planets: The case for Venus Exploration." M. V. Sykes (Ed.), *The Future of Solar System Exploration 2003-2013*, 2003.
- Crisp, D. Personal communication. 1996.
- Crisp, D. and D. Titov. "The thermal balance of the Venus atmosphere." S. W. Bouger, et al., Eds.), *Venus II*. University of Arizona Press, Tucson, pp 353-384. 1997.
- Cutts, J. A., Neck, K. T., Jones, J. A., Guillermo, R., Balaram, J., Powell, G. E., Synott, S. P. "Aerovehicles For Planetary Exploration." *Journal of Autonomous Robots* 2, 261–282. 1996.
- Cutts, J. A., Balint T. S., Hall, J. L., Kerzhanovich, V., Jones, J., Kolawa, E. A., Nott, J. "Technology challenges for exploration of planets with aerial platforms." 37th COSPAR

- Scientific Assembly, Symposium B06: Scientific investigations from Planetary Probes and Aerial Platforms, Montreal, Canada. July 13–20, 2008.
- Cutts, J. A., Balint, T. S. Chassefiere, E., Kolawa, E. A. “Chapter 13: Technology perspectives in the future exploration of Venus.” Chapman Monograph – Exploring Venus as a Terrestrial Planet. AGU, Editors: L. W. Esposito, E. R. Stofan, R. E. Cravens, ISBN 978-0-87590-441-2, 2007 (Book Chapter: 21). 2007.
- Dahlen, F. A. and J. Tromp. “Theoretical global seismology.” Princeton University Press. 1998.
- Daumiller, I., C. Kirchner, M. Kamp, K. J. Ebeling and E. Kohn. “Evaluation of the temperature stability of AlGaN/GaN heterostructure FETs.” IEEE Electron Device Letters, Vol. 20, No. 9, pp 448-450. September 1999.
- Davies, J. H. “Is the interior of Venus dry due to a Mega-collision?” AGU, pp P33A-1426. Fall 2008.
- Del Castillo, L., D. V. Schatzel, C. Tudry, T. Hatake, Y. Chen, M. M. Mojarradi and E. A. Kolawa. “Extreme environment electronic packaging for Venus and Mars landed missions.” 4th International Planetary Probe Workshop, Pasadena, CA. June 2006.
- Del Castillo, L., T. Hatake, M. Mojarradi, T. Vo, W. West, J. Yager. “Extreme Temperature Sensing System for the Venus Ambient Environment.” R&TD Annual Report. September 2007.
- Del Castillo, L., T. W. Johnson, T. Hatake, M. M. Mojarradi and E. A. Kolawa. “Sensor amplifier for the Venus ground ambient.” International Conference on High Temperature Electronics (HiTEC), May 15–18, 2006, Santa Fe, NM: International Microelectronics and Packaging Society. 2008.
- Dickey, J. O., Bender, P. L., Faller, J. E., Newhall, X. X., Ricklefs, R. L., Ries, J. G., Shelus, P. J., Veillet, C., Whipple, A. L., Wiant, J. R., Williams, J. G., Yoder, C. F. “Lunar laser ranging: A continuing legacy of the Apollo Program.” *Science* **265**, 482-490. 1994.
- Dochat, G. “Venus lander stirling cooler.” Mechanical Technology Inc. Company Report. August 1992.
- Donahue, T. M. and R. R. Hodges. “Past and present water budget of Venus.” *Journal of Geophysical Research* **97**, 6083-6091. 1992.
- Donahue, T. M., Hoffman, J. H., Hodges, R. R., Watson, A. J. “Venus was wet: A measurement of the ratio of D to H.” *Science* **216**, 630-633. 1982.
- Dudzinski, L. “Radioisotope Power for NASA’s Space Science Missions.” NASA briefing to the Outer Planets Advisory Group. March 31, 2008.
- Dupont Fluoroproducts. “HFC-235fa clean agent: Properties, uses, storage and handling.” Data sheet 3024498A, available as [http://refrigerants.dupont.com/Suva/en\\_US/pdf/h77974.pdf](http://refrigerants.dupont.com/Suva/en_US/pdf/h77974.pdf). See also Dupont Fluorochemicals Technical Information Sheet TN-236fa ENG, Thermodynamic Properties of HFC-236fa (1,1,1,3,3-hexafluorpropane). 1999.

- Dziewonski, A. M. and D. L. Anderson. "Preliminary Reference Earth Model." *Phys. Earth Planet. Int.* **25**, 297-356. 1981.
- ESA. "Cosmic Vision, Space Science for Europe 2015-2025." Technical Report ESA BR-247. 2005.
- ESA, 2009. Instrument descriptions for the Herschel mission. <http://sci.esa.int/science-/www/object/index.cfm?fobjectid=34691&fbodylongid=1593>
- ESKOS. "The Venera/VEGA Projects: An analysis of the operational experience obtained in the study of the atmosphere and surface of Venus." 1994.
- Esposito, L. W., Bertaux, J. L., Krasnopolsky, V. A., Moroz, V. I., Zasova, L. V. "Chemistry of lower atmosphere and clouds." *Venus II* (S. W. Bougher, et al., Eds.). University of Arizona Press, Tucson, pp 415-458. 1997.
- Esposito, L. W., Knollenberg, R. G., Marov, M. Y., Toon, O. B., Turco, R. P. "The clouds and hazes of Venus." *Venus* (D. M. Hunten, et al., Eds.). University of Arizona Press, Tucson, pp 484-564. 1983.
- Fegley, B. Jr. "Venus." 487–507 in Holland HD and Turekian KK (eds.) *Treatise on Geochemistry*, vol. 1, Oxford: Elsevier. 2003
- Fegley, B. and R. G. Prinn. "Estimation of the rate of volcanism on Venus from reaction rate measurements." *Nature* **337**, 55-58. 1989.
- Fegley, B. and A. H. Treiman. "Chemistry of atmosphere-surface interactions on Venus and Mars." *Venus and Mars: Atmospheres, Ionospheres and Solar Wind Interactions*. American Geophysical Union (J. G. Luhmann, et al., Eds.), Washington, DC, pp 7-71. 1992.
- Fegley, B., Treiman, A. H., Sharpton, V. L. "Venus surface mineralogy: Observational and theoretical constraints." *Proceedings of the 22nd Lunar and Planetary Science Conference*, Vol. 22. Lunar and Planetary Institute, Houston, pp 3-19. 1992.
- Fegley, B., Zolotov, M. Y., Lodders, K. "The oxidation state of the lower atmosphere and surface of Venus." *Icarus* **125**, 416-439. 1997.
- Fimmel, R. O., Colin, L., Burgess, E., Mark, H., Guastaferro, A. *Pioneer Venus*. National Aeronautics and Space Administration, Washington, DC. 1983.
- Florensky, C. P., Nikolaeva, O. V., Volkov, V. P., Kudryashova, A. F., Pronin, A. A., Gektin, Y. M., Tchaikina, E. A., Bashkiro, A. S. "Redox indicator 'contrast' on the surface on Venus." *Lunar and Planetary Science* 2030204. 1983.
- Folkner, W. M., Yoder, C. F., Yuan, D. N., Standish, E. M., Preston, R. A. "Interior structure and seasonal mass redistribution of Mars from radio tracking of Mars Pathfinder." *Science* **278**, 1749-1752. 1997.
- Gao, G.-b., J. Sterner, H. Morkoc. "High frequency performance of SiC heterojunction bipolar transistors." *IEEE Transactions on Electron Devices*, vol. 41, pp 1092-1097. 1994.
- Garvin, J. B. "Dust cloud observed in Venera 10 panorama of Venusian surface: Inferred surface processes." *Lunar and Planetary Science*. 1981.

- Garvin, J. B., Head, J. W., Zuber, M. T., Helfenstein, P. "Venus: The nature of the surface from Venera panoramas." *Lunar and Planetary Science* 296-297. 1984.
- Gellert, R., Rieder, R., Anderson, R. C., Bruckner, J., Clark, B. C., Dreibus, G., Economou, T., Klingelhofer, G., Lugmair, G. W., Ming, D. W., Squyres, S. W., d'Uston, C., Wanke, H., Yen, A., Zipfel, J., 2004. Chemistry of Rocks and Soils in Gusev Crater from the Alpha Particle X-ray Spectrometer. *Science*. 305, 829-832.
- Ghent, R., Hansen, V. L. "Structural and kinematic analysis of eastern Ovda Regio, Venus: Implications for crustal plateau formation." *Icarus* **139**, 116-136. 1999.
- Gierasch, P. J. "Meridional circulation and the maintenance of the Venus atmospheric circulation." *Journal of the Atmospheric Sciences* **32**, 1038-1044. 1975.
- Gierasch, P. J., Goody, R. M., Young, R. E., Crisp, D., Edwards, C., Kahn, R., Rider, D., Del Genio, A., Greeley, R., Hou, A., Leovy, C. B., McCleese, D., Newman, M. "The general circulation of the Venus atmosphere: An assessment." *Venus II* (S. W. Bougher, et al., Eds.). University of Arizona Press, Tucson, pp 459-500. 1997.
- Gilmore, G. "Practical Gamma-Ray Spectrometry." Wiley. 2008.
- Gilmore, M. S., Collins, G. C., Crumpler, L. S., Cutts, J. A., deCharon, A. V., Head, J. W., Nock, K. T., Parry, M., Yingst, R. A. "Investigation of the application of aerobot technology at Venus." *Acta Astronautica*. 56, 477-494. 2005.
- Goldstein, R. M., Green, R., Rumsey, H. C. "Venus radar brightness and altitude images. *Icarus* **36**, 334-352. 1978.
- Gregg, T. K. and R. Greeley. *Journal of Geophysical Research* **98**, 10,873-10,882. 1993.
- Grimm, R. E. and G. T. Delory. "Magnetotelluric sounding of the interior of Venus." *Venus Geochemistry Workshop*, Abstract 2015. 2009.
- Grimm, R. E. and P. C. Hess. "The crust of Venus." *Venus II: Geology, Geophysics, Atmosphere, and Solar Wind Environment* (S. W. Bougher, et al., Eds.). University of Arizona Press, Tucson, pp 1205-1244. 1997.
- Grinspoon, D. H. "Implications of the high D/H ratio for the sources of water in Venus' atmosphere." *Nature* **363**, 428-431. 1993.
- Grinspoon, D. H. and M. A. Bullock. "Astrobiology and Venus Exploration." *Exploring Venus as a Terrestrial Planet* (L. W. Esposito, Ed.). AGU, Washington, DC. 2007.
- Grinspoon, D. H., Pollack, J. B., Sitton, B. R., Carlson, R. W., Kamp, L. W., Baines, K. H., Encrenaz, T., Taylor, F. W. "Probing Venus' cloud structure with Galileo NIMS." *Planetary and Space Science* **41**, 515-542. 1993.
- Grotzinger, J. P., Arvidson, R. E., Bell III, J. F., Calvin, W., Clark, B. C., Fike, D. A., Golombek, M., Greeley, R., Haldemann, A., Herkenhoff, K. E. "Stratigraphy and sedimentology of a dry to wet eolian depositional system, Burns formation, Meridiani Planum, Mars." *Earth and Planetary Science Letters* **240**, 11-72. 2005.

- Guest, J. E. and E. R. Stofan. "A new view of the stratigraphic history of Venus." *Icarus* **139**, 55-66. 1999.
- Guhel Y., B. Boudart, V. Hoel, M. Werquin, C. Gaquiere, J. C. De Jaeger, M. A. Poisson, I. Daumiller, and E. Kohn. "Effects of High Temperature on the Electrical Behavior of AlGaN/GaN HEMTs." *Microwave Opt. Technol. Lett.* **34**, 4. 2002.
- Guynn, M.D., M. Croom, S. Smith, R. Parks, and P. Gelhausen. "Evolution of a Mars airplane concept for the ARES Mars Scout mission." paper AIAA 2003-6578, 2nd AIAA Unmanned Unlimited Systems, Technologies, and Operations Conf., 15-18 September 2003, San Diego, CA. 2003.
- Hagedorn, N.H. "Alkali metal carbon dioxide electrochemical system for energy storage and/or conversion of carbon dioxide to oxygen." Patent 5213908, 1993.
- Hall, J. L., D. Fairbrother, T. Frederickson, V. V. Kerzhanovich, M. Said, C. Sandy, C. Willey and A. H. Yavrouian. "Prototype design and testing of a Venus long duration, high altitude balloon." *Advances in Space Research*, Vol. 42, pp 1648-1655. 2008.
- Hall, J. L., V. V. Kerzhanovich, A. H. Yavrouian, G. A. Plett, M. Said, D. Fairbrother, C. Sandy, T. Frederickson, G. Sharpe, and S. Day. "Second generation prototype design and testing for a high altitude Venus balloon." *Advances in Space Research* (in press). 2009.
- Hamill, P., Kiang, C. S., Cadle, R. D. "The nucleation of H<sub>2</sub>SO<sub>4</sub>-H<sub>2</sub>O solution aerosol particles in the stratosphere." *Journal of the Atmospheric Sciences* **34**, 150-162. 1977.
- Hansen, J. E. and J. W. Houvenier. "Interpretation of the polarization of Venus." *Journal of the Atmospheric Sciences* **31**, 1137-1160. 1974.
- Hansen, V. L. "Geologic mapping of tectonic planets." *Earth and Planetary Science Letters* **176**, 527-542. 2000.
- Hansen, V. L. "Artemis: Surface expression of a deep mantle plume on Venus." *Geological Society of America* **114**, 839-848. 2002.
- Hansen, V. L., Phillips, R. J., Willis, J. J., Ghent, R. R. "Structures in tessera terrain, Venus: Issues and answers." *Journal of Geophysical Research* **105**, 4135-4152. 2000.
- Hansen, V. L. and J. J. Willis. "Structural analysis of a sampling of tessera: Implications for Venus geodynamics." *Icarus* **123**, 296-312. 1996.
- Harrison, K. P. and M. G. Chapman. "Evidence for ponding and catastrophic floods in central Valles Marineris, Mars." *Icarus*. 2008.
- Harrison, R. and G. A. Landis. "Batteries for Venus surface operation." 6th International Energy Conversion Engineering Conference (IECEC), Cleveland, OH, AIAA 2008-5796. July 28-30, 2008.
- Hashimoto, G. L. and Y. Abe. "Venus' surface temperature controlled by a chemical-albedo feedback." LPSC XXIX, Abstract 1593. 1998.

- Hashimoto, G. L., Roos-Serote, M. C., Sugita, S., Gilmore, M. S., Kamp, L. W., Carlson, R. W., Baines, K. H. "Galileo near infrared mapping spectrometer (NIMS) data suggest felsic highland crust on Venus." *Journal of Geophysical Research* **113**. 2008.
- Head, J. W. and A. T. Basilevsky. "Sequence of tectonic deformation in the history of Venus: Evidence from global stratigraphic relationships." *Geology* **26**, 35-38. 1998.
- Helbert, J., Muller, N., Kostama, P., Marinangeli, L., Piccioni, G., Drossart, P. "Surface brightness variations seen by VIRTIS on Venus Express and implication for the evolution of the Lada Terra region, Venus." *Geophysical Research Letters* **35**, L11201, doi:10.1029/2008GL033609. 2008.
- Helffrich, G. "Topography of the transition zone seismic discontinuities." *Reviews of Geophysics* **38**, 131-158. 2000.
- Herrick, R. R. and V. L. Sharpton. "Implications from stereo-derived topography of Venusian impact craters." *Journal of Geophysical Research* **105**, 20,245–20,262. 2000.
- [http://www.sti.nasa.gov/tto/Spinoff2008/ip\\_2.html](http://www.sti.nasa.gov/tto/Spinoff2008/ip_2.html)
- <http://www.techbriefs.com/content/view/2241/32/>
- Hunter G. W., Okojie R. S., Oberle L., Krasowski M., Neudeck P. G., Beheim G. M., Fralick G., Wrbanek J., and Greenberg P. "Microsystems, instrument electronics and mobile sensor platforms. "Fourth Annual International Planetary Probe Workshop, Pasadena, CA. June 27–30, 2006.
- Hunter, G. W., Liu C. C., Makel D. "MEMS handbook, second edition, design and fabrication." CRC Press LLC, ed. M. Gad-el-Hak, Boca Raton, FL, Ch. 11. 2006.
- Hunter, G. W., P. G. Neudeck, R. S. Okojie, G. M. Beheim, M. Kraskowski, G. E. Ponchak and L. Y. Chen. "High temperature electronics, communications, and supporting technologies for Venus missions." 5th International Planetary Probe Workshop, Bordeaux, France. June 23–29, 2007.
- Hunter, G. W., R. S. Okojie, M. Krasowski, P. G. Neudeck, G. M. Beheim, G. Fralick, J. Wrbanek, J. Xu, and P. Greenberg. "Microsystems, space qualified electronics, and mobile sensor platforms for harsh environment applications and planetary exploration." 5th International Planetary Probe Workshop, Bordeaux, France. June 23–29, 2007.
- Hyder, A. K., Wiley, R. L., Halpert, G., Flood, D. J., and Sabripour, S. "Spacecraft power technologies." Imperial College Press, London, Ch. 5–6. 2000.
- Inproxtechnology website: <http://www.inproxtechnology.com/>. 2009.
- IPCC 2007. Climate Change 2007: The physical science basis. Intergovernmental Panel on Climate Change. 1. 2007.
- Ji, Jerri. Presentation at the 6th International Planetary Probe Work shop, Atlanta, Georgia, Short Course on Extreme Environments Technologies, "High temperature Mechanisms-A breakthrough development" <http://smartech.gatech.edu/bitstream/1853/26384/1/148-243-1-PB.pdf>. 2008.

- Jimenez, J. L. and U. Chowdhury. "X-band GaN FET reliability." IEEE 46th Int. Reliability Physics Symp., Phoenix, AZ, pp 429-435. 2006.
- Johnson, R. W., Wang, C., Liu, Y., Scofield, J. D. "Power Device Packaging Technologies for Extreme Environments." Electronics Packaging Manufacturing, IEEE Transactions on (1521-334X), Vol. 30, Issue 3; p. 182. July 2007.
- Jones, A. P. and K. T. Pickering. "Evidence for aqueous fluid–sediment transport and erosional processes on Venus." Journal of the Geological Society **160**, 319-327. 2003.
- JPL MSL RAD website 2009 <http://msl-scicorner.jpl.nasa.gov/Instruments/RAD/>
- Kang B. S., F. Ren, B. P. Gila, C. R. Abernathy, J. Lin, S. N. G. Chu. "GaN-based diodes and transistors for chemical, gas, biological and pressure sensing." *J. Phys. Condens. Matter* **16** R961-R994. 2004.
- Kargel, J. S., Kirk, R. L., Fegley, B., Treiman, A. H. "Carbonate-sulfate volcanism on Venus?" *Icarus* **112**, 219-252. 1994.
- Kargel, J. S., Komatsu, G., Baker, V. R., Strom, R. G. "The volcanology of Venera and VEGA landing sites and the geochemistry of Venus." *Icarus* **103**, 253-275. 1993.
- Kasting, J. F. "Runaway and moist greenhouse atmospheres and the evolution of Earth and Venus." *Icarus* **74**, 472-494. 1998.
- Kasting, J. F., Pollack, J. B., Ackerman, T. P. "Response of Earth's atmosphere to increases in solar flux and implications for loss of water from Venus." *Icarus* **57**, 335-355. 1984.
- Kaula, W. M. "Formation of the Terrestrial Planets." *Planetary Systems—the Long View*, pp 1–8. 1997.
- Kawabata, K., Coffeen, D. L., Hansen, J. E., Lane, W. A., Sato, M., Travis, L. D. "Cloud and haze properties from Pioneer Venus polarimetry." *Journal of Geophysical Research* **85**, 8129-8140. 1980.
- Kerzhanovich, V. V., Hall, J., Yavrouian, A., Cutts, J. "Two balloon system to lift payloads for the surface of Venus." AIAA-200507322, AIAA 5th ATIO and 16th Light-Thanp-Air Sys Tech. and Balloon Systems Conferences, Arlington, VA. September 26–28, 2005.
- Kerzhanovich, V. V. and M. Y. Marov. "The atmospheric dynamics of Venus according to Doppler measurements by the Venera entry probes." *Venus* (D. M. Hunten, et al., Eds). University of Arizona Press, Tucson, pp 766-778. 1983.
- Kiefer, W. S. and B. H. Hager. "A Mantle Plume Model for the Equatorial Highlands of Venus." *Journal of Geophysical Research* **96**, 20,947-20,966. 1991.
- Kiefer, W. S. and L. H. Kellogg. "Geoid anomalies and dynamic topography from time-dependent, spherical axisymmetric mantle convection." *Phys. Earth Planet. Int.* **q06**, 237-256. 1998.
- Klose, K. B., Wood, J. A., Hashimoto, A. "Mineral equilibria and the high radar reflectivity of Venus mountaintops." *Journal of Geophysical Research* **97**, 16353-16369. 1992.

- Kolawa, E., Balint, T.S., Birur, G. Brandon, E., Del Castillo, L., Hall, J., Johnson, M., Kirschman, R., Manvi, R., Mojarradi, M., Moussessian, A., Patel, J., Pauken, M., Peterson, C., Whitacre, J., Martinez, E., Venkapathy, E., Newdeck, P., Okojie R. "Extreme environment technologies for future space science missions." Technical Report JPL D-32832, National Aeronautical and Space Administration, Washington, DC. 2007.
- Komatsu, G., Gulick, V. C., Baker, V. R. "Valley networks on Venus." *Geomorphology* **37**, 225-240. 2001.
- Konopliv, A. S., Banerdt, W. B., Sjogren, W. L. "Venus gravity: 180th degree and order model." *Icarus* **139**, 3-18. 1999.
- Konopliv, A. S. and C. F. Yoder. "Venusian k2 tidal love number from Magellan and PVO tracking data." *Geophysical Research Letters* **23**, 1857-1860. 1996.
- Kreslavsky, M. A. and A. T. Basilevsky. "Tentative analysis of reflectivity map of Venus surface based on Venera-15, -16 measurements: Comparison with Pioneer Venus data." *Lunar and Planetary Science Conference*, Vol. 20, p 542. 1989.
- Landis, G. A. "Robotic Exploration of the Surface and Atmosphere of Venus." *Acta Astronautica*, Vol. 59, 7, 517-580 (October 2006). Presented as paper IAC-04-Q.2.A.08, 55th International Astronautical Federation Congress, Vancouver, BC, (Oct. 4-8 2004).
- Landis, G. A., LaMarre, C., Colozza, A. "Atmospheric flight on Venus: A conceptual design." *Journal of Spacecraft and Rockets* **40**, 672-677. 2003.
- Landis, G. A. "Robotic exploration of Venus." VEXAG/Venus STDT meeting. 2008.
- Landis, G. and K. C. Mellott. "Venus surface power and cooling system design." Paper IAC-04-R.2.06, *Acta Astronautica*, Vol. 61, No. 11-12, pp 995-1001. 2007.
- Landis, G. A. "Revolutionary aerospace systems concepts study, Robotic exploration of Venus." NASA Glenn Research Center (summary version presented at the VEXAG/Venus-STDT meeting, May 5-8, 2008). 2003.
- Landis, G. and T. Vo. "Photovoltaic Performance in the Venus Environment." 34th IEEE Photovoltaic Specialists Conference, Denver, CO. June 8–12, 2008.
- Lay, T. and T. C. Wallace. "Modern global seismology." Academic Press. 1995.
- Lei, J. F., Fralick G. C., Krasowski M. J. "Microfabricated multifunction strain-temperature gauge." US Patent 5,979,243, November 9, 1999.
- Levine, J.S. et al. "Science from a Mars airplane: The aerial regional scale environmental survey (ARES) of Mars." Paper AIAA 2003-6576, 2nd AIAA Unmanned Unlimited Systems, Technologies, and Operations Conference, San Diego, CA. September 2003.
- LEW- 18256-1 Patent Application, "An N Channel JFET Based Digital Logic Gate Structure Using Resistive Level Shifters And Having Direct Application To High Temperature Silicon Carbide Electronics"
- Lewandowski, E. J., J. G. Schreiber, S. D. Wilson, S. M. Oriti, P. Cornell, N. Schifer. "Extended operation testing of Stirling convertors in support of Stirling radioisotope power system

- development.” 6th International Energy Conversion Engineering Conference (IECEC), AIAA 2008-5791, Cleveland, OH. July 2008.
- Lewis, J. S. “Venus: Atmospheric and lithospheric composition.” *Earth and Planetary Science Letters* **10**, 73-80. 1970.
- Limaye, S. S. “Venus atmospheric circulation: Observations and implications of the thermal structure.” *Advances in Space Research* **5**, 51-62. 1985.
- Limaye, S. S., Kossin, J. P., Rozoff, C., Piccioni, G., Titov, D. V., Markiewicz, W. J. “Vortex circulation on Venus: Dynamical similarities with terrestrial hurricanes.” *Geophysical Research Letters* **36**, 04204. 2009.
- Limaye, S. S. and V. E. Soumi. “Cloud motions on Venus—Global structure and organization.” *Journal of the Atmospheric Sciences* **38**, 1220-1235. 1981.
- Liu Y., M. Z. Kauser, D. D. Schroepfer, P. P. Ruden, J. Xie, Y. T. Moon, N. Onojima, H. Morkoç, K.-A. Son, M. I. Nathan. “Effect of hydrostatic pressure on the current-voltage characteristics of GaN/AlGaN/GaN heterostructure devices.” *J. Appl. Phys.* **99**, 113706. 2006.
- Liu Y., P. P. Ruden, J. Xie, H. Morkoç, K.-A. Son. “Effect of hydrostatic pressure on the dc characteristics of AlGaN/GaN heterojunction field effect transistors.” *Appl. Phys. Lett.* **88**, 013505. 2006.
- Lodders, K. and B. Fegley. “The planetary scientist’s companion.” Oxford University Press, New York. 1998.
- Lognonné, P. “Planetary seismology.” *Annual Review of Earth and Planetary Sciences* **33**, 571-604. 2005.
- Lognonné, P., Giardini, D., Banerdt, B., Gagnepain-Beyneix, J., Mocquet, A., Spohn, T., Karczewski, J. F., Schibler, P., Cacho, S., Pike, W. T., Cavoit, C., Desautez, A., Favède, M., Gabsi, T., Simoulin, L., Striebig, N., Campillo, M., Deschamp, A., Hinderer, J., Lévéque, J. J., Montagner, J. P., Rivéra, L., Benz, W., Breuer, D., Defraigne, P., Dehant, V., Fujimura, A., Mizutani, H., Oberst, J. “The NetLander very broad band seismometer.” *Planetary and Space Science* **48**, 1289-1302. 2000.
- Lorenz, R. D. “A review of balloon concepts for Titan.” *JBIS* **61**, 2-13. 2008.
- Lorenz, R. D. “Design considerations for Venus microprobes.” *Journal of Spacecraft and Rockets* **36**, 228-230. 1998.
- Maki, J. N., et al. “Mars Exploration Rover engineering cameras.,” *JGR* **108**, E12. 2003.
- Manohara, H. M., M. Mojarradi, R. Toda, R. Lin, A. Liao, M. Kanik. “‘Digital’ vacuum microelectronics: Carbon nanotube-based inverse majority gates for high temperature applications.” DARPA-MTO Technological Symposium, San Jose, CA. March 2009.
- Manohara, H. M. and M. Mojarradi. “Radiation-insensitive inverse majority gates.” *New Technology NPO 45388, NASA Tech Brief*, Vol. 32 (6), p 42. 2008.

- Markiewicz, W. J., Titov, D. V., Limaye, S. S., Keller, H. U., Ignatiev, N., Jaumann, R., Thomas, N., Michalik, H., Moissl, R., Russo, P. "Morphology and dynamics of the upper cloud layer of Venus." *Nature*. 450, 633-636. 2007.
- Marov, M. Y., Avdnevsy, V. S., Kerzhanovich, V. V., Rozhdestvensky, M. K., Borodin, N. F., Ryabov, O. L. "Venera 8: Measurements of temperature, pressure, and wind velocity on the illuminated side of Venus." *Journal of Atmospheric Sciences* **30**, 1210-1214. 1973.
- Marov, M. Y. and D. H. Grinspoon. "The planet Venus." Yale University Press, New Haven, CT. 1998.
- Mason, S. "Realistic specific power expectations for advanced radioisotope power systems." Proceedings of the 4th International Energy Conversion Engineering Conference (IECEC-2006), San Diego, CA. June 2006.
- McCluskey, F. P., R. Grzybowski, T. Podlesak. "High temperature electronics." CRC Press, Boca Raton, FL. 1996.
- McKinnon, W. B., Zahnle, K. J., Ivanov, B. A., Melosh, H. J. "Cratering on Venus: Models and observations. *Venus II* (S. W. Bougher, et al., Eds.). University of Arizona Press, Tucson, AZ, pp 969-1014. 1997.
- Meadows, V.S. and D. Crisp. "Ground-based near-infrared observations of the Venus nightside: The thermal structure and water abundance near the surface." *JGR* **101**, E2, 4595-4622. February 1996.
- Mellott, K. D. "Electronics and sensor cooling with a Stirling cycle for Venus surface mission," AIAA 2nd International Energy Conversion Engineering Conference, AIAA 2004-5610, Providence, RI. August 2004.
- Mellott, K. D. "Power conversion with a Stirling cycle for Venus surface mission." AIAA 2nd International Energy Conversion Engineering Conference, AIAA 2004-5622, Providence, RI. August 2004.
- Milbrath, B. D., Choate, B. J., Fast, J. E., Hensley, W. K., Kouzes, R. T., Schwepp, J. E., Comparison of LaBr<sub>3</sub>:Ce and NaI(Tl) scintillators for radioisotope identification devices. Vol. PIET-43741-TM-488, PNNL-15831. Pacific Northwest National Laboratory Report, p 18. 2006.
- Mocquet, A. "A search for the minimum number of stations needed for seismic networking on Mars." *Planetary and Space Science* **47**, 397-409. 1999.
- Moissl, R., Khatuntsev, I., Limaye, S. S., Titov, D., Markiewicz, W. J., Ignatiev, N., Roatsch, T., Matz, K. D., Jaumann, R., Almeida, M., Portyankina, G., Behnke, T., Hviid, S. "Venus cloud top winds from tracking UV features in VMC images." *Journal of Geophysical Research* **113**. 2008.
- Molina, M. J. and F. S. Rowland. "Chlorine atom-catalysed destruction of ozone." *Nature* **249**, 810-812. 1974.

- Mondt, J., Burke, K., Bragg, B., Rao, G., Vukson, S. "Energy storage technology for future space science missions." National Aeronautics and Space Administration, Technical Report, JPL D-30268 Rev. A. 2004.
- Morbidelli, A., Chambers, J., Lunine, J. I., Petit, J. M., Robert, F., Valsecchi, G. B., Cyr, R. E. "Source regions and timescales for the delivery of water to Earth." Meteoritics and Planetary Science **35**, 1309-1320. 2000.
- Moroz, V. I. "Estimates of visibility of the surface of Venus from descent probes and balloons." Planetary and Space Science **50**, pp 287-297. 2002.
- Morrison, C. R.. Siebert, M. W., Ho, E. J. "Electromagnetic Forces in a Hybrid Magnetic-Bearing Switched-Reluctance Motor," IEEE Transactions on Magnetics, Vol. 44, Issue 12, pp 4626-4638/ 2008.
- Mueller, N., Helbert, J., Hashimoto, G. L., Tsang, C. C. C., Erard, S., Piccioni, G., Drossart, P. "Venus surface thermal emission at one micrometer in VIRTIS imaging observation—evidence for variation of crust and mantle differentiation conditions." Journal of Geophysical Research **1117**. 2008.
- Nakamura, M. and P.-C. P. Team. "Present status of Venus Climate Orbiter (Planet-C)." 37th COSPAR Scientific Assembly, Symposium C31: Planetary Atmospheres. 2008.
- NASA-CheMin. <http://msl-scicorner.jpl.nasa.gov/Instruments/CheMin/>. 2009.
- NASA, Solar System Exploration Roadmap. Washington, DC, 2006.
- NASA, Solar System Exploration Roadmap. Washington, DC, 2006. Nock, K. T., Aaron, K. M., Jones, J. A., McGee, D. P., Powell, G. E., Yavrouian, A. H. and Wu, J. J., "Balloon Altitude Control Experiment (ALICE)", AIAA Paper 95-1632, 1995.
- National Research Council. "New frontiers in the solar system: An integrated exploration strategy." The National Academy Press, Washington, DC. 2003.
- National Research Council. "Committee on new opportunities in solar system exploration: An evaluation of the New Frontiers Announcement of Opportunity." The National Academies Press, Washington, DC. 2008.
- Navair, Multi-Species Gas Sensor Array project, Test and Evaluation/Science and Technology Program, Navair, Naval Undersea Warfare Center, Newport, RI, contract N66604-07-C-1828.
- Neudeck, P. G., Okojie, R. S., Chen, L.-Y. "High-temperature electronics—A role for wide bandgap semiconductors." Proceedings of the IEEE, vol. 90, pp 1065-1076. 2002.
- Neudeck, P. G. "SiC technology." *The VLSI Handbook*, the Electrical Engineering Handbook Series (W.-K. Chen, Ed.), pp 6.1-6.24. CRC Press and IEEE Press, Boca Raton, FL. 2000.
- Neudeck, P. G., D. J. Spry, L.-Y. Chen, C. W. Chang, G. M. Beheim, R. S. Okojie, L. J. Evans, R. Meredith, T. Ferrier, M. J. Krasowski, N. F. Prokop. "6H-SiC transistor integrated circuits demonstrating prolonged operation at 500 °C. 2008 IMAPS International

- Conference on High Temperature Electronics, May 12-15, Albuquerque, NM: International Microelectronics and Packaging Society, pp 95-101. 2008.
- Neudeck, P. G., D. J. Spry, L.-Y. Chen, C. W. Chang, G. M. Beheim, R. S. Okojie, L. J. Evans, R. Meredith, T. Ferrier, M. J. Krasowski, N. F. Prokop. "Long-term characterization of 6H-SiC transistor integrated circuit technology operating at 500 °C." Silicon Carbide 2008 - Materials, Processing and Devices, vol. 1069, Materials Research Society Symposium Proceedings (M. Dudley, A. R. Powell, C. M. Johnson, and S.-H. Ryu, Eds). Warrendale, PA: Materials Research Society. 2008.
- Neudeck, P. G., D. J. Spry, L.-Y. Chen, G. M. Beheim, R. S. Okojie, C. W. Chang, R. D. Meredith, T. L. Ferrier, L. J. Evans, M. J. Krasowski, N. F. Prokop. "Stable electrical operation of 6H-SiC JFETs and ICs for thousands of hours at 500 °C." IEEE Electron Device Letters, Vol. 29, No. 5. May 2008.
- Neudeck, P. G., R. S. Okojie, L.-Y. Chen. "High-temperature electronics—A role for wide bandgap semiconductors." Proceedings of the IEEE, vol. 90, pp 1065-1076. 2002.
- Newall, H. "Beyond the atmosphere: Early years of space science." NASA SP-4211, Washington, DC. 1980.
- Ni, X., J. Xie, Y. Fu, H. Morkoç, I.P. Steinke, Y. Liu, P.P. Ruden, K.-A. Son, B. Yang. "Investigation of current-voltage characteristics of n-GaN/i-Al<sub>x</sub>Ga<sub>1-x</sub>N/n-GaN structures." SPIE 6473, 11. 2007.
- Nimmo, F. "Constraining the crustal thickness on Mercury from viscous topographic relaxation." Geophysical Research Letters **29**, 7-1-7-4. 2002.
- Nock, K. T., Aaron, K. M., Jones, J. A., McGee, D. P., Powell, G. E., Yavrouian, A. H., Wu, J. J. "Balloon altitude control experiment (ALICE) project." AIAA Paper 95-1632. 1995.
- Ohme, .W., M. R. Larson, J. Riekels, S. Schlesinger, K. Vignarajah, M. N. Ericson. "Progress update on Honeywell's Deep Trek high temperature electronics project." International Conference on High Temperature Electronics, HiTEC. 2006.
- Ohme, B., T. Lucking, T, G. R. Gardner, E. Vogt, J. C. Tsang. "High temperature 0.8 micron 5V SOI CMOS for analog/mixed signal applications." 7th International HiTEC Conference, May 2004.
- Okojie, R. S., A. R. Atwell, K. T. Kornegay, S. L. Roberson, A. Beliveau. "Design considerations for bulk micromachined 6H-SiC high-G piezoresistive accelerometers." Tech. Digest 15th IEEE Intl. Conf. on MEMS, Las Vegas, NV, pp 618-622. Jan. 2002.
- Okojie, R. S., Beheim G. M., Saad G. J., Savrun E. "Characteristics of hermetic 6H-SiC pressure sensor at 600°C." AIAA Space 2001 Conference and Exposition, AIAA Paper No. 2001-4652, Albuquerque, NM. August 2001.
- Okojie, R. S., Fralick G. C., Saad G. J., Blaha C. A., Adamczyk J. J., Feiereisen J. M. "A single crystal SiC plug-and-play high temperature drag force transducer." *Digest of Technical Papers for Transducers 2003*, pp. 400-403, IEEE Catalog Number 03TH8664C, The 12th International Conference on Solid State Sensors, Actuators and Microsystems, Boston, MA. June 2003.

- Okojie, R. S., S. M. Page, M. Wolff. "Performance of MEMS-DCA SiC pressure transducers under various dynamic conditions." 2006 IMAPS International High Temperature Electronics Conference, Santa Fe, NM, pp 70-75. May 2006.
- Owen, T., Bar-Nun, A., Kleinfeld, I. "Possible cometary origin of heavy noble gases in the atmospheres of Venus, Earth and Mars." *Nature* **358**, 43-46. 1992.
- P. G. Neudeck, H. Du, M. Skowronski, D. J. Spy, A. J. Trunek. "Growth and characterization of 3C-SiC and 2H-AlN/GaN films and devices produced on step-free 4H-SiC mesa substrates." *J. Phys. D. Appl. Phys.* **40**, 6139-6149. 2007.
- Pace, N. "The universal nature of biochemistry." *Proceedings of the National Academy of Sciences* **98**, 805-808. 2001.
- Pearce, J. A. "Statistical analysis of major element patterns in basalts." *Journal of Petrology* **17**, 15-43. 1976.
- Pearce, J. A. "Geochemical fingerprinting of oceanic basalts with applications to ophiolite classification and the search for archean oceanic crust." *Lithos* **100**, 14-48. 2008.
- Penswick, L. B. and I. Urieli. "Duplex Stirling machines." QP-051082-A presented at the 19th Annual Intersociety Energy Conversion Engineering Conference, San Francisco, CA. 1984.
- Pepin, R. O. "On the origin and early evolution of terrestrial planet atmospheres and meteoritic volatiles." *Icarus* **92**, 2-79. 1991.
- Pepin, R. O. "Atmospheres on the terrestrial planets: Clues to origin and evolution." *Earth and Planetary Science Letters* **252**, 1-14. 2006.
- Pepin, R. O. "Atmospheric compositions: Key similarities and differences. *Origin and Evolution of Planetary and Satellite Atmospheres* (S. K. Atreya, et al., Eds.). University of Arizona Press, Tucson, AZ, pp 291-305. 1989.
- Peralta, J., Hueso, R., Sanchez-Lavega, A. "A reanalysis of Venus winds at two levels from Galileo SSI images." *Icarus* **190**, 469-477. 2007.
- Peterson, C., Cutts, J., Balint, T., Hall, J. "Rapid cost assessment of space mission concepts through application of complexity-based cost indices." IEEE Aerospace Conference, Big Sky, Montana, paper #1632. 2008.
- Pettengill, G. H., Dyce, R. B., Campbell, D. B. "Radar measurements at 70 CM of Venus and Mercury." *Astronomical Journal* **72**, 330. 1967.
- Pettengill, G. H., Ford, P. G., Chapman, B. "Venus: Surface electromagnetic properties." *Journal of Geophysical Research* **93**, 14881-14892. 1988.
- Pettengill, G. H., Ford, P. G., Nozette, S. "Venus: Global surface radar reflectivity." *Science* **217**, 640-642. 1982.
- Phillips, R. J., Arvidson, R. E., Boyce, J. M., Campbell, D. B., Guest, J. E., Schaber, G. G., Soderblom, L. A. "Impact craters on Venus: Initial analysis from Magellan." *Science* **252**, 288-297. 1991.

- Phillips, R. J., Bullock, M. A., Hauck, S. A. "Climate and interior coupled evolution on Venus." *Geophysical Research Letters* **28**, 1779-1782. 2001.
- Phillips, R. J. and V. L. Hansen. "Geological evolution of Venus: Rises, plains, plumes and plateaus." *Science* **279**, 1492-1497. 1998.
- Phillips, R. J., Raubertas, R. F., Arvidson, R. E., Sarker, I. C., Herrick, R. R., Izenberg, N. R., Grimm, R. E. "Impact craters and Venus resurfacing history." *Journal of Geophysical Research* **97**, 15,923-15,948. 1992.
- Phillips, R., J. Johnson, C. L., Mackwell, S. L., Morgan, P., Sandwell, D. T., Zuber, M. T. "Lithospheric mechanics and dynamics of Venus." *Venus II: Geology, Geophysics, Atmosphere, and Solar Wind Environment* (S. W. Bougher, et al., Eds.). University of Arizona Press, Tucson, pp 1163-1204. 1997.
- Piccialli, A., Titov, D. V., Grassi, D., Khatuntsev, I., Drossart, P., Piccioni, G., Migliorini, A. "Cyclostrophic winds from the Visible and Infrared Thermal Imaging Spectrometer temperature sounding: A preliminary analysis." *Journal of Geophysical Research-Planets* **113**. 2008.
- Piccioni, G., Drossart, P., Sanchez-Lavega, A., Hueso, R., Taylor, F. W., Wilson, C. F., Grassi, D., Zasova, L., Moriconi, M., Adriani, A., Lebonnois, S., Coradini, A., Bezard, B., Angrilli, F., Arnold, G., Baines, K. H., Bellucci, G., Benkhoff, J., Bibring, J. P., Blanco, A., Blecka, M. I., Carlson, R. W., Di Lellis, A., Encrenaz, T., Erard, S., Fonti, S., Formisano, V., Fouchet, T., Garcia, R., Haus, R., Helbert, J., Ignatiev, N. I., Irwin, P. G. J., Langevin, Y., Lopez-Valverde, M. A., Luz, D., Marinangeli, L., Orofino, V., Rodin, A. V., Roos-Serote, M. C., Saggin, B., Stam, D. M., Titov, D., Visconti, G., Zambelli, M. "South-polar features on Venus similar to those near the north pole." *Nature* **450**, 637-640. 2007.
- Pollack, H. N., Hurter, S. J., Johnson, J. R. "Heat flow from the Earth's interior: Analysis of the global data set." *Reviews of Geophysics* **31**, 267-280. 1993.
- Pollack, J. B. and C. Sagan. "An analysis of the Mariner 2 microwave observations of Venus." *Astrophysical Journal* **150**, 327. 1967.
- Pollack, J. B., Toon, O. B., Boese, R. "Greenhouse models of Venus' high surface temperature, as constrained by Pioneer Venus measurements." *Journal of Geophysical Research* **85**, 8223-8231. 1980.
- Powell, A.J., Neudeck, P. G., Trunek, A. J., Spry, D. J. "Method for the growth of large low-defect single crystals." United States Patent 7449065. 2008.
- Prinn, R. G. "Climate change on Venus." *Nature* **412**, 36-37. 2001.
- Prinn, R. G. "The sulfur cycle and clouds of Venus." *Recent Advances in Planetary Meteorology* (G. E. Hunt, Ed.). Cambridge University Press, Cambridge. 1985.
- Radebaugh, R. "Pulse tube cryocoolers for cooling infrared sensors." *Proceedings of SPIE, The International Society for Optical Engineering, Infrared Technology and Applications XXVI*, Vol. 4130, pp 363-379 (see in particular Fig. 7). 2000.

- Raymond, S. N., Mandell, A. M., Sigurdsson, S. "Exotic Earths: Forming habitable worlds with giant planet migration." *Science* **313**, 1413-1416. 2006.
- Ringwood, A. E. and D. L. Anderson, D. L. "Earth and Venus: Comparative study." *Icarus* **30**, 243-253. 1977.
- Rosado, L., Forster, N.H., Trivedi, H.K., King, J.P. "Solid lubrication of silicon nitride with cesium-based compounds: Part I—Rolling contact endurance, friction and wear tribology transactions." Volume 43, Issue 3, pp 489–497. July 2000.
- Ross, R. and R. F. Boyle. "NASA space cryocooler program: An overview." International Cryocooler Conference. 2002.
- Rowland, F. S. "Stratospheric ozone depletion." *Philosophical Transactions of the Royal Society* **361**, 769-790. 2006.
- Russell, C. T., Elphic, R. C., Slavin, J. A. "Limits on the possible intrinsic magnetic field of Venus." *Journal of Geophysical Research* **85**, 8319-8332. 1980.
- Russell, C. T., Zhang, T. L., Delva, M., Magnes, W., Strangeway, R. J., Wei, H. Y. "Lightning on Venus inferred from whistler mode waves in the ionosphere." *Nature* **450**, 661-662. 2007.
- Russell, C. T., Zhang, T. L., Wei, H. Y. "Whistler mode waves from lightning on Venus: Magnetic control of ionospheric access." *Journal of Geophysical Research-Planets* **113**. 2008.
- Sagdeev, R. V., Linkin, V. M., Blamont, J. E., Preston, R. A. "The VEGA Venus balloon experiment." *Science* **231**, 1407-1408. 1986.
- Sanchez-Lavega, A., Hueso, R., Piccioni, G., Drossart, P., Peralta, J., Perez-Hoyos, S., Wilson, C. F., Taylor, F. W., Baines, K. H., Luz, D., Lebonnois, S. "Variable winds on Venus mapped in three dimensions." *Geophysical Research Letters* **35**, L13204, doi:10.1029/2008GL033817. 2008.
- Sarrazin, P., Blake, D. F., Feldman, S., Chipera, S., Vaniman, D. T., Bish, D. L. "Field deployment of a portable X-ray diffraction/S-ray fluorescence instrument on Mars analog terrain." *Powder Diffraction* **20**, 128-133. 2005.
- Sato, M., Travis, L. D., Kawabata, K. "Photopolarimetry analysis of the Venus atmosphere in polar regions." *Icarus* **124**, 569-585. 1996.
- Saunders, R. S., Spear, A. J., Allin, P. C., Austin, R. S., Berman, A. L., Chandler, R. C., Clark, J., deCharon, A. V., DeJong, E. M., Griffith, D. G., Gunn, J. M., Hensley, S., Johnson, W. T. K., Kirby, C. E., Leung, K. S., Lyons, D. T., Michaels, G. A., Miller, J., Morris, R. B., Pierson, R. G., Scott, J. F., Schaffer, S. J., Slonski, J. P., Stofan, E. R., Thompson, R. W., Wall, S. D. "Magellan mission summary." *Journal of Geophysical Research* **97**, 13067-13090. 1992.
- SBIR Final Report. "Miniature solid-state sulfur oxide sensor for emission measurement." Contract # NNC04CA39C, Phase I SBIR. 2004.

- SBIR Sunpower. "High specific power multiple-cylinder free-piston alpha Stirling, sunpower, Inc." SBIR contract NNC07CA11C.
- Schaefer, L. and B. Fegley. "Volatile element geochemistry in the lower atmosphere of Venus." *Lunar and Planetary Science XXXV*, 1182. 2004.
- Schlwig J., G. Muller, M. Eickhoff, O. Ambacher, M. Stutzmann. "Gas sensitive GaN/AlGaN heterostructures." *Sensors and Actuators B87*, 425-430. 2002.
- Schofield, J. T. and F. W. Taylor. "Net global thermal emission from the Venus upper atmosphere." *Icarus* **52**, 245-262. 1982.
- Schreiber, J. G. "Developmental considerations on the free-piston Stirling power convertor for use in space." Proceedings of the 4th International Energy Conversion Engineering Conference (IECEC-2006), San Diego, CA. June 2006.
- Schreiber, J. G. "Assessment of the free-piston Stirling convertor as a long life power convertor for space." AIAA-2000-3021. 2000.
- Schubert, G., Covey, C., Del Genio, A., Elson, L. S., Haskins, R. D., McCleese, D. J., Martonchik, J. V., Reichley, P. E., Bradley, S. P., Delderfield, J., Schofield, J. T., Farmer, C. B., Froidevaux, L., Leung, J., Coffey, M. T., Gille, J. C. "Structure and circulation of the Venus atmosphere." *Journal of Geophysical Research* **85**, 8007-8025. 1980.
- Schubert, G. "General circulation and the dynamical state of the Venus atmosphere." *Venus* (D. M. Hunten, et al., Eds.). University of Arizona Press, Tucson, AZ, pp 681-765. 1983.
- Schubert, G. and D. T. Sandwell. "A global survey of possible subduction sites on Venus." *Icarus* **117**, 173-196. 1995.
- Schubert, G., Solomatov, V. S., Tackley, P. J., Turcotte, D. L. "Mantle convection and the thermal evolution of Venus." *Venus II* (S. W. Bougher, et al., Eds.). University of Arizona Press, Tucson, AZ, pp 1245-1288. 1997.
- Schulze-Makuch, D., Grinspoon, D. H., Abbas, O., Irwin, L. N., Bullock, M. A. "A sulphur-based survival strategy for putative phototrophic life in the Venusian atmosphere." *Astrobiology* **4**, 11-18. 2004.
- Schwartz, D. Z. and E. G. Ponchak. "1 GHz, 200 °C, SiC MESFET Clapp oscillator." *IEEE Microwave and Wireless Component Lett.* Vol. 15, No. 11, pp 730-732. 2005.
- Schwartz, Z. D. and G. E. Ponchak, "High temperature performance of a SiC MESFET based oscillator," 2005 IEEE MTT-S Int. Microwave Symp. Dig. Long Beach, CA, pp 1179-1182. June 2005.
- Seghi, S. "Venus lander experiment vessel: Design and modeling." National Space and Missile Material Symposium, Keystone, CO. 2007.
- Seiff, A., Kirk, D. B., Young, R. E., Blanchard, R. C., Findlay, J. T., Kelly, G. M., Sommer, S. C. "Measurements of thermal structure and thermal contrasts in the atmosphere of Venus and related dynamical observations: Results from the four Pioneer Venus probes." *Journal of Geophysical Research* **85**, 7903-7933. 1980.

- Seiff, A. "The thermal structure of the atmosphere." *Venus* (D. M. Hunten, et al., Eds.), University of Arizona Press, Tucson, AZ, pp 215-279. 1983.
- Shaltens, R. K. and W. A. Wong. "Advanced Stirling technology development at NASA Glenn Research Center." NASA/TM—2007-214930. 2007.
- Shaltens, R. K. "Future opportunities for dynamic power systems for NASA missions." Proceedings of the International Stirling Forum 2006, Osnabruck, Germany, NASA/TM-2007-214707. September 2006.
- Shearer, P. M. "Introduction to Seismology." Cambridge University Press. 1999.
- Simms, L., et al. "First use of a HyViSI H4RG for astronomical observations." Proc. of SPIE 6690. 2007.
- Simons, M., Solomon, S. C., Hager, B. H. "Localization of Gravity and Topography: Constraints on the Tectonics and Mantle Dynamics of Venus." *Geophys. J. Int.* **131**, 24-44. 1997.
- Sleep, N. H. "Evolution of the mode of convection within terrestrial planets." *Journal of Geophysical Research* **105**, 17,563-17,578. 2000.
- Smith, D. E., Zuber, M. T., Frey, H. V., Garvin, J. B., Head, J. W., Muhleman, D. O., Pettengill, G. G., Phillips, R. J., Solomon, S. C., Zwally, H. J., Banerdt, W. B., Duxbury, T. C., Golombek, M. P., Lemoine, F. G., Neumann, G. A., Rowlands, D. D., Aharonson, O., Ford, P. G., Ivanov, A. B., Johnson, C. L., McGovern, P. J., Abshire, J. B., Afzal, R. S., Sun, X. "Mars Orbiter laser altimeter: Experiment summary after the first year of global mapping of Mars." *Journal of Geophysical Research* **106**, 23,689-23,722. 2001.
- Smith, M., Schallenkamp, R. S., Ekstein, C. J., Blizzard, K. "Development of Venus aerobots." AIAA International Balloon Technology Conference, San Francisco, CA, paper AIAA-97-1446. June 1997.
- Smith, P. H. "The Phoenix mission explores the Martian arctic." Fall 2008 AGU Meeting, Abstract P13F-01. 2008.
- Smrekar, S. E., Kiefer, W. S., Stofan, E. R. "Large volcanic rises on Venus." *Venus II: Geology, Geophysics, Atmosphere, and Solar Wind Environment* (S. W. Bougher, et al., Eds.), University of Arizona Press, Tucson, AZ, pp 845-878. 1997.
- Solomatov, V. S. and L. N. Moresi. "Stagnant lid convection on Venus." *Journal of Geophysical Research* **101**, 4737-4753. 1996.
- Solomon, S. C., Bullock, M. A., Grinspoon, D. H. "Climate change as a regulator of tectonics on Venus." *Science* **286**, 87-89. 1999.
- Solomon, S. C. and J. W. Head. "Fundamental issues in the geology and geophysics of Venus." *Science* **252**, 252-260. 1991.
- Solomon, S. C., Smrekar, S. E., Bindschadler, D. L., Grimm, R. E., Kaula, W. M., McGill, G. E., Phillips, R. J., Saunders, R. S., Schubert, G., Squyres, S. W., Stofan, E. R. "Venus tectonics: An overview of Magellan observations." *Journal of Geophysical Research* **97**, 13199-13256. 1992.

- Son K.-A., Y. Liu, P. P. Ruden, J. Xie, N. Biyikli, Y. T. Moon, N. Onojima, H. Morkoç. “GaN-based micro pressure sensor for extreme environments.” Proc. IEEE Sensors, 1259. 2005.
- Son K.-A., B. H. Yang, A. Liao, N. Prokopuk, J. S. Moon, T. M. Katona, M. A. Khan. “Novel GaN micro chemical sensor nodes for long-range trace chemical agent detection and mapping.” Proceedings of 2008 Chemical and Biological Defense Physical Science and Technology. 2008.
- Son K.-A., B. Yang, N. Prokopuk, J.S. Moon, A. Liao, M. Gallegos, J. Yan, M.A. Khan. “GaN-based micro chemical sensor nodes for early warning of chemical agents.” Proceedings of SPIE 6556 Micro (MEMS) and Nanotechnologies for Defense and Security, paper # 6556-36. 2007.
- Space Sciences Board. “Review of planetary quarantine policy.” ad hoc Committee for Review of Planetary Quarantine Policy, Space Science Board of the National Research Council, National Academy of Sciences, Washington, DC, pp 3-4. 1972.
- Space Sciences Board. “Venus: Strategy for exploration.” Report of a study by the Space Science Board of the National Research Council, National Academy of Sciences, Washington, DC, pp 12-13. 1970.
- Space Studies Board. “New frontiers in the solar system: An integrated exploration strategy.” National Research Council, National Academy Press, Washington, DC. 2003.
- Spry, D. J., P. G. Neudeck, L.-Y. Chen, G. M. Beheim, R. S. Okojie, C. W. Chang, R. D. Meredith, T. L. Ferrier, L. J. Evans. “Fabrication and testing of 6H-SiC JFETs for prolonged 500 °C operation in air ambient.” *Silicon Carbide and Related Materials 2007*, Materials Science Forum, T. Kimoto, Ed., Switzerland: Trans Tech Publications. 2008.
- Squyres, S. W., Arvidson, R. E., Bell, J. F., III, Bruckner, J., Cabrol, N. A., Calvin, W., Carr, M. H., Christensen, P. R., Clark, B. C., Crumpler, L., Des Marais, D. J., d'Uston, C., Economou, T., Farmer, J., Farrand, W., Folkner, W., Golombek, M., Gorevan, S., Grant, J. A., Greeley, R., Grotzinger, J., Haskin, L., Herkenhoff, K. E., Hviid, S., Johnson, J., Klingelhofer, G., Knoll, A., Landis, G., Lemmon, M., Li, R., Madsen, M. B., Malin, M. C., McLennan, S. M., McSween, H. Y., Ming, D. W., Moersch, J., Morris, R. V., Parker, T., Rice, J. W., Jr., Richter, L., Rieder, R., Sims, M., Smith, M., Smith, P., Soderblom, L. A., Sullivan, R., Wanke, H., Wdowiak, T., Wolff, M., Yen, A. “The Spirit rover's Athena science investigation at Gusev Crater, Mars.” *Science* **305**, 794-799. 2004a.
- Squyres, S. W., Arvidson, R. E., Bell, J. F., III, Bruckner, J., Cabrol, N. A., Calvin, W., Carr, M. H., Christensen, P. R., Clark, B. C., Crumpler, L., Marais, D. J. D., d'Uston, C., Economou, T., Farmer, J., Farrand, W., Folkner, W., Golombek, M., Gorevan, S., Grant, J. A., Greeley, R., Grotzinger, J., Haskin, L., Herkenhoff, K. E., Hviid, S., Johnson, J., Klingelhofer, G., Knoll, A. H., Landis, G., Lemmon, M., Li, R., Madsen, M. B., Malin, M. C., McLennan, S. M., McSween, H. Y., Ming, D. W., Moersch, J., Morris, R. V., Parker, T., Rice, J. W., Jr., Richter, L., Rieder, R., Sims, M., Smith, M., Smith, P., Soderblom, L. A., Sullivan, R., Wanke, H., Wdowiak, T., Wolff, M., Yen, A. “The Opportunity rover's Athena science investigation at Meridiani Planum, Mars.” *Science* **306**, 1698-1703. 2004b.

- Squyres, S. W., Grotzinger, J. P., Arvidson, R. E., Bell, J. F., III, Calvin, W., Christensen, P. R., Clark, B. C., Crisp, J. A., Farrand, W. H., Herkenhoff, K. E., Johnson, J. R., Klingelhofer, G., Knoll, A. H., McLennan, S. M., McSween, H. Y., Jr., Morris, R. V., Rice, J. W., Jr., Rieder, R., Soderblom, L. A. "In situ evidence for an ancient aqueous environment at Meridiani Planum, Mars." *Science* **306**, 1709-1714. 2004.
- Squyres, S. W. and A. H. Knoll. "Sedimentary rocks at Meridiani Planum: Origin, diagenesis, and implications for life on Mars." *Earth and Planetary Science Letters* **240**, 1-10. 2005.
- Squyres, S. W., Knoll, A. H., Arvidson, R. E., Clark, B. C., Grotzinger, J. P., Jolliff, B. L., McLennan, S. M., Tosca, N., Bell, J. F., III, Calvin, W. M., Farrand, W. H., Glotch, T. D., Golombek, M. P., Herkenhoff, K. E., Johnson, J. R., Klingelhofer, G., McSween, H. Y., Yen, A. S. "Two years at Meridiani Planum: Results from the Opportunity rover." *Science* **313**, 1403-1407. 2006.
- Sternowski, R. H. "Extreme temperature design techniques for a Venus exploration S-band transmitter." 6th International Planetary Probe Workshop, Atlanta, GA. June 2008.
- Stevenson, D. J., Spohn, T., Schubert, G. "Magnetism and thermal evolution of the terrestrial planets." *Icarus* **54**, 466-489. 1983.
- Stofan, E. R., Brian, A. W., Guest, J. E. "Resurfacing styles and rates on Venus: Assessment of 18 Venusian quadrangles." *Icarus* **173**, 312-321. 2005.
- Stofan, E. R., Hamilton, V. E., Janes, D. M., Smrekar, S. E. "Coronae on Venus: Morphology and origin." *Venus II: Geology, Geophysics, Atmosphere, and Solar Wind Environment* (S. W. Bougher, et al., Eds.). University of Arizona Press, Tucson, AZ, pp 931-965. 1997.
- Strom, R. G., Schaber, G. G., Dawson, D. D. "The global resurfacing of Venus." *Journal of Geophysical Research* **99**, 10899-10926. 1994.
- Suomi, V. E. and S. S. Limaye. "Venus—Further evidence of vortex circulation." *Science* **201**, 1009-1011. 1978.
- Surkov, Y. A., Barsukov, V. L., Moskalyeva, L. P., Kharyukova, V. P., Kemurdzhian, A. L. "New data on the composition, structure and properties of Venus rock obtained by Venera 13 and Venera 14." Proceedings of the 14th Lunar and Planetary Science Conference, Vol. 89, *Journal of Geophysical Research*, pp B393-B402. 1984.
- Suryanarayana, C. and M. G. Norton. "X-ray diffraction: A practical approach." Plenum Press, New York. 1998.
- Svedhem, H., Titov, D. V., McCoy, D., Lebreton, J. P., Barabash, S., Bertaux, J. L., Drossart, P., Formisano, V., Häusler, B., Koralev, O., Markiewicz, W. J., Nevejans, D., Pätzold, M., Piccioni, G., Zhang, T. L., Taylor, F. W., Lellouch, E., Koschny, D., Witasse, O., Eggel, H., Warhaut, M., Accomazzo, A., Rodriguez-Canabal, J., Fabrega, J., Schirrmann, T., Clochet, A., Coradini, M. "Venus Express—The first European mission to Venus." *Planetary and Space Science* **55**, 1636-1652. 2007.
- Titov, D. V., Bullock, M. A., Crisp, D., Renno, N. O., Taylor, F. W., Zasova, L. V. "Radiation in the atmosphere of Venus." *Exploring Venus as a Terrestrial Planet* (L. W. Esposito, Ed.). American Geophysical Union, Washington, DC. 2007.

- Tobie, G., Forget, F., Lott, F. "Numerical simulation of the winter polar wave clouds observed by Mars Global Surveyor Mars Orbiter Laser Altimeter." *Icarus* **164**, 33-49. 2003.
- Treiman, A. H. "Compositions of igneous rocks on Venus." AGU Fall Meeting, San Francisco, pp. P31A-04. 2007.
- Trenberth, K. E. (Ed.) "Climate System Modeling." Cambridge University Press, Cambridge. 1992.
- Urey, H. C. "The Planets." Yale University Press, New Haven, CT. 1952.
- Vaniman, D. T., Bish, D. L., Blake, D. F., Elliott, S. T., Sarrazin, P., Collins, S. A., Chipera, S. "Landed XRD/XRF analysis of prime targets in the search for past or present Martian life." *Journal of Geophysical Research* **103**, 31,477-31,490. 1998.
- Venkatapathy, E., Laub, B., Hartman, G. J., Arnold, J. O., Wright, M. J., and Allen, G. A. "Selection and certification of TPS: Constraints and considerations for Venus missions." 6th International Planetary Probe Workshop, Atlanta, GA, June 2008.
- Verma, S. P., Guevara, M., Agrawal, S. "Discriminating four tectonic settings: Five new geochemical diagrams for basic and ultrabasic volcanic rocks based on log-ratio transformation of major-element data." *Journal of Earth System Science* **115**, 485-525. 2006.
- Vermeesh, P. "Tectonic discrimination of basalts with classification trees." *Geochemica et Cosmochimica Acta* **70**, 1839-1884. 2006.
- VEXAG. "Venus scientific goals, objectives, investigations, and priorities: 2007." S. Atreya, J. Luhman, eds. 2007.
- Volkov V. P., Zolotov M. Yu., Khodakovsky I. L. "Lithospheric-atmospheric interaction on Venus." *Chemistry and Physics of Terrestrial Planets* (S.K. Saxena ed.), Chapter 4 (136-190), Springer, NY. 1986.
- Waite, J. H., Lewis, W. S., Kasprzak, W. T., Anicich, V. G., Block, B. P., Cravens, T. E., Fletcher, G. G., Ip, W.-H., Luhmann, J. G., McNutt, R. L., Niemann, H. B., Parejko, J. K., Richards, J. E., Thorpe, R. L., Walter, E. M., Yelle, R. V. "The Cassini Ion and Neutral Mass Spectrometer (INMS) Investigation", *Space Science Reviews*, Vol. 114, Nos 1-4, pp.113-231. 2008.
- Waite, J. H., Jr., Combi, M. R., Ip, W.-H., Cravens, T. E., McNutt, R. L., Jr., Kasprzak, W., Yelle, R., Luhmann, J., Niemann, H., Gell, D., Magee, B., Fletcher, G., Lunine, J., Tseng, W.-L. "Cassini Ion and Neutral Mass Spectrometer: Enceladus plume composition and structure. *Science* **311**, 1419-1422. 2006.
- Walker, J. C. G., Hays, P. B., Kasting, J. F. "A negative feedback mechanism for the long-term stabilization of Earth's surface temperature." *Journal of Geophysical Research* **86**, 9776-9782. 1981.
- Wang, R., W. H. Ko, D. J. Young. "Silicon-carbide MESFET-based 400 °C MEMS sensing and data telemetry." *IEEE Sensors Journal*, Vol. 5, No. 6, pp 1389-1394. Dec. 2005.

- Wanke, H., Bruckner, J., Dreibus, G., Rieder, R., Ryabchikov, I. Chemical composition of rocks and soils at the Pathfinder site. *Space Science Reviews*. **96**, 317-330. 2001
- Ward, S. T. Allen and J. Palmour. "Reliability assessment of production SiC MESFETS." *GaAs MANTECH Technical Digest*, New Orleans, LA. 2005.
- Watson, E. B., Thomas, J. B., Cherniak, D. J. "40 Ar retention in the terrestrial planets." *Nature* **449**, 299-304. 2007.
- Wierzchos, D. M. and C. Ascaso. "Microbial fossil record of rocks from the Ross Desert, Antarctica: Implications in the search for past life on Mars." *International Journal of Astrobiology* **1**, 51-59. 2002.
- Wilson, C., O'Neill, A., Baier, S., Nohawa, J. "A complementary III-V heterostructure field effect transistor technology for high temperature integrated circuits." vol.29, p.54-57. 1995.
- Winchester, J. A. and P. A. Floyd. "Geochemical discrimination of different magma series and their differentiation products using immobile elements." *Chemical Geology* **20**, 325-343. 1977.
- Wong, W.A. "Advanced radioisotope power conversion technology research and development." Second International Energy Conversion Engineering Conference, Providence, RI, NASA/TM-2004-213352; paper AIAA-2004-5515. August 2004.
- Wood, J. A. "Rock weathering on the surface of Venus." *Venus II* (S. W. Bougher, et al., Eds.). University of Arizona Press, Tucson, AZ, pp 637-664. 1997.
- Wrbanek, J.D. and G. C. Fralick. "Thin film physical sensor instrumentation research and development at NASA Glenn Research Center." NASA TM-2006-214395, ISA# TP06IIS023. September 2006.
- Würfl, J., Hilsenbeck, J., Nebauer, E., Tränkle, G., Obloh, H., Österlem W. "Reliability of AlGaN/GaN HFETs comprising refractory ohmic and Schottky contacts." *Microelectronics Reliability*, Volume 40, Issues 8-10, pp 1689-1693. 2000.
- [www.honeywell.com/sites/portal?smap=aerospace&page=Hi](http://www.honeywell.com/sites/portal?smap=aerospace&page=Hi) - Honeywell high temperature electronic components website
- Yan, Z. and R. W. Clayton. "Regional mapping of the crustal structure in Southern California from receiver functions." *Journal of Geophysical Research* **112**, B05311, doi:10.1029/2006JB004622. 2007.
- Yavrouian, A., Plett, G., Yen S. P. S., Cutts, J., Baek, D. "Evaluation of materials for Venus aerobot applications." AIAA International Balloon Technology Conference, Norfolk, VA, AIAA-1999-3859. 1999.
- Yung, Y. L. and M. Liang. "Modeling the distribution of CO in the atmosphere of Venus." *B.A.A.S.* **40**, Abstract 62.05. 2008.
- Zacny, K., Bar-Cohen, Y., Brennan, M., Briggs, G., Cooper, G., Davis, K., Dolgin, B., Glaser, D., Glass, B., Gorevan, S., Guerrero, J., McKay, C., Paulsen, G., Stanley, S., Stoker, C. *Astrobiology*. 8(3): 665-706. 2008/

- Zahnle, K. J. "Earth after the moon forming impact." *Geochimica et Cosmochimica Acta* **70**, A729-A729. 2006.
- Zahnle, K. J. "Planetary noble gases." *Protostars and Planets III* (E. H. Levy, J. I. Lunine, Eds.). University of Arizona Press, Tucson, AZ, pp 1305-1338. 1993.
- Zuber, M. T., Smith, D. E., Solomon, S. C., Phillips, R. J., Peale, S. J., Head, J. W., III, Hauck, S. A., II, McNutt, R. L., Jr., Oberst, J., Neumann, G. A., Lemoine, F. G., Sun, X., Barnouin-Jha, O., Harmon, J. K. "Laser altimeter observations from MESSENGER's first Mercury flyby." *Science* **321**, 77-79. 2008.

## A Choosing the Mission Architecture

The Chapter 2 describes far more science investigations than can possibly be accomplished in any given flagship mission to Venus. Therefore, it is necessary to take that overarching scientific framework and synthesize a viable flagship mission for the 2020 - 2025 time frame that satisfies the key constraint of not exceeding a total mission cost of \$3 B to \$4 B. This chapter will describe the process by which the study team achieved this synthesis and selected the mission architecture for the Design Reference Mission (DRM). At the core of this process was a trade study that generated, for a variety of candidate mission architectures, numerical ratings for scientific merit, technological difficulty, and mission complexity. The scientific merit metrics were developed by the STDT starting from the

scientific framework described in Chapter 2. The technological difficulty and mission complexity ratings were developed and then translated into predicted mission costs using the rapid cost assessment methodology described in Peterson et al. (2008). The final result was a set of candidate mission architectures using various platforms (orbiters, landers, balloons, probes, etc.) in different combinations that were rated for both scientific merit and mission cost. These candidates were then compared to each other, and a final choice made that maximized the science return subject to the \$3 B to \$4 B mission cost constraint. The overall analysis process is schematically illustrated in Figure A.1.

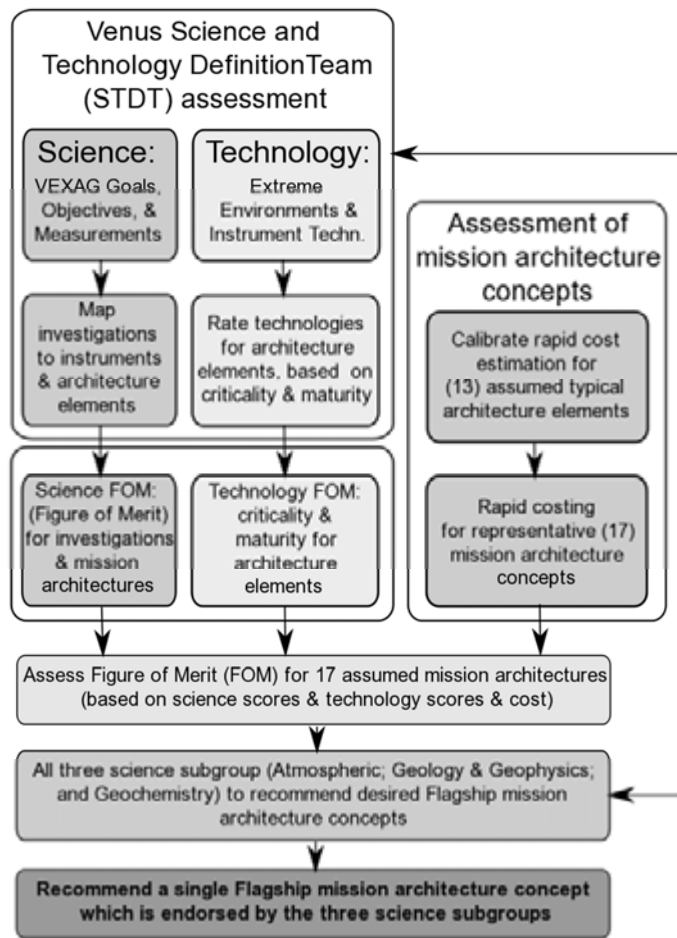


**Figure A.1:** Flowchart of the selection process used by the STDT to define a single Venus flagship mission architecture.

The STDT adopted the assumption that there would be no other Venus missions between the time of this study report and the execution of the Venus flagship mission in the 2020 - 2025 time frame. This assumption implies that the current scientific understanding of Venus can provide the basis on which to assess the relative merits of proposed Venus science investigations for the flagship mission. One consequence of this approach is that the science and mission architecture recommendations produced in this study will have to be re-assessed in light of any science data return from other new missions to Venus. It seems likely that such a re-assessment will include the removal of some investigations and the addition of others to the flagship mission, with attendant changes to the mission architecture and technology development needs. The possibility of such changes underlies the discussion presented in Chapter 5 in which are discussed the high-priority science investigations that were not selected for the Design Reference Mission but could be added later in response to results from one or more precursor missions. The technology requirements associated with those alternate science investigations are also discussed in Chapter 5.

### A.1 Venus Flagship Mission Science

The STDT began its study to determine the most valuable science that could be achieved by a flagship mission to Venus by referring to recent NASA and National Research Council (NRC) science planning documents. The 2003 Solar System Decadal Survey, *New Frontiers in the Solar System: An Integrated Exploration Strategy* (Space Studies Board, 2003), was the first effort by the NRC to prioritize planetary science and medium- to large-class missions for planetary exploration. The most recent NASA Solar System exploration roadmap, which establishes the investigative framework and objectives for NASA's Science Mission Directorate (NASA, 2006), was also used to guide the STDT's assessment of important flagship mission science at Venus. The Venus Exploration Analysis Group (VEXAG) has

also undertaken a community-wide effort to define and prioritize scientific objectives for the exploration of Venus. The latest report from this NASA-sponsored body, entitled *VEXAG Goals, Objectives, Investigations, and Priorities: 2007* (VEXAG, 2007), presents a reviewed science consensus of Venus exploration goals, objectives, investigations, and priorities. VEXAG determined that the highest-level issues to be addressed by the exploration of Venus are expressed by three overarching goals:

- *Origin and Early Evolution of Venus:* How did Venus originate and evolve, and what are the implications for the characteristic lifetimes and conditions of habitable environments on Venus and similar extrasolar systems?
- *Venus as a Terrestrial Planet:* What are the processes that have shaped and still shape the planet?
- *Implications for Earth:* What does Venus tell us about the fate of the Earth's environment?

Each VEXAG goal is divided into high-level science objectives, and each objective is addressed by investigations or experiments. These VEXAG science objectives and investigations were taken as the starting point in assessing the science that could be accomplished with a flagship mission to Venus.

The process of prioritizing science experiments at Venus and indicating what instruments and spacecraft architecture elements can best execute them is described in the sections that follow. The results of this effort are summarized in Chapter 2, Foldout 1. The investigations are mapped to instruments and spacecraft architecture elements in Foldout 1. Architecture elements are the orbiters, landers, balloons, or other in situ and mobile elements that can make up a flagship mission to Venus and are presented in Table A.1.

**Table A.1:** Mission architecture elements, FOMs, and cost estimates.

Architecture Element	Description	Science FOM	Tech. FOM	Cost est.
Orbiter	Self-evident, but can dip into the exosphere for in situ sampling	177	0	\$0.53B
High-Level Aerial	Altitude >70 km, above clouds	169	3	\$0.47B
Mid-Level Aerial	Altitude 52–70 km, in clouds (about the same altitude as the VEGA balloons)	191	3	\$0.42B
Low-Level Aerial	Altitude 15–52 km, below clouds, limited view of surface due to attenuation	176	14	\$1.7B
Near-Surface Aerial	Altitude 0–15 km, NIR imaging of surface is possible, no surface access	170	20	\$3.1B
Single Entry Probe	No surface access, descent science only	136	2	\$0.45B
Multiple Entry Probes	No surface access, descent science only	171	2	\$0.47B
Short-Lived Lander	Single lander, about 5–10 hours lifetime on surface, passive cooling	153	12	\$1.1B
Short-Lived Landers	Multiple landers, about 5–10 hours lifetime on surface, passive cooling	214	12	\$0.94B
Long-Lived Lander	Single lander, days to weeks lifetime, may require active cooling and RPS	223	21	\$3.5B
Long-Lived Landers	Multiple landers, days to weeks lifetime, may require active cooling and RPS, long lived network possible	264	21	\$3.5B
Surface System with Mobility	Active or passive cooling, mobility with surface access at multiple locations (e.g., rover with short traverse or metallic bellows with long traverse)	209	53	\$7.1B
Coordinated Atmospheric Platforms	Large number (e.g., swarm) of in situ elements, with simultaneous measurements	129	21	\$12.9B

There are some artifacts from this approach as presented. In considering single versus multiple identical elements, it must be borne in mind that it costs more *per element* to develop one lander or probe than it does to develop multiple landers or probes (due to the fact that all design and some test costs can be amortized over the multiple copies). Therefore, the single versions of landers and probes shows a higher cost than the multiple versions, as these results show the *per element* cost. Also, the costs shown in Table A.1 do not include launch vehicles or the science payload costs, which could vary substantially.

## A.2 Constructing the Science Analysis Matrix

The VEXAG report (VEXAG, 2007) contains 104 detailed science investigations that fall under the three primary science goals for Venus exploration; many investigations support multiple science objectives and are combined where such commonality was found. Note that some VEXAG investigations are described more as basic measurement needs than as science investigations. Where possible, these are combined with the more science-focused investigations that the measurements

address (e.g., “measure topography and gravity” is combined with “determine structure of the crust”), resulting in a single list of unique investigations, where each investigation often can be traced back to multiple VEXAG objectives.

The investigations recommended in the VEXAG document were roughly prioritized within each goal by objective number (i.e., objective 1 within each goal is the highest priority). Because investigations were combined from multiple VEXAG objectives, the STDT assigned a VEXAG priority based on the highest priority VEXAG objective ranking. For example, if an investigation appears within objective 1 under goal 2 and objective 7 in goal 1, the investigation was assigned a VEXAG priority 1. This convention worked very well for those investigations found in goals 1 and 2, both of which had approximately equal numbers of objectives. However, goal 3 contains only half as many objectives, and all of the investigations found in goal 3 can be grouped with investigations from the other two goals. Thus, only the priority rankings from goals 1 and 2 were used to assign VEXAG priorities.

Based on its reading of the NRC Decadal Survey, the NASA Roadmap for Solar System Exploration, and its own research, the STDT also assigned priorities, independent of the VEXAG assessments, to each investigation. Four levels of priority for inclusion on the Venus flagship mission were defined such that each science investigation was:

1 = Essential to have

2 = Highly desirable

3 = Desirable

4 = Very Good to have

No additional prioritization was done within each of these four categories. The flagship investigation priorities differ somewhat from the VEXAG priorities. To first order, the rankings reflect the importance of investigations that could be carried out by a single flagship mission. The rationale for these differences is as follows:

- a. When similar VEXAG science investigations appeared under multiple objectives, the STDT interpreted these to have an increased level of priority.
- b. While the search for more habitable climates is certainly a very important science objective, it was not seen as an overall driver for the flagship mission; therefore, these objectives were systematically ranked lower.

Nevertheless, achieving the highest priority science objectives themselves would vastly increase our understanding of terrestrial climate habitability.

General measurement techniques were identified for each science investigation, regardless of priority. (Note that all investigations were considered, even though it is recognized that some very-high-priority investigations might not be feasible within the timeframe being considered for this flagship mission concept). Specific instruments (more than one in many instances) were identified within each measurement technique category. In many cases, there were inherent assumptions as to what type of platform should be used for each measurement. Chapter 2, Foldout 1 explicitly indicates for each

instrument whether the data are assumed to be collected from orbit (o), an aerial platform (a), or a landed asset (l).

Within Foldout 1, each instrument is rated as to how well it addresses each science investigation. This numerical value is defined as ‘goodness.’ Rating categories are:

- 3 Directly answers the question
- 2 Makes a major contribution toward answering the question
- 1 Makes a minor contribution toward answering the question or provides important supporting data needed by the primary measurement
- 0 Does not address the investigation at all

The assigned ratings assume that the instruments can operate at the level of fidelity required to achieve the specific investigation. Further, relative ratings make assumptions regarding areal coverage, time required to make observations, sample preparation, integration time, and other instrument-specific performance.

The right section of Foldout 1 further refines the assumed measurement platform to a range of mission architecture elements. These elements distinguish between balloons that operate within specific altitude ranges, descent probes that do not land, short-lived landed elements, and long-lived landed elements. In the cases of aerial and landed elements, distinction is also made between the contribution that can be made to each investigation from a single element and from multiple elements (allowing for samples in at least two locations in the atmosphere or on the surface). The aerial platforms are assumed to drift with the wind and are divided into four categories:

- High-level aerial platforms are those that operate at altitudes greater than 70 km. Such balloons or aircraft could observe the atmosphere from above the cloud tops and can be designed for fairly benign environmental conditions where solar power can be used and thermal conditions are not as extreme as in the deeper atmosphere.

- Mid-level aerial platforms would operate between 52 and 70 km, within the sulfuric acid/water cloud layer. These platforms would require their own power, making atmospheric measurements as well as some possible limited surface observations.
- Low-level aerial platforms would make measurements of the lower atmosphere between 15 and 52 km. It is likely that some limited observations of the surface could be made from this altitude; however, power and substantial thermal control would be required for extended life.
- Near-surface aerial platforms would operate below 15 km. These platforms would be ideal for making observations of the surface and near surface atmosphere, but survival might be an issue (analogous to the issues associated with landed platforms).

The same scheme used for the instruments was used to quantify the effectiveness of each architecture element toward addressing each science investigation. All of the scores in Foldout 1 were assigned by the STDT and then used to develop quantitative figure of merit (FOM) scores associated with each platform (see Section A.3 and Table A.2).

### A.3 Mission Architecture Assessment Methodology

This section describes the methodology used by the Venus STDT to derive a final mission architecture for a design reference mission (Chapter 4) (Bullock et al., 2008).

#### A.3.1 Science Figures of Merit

The science priorities and goodness scores discussed in Section A.2 were used to develop quantitative figures of merit (FOM) that allowed the STDT to compare how well each instrument and architectural element could address each of the science investigations in Chapter 2, Foldout 1. This simple science figure of merit ( $FOM_S$ ) was constructed for each investigation and platform combination using the formula:

$$FOM_S = (5-P) \times G$$

where  $P$  is the priority and  $G$  is goodness.

The priority ranking represents the scientific ranking of a given investigation and assigns a numerical value between 1 and 4, as described in Section 3.2. The goodness value, summed for each instrument or measurement technique, yields a science value against a given mission science goal. The assigned values, also discussed in Section 3.2, scale upward from (0) to (3). Summing up these  $FOM_S$  values for each architecture element provides an overall  $FOM_S$  for that element. Higher values of  $FOM_S$  for a particular architecture element suggest that the element might result in higher science return.

#### A.3.2 Technological Difficulty

In parallel to the science  $FOM_S$ , a technology Figure of Merit ( $FOM_T$ ) was also constructed by the technology members of the STDT for each mission architecture element using the formula:

$$FOM_T = C / M$$

where  $C$  is technology criticality and  $M$  is technology maturity.

For criticality, the ranking from (0) to (3) is assigned to each architecture element for every investigation. Assigned values are:

- 0 Not needed for that investigation
- 1 Useful
- 2 Desirable
- 3 Must have

Similarly, maturity was defined on the basis of technology readiness levels (TRL), and ranked from (0) to (3), representing the following TRL ranges:

- 0 TRL 1 – 2
- 1 TRL 3 – 4
- 2 TRL 5 – 6
- 3 TRL 7 – 9

The STDT assessed criticality on the basis of mission impact, and the STDT technology subgroup assigned maturity values. Higher values of  $FOM_T$  meant higher technology development requirements. While the technology  $FOM_T$  does not impact the science-driven selection of mission architectures, it indicates how much technology needs to be developed to achieve them.

### A.3.3 Mission Architecture Elements

The science and technology FOMs described above are mapped against 13 mission architecture elements as defined in Table A.1. The 13 elements are meant to represent the vast majority of plausible exploration platforms for a Venus flagship mission in the 2020 - 2025 time frame. Table A.1 also shows the estimated mission architecture element costs, whose derivation are described in Subsection A.3.4. These mission architecture elements consist of an orbiter or flyby spacecraft and a set of *in situ* platforms from which science measurements could be taken (Figure A.1). *In situ* mission architecture element complexities vary from a simple descent probe to a highly complex, near-surface mobile aerial platform with long traverse and periodic access to the surface. Single element and multiple elements of the same kind are differentiated because the latter could significantly enhance science by performing synergistic measurements at different locations. Mission lifetime — short or long — is an important differentiator. On one hand, long lifetime enables observations over an extended time (multiple Earth days to months); on the other, it introduces significant technology challenges in high-temperature operation, thus increasing mission cost and complexity.

### A.3.4 Rapid Cost Estimates

Approximate mission costs were estimated by the mission architecture team at JPL using a rapid cost assessment method customized for Venus missions. This approach was developed and successfully used during NASA's Solar System exploration roadmap process (NASA, 2006) and documented in Peterson et al., 2008.

For each Venus mission architecture concept, a set of cost drivers was established identifying key capabilities that a mission would require to achieve its objectives. The three primary cost driver categories include:

1 Launch operations

2 Flight systems

3 Mission operations

Additional categories account for:

- 1 The operating environment
- 2 Technologies
- 3 Flight heritage from past missions
- 4 Technology feed forward to future missions

These categories divide potential missions into distinct categories and non-overlapping and comprehensive cost contributors. This ensures a detailed accounting of the various mission cost contributors, while eliminating potential double-counting of these factors. Each applicable cost driver is associated with a *cost driver index* acting as a measure for the overall magnitude of the perceived complexity. Cost driver indices were allocated based on a five-level exponential scale, where Levels 1 to 5 were assigned points from  $2^1$  (= 2) to  $2^5$  (= 32).

Using these definitions, the rapid cost assessment process consists of four steps:

1. *Establishing a Reference Mission Set*, which includes (a) identifying historic reference missions (e.g., MER, Stardust, Viking, Galileo, Cassini-Huygens); (b) assigning cost indices to each cost driver; (c) summing the cost indices; (d) plotting the cost indices against historic mission costs; and (d) calculating the slope of the curve fit over the data set.
2. *Calculating cost indices* for each of the 13 Venus mission architecture elements (see Figure A.3 and Table A.2).
3. *Identifying new Venus flagship class architectures* by combining multiple mission architecture elements that stay within the cost cap (assumed to be between \$3 B and \$4 B). This assumed cost cap also includes a 10% allocation for science payload.
4. *Estimating costs for these mission architectures* from the slope of the reference missions multiplied by the cost indices.

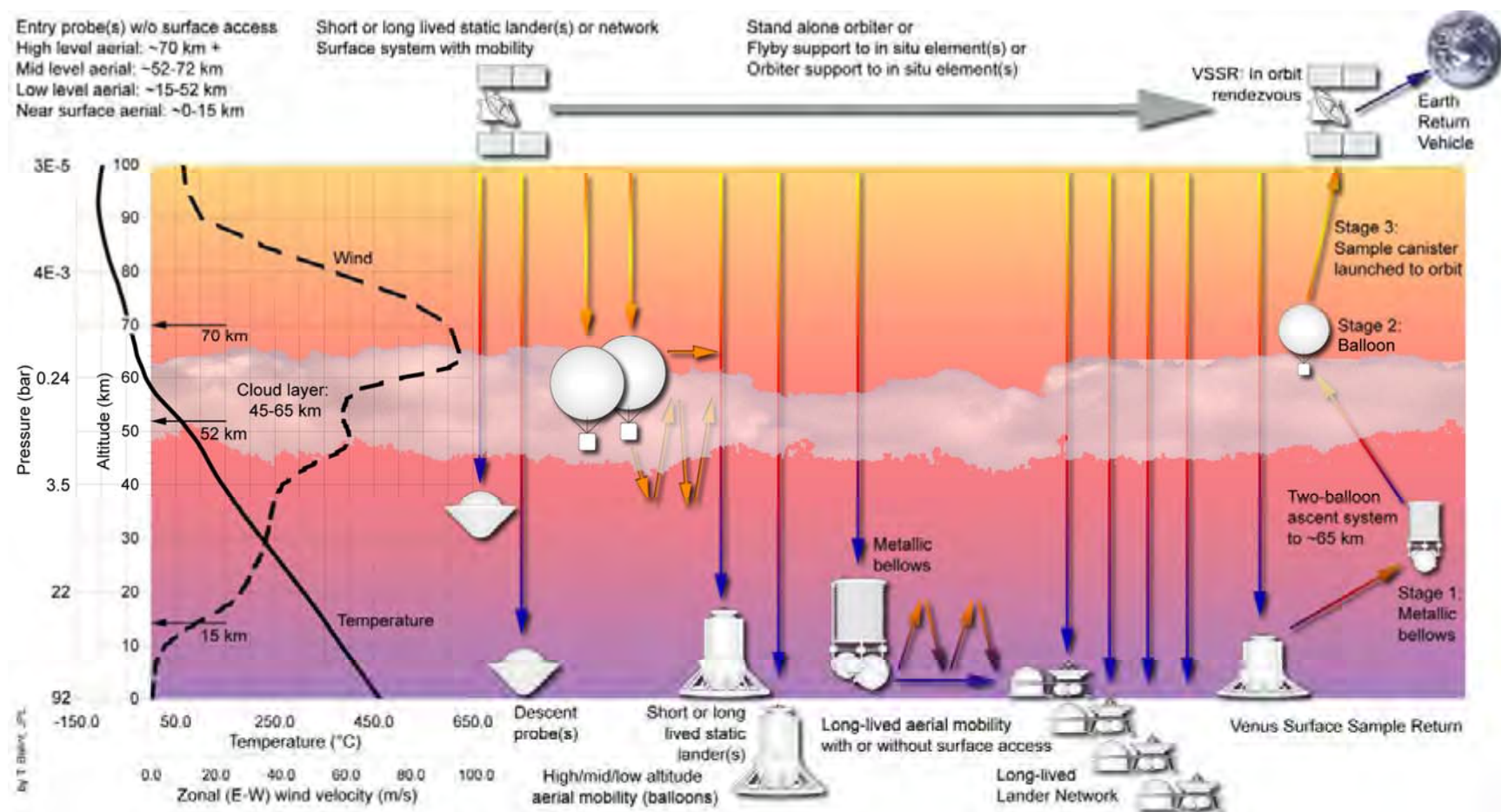
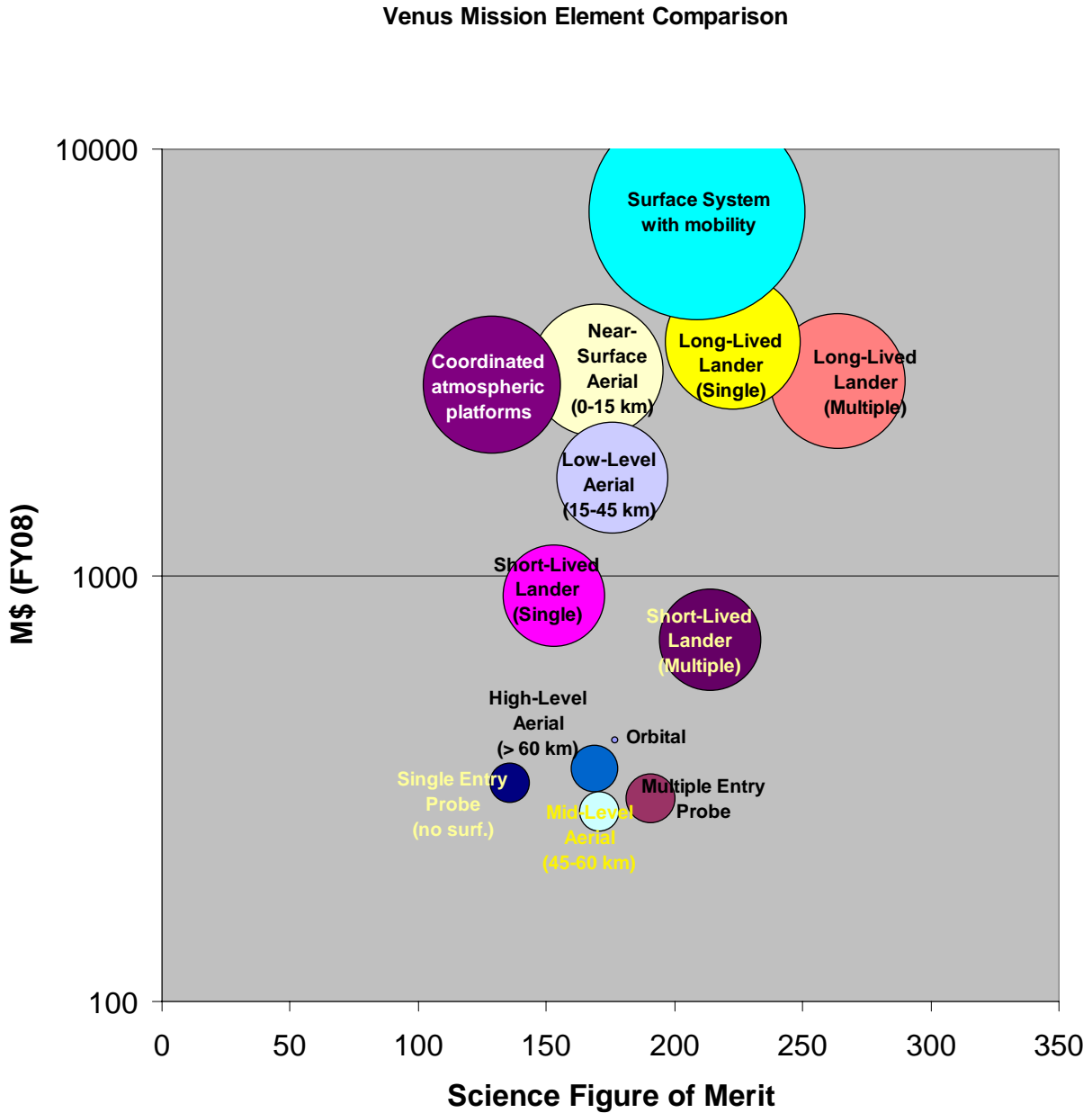


Figure A.2: Venus mission architecture elements: Orbiters, balloons, landers, and mobile platforms. Venus Surface Sample Return is shown for completeness, although it was beyond the scope of this mission study.



**Figure A.3:** Venus flagship mission architecture element costs as a function of science figure of merit. The size of each bubble (and the number with the bubbles) represent the level of technological challenge necessary to fly each architecture element.

Estimated costs as a function of science figures of merit for each of the 13 architecture elements are shown graphically in Figure A.3. The size of the bubbles (and the number within the bubbles) represents the level of technological challenge necessary to fly each architecture element.

It was found that this approach could predict relative mission costs between the various

architectures when the missions are still in their preliminary study phase and not yet fully defined. However, this method should be used for scoping only and should not to replace higher fidelity methods, such as parametric costing or a grass-roots method. The estimated accuracy of the rapid cost assessment is ~10% – 20% for relative costs and ~30%–40% for absolute costs.

**Table A.2:** Flagship mission architectures and FOMs

Mission Architecture	Science	Tech	Components	
Flagship Venera like	153	12	Flyby Short lived lander	
Venus Mobile Explorer	386	53	Orbiter Surface System w. mobility	
Pioneer-Venus plus	708	8	Orbiter Multiple (4) Entry Probes	1 High Level Balloon      1 Mid-level Balloon
Seismic Network	264	21	Flyby Long-lived multiple landers (4)	
Hi-Lo Balloons	516	23	Orbiter High-Level Aerial (> 60 km)	Near-Surface Aerial (0-15 km)
Mid-level Balloons	544	17	Orbiter Mid-Level Aerial (45-60 km)	Low-Level Aerial (15-45 km)
Mult. Short Lived Landers plus	582	15	Orbiter Short-Lived Lander (4)	Mid-Level Aerial (45-60 km)
Coord. Atmos. Platforms	306	21	Orbiter Multiple (4) coord. Platforms	
EVE-like concept	690	18	Orbiter Short-Lived Lander (Single)	High-Level Aerial (>60 km)      Mid-Level Aerial (45-60 km)
Pioneer-Venus w. landers	562	14	Orbiter Multiple (4) Entry Probes	Short-Lived Lander (Multiple)
Long-Lived Lander	400	21	Orbiter Long-Lived Lander (Single)	
EVE-Variant	635	17	Orbiter Short-Lived Lander (Single)	High-Level Aerial (> 60 km)      Single Entry Probe (no surf.)
New Frontiers VISE like	76.5	6	Flyby Short lived lander	
<b>STDT Flagship</b>	753	15	Orbiter 2 Mid-Level Aerial (52-70 km)	Short-Lived Lander (2)
Geology Choice	347	20	Orbiter Near-Surface Aerial (0-15 km)	
Atmosphere Choice	539	5	Orbiter 2 Mid-Level Aerial (52-70 km)	Multiple (2) Entry Probes
GeoChem Choice	214	12	Flyby Short-Lived Lander (2)	

#### A.4 Mission Architectures

This section provides an overview of candidate Venus mission architectures that were created by combining one or more of the elements described in the previous subsection. This is followed by a discussion of the STDT-recommended mission architecture that serves as the basis for the detailed Design Reference Mission discussed in Chapter 4.

To date, a significant number of Venus missions have either flown or been proposed using mission architectures that included orbiters (Magellan), probes (Pioneer Venus), balloons (VEGA), and short-lived landers (Venera). The total range of architecture elements is schematically shown in Figure A.4.

While the mission architecture elements of these past missions are very similar to those of potential Venus Flagship mission, there will be major differences in the science instrument

payloads and, hence, the kinds of science questions that can be addressed. The technological readiness of these previously used platforms is clearly high and results in low challenge ratings in the Venus flagship trade study. The opposite is true for platforms not previously used, particularly those involving long durations in the high-temperature regions of the lower atmosphere and on the surface.

The STDT and the JPL engineering team synthesized 17 multi-element mission architectures that spanned a large part of the design space that could conceivably fit within the assumed cost cap of a Venus Flagship mission. Science figures of merit and total mission cost estimates were compiled for all of these architectures using the methodology describe above. The results are listed in Table A.2 and plotted in Figure A.5.

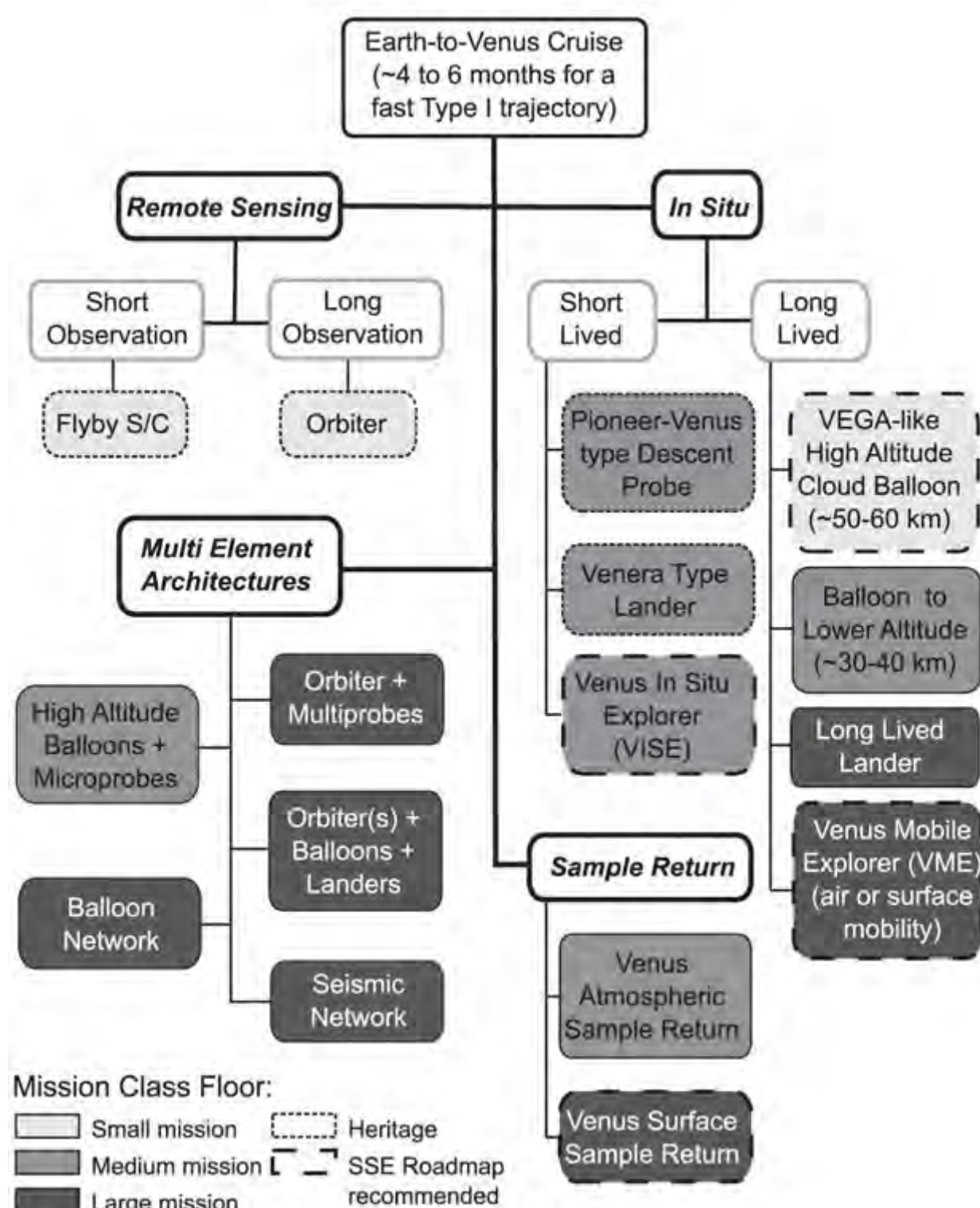
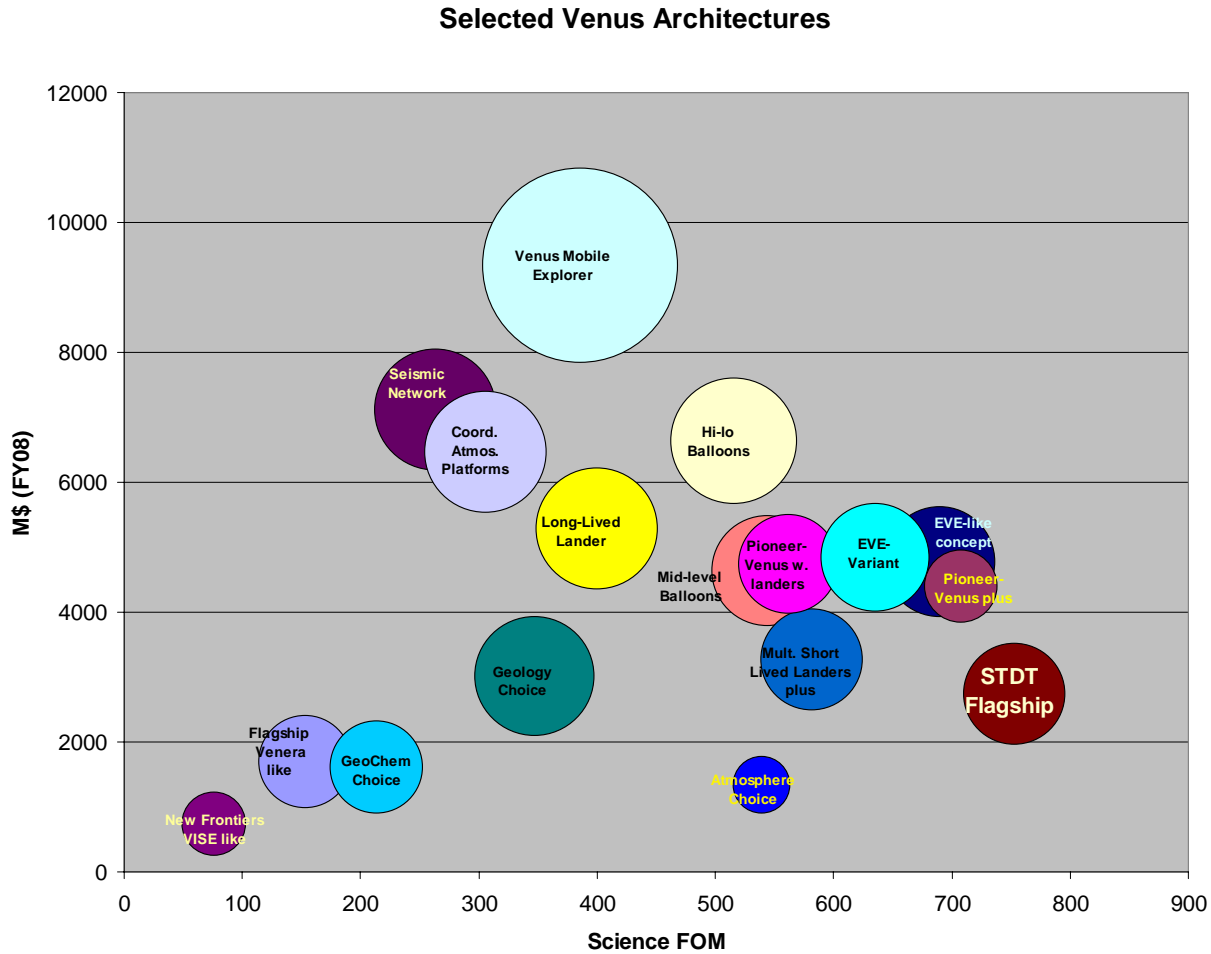


Figure A.4: Venus mission architecture examples (Balint et al., 2008).



**Figure A.5:** Venus flagship mission architecture costs as a function of science figure of merit. The size of each bubble (and the number with the bubbles) represent the level of technological challenge necessary to fly each mission type.

Each of the three STDT science subgroups, (geology and geophysics, atmosphere, and geochemistry) had its preferred mission architecture chosen from the group of 17 that maximized the scientific return for its own subgroup. A fourth was jointly proposed by the STDT that represented a balanced compromise across the subgroups. The science and technology FOMs and estimated costs for these four architectures are shown in Table A.3. The STDT found that single-element architectures, such as a near-surface mobility platform alone, cannot answer a majority of the key science questions for Venus and, thus, were not selected for the Design Reference Mission.

It is evident from Table A.3 that the STDT-recommended multi-element mission architecture has the highest science FOM and provides flexibility for payload accommodation on the various mission architecture elements. This allows for scalability in response to mission cost cap changes and readily lends itself to international collaboration because partners can take responsibility for different elements that are highly independent. In addition, this architecture supports science measurement synergies between the different platforms with little or no time difference, an advantage not afforded by individual missions that make measurements at different locations and altitudes many years apart.

**Table A.3:** Potential flagship mission architectures, FOMs, and costs.

Recommended by	Mission architecture concept	Science FOM	Tech. FOM	Cost est.
<b>Mission architecture choices by STDT Science Subgroups</b>				
Geology Subgroup	Multi-element architecture with 1 orbiter; and 1 near surface aerial platform	347	20	\$3.0 B
Atmospheric Subgroup	Multi-element architecture with 1 orbiter; 2 mid-level aerial platforms; and 2 entry probes	539	5	\$1.3 B
Geochemistry Subgroup	Multi-element architecture with 1 flyby; and 1 short lived lander	214	12	\$1.6 B
<b>STDT recommended mission architecture for detailed Flagship study</b>				
Full STDT	Multi-element architecture with 1 orbiter; 2 mid-level aerial platforms; and 2 short lived landers (could include long lived elements)	753	15	\$2.7B

To summarize, the *recommended architecture* includes a highly capable *orbiter* with a design lifetime of up to 4 years; *two cloud level super-pressure balloons* floating at a constant altitude between 52 and 70 km, each with a design lifetime of 1 month; and *two landers* that would also perform science measurements during atmospheric descent. The baseline architecture calls for short-lived landers because most of the critical landed science can be carried out during the expected 5- to 10-hour lander lifetime. However, two instruments that are not included in the recommended architecture — a long-lived seismometer and a long-lived meteorology station — would significantly enhance the science return. Their exclusion was primarily a result of technological difficulty and cost constraints, objections that would go away once the requisite technology development program were executed. Chapter 5 discusses the seismometry and meteorology options in further detail.

## B Advanced In Situ Exploration Concepts

---

As spectacularly demonstrated by the (so far) 5-year mission of the Mars Exploration Rovers, the ability to move from one location to another to explore a planet allows a variety of terrains to be investigated, thereby enabling a broader understanding of the rich diversity of a planet's surface (Arvidson et al., 2006; Squyres et al., 2006a). Exploration by a mobile explorer further allows a sense of accessible exploration and discovery, as multiple new features are investigated beyond the initial landing site and the progress of the mobile system is followed. While a landing or entry site can be chosen for its initial interest, the scientific investigations with mobile systems, such as a rover, can extend far beyond the initial point of interest. This section discusses two mobile platform systems and related solar cell technology that could significantly affect Venus exploration.

Much like the geology seen from an airplane during a flight on Earth, aerial perspectives of the planet Venus can yield a unique understanding of the planetary geology. Airplane-based observations of the Venus surface can complement the balloon missions at different altitudes and with an increased level of directional control.

A limitation of the Design Reference Mission architecture is the stationary nature of the lander elements as well as the relatively high altitude of the balloons operational above the Venus surface. A significant problem with the stationary lander is that if the nature of the site is different from that expected (for example, a regolith-covered landing site if the instrument set is optimized for drilling into rock or a high-slope landing site if the lander is optimized for an expected level landing site), the results of the short-duration mission could be compromised.

Likewise, if the initial landing site images show a target of high scientific interest only a few meters outside the reach of the lander system, mobility would be highly desired and would enable the lander system to reach and analyze the target. A stationary lander must be designed to achieve science results from

"average" landing site conditions and cannot be targeted to specific geological settings within a site. Long lifetime and surface mobility would, therefore, provide a significant enhancement to the landed mission.

Additionally, increased correlation between low-level mobile platforms, mid-level balloons, and high-level orbiters could improve the science provided by each element even more than a stationary lander. For example, correlation between the orbiter InSAR mapping activities and the mobile systems can significantly enhance the science returned if features of high geologic interest are identified near the landing site; specifically, the orbiter could identify locations of interest that could then be investigated in more detail by the mobile systems. Likewise, a low-level mobile system could identify regional geology that could then be further investigated on a broader scale by the orbiter. Integration with balloon data, as well as investigation of sites identified by the balloons, allows a three-level investigation of the Venus environment, but at various locations and in a controlled manner.

### B.1 Rovers

A lander platform could provide either short-term scientific investigations (the Design Reference Mission) or long-term investigations (using Stirling power and cooling) of the Venus surface. However, these investigations would be limited to the immediate surroundings of the landing site. To facilitate a broader sampling of data and to allow investigation of specific sites of interest on the surface, the operation of a rover system is necessary. Such a rover system could either replace the lander or be a subset of the lander's instrument package (Landis and Mellot, 2007). The fundamental approach is to be able to move from place to place in order to investigate features of the Venus surface that are not present at the initial landing site or easily investigated with the mid-atmosphere balloon. The operation of a rover on the Venus surface would require a range of high-

temperature technologies as well as a significant power source capable of long-term operation.

The overall objective of a rover for the Venus surface would be to provide mobility and scientific instrumentation of a set comparable to the scientific goals of the Mars Exploration Rovers (MER) mission. The original goal of the Athena payload — to put a ‘mobile field geologist’ on the surface — has succeeded spectacularly in understanding the local and global geology of Mars (Squyres and Team, 2001). If this could be accomplished on Venus in the future, the extraordinary scientific returns will reveal the nature of Venus’ local geology using robotic field geological investigations. Although this objective is challenging, it is within the capabilities of existing technologies if appropriate investments are made to achieve flight readiness.

### **B.1.1 Scientific Objectives of a Venus Rover**

The scientific objectives of a Venus rover would be as follows:

- Acquire multi-color images and elemental and geochemical data over traverses that cross individual flows or lithologies. Piecing together the local stratigraphy and connecting this with what is seen in the Magellan radar dataset will provide an enormous improvement in the geologic analyses of Venus.
- Provide scientific advances in understanding in great detail the local geology and geochemistry of Venus in the way that the Mars Exploration Rovers have done for Mars.
- Provide a delivery system for *in situ* experiments, such as placement of the seismometer network.
- Provide long-lived operation of a planetary outpost on Venus that can characterize the Venus environment over an extended period of time.

One rover approach would be a Radioactive Power Source (RPS)-powered system with

high-temperature actuation to allow mobility. In this example, the rover system would have the same instrumentation suite as the lander, powered and refrigerated by Stirling systems, but mobile and able to investigate a variety of locations. In effect, this rover would have many of the advantages of the lander, but with the added capabilities of mobility. The rover could also serve as a delivery system for the placement of *in situ* elements, such as seismometers, in specific locations.

The history of Mars rover investigations serves as a model for the surface investigation of Venus. A rover would allow comparison of Venus features with those of both the Earth and Mars over a wider scale than available with the lander. For example, this would enable sampling of multiple rock types and soils, rather than only the specific types at the landing location, allowing the distribution of surface features to be categorized. Given the wide range of surface variability on Earth and Mars as one goes from region to region, there will almost certainly be significant geologic differences over the scale of a rover’s traverse.

Deployed elements could use the rover as a relay station to transmit data. This decreases the complexity of the *in situ* elements without increasing significantly the complexity of the rover system. Information on rover engineering performance and failure mechanisms can lead to better design of such structures for future missions, such as a Venus Surface Sample Return (VSSR).

### **B.1.2 Technologies for Venus Rovers**

There are two main branches to the Venus rover design space: 1) designs that require refrigeration to cool onboard science instruments and other components and 2) designs that do not. This is similar to the situation for fixed landers, but with two major differences. First, rovers require motors and other actuators to move around; these actuators typically are exposed to the environment and require high-temperature compatibility. Second, rovers only become truly useful if capable of extended mission lifetimes of days or weeks. This tends to preclude advanced but passive, non-refrigerated thermal designs that

could enable landers to survive up to a day or two.

Except for the drive mechanisms, non-refrigerated rovers mimic the technological challenges of non-refrigerated landers. All components, including science instruments, computers and electronics and telecommunications equipment, must be compatible with the 460° C Venus surface temperature. Therefore, it is more likely that a Venus rover will require radioisotope-powered refrigeration similar to that discussed above for the long-duration lander. A preliminary design of such a rover was developed as part of a 2003 NASA study (Landis et al, 2006). The Venus rover is shown in Figure B.1. The candidate rover design shown utilizes a four-wheel design, with each wheel mounted on a parallelogram-suspension strut. The four-wheel parallelogram-strut design shown offered the advantage of minimizing the number of joints and moving parts, while at the same time allowing good clearance over rocky terrain and incorporating a high-flexure suspension for the landing loads. The total mass is estimated to be 330 kg.



**Figure B.1:** Conceptual design of the Venus Rover CAD model with wheels deployed, perspective view (visualization by Shawn Krizan).

The rover lands directly on its wheels while descending under a parachute. The electronic components of the rover are packaged into a spherical electronics enclosure, shown mounted at the front of the rover. A spherical shape was chosen to minimize the surface area for thermal design purposes. The power supply

and cooling radiators are mounted at the back in order to keep the heat-rejection radiators far from the cooled electronics.

Both thermoelectric and dynamic (Stirling conversion) radioisotope power options were analyzed; the Stirling converter was selected on the basis of its the higher efficiency (Mellott, 2004; Landis and Mellott, 2007). To cool the primary electronics, a two-stage Stirling cooling system was chosen. The power level of this system was selected to allow the upper-stage electronics enclosure to be cooled to 300° C and the lower-stage electronics enclosure to be cooled to 50° C. The rover surface elements were designed to use high-temperature discrete electronics operating at the Venus ambient temperature for as much of the operation as possible. Further details on this design, including discussion of high-temperature motors, actuators, and extended pressurization, can be found in Landis et al. (2006) and Dupont (1999).

Further, if a high-temperature rover is to operate in-situ in Venus environments, operate autonomously, or even provide human in the loop interaction, a basic ability to understand the system's current status and operational capabilities is needed. In a simple example, a rover investigating a rock deposit needs to know its position related to the rock deposit and barriers to arriving at the destination. It needs to know if the wear on, for example, the exterior gear system (due to the harsh environment) is limiting the amount of time left to the mission or if the system is operating outside of normal parameters. These measurements combined with other measurements could evaluate the state of the system and warn of impending mission failure and allow scientists to optimize the remaining mission time. These types of measurements have been done previously on Mars regarding engineering evaluation of the rovers. Further, if a mission fails prematurely, this information helps answer why and also provides engineering information for the design of future systems leading to, for example, a Venus Surface Sample Return. Similar

considerations also hold for other platforms being exposed to new, harsh environment operational conditions.

In summary, the conceptual analysis suggests that a Venus surface rover is feasible. Nonetheless, the technical challenges for a Venus rover are significant; however, work to date provides a starting point design and technology pathway to go forward.

## B.2 Atmospheric Exploration by Aircraft

Balloons with capable payloads can be flown from above the clouds to near the surface. However, there are some compelling scientific experiments that can and should be performed by a vehicle that can be directed to locations of interest for in situ and remote investigations. A prime example is the haze-rich environment above the clouds, which varies dramatically with latitude and time and has a major influence on the global energy balance of the atmosphere.

In-situ investigations of unparalleled scope and duration could be accomplished by properly equipped aircraft. The chemical and radiative environment could be continuously monitored for many tens of revolutions around the planet at a variety of altitudes. The above cloud hazes, which vary in time and are more prevalent at the poles, could be characterized sufficiently to understand their affects on climate, clouds, and atmospheric circulation. Flights within the clouds, much like the

exploratory aircraft that sample the Earth's clouds, would give us a detailed understanding of the formation and structure and chemistry of the Venus clouds. Finally, an aircraft that can be controlled to search for regions of vertical winds or other dynamical phenomena can probe the poorly-understood dynamics of Venus' atmosphere.

Table B.1 compares some of the advantages and disadvantages of three types of airborne platforms: balloons, airships, and airplanes. The atmospheric pressure and density found near the surface of Earth occurs at an altitude of just over 50 km on Venus. For a flight vehicle, this means that flying at 50 km on Venus is similar aerodynamically to flying near the surface on Earth. Above the cloud layer, there is an abundant amount of solar energy. The solar flux at the orbit of Venus is  $2600 \text{ W/m}^2$ , which is much greater than the  $1360 \text{ W/m}^2$  available at Earth orbit. This nearly 100% increase in solar flux can significantly increase the performance of solar-powered vehicles. Even within or below the cloud layer, there might be sufficient solar energy to power a vehicle. At the bottom of the cloud layer (48 km altitude), the solar intensity is comparable to the solar intensity at Mars or Earth. Therefore, even within the cloud layer, the ability to fly under solar power on Venus will be no worse than it is to fly on Earth or Mars.

**Table B.1:** Summary: Airborne Platform Concept Trade-offs.

Balloon	Airship	Airplane
<ul style="list-style-type: none"> <li>Simple technology</li> <li>No power required to maintain altitude; power only for instruments and payload</li> <li>Demonstrated on Venus by the Russian "VEGA" mission</li> <li>Altitude change possible within limits by dropping ballast or venting gas, but repeated altitude change is difficult</li> <li>Location change not controllable</li> <li>Cannot stationkeep over surface; cannot stay in sunlight</li> </ul>	<ul style="list-style-type: none"> <li>Difficult to stow and deploy</li> <li>Altitude change possible, but difficult</li> <li>Speed is slow</li> <li>Cannot stationkeep over surface; cannot stay in sun</li> </ul>	<ul style="list-style-type: none"> <li>Airplane design uses terrestrial experience</li> <li>Stow and deploy concepts demonstrated by ARES Mars airplane (Landis, 2003; Levine et al., 2003)</li> <li>Altitude change is possible above range defined by temperature limits and below altitude limit defined by atmospheric density</li> <li>Speed allows stationkeeping over surface feature or continuous sun flight</li> </ul>

The winds within the atmosphere blow fairly consistently in the same direction as the planetary rotation (East to West) over all latitudes and altitudes up to 100 km. Above 100 km, the winds shift to blow from the dayside of the planet to the night side. The wind speeds decrease as a function of altitude from ~100 m/s at the cloud tops (60 km) to ~0.5 m/s at the surface. These high wind speeds and the slow rotation of the planet produce a super rotation of the atmosphere (nearly 60 times faster than the surface) (Schubert, 1983). The gravitational acceleration on Venus ( $8.87 \text{ m/s}^2$ ) is slightly less than that on Earth, which aids somewhat in the lifting capability of an air vehicle.

### ***B.2.1 Scientific Objectives for the Exploration of Venus by Aircraft***

A flight vehicle operating within Venus' atmosphere can carry out a number of potential science missions. Some examples of these are:

- The determination of atmospheric properties over a region of the atmosphere.
- Direct sampling and analysis of the atmosphere.
- Characterization of trace gasses as possible biogenic indicators of life.
- Searching for volcanic emissions in specified regions of the planet.
- Magnetic field mapping over a region of the planet.
- Platform for radar investigations of the surface.
- Magneto-telluric sounding of the interior.
- Correlation of atmospheric motion between different locations by two or more aircraft.
- Communications and command relay for balloons, landers, and possible surface vehicles.

Flight vehicles can provide a unique perspective for the exploration of Venus. Ideally a flight vehicle would be capable of operating for long durations, on the order of months, within the atmosphere. Possible flight

altitudes are 50 km to 75 km above the surface, at and slightly above the cloud layer.

The addition of controlled flight in the Venus atmosphere can allow for targeted investigation of specific Venus atmospheric features that uncontrolled flight would have difficulty investigating. One recent example is the apparent difference in composition between the tessera and plains, deduced from emissivity differences apparent in VIRTIS images of the surface (Helbert et al., 2008; Mueller et al., 2008).

While the Design Reference Mission involves balloons that are carried by atmospheric currents, there is no control of the direction of the balloons in these currents. In contrast, an airplane mission would have independent flight unrestricted by such currents. In principle, the airplane mission could last considerably longer than the balloon mission, given the airplane's ability to fly higher to retrieve solar power and then lower for investigation purposes. The operation of the airplane could be coordinated with the balloon mission to first investigate different altitudes than the balloon as well as to target specific areas of interest identified by other components of the mission (e.g., lower-level balloons). The airplane mission could also repeatedly go through layers of the atmosphere to characterize atmospheric conditions at different altitudes.

### ***B.2.2 Technologies for Venus Aircraft***

A number of studies have been conducted to assess the possibility of solar-powered flight on Venus (e.g., Colozza et al., 2004; Landis et al., 2003, 2005, 2006). These studies suggested the feasibility of making a solar-powered aircraft for flight at levels above the middle cloud level; that is, roughly above an altitude of 50 - 60 km. At this altitude, the conditions on Venus are similar to terrestrial conditions. Consequently, the resulting Reynolds numbers for flight are comparable, thus simplifying the task of propeller and wing design. Furthermore, the solar intensity is about twice of that on Earth, high enough that solar arrays can provide not only adequate power for flight during daylight, but also the

power required for more difficult maneuvers, such as hovering over a particular ground location despite the very high 60+ m/s wind speeds encountered at the cloud altitude of 50 - 60 km. This kind of maneuverability enables exploration scenarios not possible with balloons or even propeller-driven blimps. For example, it would be possible for the aircraft to loiter at high altitudes, flying at sufficient speed to stay at the subsolar point where it receives maximum solar intensity, and then conduct a sortie mission to lower altitudes, where it could spend extended periods (dozens of hours of operation) making measurements at levels down to approximately 47 km for a 100° C temperature limit and an altitude of 33 km with a 200° C temperature limit.

A significant requirement for a Venus aircraft design is that the wing and tail must be designed to fold and fit into the aeroshell for transport to Venus and entry into its atmosphere. The unfolding of a candidate design is shown in Figure B.2, which illustrates the placement of solar cells on top and bottom surfaces of the wings. Folding-wing deployment has been demonstrated on a similar-sized test airplane in the ARES project, a demonstrator for a proposed Scout mission to Mars (Guynn et al., 2003). The configuration chosen is a conventional aircraft platform, with each wing folded about halfway out the span, and a folding propeller. The vertical tail is doubled and mounted on the bottom surface, rather than the top, to fit in the aeroshell. Figure B.2 (right side) shows the airplane unfolded for flight. In the current design for Venus, the aircraft has a 12-m wingspan, allowing it to be folded into a 3.7-m aeroshell for entry. The baseline airplane mass is 103 kilograms, including instruments.

The Venus airplane requires development of technologies for long-duration, solar-powered flight in the Venus atmosphere. Although solar-powered flight has been demonstrated by a number of investigators on Earth, the technology needs to be developed further to

reduce the size and increase the operational envelope for use on Venus and to increase the latitude range of operation (that is, develop new solar airplane designs that operate at lower Sun angles). The speed range for operation of the Venus airplane is higher than that used for solar airplanes on Earth; this will require some changes in design. In addition, the carbon dioxide atmosphere provides some differences in performance that will have to be studied. In particular, since the speed of sound is lower in the Venus atmosphere, at a given Reynolds number of operation the propeller will operate at a higher Mach numbers. This will require some computational fluid dynamic modeling to optimize a propeller for Venus.

At cloud-level altitudes (50 - 60 km), conventional space solar cell technology should operate at good efficiencies. However, the solar spectrum changes with altitude because cloud particles preferentially scatter infrared light and, at low altitudes, Rayleigh scattering removes the shortest wavelength (blue) component of the spectrum. This means that the optimization of the solar cell design will be a function of altitude. There is also a strong interaction with the temperature, since the type of semiconductor technology that is least sensitive to temperature is inherently most responsive to the short-wavelength illumination and does not convert to red and infrared; thus, the selection of technology is a trade-off between the higher efficiency of short-wavelength-sensitive semiconductors and the reduction of short-wavelength spectrum available.

Protection of the solar arrays against the sulfuric acid droplets in the clouds will be needed. The most likely solution will consist of coating the arrays with Teflon, which is commonly done in the terrestrial thin-film solar array industry for environmental protection. It is also necessary to make sure that all exposed surfaces of the airplane be either Teflon-coated or constructed from a sulfuric acid tolerant material.



**Figure B.2:** Left Side: Artist's conception of the unfolding sequence of the airplane tail and wing for an early conceptual design of a Venus aircraft, showing solar cells on the top and bottom surface of the wings and tail; Right Side. Visualization of the final design configuration of the Venus airplane, showing perspective and side views.

### **B.2.3 Solar Power Generation Technology for Venus Exploration**

Photovoltaic power could be extremely valuable for Venus atmospheric and surface missions; however, the Venus environment provides significant challenges to photovoltaic operation (Landis and Vo, 2008). The problems with solar power generation for in situ Venus missions become increasingly difficult as the altitude decreases. Four effects make the Venus environment challenging when considering solar panels:

1. Temperature.
2. Solar intensity.
3. Solar spectrum.
4. Corrosive environment.

Temperature is the most significant problem. Solar cells have a fundamental decrease in performance as temperature increases; at very high temperatures, solar panels can experience catastrophic degradation. The performance decrease with temperature is a fundamental property of semiconductors; however, it is dependent on the material technology chosen. Different technologies will have different performance in the Venus environment. If solar cells are to be operated at extremely low altitudes, dealing with the catastrophic degradation at high temperatures is a matter of utilizing the appropriate technology (e.g., metallization

chosen not to interact with the semiconductor, use of barrier technologies, etc.). Operation of existing technologies has been demonstrated up to temperatures of 227° C, corresponding to about 30-km altitude above the Venus surface. Higher temperature operation will require validation testing; at some temperature this will also require technology development. While this is not a fundamental problem, and technologies to deal with high-temperature operation have been developed for other applications, the technology required has been demonstrated only on small-scale test devices and is not currently employed on solar cells. Likewise, the encapsulation technology for the solar array will also require some technology validation and development, since existing solar cell cover glasses are affixed to the cells by silicon adhesives, which have not been qualified for operation at high temperatures.

Solar intensity decreases as the altitude decreases. This fact puts a fundamental limit on the amount of power that can be generated per unit area, a fact exacerbated by the fact that the solar spectrum narrows with altitude. At the cloud level, cloud particles preferentially scatter out infrared light; at low altitudes, Rayleigh scattering removes the shortest wavelength (blue) component of the spectrum. This effect adjusts the optimum technology choice as a function of altitude. This effect also has a strong interaction with the temperature, since the type of

semiconductor technology that is least sensitive to temperature is inherently most responsive to the short-wavelength illumination and does not convert to red and infrared. Therefore, the selection of solar panel technology is a trade off between the higher efficiency of short-wavelength-sensitive semiconductors and the reduction of short-wavelength spectrum available.

An additional challenge is the possible corrosive effect of the Venus environment, most notably the sulfuric acid droplets at the cloud level and the supercritical carbon dioxide at the low altitudes. Mitigation of the sulfuric acid problem does not represent a significant challenge. Solar cells used in space are shielded behind transparent cover glass, a material that is not attacked by sulfuric acid; therefore, the large exposed area is already covered with a resistant material in the standard approach. In this approach, encapsulation against the acid comprises enlarging the size of the glass cover to make a single continuous sheet (a technique used in terrestrial solar arrays) and making sure that the edges and interconnects are sealed with an acid-resistant seal. An alternative solution is to use transparent Teflon. Teflon is a material commonly used in applications requiring sulfuric acid resistance, and was used on the VEGA mission. Teflon encapsulation is done commercially in the terrestrial thin-film solar array business because it is cheap and simple, and FEP Teflon encapsulation for space solar arrays has been developed and tested. It would be a low-cost, lightweight alternate method to

encapsulate cells for Venus. Glass-cover encapsulation is expected to provide protection from supercritical carbon dioxide as well.

The optimum solar cell technology for Venus and the performance possible (in terms of watts per square meter) depends on the operating altitude. For altitudes down to about 25 - 30 km, well below the base of the clouds, conventional triple-cell technology remains the best choice. Below 25 km, the germanium subcell of the triple-junction cell is no longer producing power, and a dual-junction (GaInP/GaAs) cell technology would be preferred. At the surface, the short-wavelength light intensity is no longer great enough to fully power the GaInP sub-cell; in that situation, a single-junction cell becomes a slightly higher-performing technology.

Table B.2 shows an example calculation (Landis and Vo, 2008) showing the area of solar array required to produce one watt at solar noon as a function of altitude for the three cell technologies considered. Below about 30 km, significant technology development will be required, since the cell technology commercially available today does not incorporate metallization or cell encapsulation designed for the temperatures. Note that at low altitudes, however, it takes very large solar panels to produce even small amounts of electrical power. Therefore, photovoltaic power generation is likely to be restricted to higher altitude applications except, perhaps, for very specialized applications requiring just a few Watts of power for long durations.

**Table B.2:** The Solar Array Area Required to Produce One Watt of Power at Various Altitudes in the Venus Atmosphere at Solar Noon. (Note that solar arrays for altitudes below about 30 km will require technology development to avoid thermal degradation.)

Altitude(km)	Cell type		
	Triple junction Area (m <sup>2</sup> )	Dual Junction Area (m <sup>2</sup> )	Single Junction Area (m <sup>2</sup> )
0	-	1.56	1.17
10	1.34	0.37	0.97
20	0.47	0.20	0.63
30	0.08	0.09	0.32
40	0.05	0.04	0.25
50	0.02	0.03	0.17
60	0.01	0.01	0.09